Identification and regulation of receptors involved in plant immunity

---

by

Isabel Marie-Luise Saur

Canberra, March 2015

A thesis submitted for the degree of

Doctor of Philosophy of

The Australian National University

Declaration

This thesis is my own work and does not contain any results that have been generated by persons other than myself, expect where due reference and acknowledgment has been provided. Results presented in this thesis have not been used for the award of any other degree at any other institution.

Isabel S

Isabel ML Saur

Acknowledgements

Firstly, I would like to thank John Rathjen who proved himself a helpful supervisor and friend, always having time for my questions. Thanks for supporting me throughout my PhD studies which incorporated a difficult period in my personal life. I admire and respect your teaching and am grateful for the guidance.

Secondly, I would like to thank Cyril Zipfel from The Sainsbury Laboratory for hosting me for a portion of time during my studies. Several results included in this thesis were generated in his laboratory and with no doubt many outcomes would not have been achieved if Cyril had not shared his knowledge with me.

Thanks also to my advisory panel consisting of David Jones and Peter Dodds for questions, suggestions and discussions regarding my project. I must express special gratitude and recognition to my advisor Warwick Hillier who has since passed on. Despite experiencing the most difficult challenges himself, he always found the words to support and encourage.

I would also like to express my gratitude to all members of Cyril Zipfel's team and everyone from the Rathjen Lab. Special mention goes to Brendon Conlan, who was most useful for discussions regarding the Pto/Prf project.

Thanks to my colleagues from 3rd floor South Wing and my friends at the ANU Research School of Biology for providing such a friendly and supportive working environment. Special thanks to my friends Lauren Du Fall and Bianca Haberl for their support, proof reading of several documents and their friendship.

Special thanks also to my brother Michael and his family without whom I am positive I would not have finished my PhD. Thank you for shouldering responsibilities in Germany while I was overseas and for supporting me throughout the years. For the same, I would also like to acknowledge my extended family.

Most importantly, I would like to thank my parents for their love and guidance and being with me for as long as they could. Thank you for raising me to be self sufficient and independent, teaching me the important values in life. I wish I had longer with you both and hope you would still approve of my choices in life.

Abstract

Plants sense invading microbes using surface-localised transmembrane receptors (pattern recognition receptors, PRRs) and intracellular nucleotide-binding – leucine-rich repeats proteins (NB-LRR). PRRs detect elicitors conserved amongst whole classes of microbes (pathogen-associated molecular patterns, PAMPs), such as bacterial flagellin. PAMP perception initiates cellular reactions collectively called PAMP-triggered immunity (PTI). Considering the number of transmembrane receptors present in plant genomes, only few PRRs have been identified to date. Identification of novel PRRs is important from a basic knowledge standpoint and because interfamily transfer of PRRs can confer broad-spectrum disease resistance.

I used the common PRR co-factor BAK1 as bait to purify new PRRs after PAMP treatment. The success of this novel strategy was confirmed by the identification of the receptor for the bacterial PAMP cold shock protein (CSP) from *Nicotiana benthamiana* (Cold Shock Protein Receptor; NbCSPR). Perception of CSP is potentiated by earlier flagellin recognition, confers resistance to bacteria in an age-dependent manner, and limits *Agrobacterium*-mediated transformation of flowering *N. benthamiana* plants. Transfer of *NbCSPR* to *Arabidopsis thaliana* confers CSP recognition, suggesting that the gene can be transferred into other plant species to confer anti-bacterial resistance.

I further studied recognition of the fungal pathogen *Puccinia striiformis f.sp. tritici* in non-host species. Treatment of *N. benthamiana and A. thaliana* with stripe rust PAMP-preparations suggested the existence of PRRs that recognise this wheat pathogen. Using the above BAK1 strategy, I identified candidates for such PRRs and their

potential roles in restricting rust diseases in non-host plants through PTI may now be determined.

PTI can be suppressed by pathogenic microbes through the secretion of virulence effector proteins, which target defence components and lead to disease development in susceptible plants. The recognition of effectors by intracellular NB-LRR resistance (R) protein can however initiate effector-triggered immunity (ETI), usually associated with a localised cell death that can prevent pathogen spread. How effector recognition translates to cell death is not well understood. Because of the dramatic outcome of ETI, R proteins have to be tightly regulated, and understanding these mechanisms is crucial for engineering durable resistance to crop pathogens.

The tomato R protein complex composed of the Pto kinase and the NB-LRR protein Prf confers resistance to the bacterium *Pseudomonas syringae* pathovar *tomato* (*Psto*), the causal agent of bacterial speck disease. The Pto/Prf complex is tightly regulated: In the absence of the *Psto* effectors AvrPto and AvrPtoB, Pto negatively regulates Prf and *vice versa*. Effector binding to Pto triggers a number of conformational changes within the complex for which the structural basis is largely undetermined. The unique N-terminal domain of Prf (N) is the Pto binding site, and must play an important role in regulation of the complex. I analysed the interactions between Pto and N using a co-immunoprecipitation strategy. I developed a schematic model of the complex, which includes a novel interaction between the N and LRR domains. Finally, using the Pto homolog Fen, I develop a model suggesting that Fen (and by analogy Pto) together with N, encodes the module for downstream signalling, leading to cell death and resistance.

List of Abbreviations

aa	Amino acid
ABA	Abscisic acid
Adi3	AvrPto-DEPENDENT Pto INTERACTOR 3
APAF-1	APOPTOTIC PROTEASE-ACTIVATING FACTOR 1
At	*Arabidopsis thaliana*
Avr	Avirulence
BAK1	BRI1-ASSOCIATED KINASE1
BAK1-5	BRI1-ASSOCIATED KINASE1 C508Y
BIK1	BOTRYTIS-INDUCED KINASE 1 (BIK1)
BIR	BAK1-INTERACTION RECEPTOR
BKK1	BAK1-like
BR	Brassinosteroid
BRI1	BRASSINOSTEROID INSENSITIVE 1
CaMK	Calcium/calmodulin-dependent protein kinase
CaMV	Cauliflower mosaic virus
CBB	Coomassie brilliant blue
CC	Coiled-coil
CDPK	Calcium-dependent protein kinase
CEBiP	CHITIN ELICITOR BINDING PROTEIN
CED-4	CELL DEATH PROTEIN 4
CERK1	CHITIN ELICITOR RECEPTOR KINASE 1
Cfu	colony forming units
CGF	Constitutive gain-of-function
CNL	Prf lacking the N-terminal and Solanaceous domain
coIP	Co-Immunoprecipitation
COR	coronatine
CP	potato virus X coat protein
CRT1	COMPROMISED RECOGNITION OF TCV

CS	CRYSTALLINE AND SMALL HEAT SHOCK PROTEIN-LIKE
CSD	Cold shock domain
CSP	Cold shock protein
CSPR	COLD-SHOCK PROTEIN RECEPTOR
CSPRC	COLD-SHOCK PROTEIN RECEPTOR CANDIDATE
CP	coat protein of the potato virus X
DAMP	Danger/damage-associated molecular patterns
DEX	Dexamethasone
dpi	Day post infiltration/infection
EDS1	ENHANCED DISEASE SUSCEPTIBILITY 1
EFR	EF-Tu receptor
EF-Tu	Bacterial elongation factor-thermo unstable
EIX	Ethylene-inducing xylanase/ Receptor for EIX
ET	Ethylene
ETI	Effector-triggered immunity
EV	Empty vector
EVR	EVERSHED
FLS2	Flagellin sensing 2
GSL5	glucan synthase-like 5
GUS	β-glucuronidase
h	hour(s)
HA	Hemagglutinin
HR	Hypersensitive response
Hrc	Hypersensitive response and conserved
Hrp	Hypersensitive response and pathogenicity
HSP	HEAT-SHOCK PROTEIN
IP	Immunoprecipitation
JA	Jasmonic acid
Le	*Leycopersicum esculentum*
LPS	Lipopolysaccharide
LRR	Leucine-rich repeats

LysM/LYM	Lysine motif
MAMP	Microbe-associated molecular pattern
MAPK	Mitogen-activated protein kinase
MAPKK	MAPK kinase
MEK	MAPKK kinase
MKS1	MAPK kinase substrate 1
MW	Molecular weight
N	Prf N-terminal domain
NADP	Nicotinamide adenine dinucleotide phosphate
NB	Nucleotide-binding
Nb	*Nicotiana benthamiana*
NBARC	NB adaptor shared by APAF-1, certain R proteins and CED-4
NbN	*Nicotiana benthamiana* Prf N-terminal domain
NbPth1	*N. BENTHAMIANA* Pto homolog1
NBS	Nucleotide-binding site
NDR1	NON-RACE-SPECIFIC DISEASE RESISTANCE 1
NLR	NOD-like receptor
NmL	Prf N–terminal domain N middle long
NmS	Prf N –terminal domain N middle short
NOD	Nucleotide binding and oligomerisation domain
NPR1	Non-expressor of Pathogenesis-Related 1
NRC	NB-LRR PROTEIN REQUIRED FOR HR-ASSOCIATED CELL DEATH
NRIP1	N-RECEPTOR INTERACTING PROTEIN 1
NRP	Negative regulatory patch
Nt	*Nicotiana tabacum*
OG	Oligo-α-galacturonide
Os	*Oryza sativa*
p50	Helicase domain of the Tobacco mosaic virus replicase
PAD4	PHYTOALEXIN DEFICIENT 4
PAMP	Pathogen-associated molecular pattern
PEPR	PEP RECEPTOR

PGN	Peptidoglycan
PIGs	Pathogen induced genes
PMR4	Powdery mildew resistant 4
PP2A	SER/THR PHOSPHATASE TYPE 2A
Pph	*Pseudomonas syringae* pv *phaseolicola*
Prf	PTO RESISTANCE AND FENTHION SENSITIVITY
PRR	Pattern-recognition receptor
Ps	*Pseudomonas syringae*
Pst	*Puccinia striiformis f. sp. tritici*
Psto	*Ps* pv *tomato*
Pta	*Ps* pv *tabaci*
Pti	Pto interacting protein
Pto	RESISTANCE TO PSEUDOMONAS SYRINGAE PATHOVAR TOMATO
Pto/N site1	Pto binding site 1 (residues 1-159) of the Prf N-terminal domain
Pto/N site2	Pto binding site 2 (residues 410-546) of the Prf N-terminal domain
pv.	Pathovar
PVX	potato virus X
qPCR	Quantitative polymerase chain reaction
R	Resistance
RAR1	REQUIRED FOR MLA12 RESISTANCE
RBOH	RESPIRATORY BURST OXIDASE HOMOLOGS
RBPG1	RESPONSIVENESS TO BOTRYTIS POLYGALACTURONASES1
RE	Restriction enzyme
RIN4	RPM1-INTERACTING PROTEIN 4
RK	Receptor kinase
RLK	Receptor-like kinase
RLP	Receptor-like protein
ROS	Reactive oxygen species
RPM1	RESISTANCE TO PSEUDOMONAS MACULICOLA1
RPP1	RESISTANCE TO PODOSPHAERA PANNOSA 1
RPS	RESISTANCE TO PSEUDOMONAS SYRINGAE PROTEIN

RT	Room temperature
RT-PCR	Reverse-transcriptase polymerase chain reaction
SA	Salicylic acid
SAG101	SENESCENCE-ASSOCIATED GENE101
SAR	Systemic acquired resistance
SCNL	Prf lacking the N-terminal domain
SD	*Solanaceous* domain
SERK	SOMATIC EMBRYOGENESIS-RELATED KINASE
SGI	Seedling growth inhibition
SGT1	SUPPRESSOR OF G2 ALLELE OF skp1
Sl	*Solanum lycopersicum*
SOBIR1	SUPPRESSOR OF BAK1-INTERACTION RECEPTOR1
ssp.	Subspecies
TFT	Tomato 14-3-3 protein
TIR	Toll/Interleukin-1 receptor
TMV	Tobacco mosaic virus
TRV	Tobacco rattle virus
TTSS	Type Three Secretion System
VIGS	Virus-induced gene silencing
WAK1	CELL WALL ASSOCIATED KINASE 1
WB	Western blot
x g	Times gravitational force

Table of Contents

1. Introduction. 17

1.1. General Introduction. 17

1.2. PAMP-triggered immunity. 22

1.2.1. Pattern-associated-molecular patterns (PAMPs) and pattern recognition receptors (PRRs). 23

1.2.2. Danger- or damage-associated molecular patterns and danger-associated-recognition receptors. 24

1.2.3. Lysin motif receptors recognising polysaccharides. 25

1.2.4. Leucine-rich repeat receptors. 25

1.2.5. PRR activation by ligand perception and the importance of BRI1-ASSOCIATED KINASE 1 (BAK1). 27

1.2.6. Other receptor kinases with potentially important roles for the PRR-BAK1 receptor complexes. 29

1.2.7. Responses downstream of PRR-BAK1 receptor complexes. 32

1.3. Effector-triggered immunity. 39

1.3.1. Bacterial pathogen effectors. 39

1.3.2. Effector recognition. 40

1.3.3. The structural basis of NB-LRR protein function. 45

1.3.4. Chaperones involved in ETI signalling. 49

1.3.5. NB-LRR signalling. 50

1.4. The Prf protein of tomato, required for resistance to bacterial speck disease. 51

1.4.1. AvrPto and AvrPtoB block PTI. 52

1.4.2. Recognition of AvrPto and AvrPtoB by the Pto kinase. 53

1.4.3. Fen and the insecticide fenthion. 56

1.4.4. Prf (Pto resistance and fenthion sensitivity). 57

1.4.5. Pto and Prf regulate each other through the unique Prf N-terminal domain. 59

1.4.6. The Prf multimerisation through the unique N-terminal domain brings two Pto molecules together and sets a molecular trap for the effectors. 61

1.4.7. Pto/Prf signalling. 63

1.5. Summary 64

1.6. Aims of this project 66

2. Materials and Methods 67

2.1. Chemicals 67

2.2. Plant material and growth conditions. 67

2.2.1. Arabidopsis thaliana. 67

2.2.2. Nicotiana benthamiana. 69

2.3. Bacterial strains. 70

2.4. Antibiotics. 71

2.5. Molecular biology techniques. 71

2.5.1. Vectors and constructs. 71

2.5.2. Primer design. 74

2.5.3. Polymerase chain reaction. 79

2.5.4. DNA-gel electrophoresis. 82

2.5.5. Plasmid isolation and purification from bacterial cells. 83

2.5.6. Cloning. 86

2.5.7. DNA sequencing using the Sanger method. 91

2.5.8. RNA isolation and cDNA synthesis 92

2.5.9. Quantitative real time PCR. 93

2.5.10. Transformation of *E. coli* DH5α and *Agrobacterium tumefaciens* GV3101 pMp90. 95

2.6. Plant methods. 96

2.6.1. Transformation of *Arabidopsis thaliana* protoplasts. 96

2.6.2. *Agrobacterium tumefaciens*-mediated transformation of *Arabidopsis thaliana*. 99

2.6.3. *Agrobacterium tumefaciens*-mediated transient transformation of *Nicotiana benthamiana* leaves. 100

2.6.4. Bacterial growth assays. 102

2.6.5. Trypan blue staining to detect cell death. 103

2.6.6. β-glucuronidase (GUS) staining of leaves. 103

2.6.7. Assays to measure Pathogen-associated molecular pattern-triggered immunity. 104

2.7. Biochemical methods. 108

2.7.1. Heterologous expression and purification of proteins fused to glutathione-S-transferase (GST) using the pGEX-2TK expression vector. 108

2.7.2. Protein extraction from plant material and protein co-immunoprecipitation (co-IP) assay. 109

2.7.3. Bradford assay for determination of protein concentration. 112

2.7.4. *In vitro* receptor-peptide binding assay. 113

2.7.5. Sodium dodecyl sulphate (SDS) polyacrylamide gel electrophoresis (PAGE). 115

2.7.6. Staining and detection of proteins on SDS-PAGE gels. 117

2.7.7. Immuno-blotting of membrane-immobilised proteins. 118

2.7.8. De novo identification of BAK1-interacting receptor proteins by mass spectrometry. 121

3. Identification of the receptor for the bacterial PAMP cold shock protein from *Nicotiana benthamiana* using BAK1 as molecular bait. 129

3.1. Introduction. 129

3.2. Results. 132

3.2.1. csp22-induced responses are dependent on the plant age in *Nicotiana benthamiana*. 132

3.2.2. Identification of the CSP receptor from *Nicotiana benthamiana* using NbBAK1 as molecular bait. 135

3.2.3. NbCSPR binds csp22 and is required for csp22 responses. 140

3.2.4. NbCSPR does not require NbSOBIR1 for csp22 responses. 144

3.2.5. *NbCSPR* confers responsiveness to csp22 in transgenic *Arabidopsis thaliana* plants dependent on *AtBAK1/AtBKK1*. 147

3.2.6. NbCSPR confers age-related resistance to bacterial pathogens and restricts *Agrobacterium*-mediated transformation of *Nicotiana benthamiana* in flowering plants. 149

3.2.7. Potentiation of csp22 responses by flg22 pre-treatment. 153

3.3. Discussion. 155

4. Molecular events underlying non-host resistance to wheat stripe rust in *Nicotiana benthamiana* and *Arabidopsis thaliana*. 161

4.1. Introduction. 161

4.2. Results. 164

4.2.1. *Puccinia striiformis f. sp. tritici* (*Pst*) induces PTI responses in *Nicotiana benthamiana* and *Arabidopsis thaliana*. 164

4.2.2. *Pst* spore extract contains several PAMPs perceived by *Nicotiana benthamiana* and *Arabidopsis thaliana*. 168

4.2.3. The perception of PAMPs present in *Pst* spore extract is partly BAK1 dependent. 170

4.2.4. Identification of BAK1-interacting proteins from leaves responding to *Pst* spore extract. 173

4.3. Discussion. 181

5. The structure of the Pto/Prf protein complex. 189

5.1. Introduction. 189

5.2. Results. 190

5.2.1. Heterologous expression of Prf N (experiments carried out by Dayna Scott, ANU Summer Scholar under my supervision). 190

5.2.2. Generating deletion fragments of Prf N (N deletants). 192

5.2.3. Homodimerisation of the Prf N domain. 195

5.2.4. Prf N interacts with the Pto kinase through two separate binding sites. 203

5.2.5. Results 'A P+1 loop mutation in Pto abrogates interaction with the Pto/N site1'. 210

5.2.6. The Fen kinase is regulated by tomato Prf N but not its homologue from *Nicotiana benthamiana* NbN 219

5.2.7. The N domain of Prf interacts with SCNL via the LRR domain. 228

5.3. Conclusion. 244

6. General Conclusions and Discussion. 248

Literature 260

Attachments 283

Attachment 1 283

Attachment 2 309

Attachment 3 310

Attachment 4 311

Attachment 5 313

Attachment 6 317

Attachment 7 337

Attachment 8 340

1. Introduction.

1.1. General Introduction.

Plants are constantly exposed to microbes and provide diverse niches that can be invaded by microorganisms, notably the roots and leaves. Leaf pathogens must first enter the plant apoplast by penetrating the leaf surface. Most plant microbes enter though stomatal openings or by open wounds, which provides them with nutrients and a favourable environment for microbial growth (Jones & Dangl, 2006). The ability of a plant to sense an attacking microbe and avoid subsequent disease is crucial for its survival.

In the apoplast, microbes are faced with the plant immune system. Unlike mammals, plants lack defender cells or an adaptive immune system (Jones & Dangl, 2006). Plants possess a range of pre-established passive defences, such as the leaf waxy cuticle and lignified cell walls. These non-targeted defences provide the front line of plant defence and most likely prevent the majority of potential pathogen-related infections.

Active defence mechanisms are those that are induced by the plant upon microbial detection and thus depend on the recognition of potential pathogens. Those active defences rely on primary and secondary levels of pathogen perception, comprising pattern-triggered immunity (PTI) and effector-triggered immunity (ETI), respectively (Dodds & Rathjen, 2010). The primary strategy includes externally-faced transmembrane proteins including receptor kinases (RKs) and receptor-like proteins (RLPs), collectively called pattern recognition receptors (PRRs), which allow perception of microbial elicitors also called pathogen associated molecular patterns (PAMPs) (Jones & Dangl, 2006). PAMPs are generally crucial components or commonly released

molecules of all microbes, including non-pathogens. Two well studies PAMPs are the bacterial flagellin and the fungal chitin (Enkerli *et al.*, 1999; Wan *et al.*, 2008b). As such, PAMPs are also referred to as microbe-associated-molecular-patterns (MAMPs); in this work the term PAMPs will be used throughout. Detection of PAMPs by PRRs activates signal transduction across the plasma membrane into the cytoplasm and ultimately induces PTI. PTI includes defence mechanisms such as the production of antimicrobial compounds (e.g. cationic peptides and reactive oxygen species (ROS)) and defence-related peptides or proteins (e.g. defensins, chitinases and proteinases) (Jalali *et al.*, 2006) (Figure 1.1 a).

PTI is a conserved evolutionary strategy and highly important for basal immunity to microbial infection of plants (Nurnberger & Lipka, 2005; Bittel & Robatzek, 2007). Consequently, PTI should normally halt the progress of infection. However, some microbes such as Agrobacterium and Rhizobia have a modified flagellin sequence, which allows *Agrobacterium*-mediated transformation and root-nodule symbiosis (Enkerli *et al.*, 1999; Clarke *et al.*, 2013). Additionally, bacterial cell wall and cell membrane components including lipopolysaccharides derived from Gram-negative bacteria, and peptidoglycans (e.g. muropeptides) from both Gram-positive and Gram-negative bacteria, can undergo structural modifications to mimic the host or to suppress or prevent recognition (Erbs & Newman, 2003; Liu *et al.*, 2014). Invading bacteria can be protected from host defences by exterior polysaccharides to form a shielding layer that stops the entry of toxic hydrogen peroxide (D'Haeze *et al.*, 2003). In addition, microbes can produce antioxidants (e.g. ascorbic acid and glutathione) and enzymes (e.g. catalase and superoxide dismutase to scavenge or detoxify toxic reactive oxygen species), which provide protection from the PTI induced basal defence mechanisms (Storozhenko *et al.*,

2002; Imlay, 2003). For example, fungal endochitinases are secreted into the host apoplast and scavenge small chitin oligomers thereby, preventing binding to the cognate PRR (de Jonge *et al.*, 2010).

Most importantly, invading pathogens can reduce the PTI response by secreting virulence effector proteins into the plant apoplast or cytoplasm. Effectors target the microbial recognition machinery or signalling components downstream of PAMP recognition (Mudgett, 2005; Grant *et al.*, 2006; da Cunha *et al.*, 2007). Bacteria have a number of secretion systems with uncharacterised roles in virulence. To date, the best characterised effector delivery system is that of gram-negative bacterial pathogens, which use a type III secretion system (TTSS) to allow the deposition of effectors directly into the host cytoplasm. Secretion systems used by eukaryotic pathogens are more diverse and not fully understood yet. In the host cytoplasm, effector molecules interfere with PTI, which makes them virulence factors (Figure 1.1 b) (Hann *et al.*, 2010; Deslandes & Rivas, 2012). A broader overview of well-studied bacterial effectors and their targets can be found in Hann *et. al.* 2010 and Deslandes & Rivas 2012.

The second pathogen defence mechanism is known as ETI. The genetic concept underlying this phenomenon was first described by Flor in 1956, who investigated the genetic basis of resistance in flax (*Linum usitatissimum*) to the fungal pathogen *Melampsora lini* (Flor, 1956). Flor's investigations led to development of the gene-for-gene theory, wherein resistance to a specific pathogen relies on two critical genes; a *Resistance* (*R*) gene in the plant, and a corresponding *Avirulence* (*Avr*) gene in the pathogen. Subsequently it has become clear that *Avr* genes usually encode effector proteins with roles in virulence. It is thought that the evolution of secreted effector proteins, themselves an evolutionary response to the innate immune system, led to the

acquisition of plant resistance (*R*) genes that encode proteins for effector recognition (Dangl & Jones, 2001). As such, *R* genes are the evolutionary answer to adapted plant pathogens.

Most plant R proteins encode nucleotide-binding (NB) leucine-rich repeat (LRR) domains, which detect effector proteins either directly or indirectly, mediated by an accessory protein (Figure 1.1 c). In an indirect detection mechanism, the accessory protein is targeted and subsequently modified by pathogen effectors. These modifications in turn activate the NB-LRR protein, and lead to further downstream signalling. Models such as these are also known as guard or decoy models as the accessory is thought to mimic the virulence target of pathogen effectors.

As for PTI, ETI induces a host of cellular responses, which are correlated with disease resistance, but overall the basis of active resistance against the different classes of pathogen is not understood. One hallmark response is cellular suicide/localised cell death known as the hypersensitive response (HR) (Meyers *et al.*, 1999; van Doorn & Woltering, 2005). The HR is believed to play a crucial role in arresting the invasion of pathogens that require a living host for growth (biotrophic pathogens) (Greenberg & Yao, 2004).

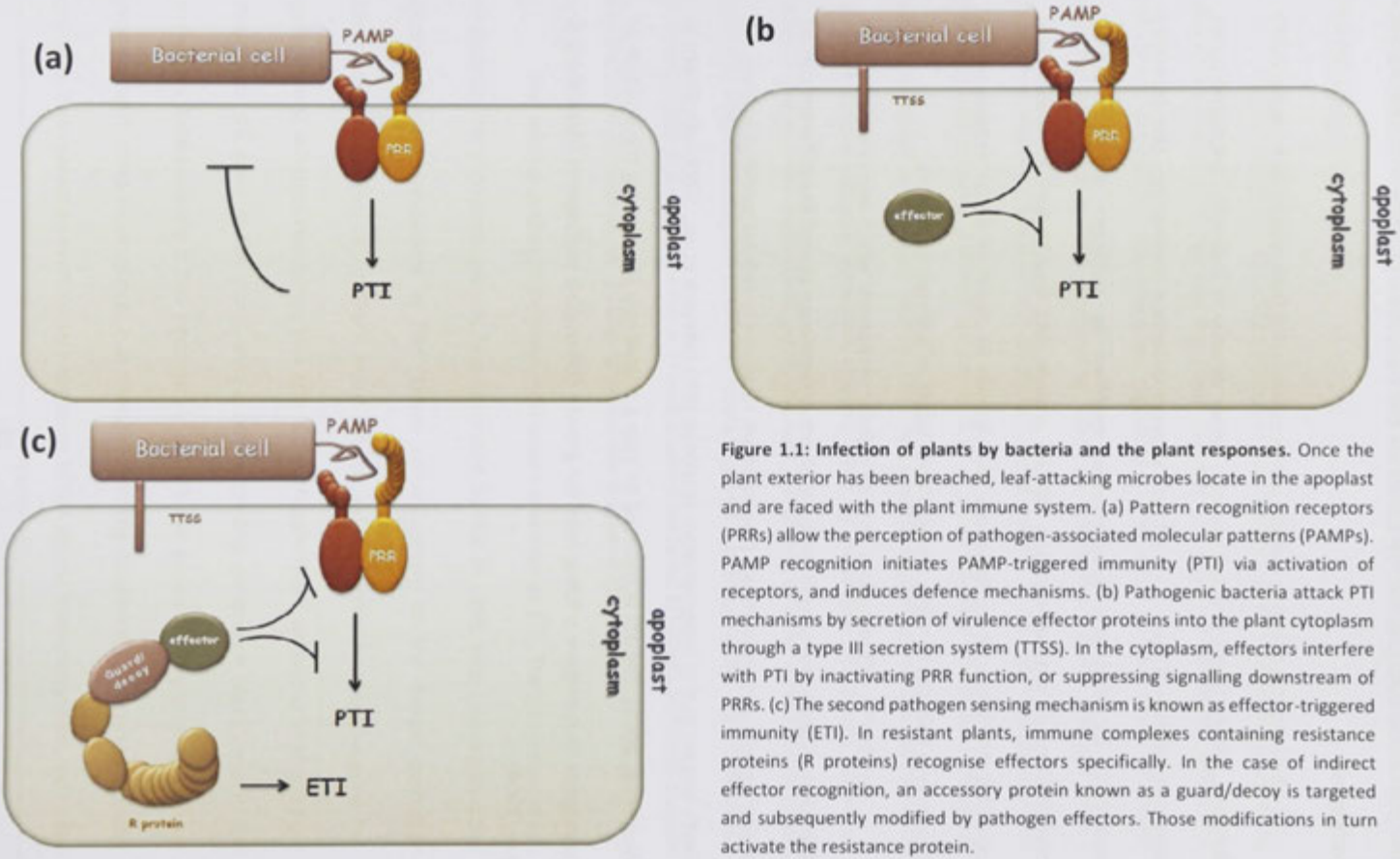

Figure 1.1: Infection of plants by bacteria and the plant responses. Once the plant exterior has been breached, leaf-attacking microbes locate in the apoplast and are faced with the plant immune system. (a) Pattern recognition receptors (PRRs) allow the perception of pathogen-associated molecular patterns (PAMPs). PAMP recognition initiates PAMP-triggered immunity (PTI) via activation of receptors, and induces defence mechanisms. (b) Pathogenic bacteria attack PTI mechanisms by secretion of virulence effector proteins into the plant cytoplasm through a type III secretion system (TTSS). In the cytoplasm, effectors interfere with PTI by inactivating PRR function, or suppressing signalling downstream of PRRs. (c) The second pathogen sensing mechanism is known as effector-triggered immunity (ETI). In resistant plants, immune complexes containing resistance proteins (R proteins) recognise effectors specifically. In the case of indirect effector recognition, an accessory protein known as a guard/decoy is targeted and subsequently modified by pathogen effectors. Those modifications in turn activate the resistance protein.

1.2. PAMP-triggered immunity.

PTI is a defence mechanism that relies on the perception of PAMPs by their respective PRRs and is explained here in detail. All examples of PAMP/PRR pairs mentioned here are summarised in Table 1.1.

Table 1.1 PAMPs and corresponding PRRs

PAMP	pathogen	PRR	receptor class	recognising host(s)	detail	reference
flagellin	Bacteria general	FLS2	Leucine rich repeats (LRR)-RK	Most plants	Direct binding confirmed	(Enkerli *et al.*, 1999; Chinchilla *et al.*, 2006)
elongation factor-Tu	Bacteria general	EFR	LRR-RK	*Brassica*	Interfamily transfer confers recognition	(Nurnberger & Kemmerling, 2006; Lacombe *et al.*, 2010)
peptidoglycan	Bacteria general	CERK1, LYM1, LYM3	Lysin M motif (LysM)-RK, LysM-RLPs	*Arabidopsis* and possibly others		(Willmann *et al.*, 2011)
lipopolysaccharides	Bacteria (*Pseudomonas and Xanthomonas* ssp.)	LORE	Lectin S-domain-RK	*Arabidopsis* and possibly others	Interfamily transfer confers recognition	(Ranf *et al.*, 2015)
cold shock protein	Bacteria general	unknown		*Solanaceae*		(Felix & Boller, 2003)
eMAX (elicitor fraction)	bacteria (*Xanthomonas* ssp.)	ReMAX	LRR-RLP	*Arabidopsis* and possibly others	Recognition specificity confirmed	(Jehle *et al.*, 2013b)
endopolygalacturonase	Fungi	RLP42	LRR-RLP	*Arabidopsis* and possibly others	Direct binding confirmed	(Hou *et al.*, 2014)
chitin	Fungi	CERK1, LYK4, LYK5	LysM-RKs	Most plants	Direct binding confirmed	(Miya *et al.*, 2007) (Wan *et al.*, 2012; Cao *et al.*, 2014)
chitin	Fungi	CEBiP, CERK1	LysM-RLP, LysM-RK	Rice	Direct binding confirmed	(Kaku *et al.*, 2006; Shimizu *et al.*, 2010)
xylanase	Fungi	EIX1,EIX2	LysM-RLPs	Tomato, tobacco and possibly others	Interfamily transfer confers recognition	(Ron & Avni, 2004)
SCFE1 (elicitor fraction)	*Sclerotinia sclerotiorum*	RLP30	LRR-RLP	*Arabidopsis* and possibly others		(Liebrand *et al.*, 2014)
INF1	*Phytophthora infestans*	unknown		*Nicotiana* and possibly others	Unknown	(Chaparro-Garcia *et al.*, 2011)
Avr4	*Cladosporium fulvum*	Cf-4	LRR-RLP	Tomato	Interfamily transfer confers recognition	(Joosten *et al.*, 1997)
Ave1	*Verticillium dahliae* and *V. albo-atrum*	Ve1	LRR-RLP	Tomato	Interfamily transfer confers recognition	(Fradin *et al.*, 2011)

1.2.1. Pattern-associated-molecular patterns (PAMPs) and pattern recognition receptors (PRRs).

PRRs perceive PAMPs to sense invading microbes. PAMPs are molecules with conserved structures characteristic of whole classes of microbes and are typically absent from the host organism (Medzhitov & Janeway, 1997). This enables the host to distinguish non-self and hence sense microbial attack. Fungal chitin (fungal cell wall component) and bacterial flagellin (building block of the flagellum of mobile bacteria) are probably so far the best studies examples (Zipfel *et al.*, 2004; Chinchilla *et al.*, 2006; Kaku *et al.*, 2006; Miya *et al.*, 2007). PAMPs are ligands for extracellular receptor domains of host plasma-membrane localised PRRs. Known PRR are either receptor kinases (RKs) or receptor-like proteins (RLPs). Both contain external membrane-embedded domains, but only RKs have internal protein kinase domains. Receptor-like proteins may generally pair with RKs to acquire the trans-membrane signalling capability (Gust & Felix, 2014). The recognition domains may consist of LRR domains as described for the perception of the bacterial ligands flagellin or elongation factor-Tu, or Lysin motif (LysM or LYM) domains as described for fungal chitin (Miya *et al.*, 2007; Wan *et al.*, 2008a). Other receptor domains remain to be identified because these classes of genes are highly expanded in plant genomes. The PRRs explained here are well-studied examples, however recently a number of novel PRRs have been identified (Table 1.1) (Zipfel, 2014).

1.2.2. Danger- or damage-associated molecular patterns and danger-associated-recognition receptors.

A key feature of PAMPs is that they are absent from the host organism. Some host molecules can however induce a similar set of responses to PAMPs (Denoux *et al.*, 2008; Galletti *et al.*, 2008). Those molecules are generated and released from the host at the injury site in response to cellular damage and/or pathogen attack; they are therefore named danger- or damage-associated molecular patterns (DAMPs) (Matzinger, 2002). For example, the DAMPs oligo-α-galacturonides (OGs) are released from the host cell wall by fungal hydrolases attacking the integral component pectin (Nothnagel *et al.*, 1983; Ferrari *et al.*, 2008). The receptor for OGs is the CELL WALL ASSOCIATED KINASE 1 (WAK1) (Brutus *et al.*, 2010) but other known DAMPs are perceived by transmembrane receptor kinases similar to PAMP perception by PRRs, which has been demonstrated for the DAMP AtPep1. The AtPep1 precursor protein PROPEP1 is induced in response to wounding and wounding responses, and AtPep1 peptide is processed from the precursor after its transport to the apoplast, where it is detected by the LRR-RKs PEP RECEPTOR 1 and 2 (PEPR1 and PEPR2) (Huffaker *et al.*, 2006; Yamaguchi *et al.*, 2006; Krol *et al.*, 2010). Importantly, AtPEPR1 and the bacterial flagellin may act synergistically in PAMP triggered responses (Ma *et al.*, 2012). Similarly, the host peptides PIP1 and PIP2 are able to activate immune responses in a receptor-like kinase 7 (RLK7) -dependent manner in *Arabidopsis thaliana* and their perception amplifies flagellin-induced immunity (Hou *et al.*, 2014).

1.2.3. Lysin motif receptors recognising polysaccharides.

LysM domains bind polysaccharide containing PAMPs, such as the essential bacterial cell wall component (PGN). Nevertheless, the *A. thaliana* receptor for bacterial lipopolysaccharides (LPS) from the genera *Pseudomonas* belongs to lectin S-domain receptor class of proteins (Ranf *et al.*, 2015). The LysM receptors for the fungal cell was component chitin include the RK CHITIN ELICITOR RECEPTOR KINASE 1 (CERK1) in *A. thaliana* and CHITIN ELICITOR BINDING PROTEIN (CEBiP) in rice (*Oryza sativa*) (Miya *et al.*, 2007). Both are essential for chitin perception, and the chitin N-acetyl-D-glucosamine pentamer interacts directly with the three extracellular lysine motif (LysM or LYM) domains of CERK1 (Iizasa *et al.*, 2010; Liu *et al.*, 2012). In rice, the LysM domain-containing protein CEBiP also binds chitin directly, and upon binding interacts with the rice homolog of CERK1 (Kaku *et al.*, 2006). OsCEBiP forms a homo-oligomer, and homo-dimerisation of CERK1 is also essential for PTI responses in *A. thaliana*. The CERK1 homo-dimerisation is a result of binding either end of a chitin octamer, which acts as a so called "bivalent ligand" (Liu *et al.*, 2012). Notably, other LysM receptors have been implicated in chitin binding (Cao *et al.*, 2014) and LysM1, LysM3 as well as CERK1 mediate bacterial peptidoglycan sensing and immunity to bacterial infection (Gimenez-Ibanez *et al.*, 2009b; Willmann *et al.*, 2011).

1.2.4. Leucine-rich repeat receptors.

Two of the best understood PRRs are the LRR-RKs, FLAGELLIN SENSING 2 (FLS2) and ELONGATION FACTOR- THERMO UNSTABLE (EF-Tu) RECEPTOR (EFR), which belong to the *A. thaliana* LRR-XII RK subfamily and are essential for recognition of and immunity to bacteria (Felix *et al.*, 1999; Kunze *et al.*, 2004). The extracellular LRR domains of FLS2

and EFR specifically bind the bacterial PAMPs flagellin and elongation factor Thermo unstable (EF-Tu), or their synthetic peptide derivatives flg22 and elf18, respectively (Chinchilla *et al.*, 2006; Zipfel *et al.*, 2006). Both, flg22 and elf18 encode the minimal region of the bacterial flagellin and EF-Tu that initiate immune responses in *Arabidopsis thaliana*. In tomato (*Solanum lycopersicum*), the N-terminal 15 amino acids (aa) of the bacterial flagellin are sufficient for recognition, whereas EF-Tu recognition is specific to members of the *Brassicaceae* family, and it is not recognised in tomato (Felix *et al.*, 1999; Bauer *et al.*, 2001; Zipfel *et al.*, 2006). However, expression of *A. thaliana EFR* in the *Solanaceous* species *Nicotiana benthamiana* and tomato as well as rice, which normally lack this recognition capability, confers EF-Tu recognition and increases their resistance to virulent bacterial pathogens (Lacombe *et al.*, 2010; Holton *et al.*, 2015). The importance of these recognition events is further underlined by the higher susceptibility to the bacterial plant pathogen *Pseudomonas syringae (Ps)* when *A. thaliana* plants are impaired in flagellin and/or EF-Tu perception (Nekrasov *et al.*, 2009; Zipfel, 2009).

LRR receptors are not restricted to the perception of bacterial PAMPs. The LRR receptors from tomato LeEIX1 and LeEIX2 recognise the fungal elicitor ethylene-inducing xylanase (EIX). EIX is a 22 kDa protein from the fungus *Trichoderma viride,* which degrades the host carbohydrate cell-wall component xylan during infection. It induces ethylene production in tobacco (*Nicotiana tabacum*) and tomato and other defence signals associated with PTI independent of this enzymatic activity, (Fuchs *et al.*, 1989; Bailey *et al.*, 1990; Bailey *et al.*, 1993; Enkerli *et al.*, 1999; Furman-Matarasso *et al.*, 1999; Bargmann *et al.*, 2006). The two receptors show high sequence similarity; like FLS2 and EFR they encode an extracellular LRR domain and a transmembrane domain but lack an intracellular kinase domain and encode a cytoplasmic tail (Bailey *et al.*, 1993; Ron & Avni,

2004). When transiently overexpressed in tobacco both LeEIX1 and LeEIX2 bind xylanase and heterodimerise, but only LeEIX2 activates downstream defences (Ron & Avni, 2004). Signal transduction might be dependent on associated kinases such as Suppressor of BAK1-INTERACTION RECEPTOR1 (SOBIR1), which is described in detail later (Liebrand *et al.*, 2013).

1.2.5. PRR activation by ligand perception and the importance of BRI1-ASSOCIATED KINASE 1 (BAK1).

Perception of flg22 and elf18 by FLS2 and EFR is dependent on the regulatory co-receptor BRI1-ASSOCIATED KINASE1 (BAK1) as the *A. thaliana bak1-4* null mutants and plants silenced for *BAK1* in *N. benthamiana* are compromised in their responsiveness to flg22 and elf18 (Chinchilla *et al.*, 2007b; Heese *et al.*, 2007; Postel & Kemmerling, 2009; Bar *et al.*, 2010; Postel *et al.*, 2010; Schulze *et al.*, 2010; Roux *et al.*, 2011). BAK1 belongs to the LRR-RK subfamily II and is a member of the SOMATIC EMBRYOGENESIS-RELATED KINASE (SERK) family, and thus also known as SERK3 (Hecht *et al.*, 2001; Albrecht *et al.*, 2008). Notably, other SERK family members may act similarly to BAK1 as the transcription of all SERK genes is affected by pathogens. Also, the mutant line *bak1-5/bkk1* (point mutation in the BAK1 gene (*bak1-5*) and a null mutation in the *BAK1-like (BKK1)/SERK4* gene is less responsive to flg22 than the single b*ak1-5* or *bak1-4* mutants (Song et al., 2008; Santos et al., 2009)(Roux *et al.*, 2011; Schwessinger *et al.*, 2011).

Interestingly, BAK1 was first identified as a positive regulator of brassinosteroid signalling. It binds and regulates the brassinosteroid (BR) receptor BRASSINOSTEROID

INSENSITIVE 1 (BRI1) (Li & Nam, 2002; Nam & Li, 2002; Russinova *et al.*, 2004; Karlova & de Vries, 2006; Wang *et al.*, 2008). Unlike FLS2 and EFR, BRI1 belongs to the LRR-RK subfamily X. SERK1 and SERK4/BKK1 also interact with BRI1 to regulate BR signalling (Karlova *et al.*, 2006; He *et al.*, 2007; Albrecht *et al.*, 2008; Jeong *et al.*, 2010; Roux *et al.*, 2011). Notably, the *bak1-5* allele is impaired in flg22 and elf18 but not BR signalling (Schwessinger *et al.*, 2011).

BAK1 also binds FLS2 and EFR through interaction with both receptors within minutes after ligand perception (Figure 1.2) and plays a role in flg22 binding with contacts between the C- terminus (residue L19) of the peptide and BAK1 (residues Thr52 and Val54) (Sun, Y *et al.*, 2013). Interestingly, a ligand-independent interaction of BAK1-5 (BAK1C508Y protein encoded by *bak1-5*) from both, *A. thaliana* and *N. benthamiana* with AtFLS2 has been observed ((Schwessinger *et al.*, 2011), Chapter 3 this study). BAK1 seems to act as a signal amplifier for its interacting receptor kinases, but the exact phosphorylation and signalling events involving BAK1 are not yet fully understood, especially considering that the function of BAK1 in innate immunity seems to be independent of its function in BR signalling (Schwessinger *et al.*, 2011). In contrast with the theory that the major role of BAK1 to enhance the kinase activity of the interacting RK (Heese *et al.*, 2007; Roux *et al.*, 2011; Schwessinger *et al.*, 2011) is the requirement of BAK1 for the function of the tomato RLPs Ve1 and EIX1, which lack an intracellular kinase domain and are involved in recognition of fungal elicitors (Ron & Avni, 2004; Fradin *et al.*, 2009; Bar *et al.*, 2010). However, Ve1- and EIX interact with the RK SOBIR1 (Liebrand *et al.*, 2013).

Additionally, BAK1 plays a role in cell death control. This is based on the observation that the *bak1-4* null mutants show early senescence (Colcombet *et al.*,

2005; He *et al.*, 2007; Kemmerling *et al.*, 2007). Whereas this phenotype is weak, a double-mutant combination with the closest *BAK1* homolog, *BKK1*, exhibits a seedling-lethality phenotype (He *et al.*, 2007; Jeong *et al.*, 2010). The finding of the *bak1-5* allele enabled study of non-lethal *bak1-5/bkk1* double mutant (Roux *et al.*, 2011; Schwessinger *et al.*, 2011). Antagonistically, transient overexpression of *NbBAK1* in *N. benthamiana* leaves caused a cell death phenotype (this study) and the biological relevance of this is unknown.

Besides its involvement in BR signalling and cell death control, BAK1 is clearly an important component of plant immunity and likely acts as a co-receptor for a number of PRRs. The receptors for the elicitor INF1 from *Phytophthora infestans* and the peptide derivative of bacterial cold shock protein (CSP) known as csp22 likely bind BAK1, as NbBAK1 is required for inducing INF1 and csp22-dependent responses in *N. benthamiana* (Felix & Boller, 2003; Heese *et al.*, 2007; Chaparro-Garcia *et al.*, 2011).

1.2.6. Other receptor kinases with potentially important roles for the PRR-BAK1 receptor complexes.

1.2.6.1. BAK1 interaction receptor like kinases (BIR) involved in BAK1 dependent cell death control.

Through a reverse genetic screen, a constitutively active defence mutant (*bir1-1*) was identified (Gao *et al.*, 2009). The respective gene codes for BAK1-INTERACTING RECEPTOR 1 (BIR1), belongs to the LRR X – RK subfamily and constitutively interacts with BAK1. It is currently unknown if *BIR1* actually plays a role in a PAMP-induced signalling pathway. Recently, additional BIR proteins were identified biochemically and named

BIR2, BIR3 and BIR4, all of which belong to the LRR subgroup X along with BIR1 (Halter *et al.*, 2014). In directed co-immunoprecipitations (coIPs) of transiently expressed proteins in *N. benthamiana*, all four BIR family members show an association with BAK1. The biological function of BIR3 and BIR4 remains unknown, but BIR2 negatively regulates BAK1 signalling by physical interaction prior to PAMP perception (Halter *et al.*, 2014). It is involved in regulating PAMP induced responses, can control BAK1-FLS2 complex formation in a ligand-dependent manner and is released for BAK1 after ligand perception (Halter *et al.*, 2014). Notably, a role in BR signalling has not been found for BIR2. Additionally, *A. thaliana bir2* mutant alleles show enhanced cell-death responses and are more susceptible to necrotrophic fungi (induce host cell death) infection but show enhanced resistance to the virulent bacterium *Pseudomonas syringae* pathovar *tomato* (*Psto*) DC3000 (Halter *et al.*, 2014).

1.2.6.2. SUPPRESSOR OF BIR1-1 (SOBIR1) involved in BAK1-dependent cell death control.

A screen for genetic suppressors of *bir1-1* in *A. thaliana* identified a mutation in another RK gene, *SUPPRESSOR OF BIR1-1 (sobir1-1),* which suppresses the cell death phenotypes of *bir1-1* plants (Gao *et al.*, 2009). SOBIR1 encodes a LRR-RK of the family XI and is also known as EVERSHED (EVR) (Gao *et al.*, 2009). EVR was originally identified as a regulator of floral organ shedding. The fact that BAK1 has been implicated in cell death control may suggest that *SOBIR1* plays an important role in positively regulating cell death and disease resistance. SOBIR1 overexpression indeed activates cell death and defence responses, but SOBIR does not interact with BAK1 (Gao *et al.*, 2009). Importantly, studies in tomato and *A. thaliana* showed that SlSOBIR1 and AtSOBIR1 are

essential for defence responses triggered by certain LRR-RLPs that act as immune receptors, respectively (Jehle *et al.*, 2013a; Liebrand *et al.*, 2013; Zhang *et al.*, 2013; Zhang, LS *et al.*, 2014). SOBIR1 interacts with the anti-fungal RLPs Cf-4 and Ve1 and is required for their accumulation when they are expressed transiently in *N. benthamiana* (Liebrand *et al.*, 2013). Wheather this interaction is maintained in the presence of the elicitor is unknown. Additionally, AtSOBIR1, AtBAK1 and AtRLP30 are required for signalling in response to an elicitor-containing fraction from the necrotrophic fungus *Sclerotinia sclerotiorum,* but whether the three proteins interact *in planta* remains to be determined (Zhang *et al.*, 2013). SOBIR1 is also required for the fungal PAMP endopolygalacturonase binding RLP RESPONSIVENESS TO BOTRYTIS POLYGALACTURONASES1 (RBPG1/ AtRLP42) (Zhang, L *et al.*, 2014). Finally, SOBIR1 is required for the perception of the PAMP eMax from the bacterium *Xanthomonas* by the RLP ReMAX in *A. thaliana* (Jehle et al., 2013a). These results suggest that SOBIR1 generally functions in combination with RLPs, potentially as signal transducer (Gust & Felix, 2014), but its exact role in activation of PAMP dependent signalling pathways remains to be determined.

1.2.6.3. Botrytis-induced kinase 1 (BIK1).

BAK1 and FLS2 interact with the membrane associated, cytoplasmic kinase BOTRYTIS-INDUCED KINASE 1 (BIK1), first implicated in resistance to the necrotrophic fungus *Botrytis cinerea* and other necrotrophic pathogens (Veronese *et al.*, 2006; Lu *et al.*, 2010). Surprisingly, the *bik1* mutant is also impaired in immune responses to *Psto* DC3000 (Zhang, J *et al.*, 2010). BIK1 constitutively associates with FLS2 and BAK1 and is phosphorylated and released from the complex after flg22 treatment to directly phosphorylate the NADPH oxidase RbohD (required for

defence related ROS induction) (Lu *et al.*, 2010; Schulze *et al.*, 2010; Laluk *et al.*, 2011; Kadota *et al.*, 2014). Notably, an interaction of BIK1 with FLS2 and BAK1 has not always been detected (Lu *et al.*, 2010; Zhang, J *et al.*, 2010).

1.2.6.4. Other negative regulators of BAK1.

Because of its importance in defence and cell death signalling, it is not surprising that BAK1 is tightly regulated by phosphorylation. Recently, the protein SER/THR PHOSPHATASE TYPE 2A (PP2A) was found to negatively regulate BAK1 by constitutive interaction and modulation of the BAK1 phospho-status (Segonzac *et al.*, 2014). Additionally, the two U-BOX E3 UBIQUITIN LIGASES, PUB12 and PUB13 were also identified as negative regulators of BAK1 (Lu *et al.*, 2011). BAK1 binds and phosphorylates PUB12/13 and is required for FLS2-PUB12/13 association that facilitates flagellin-induced FLS2 degradation. *pub12* and *pub13* mutants displayed elevated immune responses to flagellin treatment (Lu *et al.*, 2011).

1.2.7. Responses downstream of PRR-BAK1 receptor complexes.

Activation of PRRs leads to different measurable downstream signals, which can be separated into early and late responses. Several of them are used to assay PAMP responses and collectively comprise resistance but the actual mechanisms are poorly understood. Not all downstream signalling components are shared between all PAMP perception pathways or all plant species, but most or all of those responses are shared with ETI and have been studied most comprehensively in response to the PAMPs flg22 and elf18 in *A. thaliana*.

1.2.7.1. Ion fluxes and Ca^{2+} signalling.

Some of the earliest responses associated with PRR activation include ion exchanges across the plasma membrane. PAMP perception elicits a rapid K^+ efflux alongside the influx of Ca^{2+} ions (Atkinson *et al.*, 1990), leading to alkalinisation of the external medium (Felix *et al.*, 1999; Kunze *et al.*, 2004; Jeworutzki *et al.*, 2010) and a localised increase in cytosolic calcium, respectively. Such a rapid influx of calcium can be quantitatively measured using transgenic lines overexpressing the jellyfish reporter protein Aequorin and adding the substrate coelenterazine during elicitation (Knight *et al.*, 1991; Segonzac *et al.*, 2011). Aequorin and coelenterazine form a complex that, in response to Ca^{2+} ions, releases coelenteramide, which can be measured at a wavelength of 469 nm. Using this assay, it was found that different PAMPs cause different intracellular Ca^{2+} ion concentrations. Changes in Ca^{2+} concentration are specifically recognised by calcium dependent protein kinases (CDPKs) and several other calcium binding proteins including calmodulin, which have been implicated in PTI signalling (Keller *et al.*, 1998; Sagi & Fluhr, 2001; Boudsocq *et al.*, 2010; Dodd *et al.*, 2010; Jeworutzki *et al.*, 2010; Kudla *et al.*, 2010; Monaghan *et al.*, 2014). Further, Ca^{2+} is required for the PAMP-triggered ROS burst and activation of Mitogen activated protein kinases (MAPKs), described below in detail.

1.2.7.2. The oxidative burst.

A hallmark of pathogen attack in both plant and animal systems is the production of ROS and Nitric Oxide (Zhang *et al.*, 2007). Notably, the production of ROS also plays a role in other biotic and abiotic stress responses and several plant developmental processes (Bailey-Serres & Mittler, 2006). The oxidative burst is a product of ten different membrane-localised NADPH oxidases known as RESPIRATORY BURST OXIDASE

HOMOLOGS (RBOH) (Torres *et al.*, 2002; Torres & Dangl, 2005). Although the oxidative burst is a long-described phenomenon, its biological mechanism in PTI signalling has only been elucidated recently. In *A. thaliana*, AtRBOHD is the most important NADPH oxidase for the production of ROS as a PTI response (Meszaros *et al.*, 2006). RBOHD is activated through phosphorylation by BIK1 in response to flg22 and elf18 perception by FLS2 and EFR, respectively (Kadota *et al.*, 2014). Fungi and oomycetes are also more pathogenic on *rbohB*-silenced (closest *AtrbohD homolog*) *N. benthamiana* plants (Asai *et al.*, 2008).

1.2.7.3. PAMP-induced MAPK cascades and changes in gene expression.

Within 5-10 minutes of PAMP perception, MAPK signalling cascades are activated. Activation seems to act downstream of ROS and Ca^{2+} signalling (Felix *et al.*, 1991; Schulze *et al.*, 2010). MAPK cascades depend on sequential phosphorylation between MAPKK kinases (MEKK), MAPK kinases (MKK) and MAPKs (MAPK). Two MAPK cascades act coincidently in *A. thaliana* after flg22 perception: The MEKK-MKK4/MKK5-MPK3/MPK6 and MEKK1-MKK1-MKK2/MPK4 cascades. The first of these acts positively, and the latter negatively on PTI, which may provide a way for the plant to balance the outputs of signalling (Meszaros *et al.*, 2006; Su *et al.*, 2007; Suarez-Rodriguez *et al.*, 2007). However, both cascades lead to the activation of WRKY transcription factors, which contain a conserved domain that binds to W-box (TTGACC/T) motifs present in the promoters of some defence-related genes (Navarro *et al.*, 2004; Eulgem & Somssich, 2007; Pandey & Somssich, 2009). The MEKK/MKK4/MKK5-MPK3/MPK6 cascade activates WRKY22 and WRKY29, which are positive regulators of PTI (Asai *et al.*, 2002). The activation of the second cascade results in the disruption of the interaction between MPK4, WRKY33 and MAPK kinase substrate 1 (MKS1). This is turn releases the

transcription factors to modify gene expression (Andreasson *et al.*, 2005; Zheng *et al.*, 2006; Qiu *et al.*, 2008).

Activation of MAPKs is easily detected. Two assays are commonly used: the direct detection of MAPK phosphorylation using phospho-specific MAPK antibodies in immuno-blot analyses, and indirectly, the detection of transcriptional up-regulation of certain pathogen induced genes (PIGs, usually WRKY genes) by qRT-PCR.

1.2.7.4. Hormone signalling.

PAMP perception triggers changes in plant hormone accumulation. Especially salicylic acid (SA), jasmonic acid (JA), and ethylene (ET) have been implicated in the resistance pathways (Felix *et al.*, 1999; Durrant & Dong, 2004; Glazebrook, 2005; Mishina & Zeier, 2007; Tsuda *et al.*, 2008; Mukherjee *et al.*, 2010; Sun, F *et al.*, 2013). SA is mainly involved in restriction of biotrophic pathogens and plants deficient in SA production or insensitive to SA show enhanced susceptibility to those pathogens (Jalali *et al.*, 2006). JA and ET-signalling mainly function against necrotrophic pathogens. As such, SA and JA/ET mainly act antagonistically, and in agreement with that, MPK4 acts as a negative regulator of SA-dependent resistance and as an activator of JA-dependent defence gene expression (Petersen *et al.*, 2000). In addition, a virulence strategy of *Psto* is the production of the toxin coronatine (COR). COR mimics jasmonate-isoleucine and consequently promotes bacterial infection while activating defences against fungal pathogens (Gimenez-Ibanez *et al.*, 2014). Notably, all three hormones are involved in local and systemic-acquired immunity (SAR). SAR is a mechanism that confers resistance in non-infected tissues of an infected host plant to prevent subsequent microbial colonisation (Grant & Lamb, 2006). Other plant hormones involved in defence are auxin and abscisic acid (ABA). flg22 treatment leads to reduction of auxin receptor levels, and

SA signalling stabilises auxin-response repressors (Navarro *et al.*, 2006; Wang *et al.*, 2007). The exact biological relevance of these remains to be determined. ABA is mainly required for stomatal closure (Melotto *et al.*, 2006) and exogenous ABA application resulting in inhibition of SAR (Yasuda *et al.*, 2008). ETI also relies on plant hormone signalling, further confirming the overlap between PTI and ETI responses (Jones & Dangl, 2006).

1.2.7.5. Stomata closure.

Bacteria frequently use stomata as a point of ingress to the leaf. Consequently, PAMP perception leads to stomatal closure as a means of excluding bacteria from the leaf interior (Melotto *et al.*, 2006). As mentioned above, stomatal closure relies on absicic acid (ABA) signalling as components of this signalling pathway are required for the flg22-induced closure of stomata (Melotto *et al.*, 2006; Zeng & He, 2010; Zeng *et al.*, 2010). Importantly, JA signalling is also involved in the regulation of stomata opening and closure, as COR and the *Pseudomonas* effector protein HopX1 can prevent stomata closure by interfering with the JA signalling pathway (Melotto *et al.*, 2006; Gimenez-Ibanez *et al.*, 2014).

1.2.7.6. Callose deposition.

In response to pathogen recognition, the host plant deposits callose. Callose deposition is the accumulation of β-1,3-glucans between the plasma membrane and the plant cell wall, which is thought to restrict the distribution and growth of microbes (Bestwick *et al.*, 1997; Gomez-Gomez *et al.*, 1999). In *A. thaliana* the callose synthase glucan synthase-like 5 (GSL5) / powdery mildew resistant 4 (PMR4) is the key enzyme for the synthesis of this polymer in response to PAMPs and fungal pathogens

(Ostergaard *et al.*, 2002; Jacobs *et al.*, 2003) and its transcript is up-regulated in response to SA signalling. The *Psto* effector AvrPto, which inhibits expression of genes involved in the deposition of callose underlines the importance of this physical barrier (Hauck *et al.*, 2003).

1.2.7.7. Seedling growth inhibition.

One effect of PAMP perception is the inhibition of plant growth. Generally, it is thought that plants inhibit pathways that promote growth to support defence mechanisms. As BAK1 is a central regulator of both BR and PAMP induced signalling, it was proposed that BAK1 plays a critical role in promoting one signalling cascade whilst inhibiting the other (Lozano-Duran *et al.*, 2013). Several studies have tried to identify mechanisms underlying this phenomenon (Albrecht *et al.*, 2012; Belkhadir *et al.*, 2012). Recently, the two key regulators BRASSINAZOLE-RESISTANT 1 (BZR1) and HOMOLOG OF BR ENHANCED EXPRESSION2 INTERACTING WITH INCREASED LEAF INCLINATION1 BINDING bHLH1 (HBI1) and were identified, which tightly balance BR and PTI signalling (Lozano-Duran *et al.*, 2013; Fan *et al.*, 2014).

The inhibition of seedling growth in response to treatment with PAMPs is a convenient response to measure pathway activation. Seedlings can be subjected to PAMP treatment, and inhibition of seedling growth can be assayed after about one week. Using a collection of homozygous T-DNA insertion mutants for LRR-RK and RLP genes that are up-regulated upon induction with flg22 and elf18 in *A. thaliana*, could identify BAK1, EFR and chaperones of the endoplasmic reticulum, required for EFR accumulation (Kunze *et al.*, 2004; Zipfel *et al.*, 2006; Chinchilla *et al.*, 2007b; Wang *et al.*, 2008; Li *et al.*, 2009) .

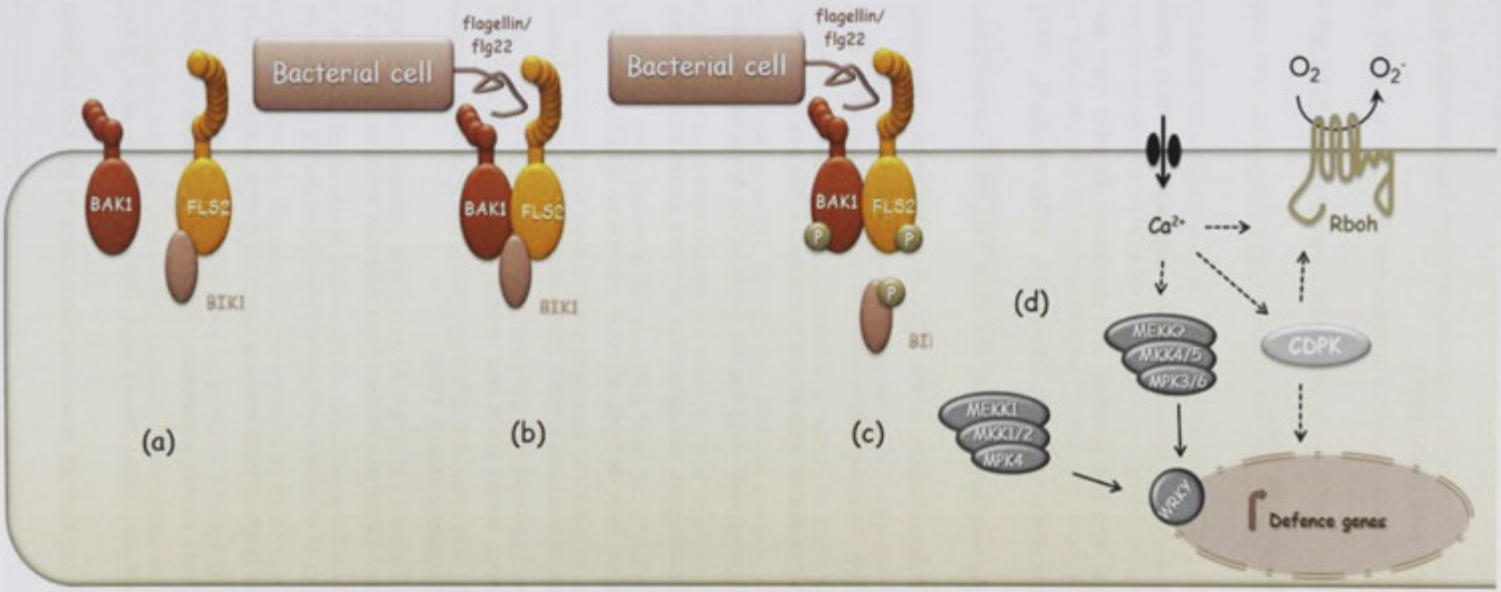

Figure 1.2: Infection of plants by bacteria and flagellin-induced host responses. The diagram shows PRR activation and early molecular signalling mechanisms in response to the bacterial PAMP flagellin as an example. **(a)** BAK1 and FLS2 span the plasma membrane with the receptor domains oriented into the apoplast. BIK1 is intracellular and directed to the plasma membrane by N-acylation. **(b)** The bacterial flagellin in the apoplast is recognised by FLS2, leading to hetero-complex formation with BAK1. **(c)** The kinase domains of BAK1, FLS2, and BIK1 undergo trans-phosphorylation, leading to the activation and release of BIK1 **(d).** Trans-phosphorylation events activate downstream signalling responses including the influx of calcium ions, activation of CDPKs and other calcium binding proteins, activation of RBOHD and the oxidative burst, the MAPK cascades and subsequent changes of gene expression by WRKY transcription factors, amongst others. Not shown: Hormone signalling, stomatal closure and callose deposition. Cartoon adapted from (Segonzac & Zipfel, 2011).

1.3. Effector-triggered immunity.

1.3.1. Bacterial pathogen effectors.

Adapted plant pathogens secrete numerous proteins, peptides and other small molecules (so-called effectors) into the apoplast and cytoplasm to alter host cell structure and function to aid their virulence (Staskawicz, 2001; Mudgett, 2005; Panstruga & Dodds, 2009). As mentioned above, the most important translocation system for Gram-negative phytopathogens is the TTSS. A pathogenicity-associated island (or gene cluster) called "hypersensitive-response and pathogenicity" (*hrp*) encodes the machinery for this secretion system and is induced in the plant apoplast. "hypersensitive-response and conserved" (hrc) are the genes of the *hrp* genes that are conserved amongst bacterial pathogens and activation of those genes promotes the formation of an infection pilus that delivers effector molecules directly into the cytoplasm of the host (Salmeron & Staskawicz, 1993; Staskawicz, 2001; Buttner & Bonas, 2002). This system is conserved across plant and animal pathogenic bacteria, and generally underlies basic pathogenesis (Hueck, 1998).

Upon secretion into the host, bacterial effectors have different activities. So far as is known, one of the primary roles of effectors is to promote virulence during infection by suppression of PTI. Their ability to attack host immune targets is diverse. Some effectors bind directly to PRRs to inactivate elicitor perception, whilst others are able to disturb signalling downstream of PAMP perception (Hauck *et al.*, 2003; Keshavarzi *et al.*, 2004; Kim, HS *et al.*, 2005). AvrPto and AvrPtoB from *Psto* were some of the first bacterial

effectors shown to suppress PTI-associated responses (He *et al.*, 2006). Both effectors block PAMP-induced signal transduction cascades upstream of MAPK activities (He *et al.*, 2006). AvrPto is a kinase inhibitor and can inhibit the intra-cellular kinase domains of the FLS2/BAK1 heterocomplex (Xiang *et al.*, 2008). AvrPtoB encodes an E3 ubiquitin ligase that can indirectly degrade FLS2 and other proteins involved in the elicitation of plant defence (Janjusevic *et al.*, 2006; Gohre *et al.*, 2008). Understanding the molecular function of effectors and their targets will undoubtedly be essential to fully understand the machineries of different pathogens to promote plant infection.

1.3.2. Effector recognition.

Pathogen virulence is compromised through the intracellular recognition of effectors by host receptor complexes, which in turn elicit downstream signalling responses leading to ETI. Recognised effectors are often said to be avirulence (Avr) proteins, because they change the phenotype of infection from virulence to avirulence on resistant hosts (Jones & Dangl, 2006). Such intracellular recognition complexes can be understood as an evolutionary response to inhibition of PTI by effectors (Dangl & Jones, 2001). Often R proteins contain NB-LRR domains that either directly or indirectly recognise the respective effector proteins (Chisholm *et al.*, 2006). NB-LRR genes show a high degree of variation, which may be due to the diversification of effectors (Chisholm *et al.*, 2006; Deslandes & Rivas, 2012). The mechanisms of recognition of effectors by such R proteins are diverse, and are thought to result from the virulence target of the effector (Dangl *et al.*, 2013), but in general, NB-LRR proteins either bind effectors themselves (direct), rely on an accessory for effector binding (indirect) or recognise

effectors by hetero-complex formation with other NB-LRRs (paired). Table 1.2 contains the examples for NB-LRR proteins and their respective effectors mentioned here.

Table 1.2: Pathogen effectors and NB-LRR resistance proteins

effector	pathogen	recognition	accessory	NB-LRR	recognising host(s)	reference
AvrB	*Pseudomonas syringae (Ps)*	Indirect	RIN4	RPM1	*Arabidopsis thaliana*	(Grant *et al.*, 1995; Mackey *et al.*, 2002)
AvrRpm1	*Ps*	Indirect	RIN4	RPM1	*A. thaliana*	(Grant *et al.*, 1995; Mackey *et al.*, 2002)
AvrRps2	*Ps*	Indirect	RIN4	RPS2	*A. thaliana*	(Kunkel *et al.*, 1993; Kim, HS *et al.*, 2005)
AvrPphB	*Pseudomonas syringae* pathovar *tomato (Psto)*	Indirect	PBS1	RPS5	tomato	(Shao *et al.*, 2003; Ade *et al.*, 2007)
AvrRps4	*Pseudomonas syringae pv. pisi*	Paired	RRS1	RPS4	*A. thaliana*	(Hinsch & Staskawicz, 1996; Narusaka *et al.*, 2009)
PopP2	*Ralstonia solanacearum*	Paired	RRS1	RPS4	*A. thaliana*	(Deslandes *et al.*, 2003; Narusaka *et al.*, 2009)
unknown	*Hyaloperonospora parasitica*	Unknown	n/a	RPP1A	*A. thaliana*	(Botella *et al.*, 1998)
Avr2	*Fusarium oxysporum*	Unknown	n/a	I-2	tomato	(Houterman *et al.*, 2009)
AvrPto	*Psto*	Indirect	Pto	Prf	tomato	(Salmeron *et al.*, 1996; Kim *et al.*, 2002; Martin *et al.*, 2003)
AvrPtoB	*Psto*	Indirect	Pto	Prf	tomato	(Salmeron *et al.*, 1996; Kim *et al.*, 2002; Martin *et al.*, 2003)
coat protein	PVX	Indirect	RanGap2	Rx	potato	(Kavanagh *et al.*, 1992; Tameling *et al.*, 2010)
p50	*Tobacco Mosaic Virus*	Indirect	NRIP1	N	tobacco	(Caplan *et al.*, 2008)
AvrPita	*Magnaporthe oryzae*	Direct	-	Pi-ta	rice	(Jia *et al.*, 2000)
AvrPia	*Magnaporthe oryzae*	Paired	RGA4	RGA5	rice	(Cesari *et al.*, 2013)
AvrCO39	*Magnaporthe grisea*	Paired	RGA4	RGA5	rice	(Cesari *et al.*, 2013)
unknown	*Blumeria graminis*	Unknown	n/a	MLA10	barley	(Seeholzer *et al.*, 2010)
Avr567	*Melampsora lini*	Direct	-	L7, L6, L5	flax	(Dodds *et al.*, 2006)
AvrM	*Melampsora lini*	Direct	-	M	flax	(Catanzariti *et al.*, 2010)

1.3.2.1. Direct recognition.

The simplest mechanism of effector perception is the direct one, in which the R protein itself directly identifies the respective effector and translates this into defence signalling (Rairdan & Moffett, 2006; Padmanabhan *et al.*, 2009). Examples for direct interaction between a NB-LRR protein and its cognate effector come from studies of *Pi-ta*, an *R* gene from rice that specifies resistance to strains of the rice blast fungus *Magnaporthe grisea* expressing the effector gene *AvrPita* (Jia *et al.*, 2000), and the flax *R genes* L5, L6, L7 and M recognising *Melampsora lini* effector AvrL567 and M, respectively (Dodds *et al.*, 2006; Catanzariti *et al.*, 2010).

1.3.2.2. Indirect recognition.

In many cases, R proteins recognise effectors indirectly. In these examples, an accessory protein of the NB-LRR interacts directly with the effector molecule and transduces this signal to the NB-LRR protein. Different models have been developed to describe indirect recognition mechanisms and are described below.

1.3.2.2.1. Guard hypothesis.

The guard hypothesis suggests the activation of the NB-LRR protein by the detection of changes in the virulence effector target, the guardee (Van der Biezen & Jones, 1998). For example, the *Pseudomonas* effectors AvrRpm1 and AvrB bind to the accessory protein RPM1-INTERACTING PROTEIN 4 (RIN4) and AvrRpt2 cleaves RIN4. RIN4 modification functions as an activator of the NB-LRR proteins RPS2 (RESISTANCE TO PSEUDOMONAS SYRINGAE PROTEIN 2) (in response to AvrRpt2) or RPS3/RPM1

(RESISTANCE TO PSEUDOMONAS MACULICOLA1) (in response to AvrRpm1 and AvrB), to trigger plant defence. RIN4 is involved in negatively regulating PTI in *A. thaliana*. However, the respective contributions of AvrRpm1 and AvrRpt2 to virulence are far greater in mutants lacking RIN4; it is therefore not completely understood whether RIN4 is the major target of those effectors (Mackey *et al.*, 2002; Axtell & Staskawicz, 2003; Day *et al.*, 2005; Kim, HS *et al.*, 2005). Another example is the NB-LRR protein N from *Nicotiana glutinosa*. N confers resistance to the Tobacco Mosaic Virus (TMV) by binding to the accessory N-RECEPTOR INTERACTING PROTEIN 1 (NRIP1), the target of the TMV effector p50 (Caplan *et al.*, 2008).

1.3.2.2.2. Decoy model.

The decoy model is a refinement to the guard hypothesis. Similarly, to the guard hypothesis, the decoy model proposes the R protein again detects effector-induced changes in the accessory protein, mediated by effector recognition. This model implies that the accessory protein acts as a decoy and mimics the effector virulence target (van der Hoorn & Kamoun, 2008). Evidence for the decoy model comes from the *Psto* protease effector AvrPphB, which cleaves the *A. thaliana* PBS1 (AvrPphB SUSCEPTIBLE 1) kinase to activate the NB-LRR protein RPS5 (Swiderski & Innes, 2001; Shao *et al.*, 2003). PBS1 is thought to be a decoy, as AvrPphB can also cleave PBS1-related kinases involved in PTI, namely BIK1 and PBS1-like (Zhang, J *et al.*, 2010). Another example is the interaction of the Pto (RESISTANCE TO PSEUDOMONAS SYRINGAE PATHOVAR TOMATO) kinase and the *Psto* effectors AvrPto and AvrPtoB. The accessory Pto shows homology to the BAK1 kinase domain, a virulence target of AvrPto and AvrPtoB and requires the NB-LRR protein Prf (PTO RESISTANCE AND FENTHION SENSITIVITY) for resistance (Scofield

et al., 1996; Tang *et al.*, 1996; Van der Biezen & Jones, 1998; Ntoukakis *et al.*, 2014). This protein complex and its effector recognition mechanism are described in detail later.

1.3.2.2.3. Bait and switch model.

The bait and switch model proposes that the interaction between effector and accessory protein (bait) is a fishing mechanism to facilitate effector binding to the NB-LRR protein (Collier & Moffett, 2009). This model is based on the R protein Rx (RESISTANCE TO POTATO VIRUS X) from potato conferring resistance to the potato virus X (PVX), which directly recognises the coat protein (CP) of PVX, but requires the bait RanGap2 for interaction (Rairdan & Moffett, 2006).

1.3.2.2.4. NB-LRR pairs.

In some cases, NB-LRR protein pairs have been identified, where one NB-LRR acts as accessory (Eitas & Dangl, 2010). For example, the *A. thaliana* TIR-NB-LRRs RPS4 (RESISTANCE TO PSEUDOMONAS SYRINGAE PROTEIN 4) and RRS1 (resistance to *Ralstonia solanacearum 1*) interact and recognise bacterial effectors AvrRps4 from *P. syringae* pv. *pisi* and PopP2 from *Ralstonia solanacearum* and at least one unknown effector from the fungal pathogen *Colletotrichum higginsianum* (Birker *et al.*, 2009; Narusaka *et al.*, 2009; Williams *et al.*, 2014). The CC-NB-LRR protein RGA5 from rice also forms a hetero-complex with CC-NB-LRR protein RGA4 and directly binds the *Magnaporthe oryzae* effectors Avr-Pia and AvrCO39 to confer resistance (Cesari *et al.*, 2013; Cesari *et al.*, 2014).

1.3.3. The structural basis of NB-LRR protein function.

The predominant class of plant *R genes* encodes a conserved NBARC (for nucleotide binding domain shared by APAF-1, certain R gene products, and CED-4) ATPase domain fused to C-terminal leucine-rich repeats (here referred to as NB-LRR proteins) (Leipe *et al.*, 2004).

NB-LRR proteins are further distinguished into two dominant classes that possess either a coiled-coil (CC) or Toll-interleukin 1 receptor and resistance (TIR) domain N-terminal of the NB-LRR domain (Collier & Moffett, 2009). Whereas most plant NB-LRRs homo- or hetero-multimerise thought those conserved N-terminal domains (examples are given below), mammalian NB-LRRs proteins usually oligomerise through this central NBARC domain.

1.3.3.1. The N-terminal coiled-coil and Toll interleukin 1 receptor and resistance (TIR) domains.

The TIR domain is similar to the cytoplasmic signalling domain utilised by the *Drosophila* TOLL AND MAMMALIAN INTERLUEKIN-1 receptor proteins involved in animal PTI (Underhill & Ozinsky, 2002). TIR domains typically specify homo- or hetero-dimerization interactions with other TIR domain-containing proteins. Overexpression of flax L6, *A. thaliana* RPS4, RPP1A (RESISTANCE TO PODOSPHAERA PANNOSA 1) and tobacco N TIR domains cause effector-independent HR in tobacco and/or *N. benthamiana* leaves, suggesting that the TIR domain is the signalling moiety of TIR-NB-LRRs (Jebanathirajah *et al.*, 2002; Frost *et al.*, 2004; Weaver *et al.*, 2006; Swiderski *et al.*, 2009; Krasileva *et al.*, 2010; Bernoux *et al.*, 2011; Williams *et al.*, 2014). Deletions and point mutations that de-stabilise homo- or hetero-dimerisation of TIR domains usually

affect signalling underlining correlations between oligomerisation and signalling abilities of TIR-NB-LRR proteins (Mestre & Baulcombe, 2006; Bernoux *et al.*, 2011; Williams *et al.*, 2014).

The coiled-coil (CC) domain is a common structural domain of amphipathic α-helices involved in protein-protein interactions. In the case of indirect effector recognition, the CC domain can mediate the physical interaction between the NB-LRR and the accessory protein. This has been shown for the RPM1-RIN4, RPS5-PBS1 and Rx-RanGAP2 interactions (Mackey *et al.*, 2002; Ade *et al.*, 2007; Hao *et al.*, 2013), whereas the CC domain of barley MLA10 (conferring resistance to certain races of *Blumeria graminis*) forms a rod-shaped dimer (Maekawa *et al.*, 2011). Overexpression of the MLA10 CC domain in *N. benthamiana* leaves leads to an effector independent HR (Maekawa *et al.*, 2011). Additionally, the CC domains of the rice CC-NB-LRR pair RGA4-RGA5 mediate homo- and hetero-dimerisation between the NB-LRR pair, but overexpression of only the CC domains in *N. benthamiana* is not sufficient for effector independent HR (Cesari *et al.*, 2013; Cesari *et al.*, 2014).

1.3.3.2. Nucleotide binding site.

The NB domain usually occupies a central position in the NB-LRR protein family and in mammalian systems it is also known as NOD (for nucleotide binding oligomerisation domain) as it mediates oligomerisation of mammalian but not plant NB-LRRs (Takken *et al.*, 2006; Franchi *et al.*, 2009; Dagenais *et al.*, 2010). The ARC domain is conserved between plant NB–LRR proteins and animal cell death proteins. The mammalian protein Apaf-1 contains four subdomains: a P-loop (nucleotide binding) domain (ARC1), helical domain (ARC2), an extended winged-helix domain and a second

helical domain (ARC3). The structure of CED-4 is similar to that to APAF-1, but lacks ARC3 (Albrecht & Takken, 2006). Despite their structural connection, APAF-1 and CED-4 have different mechanisms of activation, but both their crystal structures indicate that an ATP or ADP is bound in a buried pocket, the P-loop (Riedl *et al.*, 2005) and mutations of conserved P-loop residues result in an inactive proteins. For plant NB-LRRs, the MHD motif within the ARC2 domain is conserved and affects nucleotide binding. The highly conserved Histidine coordinates binding of ADP and the less conserved Methionine and Aspartate may stabilise this interaction. Substitutions within this motif can lead to constitutive activity as shown for most plant NB-LRR proteins (DeYoung & Innes, 2006) and reduced for ATP hydrolysis to ADP, as shown for tomato I-2 (conferring resistance to *Fusarium oxysporum* (Tameling *et al.*, 2002). As such, the ATP-bound configuration is thought to be the active form (Tameling *et al.*, 2006).

1.3.3.3. Leucine-rich repeats.

In NB-LRR proteins, LRR domains are located immediately C-terminal of the NB domain, and are composed of tandem LRRs. Usually they comprise the most C-terminal domain of the protein. LRR domains provide a structural platform for protein-protein interactions in a wide range of diverse proteins (Kobe & Deisenhofer, 1994; Kobe & Kajava, 2001; Bella *et al.*, 2008). Generally, LRRs have been implicated with recognition as well as signalling, and both the negative and positive regulation of a number of R proteins (Warren *et al.*, 1998; Banerjee *et al.*, 2001; Du *et al.*, 2012). The perception of proteinacous PAMPs by the LRR domain of LRR-RKs and LRR-RLPs suggests a role of the LRR domain of NB-LRRs in effector binding. This however, is not the case for mammalian NB-LRR proteins and in plants it is true for only few effector - NB-LRR protein

interactions; for example, the perception of AvrL567 by L6 and Avr-Pita by Pi-ta (Jia *et al.*, 2000; Bernoux *et al.*, 2011). In the case of mammalian NOD2, tomato Prf and Mi1.2 (conferring resistance to root-knot nematodes), potato Rx, and *A. thaliana* RPS2, RPS5 (RESISTANCE TO PSEUDOMONAS SYRINGAE PROTEIN 5) and RPP1A, the LRR domain negatively regulates signalling (Tao *et al.*, 2000; Bendahmane *et al.*, 2002; Tanabe *et al.*, 2004; Weaver *et al.*, 2006; Du *et al.*, 2012).

1.3.3.4. Intramolecular interactions and regulation of NB-LRR proteins.

Intramolecular interactions between NB-LRR protein subdomains appear to be an important aspect of their regulation. The NB domain of Rx can physically interact with the Rx CC and LRR domains. Importantly, and those interactions reconstitute the Rx protein but are disrupted in the presence of the effector protein (Moffett *et al.*, 2002; Leister *et al.*, 2005; Rairdan & Moffett, 2006). Interestingly, a non-functional Rx protein containing a mutation in the conserved P-loop disrupted the interaction with the CC, but not its interaction with the LRR domain (Rairdan & Moffett, 2006). The RPS5 NB domain also associates with both its CC and LRR domains (Ade *et al.*, 2007; Qi *et al.*, 2012), and the isolated unique N-terminal domain of Prf interacts with the other Prf moiety (Gutierrez *et al.*, 2010), but those interactions are not affected by the respective effectors.

NB-LRR activation by effector recognition is diverse and the function of individual domains cannot be generalised. However, certain substitutions with the MHD motive or the P-loop within the conserved NB site lead to gain- and loss-of function, respectively, suggesting that this mechanism plays an important role in the activation and/or loss of negative regulation. These mechanisms have been associated with conformational

changes and as the LRR domain also has been implicated the regulation of the NB-LRR activation status, it is possible that those changes affect interplay between the NB and the LRR domain. Despite the strong conservation of NB-LRRs is plant and animal disease resistance, the activation of signalling downstream of the molecular NB on/off switch still remains to be determined.

1.3.4. Chaperones involved in ETI signalling.

NB-LRRs exist in large complexes and it is thus not surprising that they rely on chaperones. Especially the chaperone proteins REQUIRED FOR MLA12 RESISTANCE (RAR1), SUPPRESSOR OF G2 ALLELE OF skp1 (SGT1) and HEAT-SHOCK PROTEIN 90 (HSP90) have been implicated in NB-LRR signalling. All interact with one another and are fundamental for the accumulation and function of some CC and TIR domain containing NB-LRRs in plants (Freialdenhoven *et al.*, 1994; Azevedo *et al.*, 2002; Shirasu & Schulze-Lefert, 2003). This includes barley MLAs; *Arabidopsis* RPP4, RPP5, RPM1, RPS2, RPS4 and RPS5; soybean Rpg1b; potato Rx; and tomato Prf (Muskett *et al.*, 2002; Tor *et al.*, 2002; Tornero *et al.*, 2002; Bieri *et al.*, 2004) .

RAR1 contains two cysteine and histidine-rich domains (CHORDs) and SGT1 contains a crystalline and small heat shock protein-like (CS) domain. Heat shock protein 90 (Hsp90) is a member of the GHKL (Gyrase, Hsp90, histidine kinase, MutL) ATPase/kinase superfamily. The CS domain of SGT1, and the CHORDI domain of RAR1 can interact with the N-terminal ATPase domain of Hsp90; the CHORDII domain of RAR1 also interacts with the CS domain of SGT1 (Takahashi *et al.*, 2003). The interaction between Hsp90 and SGT1 is mandatory for SGT1 function (Boter *et al.*, 2007) and the

crystal structure of the SGT1 CS domain, the RAR1 CHORD domain and the N domain of Hsp90 protein complex suggests that RAR1 structurally influence SGT1 and HSP90 (Zhang, M *et al.*, 2010). Those inter-complex interactions may thus have an important biological function. The complex might stabilise NB-LRRs by direct interaction as the SGT1-specific domain of SGT1 facilitates interaction with mammalian Nod1, potato Rx as well as other plant NB-LRRs (Bieri *et al.*, 2004; Correia *et al.*, 2007; Shen & Schulze-Lefert, 2007).

Interestingly, CRT1 (COMPROMISED RECOGNITION OF TURNIP CRINKLE VIRUS1) is structurally similar to Hsp90 (Kang *et al.*, 2008) and interacts with the NB domain of CC-NB-LRRs and TIR-NB-LRRs (including Rx, RPS2 and RPM1) (Kang *et al.*, 2010). Additionally, CRT2 and CRT3 are also required for tobacco N for its function in TMV resistance (Caplan *et al.*, 2009).

1.3.5. NB-LRR signalling

How NB-LRRs initiate cell death and resistance is not fully understood to date. Some NB-LRR proteins act in the plant nucleus, where they were suggested to interfere with the WRKY transcriptional network involved in defense gene expression. Examples include barley MLAs and *A. thaliana* SNC1 (Shen *et al.*, 2007; Zhu *et al.*, 2010; Chang *et al.*, 2013). *A. thaliana* RRS1 contains a WRKY domain and directly binds DNA (Deslandes *et al.*, 2002). The RRS1 susceptible allele shows the same DNA binding activity, suggesting that the RRS1 WRKY domain acts as integrated effector decoy rather than as a resistance signalling moiety (Le Roux *et al.*, 2015). The membrane-localised protein NON-RACE-SPECIFIC DISEASE RESISTANCE 1 (NDR1) is required for the function of many CC-NB-LRRs, while many TIR-NB-LRR proteins require the lipase-like proteins ENHANCED DISEASE SUSCEPTIBILITY 1 (EDS1) (Aarts *et al.*, 1998; Falk *et al.*, 1999), describing at least

two separate pathways for ETI signalling. Especially the EDS1 pathway has been studies extensively. EDS1 interacts with either of two related proteins, PHYTOALEXIN DEFICIENT 4 (PAD4) or SENESCENCE-ASSOCIATED GENE101 (SAG101) (Feys *et al.*, 2001). A physical interaction between EDS1 and TIR-NB-LRRs suggests that EDS1 links TIR-NB-LRRs to downstream responses (Bhattacharjee *et al.*, 2011; Heidrich *et al.*, 2011). Additionally, EDS1 may be a virulence target for effector molecules (Heidrich *et al.*, 2011). The exact molecular function of EDS1 and NDR1 is currently unknown, especially as EDS1 is also involved in resistance mediated by the RLP Ve1 (Hu *et al.*, 2005) and plays a role in innate immunity (Feys *et al.*, 2005; Lipka *et al.*, 2005).

Another component that plays a role in PTI and ETI downstream of receptor proteins, is NB-LRR PROTEIN REQUIRED FOR HR-ASSOCIATED CELL DEATH 1 (NRC1). NRC1 encodes a CC-NB-LRR protein itself and silencing of NRC1 in *N. benthamiana* compromises HR induced by the R proteins Pto, Rx and Mi and the RLPs Cf4 and EIX. Importantly, only in the case of Avr4/Cf4, lack of NCR1 lead to enhanced susceptibility. The exact role of NRC1 and the physical interaction of NRC1 with either of those defence related proteins remains to be determined (Gabriels *et al.*, 2007).

1.4. The Prf protein of tomato, required for resistance to bacterial speck disease.

Bacterial speck disease of tomato is caused by *Psto*. The bacteria are able to enter leaves through stomata or wounds where they reproduce in the apoplast, which leads to disease symptoms characterised by small (~1 mm) black or brown necrotic lesions

(specks), that can become surrounded by yellow haloes caused by the phytotoxin coronatine (Bender & Cooksey, 1987; Preston, 2000). Likewise, lesions form on both unripe and ripe tomato fruit, and this manifestation of the disease can decrease fruit marketability. Two of the *Psto* effectors, AvrPto and AvrPtoB, promote virulence by blocking PAMP-induced signal transduction cascades upstream of the MAPK pathway (He *et al.*, 2006).

1.4.1. AvrPto and AvrPtoB block PTI.

The AvrPto gene encodes a small (18.3-kDa) hydrophilic triple-helix protein that is N-myristoylated *in vivo*. AvrPto functions as a kinase inhibitor that restricts PRR signalling, as demonstrated by its ability to inhibit the kinase activity of PRR kinase domains (Xing *et al.*, 2007; Xiang *et al.*, 2008). Ectopic over-expression of AvrPto also suppresses the host cell wall strengthening in *A. thaliana* (Hauck *et al.*, 2003; DebRoy *et al.*, 2004), which is a typical defence response. Localisation of AvrPto to the plasma membrane by N-myristoylation is indispensable for its virulence functions (Shan *et al.*, 2000).

AvrPtoB is a cytoplasmic protein of 59 kDa (Kim *et al.*, 2002). It possesses a C-terminal E3 ubiquitin ligase domain indicating the ability to ubiquitinate and indirectly degrade target proteins. AvrPtoB interacts with the kinase domain of BAK1 and FLS2 and CERK1 to supress defence signalling (Gohre *et al.*, 2008; Shan *et al.*, 2008; Gimenez-Ibanez *et al.*, 2009a). AvrPtoB deletion fragment encoding aa 1-387 can bind BAK1 and FLS2 to inhibit flagellin signalling and crystallographic analysis mapped the interface of BAK1 and AvrPtoB to the AvrPtoB residues 250-359. Shorter fragments such as AvrPtoB $_{1\text{-}307}$, are unable to suppress BAK1/FLS2 but interact with CERK1 in *N. benthamiana* (Shan *et al.*, 2008; Gimenez-Ibanez *et al.*, 2009a; Zeng *et al.*, 2012).

1.4.2. Recognition of AvrPto and AvrPtoB by the Pto kinase.

Resistance in tomato is mediated by the recognition of AvrPto and AvrPtoB in tomato lines expressing Pto (resistance to *Pseudomonas syringae* pathovar *tomato*). *Pto* is a member of a small, clustered family (*Pto* and the *Pto* homologs *Fen* and *Pth2/3/4/5*) (Martin *et al.*, 1993). Fen is responsive for perception of the insecticide fenthion and is described below in detail. The biological function of *Pth2, Pth3, Pth4* and *Pth5* is not fully determined but they potentially provide recognition of yet unknown pathogen elicitors to expand recognition (Mucyn *et al.*, 2009). *Pto* itself encodes an N-myristoylated serine/threonine kinase structurally similar to the kinase domains of PRRs enforcing the idea that Pto acts as a decoy for the virulence target (Cheng *et al.*, 2011; Ntoukakis *et al.*, 2014). The Pto kinase domain contains a high degree of amino acid similarity with those of human IRAK-1 and *Drosophila* Pelle, both with roles in immunity (Shelton & Wasserman, 1993; Cao *et al.*, 1996; Sessa *et al.*, 2000a; Cohn *et al.*, 2001). In plants, this class of kinase genes has proliferated dramatically which has been postulated to be crucial for plant-specific adaptations (Lehti-Shiu *et al.*, 2009). Pto recognises both effectors directly though a common interface at the Pto activation segment (Figure 1.3) (Wulf *et al.*, 2004; Xing *et al.*, 2007; Dong *et al.*, 2009; Wirthmueller *et al.*, 2013; Mathieu *et al.*, 2014). The activation segment is a loop region, which lies in the catalytic cleft of the enzyme, inhibiting the kinase in the inactive conformation, and in a structured open conformation when the kinase is active. Within the activation loop are smaller regulatory subdomains, including the T-loop in which regulatory phosphorylation events often occur, and the C-terminal P+1 loop, which binds and orients protein substrates (Taylor *et al.*, 1993; Johnson *et al.*, 1996). The GINP residues of AvrPto and the AVAF residues of AvrPtoB or its deletion fragment $AvrPtoB_{121\text{-}205}$ bind the P+1 loop of Pto (Wu

et al., 2004). Additionally, either effector encodes a second Pto interface. AvrPto binds with its helical bundle to Pto residues 49-52, N-terminal of the P+1 loop and AvrPtoB with L1 and helix a1 C-terminal to the P+1 loop (Figure 1.3).

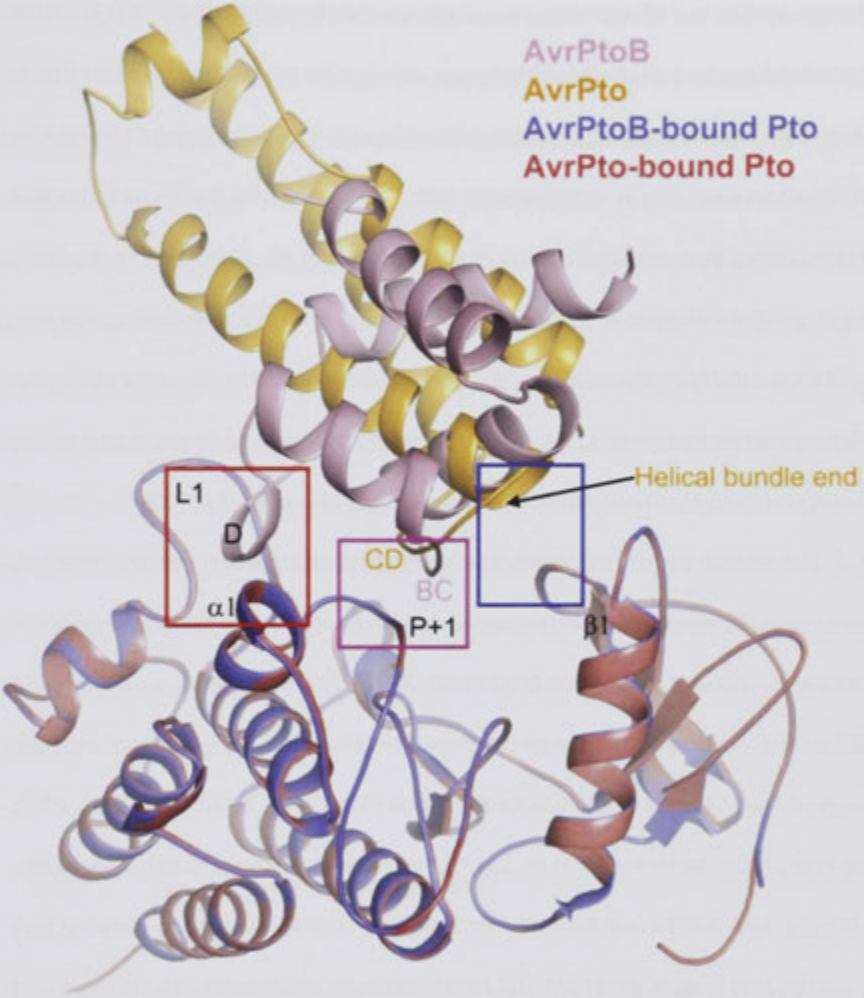

Figure 1.3: Structural comparison of the AvrPtoB$_{121-205}$-Pto and AvrPto-Pto complexes (Dong *et al.*, 2009). The pink square highlights the Pto P+1 loop interaction with the AvrPtoB AVAF residues (BC) and AvrPto GINP (CD) residues. The red square shows interaction of AvrPtoB helix with Pto loop L1 and helix a1. The blue square highlights the unique interface between the Pto residues H49/V51 and AvrPto.

In response to the effectors, Pto activates downstream signal transduction pathways, leading to a HR and resistance. Correspondingly, mutations in residues within the Pto P+1 loop lead to the constitutive induction of HR in the absence of AvrPto or AvrPtoB (also known as constitutive gain-of-function (CGF)) when expressed transiently in *N. benthamiana*. This is in agreement with the P+1 loop as the most important effector-binding determinant (Rathjen *et al.*, 1999; Wu *et al.*, 2004; Xing *et al.*, 2007; Dong *et al.*, 2009; Wirthmueller *et al.*, 2013). The P+1 loop is also known as negative regulatory patch (NRP) based on a speculative model in which Pto is repressed by an inhibitory peptide that binds to the P+1 loop, and that effector binding at the same site de-represses this negative regulation (Wu *et al.*, 2004; Mucyn *et al.*, 2009).

The crystal structures, which elucidated binding between Pto and effector, showed that phosphorylation of threonine-199 within the Pto activation segment is necessary for effector interaction (Xing *et al.*, 2007). Phosphorylation on this residue stabilises the kinase activation segment through interaction via a salt bridge with the conserved Arg-163 within the kinase catalytic loop (Sessa *et al.*, 2000b; Xing *et al.*, 2007; Dong *et al.*, 2009; Wirthmueller *et al.*, 2013). Yet, Pto kinase activity itself is dispensable for binding both AvrPto and AvrPtoB. The point was recently clarified by showing that the substitution mutant ptoT199A still recognises both effectors *in vivo* (Ntoukakis *et al.*, 2013). Nevertheless, phosphorylation on residues S198 and T199 is still required for signal transduction. Importantly, Pto mutants that cause CGF signalling in *N. benthamiana* are usually kinase-deficient but are believed to signal due to their trans-phosphorylation by the *N. benthamiana* Pto homolog (NbPth1). Notably, a phosphor-mimic form of Pto, the ptoS198D/T199D mutant, does not display the CGF phenotype

but still responds to the effectors. Thus, both disruption of the negative regulatory patch and phosphorylation (mainly at S198 and T199) are required for Pto signalling, whereas phosphorylation alone is not sufficient (Sessa *et al.*, 2000b; Ntoukakis *et al.*, 2013).

Pto is N-myristoylated on residue Glycine-2, but it has not yet been possible to show that Pto is localised to the plasma membrane although the N-myristoylation motif is required for Pto function (Rathjen *et al.*, 1999; Andriotis & Rathjen, 2006; de Vries *et al.*, 2006; Balmuth & Rathjen, 2007; Ntoukakis *et al.*, 2009). The essential nature of this modification, and the observation that the AvrPto and AvrPtoB virulence targets are also plasma membrane proteins, makes this the most likely hypothesis. Myristoylation confers rather weak affinity for membrane structures, which may explain why Pto has not been visualised in membrane fractions, and because of this is usually coupled with other acyl modifications such as palmitoylation, as for AvrPto and several other effectors localised to the plasma membrane. This area requires further study but is particularly interesting not least because of the strict requirement for Pto N-myristoylation for signalling, and the ability of myristate to inhibit Pto kinase activity (Andriotis & Rathjen, 2006).

1.4.3. Fen and the insecticide fenthion.

One member of the Pto gene family, *Fen*, mediates HR-like cell death in response to the insecticide fenthion. The *Fen* gene lies within the *Pto* cluster in a region of 25 kb 5' from Pto, which explains the genetic co-segregation of bacterial speck resistance and sensitivity to fenthion (Carland & Staskawicz, 1993). Fen and Pto share 80% amino acid identity including the kinase and the N-myristoylation motif. However, AvrPto cannot interact with the Fen kinase as it contains substitutions in three key residues that

correspond to Pto His-49, Val-51, and Thr-204 (Scofield *et al.*, 1996; Frederick *et al.*, 1998; Kim *et al.*, 2002; Xing *et al.*, 2007; Tang *et al.*, 2008). Interestingly, AvrPtoB interacts with Fen, and its E3 ubiquitin ligase activity causes degradation of Fen but not Pto (Janjusevic *et al.*, 2006; Rosebrock *et al.*, 2007). This can be explained by enhanced kinase activity of Pto when compared to Fen, as the phosphorylation of AvrPtoB diminished its E3 ligase activity (Ntoukakis *et al.*, 2009). Alternatively, the relative distance of the kinase interaction site may play a role, as in a linear molecule, the Pto-AvrPtoB interface would lie further from the E3-ligase domain of AvrPtoB than the AvrPtoB-Fen interface (Mathieu *et al.*, 2014). At this point, neither explanation excludes the other, and as substrate binding is a component of kinase activity, both may be real. Remarkably, a shortened form of AvrPtoB lacking its E3 ligase subdomain binds Fen, leading to resistance to bacterial speck (Rosebrock *et al.*, 2007). Similar to Pto CGF mutants, Fen causes the HR when expressed transiently in *N. benthamiana.* Whereas autoactive Pto mutants are generally kinase inactive (through mutation-induced disruption of the activation segment), Fen is an active kinase that requires kinase activity for the CGF HR in *N. benthamiana* (Mucyn *et al.*, 2009).

1.4.4. Prf (Pto resistance and fenthion sensitivity).

The *Prf* gene encoding a NB-LRR protein resides in the Pto gene cluster, 24 kb 5' from *Pto* and 500 bp 5' from *Fen* (Salmeron *et al.*, 1996; Oldroyd & Staskawicz, 1998; Chang *et al.*, 2002). *Prf* occurs in both resistant and susceptible tomatoes, but *Pto* is present only in resistant lines and Pto mutants show reduced resistance. For this reason, Pto is the polymorphic determinant of resistance and hence is designated the resistance gene. However, a lack of *Prf* leads to full susceptibility to *Psto* and sensitivity to fenthion.

(Tobias *et al.*, 1999). Complementation of the *prf-3* allele (lacking 1.1 kbp of the Prf gene) with the full-length *Prf* gene can restore responsiveness to *Psto* and fenthion. Correspondingly, Fen and Pto physically associate with Prf for signal transduction (Mucyn *et al.*, 2006) but a role for Prf in effector or fenthion binding has not been described (Salmeron *et al.*, 1996; Wu *et al.*, 2004). Prf may be also bind the Pto-like kinases to provide recognition of yet unknown pathogen elicitors (Mucyn *et al.*, 2009).

Prf is a typical NB-LRR protein but contains a huge N-terminal extension that doubles the length of the protein to almost 2,000 amino acids (**Error! Reference source not found.**) (Oldroyd & Staskawicz, 1998; Mucyn *et al.*, 2009). The very N-terminal

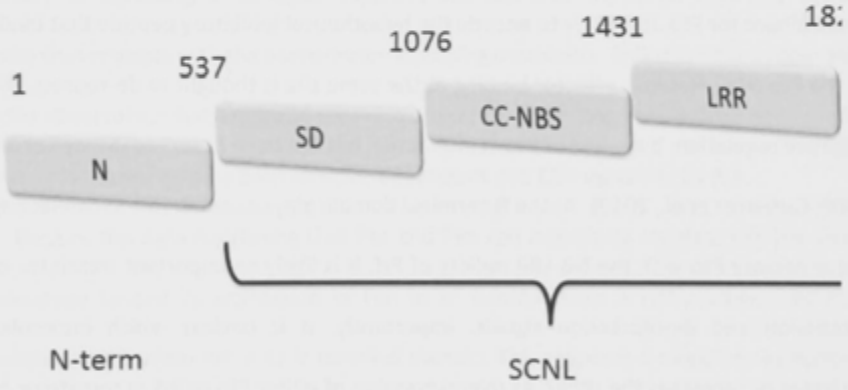

Figure 1.4 Schematic structure of the Prf protein illustrating the individual Prf domains. N, N-term: N-terminal domain; SD: *Solanaceous* domain; CC: coiled-coil, NBS: nucleotide binding site; LRR: leucine-rich repeats domain. SCNL: SD-CC-NB-LRR. aa: Amino acid.

domain (N, aa 1-546) shows no similarity to other proteins. Directly C-terminal leis a domain with unknown function that shows similarities to regions found in other *Solanaceous* proteins (Solanaceous domain, (SD)). Between the SD domain and the NB-

LRR region of Prf leis a region, which has been predicted to contain a CC domain (Mucyn *et al.*, 2006). The Prf N domain is involved in intramolecular interactions within the Prf molecule. Co-expression of the N- domain and the remainder of the protein comprising the SD-CC-NB-LRR moiety (SCNL) functionally restores the Prf molecule. Such functional complementation is correlated with physical interaction between the Prf sub-domains *in planta* (Mucyn *et al.*, 2006).

1.4.5. Pto and Prf regulate each other through the unique Prf N-terminal domain.

The Prf N domain mediates binding of the accessory Pto, Fen and potentially other members of the Pto family (Mucyn *et al.*, 2006; Mucyn *et al.*, 2009). As the direct binding determinant for Pto, it is likely to encode the hypothetical inhibitory peptide that binds to the Pto NRP. Notably, effector binding at the same site is thought to de-repress this negative regulation, but a loss of Pto-N interaction has not been observed (Mucyn *et al.*, 2006; Gutierrez *et al.*, 2010). As the N-terminal domain plays a central role in connecting the accessory Pto with the NB-LRR moiety of Prf, it is likely an important translator of repression and de-repression signals. Importantly, it is unclear which molecules activates or represses the other, as overexpression of either Pto or Prf in tomato or *N. benthamiana* causes a ligand-independent HR in both tomato and *N. benthamiana* (Tang *et al.*, 1999; Xiao *et al.*, 2003; Mucyn *et al.*, 2006). Pto was thought to negatively regulate Prf because in *N. benthamiana,* constitutive Prf signalling can be inhibited by co-expression of the *Pto* mutants *ptoG2A* and *ptoD164N*, deficient in N-myristoylation and kinase activity respectively (Mucyn *et al.*, 2006; Ntoukakis *et al.*, 2013). Constitutive Prf signalling results from extreme overexpression of *Prf* from to the strong

dexamethasone-inducible promoter (*Dex:Prf*) and a mutation in the sequence encoding the conserved MHD motif (IHD for Prf, mutated to IHV for CGF) within the NB-ARC domain. Interestingly, Fen mutants deficient in kinase activity and myristoylation are also capable of inhibiting the *Dex:Prf* dependent HR. This supports the idea of a regulatory effect of Fen and Pto on Prf, which seems likely to be mediated through the Prf N-terminal domain as it encodes the interaction site for both kinases (Mucyn *et al.*, 2006; Mucyn *et al.*, 2009). Importantly, this cannot explain why Fen signalling is deregulated in the absence of fenthion in *N. benthamiana*. It has been speculated that Fen binds to the *N. benthamiana* homolog of Prf (NbPrf), forming a mis-regulated complex, which signals constitutively. So far, no direct evidence to challenge or support this model is available. CGF Pto mutants also require the *N. benthamiana* Prf homolog (NbPrf) for signalling, which again supports that fact that Prf, rather than Pto, is the entity that engages with the downstream signalling machinery. This is further supported by the observation that a mutation of Prf in the conserved P-loop required for nucleotide binding (K1128A) inhibits both effector-dependent and CGF signalling by Pto.

Despite the data suggesting that Pto and Fen can negatively regulate Prf, the CGF phenotype caused by expression of Fen in *N. benthamiana* is compromised by co-expression of tomato Prf or its N-terminal domain. This proposes a negative regulatory effect of Prf on Fen and possibly Pto (Mucyn *et al.*, 2009), which is in agreement with the hypothesis of Prf containing the peptide sequence complementary to the Pto NRP. As Fen requires its kinase activity for the CGF phenotype, tomato Prf may additionally inhibit Fen kinase activity whereas NbPrf is unable to do so.

1.4.6. The Prf multimerisation through the unique N-terminal domain brings two Pto molecules together and sets a molecular trap for the effectors.

The regulatory interplay between Prf and Pto (and by analogy Fen) can be at least partly explained by Prf multimerisation, which is also mediated by its unique N-terminal domain and independent of Pto (Gutierrez *et al.*, 2010). Although it has not been shown directly, Prf multimerisation is likely a crucial adaptation for sustainable effector recognition as it brings at least two Pto molecules into close proximity. Both AvrPtoB and AvrPto are able to inhibit or degrade their known virulence targets, which are PRRs and Pto kinase activity is compromised by the interacting effectors, but neither effector is able to inhibit Pto/Prf-mediated resistance in the same way (Ntoukakis *et al.*, 2009; Ntoukakis *et al.*, 2013). This can be explained by the oligomeric occurrence of the Pto/Prf complex in which one Pto molecule acts as the effector sensor and the other Pto molecule as the helper-Pto for trans-phosphorylation (Ntoukakis *et al.*, 2014). In this model, the effectors bind the sensor Pto molecule, leading to inactivation of its kinase activity through disruption of the P+1 loop and the negative regulation imposed by Prf through a potential peptide sequence. De-repression of the P+1 loop activates a second helper Pto molecule in the Prf complex to trans-phosphorylate the first on threonine-199, leading to full activation of the complex, which at this point is believed to be an unknown signal transduction pathway (Figure 1.5) (Wu *et al.*, 2004; Mucyn *et al.*, 2009). Importantly, the NB of Prf is required for Pto trans-phosphorylation events (Ntoukakis *et al.*, 2013). This suggests that the molecular on/off switch of the NB-LRR moiety of Prf acts down-stream of effector mediated activation of the sensor Pto but up-stream of Pto trans-phosphorylation (Ntoukakis *et al.*, 2014).

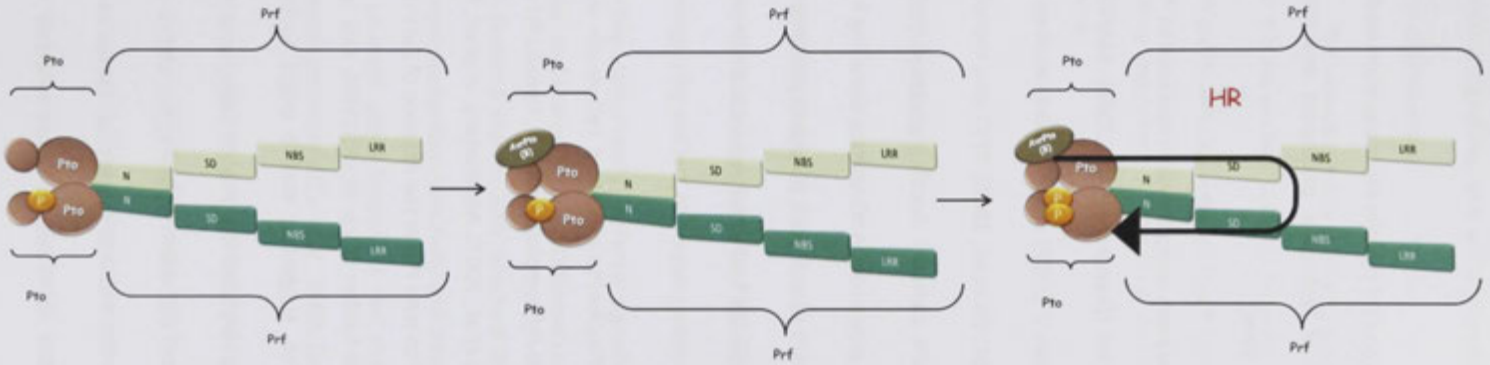

Figure 1.5: A schematic model explaining the Pto/Prf protein complex regulation. The Pto/Prf complex is composed of at least two Pto and two Prf molecules, with the Prf N domain as the primary interaction site. Upon recognition of the effector molecules AvrPto or AvrPtoB by one Pto molecule, which undergoes a conformational change. This in turn is detected by the Prf N domain, and hence Prf disrupts its negative regulation of the Pto molecules. De-repression of the P+1 loop activates a second Pto-helper molecule in the Prf complex that trans-phosphorylates the first sensor-kinase, leading to complex activation and to the hypersensitive response. The model was developed in 2010 and is based predominately on the results of Mucyn *et. al.* 2006, Gutierrez *et. al.* 2010 and Ntoukakis *et. al.* 2013. N: N-terminal domain; SD: *Solanaceous* domain; CC: coiled-coil, NBS: nucleotide binding site; LRR: leucine-rich repeats domain.

1.4.7. Pto/Prf signalling.

As for other R proteins, activation of Pto and Prf by effector recognition leads to the HR as cellular suicide to restrict growth of biotrophic pathogens and confer resistance (Morel & Dangl, 1997; Rathjen *et al.*, 1999).

Silencing of MAPKKKα and MAPKKKε have been compromised resistance to *Psto*, and ectopic overexpression have lead to the HR (Ekengren *et al.*, 2003). MAPKKKα interacts directly with the tomato 14-3-3 protein 7 (TFT7) which is also required for Pto/Prf-mediated cell death (del Pozo *et al.*, 2004; Oh *et al.*, 2010). TFT7 may therefore act as a linker between Pto/Prf and the MAPK cascade. Another protein, AvrPto-DEPENDENT Pto INTERACTOR 3 (Adi3) may also play a role in translating signalling from the Pto/Prf complex to the MAPK cascade. Adi3 is a kinase itself, phosphorylated by Pto in the absence of AvrPto and silencing of Adi3 causes MAPKKKα-dependent cell death signalling (Devarenne *et al.*, 2006).

NCR1 is also required for the weak Pto/AvrPto-mediated cell death in *N. benthamiana* (dependent on the *N. benthamiana Prf* homolog), Notably, tomato Prf was not co-expressed in those experiments (Gabriels *et al.*, 2007). Additionally, in yeast, Pto-interacting proteins have been identified (Pti). Ptis bind Pto in the absence of AvrPto or AvrPtoB. The role of Pti1 has been investigated further (Zhou *et al.*, 1995). Pti1 is an active kinase but does not phosphorylate Pto, suggesting that it might function downstream of Pto *in vivo*. Pti1 was phosphorylated by Pto *in vitro*, and *Pti1* overexpression leads to enhanced Pto-mediated cell death (Zhou *et al.*, 1995). Pti1 substitutions or Pto kinase mutations abolish the Pto-Pti1 interaction (Sessa *et al.*, 2000a). Importantly, silencing of neither of the identified Pti genes affected *Pto*-

dependent signalling, and understanding a clear role for Pti1 in resistance requires further experiments.

The immediate downstream signalling partner of Pto and Prf is still unknown and in fact it is still unclear whether Prf or Prf causes activation of this unknown component. Identification of links between Pto/Prf as well as other R proteins with the downstream signalling machinery is therefore one of the outstanding goals in plant immunity research.

1.5. Summary.

Receptors build the frontline in the initiation of plant immunity. Most of those immune receptors belong to the RLPs, RKs (PRRs) or NB-LRR (R protein) class of proteins for recognising distinct pathogen component and translating recognition into defence signalling. Importantly, defence signalling pathways are conserved amongst plant families and shared between different receptors (Nimchuk *et al.*, 2003; Belkhadir *et al.*, 2004; Pedley & Martin, 2005; Macho & Zipfel, 2014). As such, the receptors itself confer pathogen recognition specificity and transfer of immune receptors within plant species and amongst plant families is the most common strategy to engineer pathogen resistance genetically (Tai *et al.*, 1999; Jones *et al.*, 2014).

Because components recognised by PRRs are usually crucial, loss of those components is likely lethal; although few cases exist where patterns have successfully changed to retain their biological function but avoid host recognition (Felix *et al.*, 1999). Nevertheless, this makes interfamily transfer of PRRs an important strategy to confer

broad-spectrum disease resistance (Fradin *et al.*, 2009; Lacombe *et al.*, 2010; Wulff *et al.*, 2011; Dangl *et al.*, 2013; Holton *et al.*, 2015; Schoonbeek *et al.*, 2015). Importantly, plants possess a large number of RLPs and RKs (Shiu & Bleecker, 2001; Fritz-Laylin *et al.*, 2005) and many of those may act as PRRs (Zipfel, 2014). Considering this, only few PRRs have been identified with the capacity to identify more in the future. PRRs are commonly targets of effector molecules, which in turn can be recognised by NB-LRRs (Chisholm *et al.*, 2006; Jones & Dangl, 2006). Importantly, the effector reservoir of single pathogens is large and loss of single effectors only weakly compromises pathogenicity but can lead to full susceptibility of the host (Kamoun, 2006; McCann & Guttman, 2008; Hann *et al.*, 2010). Loss or change of effectors are therefore important virulence strategies of pathogens (Stam *et al.*, 2014). In addition, the rapidly evolving pathogen may possess new effectors targeting R proteins or their respective downstream components. This is why *R* gene transfer alone may be overcome by pathogens quickly. One of the emerging strategies to engineer a more durable resistance is "stacking" of R genes with different specificities against one or more pathogens (Naqvi *et al.*, 2010; Olson *et al.*, 2013; Jo *et al.*, 2014). Identification and transfer of immune receptors alone is not always sufficient, especially because they often occur in multi-protein complexes. Understanding receptor interactions, regulations and signalling pathways is therefore crucial. For examples, Pto genetically confers resistance to *Psto* in tomato, but transfer of Pto alone is insufficient for resistance, because it requires Prf for function (Rommens *et al.*, 1995; Oldroyd & Staskawicz, 1998; Mucyn *et al.*, 2006).

1.6. Aims of this project.

The work presented in this thesis addresses two major aspects in plant immunity: Identification of novel receptors for pathogen elicitors, as well as the regulation mechanisms of a known protein complex. Precisely, the objectives are:

- The development of a novel general method to identify BAK1-dependent PRRs biochemically, using BAK1 as molecular bait.
- The identification of the PRR recognising the bacterial PAMP csp22 in *N. benthamiana*.
- Adressing the question whether non-host species can detect and confer PTI to the obligate biotrophic wheat rust fungus *Puccinia striiformis forma specialis tiritici* (*Pst*) , and identification of putative PRR candidates that recognise *Pst* in *A. thaliana* or *N. benthamiana*.
- An investigation of inter-domain interaction within the Pto/Prf complex with a particular focus on the unique Prf N-terminal domain, to understand the Pto/Prf mode of activation.

2. Materials and Methods.

2.1. Chemicals.

All chemicals used were of the highest obtainable grades. Deionised water (Milli-Q water, Millipore, Bedford, MA) with resistance of greater than 18 megaOhm/cm was used throughout.

2.2. Plant material and growth conditions.

2.2.1. Arabidopsis thaliana.

Arabidopsis thaliana plants (Table 2.1) were grown as 1 seedling per pot in controlled environment chambers with a 10 h (short day) or 16 h (long day) photoperiod at 20-22°C and 65 % humidity.

Table 2.1: Arabidopsis thaliana *lines used in this study.*

Plant line	Use	Reference
Wild type, ecotype Columbia (Col-0)	Reactive Oxygen Species (ROS) assay, Seedling growth inhibition (SGI) assay, Mitogen-activated protein kinase (MAPK) assay, transformation	
rbohD, background: Col-0	Reactive Oxygen Species (ROS) assay,	(Torres *et al.*, 2002)
bak1-4, background: Col-0	ROS assay, SGI assay, MAPK assay, transformation	(Kemmerling *et al.*, 2007)
bak1-5/bkk1-1, background: Col-0	ROS assay, SGI assay, MAPK assay, transformation	(Roux *et al.*, 2011)

Table 2.1 continued: Arabidopsis thaliana lines used in this study.

sobir1-1, background: Col-0	MAPK assay, transformation	(Gao *et al.*, 2009)
bak1-4/pAtBAK1:AtBAK1-YFP, background: Col-0	Identification of AtBAK1-interacting proteins	(Schwessinger PhD thesis, University of East Anglia, Norwich UK, 2010)
bak14/pAtBAK1:AtBAK1-5-YFP, background: Col-0	Identification of AtBAK1-5 interacting proteins	(Schwessinger PhD thesis, University of East Anglia, Norwich 2010)
Receptor-like kinase T-DNA insertion library	SGI assay	(Danna *et al.*, 2011)
Receptor-like Protein T-DNA insertion library	SGI assay	(Wang *et al.*, 2008)
35S:EV-5xMyc-1 background: Col-0	ROS assay, SGI assay, MAPK assay, transformation, bacterial growth assay	This thesis
35S:NbCSPR-5xMyc-5 background: Col-0	ROS assay, SGI assay, MAPK assay, transformation, bacterial growth assay	This thesis

2.2.1.1. Seed sterilisation and in vitro *growth of* Arabidopsis thaliana.

In a desiccator, chlorine gas was generated by supplementing 100 mL of 12.5% v/v sodium hypochlorite solution with four mL hydrochlorate solution. Seed-containing tubes were opened and treated with chlorine gas in the desiccator for three to six hours, before letting the gas evaporate under sterile conditions. Seeds were transferred onto solid MS media (Table 2.2) (Murashige & Skoog, 1962) supplemented with 25 µg/mL of

the anti-fungicide Nystatin (Sigma, Castle Hill, Australia). Seeds were stratified for two days at 4°C in the dark before they were moved for germination to growth chambers with a or 16 h (long day) photoperiod at 20-22°C and 65 % humidity.

Table 2.2: Preparation of MS salt medium.

Reagents	Final concentration
MS salts (Sigma)	4.3 g/L
N-morpholinoethanesulfonic acid (MES)	0.59 g/L
Agar (for solid media only)	8 g/l
pH adjusted to 5.7 with HCl	

2.2.2. Nicotiana benthamiana.

Nicotiana benthamiana (Table 2.3) was sown in soil and germinated under standard greenhouse conditions. Two week old seedlings were transplanted to larger pots (one seedling per pot) and grown in controlled environment chambers at an average temperature of 22°C, with 45-65 % relative humidity under long day conditions (16 h light) for another 3-5 weeks before use in biological or molecular assays.

Table 2.3: Nicotiana benthamiana *lines used for transient expression of proteins and VIGS.*

Plant line	Use	Reference
Nicotiana benthamiana wild-type	Transient expression using agroinfiltration	(Scofield *et al.*, 1996)
Nicotiana benthamiana SLJR15 (*35S:aequorin*)	Calcium influx assay	(Albrecht *et al.*, 2012)

2.3. Bacterial strains.

Bacterial strains used in this study are listed in Table 2.4.

Table 2.4: Bacterial strains used for cloning and transformation

Bacterial strain	Genotype	Applications	Reference or source
Escherichia coli DH5α	F', ϕ80d*lacZ*ΔM15, Δ(*lacZYA-argF*)U169, *deoR*, *recA*1, *endA*1, *hsdR*17(rk⁻, mk⁺), *phoA*, *supE*44, λ⁻, *thi*-1, *gyrA*96, *relA*1GAL-	molecular cloning	(Hanahan, 1983)
Escherichia coli BL21(DE3)	F– ompT gal dcm lon hsdSB(rB- mB-) λ[DE3 [lacI lacUV5-T7 gene 1 ind1 sam7 nin5])	heterologous expression of proteins	(Daegelen *et al.*, 2009)
Escherichia coli Shuffle B	*fhuA2 [lon] ompT ahpC gal* λatt::pNEB3-r1-*cDsbC* (SpecR, *lacI*^{q}) *ΔtrxB sulA11 R(mcr-73::miniTn10*--Tet^{S})*2 [dcm] R(zgb-210::Tn10* --Tet^{S}) *endA1 Δgor Δ(mcrC-mrr)114::IS10*	heterologous expression of proteins	(Lobstein *et al.*, 2012)
Escherichia coli Shuffle K12	F' *lac, pro, lacI*^{q} */ Δ(ara-leu)7697 araD139 fhuA2 lacZ::T7 gene1 Δ(phoA)PvuII phoR ahpC* galE (or U) galK* λ*att*::pNEB3-r1-*cDsbC* (Spec^{R}, *lacI*^{q}) *ΔtrxB rpsL150*(Str^{R}) *Δgor Δ(malF)3*	heterologous expression of proteins	(Lobstein *et al.*, 2012)
Agrobacterium tumefaciens GV3101 (pMp90)	Gm^{r}, Rif^{r}	Plant transformation	(Koncz & Schell, 1986)
Pseudomonas syringae pathovar *tabaci* 6605	Rif^{r}	Pathogen assays	(Shimizu *et al.*, 2003)
Pseudomonas syringae pv. *tabaci* 6605 - *hrcC*	Δ hrpC, Rif^{r}	Pathogen assay	(Shimizu *et al.*, 2003)
Pseudomonas syringae pv. *tabaci* 6605 - *fliC*	Δ fliC, Rif^{r}	Pathogen assay	(Shimizu *et al.*, 2003)
Pseudomonas syringae pv. *phaseolicola* 1448α	Rif^{r}	Pathogen assay	(Arnold *et al.*, 2011)
Pseudomonas syringae pv. *tomato* DC300	-	Pathogen assay	

2.4. Antibiotics.

Antibiotics used for bacterial and plant selection of positive transformants are listed with respective final concentrations in Table 2.5.

Table 2.5: Antibiotics used as selective markers

Antibiotic	Concentration in liquid and solid media
Kanamycin	25–50 µg/mL
Tetracycline	1.5-10 µg/mL
Chloramphenicol	100 µg/mL
Carbenicillin	100 µg/mL
Rifampicin	50 µg/mL
Spectinomycin	100 µg/mL
Gentamycin	50 µg/mL

2.5. Molecular biology techniques.

2.5.1. Vectors and constructs.

Constructs for which template sequences existed are listed in Table 2.6. Vectors used for cloning are listed in Table 2.7. For most cloning procedures, the pT70 vectors were used. pT70 vectors are pTFS-40 derivatives intended for insertion of a promoter-gene fusion in frame with an epitope tag for *in planta* overexpression using the cauliflower mosaic virus (CaMV) 35S promoter. In pT70, the *35S* promoter from pSLJ4D4 (parent clone of all p4D4.1 vectors, (Jones *et al.*, 1992) was excised and inserted into pTFS-40 using the *EcoRI* and *Xho*I sites (thus deleting the *BamHI* site, (Rathjen *et al.*,

1999)). The epitope tag fuses in frame with an XbaI site (Figure 1) (Balmuth & Rathjen, 2007). For gene insertion, XhoI (or SalI) is used at the 5' end, and XbaI (or AvrII or SpeI) at the 3' end (Figure 2.1).

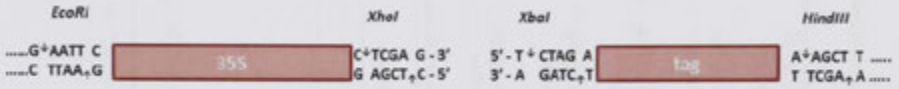

Figure 2.1: The polylinker of pT70. For gene insertion, XhoI (or SalI) is used at the 5' end, and XbaI (or AvrII or SpeI) at the 3' end

Table 2.6: Pre-existing constructs for direct use in pT70 vectors, or ready for sub-cloning into pT70.

construct	Reference
Pto	(Rathjen *et al.*, 1999)
ptoL205D	(Wu *et al.*, 2004)
ptoD164N	(Wu *et al.*, 2004)
Prf SD-CC-NB-LRR deletion construct	(Mucyn *et al.*, 2006)
Prf CC-NB-LRR deletion construct	(Mucyn *et al.*, 2006)

Table 2.7: Vectors used for cloning

Vector	Description	Selection	Reference or source
pT70	Low copy number binary vector carrying the *35S* promoter sequence	*Agrobacterium*: 50 µg/mL kanamycin, 1.5 µg/mL tetracycline, *E. coli*: 10 µg/mL tetracycline	(Rathjen *et al.*, 1999)
pT70-3xHA-FLAG	pT70 vector carrying sequence for three C-terminal HA epitopes fused to the FLAG octapeptide	*Agrobacterium*: 50 µg/mL kanamycin, 1.5 µg/mL tetracycline, *E. coli*: 10 µg/mL tetracycline	(Rathjen *et al.*, 1999; Balmuth & Rathjen, 2007)
pT70-5xMyc	pT70 vector carrying sequence for five C-terminal c-Myc epitopes	*Agrobacterium*: 50 µg/mL kanamycin, 1.5 µg/mL tetracycline, *E. coli*: 10 µg/mL tetracycline	(Rathjen *et al.*, 1999; Balmuth & Rathjen, 2007)
pT70-sGFP	pT70 vector carrying sequence for a C-terminal synthetic GFP tag	*Agrobacterium*: 50 µg/mL kanamycin, 1.5 µg/mL tetracycline, *E. coli*: 10 µg/mL tetracycline	(Rathjen *et al.*, 1999; de Vries *et al.*, 2006)
pT60-FLAG	Low copy number binary vector carrying the tomato Pto promoter sequence	*Agrobacterium*: 50 µg/mL kanamycin, 1.5 µg/mL tetracycline, *E. coli*: 10 µg/mL tetracycline	(Rathjen *et al.*, 1999; Balmuth & Rathjen, 2007)
pGWB414	Gateway destination binary vector carrying the *35S* promoter sequence and the sequence for three C-terminal HA epitopes	100 µg/mL spectinomycin	(Nakagawa *et al.*, 2008)
pYY13	TRV RNA2 silencing vector for VIGS	50 µg/mL kanamycin	(Dong *et al.*, 2007)
pENTR/D-TOPO	Commercial cloning vector for Gateway cloning	100 µg/mL carbenicillin	Life Technologies
pGem-Teasy	Commercial cloning vector for TA cloning	100 µg/mL carbenicillin	Promega
pGEX-2TK	Commercial vector for N-terminal GST fusion and heterologous expression of protein in *Escherichia coli*	100 µg/mL carbenicillin	(Kaelin *et al.*, 1992), GE Healthcare

2.5.2. Primer design.

All oligonucleotide primers (Table 2.8, Table 2.9Table 2.) were chosen to have a GC content between 40% to 70%, a theoretical melting temperature above 50°C, and a minimal chance of self-priming or forming strong hairpin structures. Primers were purchased from Integrated DNA Technologies.

Table 2.8: Primers used for cloning described in Chapter 3, restriction enzyme sites or overhangs are in lower case, gene-specific sequences in uppercase; start codons underlined. /5'PHOS/ indicates phosphorylation of 5 prime ends used in whole vector amplification for side-directed mutagenesis.

Gene	Forward primers	Details	Reverse primers	Details
Primers used for amplification of NbBAK1b from *Nicotiana benthamiana* cDNA, for cloning into pT70 and for Primers used for generating NbBAK1b-5				
NbBAK1b	5'- tacctctcgagccATGATTCCTGCTTGGTATTACACA -3'	XhoI restriction enzyme (RE) site	5'- ttctctagaAGAGTCAAGGGGCTGTTCTTT -3'	XbaI RE site – STOP codon
NbBAK1b C408Y (NbBAK1-5)	/5'PHOS/GTGATGTCAAAGCCGCAAATATCTTATTGGATG-3'	-	/5'PHOS/GATGAATAATCTTAGGATcatAATGATCATGCAAGT AAGA -3'	TGC to TAC mutation
Primers used for amplification of NbCSPR (NbCSPR2) from *N. benthamiana* cDNA for cloning into pENTR/D-TOPO and subcloning into pGWB vectors				
NbCSPR (NbCSPRC2)	5'- caccATGAAAAGTGAGAGATTTTTATTTCTCAATATTG -3'	CACC overhang	5'- ACTCCAGAGCACCTTCAATCTGTG -3'	- STOP codon
Primers used for amplification of NbCSPR (NbCSPR2) from *N. benthamiana* cDNA for cloning into pT70				
NbCSPR (NbCSPRC2)	5'- ttctcgagccATGAAAAGTGAGAGATTTTTATTTCTCAATATTG -3'	XhoI RE site	5'- ttctctagaACTCCAGAGCACCTTCAATCTGTG -3'	XbaI RE site, –STOP Codon

Table 2.8 continued: Primers used for cloning described in Chapter 3, restriction enzyme sites or overhangs are in lower case, gene-specific sequences in uppercase; start codons underlined. /5'PHOS/ indicates phosphorylation of 5 prime ends used in whole vector amplification for side-directed mutagenesis.

Primers used for amplification of NbSOBIR1 from *N. benthamiana* cDNA for cloning into pT70				
NbSOBIR	5'- ttctcgagccATGGCCTTCACTGCTT-'3	XhoI RE site	5'- ttctctagaATGCTTGATCTGAGTTAACATACACC-'3	XbaI RE site, –STOP Codon
Primers used for generating the genetic sequence for csp22 and flg22 and subsequent cloning into pGex-2TK for Glutahione-S-Transferase (GST) fusion				
flg22	/5'Phos/gatccCAGAGGCTGAGCACCGGCAGCAGGATCAACAGCGCCAAGGACGACGCCGCCGGCCTGCAGATCGCCg – 3'	5" EcoRI and 3' BamHI RE site (post digest)	/5'Phos/aattcGGCGATCTGCAGGCCGGCGGCGTCGTCCTTGGCGCTGTTGATCCTGCTGCCGGTGCTCAGCCTCTGg -3"	3" EcoRI and 5' BamHI RE site (post digest)
csp22	/5'Phos/gatccGCCGTGGGCACCGTGAAGTGGTTCAACGCCGAGAAGGGCTTCGGCTTCATCACCCCCGACGGCGGCg – 3"	5" EcoRI and 3' BamHI RE site (post digest)	/5'Phos/aattcGCCGCCGTCGGGGGGTGATGAAGCCGAAGCCCTTCTCGGCGTTGAACCACTTCACGGTGCCCACGGCg -3'	3" EcoRI and 5' BamHI RE site (post digest)
Primers used for generating virus-induced gene silencing constructs				
NbCSPR (NbCSPRC2) silencing construct 1	5'-cgacgacaagaccctCATTACTCCTTCATTGCTTGAATTG-3'	Ligase independent cloning (LIC) forward region	5'-gaggagaagagccctGATAAGCTCAGAA ACAATTCAGGAAG-3'	LIC reverse region
NbCSPR (NbCSPRC2) silencing construct 2	5'-cgacgacaagaccctTGAAAAGTGAGAGATTTTTATTTC -3'	LIC forward region	5'-gaggagaagagccct GTTACCTCTCAAATGTTGACTATAG -3'	LIC reverse region
NbFLS2 silencing construct	5'-cgacgacaagaccctTACCTTTTTCATACCTTTG-3'	LIC forward region	5'-gaggagaagagccctGGTGGAATATTTCC-3'	LIC reverse region

Table 2.9: Primers used for cloning described in Chapter 5, restriction enzyme sites or overhangs are in lower case, gene-specific sequences in uppercase; start codons underlined. /5'PHOS/ indicates phosphorylation of 5 prime ends used in whole vector amplification for side-directed mutagenesis.

Gene	Forward primers	Details	Reverse primers	Details
Primers used for generating Prf N-terminal domain regions and subsequent cloning into pT70 vectors.				
N1	5'-gggcgaattgggtaccctcgagccATGGCGAAAGAATGCCGTGAT-'3	XhoI RE site	5'-ttctctagaAATCAGGGCGTTCAGATAAA –3'	XbaI RE site, no STOP codon
N2	5'-gggcgaattgggtaccctcgagccATGGCGAAAGAATGCCGTGAT-'3	XhoI RE site	5'- ttctctagaAATCAGGGCGTTCAGATAAA –3'	XbaI RE site , no STOP codon
N3	5'-gggcgaattgggtaccctcgagccATGGCGAAAGAATGCCGTGAT-3'	XhoI RE site	5'- ttctctagaATCGTAGCTGTAGATGGCATTG–3'	XbaI RE site, no STOP codon
N4	5'-gggcgaattgggtaccctcgagccATGGCGAAAGAATGCCGTGAT-3'	XhoI RE site	5'- ttctctagaGCTCTGAATATAGTTCAGGATA–3'	XbaI RE site , no STOP codon
C1	5'- taccctcgagccATGCCGAGTCGCTCTAGCAG-3'	XhoI RE site	5'- ttctctagaCAGCAGGTTCACCAGAATG–3'	XbaI RE site – STOP codon
C2	5' -taccctcgagccATGGGTAGCAGCTGCCATATGG-3'	XhoI RE site	5'- ttctctagaCAGCAGGTTCACCAGAATG-3'	XbaI RE site – STOP codon
C3	5' -taccctcgagccATGGATATTGAAAGCTATC–3'	XhoI RERE site	5'- ttctctagaCAGCAGGTTCACCAGAATG–3'	XbaI RE site – STOP codon
C4	5' -taccctcgagccATGGTTTGGGAAGAACTGAT-3'	XhoI RE site	5'- ttctctagaCAGCAGGTTCACCAGAATG-3'	XbaI RE site – STOP codon

Table 2.9 continued: Primers used for cloning described in Chapter 5, restriction enzyme sites or overhangs are in lower case, gene-specific sequences in uppercase; start codons underlined. /5'PHOS/ indicates phosphorylation of 5 prime ends used in whole vector amplification for side-directed mutagenesis.

Primers used for generating N-terminal domain regions and subsequent cloning into pGEX-2TK for GST-fusion				
N	5'- gatggatccGCGAAAGAATGCCGTGAT -'3	EcoRI RE site – ATG	5'-ctagaattcCAGCAGGTTCACCAGAATGA–3'	BamHI RE site no STOP codon
N1	5'- gatggatccGCGAAAGAATGCCGTGAT -'3	EcoRI RE site, – ATG	5'- ctagaattcCGGACCGGCGCTAATAAAAAA–3'	BamHI RE site no STOP codon
N2	5'- gatggatccGCGAAAGAATGCCGTGAT -'3	EcoRI RE site – ATG	5'-ctagaattcAATCAGGGCGTTCAGATAAA–3'	BamHI RE site no STOP codon
N3	5'- gatggatccGCGAAAGAATGCCGTGAT -3'	EcoRI RE site – ATG	5'-ctagaattcATCGTAGCTGTAGATGGCATTG–3'	BamHI RE site no STOP codon
N4	5'- gatggatccGCGAAAGAATGCCGTGAT -3'	EcoRI RE site – ATG	5'-ctagaattcGCTCTGAATATAGTTCAGGATA–3'	BamHI RE site, no STOP codon
C1	5'- gatggatccCCGAGTCGCTCTAGCAG-3'	EcoRI RE site , NO ATG	5'-ctagaattcCAGCAGGTTCACCAGAATG–3'	BamHI RE site, – STOP codon
C2	5' -gatggatccGGTAGCAGCTGCCATATGG-3'	EcoRI RE site, NO ATG	5'-ctagaattcCAGCAGGTTCACCAGAATG-3'	BamHI RE site, – STOP codon
C3	5'- gatggatccGATATTGAAAGCTATC–3'	EcoRI RE site, NO ATG	5'-ctagaattcCAGCAGGTTCACCAGAATG–3'	BamHI RE site, – STOP codon
C4	5' -gatggatccGTTTGGGAAGAACTGAT-3'	EcoRI RE site, no ATG	5'- ctagaattcCAGCAGGTTCACCAGAATG-3'	BamHI RE site, – STOP codon
Primers used for cloning deletion fragments of the Prf gene and subsequent cloning into pT70 vectors.				
Prf CC-NB	5'- taccctcgagccATGATTCCTGCTTGGTATTACACA -'3	XhoI RE site, + ATG	5'- ttctctagaCTCTTGTTTGGCCTTTTCCAT -3'	XbaI RE site, no STOP codon
Prf LRR	5'- taccctcgagccATGAACAAGAGGATTTTCTTCTCCAA -'3	XhoI RE site, + ATG	5'- ttctctagaGTCAAGGGGCTGTTCTTT -3'	XbaI RE site, - STOP codon

Table 2.9 continued: Primers used for cloning in Chapter 5, restriction enzyme sites or overhangs are in lower case, gene-specific sequences in uppercase; start codons are underlined./5'PHOS/ indicated phosphorylation of 5 prime ends used in whole vector amplification for side-directed mutagenesis.

Primers used for generating Pto phospho-null mutants (ptoS198A/T199A, ptoD164N/S198A/T199A ptoS198A/T 199A/ L205D) via site directed mutagenesis, using Pto, ptoL205D, ptoD164N as templates and subsequent cloning into pT70 vectors.				
Pto phospho- dead mutants	/5'PHOS/CAAACCCATCTTgccgcaGTAGTGAAAGG -3'	AGC to GCC and ACA to GCA	/5'PHOS/ATCAAGCTCAGTCCCTTTCTTGGATATTCC -3'	-
Primers used for generating Pto phospho-mimic mutants (pto S198D/T199D, pto D164N/S198D/T199D ptoS198D/T 199D/ L205D) via site directed mutagenesis using pto S198A/T199A, pto D164N/S198A/T199A ptoS198A/T 199A/ L205D in as templates and subsequent cloning into pT70 vectors.				
Pto phospho-mimic mutants	/5'PHOS/GAGCTTGATCAAACCCATCTTgatgatGTAGTGAAAGG-3'	GCC to GAT and GCA to GAT	/5'PHOS/ AGTCCCTTTCTTGGATATTCCAAATCAGTAATTTTTG-3'	-
Primers used for amplification of the *N. benthamiana* Prf N-terminal domain (NbN) from cDNA and subsequent cloning into pT70 vectors.				
NbPrf N-term (NbN)	5'- ccctcgagccATGGCCGAGGAGTGTCGC-'3	XhoI RE site	5'- ttcaactagtTAGCAGATTTTCGAGAATATATTCATGAAACCC-'3	SpeI RE site, - STOP codon

2.5.3. Polymerase chain reaction.

Polymerase chain reactions (PCR) were performed in a S1000 thermal cycler (Bio-Rad). The initial denaturation was carried out at 98°C for five minutes followed by a total of 35 cycles as follows: denaturation at 98°C for 10 seconds, annealing between 40°C and 60°C for 30 seconds, and extension at 72°C for 0.5-1 min/kb. The final extension was carried out at 72°C for 5 minutes. PCR products were visualised by agarose gel electrophoresis and purified from PCR components using the Promega Gel extraction kit (Promega) according to the manufacturer's instructions.

2.5.3.1. Polymerase chain reaction for PCR-based cloning.

For PCR based cloning, Phusion Hot Start II High-Fidelity DNA Polymerase (Thermo Scientific) and specific primers for each gene were used (Table 2.9).

Table 2.9: Chemical composition of polymerase chain reactions for PCR-based cloning.

Reagents	Quantity
Phusion™ Hot Start DNA Polymerase (2 U/µl)	0.5 µL
5x Phusion™ HF Buffer	5 µL
10 mM dNTPs	1 µL
10 µM forward primer	1 µL
10 µM reverse primer	1 µL
template DNA	~50 ng
H_2O	Up to 50 µL

2.5.3.2. Polymerase chain reaction for site-directed mutagenesis.

Site-directed mutagenesis of genes within vectors was performed using Phusion™ Site-Directed Mutagenesis Kit (Table 2.10, Finnzymes), which uses Phusion™ Hot Start High-Fidelity DNA Polymerase for exponential PCR amplification of the dsDNA plasmid to be mutated. The primers containing the desired point mutations were designed with 5-prime phosphorylation to allow annealing back to back on the plasmid according to the Phusion™ Site-Directed Mutagenesis Kit manufactor's instructions.

Table 2.10: Composition of site-directed polymerase chain reactions using the Phusion™ Site-Directed Mutagenesis Kit.

Reagents	**Quantity**
Phusion™ Hot Start DNA Polymerase (2 U/µl)	0.5 µL
5x Phusion™ HF Buffer	10 µL
10 mM dNTPs	1 µL
10 µM forward primer	1 µL
10 µM reverse primer	1 µL
1:10 dilution of isolated plasmid	2 µL
H_2O	32.5 µL

2.5.3.3. Polymerase chain reaction for screening of positive clones (colony PCR).

Colony screening was carried out by PCR using primers (Table 2.11) for the promoter and epitope tag of the vector were used. For pT70-sGFP, a forward primer for the promoter region and a gene specific reverse primer were used.

Colonies grown overnight were transferred into 30 µL sterile Milli-Q water and boiled for 10 min. Subsequently, insoluble material was collected at the bottom of the tube by a short centrifugation. Five µL of the supernatant was used for a 25 µL colony PCR reaction (Table 2.12). PCR products were visualised by DNA-gel electrophoresis.

Table 2.11: Primers used for screening clones and sequencing reactions.

Vector	Forward primers	Details	Reverse primers	Details
pT70-3xHA-FLAG	5'-GATGTGATATCTCCACTGACGTAA-3'	35S promoter	5'-AGCGGATAACAATTTCACACAGGA-3' or 5'-CTTATCATCATCATCCTTATAATC-3''	3x HA – Tag or FLAG- Tag
pT70-5xMyc	5'-GATGTGATATCTCCACTGACGTAA-3'	35S promoter	5'-TTACATGGTGAGGTCGCC-3'	5x Myc - Tag
pYY13 RNA2 vector	5'- ATTACGGACGAGTGGACTTAGATTC – 3'	pYY13 forward	5'-ATTACGGACGAGTGGACTTAGATTC-3'	pYY13 reverse
pGem-Teasy pENTR/D-TOPO	5'- CGCCAGGGTTTTCCCAGTCACGAC– 3'	M13 forward primer	5'- AGCGGATAACAATTTCACACAGGA-3'	M13 reverse primer
pGex-T2K	5'- GGGCTGGCAAGCCACGTTTGGTG – 3'	GST tag	5'- CCGGGAGCTGCATGTGTCAGAGG- 3'	pGex reverse primer

Table 2.12: Chemical composition of polymerase chain reactions for colony PCR screening.

Reagents	Quantity
Promega Master Mix	12.5 µL
10 µM forward primer	1 µL
10 µM reverse primer	1 µL
Colony lysate	3 µL
H_2O	Up to 25 µL

2.5.4. DNA-gel electrophoresis.

DNA gel electrophoresis was performed using 0.7 - 2 % (w/v) agarose gels in Tris-borate-Ethylenediaminetetraacetic acid (EDTA) (TBE) buffer (Table 2.13). To 5 µl of DNA sample, 1 µl of 6x loading buffer (Table 2.14) was added before loading the sample on the gel. The gel was run at 5 V/cm for 1 h or until the dark blue running front reached the end of the gel.

The gel was visualised by red safe (ABCScientific), documented on the ChemiDoc™ XRS+ System (Bio-Rad), and analysed using the QuantityOne software (Bio-Rad). For subsequent extraction of nucleic acids (Life Technologies), gels were supplemented with SybrSafe (Life Technologies) instead of red safe and cut on a blue box (Life Technologies).

Table 2.13: Chemical composition of Tris borate EDTA (TBE) buffer (1x).

Reagents	Concentration
Tris	90 mM
H_3BO_3	90 mM
EDTA	2 mM

Table 2.14: Chemical composition of 6x loading dye

Reagents	Concentration
Sucrose	40 %
Urea	4 M
EDTA	10 mM
Tris	120 nM
Orange G or Bromophenole blue	0.25 %
Adjust pH to 7.5	2 mM

2.5.5. Plasmid isolation and purification from bacterial cells.

2.5.5.1. Small-scale isolation of plasmid vectors (miniprep).

A 10 mL liquid culture of *E. coli* DH5α containing the respective vector construct was cultivated overnight at 37°C in Luria-Bertani (LB, Table 2.15) medium. Cells were centrifuged at 5,000 *x g* for 5 minutes and the supernatant was discarded. The bacterial pellet was resuspended in 1 mL of Milli-Q water and 1 mL of 1 M lysis buffer (1 M Sodium hydroxide, 1% SDS) was added and samples were mixed gently. After incubation for 2 minutes at room temperature (RT), 1 mL of protein precipitation solution (1.5 M

potassium acetate, 2.55 % (v/v) formic acid) was added. Proteins were removed by centrifugation at 15,000 *x g* for 10 min. The supernatant was transferred to a new tube and nucleic acids were precipitated by the addition of 2 mL of 100% isopropanol, followed by centrifugation at 15,000 *g* for 10 min. The pellets were washed once with 1 ml 70% ethanol and air dried before resuspending in 80 µL of sterile Milli-Q-water containing 2 µg RNAseA (Sigma).

Table 2.15: Composition of Luria – Bertani (LB) medium.

Reagents	Final Concentration
Tryptone	10 g/L
Yeast extract	5 g/L
NaCl	10 g/L
Agar	14 g/L
pH adjusted to 7.0	

2.5.5.2. Isolation of low copy number binary vectors for ligation reactions.

A 100 mL liquid culture of *E. coli* DH5α containing the respective vector construct was cultivated overnight at 37°C in Terrific Broth (TB) medium (Table 2.16). Cells were centrifuged at 5,000 *x g* for 10 minutes and the supernatant was discarded. The bacterial pellet was washed once in Milli-Q-water and subsequently resuspended in 10 mL of Milli-Q water, and 20 mL of lysis buffer (1 M Sodium hydroxide, 1% SDS) was added and samples were mixed gently. After incubation for two minutes at RT, 15 mL of protein precipitation solution (1.5 M potassium acetate, 2.55 % (v/v) formic acid) was added.

Precipitated material including genomic DNA and denatured proteins were removed by filtering the extract through Miracloth (Merck). Nucleic acids were precipitated by the addition of 30 mL of 100% isopropanol to the filtrate and centrifugation at 15,000 *x g* for 10 min. The pellet was resuspended in 5 mL of 2.5 M LiCl and incubated on ice for 20 minutes before centrifugation at 15,000 *x g* for 5 min, to pellet the majority of ribonucleic acids. For further purification, the soluble nucleic acids were precipitated by the addition of 3 mL 100% isopropanol. The pellet was resuspended in 1 mL of nuclease-free water containing 2 µg RNAseA (Sigma) and incubated at 37°C for 4 h. Subsequently, 1 mL of 13% (w/v) PEG/1.6 M NaCl was added and samples were centrifuged for 5 minutes at 15,000 *x g*. The pellet was resuspended in 200 µl H_2O, then 20 µL of 3 M Sodium Acetate pH 5.6 and 220 µL of 100% isopropanol was added and samples were centrifuged for 5 minutes at 15,000 *x g*. The pellets were washed once with 70% ethanol and air dried before resuspending in 100 µL of nuclease-free water (Sigma).

Table 2.16: Composition of Terrific Broth (TB) medium.

Reagents	Final Concentration
Tryptone	12 g/L
Yeast extract	24 g/L
Glycerol	0.4 %
pH adjusted to 7.0	

2.5.6. Cloning.

2.5.6.1. TA and Gateway cloning.

TA cloning into the pGem-Teasy vectors, Gateway cloning into pENTR/D-TOPO as well as the Gateway LR reaction for cloning into the pGWB destination vector was carried out according to manufacturer's instructions (Promega, Life Technologies).

2.5.6.2. Restriction endonuclease based cloning into pT70 and pT60 vectors.

2.5.6.2.1. Digestion of pT70 and pT60 vectors.

Restriction endonuclease digestions of pT70 and pT60 (pT70 vector with the genomic *Pto* promoter instead of the *35S* promoter) vectors were carried out using XhoI, XbaI and/or SalI, AvrII, SpeI (New England Biolabs) according to Table 2.21. The reaction mixture was incubated overnight at 37°C and heat inactivated at 65°C for 20 minutes.

Table 2.17: Chemical composition of DNA digestions

Reagents	Quantity
Restriction enzyme 1 (New England Biolabs)	200 U
Restriction enzyme 2 (New England Biolabs)	200 U
10x CutSmart Buffer	20 µL
Template DNA	2 µg
H_2O	Up to 200 µL

Digested vectors were desalted (2.5.6.2.4), dephosphorylated by 100 U antarctic phosphatase (New England Biolabs) at 37°C for 6 hours, and subsequently purified by phenol/chloroform extraction. In brief, twice the volume of Phenol:Chloroform-Isoamyl alcohol was added to the digestion/dephosphorylation and mixture was vortexed well. The suspension was centrifuged at 15,000 *x g* for 10 minutes to separate phases. The upper phase was removed and added to the same volume of 100 % Isopropanol for DNA precipitation. Precipitates were recovered by centrifugation at 15,000 *x g* for 10 minutes, washed in 200 µl 70% Ethanol and air dried before resuspending pellet in 100 µl of nuclease-free water. The purified DNA was quantified visually by agarose gel electrophoresis using the ladder bands (New England Biolabs) as weight standard.

2.5.6.2.2. Digestion of DNAs.

Restriction endonuclease digestions were carried out using XhoI, XbaI SalI, AvrII and/or SpeI (New England Biolabs) according to Table 2.18. The reaction mixture was incubated overnight at 37°C and heat inactivated at 65°C for 20min.

Table 2.18: composition of DNA digestions

Reagents	Quantity
Restriction enzyme 1	20 U
Restriction enzyme 2	20 U
10x Cut Smart Buffer	2 µL
Template DNA	~500 ng
H_2O	Up to 20 µL

The success of the digestion reactions was determined by agarose gel electrophoresis. Specific DNA bands corresponding to the species of interest was excised from the gel (supplemented with SybrSafe) using a sterile scalpel on a blue box (Life Technologies). Gel slices were collected in sterile pre weighed 2.0 mL micro-centrifuge tubes. The Promega Gel extraction kit (Promega) was used to elute the DNA from the agarose block as described in the user's manual. The purified DNA was quantified visually by agarose gel electrophoresis using the ladder bands (New England Biolabs) as weight standard.

2.5.6.2.3. DNA ligation reactions.

Ligations were carried out using the T4 DNA ligase (Promega) according to the user's manual (Table 2.19). For ligation reactions, a molar ratio of 1:5 vector: insert was calculated using the following formula. The reaction mixture was incubated overnight at RT and subsequently heat inactivated at 65°C for 20 min.

$$\frac{\text{ng of vector} \times \text{kb size of insert}}{\text{kb size of vector}} \times \frac{\text{molar ratio of insert}}{\text{vector}} = \text{ng of insert DNA}$$

Table 2.19: composition of ligation reactions.

Reagents	Quantity
T4 DNA ligase (1 U/µL)	1 µL
10x Ligation Buffer	2 µL
Vector DNA	200 ng
Insert DNA	See formula
H_2O	Up to 20 µL

2.5.6.2.4. Desalting of ligation reactions.

For electroporation, DNA samples and ligation mixtures were desalted using a 30% (w/v) Sephadex G-25 column. Sephadex stock was prepared by equilibrating 60 g Sephadex G-25 in 1 L sterile 1x TE buffer *(Table 2.20)* overnight. TE buffer was decanted and was replaced by 1 L of 0.2 M NaOH. Sephadex was left to settle at RT for 20 minutes before decanting NaOH and washing five times 1 L of sterile Milli-Q water. Equilibrated and washed Sephadex was stored in 500 ml of 1x TE buffer.

For one desalting reaction, 200 µl of well-suspended Sephadex was transferred into a PCR tube. With a sterile needle, a hole was punched into the bottom and TE buffer was removed by centrifugation of the open tube at 2,000 *x g* for two minutes. Column was transferred into a fresh 1.5 ml tube adding DNA samples or ligation reactions to the tube. DNA samples or ligation reactions were recovered by centrifugation of the open tube at 2,000 *x g* for two minutes.

Table 2.20: composition of TE buffer (1x)

Reagents	Quantity
Tris	10 mM
EDTA	1 mM
Adjust pH to 7.5 with HCL	

2.5.6.3. Ligation-independent cloning (LIC) into the pYY13 vector for virus-induced-gene-silencing (VIGS).

Two non-overlapping regions with a length of approximately 200-700 base pairs from each gene to be silenced were amplified by PCR using the respective primers. The pYY13 TRV RNA2 binary vector was isolated using the Promega Miniprep kit according to manufactur's instructions and digested using with PstI in a 20 µL reaction at 37°C for two hours.

Vector and insert DNAs were pre-treated with dTTP and dATP, respectively for 30 minutes at room temperature according to Table 2.21 and Table 2.22. Next, 2.5 µL of the vector and 2.5 µL of the insert pre-treatment reactions were mixed and incubated for 30 minutes at RT, and 1 µL was directly transformed according to 2.5.10. This protocol was adapted from (Dong *et al.*, 2007).

Table 2.21: Chemical composition of vector pre-treatment reaction for ligase independent cloning into the VIGS RNA2 vector pYY13.

Reagents	Quantity
pYY13 PstI restricted vector	50 ng
10x NEB BUFFER 2	1 µL
100 nM Dithiothreitol (DTT)	0.5 µL
100 mM dTTP	0.5 µL
T4 DNA polymerase	1 µL
H_2O	up to 10 µL

Table 2.22: Chemical composition of insert pre-treatment reaction for ligase independent cloning into the VIGS RNA2 vector pYY13.

Reagents	Quantity
Insert	50 ng
10x NEB BUFFER 2	1 µL
100 nM DTT	0.5 µL
100 mM dATP	0.5 µL
T4 DNA polymerase	1 µL
H_2O	up to 10

2.5.7. DNA sequencing using the Sanger method.

The sequences of constructs were confirmed by DNA sequencing using the ABI Prism BigDye terminator v3.1 sequencing protocol with specific primers (Table 2.23).

Table 2.23: Composition of a sequencing reaction using BigDye v3.1.

Reagents	Final Concentration
BigDye terminator	1 µL
10 µM primer	0.4 µL
5 x Sequencing Buffer	3.6 µL
PCR product (template)	40 ng
H_2O	Up to 20 µL

The initial denaturation step was carried out at 95°C for 5 minutes followed by a total of 30 cycles as follows: denaturation 96°C for 10 seconds, annealing between 50°C for 5 seconds, and 60°C for 4 min.

The sequencing reactions were purified by adding a precipitating solution containing 2.5 µL of 3 M Sodium Acetate, pH 5.6, 5.0 µL 100 mM EDTA, and 70 µL of 95% Ethanol. The samples were incubated at RT for 15 minutes before centrifugation at 15,000 *x g* for 10 min. Subsequently, the pellets were washed once with 70% ethanol and air dried. The dried pellets were dissolved in 20 µL Hi-Di formamide and transferred into clear optical 96-well sequencing plates (Axygen Scientific). The sequence analysis was performed using an ABI 3130x1 Genetic Analyzer (Life Technologies) at the Bio Molecular Resource Facility of the John Curtin School of Molecular Biology, The Australian National University.

2.5.8. RNA isolation and cDNA synthesis.

Trizol (Life Technologies) was used for high quantity and quality RNA isolation tissue. One hundred milligrams (dry weight) of biological material was ground in liquid nitrogen and mixed with one mL Trizol reagent. Samples were homogenised by vortexing and incubated in the fume hood for five minutes. Subsequently, 200 µL chloroform was added, vortexed, and each tube was incubated for three minutes in the fume hood before separating the phases and insoluble material by centrifugation at 12,000 *x g* for 15 minutes at 4°C. The aqueous supernatant was transferred to a new tube containing 500 µL isopropanol to precipitate nucleic acids. After mixing well, the tube was centrifuged at 15,000 *x g* for 10 minutes at 4°C. The pellet containing total cellular RNA was washed in one mL 70% ethanol and centrifuged at 7,500 *x g* for five minutes at 4°C. The pellet was air-dried after removing the ethanol before resuspension

in 85 µL nuclease-free water. Contaminating DNA was removed using the Ambion TURBO DNA-free Kit (Life Technologies). First strand cDNA was prepared using random or oligo(dT)$_{12-18}$ primers and SuperScript III Reverse Transcriptase (Life Technologies) according to Table 2.24. For amplification of fragments via PCR, two µL of each cDNA reaction was used in a 50 µL PCR reaction.

Table 2.24: Protocol for cDNA synthesis from extracted RNA samples.

Reagents	Quantity	Incubation
Total RNA	2-5 µg	
100 µM random or oligo (dT)$_{12-18}$ primers	1 µL	65°C for 5 minutes, and on ice for 1 minute
10 mM dNTP mix	1 µL	
H_2O	Up to 13 µL	
5x first strand buffer	4 µL	55°C for 90 minutes inactivate reaction at 70°C for 15 minutes
0.1 M DTT	1 µL	
SuperScript III RT	0.5-1 µL	

2.5.9. Quantitative real time PCR.

Total RNA was isolated and cDNA was synthesised using 3 µg of total RNA for cDNA synthesis in a 20 µL reaction. qPCR was performed using gene-specific primers (Table 2.25) and at least three biological and three technical repeats were performed for each biological sample.

Table 2.25: Primers used for quantitative RT-PCR analysis.

Gene	Forward primers	Reverse primers
NbEF1 α	5 - AAGGTCCAGTATGCCTGGGTGCTTGAC-3	5 - AAGAATTCACAGGGACAGTTCCAATACCAC-3
NbWRKY22	5 - AAGGTCCAGCGAAGTCTCTGAGGGTGA-3'	5 - AAGAATTCCAATCCTAGCTCTGGCTCCTG- 3'
NbACRE31	5 - AAGGTCCCGTCTTCGTCGGATCTTCG -3	5 - AAGAATTCGGCCATCGTGATCTTGGTC-3
NbCYP71D20	5'- AAGGTCCACCGCACCATGTCCTTAGAG -3'	5'- AAGAATTCCTTGCCCCTTGAGTACTTGC-3'
NbCSPR	5' - GTCTCTTCCCGTTTGCTTTC – 3'	5' - GATGTCAGGCAATGAACCAC –3'
NbSOBIR1	5' - ATGGCCTTCACTGCTTCACAAATTC– 3'	5' - ATTCGAAGGCGGAGTAGAGA–3'
NbFLS2	5' - CTGTGTACAAGGGTAGACTGGAAGATGG – 3'	5' - GGAGAGGTGCAAGGACAAAGCCAATTT–3'
Pta 16S RNA	5' - CAATGGGCGAAAGCCTGATCCAGC– 3'	5' - CTCTGTATTACCGCGGCTGCTGG–3'
Pta csp	5' - ACCGTYAAGTGGTTCAACGAYGAAAAAGGTTT– 3'	5' - TGGCCTTCTTTCAGGCTYTTGAAGCCGT–3'

The qPCR reactions were performed in a total volume of 10 µL containing 0.5 µL template (of a 20 µL cDNA reaction with 3 µg total RNA), 0.25 µM of each primer (Table 2.25) and 5 µL SYBR green PCR master mix (Life Technologies). Reactions were amplified as follows: 50°C for 2 minutes, then 95°C for 10 minutes; then 40 cycles of 95°C for 15 seconds and 51°C for 1 minute; followed by a dissociation step of 95°C for 15 seconds, 60°C for 15 seconds and 95°C for 15 seconds. Amplifications were performed using an ABI PRISM 384-well clear optical reaction plate with a ViiA™ 7 system PCR analyzer (Life Technologies). Threshhold cycles (C_T) was set automatically by the ViiA™ 7 system PCR analyser software. Amplification cycles were normalised against the *NbEF1α* or *Pta 16S RNA* gene by calculating differences between the C_T of the target gene and the C_T of *NbEF1α* or *Pta 16S RNA*.

2.5.10. Transformation of *E. coli* DH5α and *Agrobacterium tumefaciens* GV3101 pMp90.

2.5.10.1. Preparation of electro-competent cells.

Using sterile technique, 100 mL Super Optimal Broth (SOB) medium (Table 2.26) was inoculated with 3 to 4 bacterial colonies and grown for 24-30 h at 22°C. This starter culture was diluted 1:100 in SOB medium and grown at 22°C (*E. coli*) or 16°C (*A. tumefaciens*) for 12-18 h or until the OD_{600} reached 0.7. The cells were pelleted by centrifugation at 2500 *x g* for 20 minutes at 4°C, and washed six times with 200 ml ice cold sterile Milli-Q water. After the last wash, pelleted cells were resuspended in 3 mL ice-cold Milli-Q-water and DMSO was added to a final concentration of 7% (v/v). The cells were dispensed into 21 µL aliquots in 200 µL tubes, snap frozen in liquid nitrogen, and stored at -80°C until use.

Table 2.26: Composition of Super Optimal Broth (SOB) medium.

Reagents	Final Concentration
Tryptone	20 g/L
Yeast extract	5 g/L
NaCl	0.6 g/L
KCl	0.6 g/L
pH adjusted to 7.0	

2.5.10.2. Electroporation of Escherichia coli DH5α and Agrobacterium tumefaciens GV3101 pMp90 cells.

After the electro-competent bacteria cells were thawed on ice, 5 µL of desalted ligation reaction mixture or 1 µL of pure plasmid was added, and the mixture was transferred to an ice cold 0.2 cm electroporation cuvette and electroporated with 1.25 kV/0.1 cm for about five mseconds in a Bio-Rad Gene Pulser (Bio-Rad). Cells were diluted in 1 mL LB medium and incubated at 37°C for 1 h for *E. coli* or 28°C for 2 h for *A. tumefaciens* to allow recovery and expression of the antibiotic resistance markers. The cultures were spread onto pre-warmed LB agar plates containing the appropriate antibiotic(s) and incubated overnight at 37°C (*E. coli*) or 28°C for two to three days (*A. tumefaciens*).

2.6. Plant methods.

2.6.1. Transformation of *Arabidopsis thaliana* protoplasts.

2.6.1.1. Plant material and growth.

A. thaliana plants were grown as described in section 2.2.1 under 12 h daylight for approximately four to five weeks.

2.6.1.2. Protoplast isolation.

Protoplast transformation was carried out at room temperature unless otherwise indicated. Room temperature should not exceed 25 °C. For each transformation, well-expanded leaves (five to six per plant) of approximately 24 *A. thaliana* plants were harvested and cut with a razor blade or scalpel into 0.5-1 mm leaf strips, and transferred into a glass beaker with 100 mL of protoplast isolation solution (Table 2.27).

Table 2.27: Composition and preparation of protoplast isolation solution.

Reagents	Final concentration
cellulase R10 (Sigma)	1-1.5% (w/v)
macerozyme R10 (Sigma)	0.2-0.4% (w/v)
mannitol	0.4 M
KCl	20 mM
MES (pH 5.7)	20 mM
Heat to 55°C for 10 min, cool to RT before adding the components below:	
$CaCl_2$	10 mM
bovine serum albumin	0.1% (w/v)

The protoplast isolation solution was infiltrated into leaf strips for 5-10 minutes using a vacuum pump, before gentle swirling at 40 rounds per minute (rpm) of the strips in the solution on a rotary shaker at room temperature for 90 minutes. The protoplasts were separated from the enzyme solution by filtering through a 75 µm nylon mesh. To

release remaining protoplasts from the leave strips, twenty millilitres of protoplast wash solution (Table 2.28) was added to the leave strips and was solution including the protoplasts was separated from leave material by filtering through a 75 µm nylon mesh. Both protoplast suspensions were pooled. Protoplasts were recovered by centrifugation at 100 *x g* for three minutes in round-bottomed tubes. Ten millilitres of protoplast wash solution was added to the protoplast pellet and mixed gently. Suspensions of protoplasts were aliquoted equally into round bottom tubes, if performing more than one transformation. In the wash solution, protoplasts were incubated on ice for 20 minutes.

Table 2.28: Composition of protoplast wash solution.

Reagent	Final concentration
NaCl	154 mM
$CaCl_2$	125 mM
KCl	5 mM
MES (pH 5.7)	2 mM

For each transformation, protoplasts were recovered from the wash solution by centrifugation at 100 *x g* for three minutes and resuspended gently in two mL transformation solution I (Table 2.29). Transformation was carried out with 200 µL of plasmid DNA (pGWB414 vectors) at a concentration of 500 ng/µl for 2 mL of protoplasts. An equal volume (~ 2 mL) of transformation solution II (Table 2.29) was added. Tubes were mixed well by gentle shaking. After incubation for 10 minutes at RT, the transformation was stopped by adding the same volume (~4-5 mL) of wash solution.

Table 2.29: Composition of protoplast transformation solutions I and II

Reagent	Final Concentration	
	Protoplast transfection solution I	Protoplast transfection solution II
Mannitol	0.4 M	0.2 M
$MgCl_2$	15 mM	-
$CaCl_2$	-	100 mM
PEG4000 (Fluka, Sigma)	-	40%(w/v)
MES (pH 5.7)	4 mM	-

Protoplasts were harvested by centrifugation at 100 *x g* for 3 min, resuspended in the desired volume of wash solution and aliquoted for PAMP-induced mitogen-activated protein kinase (MAPK) activation (1 mL/tube). Plates and tubes were incubated horizontally for 16 h before PAMP treatment according to 2.6.7.5.

2.6.2. *Agrobacterium tumefaciens*-mediated transformation of *Arabidopsis thaliana.*

2.6.2.1. Plant material and growth conditions.

A. thaliana plants for *Agrobacterium*-mediated transformation by floral dipping (Clough & Bent, 1998) were grown as described in section 2.2 under 16 h daylight for approximately four weeks.

2.6.2.2. Preparation of A. tumefaciens for floral dipping.

The *A. tumefaciens* strain GV3101 pmp90 was transformed with each vector as described in 2.5.10. Recombinant *A. tumefaciens* containing the respective binary plasmids were grown to stationary phase (~2 days) at 28°C in LB medium containing the appropriate antibiotics. Bacteria were subcultured into 50-100 mL LB using a 1/100 dilution of the starter culture, and grown overnight at 28°C with shaking. Bacterial cultures were harvested by centrifugation (4,000 *x g* for 10 minutes at RT) and diluted in 5% sterile sucrose solution with 0.02% (v/v) Silwet L-77.

Flowering *A. thaliana* plants were dipped into the *Agrobacterium tumefaciens* suspension carrying the respective plasmid. Dipping was repeated four to seven days after the first transformation (Clough and Bent, 1998). Plants were grown until they developed seeds and putative transformants were selected on MS media containing the appropriate antibiotic (here; 50 µg/mL kanamycin for pT70 binary vectors).

2.6.3. *Agrobacterium tumefaciens*-mediated transient transformation of *Nicotiana benthamiana* leaves.

2.6.3.1. Plant material and growth.

N. benthamiana plants for *Agrobacterium tumefaciens*-mediated transient gene expression experiments were grown for four to five weeks according to 2.2.

2.6.3.2. Preparation of A. tumefaciens for agroinfiltration.

The *A. tumefaciens* strain GV3101 pmp90 was transformed with an individual binary vector. Recombinant *A. tumefaciens* strains were grown separately to stationary phase

(~2 d) at 28°C in 3 mL of LB medium containing the appropriate antibiotics. Bacteria were subcultured into fresh LB media using a 1/100 dilution and grown for 24 h as described above. Bacterial cultures were harvested by centrifugation (4,000 *x g*, 10 min), washed once in infiltration buffer (Table 2.30) and subsequently diluted to an OD_{600} = 0.4-1.0 depending on the level of expression of the transgene within each construct. For co-expression experiments, *Agrobacterium* strains were mixed prior to infiltration.

Table 2.30: Composition of Infiltration buffer for Agrobacterium tumefaciens-mediated transient expression.

Reagents	Final Concentration
N-morpholinoethanesulfonic acid (MES) pH 5.6	10 mM
$MgCl_2$	10 mM
Acetosyringone (4'-hydroxy-3',5'-dimethoxyacetophenone)	100-200 µM

2.6.3.3. Agrobacterium-*mediated transformation by infiltration (agroinfiltration) for transient expression of proteins in* Nicotiana benthamiana.

The *Agrobacterium* cultures for leaf infiltration were pressure infiltrated into the mesophyll of four week old *N. benthamiana* leaves using a 1 mL disposable syringe without a needle. The two youngest, fully-expanded leaves were chosen for infiltration. For cell death assays, the leaves were superficially wounded with a needle to improve infiltration and the approximate area of infiltration was outlined with a permanent marker pen.

2.6.3.4. *Virus-induced gene-silencing of* Nicotiana benthamiana *plants.*

Agrobacterium tumefaciens GV3101 pMp90 cultures carrying the TRV RNA1 construct pTRV1, and the respective TRV RNA2 vectors containing gene fragments to be silenced, were mixed in a 1:2 ratio (RNA1:RNA2) in infiltration buffer (Table 2.30) to a final of OD= 1.0.

Leaves of two week old *N. benthamiana* plants were infiltrated with the *A. tumefaciens* mixtures and systemic spread of the virus was monitored based on the phenotypic changes that were evident when silencing NbBAK1a and NbBAK1b (Chaparro-Garcia *et al.*, 2011). Systemic TRV infection in *N. benthamiana* developed 5 to 10 days post-inoculation and systemic silencing after 3 to 4 weeks. The TRV vectors were kindly provided by Prof. A. Hardham (Research School of Biology, The Australian National University).

2.6.4. Bacterial growth assays.

The bacteria of interest comprising *Pseudomonas syringae* strains were grown in LB media supplemented with appropriate antibiotics and harvested by centrifugation. Pellets were resuspended in 10 mM $MgCl_2$ to a final OD_{600} = 0.1. Immediately prior to infection, the surfactant Silwet L-77 was added to bacteria to a final concentration of 0.02 % (v/v). *N. benthamiana* leaves were dipped for approximately 20 seconds in the bacterial suspensions. *A. thaliana* plants were spray-infected.

Three days after infection, three leaf disks (7.8 mm in diameter surface area) of a minimum of six individual leaves were taken per bacterial strain and plant genotype, and ground in 200 µL 10 mM $MgCl_2$ using a tissue lyser (Qiagen). Samples were diluted to 10^{-1}, 10^{-2}, 10^{-3}, 10^{-4}, 10^{-5}, 10^{-6}, and 10^{-7} in a total volume of 500 µL per dilution, and 20 µL of each dilution was plated on LB agar with appropriate antibiotic selection in a 24-well plate. Plates were incubated at 28°C and colonies counted after two days.

2.6.5. Trypan blue staining to detect cell death.

Leaf tissue was covered in lactophenol (Table 2.31) containing 0.067% (v/v) trypan blue and boiled for 2 min, then cooled to 25°C over 30 min, then destained in 50% ethanol to remove chlorophyll.

Table 2.31: Composition of lactophenol for trypan blue staining of leaf tissue

Reagents	Final concentration
Lactic Acid	10 (v/v) %
Glycerol	10 (v/v) %
Ethanol absolute	60 (v/v) %
Phenol, solid	10 (w/v) %

2.6.6. β-glucuronidase (GUS) staining of leaves.

Leaves were vacuum infiltrated with X-gluc (5-bromo-4-chloro-1H-indol-3-yl β-D-glucuronide) substrate solution (Table 2.32), incubated at 37°C overnight, then destained in 50% ethanol to remove chlorophyll.

Table 2.32: Composition of X-gluc staining solution for GUS staining of leaf tissue.

Chemical	Final concentration
X-gluc (5-bromo-4-chloro-3-indolyl ß-D-glucuronide)	
(100mM stock in N,N-dimethylformamide)	2 mM
$K_3Fe(CN)_6$	5 mM
$K_4Fe(CN)_6$	5 mM
NaH_2PO_4 – Na_2HPO_4 (pH 7) buffer	50 mM

2.6.7. Assays to measure Pathogen-associated molecular pattern-triggered immunity.

2.6.7.1. PAMPs used in this study.

Purified elicitors or their active derivatives used in this study are described in Table 2.33. Extracts of *Puccinia striiformis f.sp. tritici* (*Pst*) urediniospores (1x spore extract; SE) were prepared as follows: In a safe lock tube, 35 mg of fresh *Pst* urediniospores were supplemented with glass powder and one stainless steel bead (Qiagen) and ground for 6 minutes in a tissue lyser (Qiagen). Tubes were kept cold by freezing in liquid nitrogen every two minutes. For the preparation of spore extract (SE), the ground spores were suspended in 8 mL of sterile water (resulting in a concentration of 4 mg ground spores/mL water) and mixed well. Spore debris was removed by centrifugation at 15,000 *x g* and subsequent sterile filtration using a 0.2 µm cut off filter. The filtrate was boiled for 10 minutes before use.

Table 2.33: PAMPs used for elicitation of PTI responses

elicitor	Final concentration	Description/ peptide sequence	source
chitin	100 µg/mL	from crab shell	Sigma
chitin	1 µg/mL	from crab shell	Yaizu Suisankagaku Industry
flg22 (flagellin peptide derivative)	100 nM	CKANSFREDRNEDREV	Mimotopes, Melbourne
csp22 (bacterial cold shock protein peptide derivative)	100 nM	AVGTVKWFNAEKGFGF ITPDGG	Mimotopes, Melbourne
spore extract	as described above	as described above	NIAB, Cambridge, UK

2.6.7.2. PAMP treatment for reactive oxygen species (ROS) burst assay.

Leaf discs (3.8 mm in diameter) of four to five week old *A. thaliana* or *N. benthamiana* plants were excised using a cork borer and floated overnight on 100 µL of sterile water in white 96-well plates. The following day the water was replaced with either spore extract or water containing the respective PAMP at the appropriate concentration, supplemented with 17 µg/mL luminol (Sigma) or L-012 (Wako Pure Chemicals, Japan) and 10 µg/mL horseradish peroxidase (Sigma). Luminescence was captured using a Photek camera (East Sussex, UK) or a TECAN plate reader (TECAN). Sterile water without added PAMP was used as a control.

2.6.7.3. PAMP treatment for Ca^{2+} ion influx assay.

Leaf discs (3.8 mm in diameter) of four to five week old *N. benthamiana* SLJR15 plants were excised using a cork borer and floated overnight on 100 µL of sterile water in white 96-well plates. The following day the water was replaced with water containing the respective PAMP at the appropriate concentration, supplemented with 25 µM coelenterazine. Light emission was captured using a Photek camera (East Sussex, UK) or Infinite M200 PRO TECAN plate reader (TECAN). Sterile water without added PAMP was used as a control.

2.6.7.4. PAMP treatment for MAPK activation assays and qRT-PCR analysis using leaf disks.

For each treatment, 15 leaf discs (3.8 mm in diameter) from four to five week old N. benthamiana or A. thaliana plants were sampled using a cork borer and floated overnight on two mL sterile water in 6-well plates. Leaf discs were treated with 2 mL sterile water containing the respective PAMP (Table 2.33) for five and 15 minutes and frozen in liquid nitrogen for protein extraction and immunoblot analysis. For 15 leaf discs, 150 µL of protein extraction buffer (

Table 2.36) was used. For qRT-PCR analysis (2.5.9), leave disks were incubated in PAMP containing solution for one hour before harvesting.

2.6.7.5. PAMP treatment for MAPK activation assays using Arabidopsis thaliana protoplasts.

A. thaliana protoplasts were isolated and transformed according to 2.6.1. After a recovery period of approximately 16 h, the protoplasts were supplemented with the respective PAMP to the final concentration stated in Table 2.33.

For harvesting, protoplasts were recovered from suspensions by centrifugation for three minutes at 100 *x g* after the respective incubation time, and frozen in liquid nitrogen for protein extraction and immunoblot analysis. For 1 mL of protoplast suspension, 100 µL of protein extraction buffer was used.

2.6.7.6. Assay to measure changes in bacterial gene expression by PAMP-induced plant defence responses.

For every treatment, 20 leaf discs (3.8 mm in diameter) from *N. benthamiana* plants were sampled using a cork borer and floated overnight on two mL sterile water in 12-well plates.

Pseudomonas syringae pv. *tabaci* fliC- was grown overnight, harvested by centrifugation at 2,500 *x g* for 5 minutes, resuspended in sterile 10 mM $MgCl_2$ to an OD_{600} = 1. Two mL of bacterial suspension supplemented with or without 100 nM flg22 were added to 20 leaf discs and incubated for 2 h. Bacterial suspensions were removed, harvested by centrifugation at 2,500 *x g* for 5 minutes, and frozen in liquid nitrogen for subsequent qRT-PCR analysis (2.5.9).

2.6.7.7. Seedling growth inhibition (SGI) assays.

A. thaliana seeds were surface sterilised and grown as described in 2.2.1.1. Four-day old seedlings were transferred into liquid MS containing 10% sucrose and Gamborg's B5 Vitamins (100 µg/mL myo-inositol, 1 µg/mL nicotinic acid, 1 µg/mL pyridoxine hydrochloride, 10 µg/mL thiamine hydrochloride) supplemented with or without the respective PAMP at the desired concentration (Table 2.33), and incubated as described in 2.2.1. Eight days after transfer, dry weight was measured.

2.7.Biochemical methods.

2.7.1. Heterologous expression and purification of proteins fused to glutathione-S-transferase (GST) using the pGEX-2TK expression vector.

2.7.1.1. Expression of recombinant proteins in Escherichia coli.

For expression of proteins from the lac promoter of the pGEX-2TK vector, 50 mL of *E. coli* cells (BL21, Shuffle B or Shuffle K12 harbouring the pGEX-2TK vector containing the gene of interest) were grown in LB media (Table 2.16) with 100 μg/mL carbenicillin to OD_{600} = 0.6-0.9 before inducing gene expression by isopropyl β-D-1-thiogalactopyranoside (IPTG) at a final concentration of 1 mM. Cells were cultivated overnight with shaking at 20°C for expression of the recombinant protein. For harvesting, bacteria were pelleted by centrifugation at 2500 *x g* for 10 minutes, and the pellet was resuspended in 5 mL cell lysis buffer (Table 2.34), sonicated for 1 h at 4°C and subjected to six freeze-thaw cycles before separating soluble proteins from insoluble fractions by centrifugation at 15,000 *x g* for 30 minutes at 4°C.

2.7.1.2. Purification of recombinant GST proteins.

Glutathione-conjugated beads (Sigma, 200 μL for each 5 mL of soluble protein extract) were incubated in 5 mL equilibration buffer (Table 2.34) for 30 minutes at 4°C with slow but constant rotation before adding to the protein extract and subsequently mixed for 2 h at 4°C, with slow but constant rotation. The beads were washed ten times in 1 mL cold wash buffer at 4°C, with slight vortexing each time (Table 2.34), and stored in one mL wash buffer at -20 °C.

Table 2.34: Composition of cell lysis buffer, equilibration buffer and wash buffer for extraction and purification of proteins from E. coli.

Reagents	Final concentration		
	cell lysis buffer	equilibration buffer	wash buffer
Lysozyme	10 mg/mL		
Tris base	50 mM	50 mM	50 mM
NaCl	150 mM	150 mM	150 mM
EDTA	10 mM	10 mM	10 mM
DTT	20 mM	-	-
Glycerol	10 %	10 %	10 %
Protease inhibitor (Sigma)	1.5 %	-	0.5%
Bovine serum albumin	-	1.5 %	-
Adjust pH with HCl to 7.5			

2.7.2. Protein extraction from plant material and protein co-immunoprecipitation (co-IP) assay.

Leaf samples were ground frozen in liquid nitrogen to a fine powder. For a standard coIP procedure, 300 mg leaf material was thawed in 2 mL of cold plant protein extraction buffer (Table 2.36). Extracts were centrifuged at 15,000 *x g* for 10 minutes at 4°C. Supernatants were passed through a 0.2 µm sterile filter and centrifuged at 15,000 *x g* for another 30 minutes at 4°C. As an alternative to sterile filtration and subsequent

centrifugation, protein extracts were subjected to ultracentrifugation at 100,000 *x g* for 20 minutes at 4°C.

Antibody-conjugated beads (Table 2.35, 20 µL of agarose beads, or 7 µL of magnetic beads per standard co-IP samples) were incubated in plant equilibration buffer (Table 2.36) for 30 minutes at 4°C, and subsequently mixed with the filtered protein extracts for 2 h at 4°C, with slow but constant rotation. Conjugated beads were washed eight times in 1 mL cold plant wash buffer at 4°C, with slight vortexing each time (Table 2.36). With the last was, beads were trasferred low protein binding tubes before stripping the beads of bound proteins by boiling them in 40 µL SDS sample buffer (Table 2.39).

Table 2.35: Affinity matrices used for protein immunoprecipitation

Affinity matrix	Handling procedure
Anti-FLAG mouse, monoclonal (M2, magnetic, Sigma)	Use magnet for 1.5 to 2 mL tubes
Anti-HA rat, monoclonal (3F10, Roche)	Spin 15 seconds 600 *x g* in 1.5 mL tubes
Anti-FLAG mouse, monoclonal (M2, agarose, Sigma)	Spin 15 seconds 600 *x g* in 1.5 mL tubes

Table 2.36: Composition of plant protein extraction buffer, plant equilibration buffer and plant protein wash buffer.

Reagents	Final concentration		
	plant protein extraction buffer	**plant equilibration buffer**	**plant protein wash buffer**
IGEPAL (for membrane-associated proteins only)	1 % (v/v)		
Tris base	150 mM	150 mM	150 mM
NaCl	150 mM	150 mM	250 mM
Ethylenediaminetetraacetic acid	10 mM	10 mM	10 mM
Dithiothreitol	20 mM	-	-
Glycerol (v/v or w/v)	10 %	10 %	5 %
Plant protease inhibitor (Sigma)	1.5 %	-	-
Polyvinylpolypyrrolidone (PVPP), insoluble (only *for Nicotiana benthamiana* samples)	2 %	-	-
Bovine serum albumin	-	1.5 % (w/v)	-
Adjust pH with HCl to 7.5			

2.7.3. Bradford assay for determination of protein concentration.

The protein concentration of leaf extracts was determined in a microtitre plate by Bradford assay (Bio-Rad), using BSA to create a standard curve. The BSA stock (5 mg/mL) solution was diluted in protein extraction or elution buffers (Table 2.37). The Bradford dye was diluted 1:5 in extraction or elution buffer, and 245 µL was added to 5 µL of each standard or sample to a microtiter plate. The mixtures were mixed using a pipette tip until a homogenous light blue colour appeared. The plate was run through a reader (Bio-Rad Micro plate Reader model 680, λ = 595 nm). A standard curve was generated using a linear regression equation and the concentration of protein samples was interpolated.

Table 2.37: BSA standards used for protein concentration determination.

BSA standards (mg/mL)	vol. BSA stock (mL)	vol. extraction buffer (mL)
0.0	0.00	0.50
0.2	0.02	0.48
0.4	0.04	0.46
0.6	0.06	0.44
0.8	0.08	0.42
1.0	0.10	0.40

2.7.4. *In vitro* receptor-peptide binding assay.

2.7.4.1. Receptor preparation.

The respective receptor was overexpressed in *N. benthamiana* leaves as a 3xHA-FLAG fusion protein. Two days post infiltration, samples were harvested and ground in liquid nitrogen to a fine powder. For a standard binding assay, 1 g (fresh weight) of leaf material was thawed in 10 mL of cold plant protein extraction buffer (Table 2.36). Extracts were centrifuged at 15,000 *g* for 10 minutes at 4°C. Supernatants were passed through a 0.2 µm sterile filter.

Antibody-conjugated beads (Table 2.35), 200 µL of magnetic beads for 20 mL of plant extract) were incubated in plant equilibration buffer (Table 2.36) for 30 minutes at 4°C and subsequently mixed with the filtered protein extracts for 2 h at 4°C, with slow but constant rotation. At 4°C, conjugated beads were washed five times in 1 mL cold plant protein wash buffer with slight vortexing each time (Table 2.36) and five times with peptide binding buffer (Table 2.38). Receptor bound anti-FLAg beads were stored in 0.5 ml binding buffer.

Table 2.38: Composition of peptide binding buffer

Chemical	Final concentration
MES	100 mM
$MgCl_2$	3 mM
NaCl	10 mM
Adjust pH to 6.0	

2.7.4.2. Peptide preparation.

Each peptide was expressed as a GST fusion in *E. coli* BL21. GST-tagged peptides were isolated as described in 2.7.1 and subsequently washed five times with peptide binding buffer (Table 2.38).

2.7.4.3. **In vitro** *peptide binding and peptide competition.*

After isolation (2.7.4.2), 5 µg of purified peptide (flg22-GST or csp22-GST as estimated by SDS-PAGE) was stripped off Glutathione-conjugated beads by shaking for 30 minutes in 0.5 mL peptide binding buffer (Table 2.38) containing 4 mg/mL Glutahione at room temperature. Five µl of csp22-GST eluate was added to 100 µl control (EV) or NbCSPR-3xHA-FLAG Anti-FLAG conjugated beads (isolated as described in 2.7.4.1) and incubated at 4°C for 30 minutes with constant rotation. For competition, peptide binding solution was supplemented with or without 10 µM csp22 or 10 µM flg22. After binding, Anti-FLAG conjugated beads were washed once in 100 µl cold binding buffer (Table 2.34) at 4°C and transferred to low protein binding tubes, before stripping off interacting proteins from the beads by boiling them in 50 µL SDS sample buffer. Proteins interaction were analysed by SDS-PAGE and immunoblotting.

2.7.5. Sodium dodecyl sulphate (SDS) polyacrylamide gel electrophoresis (PAGE).

2.7.5.1. Sample preparation.

SDS Sample Buffer (Table 2.39) was added to solubilised samples and the samples were boiled for five minutes and centrifuged at 15,000 *x g* for 10 minutes to collect the samples and remove undissolved substances.

Tris-glycine gels were placed into a Mini-PROTEAN® 3 Cell (Bio-Rad, Gladesville, Australia). The lower and the upper buffer chambers were filled with 1xSDS Running Buffer (Table 2.41), ensuring that all wells were full of running buffer and that air bubbles were displaced from the wells. Five µL of the marker Precision Plus Protein Blue or Dual Colour pre-stained Standard (Bio-Rad, Gladesville, Australia) was added to the marker lane, and equal amounts of each sample by protein concentration were loaded onto the gel. The gel was run at a constant 100 to 200 V at 4 °C until the dye front reached the end of the gel.

Table 2.39: Composition of 2 % SDS Sample Buffer

Reagents	Final Concentration
Tris base	90 mM
Glycerol (w/v)	15%
SDS (w/v)	3%
Beta-mercaptoethanol (v/v)	5%
Bromophenol Blue (w/v)	0.1 %
Adjust pH with HCl to 6.8	

2.7.5.2. *Preparation of SDS-PAGE gels.*

SDS-PAGE gels were prepared according to Table 2.40.

Table 2.40: Composition of one 10% Tris-glycine polyacrylamide gel.

Reagents	Final concentrations
Tris base	300 mM
Acrylamide (v/v)	10 %
Ammonium persulfate (APS) (w/v)	0.1 %
N, N, N', N'-tetramethylethylenediamine (TEMED) (v/v)	0.5 %
SDS (w/v)	0.1 %
Adjust pH with HCl to 6.8	

Table 2.41: Composition of 1x SDS running buffer

Reagents	Final concentration
Tris base	25 mM
Glycine	192 mM
SDS (w/v)	0.1 %
Adjust pH with HCl to 8.3	

2.7.6. Staining and detection of proteins on SDS-PAGE gels.

2.7.6.1. Coomassie Staining.

Preparative gels or PVDF membranes were stained in 10 mL Colloidal Coomassie staining solution (Table 2.42) for 15 minutes in sealed plastic pouches with gentle shaking at room temperature and rinsed in Milli-Q water. Gels were destained in 10 mL destaining solution (Table 2.42) until the background signal was removed completely.

Table 2.42: Chemical composition of the Colloidal Coomassie staining solution

Reagents	Final Concentration	
	Staining solution	Destaining solution
Acetic Acid (v/v)	10 %	10 %
Ethanol (v/v)	40 %	10 %
Coomassie R-250 (w/v)	0.1 %	-

2.7.6.2. Detection and documentation of stained gels.

Stained gels or PVDF membranes were documented using the ChemiDoc™ XRS+ System (Bio-Rad) and analysed using the QuantityOne software (Bio-Rad).

2.7.7. Immuno-blotting of membrane-immobilised proteins.

2.7.7.1. Transfer of proteins from gels to membranes.

After SDS-PAGE, proteins were transferred from gels to polyvinylidene difluoride membranes (PVDF) for immunoblotting. The membrane and one pieces of extra-thick or three pieces of thick blot filter paper (Bio-Rad) were cut into the same dimensions as the gel (7 x 10.5 cm), and the membrane was soaked in 100% methanol for 45 s and subsequently equilibrated in 1x transfer buffer (Table 2.43) together with the filter papers for 10 minutes prior to use. The gel was rinsed in Milli-Q water and covered with the equilibrated membrane. This sandwich was stacked in between the two filter papers and two sponges (Bio-Rad) and placed into a blotting cassette with the gel facing the anode and the membrane facing the cathode. To maximise the protein transfer, all layers were aligned accurately and air bubbles were removed.

Table 2.43: Chemical composition of 1x transfer buffer.

Reagents	Final Concentration
Tris base	25 mM
Glycine	192 mM
Methanol	20 % (v/v)
SDS	0.1 %(w/v)

To transfer proteins, the blotting cassette was placed into a Mini-PROTEAN® 3 Cell (Bio-Rad) and at RT a constant current of 30 V was applied for 30 minutes followed by 100 V for 1 hour for a standard 1.5 mm gel.

2.7.7.2. Blocking transfer membranes.

Non-specific binding of antisera to the transfer membrane was blocked by immersing the membrane in 3 % (w/v) non-fat dried milk, 0.1 % (v/v) Tween 20 in TBS (Table 2.44) (TBS-T) overnight at 4°C on an orbital shaker. The membrane was rinsed once with 1x TBS-T as a washing procedure.

Table 2.44: Chemical composition of 1x Tris-Buffered Saline (TBS)

Reagents	Final concentration
Tris base	50 mM
NaCl	150 mM
Adjust pH with HCl to 7.5	

2.7.7.3. Primary antibody incubation.

The blots were probed with the primary antibody diluted to the desired concentration (Table 2.45) in TBS-T with gentle agitation for one hour at room temperature on an orbital shaker. Afterwards, the membrane was washed three times in TBS-T for 10-15 minutes at room temperature.

2.7.7.4. Secondary antibody incubation.

The membrane was probed with the secondary antibody diluted to the desired concentration (Table 2.45) in TBS-T with gentle agitation for one hour at room temperature on an orbital shaker. Afterwards, the membrane was washed twice in TBS-T, then twice in TBS for 10-15 minutes at room temperature.

Table 2.45: Antibodies used for detection of blotted proteins

Primary antibody and working dilution	Secondary antibody and working dilution
Anti-HA Rat monoclonal (3F10, Roche) (100 µg/mL) 1:2,000	Anti-rat-HRP, polyclonal Sigma (concentration not specified) 1:100,000
Anti-GST rabbit, monoclonal (SIGMA) (concentration not specified) 1:20,000	Anti-rabbit-HRP, polyclonal Sigma (concentration not specified) 1:100,000
Anti-c-myc rabbit monoclonal (A-14, Santa Cruz) (200 µg/mL) 1:5,000	Anti-rabbit-HRP, polyclonal Sigma (concentration not specified) 1:100,000
Anti-pMAPK rabbit monoclonal (Phospho p44/42 XP, Cell Signalling technologies, concentration not specified) 1:5,000	Anti-rabbit-HRP, polyclonal Sigma (concentration not specified) 1:10,000

2.7.7.5. Visualization of antibody complexes on western blots.

The blots were incubated with the SuperSignal Femto Chemiluminescent substrate (Anti-HA, Anti-c-myc, Anti-FLAG; Pierce) or ECL prime (Anti-pMAPK; GE Healthcare) for five minutes at room temperature. The membrane was semi-dried by holding it vertically and touching it against tissue paper to drain excess chemiluminescent reagent. The membranes were placed on glad wrap and exposed to the ImageQuant LAS 4000 Luminescence Image Analyser with the protein side facing upwards. The ImageQuant TL software was used for automatic blank field correction for white background.

2.7.8. De novo identification of BAK1-interacting receptor proteins by mass spectrometry.

2.7.8.1. Treatment of leaves with PAMPs.

PAMP solutions of the desired concentration were vacuum-infiltrated into leaf tissue for two minutes or until completely saturated. *N. benthamiana* leaves infiltrated with csp22 were frozen in liquid nitrogen. *A. thaliana* seedlings infiltrated with *Pst* spore extract were transferred onto wet whatman filter paper and kept in the dark for five hours before freezing in liquid nitrogen.

2.7.8.2. Co-IP for mass spectrometry.

A. thaliana seedlings or *N. benthamiana* leaf samples were ground in liquid nitrogen to a fine powder. For a standard large-scale co-IP procedure, 10 leaves or 150 seedlings were thawed in 40 mL of the respective cold plant protein extraction buffer (Table 2.46). Extracts were centrifuged at 15,000 *x g* for 20 minutes at 4°C. Supernatants were subsequently filtered through Econo-Pac® Chromatography Columns (Bio-Rad) at 4°C before measuring the protein concentration using the Bradford reagent according to 2.7.3. The protein concentration was adjusted to 3 mg/mL and the same volume of each sample was used in the subsequent co-IP procedure.

When using agarose-conjugated antibodies, for each sample 150 µL of anti-GFP conjugated beads (GFP-Trap, Chromotek) were washed once in one mL wash buffer and then added to the diluted protein extract. Conjugated beads were mixed with the protein extracts for 2 h at 4°C, with slow but constant rotation.

Beads bound to immunoprecipitated proteins were collected by centrifugation of the mixture at 3000 *x g* for one minute at 4°C. Six washes were performed with 1 mL cold wash buffer in 1.5 mL tubes by spinning at 500 *x g* for 20 seconds (

Table 2.46) before stripping off the interacting proteins by boiling the beads in 60 µL loading buffer (Table 2.47, Life Technologies). The beads were removed from the protein containing buffer by transferring into mini Bio-Rad chromatography columns (Bio-Rad) and centrifuging at 500 *x g* for 20 seconds at RT.

Table 2.46: Composition of large-scale plant protein extraction buffer and wash buffer.

Reagents	Final concentration		
	***Nicotiana benthamiana* extraction buffer**	***N. benthamiana* wash buffer**	***Arabidopsis thaliana* extraction/wash buffer**
Tris HCl pH 7.5	150 mM	150 mM	50 mM
NaCl	150 mM	150 mM	150 mM
EDTA	5 mM	5 mM	2 mM
DTT	10 mM	1 mM	5 mM
Glycerol (v/v)	10%	10%	10%
Plant protease inhibitor (Sigma)	1%	0.5%	1%
IGEPAL (v/v)	1%	0.5%	1%
Sodium molybdite (NaMoO4)	1 mM	1 mM	2 mM
Sodium fluoride (NaF)	1 mM	1 mM	2 mM
Phenylmethanesulfonylfluoride (PMSF)	0.5 mM	-	1 mM
Sodium vanadate (Na_3VO_4)	1 mM	-	1.5 mM
Polyvinylpolypyrrolidone (PVPP), insoluble (w/v)	1%	-	-

2.7.8.3. Sodium dodecyl sulphate-polyacrylamide gel electrophoresis to prepare protein samples for subsequent mass-spectrometry.

One or two 3-16% NuPAGE Bis-Tris gels were placed into an XCell SureLock Mini-Cell Electrophoresis System (Life Technologies). The inner and outer chambers were filled with 1x NuPAGE MOPS Running Buffer (Life Technologies), ensuring that all wells were full of running buffer and that air bubbles were displaced from the wells. Five µL of the marker SeeBlue Plus2 Pre-Stained Standard (Life Technologies) was added to the marker lane and equal amounts of each protein sample were loaded onto the gel. Empty wells were filled with 30 µL of sample buffer (Table 2.47). The gels were run at 100 V for 15 minutes, and current was then increased to a constant 200 V until the dye front reached the end of the gel.

Table 2.47: Preparation of 2% loading buffer (Life Technologies)

Reagents	Volume
4x sample buffer (life technologies)	2 volumes
10x Reducing reagent (life technologies)	1 volume
Milli-Q water	7 volumes

2.7.8.4. Staining of proteins on gels for mass-spectrometry.

Gels containing protein samples for mass-spectrometry were stained in Simply Blue Safe stain (Life Technologies) overnight in sealed plastic pouches with gentle shaking at 4°C, and destained in Milli-Q water until the background was removed completely. Stained gels were scanned at 300 dots per inch resolution using a Bio-Rad GS-710 Calibrated Imaging Densitometer (Bio-Rad).

2.7.8.5. Trypsin Digestion and mass spectrometry of gel-resolved protein samples.

2.7.8.5.1. Trypsin digestion.

Protein bands from stained gels were excised using sterile scalpel blades, cut into 2-4 mm pieces and transferred into a 1.5 mL tube. Tryptic digests were performed using MS-grade solutions according to Table 2.48.

Table 2.48: In-gel protein digestion

Solution (volume/sample)	Composition	Conditions
Wash (500 µL)	50% (v/v) acetonitrile, 25 mM (w/v) ammonium bicarbonate (final)	2 x 30 minutes at 56°C, shaking
Dehydration (200 µL)	100% acetonitrile	5 – 10 minutes at RT
Reduction of disulphide bonds (200 µL)	10 mM DTT 50 mM (w/v) $(NH_4)HCO_3$	30-45 minutes at 56°C, shaking
Alkylation of cysteines (200 µL)	55 mM chloroacetamide 50 mM (w/v) $(NH_4)HCO_3$	20-30 minutes in the dark
Tryptic digest (200 µL)	2 µg Trypsin (Promega) (20 µL of 100ng/ µL stock) 1% (v/v) acetonitrile 50 mM (w/v) ammonium bicarbonate	overnight, 37°C

The peptides were extracted and recovered by adding one volume (200 µL) 50% acetonitrile 5% formic acid solution and sonicating for 5-10 minutes. The extraction was repeated twice with another 150 µL 50% acetonitrile 5% formic acid solution, and the peptide containing solutions were pooled for each sample in a fresh low protein bind eppendorf tube. The solvent was evaporated away in a speedy vac until dry, and stored at -20°C for subsequent mass-spectrometry. Immediately before analysis by Liquid chromatography mass spectrometry (LC-MS), peptides were dissolved in 0.5% formic acid.

2.7.8.6. Liquid chromatography mass spectrometry (LC-MS).

LC-MS/MS analysis was performed by Dr. Jan Sklenar at the proteomics facility of The Sainsbury Laboratory, Norwich, UK, using a hybrid mass spectrometer LTQ-Orbitrap (ThermoFisher Scientific) and a nanoflow-UHPLC system (nanoAcquity, Waters Corp.) The generated peptides were applied to a reverse phase trap column (Symmetry C18, 5µm, 180µm x 20mm, Waters Corp.) connected to an analytical column (BEH 130 C18, 1.7µm, 75µm x 250mm, Waters Corp.) in vented configuration using nano-T coupling union. Peptides were eluted in a gradient of 3-40% acetonitrile in 0.1% formic (solvent B) acid over 50 minutes followed by gradient of 40-60% over three minutes at a flow rate of 250 nL min-1. The mass spectrometer was operated in positive ion mode with nano-electrospray ion source with ID 0.02 mm fused silica emitter (New Objective). Voltage +2 kV was applied via platinum wire held in PEEK T-shaped coupling union. Transfer capillary temperature was set to 200 °C, no sheath gas, and the focusing voltages in factory default setting were used.

In the Orbitrap, MS scan resolution 60,000 at 400 m/z, range 300 to 2000 m/z used, and automatic gain control (AGC) target was set to 1000000 counts.

In the linear ion trap (LTQ), MS/MS spectra were triggered with data dependent acquisition method for the five most intense ions. The threshold for collision induced dissociation (CID) above 1000 counts, normal scan rate types, and AGC accumulation target set to 30,000 counts were used.

Data dependent algorithm was used to collect as many tandem spectra as possible from all masses detected in master scan in the Orbitrap. For the latter, Orbitrap pre-scan functionality, isolation width 2 *m/z* and collision energy set to 35 % were used. The selected ions were then fragmented in the ion trap using CID. Dynamic exclusion was enabled allowing for one repeat only, with a 60 seconds exclusion time, and maximal size of dynamic exclusion list 500 items. Chromatography function to trigger MS/MS event close to the peak summit was used with correlation set to 0.9, and expected peak width 7s. Charge state screening enabled allowed only higher than 2+ charge states to be selected for MS/MS fragmentation.

2.7.8.7. Software processing and peptide identification.

Peak lists in the form of Mascot generic files (.mgf files) were prepared from raw data using Proteome Discoverer v1.2 (ThermoFisher Scientific) and if required concatenated using in house developed Perl script. Peak picking settings were as follows: m/z range set to 200-5000, minimum number of peaks in a spectrum was set to

1, S/N threshold for Orbitrap spectra set to 1.5, and automatic treatment of unrecognised charge states was used. Peak lists were searched against TAIR (*A. thaliana*) or a combined TAGC/Solgenomics (*N. benthamiana*) database with added construct if used throughout the experiments. Only tryptic peptides with up to 2 possible miscleavages and charge states +2, +3, +4, were allowed in the search. The following modifications were included in the search as well: oxidised methionine (variable), carbamidomethylated cysteine (static). Data were searched with a monoisotopic precursor and fragment ions mass tolerance 10ppm and 0.8Da respectively. Mascot results were combined in Scaffold (Proteome Software) and exported in Excel (Microsoft Office).

In Scaffold, the peptide identifications were accepted if they could be established at greater than 95.0% probability by the Peptide Prophet algorithm with Scaffold delta-mass correction. Protein identifications were accepted if they could be established at greater than 95.0% probability and contained at least two identified peptides (amongst all samples within one experiment). Protein probabilities were assigned by the Protein Prophet algorithm; proteins that contained similar peptides and could not be differentiated based on MS/MS analysis alone were grouped to satisfy the principles of parsimony (Searle, 2010).

3. Identification of the receptor for the bacterial PAMP cold shock protein from *Nicotiana benthamiana* using BAK1 as molecular bait.

3.1. Introduction.

Plants and animals sense microbes by detecting a range of their constituent molecules, so-called pathogen-associated molecular patterns (PAMPs). PAMPs are recognised directly by pattern recognition receptors (PRRs) located on the cell surface. In plants, PRRs usually belong to the receptor kinase (RK) or receptor-like protein (RLP) families, and often contain extracellular lysin motif (LysM or LYM) or leucine-rich repeats (LRR) domains (Cao *et al.*, 2014). Perhaps the best developed of these models is perception of the bacterial protein flagellin or its peptide derivative flg22 by the LRR-RK FLAGELLIN SENSING 2 (FLS2) (Gomez-Gomez & Boller, 2000; Chinchilla *et al.*, 2006; Sun, Y *et al.*, 2013). LysM receptors have been implicated in the perception of carbohydrate components such as fungal chitin, and peptidoglycan or lipopolysaccharides from bacteria (Dow *et al.*, 2000; Erbs & Newman, 2003; Gust *et al.*, 2007; Miya *et al.*, 2007; Willmann *et al.*, 2011).

FLS2 and several other LRR-receptors require the LRR-RK BRASSINOSTEROID INSENSITIVE 1 (BAK1) for signal transduction (Chinchilla *et al.*, 2007b; Heese *et al.*, 2007; Roux *et al.*, 2011; Koller & Bent, 2014). BAK1 is part of the SOMATIC EMBRYOGENESIS RECEPTOR KINASE (SERK) family (thus also known as SERK3) in *Arabidopsis thaliana* and some of its functions can be performed by SERK4/BAK1-LIKE 1 (BKK1) (Roux *et al.*, 2011). In most cases, BAK1 interacts with receptors in a ligand-induced manner (Chinchilla *et al.*, 2007a; Heese *et al.*, 2007; Krol *et al.*, 2010; Schulze *et al.*, 2010; Roux *et al.*, 2011;

Sun, Y *et al.*, 2013). FLS2 binds BAK1 within minutes after flg22 treatment. The BAK1-INTERACTING RECEPTOR-LIKE KINASES 1 and 2 (BIR1 and BIR2) negatively regulate BAK1. BIR2 is released from the BAK1-FLS2 complex during flg22 perception and BIR1 negatively regulates BAK1-mediated cell death. The *bir1-1* cell death phenotype is rescued by the *sobir1-1* mutation. SUPPRESSOR OF BIR1-1 (SOBIR1) also interacts constitutively with some RLPs from *A. thaliana* and tomato, and is required for ligand-induced signalling (Jehle *et al.*, 2013a; Liebrand *et al.*, 2013; Zhang *et al.*, 2013; Zhang, LS *et al.*, 2014). SOBIR1 may function as a signal transducer for those PRRs that lack a cytoplasmic kinase domain (Gust & Felix, 2014). *Nicotiana benthamiana* contains two SOBIR1 homologs, NbSOBIR1 and NbSOBIR1-like (Liebrand *et al.*, 2013).

Activation of PRRs by ligand binding and subsequent stimulation of the immune system is termed PAMP-triggered immunity (PTI) (Monaghan & Zipfel, 2012). PTI is associated with numerous phenomena such as extracellular alkalinisation, influx of Ca^{2+}, production of reactive oxygen species (ROS), activation of mitogen activated protein kinase (MAPK) cascades, and massive changes in host gene expression (Segonzac & Zipfel, 2011). Importantly, adapted bacterial pathogens have evolved to escape PTI by altering PAMPs to avoid recognition or by the secretion of virulence effector proteins into the host cytoplasm. Such effectors can inhibit crucial PTI signalling components (Jones & Dangl, 2006). Reduced PTI is usually associated with plant diseases (Jones & Dangl, 2006), but also allows *Agrobacterium*-mediated plant transformation and establishment of nitrogen fixing nodules in roots by rhizobial bacteria, as both *Agrobacterium ssp.* and *Rhizobium ssp.* have altered flagellin sequences that are not recognised by plants (Felix *et al.*, 1999). Such bacteria, which are not recognised by FLS2, still elicit PTI through the perception of alternative PAMPs, and while flagellin perception

by FLS2 seems to be conserved in vascular plants, several PAMPs are recognised only by certain plant families (Boller & Felix, 2009). *A. thaliana* recognises the bacterial PAMP Elongation Factor-Tu through the LRR-RK ELONGATION FACTOR-Tu Receptor (EFR) (Zipfel *et al.*, 2006). Similar to FLS2, EFR recruits BAK1 after perception of EF-Tu, illustrating the capacity of BAK1 to interact with different receptors (Schulze *et al.*, 2010). Likewise, the cold shock protein (CSP) was identified from *Staphylococcus aureus* as a bacterial PAMP that is perceived specifically by members of the plant family *Solanaceae* (Felix & Boller, 2003). CSPs encode a RNA-binding motif with a highly conserved domain, known as the cold-shock-domain (CSD). The N-terminal 22 amino acid (aa) sequence of the CSP consensus sequence, known as csp22, elicits typical immune responses in a BAK1-dependent manner (Felix & Boller, 2003; Heese *et al.*, 2007). However, the receptor for CSP has not yet been identified, despite identification of this PAMP 12 years ago.

Here, I describe a novel biochemical strategy to identify new PRRs using BAK1 as molecular bait. I confirm its utility by identification of the CSP receptor in *Nicotiana benthamiana* (NbCSPR). NbCSPR restricted the growth of adapted and non-adapted bacterial pathogens and the perception of the CSP peptide derivative csp22 is potentiated by prior flg22 perception. I further show that perception of CSP from *Agrobacterium tumefaciens* limits transformation of *N. benthamiana* plants, and that interfamily transfer of NbCSPR is a useful strategy to enhance bacterial disease resistance in non-*Solanaceaeous* plants.

3.2. Results.

3.2.1. csp22-induced responses are dependent on the plant age in *Nicotiana benthamiana.*

Four- to five-week old *N. benthamiana* plants prior to onset of flowering are commonly used to measure immunity and for transient *Agrobacterium*-mediated transformation (Goodin *et al.*, 2008; Shamloul *et al.*, 2014). Unlike flg22-induced events, csp22-dependent responses are weak and inconsistent in plants of this age. I however found that csp22-induced responses were higher in flowering *N. benthamiana* plants. Under growth conditions used here and described in Chapter 2, the plants were six weeks old when they flowered. I measured PTI responses including ROS production, cytoplasmic influx of Ca^{2+} ions from the apoplast, activation of MAPKs, and up-regulation of pathogen induced gene (PIG) expression. All responses triggered by csp22 were greater in six week old than four week old plants, but this effect was not seen for flg22 (Figure 3.1, Figure 3.2). Therefore, six-week old plants were used to identify the receptor for CSP in *N. benthamiana,* and for all subsequent experiments unless indicated otherwise.

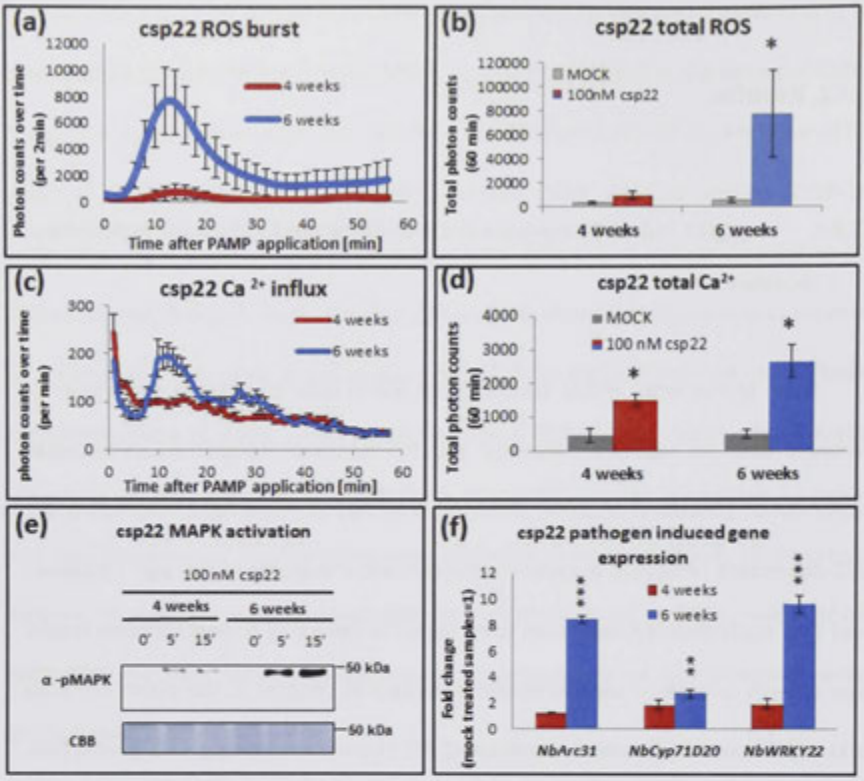

Figure 3.1: csp22 induces immune responses in *Nicotiana benthamiana* in an age-dependent manner. Comparison of responses induced by 100 nM csp22 in 4- and 6-week old *N. benthamiana* plants; **(a, b)**, ROS production **(c, d)** Cytoplasmic influx of Calcium ions, **(e)** MAPK activation and **(f)** up-regulation of PIGs. Graphed data are ± SEM, * $P < 0.05$, ** $P < 0.01$, *** $P < 0.001$ (pairwise Student's *t*-test comparing 6-week old plants to 4-week old plants, n=8 for ROS, Calcium influx, n=6 for qRT-PCR). All experiments were performed three or more times and representative results are shown.

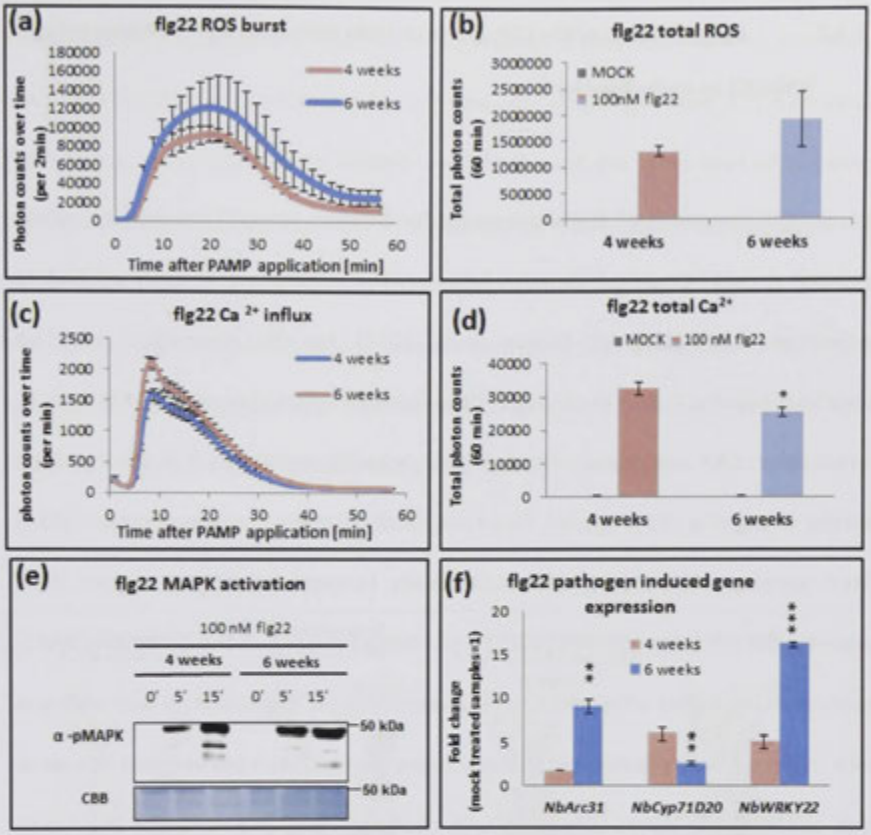

Figure 3.2: flg22-induced immune responses in *Nicotiana benthamiana* do not increase with plant age. Comparison of responses induced by 100 nM flg22 in 4- and 5-week old *N. benthamiana* plants; **(a, b)**, ROS production, **(c, d)**, Calcium ion influx **(e)** MAPK activation and **(f)** up-regulation of pathogen induced gene expression. Graphed data are ± SEM, * $P < 0.05$, ** $P < 0.01$, *** $P < 0.001$ (pairwise Student's *t*-test comparing 6-week old plants to 4-week old plants, n=8 for ROS, Calcium influx, n=6 for qRT-PCR). All experiments were performed three or more times and representative results are shown.

3.2.2. Identification of the CSP receptor from *Nicotiana benthamiana* using NbBAK1 as molecular bait.

I took advantage of the requirement for NbBAK1 in csp22 recognition, which suggested a csp22-triggered complex between the unknown CSP receptor and *N. benthamiana* BAK1 (NbBAK1) (Heese *et al.*, 2007). For this approach, I amplified NbBAK1b (Chaparro-Garcia *et al.*, 2011) (from here on referred to as NbBAK1) from *N. benthamiana* cDNA and cloned it into a binary vector for expression in *N. benthamiana* from the strong viral 35S promoter, fused genetically to green fluorescent protein (GFP) at its C-terminus (*35S:NbBAK1-GFP*). Additionally, I created the *NbBAK1* mutant allele containing the *bak1-5* mutation (C508Y) (*35S:NbBAK1-5-GFP*), as the *A. thaliana* BAK1-5 protein shows higher affinity to the FLS2 receptor in *A. thaliana* than wild type and hence might provide a better bait in this scheme (Figure 3.3). I transformed five week old *N. benthamiana* leaves transiently with each construct, and infiltrated them with csp22 peptide at the onset of flowering to induce complex formation between NbBAK1-GFP and the unknown CSP receptor. The putative NbBAK1 protein complexes were purified from leaf extracts using an anti-GFP antibody conjugated to beads, washed several times, and removed from the beads by boiling in SDS before separation on one-dimensional polyacrylamide gel electrophoresis. Fractions were excised from the gel, and isolated proteins identified by liquid chromatography-mass spectrometry (LC-MS/MS). The MS was operated by Dr. Jan Sklenar from The Sainsbury Laboratory Proteomics facility. Experiments were performed four times independently and the total number of peptides identified in all experiments is shown in Table 3.1. The list of all identified proteins can be found in the attachment (Attachment 1). Similar numbers of

peptides were identified for NbBAK1 and NbBAK1-5 in both mock-treated and csp22-treated samples. I identified *N. benthamiana* homologs of the known AtBAK1 interactors BAK1-INTERACTING RECEPTOR 1 (BIR1) and two BIR2 homologs (Table 3.1) (Gao *et al.*, 2009; Halter *et al.*, 2014). Both NbBIR2 variants showed the same level of sequence identity to AtBIR2. One variant was more abundant in NbBAK1b pull-downs hence was designated NbBIR2b, and I refer to the other as NbBIR2a (Attachment 2). NbBIR1, NbBIR2a and NbBIR2b were present in both mock and csp22 treatments. Two RLPs as potential CSPR candidates that were enriched in the csp22-treated samples were identified. They were termed NbCSPRC1 and NbCSPRC2 (Table 3.1).

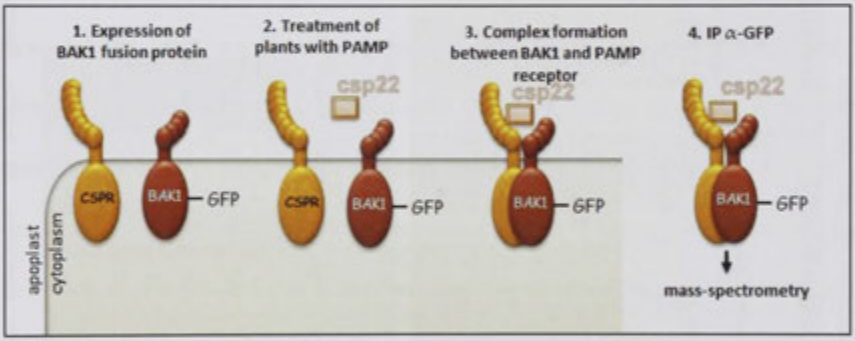

Figure 3.3: Strategy to identify the unknown CSP receptor (NbCSPR). *Nicotiana benthamiana* leaves are transiently transformed with *35S:NbBAK1-GFP* or *35S:NbBAK1-5-GFP* (1). Leaves are treated with csp22 (2) leading to complex formation between NbBAK1 and the hypothetical NbCSPR protein (3). The complex is isolated using anti-GFP conjugated beads (4), and co-purifying proteins identified by mass-spectrometry.

Table 3.1: Lists of selected proteins with their corresponding unique peptides identified by LC-MS/MS (95% peptide and protein probability, with at least two peptide identified amongst all samples) of proteins isolated from N. benthamiana that transiently expressed either NbBAK1-FLAG, NbBAK1-GFP or NbBAK1-5-GFP treated for ten minutes with sterile MQ-water (-) or 100 nM csp22 peptide by vacuum infiltration. [1]

(a)

Homologue or most sililar to	annotated as	size	experiment 1				experiment 2				experiment 3				experiment 4			
			BAK1 -	BAK1 + csp22	BAK1-5 -	BAK1-5 + csp22	BAK1 -	BAK1 + csp22	BAK1-5 -	BAK1-5 + csp22	BAK1 -	BAK1 + csp22	BAK1-5 -	BAK1-5 + csp22	BAK1 -	BAK1 + csp22	BAK1-5 -	BAK1-5 + csp22
BAK1b	BAK1b	68 kDa	18	17	33	32	44	43	39	41	47	47	42	43	54	56	38	47
BIR1	BIR1	69 kDa	1	3	7	12	9	11	9	9	18	21	12	23	16	21	13	12
BIR2a	BIR3a	66 kDa				1	1	2		1	12	10	4	4	13	16	2	5
BIR2b	BIR3b	67 kDa	3	6		11	18	22	1	10	48	50	17	20	53	45	18	19
RLP	disease resistance/LRR	68 kDa						2			1	2	1	3		2		1
RLP	LRR-RLK GSO1	112 kDa			1	2						2		1	2	4		1

(b)

Homologue or most sililar to	here referred to as	size	Total coverage	total			
				BAK1 -	BAK1 + csp22	BAK1-5 -	BAK1-5 + csp22
BAK1b	NbBAK1b	68 kDa	> 60%	163	163	152	163
BIR1	NbBIR1	69 kDa	>38%	44	56	41	56
BIR2a	NbBIR2a	66 kDa	>60%	26	28	6	11
BIR2b	NbBIR2b	67 kDa	>62%	122	123	36	60
RLP	NbCSPRC1	68 kDa	6%	1	6	1	4
RLP	NbCSPRC2	112 kDa	10%	2	6	1	4

(c)

NbCSPRC1	NbCSPRC2
GPLPDLALFPSLR	IPNFIGSFPR
MLESLDLSR	ALDLSTNNLNQPLPELFLSLSDKAEK
IPSSTQLQTFER	IHILDLSQNSLSGEIPR
NQLSGMIPK	SLEELHLSNNHLSGSLPDITR
	LESLDLSGNR

[1] **(a)** List represents results from four independent experiments. **(b)** Peptides identified for the respective protein in the individual samples were summed up from the four individual experiments. **(c)** Peptides identified corresponding specifically to the two csp22-receptor-candidates.

I cloned the *NbCSPRC1* and *NbCSPRC2* coding regions (Attachment 3 and 4) into binary vectors, under control of the 35S promoter, fused genetically to a C-terminal 5xMyc epitope tag. I co-expressed each of these constructs in *N. benthamiana* leaves with *NbBAK1* expressed also from the 35S promoter and fused C-terminally to 3xHA and 1xFLAG tags (*35S:NbBAK1-3xHAF*), and tested their ability to form complexes in the presence of csp22 by co-immunoprecipitation (coIP) experiments. Using anti-FLAG to recover NbBAK1, and probing the immune complexes by anti-Myc western blots, I found that in contrast to the MS results, NbCSPRC1 was constitutively associated with NbBAK1. On the other hand, NbCSPRC2 co-purified with NbBAK1 more abundantly after csp22 treatment, and not after addition of flg22 (Figure 3.4 a and b). I could detect a weak interaction between NbCSPR and NbBAK1 after sterile water treatment when overexposing (data not shown). Additionally, NbCSPRC1 and NbCSPRC2 bound to NbBAK1-5 independent of csp22 (Figure 3.4 c). Similar results were observed for the interaction between BAK1-5 and AtFLS2 (Figure 3.4 c) (Schwessinger *et al.*, 2011). I concluded that NbCSPRC2 is likely the receptor for CSP in *N. benthamiana* and from here on, I refer to it as NbCSPR (for *N. benthamiana* COLD SHOCK PROTEIN RECEPTOR). The predicted NbCSPR protein contains an N-terminal signal peptide, 28 extracellular tandem LRRs and a transmembrane domain followed by a short cytoplasmic tail (Figure 3.5). CSP was identified as a PAMP on *Nicotiana tabacum* suspension cultures (Felix & Boller, 2003), and correspondingly I identified a homolog to *NbCSPR* in *N. tabacum* (*NtCSPR*) with 97% nucleotide sequence (Attachment 5) and 95% aa identity. Tomato leafs respond to the csp15 peptide lacking the first seven aa of csp22 (Felix & Boller, 2003) treatment, but despite this I was unable to identify a strong *NbCSPR* homolog in tomato by searching the currently available genome (NCBI, Solgenomics) using BLAST.

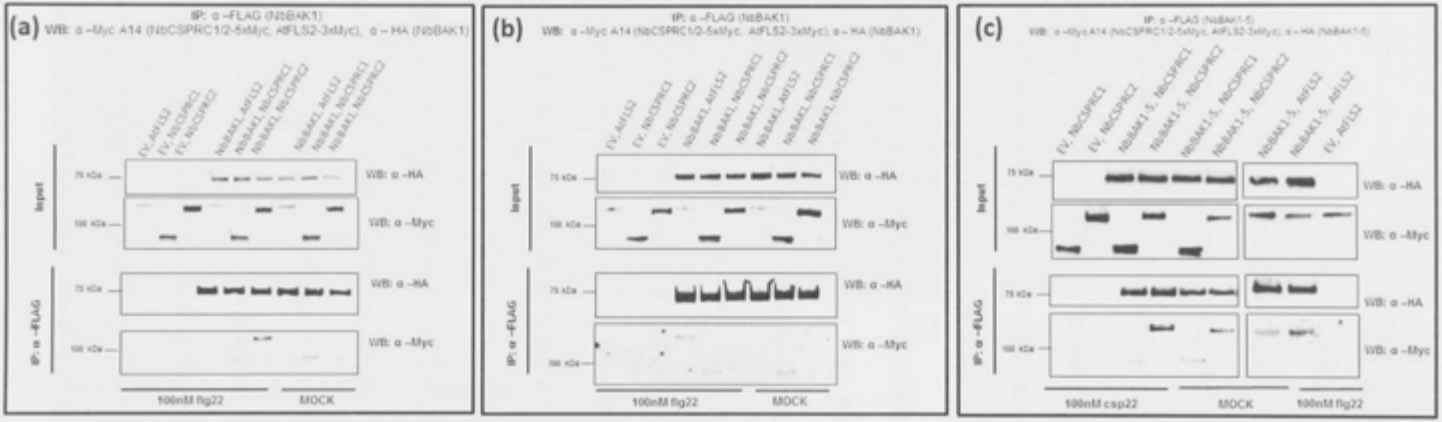

Figure 3.4 NbCSPRC2 binds NbBAK1 in a csp22-dependant manner. *N. benthamiana* was transiently transformed with *35S:NbBAK1-3xHA-FLAG*, *35S:NbBAK1-5-3xHA-FLAG* or an EV and *pAtFLS2:AtFLS2-3xMyc*, *35S:NbCSPRC1-5xMyc* or *35S:NbCSPRC2-5xMyc* and 2 days post infiltration treated with sterile water (MOCK), 100 nM flg22 or 100 nM csp22 for 10 minutes before harvesting leave tissue. **(a, b)** NbBAK1-3xHA-FLAG or **(c)** NbBAK1-5-3xHA-FLAG was recovered by anti-FLAG pull down, and the immunoprecipitates probed with anti-Myc and anti-HA western blots after gel electrophoresis. IP: Immunoprecipitated fraction.

MKSERFLFLNIAFSAFIGLVIGTSSGGDGRTTLCIERERE ALLKFKQGLIDNYGILSSWGREEEKEECCGWKGVQCSNRTGHVVVLDIH APSYSQHLRGNITPSLLELQHLKHLDLSYNDFGTSRIPNFIGSFPRLEYLFLEDASLSGEIPHALGNLTHLQILDLSLNSRLVVKNLEWL PRLAFLRDLGLSLVHIETVNWLQQIKSPSLEQLDLKHCNVPEPIISISHLSSNVSSRLLSSLNLADTGLSSSAFRWLFNLSTRFTSIDLSS NNLAGCIPEAFGYMQHLEFIDLSNTNILEGGLPKSFGNLSHLRALDLSTNNLNQPLPELFLSLSDKAEKSLEELHLSNNHLSGSLPDITRF SSLKSLYLQENQLNGSFFESYGQISKIEFLDLSLNQLTGPLPNLTAFSALRELHLNNNQFKGRLPQSIGRLSKLEMLRVESNFMEGPIT ESHLSNLSSLRVLDLSYNSFSFQLGLNWLPPFELDVESLSHCKMGPHFPQWLRTQKNYSHLDISFAGISGVAPNWFWDLSPEMMHFSIS NNQISGEVPDLSSKFVKETNYPTMDFSSNNFSGLVPSFSSNLESLNLSKNKFVGSISFLCKIANALFRTIDLSNNLLSGELHNCLMGFEE LAILNLANNNLYGKIPSSIGSLWDIQSLQLRNNNFTGDLPTSLKNCGILQILDVGGNKLSGEIPLWIGSHLTFLVVLSLRLNKFNGSIPQ NFCHLNKIHILDLSQNSLSGEIPRCLNNITSLLQNNNSSDPSILFALGGDSHNGYSYYEEYLGDALVQWKSSESVYNKTLGLLKIIDFSN NELSGNVPEEIAQLNGVLSLNLSRNNLTGNVIQGIGKMEKLESLDLSGNRLTGRIPTSLAQLHFLSVLDLSSNNLSGKIPSSTQLQSFDP SSYEGNNELCGPPLAECPEDRNTQSPSADHSKINNLDEDDKILSFEFYVCVESGFILGFWGVVFSLVLNQSFRDAYFQKLTNFAIWISATI VMFLHRLKVLWS

Figure 3.5: The NbCSPR protein sequence. Protein domains are highlighted by colour: green: signal peptide aa 1-22 (Signal P v4.1), blue: 28 LRR domains aa 111 – 885 (Bej. *et al.* 2014), red: Transmembrane domain aa 969 – 988 (tmhmm server v. 2.0).

3.2.3. NbCSPR binds csp22 and is required for csp22 responses.

To test if NbCSPR can bind csp22, I expressed NbCSPR in *N. benthamiana* leaves fused C-terminally to the 3xHAF epitope tag and purified it from leaf extracts by IP. To test for interaction with the ligand, I mixed the bead-bound receptor with csp22 expressed as a recombinant fusion with the GST protein (csp22-GST). After washing the beads, I detected a specific interaction of csp22-GST with NbCSPR-bound anti-FLAG beads (Figure 3.6 a). I could not detect an interaction of NbCSPR with flg22-GST and the interaction between csp22-GST and NbCSPR was abrogated when 10 µM free csp22 but not when 10 µM free flg22 peptide was added (Figure 3.6 b). The data indicate that NbCSPR binds specifically to csp22, consistent with the idea that NbCSPR is the CSP receptor.

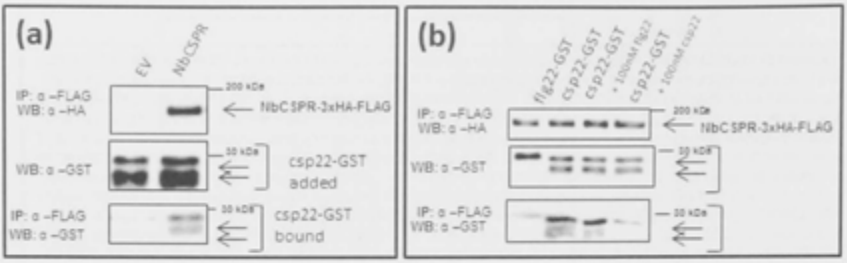

Figure 3.6 NbCSPR binds csp22 *in vitro*. Recombinant csp22-GST and flg22-GST were expressed in and purified from *Escherichia coli BL21* cells. **(a)** csp22-GST was added to NbCSPR-3xHAF bound to anti-FLAG beads or anti-FLAG beads incubated in protein extract without NbCSPR-3xHAF (EV). **(b)** flg22-GST and csp22-GST was added to NbCSPR-3xHAF bound to anti-FLAG beads with or without 10 µM unlabelled flg22 or csp22 as indicated. The presence of receptor-peptide complexes was determined by anti-HA and anti-GST western blots (WB) after gel electrophoresis. IP: Immunoprecipitated fractions.

To investigate the requirement for *NbCSPR* in csp22 responses, I generated gene fragments corresponding to nucleotides 2-299 (*TRV2:NbCSPR*) and 300-1001 (*TRV1:NbCSPR*) of the open reading frame, and cloned them into a tobacco rattle virus (TRV) vector for virus-induced gene silencing (VIGS) experiments. Successful silencing was confirmed by reduced *NbCSPR* mRNA levels and lack of detectable NbCSPR protein after transient transformation of *TRV1/2:NbCSPR* plants with *35S:NbCSPR-3xHAF* (Figure 3.7 a and b). Plants silenced for *NbCSPR* (*TRV1:NbCSPR* and *TRV2:NbCSPR,* Attachment 5), but not those silenced for the control *GFP* gene (*TRV:GFP*), showed reduced csp22 responses commensurate with the level of *NbCSPR* silencing, including diminished ROS production, activation of MAPKs, and up-regulation of PIGs expression (Figure 3.7 c to f). Silencing of *NbCSPR* did not affect flg22 responses (Figure 3.8). The activation of only one MAPK was detected in silenced plants treated with PAMPs, as reported previously (Segonzac *et al.*, 2011). The *TRV2:NbCSPR* construct was used for all subsequent experiments because of higher silencing efficiency (Figure 3.7 a); it is referred to as *TRV:NbCSPR* from here on.

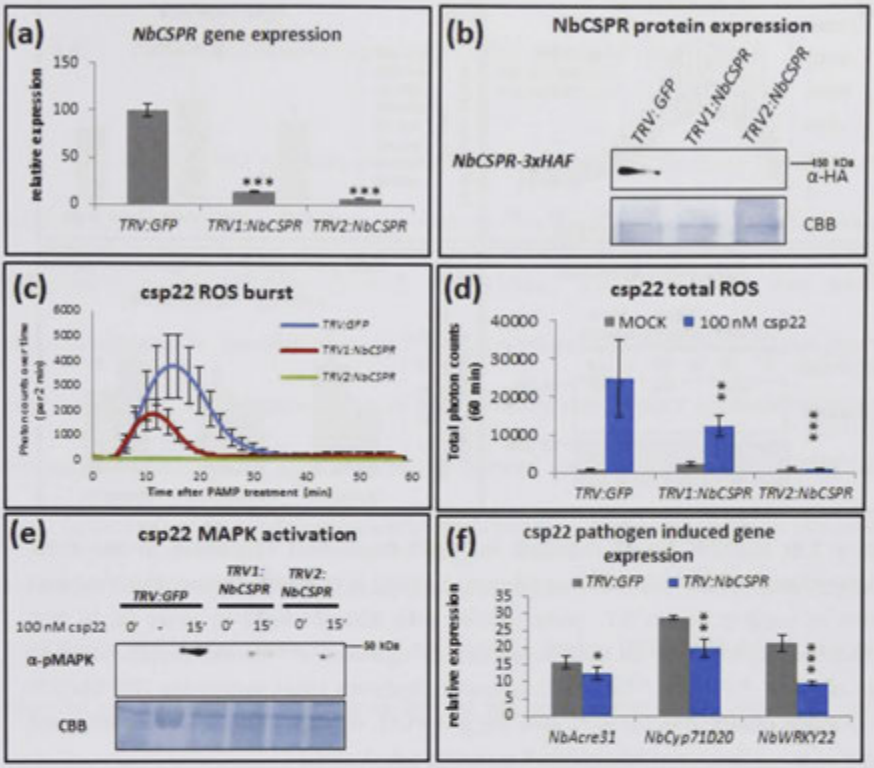

Figure 3.7 *NbCSPR* is genetically required for csp22 dependent responses. Tobacco Rattle Virus (TRV)-based Virus-induced gene silencing (VIGS) of NbCSPR was performed. Successful silencing was confirmed by **(a)** qRT-PCR and **(b)** lack of NbCSPR-3xHA-FLAG protein in *TRV:NbCSPR* plants transiently transformed with *35S:NbCSPR-3xHAF* (determined by anti-HA western blots after gel electrophoresis). *NbCSPR* is required for csp22-dependent responses as determined by VIGS of *N. benthamiana* plants, firstly measuring **(c, d)** ROS production, **(e)** activation of MAPKs, and **(f)** up-regulation of PIGs expression. Graphed data are ± SE, * P <0.05, ** P < 0.01, *** P < 0.001 (pairwise Student's *t*-test comparing *TRV:NbCSPR* to *TRV:GFP* plants, n=8 for ROS, n=6 for qRT-PCR). All experiments were performed three or more times and representative results shown.

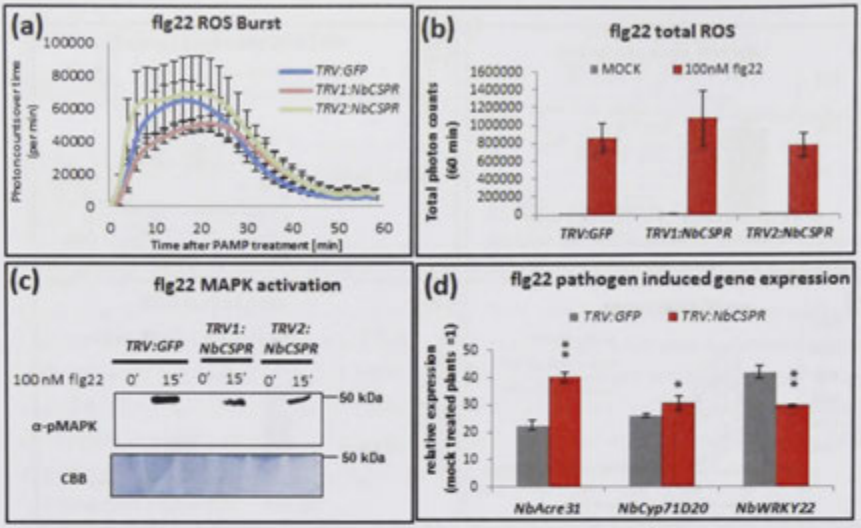

Figure 3.8: *NbCSPR* is not required for flg22-dependent responses in *Nicotiana benthamiana*. *NbCSPR* or *GFP* was silenced by VIGS in *N. benthamiana*, and the same plants as used in Figure 3.7 were treated with 100 nM flg22 to assay **(a, b)** ROS production, **(c)** activation of MAPKs, and **(d)** up-regulation of PIGs expression. Graphed data are ± SE, * P<0.05, ** P < 0.01 (pairwise Student's *t*-test comparing *TRV:NbCSPR to TRV:GFP* plants, n=8 for ROS, n=6 for qRT-PCR). All experiments were performed three or more times and representative results are shown.

3.2.4. NbCSPR does not require NbSOBIR1 for csp22 responses.

The RK NbSOBIR1 was suggested to be generally required for signal transduction by RLPs through direct interaction, perhaps by providing an intracellular signalling component to the complex (Gust & Felix, 2014). Indeed, I found that when overexpressed in *N. benthamiana*, NbCSPR co-purified with NbSOBIR1 in pull-down experiments, but AtFLS2 did not (Figure 3.9). To test a requirement of NbSOBIR1 or its homolog NbSOBIR1-like, I generated plants silenced for both genes *(TRV:NbSOBIR1(-like))* (Liebrand *et al.*, 2013). Successful silencing was confirmed through reduced *NbSOBIR1 and NbSOBIR1-like* mRNA levels and the lack of Avr4/Cf4-mediated cell death in *TRV:NbSOBIR1(-like)* plants (Figure 3.10 a and b). Such a lack of cell death may be because the RLPs Cf4 and Ve1 proteins did not accumulate when *NbSOBIR1* and *NbSOBIR1-like* were silenced (Liebrand *et al.*, 2013). NbSOBIR1 is however not required for the accumulation of the NbCSPR protein, as silencing of *NbSOBIR1(-like)* (Liebrand *et al.*, 2013) did not affect NbCSPR protein accumulation, after transient expression of *35S:NbCSPR-5xMyc* (Figure 3.10 c). Despite the interaction between NbSOBIR1 and NbCSPR, plants silenced for *NbSOBIR1* and its close homolog *NbSOBIR1-like* (Liebrand *et al.*, 2013) were not impaired in csp22- or flg22-induced production of ROS, activation of MAPKs, or PIG up-regulation (Figure 3.10 d to j). In fact, in *TRV:NbSOBIR1(-like)* plants, PIGs were induced to a higher extend after csp22 and flg22 treatment when compared to control plants. I thus conclude that csp22-triggered immune signalling is not clearly reduced in plants silenced for *NbSOBIR1* and *NbSOBIR1-like*.

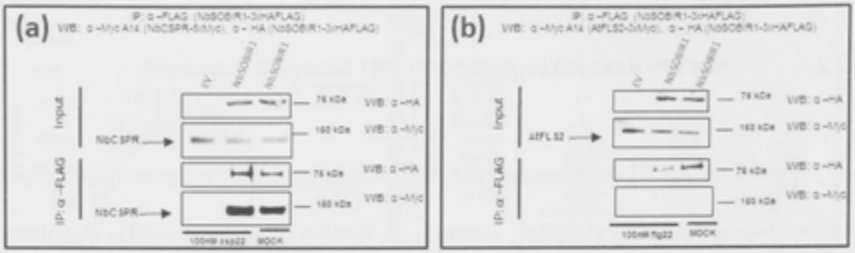

Figure 3.9 NbCSPR can bind NbSOBIR1 when overexpressed. *N. benthamiana* leaves were co-transformed transiently with *35S:NbSOBIR1-3xHAF* or EV, and one of *35S:NbCSPR-5xMyc* or *pAtFLS2:AtFLS2-3xMyc*. Two days post-infiltration the tissue was treated with sterile water (MOCK), csp22 or flg22 for 15 minutes as indicated, before harvesting the leaf tissue. NbSOBIR1-3xHAF was recovered by anti-FLAG pull down, and the immunoprecipitates probed with anti-Myc and anti-HA western blots after gel electrophoresis. IP: Immunoprecipitated fraction. **(a)** Overexpressed NbSOBIR1 interacts with NbCSPR with or without csp22 treatment. **(b)** AtFLS2 does not interact with NbSOBIR1 with or without flg22 treatment.

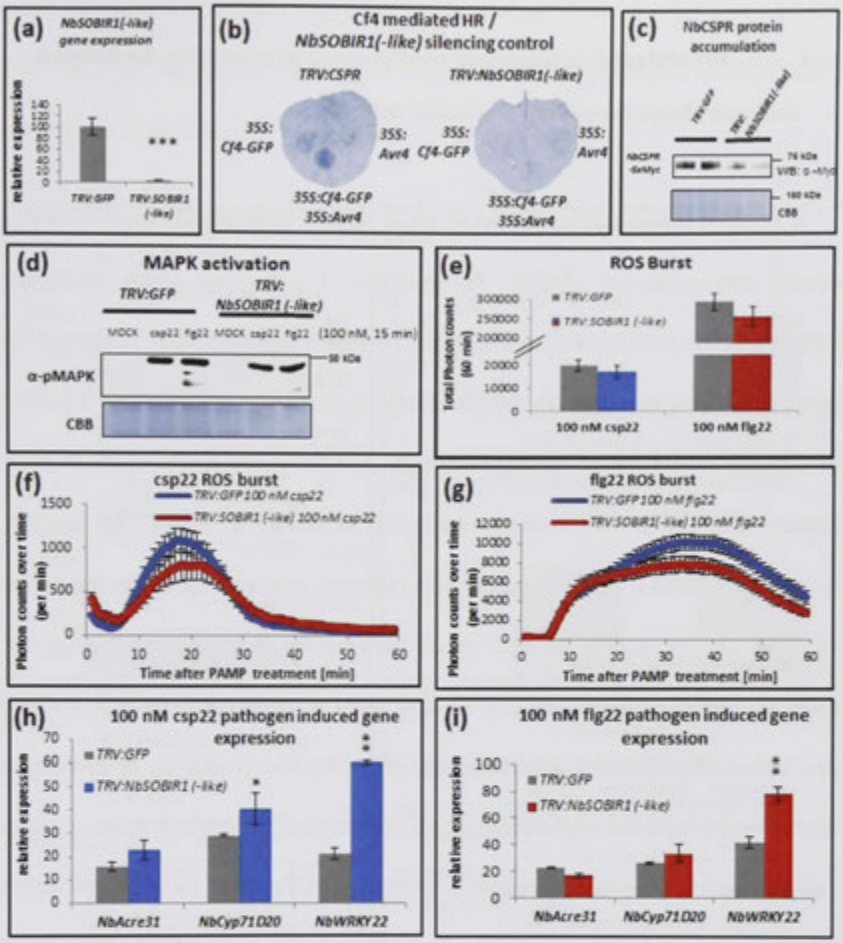

Figure 3.10: NbSOBIR1 is not required for NbCSPR protein accumulation, csp22-dependent or flg22-dependent responses. Tobacco Rattle Virus (TRV)-based Virus-induced gene silencing (VIGS) of NbSOBIR1 and NbSOBIR1-like was performed. Effective silencing of both, *NbSOBIR1* and *NbSOBIR1-like* (*TRV:NbSOBIR1(-like)*) was confirmed by **(a)** qRT-PCR and **(b)** a functional assay for the NbSOBIR1-dependent Avr4/Cf4 HR. *N. benthamiana* plants silenced for *NbCSPR* (left) or *NbSOBIR1(-like)* (right) were transformed transiently with *35S:Cf4-GFP*, *35S:Avr4* and EV as indicated. Leaves were harvested four days post transformation and cell death was detected by trypan blue staining. *NbSOBIR1/NbSOBIR1-like* is not required for NbCSPR protein accumulation **(c)**. *N. benthamiana* leaves were transformed transiently with *35S:NbCSPR-5xMyc* and NbCSPR protein levels were determined two days later by western blot using anti-Myc. *NbSOBIR1/NbSOBIR1-like* is not required for csp22- or flg22-dependent **(d)** MAPK activation, or **(e, f, g)** ROS production. **(h, j)** Up-regulation of PIGs marker genes by csp22 or flg22 treatment is not impaired in plants silenced for *NbSOBIR1 and NbSOBIR1-like*. Graphed data are ± SE, * $P < 0.05$, ** $P < 0.01$, ***$P<0.001$ (pairwise Student's *t*-test comparing *TRV:NbSOBIR1(-like) to TRV:GFP* plants, n=8 for ROS, n=6 for qRT-PCR). All experiments were performed two or more times and representative results are shown.

3.2.5. *NbCSPR* confers responsiveness to csp22 in transgenic *Arabidopsis thaliana* plants dependent on *AtBAK1/AtBKK1*.

If NbCSPR is indeed the CSP receptor, it might confer csp22 recognition to a previously non-responsive species. To test this, I generated stable transgenic *35S:NbCSPR-5xMyc A. thaliana* plants using the ecotype Columbia (Col-0). I obtained five transgenics, but only one of these, *NbCSPR-5xMyc*-5, expressed NbCSPR-5xMyc protein to a detectable level. I measured csp22-dependent responses in this line, including ROS production, seedling growth inhibition (SGI) and activation of MAPK. The *NbCSPR-5xMyc*-5 line, showed a csp22-triggered ROS response that was absent in the empty vector (line 1). The profile of ROS accumulation was aberrant compared to *N. benthamiana* leaf discs suggesting that NbCSPR is not properly regulated in *A. thaliana* (Figure 3.11 a and b), which might be related to the low frequency of productive transformation. In addition to this observation, I found that *35S:NbCSPR-5xMyc*-5 plants but not EV controls showed progressive activation of MAPK after 5 and 15 min, and a small but significant inhibition of seedling growth in response to the elicitor (Figure 3.11 c and d). In parallel, I transformed *A. thaliana* Col-0 protoplasts with *35S:NbCSPR-3xHA* to test for *bak1-5/bkk1* and *sobir1-12* dependent csp22-induced MAPK activation. Wild type Col-0 protoplasts were blind to the PAMP, whereas *NbCSPR*-expressing protoplasts activated MAPKs in a csp22-dependent manner. (Figure 3.11 e). csp-22-dependent MAPK activation was absent in transformed *bak1-5/bkk1* double mutant cells, but present in *sobir1-12* mutant cells (Figure 3.11 f). Col-0 and *sobir1-12* but not *bak1-5/bkk1* protoplasts expressing *NbCSPR* activated MAPKs in response to flg22 in the same experiments (Figure 3.11 f).

Overall, the data corroborate my findings in *N. benthamiana*, and support a model in which NbCSPR1 recognises csp22 in a complex containing NbBAK1 (or NbBKK1) but independent of SOBIR1.

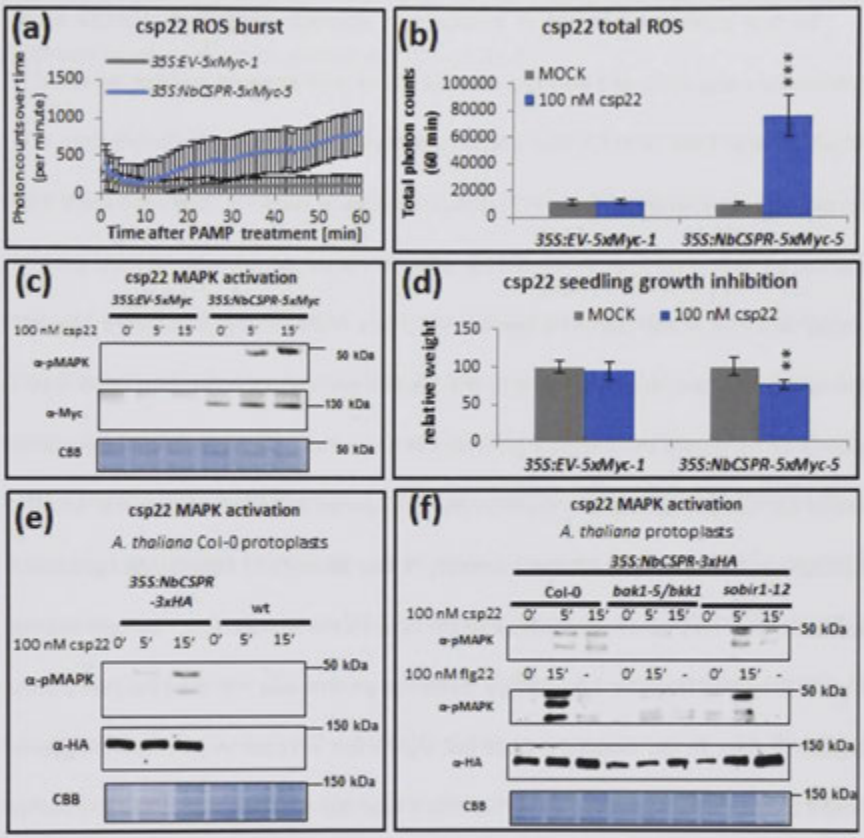

Figure 3.11: *NbCSPR* confers recognition of csp22 in *Arabidopsis thaliana*. Overexpression of *NbCSPR* in stable transgenic *A. thaliana* Col-0 plants leads to csp22–dependent responses, including **(a, b)** production of ROS, **(c)** MAPK activation, and **(d)** seedling growth inhibition (SGI). Graphed data are ± SE, ** $P < 0.01$, *** $P < 0.001$ (pairwise Student's *t*-test comparing *35S:NbCSPR-5xMyc-5 to 35S:EV-5xMyc-1* plants, n=8). All experiments were performed two or more times and representative results are shown. **(e) Transformation of Col-0 protoplasts** with *35S:NbCSPR-3HA* (left) or EV (right). Protoplasts were treated with csp22 16 hours post transfection and MAPK activation measured by anti-pMAPK western blot at the times shown. **(f)** Col-0, Col-0 *bak1-5/bkk1* and Col-0 *sobir1-12* protoplasts were transformed with *35S:NbCSPR-3xHA*. MAPK assay was performed as for (e).

3.2.6. NbCSPR confers age-related resistance to bacterial pathogens and restricts *Agrobacterium*-mediated transformation of *Nicotiana benthamiana* in flowering plants.

To test roles for *NbCSPR* in immunity, I silenced *NbCSPR* or *NbFLS2* in *N. benthamiana* using VIGS, and infected silenced plants with adapted and non-adapted *P. syringae* strains. Both *NbFLS2- and NbCSPR*-silenced plants supported more than one log growth of the adapted pathogen *P. syringae* pathovar *tabaci* 6605 (*Pta*) (Figure 3.12 a) compared to control plants silenced for *GFP*. This is consistent with *NbCSPR* playing an important role in anti-bacterial immunity. To test this further, I inoculated silenced plants with a mutant strain deficient in the Type-III secretion system (*Pta* 6605 *hrcC*-) (Figure 3.12 b). Again, the bacteria grew significantly more on *N. benthamiana* plants silenced for *NbFLS2* or *NbCSPR* than on plants silenced for *GFP*. To test the relative contribution of NbFLS2 to bacterial immunity in the absence of flagellin recognition, I inoculated four- and six-week old silenced plants with the Pta 6605 *fliC*- mutant lacking the gene encoding flagellin. Accordingly, bacterial growth was not increased on plants silenced for *NbFLS2* but showed a small but significant increase in six-week old plants silenced for *NbCSPR* (Figure 3.12 c). This effect was not seen on four-week old plants (Figure 3.12 d). For all other *Pseudomonas* strains tested, the contribution of NbCSPR in restricting bacterial growth was not dependent on the plant age. Thus, the effect of *NbCSPR* on bacterial growth is measurable even in the absence of flagellin recognition, but only in six week old, flowering *N. benthamiana* plants. To test a role for NbCSPR against non-adapted pathogens, I inoculated silenced plants with *P. syringae* pv. *phaseolicola* 1448α. Although this strain grows quite weakly on *N. benthamiana*, again growth was significantly higher on plants silenced for *NbFLS2* or *NbCSPR* when

compared with plants silenced for *GFP* (Figure 3.12 e). *NbCSPR* also contributes to bacterial resistance when transferred into *A. thaliana*. Stable transgenic Col-0 *35S:EV-5xMyc-1* or *35S:NbCSPR-5xMyc-5* were spray-infected with adapted *P. syringae* pv. *tomato* (*Psto*) DC3000 bacteria. Plants expressing the NbCSPR protein showed a slightly reduced growth of this host pathogen (Figure 3.12 f).

Flowering *N. benthamiana* plants are recalcitrant to recombinant protein expression after *Agrobacterium*-mediated transformation (Shamloul *et al.*, 2014). As *A. tumefaciens* also encode genes for CSP, I tested if *NbCSPR* restricts *Agrobacterium*-mediated transient transformation. Four-week old plants silenced for *GFP*, *NbFLS2,* or *NbCSPR,* were equally transformable by *A. tumefaciens* as judged by expression of an *intron-GUS* marker gene. Older plants were minimally transformable after silencing for *GFP* or *NbFLS2* (Figure 3.13 a and b). Strikingly, *NbCSPR*-silenced plants showed much higher GUS expression, comparable to expression in young plants. Similarly, transient expression of an arbitrary gene (35S:*N2-3xHAF*) encoding aa 1-242 of the *Solanum lycopersicum* Prf protein (Saur *et al.*, 2015) in flowering plants revealed greater N2 accumulation in plants silenced for *NbCSPR* relative to those silenced for *GFP*. N2 protein levels were unchanged by gene silencing in younger plants (Figure 3.13 c and d). Greater resistance of older plants to *Agrobacterium*-mediated transformation may be due to *NbCSPR* up-regulation of about 2-fold in six-week old relative to four-week old plants, an effect which was not seen for *NbFLS2* (Figure 3.14). Taken together, the data show that NbCSPR is an important component of the anti-bacterial immune machinery by recognising the conserved residues of the bacterial cold shock protein shared between *Pseudomonas* and *Agrobacterium* (Figure 3.15).

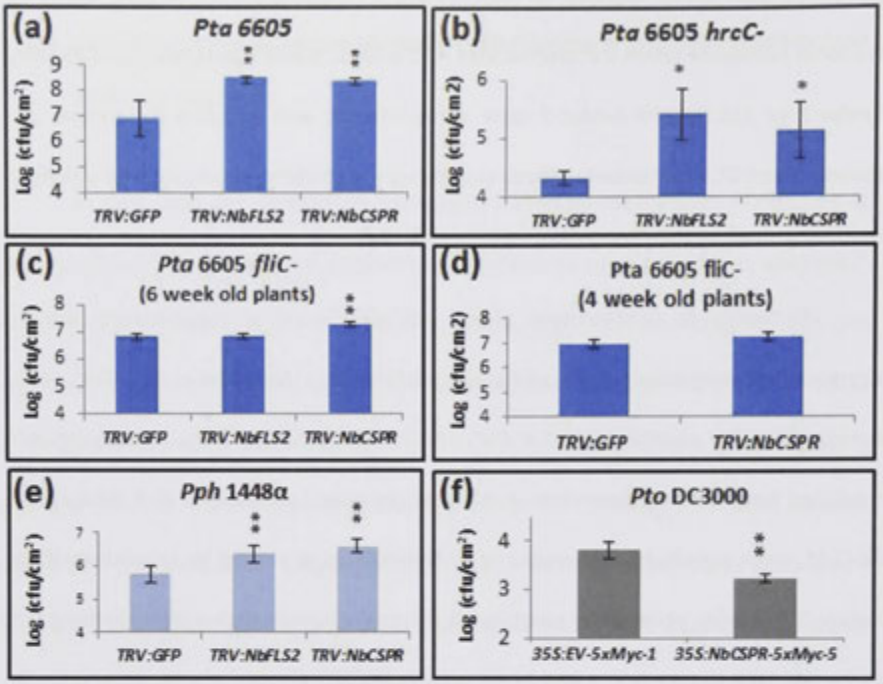

Figure 3.12: *NbCSPR* contributes to anti-bacterial immunity. *N. benthamiana* plants were silenced for *GFP*, *NbFLS2* or *NbCSPR* before infection by dipping into *P. syringae* suspensions. Infection of silenced plants with **(a)** the adapted strain *P. syringae* pv. *tabaci* (*Pta*) 6605, **(b)** the non-pathogenic strain *Pta* 6605 *hrcC-*, **(c, d)** a mutant strain lacking flagellin, *Pta* 6605 *fliC-* and **(e)** with the non-adapted pathogen *P. syringae* pv. *phaseolicola* 1448A (*Pph*). **(f)** Stable transgenic *A. thaliana* Col-0 plants transformed with *35S:EV-5xMyc* or *35S:NbCSPR-5xMyc* were spray-infected with the adapted *P. syringae* pv. *tomato* DC3000 bacteria. For all infection assays, plants were infected using a bacterial suspension containing 5 x 10^7 cfu/ mL. Graphed data are ± SEM, * P<0.05, ** P < 0.01 (pairwise Student's *t*-test comparing *TRV:NbFLS2* or *TRV:NbCSPR* to *TRV:GFP* plants, n=6).Samples for bacterial counts were taken after 3 days. All experiments were performed two or more times and representative results are shown.

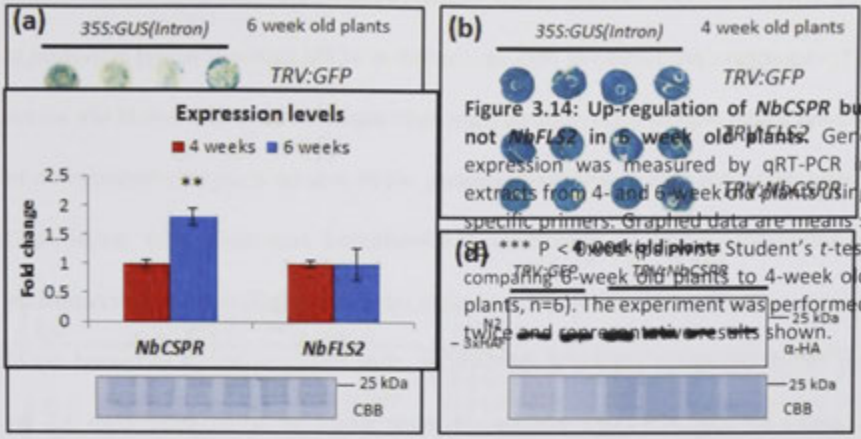

Figure 3.14: Up-regulation of *NbCSPR* but not *NbFLS2* in 6 week old plants. Gene expression was measured by qRT-PCR in extracts from 4- and 6-week old plants using specific primers. Graphed data are means ± SE. *** P < 0.001 Student's *t*-test comparing 6-week old plants to 4-week old plants, n=6). The experiment was performed twice and representative results are shown.

Figure 3.13: Transformation of six-week old *N. benthamiana* plants is restricted by *NbCSPR*. (a, b) *N. benthamiana* plants were silenced for *GFP*, *NbFLS2* or *NbCSPR* before infiltration of **(a)** six week old plants and **(b)** four week old plants with *Agrobacterium tumefaciens* GV3101 pMp90 carrying a 35S:intron-*GUS* construct. Leaves were harvested two days post infiltration and GUS activity detected by GUS staining; chlorophyll was removed using 70% Ethanol. Blue colour indicated transformation of the *GUS* gene. (c, d) Transformation of silenced **(c)** 6-week old plants and **(d)** 4-week old plants with *A. tumefaciens* GV3101 pMp90 carrying a binary construct for *35S:N2-3xHAF* expression. N2-3xHAF protein was detected by anti-HA western blot. All experiments were performed two or more times and representative results are shown.

Figure 3.15: Conservation of the csp15 and csp22 motif (Felix & Boller, 2003) in the cold shock proteins of *P. syringae* and *A. tumefaciens*. Residues critical for extracellular alkalysation of tobacco suspension cultures as described in (Felix & Boller, 2003) are highlighted red.

3.2.7. Potentiation of csp22 responses by flg22 pre-treatment.

Interestingly, I found that that treatment of *N. benthamiana* plants with flg22 2.5 before csp22 treatment, increased csp22-dependent responses, but this effect was not seen in reverse. Treatment of *N. benthamiana* leaves with 100 nM csp22 significantly up-regulated *NbCSPR* expression, but this effect was far higher upon treatment with 100 nM flg22 (Figure 3.16). Conversely, flg22 treatment up-regulated *NbFLS2* to a small extent, whereas its induction by csp22 was negligible. Consistent with these results, I

found that prior flg22 treatment (2.5 hours before csp22 treatment) caused higher csp22-dependent production of ROS, up-regulation of PIG expression, and activation of a second MAPK (Figure 3.17). Interestingly, both csp22-induced ROS and MAPK assays showed decreases after csp22 pretreatment, which may be a similar phenomenon to the refractory period of diminished FLS2-mediated responses after initial flg22 perception (Smith *et al.*, 2014). PTI responses induced by flg22 were not increased by prior csp22 treatment (Figure 3.18). Overall, prior flg22 treatment increased csp22 responses but not *vice versa* and this increase wears off when more than 3.5 lay inbetween the first and second treatment. In this way, *NbCSPR* seems to act as a client receptor for NbFLS2, perhaps consistent with the fact that flagellin and CSP are external and internal PAMPs, respectively. To extend this, I measured *CSP* gene expression in *Pta* 6605 *fliC*- bacteria incubated with *N. benthamiana* leaf discs treated with or without 100 µM flg22 (Figure 3.19). I observed up-regulation of the bacterial *CSP* gene of about 2.5

fold due to the flg22 treatment. Thus, CSP may be up-regulated in the bacteria as a response to host PTI.

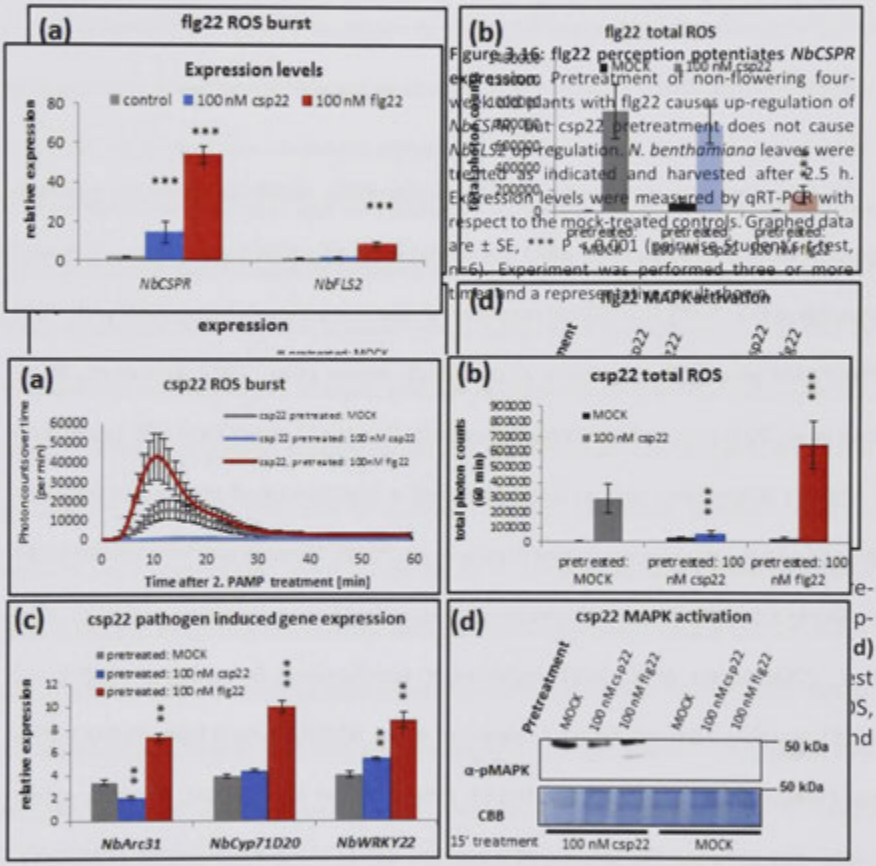

Figure 3.17: flg22 perception potentiates csp22 responsiveness in four-week old *N. benthamiana* plants. Pre-treatment of non-flowering four-week old plants with flg22 causes a later (2.5h) up-regulation of csp22-induced **(a, b)** ROS production, **(c)** expression of PIGs genes and **(d)** MAPK activation in *N. benthamiana* leaves. Graphed data are ± SE, ** $P < 0.01$, *** $P < 0.001$ (pairwise Student's *t*-test comparing flg22 or csp22 pretreated plants to MOCK pretreated plants, n=8 for ROS, n=6 for qRT-PCR). All experiments were performed three or more times and representative results are shown.

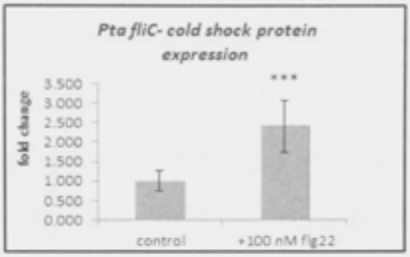

Figure 3.19: flg22-induced defence responses cause up-regulation of bacterial CSP. Plant defence responses initiated by treatment with 100 nM flg22 cause up-regulation of *Pseudomonas syringae* pv. *tabaci 6605* cold shock proteins. Graphed data are ± SEM, *** $P < 0.001$ (pairwise Student's *t*-test, n=6). Experiment was performed three or more times and representative results are shown.

3.3. Discussion.

I developed a new approach to identify PRRs, which depends on common complex components such as BAK1 for ligand-induced signal transduction. It is well established that BAK1 is a central regulator of immunity though interaction with PRRs after PAMP perception (Chinchilla *et al.*, 2007b; Heese *et al.*, 2007; Krol *et al.*, 2010; Roux *et al.*, 2011). It has been shown previously that csp22-dependent ROS production is NbBAK1 dependent, and as such predicted a csp22-induced interaction between NbBAK1 and the unknown receptor (Heese *et al.*, 2007). Through purifying NbBAK1-GFP (or NbBAK1-5-GFP) after csp22 treatment, I identified known interactors of BAK1 (Gao *et al.*, 2009; Halter *et al.*, 2014) including *N. benthamiana* homologs of AtBIR1 and AtBIR2. Notably, I did not detect a release of either NbBIR2 variant from NbBAK1 after csp22 treatment as has been reported for AtBIR2 (Halter *et al.*, 2014). This may reflect a difference between the species, or is perhaps due to the overexpression of NbBAK1. Most importantly, I identified two potential receptor candidates based on their enrichment in csp22-treated samples. The receptor for csp22 likely binds NbBAK1 only after csp22 treatment, whereas BIR proteins interact with BAK1 constitutively, which can explain the lower number of peptides found for both csp22-receptor candidates. Subsequent coIP analysis indeed confirmed the csp22-dependent interaction of

NbCSPRC2 with NbBAK1. When both receptors were transiently overexpressed, NbBAK1-5 bound NbCSPRC1 and NbCSPRC2 after MOCK or csp22 treatment. On the other hand, the interaction between NbBAK1 and NbCSPR is ligand-dependent, as confirmed by coIP. Overall, this approach was successful and offers a general strategy to identify novel PRRs.

I showed that NbCSPR expressed in *N. benthamiana* tissue bound csp22-GST *in vitro*, and that this interaction could be abrogated when the unlabelled csp22 peptides was used for competition. Secondly, genetic tests showed that *NbCSPR* is required for csp22-dependent responses and anti-bacterial immunity. Plants silenced for *NbCSPR* were deficient in csp22-triggered ROS production, MAPK activation and up-regulation of PIGs. Consistent with this, the silenced plants were more susceptible to infection by adapted and non-adapted *P. syringae* pathogens. Silencing of *NbCSPR* allowed a similar increase in bacterial growth as silencing NbFLS2, which was about a ten times difference in colony forming units (cfu)/cm^2 for adapted *Pta* 6605. Moreover, plants silenced for *NbCSPR* were transformed more efficiently by *A. tumefaciens* than control silenced plants, but this effect was not seen for *NbFLS2*. These results may reflect the fact that *A. tumefaciens* possess a conserved CSP protein containing the csp22 motif, but its flagellin is not recognised (Felix *et al.*, 1999). Recognition of *A. tumefaciens* CSP may suggest why NbCSPR peptides were recovered from NbBAK1-GFP preparations prior to csp22 treatment. Restriction of *Agrobacterium*-mediated transformation by NbCSPR is not completely unexpected because EFR also limits transformation in *A. thaliana* and *N. benthamiana* (Zipfel et al., 2006). Overall, I conclude that NbCSPR is the CSP receptor in *N. benthamiana*.

NbSOBIR1 is required for accumulation and functionality of multiple RLPs, perhaps by stabilising the respective receptor or by providing transmembrane signalling capability (Jehle *et al.*, 2013a; Liebrand *et al.*, 2013; Zhang *et al.*, 2013; Zhang, LS *et al.*, 2014). Although NbCSPR bound NbSOBIR1 in directed tests after overexpression of both proteins, neither *NbSOBIR1* nor its close homolog *NbSOBIR1-like* were required for csp22-induced responses. I used the *TRV:SOBIR1(-like)* silencing construct described by Liebrand *et. al.* 2014 that targets both genes. Co-silencing of *NbSOBIR1* and *NbSOBIR1-like* was confirmed by the lack of Avr4/Cf4 induced hypersensitive response, as shown previously (Liebrand *et al.*, 2013). The same plants exhibited all csp22-induced responses. I further found that *SOBIR1* was dispensable for NbCSPR accumulation or function, as *TRV:SOBIR1(-like) N. benthamiana* plants expressed NbCSPR to a similar extent as control silenced plants. Furthermore, *A. thaliana sobir1-12* protoplasts transformed with *35S:NbCSPR-3xHA* were responsive to csp22 and showed comparable NbCSPR accumulation as Col-0 protoplasts. Thus, although NbSOBIR1 can interact with NbCSPR, this interaction is dispensable for csp22 recognition.

csp22 responses were far greater in plants that were transitioning to flowering than in younger plants. This may be due to an increase in *NbCSPR* expression, or several other regulatory mechanisms, which were not tested here. The difference is biologically significant because older plants were more resistant to *P. syringae* bacteria lacking flagellin, and were recalcitrant to transformation by *A. tumefaciens*. Both effects were reversed by *NbCSPR* silencing. Despite the fact that csp22 generally exhibited weaker PTI responses than flg22 (Felix *et al.*, 1999; Felix & Boller, 2003; Heese *et al.*, 2007), plants silenced for *NbCSPR* showed strikingly similar levels of bacterial growth when compared to *NbFLS2*-silenced plants. This was true for adapted and non-adapted pathogens. However, I cannot exclude differential silencing levels of each receptor gene.

The *Pta fliC*- strain, which does not activate FLS2, showed similar growth in *TRV:NbFLS2* silenced plants compared to *TRV:GFP* plants, as expected. Growth of this strain was slightly but significantly higher in *NbCSPR* silenced plants, again demonstrating a role for NbCSPR in immunity. Likewise, *Agrobacterium*-mediated transformation efficiency of *TRV:GFP* plants and *TRV:NbFLS2* was similar, whereas *TRV:NbCSPR* plants showed strongly enhanced GUS activity (Zipfel *et al.*, 2006) and expression of the arbitrary N2 protein (Saur *et al.*, 2015) after transient transformation. Similarly, resistance to *Xanthomonas oryzae* pv. *oryzae* mediated by the rice PRR Xa21 is developmentally regulated and dependent on the expression level of Xa21 (Century *et al.*, 1999; Park *et al.*, 2010).

The data further showed that younger plants can compensate their deficiency in csp22-induced resistance by flagellin perception and subsequent up-regulation of *NbCSPR* expression. This and potentially other flg22-induced modifications potentiated all csp22-induced responses tested here, which may explain why NbCSPR does not restrict growth of the flagellin-deficient strain *Pta* 6605 *fliC*- in four week old plants. As such, flagellin and CSP perception may occur sequentially. At the outset of a bacterial invasion, CSPs are possibly not instantaneously detectable, as they do not reside on the surface of the bacterial cells but could be freed from early lysing bacteria. Bacterial lysis may occur due to a turnover into stationary growth phase induced by flagellin-induced plant defence responses. Importantly, flagellin-induced plant defence responses up-regulate the expression levels of bacterial CSPs. As such, the up-regulation of *NbCSPR* by flagellin perception may allow the plant to prepare for subsequent release of bacterial components, including CSPs for the preservation of immune signalling over a longer period.

The transfer of *NbCSPR* to protoplasts of *A. thaliana* allowed csp22-dependent MAPK activation in the transformed cells, whereas protoplasts transformed with the empty vector were blind to the PAMP, as are wild type Col-0 plants. Importantly, signalling by NbCSPR in *A. thaliana* protoplasts required AtBAK1 or its close paralog AtBKK1, as *bak1-5/bkk1* protoplasts transformed with NbCSPR were non-responsive to csp22. The stable transgenic *35S:NbCSPR-5xMyc-5* line of *A. thaliana* initiated csp22-dependent production of ROS, MAPK activation and SGI. Importantly, the transformation efficiency for the *35S:NbCSPR-5xMyc-5* construct was approximately 10-fold lower than for the *35S:EV-5xMyc* construct and I only obtained five lines successfully transformed with *35S:NbCSPR-5xMyc*. The expression of the NbCSPR-5xMyc protein could only be detected in the *35S:NbCSPR-5xMyc-5* line and the protein did not accumulate strongly. Robust accumulation of the NbCSPR protein may be seedling lethal, potentially by the perception of *A. thaliana* host proteins with CSDs. CSDs of plant proteins are strikingly similar to CSDs of bacterial CSPs. In fact, the CSD of a *Nicotiana sylvestris* glycine-rich RNA-binding protein elicits defence response in tobacco suspension cultures (Felix & Boller, 2003). Developmental and flagellin-dependent control of CSP perception in *N. benthamiana* may thus avoid autoimmunity by perception of the host CSP.

Taken together, I identified the receptor for the bacterial PAMP csp22 using a novel biochemical approach. *NbCSPR* encodes a previously undescribed LRR-RLP that forms a complex with NbBAK1 after elicitation. It is required for csp22 response and for immunity to pathogens, and seems to comprise the receptor moiety for the PAMP. It is active in six week old plants, where it strongly restricts the growth of adapted and non-adapted pathogens, and transient transformation by *A. tumefaciens*. NbCSPR can be transferred into other plant species to confer bacterial CSP recognition to enhance

immunity to bacterial pathogens, as shown for *A. thaliana*. Interestingly, my results suggest a mechanism in which PAMP perception is coordinated temporally as prior flagellin perception potentiates NbCSPR mediated immunity in four week old plants.

4. Molecular events underlying non-host resistance to wheat stripe rust in *Nicotiana benthamiana* and *Arabidopsis thaliana*.

4.1. Introduction.

The economically most significant diseases of wheat are caused by rust fungi, which threaten wheat agriculture all over the world. There are three main rusts that attack wheat: *Puccinia graminis* causes stem (or black) rust, *Puccinia triticina* causes leaf (or brown) rust, and *Puccinia striiformis* causes stripe (or yellow) rust (Rapilly, 1979; Saari, 1985; Roelfs *et al.*, 1992). The differentiation by '*formae specialis* (*f. sp.*)' divides the rust species depending on the host which the respective rust is specialised upon and requires to complete the asexual lifecycle. Wheat stripe rust is caused by *Puccinia striiformis f. sp. tritici* (*Pst*). Within each *formae specialis*, there are specific races or strains called pathotypes that can infect different varieties of wheat (Anikster *et al.*, 2003). The name stripe rust derives from the yellow pustules that form along the surface of wheat leaves during a successful infection.

Rust fungi are obligate biotrophic basidiomycete fungi, meaning that they require a living host to complete their lifecycles, which can involve up to five different spore stages (Kolmer J, 2009). However, in Australia, stripe rust exclusively undergoes the asexual life-cycle. Briefly, *P. striiformis* urediniospores germinate under humid and low temperature conditions on the surface of the wheat leaf, to enter the plant apoplast through the stomata (Devallavieillepope *et al.*, 1995). From the infection hyphae, a so-called haustorium mother cell forms on the plant cells, from which the specialised haustorium feeding structure originates. Unlike the mother cell, the haustorium breaches the cell wall of the plant but is separated from the plant cytoplasm through the extra-haustorial matrix (EHM), which differentiates from the existing host plasma

membrane. The fungal hyphae ramify throughout the leaf developing haustoria as they grow. About two weeks post germination, new pustules develop on the leaf surface containing urediniospores. The new spores can then be easily distributed by wind (Nagarajan & Singh, 1990). Rusts can also re-infect the same host and form several new pustules from each infection site. Therefore, under optimal conditions, the life-cycle can be recurring many times during the cropping-season. During the off-season, stripe rust can survive near wheat fields on susceptible volunteer or self-sown wheat plants and also on grass species (Stubbs, 1985; Wellings & Mcintosh, 1990). In addition to their roles as a feeding structures, haustoria deliver effectors into the host cells (Kemen *et al.*, 2005; Rafiqi *et al.*, 2010). To date, the targets and virulence strategies of rust fungal effectors are unknown but like effectors from other pathogens, the effectors secreted by rusts are thought to be essential for virulence (Panstruga & Dodds, 2009). From studies on other patho-systems, it seems likely that the rust effectors manipulate host immune responses by targeting a variety of defence mechanisms that collectively underlie PTI. Especially responses derived from plant receptors with extracellular Lysin motifs (LysM or LYM), recognising the fungal cell wall component chitin, are involved in PTI to fungal pathogens. Rust effectors may thus target plant chitin receptors and other PRRs and to promote pathogenicity as this constitutes the first layer of pathogen recognition.

Certain wheat isolates and relatives have evolved resistance genes that recognise specific rust effectors, leading to a cell death response that abrogates the infection (Bent & Mackey, 2007). Breeding for such resistant varieties of wheat is an effective way to control the pathogen until such time as the appearance of races that overcome these *R* genes. This is due in part to the enormous number of spores produced during the lifecycle coupled with a constant mutation rate. Genetic control of this

devastating pathogen is thus extremely difficult as both the pathogen and the host are complex, and genetic resources identified in model interactions cannot be easily utilised. Overall, the molecular events that underlie *Pst* pathogenicity are only beginning to be described (Garnica *et al.*, 2013). Current research focuses on identification of effectors from economically important rust isolates. It is hoped that these can be used as probes to identify new *R* genes, which can be deployed into commercial wheat cultivars.

A central tenet of plant pathology is that most plants are resistant to most pathogens, a phenomenon that is referred to as non-host resistance (NHR). The mechanisms underlying NHR are hard to break down, but generally it is thought that PRRs that have been identified in non-host systems are operative in hosts, as described for a number of PRRs (Lacombe *et al.*, 2010; Fradin *et al.*, 2011; Holton *et al.*, 2015; Schoonbeek *et al.*, 2015). Thus, identification of *NHR* genes could be a valuable source of resistance genes for cropping species. As such, the molecular mechanisms underlying NHR to *Pst* must be determined. The obligate biotrophic lifestyle of *Pst* may indicate that NHR results from physiological and nutritional incompatibilities of *Pst* and the non-host plant. Alternatively, a combination of physiological incompatibilities and active host immune responses may be required to successfully battle *Pst* infection. The aim of this study is to identify molecular mechanisms underlying NHR in *Arabidopsis thaliana* and *Nicotiana benthamiana* active against wheat stripe rust, with an emphasis on identifying PRRs that recognise rust PAMPs from these species. For this approach to be successful, the ability of the non-host species to identify *Pst* and initiate defence responses has to be detectable. Here I describe the recognition of unknown PAMPs derived from *Pst* urediniospores in the non-host species *A. thaliana* and *N. benthamiana*. I confirmed the existence of *Pst* PAMPs and attempted the identification of respective non-host PRRs. I

have identified candidate PRRs in *A. thaliana,* which may now be tested for their involvement in NHR to *Pst*.

4.2. Results.

4.2.1. *Puccinia striiformis f. sp. tritici* (*Pst*) induces PTI responses in *Nicotiana benthamiana* and *Arabidopsis thaliana.*

I first aimed to investigate the recognition and responsiveness of *A. thaliana* and *N. benthamiana* to potential PAMPs from *Pst*. On wheat, a new *Pst* infection cycle starts with urediniospores germinating on the leaf surface. I thus used urediniospores to determine the ability of *Pst* elicitors to trigger typical PTI responses on non-hosts. In order to release potential PAMPs from the robust spores, I ground the *Pst* spores in liquid nitrogen, extracted components with sterile water and removed insoluble debris through centrifugation and subsequent sterile filtration. I named the resulting extract 1x spore extract (SE). When 1x SE was infiltrated into *N. benthamiana* leaves, leaves developed a weak cell death response upon treatment with *Pst* spore extract (SE). within 24 hours after infiltration (Figure 4.1). To test responsiveness to SE in *A. thaliana*, I chose seedling growth inhibition (SGI) as an initial and reliable assay to determine the presence of bioactive PAMPs within the SE. PAMP-induced seedling growth inhibition (SGI) may be due to a negative regulation of BR perception (Albrecht *et al.*, 2012; Belkhadir *et al.*, 2012; Lozano-Duran *et al.*, 2013) and lead to the discovery of PTI components previously (Zipfel *et al.*, 2006; Chinchilla *et al.*, 2007b). I used 2x liquid MS media and diluted the media with SE to 1x MS media, resulting in a final concentration of 0.5x SE. *A. thaliana* Col-0 seedlings grown in MS media supplemented with 0.5x SE showed impaired root growth relative to mock-treated (sterile water) controls (Figure 4.2).

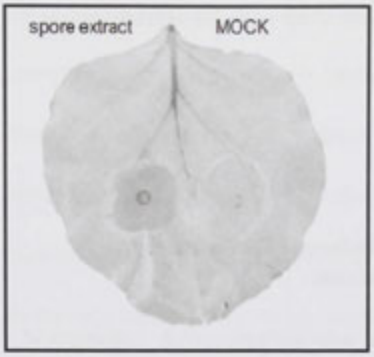

Figure 4.1: *N. benthamiana* responds to *Puccinia striiformis* f.sp. *tritici* (*Pst*) spore extract (SE). SE or a sterile water control (MOCK) was syringe-infiltrated into *N. benthamiana* leaves. The spore extract causes a weak cell death response that could be detected 24 h after infiltration. Picture was taken using a Bio-Rad Gel doc in reflective mode to detect contrast.

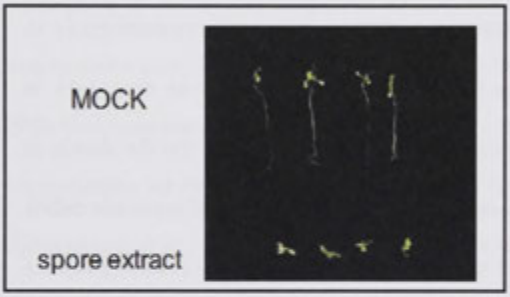

Figure 4.2: SE inhibits growth of *Arabidopsis thaliana* (Col-0) seedlings. Seedlings grown for one week in liquid MS media supplemented with 0.5x spore extract (SE) were impaired in root growth when compared to seedlings grown without spore extract (MOCK).

To quantitate the responses elicited by SE, I determined the production of reactive oxygen species (ROS) in response to SE over time (Keppler *et al.*, 1989). Both *N. benthamiana* and *A. thaliana* responded to SE with the production of ROS starting four hours post elicitation and the ROS bust continued for several hours (Figure 4.3). The ROS burst was only weakly stronger when plants were treated with SE compared to MOCK treated plants. To determine if the ROS burst was not triggered by stress responses other than pathogen elicitors, I used the *A. thaliana rbohD* mutant line. This line lacks a functional NADPH oxidase, which is specifically activated in response to PAMP perception (Torres *et al.*, 2002). The *rbohD* mutant did not produce ROS in response to SE (Figure 4.4) and I therefore conclude that the weak production of ROS is specific to the recognition of SE components in *A. thaliana*.

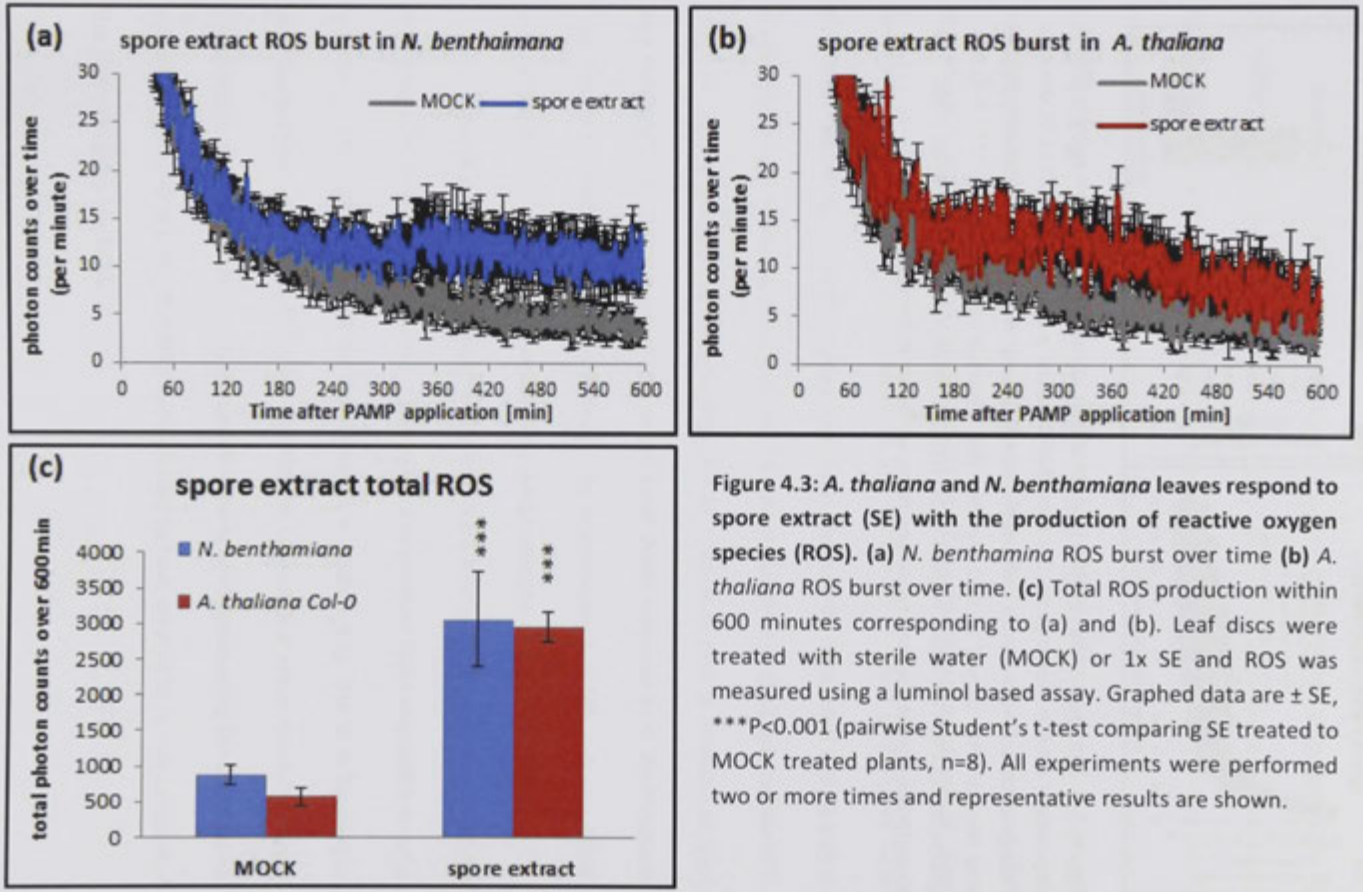

Figure 4.3: *A. thaliana* and *N. benthamiana* leaves respond to spore extract (SE) with the production of reactive oxygen species (ROS). (a) *N. benthamina* ROS burst over time **(b)** *A. thaliana* ROS burst over time. **(c)** Total ROS production within 600 minutes corresponding to (a) and (b). Leaf discs were treated with sterile water (MOCK) or 1x SE and ROS was measured using a luminol based assay. Graphed data are ± SE, ***P<0.001 (pairwise Student's t-test comparing SE treated to MOCK treated plants, n=8). All experiments were performed two or more times and representative results are shown.

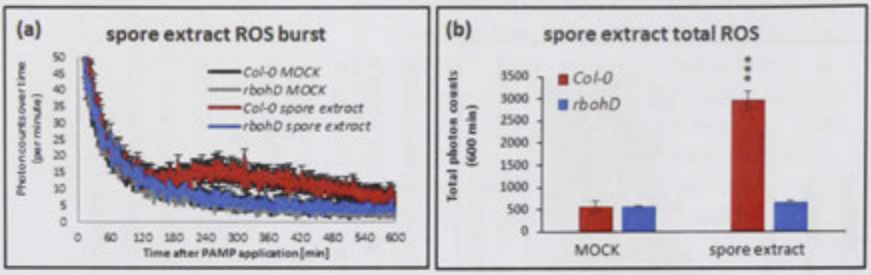

Figure 4.4: The production of ROS in *A. thaliana* in response to spore extract (SE) is dependent on the *rbohD* gene. Col-0 or *rbohD* leaves were treated with 1x SE prior to ROS detection. Photon count reflects the production of ROS over time (per minute) **(a)** and over a total period of 600 minutes **(b)**. Graphed data are ± SE, *** P<0.001 (pairwise Student's t-test comparing SE treated to MOCK treated plants, n=8). The experiment was performed twice and representative results are shown.

4.2.2. *Pst* spore extract contains several PAMPs perceived by *Nicotiana benthamiana* and *Arabidopsis thaliana*.

Bacterial suspensions elicit higher PTI responses after heat treatment (Felix *et al.*, 1999; Felix & Boller, 2003; Kunze *et al.*, 2004; Zipfel *et al.*, 2004; Gimenez-Ibanez *et al.*, 2009b). Similarly, the production of ROS in *A. thaliana* by SE increased 4-fold when the extract was heat-treated (ht) beforehand (Figure 4.5). The same phenomenon was found for *N. benthamiana* leaves (data not shown). Interestingly, heat-treated SE did not trigger cell death on *N. benthamiana* leaves (Figure 4.7). These observations suggest that one or more heat-stable and one or more heat-liable PAMPs are present in SE. The heat-stable PAMP(s) may be proteinacous and disruption of intact proteins by heat treatment may allow the plant to access the respective PAMPs. Consistent with this idea, treatment of heat-treated spore extract with 1 mg/ml Proteinase K (PK) reduced the ROS burst elicited by the SE in *A. thaliana* (Figure 4.5). I conclude that SE contains at least one heat-labile component, which can cause a cell death response in *N. benthamiana* and that heat-treated SE contains at least one proteinaceous PAMP and one PAMP resistant to Proteinase K, both of which elicit the production of ROS in *A. thaliana*.

To exclude that chitin perception by AtCERK1 is a ROS-eliciting component of the SE, I tested the *A. thaliana* line *cerk1-2* and found it to produce ROS comparably to wild-type Col-0 after treatment with the heat-treated SE (Figure 4.6). The SE is based on a water-extraction protocol and is thus unlikely to contain the water-insoluble fungal PAMP chitin. Together with the unchanged ROS burst when comparing Col-0 and *cerk1-12* lines, I can conclude that the ROS burst elicited by heat-treated SE is independent of the chitin receptor AtCERK1.

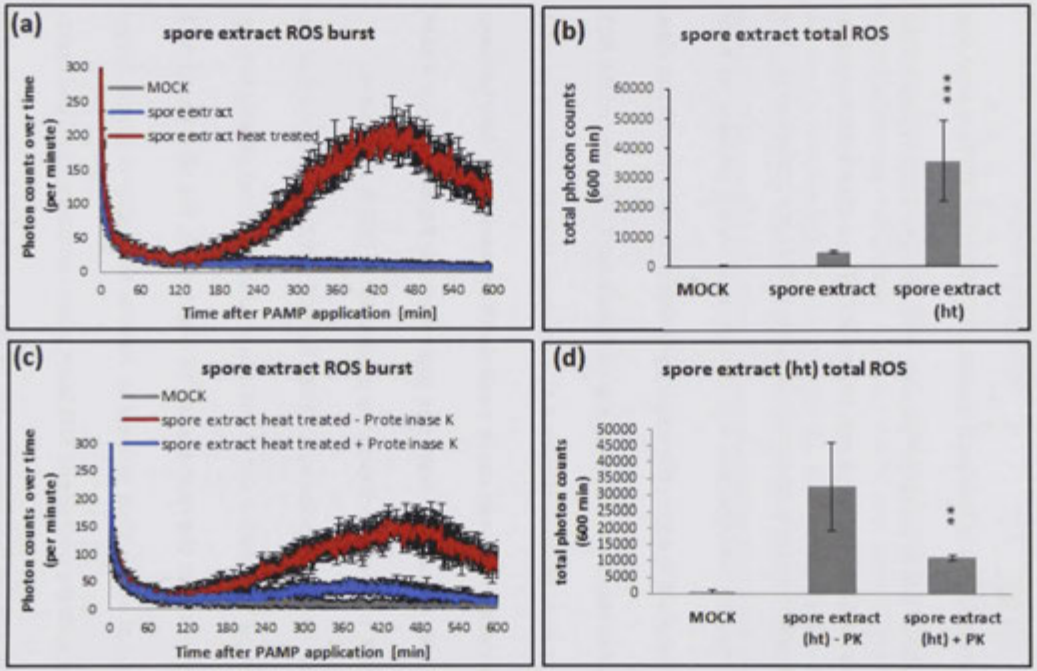

Figure 4.5: Heat treatment of spore extract (SE) increases and treatment with Proteinase K (PK) decreases ROS production in *A. thaliana*. (a, b) SE was either not treated, or heat-treated at 98°C for 10 minutes before cooling to room temperature. **(c, d)** SE was either not treated, or treated with 1 mg/ml PK overnight at room temperature. **(a, c)** SE-induced production of ROS over time **(b, d)** Total ROS induced by treated or untreated SE after 600 min. Graphed data are ± SE, ** P<0.01, *** P<0.001 (pairwise Student's t-test comparing SE treated to MOCK treated plants, n=8). The experiment was performed more than three times and representative results are shown.

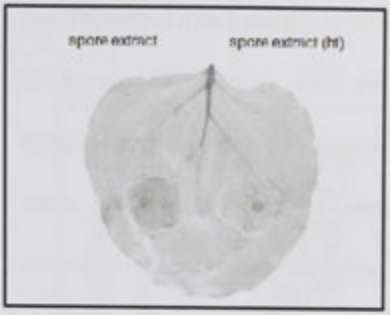

Figure 4.7: Heat treatment (ht) of spore extract (SE) diminishes cell death response in *N. benthamiana* leaves. SE was either not treated, or heat treated at 98°C for 10 minutes and cooled to room temperature, before SE was syringe-infiltrated into *N. benthamiana* leaves. The response was visualised 24 h after infiltration. Picture was taken using a Bio-Rad Gel doc in reflective mode to detect contrast.

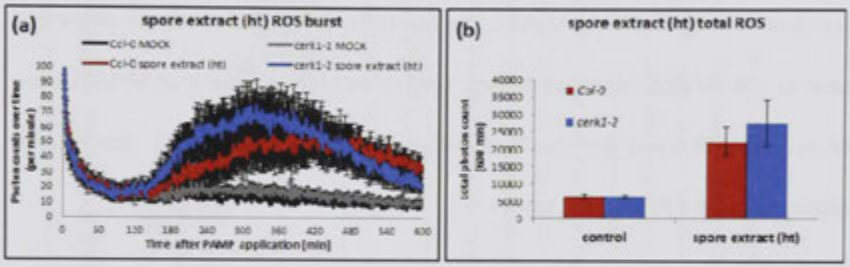

Figure 4.6: The production of ROS in *A. thaliana* in response to SE is independent of the AtCERK1 receptor. *A. thaliana* Col-0 or *cerk1-2* leaves were treated with SE (heat treated, ht), and the production of ROS measured **(a)** over time (per minute) and **(b)** over a total period of 600 min. The experiment was performed twice and representative results are shown.

4.2.3. The perception of PAMPs present in *Pst* spore extract is partly BAK1 dependent.

BAK1 is required for several PRRs that recognise proteinacous PAMPs. As such, one or more PAMPs in the heat-treated SE may thus elicit ROS, which is dependent on BAK1 or its close homolog BKK1 (Roux *et al.*, 2011). Indeed, the *bak1-5/bkk1 A. thaliana* line was impaired in the response to SE treatment in several independent experiments (Figure 4.8). Importantly, untreated SE caused a slight but insignificant reduction in the production of ROS in *bak1-5/bkk1* plants when compared to Col-0 (Figure 4.9), suggesting the presence of at least one BAK1-dependent PRR and one BAK1-independent PRR recognising spore extract PAMPs. Notably, *N. benthamiana* plants

silenced for *NbBAK1* initiated a cell death response when infiltrated with untreated (not heat treated) spore extract (Figure 4.10). Thus, the heat-labile elicitor(s) that caused the weak cell death response in *N. benthamiana* is/are likely to be detected by a receptor that functions independently of NbBAK1. *TRV:NbBAK1* plants did also not show decreased ROS burst in response to heat-treated SE when compared to control silenced plants (*TRV:GFP,* data not shown), suggesting that the SE-induced ROS burst of *N. benthamiana* is independent of NbBAK. The same plants showed a strongly decreased response to 100 nM flg22 (data not shown). Yet, I cannot fully exclude that NbBAK1 plays a role in the SE-induced cell death response, as NbBAK1 transcripts may not be sufficiently silenced *TRV:NbBAK1* plants.

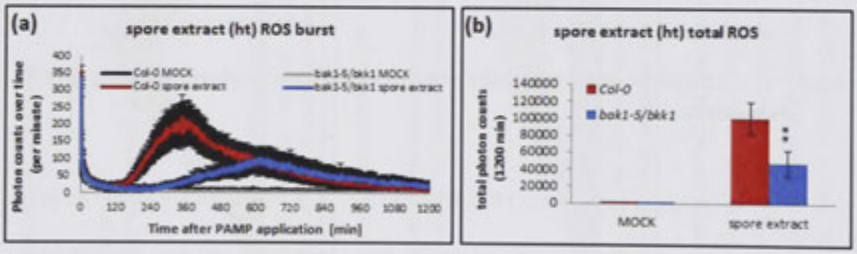

Figure 4.8: The ROS burst elicited by heat treated (ht) spore extract (SE) is dependent on *BAK1* and/or *BKK1*. (a) ROS burst elicited by SE (ht) over time in *A. thaliana* Col-0 and *bak1-5/bkk1* leaves. **(b)** Total ROS production within 600 minutes corresponding to **(a)**. Leaf discs were treated with sterile water (MOCK) or SE (ht). Graphed data are ± SE, ** P<0.01, (pairwise Student's t-test comparing *bak1-5/bkk1* to Col-0 plants, n=8). The experiment was performed four times and representative results are shown.

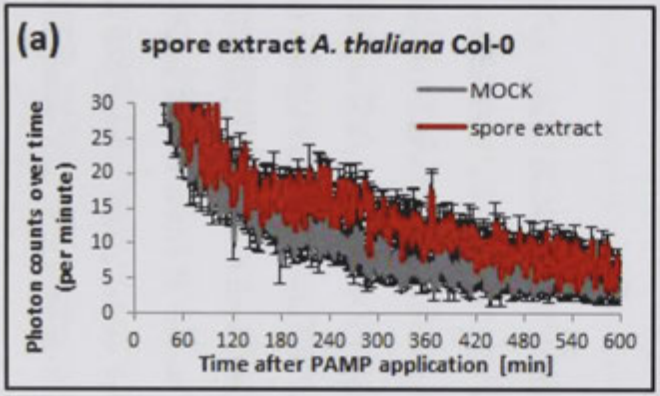

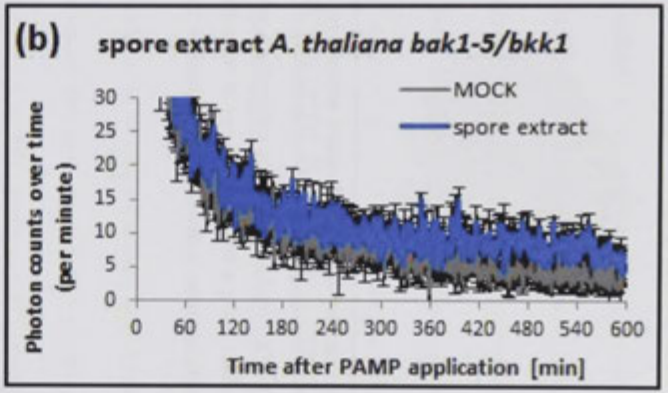

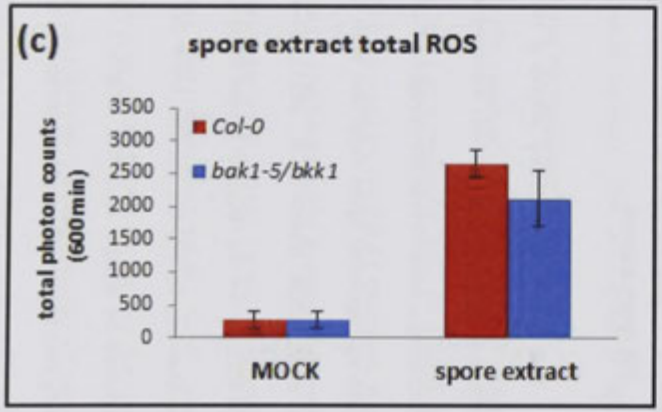

Figure 4.9: The ROS burst elicited by untreated spore extract (SE) is not dependent on *bak1* or *bkk1*. **(a)** *A. thaliana* Col-0 ROS burst over time, elicited by spore extract (not heat treated). **(b)** *A. thaliana bak1-5/bkk1* ROS burst over time, elicited by spore extract (not heat treated). **(c)** Total ROS production within 600 minutes corresponding to **(a)** and **(b)**. Leaf discs were treated with sterile water (MOCK) or SE. Experiments were performed two or more times and representative results are shown.

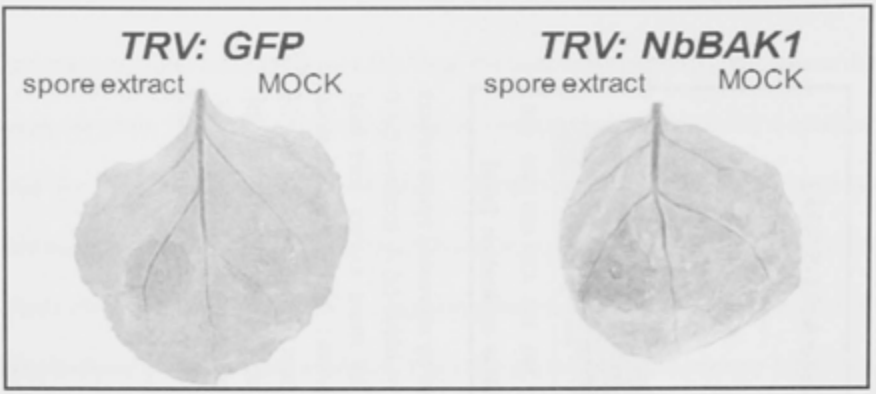

Figure 4.10: The weak cell death response caused by untreated spore extract in *N. benthamiana* is independent of *NbBAK1*. *N. benthamiana* leaves were silenced by VIGS for either *GFP* (*TRV:GFP*, control) or *NbBAK1* (*TRV:NbBAK1*) before infiltration with spore extract (not heat treated). Picture was taken using a Bio-Rad Gel doc in reflective mode. The experiment was performed twice with representative results shown.

4.2.4. Identification of BAK1-interacting proteins from leaves responding to *Pst* spore extract.

The use of *A. thaliana* allows a relatively straightforward strategy for the identification of novel components involved in PTI. In fact, BAK1 was identified from *A. thaliana* using a collection of homozygous T-DNA insertion mutants for RK and RLP genes that are up-regulated upon induction with bacterial PAMPs (Chinchilla *et al.*, 2007b; Wang *et al.*, 2008; Danna *et al.*, 2011). Using this collection of T-DNA insertion lines (Table 4.1), I screened receptor kinase (RKs) and receptor-like protein (RLP) mutants for responsiveness to PAMPs derived from SE. Because SE inhibits seedling growth as determined by weight and root length, I used seedling growth inhibition (SGI) as a primary test to identify mutants incapable of responding to SE. Such mutants would likely carry a mutation in a receptor essential for SE recognition. The obvious

disadvantage of this approach is that the spore extract likely contains more than one PAMP, consequently a clear phenotype may be challenging to identify. For example, the *bak1-5/bkk1 A. thaliana* line was impaired in htSE-mediated SGI (Figure 4.11 a and b) in two independent experiments where 0.5 x htSE was used. In another two independent experiments where a higher htSE concentrations was used, a difference between Col-0 and *bak1-5/bkk1* was not observed (Figure 4.11c and d). The This approach is thus not ideal to identify a PRR recognising an elicitor(s) from SE. Likewise, although I could identify six candidate lines in the first-round screen of the T-DNA insertion lines for non-responsiveness to SE (Table 4.1), none of these could be confirmed after repeating the experiment (data not shown). Interestingly, inhibition of root growth did not always correspond to decreased weight of the respective seedling. A slight but significant SE-dependent decrease in SGI and seedling weight could be detected only for the *At4g13900-1*, *AT2G45910-1* and *AT1G66980-2* insertion lines. Again, these results could not be confirmed when the experiments were repeated. The production of ROS in response to untreated and heat-treated SE was not measured for these lines.

In an alternative approach to identify PRR candidates that recognise a *Pst* PAMP, I used the method developed in Chapter 3 'BAK1 as a molecular bait'. As described in Chapter 3, I included the BAK1-5 mutant. BAK1-5 contains the C508Y mutation, shows higher affinity to several receptors than AtBAK1, and hence might provide a better bait for the unknown PRR(s) (Chapter 3) (Schwessinger *et al.*, 2011). I grew transgenic *A. thaliana bak1-4/pAtBAK1:AtBAK1-YFP* and *bak1-4/pAtBAK1:AtBAK1-5-YFP* plants (Schwessinger, PhD thesis University of East Anglia, 2011) to seedling stage under sterile conditions. The four-week old seedlings (150 per treatment) were infiltrated with sterile water or 1x heat treated SE, and kept on a pre-wetted filter paper in a large Petri dish

for four hours, at which point the SE-dependent ROS burst peaked. Seedlings were harvested for protein extraction and subsequent co-immunoprecipitation (coIP) using anti-GFP to isolate AtBAK1 or AtBAK1-5 fused to the YELLOW FLUORESCENCE PROTEIN (YFP). Purified proteins were released from the matrix by boiling in SDS loading buffer, and separated on one-dimensional SDS-PAGE gels. In three independent experiments, AtBAK1 and AtBAK1-5 was not strongly enriched after IP as detected by Coomassie-based staining (Safe stain, life technologies) of the gel-separated proteins. In fact, on the digitalised picture the band representing AtBAK1 and AtBAK1-5 was barely visible (Figure 4.13). Despite this, I cut the gel into slices as indicated (Figure 4.13) and extracted the proteins contained within them for liquid-chromatography mass-spectrometry (LC-MS/MS) analysis (the mass spectrometer was run by Dr. Jan Sklenar at The Sainsbury Laboratory Proteomics facility). I ranked the identified proteins according to their presence and abundance in samples treated with spore extract when compared to sterile water treated samples, with specific emphasis on receptor proteins (Table 4.2). The full summary of all four independent experiments can be found in the Attachment (Attachment 6).

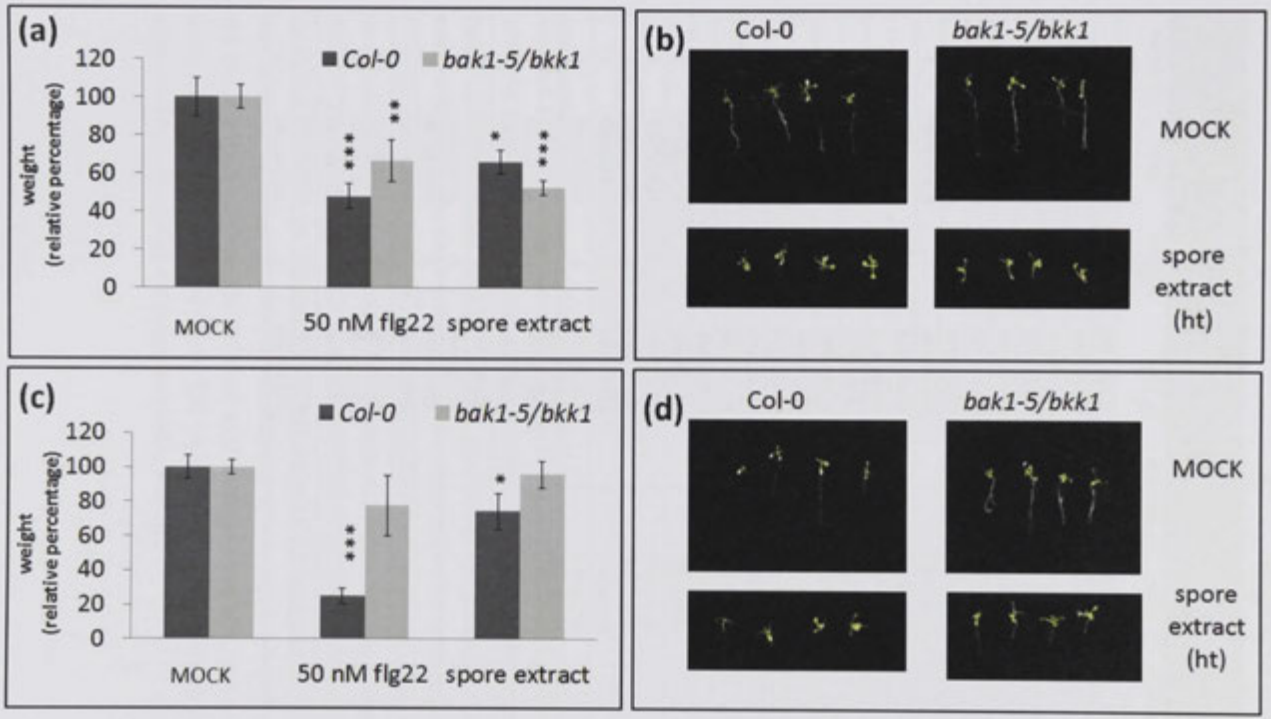

Figure 4.11: *Pst* spore extract (SE) causes growth inhibition of *A. thaliana* Col-0 seedlings (SGI), partly dependent on *bak1* and/or *bkk1*. *A. thaliana* Col-0 or *bak1-5/bkk1* seedlings were treated with sterile water (MOCK), 0.5x SE or 50 nM flg22. **(a and b)** Experiment 1: 0.5x SE and 50 nM flg22 caused SGI of Col-0 plants and *bak1-5/bkk1* mutants. **(c and d)** Experiment 2: 1x SE and 50 nM flg22 caused SGI of Col-0 plants, but not *bak1-5/bkk1* mutants. Graphed data are ± SE, * P<0.05, ** P<0.01, ** P<0.001 (pairwise Student's *t*-test comparing treated to untreated plants, n=12). Experiments were performed four times and either result was obtained twice.

Table 4.1: List of T-DNA insertions lines mutated in genes encoding LRR-RLKs and LRR-RLPs (Wang et al., 2008 and Danna et al., 2011) used to screen for non-responsiveness to Pst SE by SGI.

non RD LRR-RLKs				LRR-RLPs			
gene	Insertion line	gene	Insertion line	gene	Insertion line	gene	Insertion line
AT1G33260	1	AT4G26540	1	AT1G07390	1	AT2G33050	1
AT1G52540	1	AT4G26540	2	AT1G07390	2	AT2G33060	1
AT1G66910	1	AT4G32300	1	AT1G07390	3	AT2G33080	1
AT1G66920	2	AT5G05160	1	AT1G17240	1	AT2G42800	1
AT1G66930	1	AT5G05160	2	AT1G17250	1	AT2G05360	1
AT1G66980	1	AT5G18910	1	AT1G17250	2	AT2G05360	2
AT1G66980	2	AT5G20050	1	AT1G28340	1	AT2G05370	1
AT1G67000	1	AT5G20480	1	AT1G28340	1	AT2G05370	2
AT1G68400	1	AT5G24080	1	AT1G45616	1	AT3G05660	1
AT1G80870	1	AT5G24080	2	AT1G45616	1	AT3G05660	2
AT1G80870	2	AT5G35370	1	AT1G47890	1	AT3G11010	1
AT2G13800	1	AT5G35370	2	AT1G47890	2	AT3G11080	2
AT2G19130	1	AT5G38240	1	AT1G54480	1	AT3G23120	1
AT2G19130	2	AT5G38260	2	AT1G58190	1	AT3G24900	1
AT2G24130	1	AT5G38280	1	AT1G58190	2	AT3G24954	1
AT2G24130	2	AT5G39020	2	AT1G65380	1	AT3G25010	1
AT2G30940	1	AT5G39030	1	AT1G65380	2	AT3G25010	2
AT2G31880	1	AT5G46330	1	AT1G71390	1	AT3G25020	1
AT2G31880	2	AT5G51770	1	AT1G71400	1	AT3G25020	2
AT2G45590	1	AT5G51770	2	AT1G71400	2	AT3G28890	1
AT2G45910	1	AT5G56040	1	AT1G74170	1	AT3G49750	1
AT3G09780	1	AT5G60900	1	AT1G74170	2	AT3G53240	1
AT3G09780	2	AT5G60900	2	AT1G74180	1	AT4G13810	1
AT3G15890	1			AT1G74190	1	AT4G13880	1
AT3G26700	1			AT1G74190	2	AT4G13900	1
AT3G47090	1			AT1G74200	1	AT4G13900	2
AT3G47090	2			AT1G80080	1	AT4G13920	1
AT3G47110	1			AT1G80080	2	AT4G18760	1
AT3G47570	1			AT2G15040	1	AT4G27060	2
AT3G47570	2			AT2G25440	1	AT4G40170	1
AT3G47580	1			AT2G25470	1	AT4G45770	1
AT4G18250	1			AT2G32680	1	AT4G65830	1
AT4G18250	2			AT2G33020	1	AT3G05360	1
AT4G25390	1			AT2G33030	1	AT3G05360	2

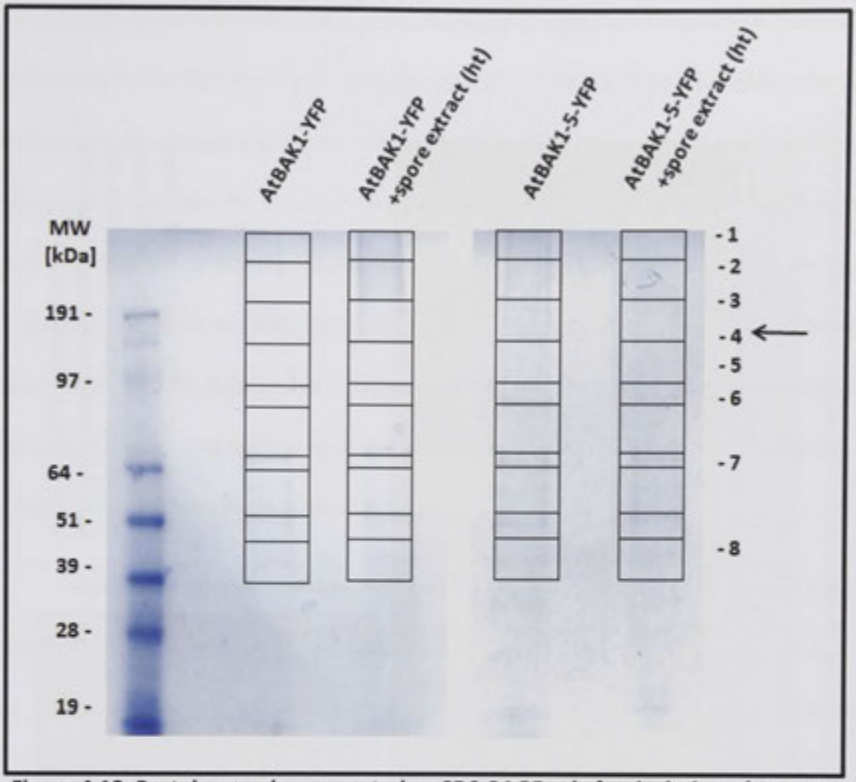

Figure 4.12: Protein samples separated on SDS-PAGE gel after isolation of AtBAK1-YFP and AtBAK1-5-YFP by anti-GFP pull down. *bak1-4/pAtBAK1:AtBAK1-YFP* and *bak1-4/pAtBAK1:AtBAK1-5-YFP* seedlings were infiltrated with sterile water or heat treated (ht) extracts, and incubated for four hours before freezing in liquid nitrogen. Proteins were extracted and AtBAK1-YFP or AtBAK1-5-YFP purified by anti-GFP pull downs. Isolated proteins were removed from the beads and separated on a 4-12% SDS gel (life technologies) and stained with Safe stain (life technologies). Proteins were cut from gel as indicated by black squares for subsequent LC-MS. Arrow indicates the expected position of the AtBAK1-YFP or AtBAK1-5-YFP protein(s) on the gel at a molecular weight (MW) of approximately 100 kDa. Gel was digitalised using a Bio-Rad Gel doc in gel mode. The highlighted squares indicate the gel pieces subjected to subsequent mass-spectrometry analysis.

Table 4.2: List of proteins with their corresponding numbers of unique peptides identified by LC-MS/MS (95% peptide and protein probability with at least two peptides identified in all samples) of proteins that co-precipitated with AtBAK1-YFP or AtBAK1-5-YFP after treatment with

(a)

Annotated as	Accession number	Size	BAK1	BAK1 + spore extract	BAK1-5 -	BAK1-5 + spore extract	BAK1	BAK1 + spore extract	BAK1-5 -	BAK1-5 + spore extract	BAK1	BAK1 + spore extract	BAK1-5 -	BAK1-5 + spore extract
BAK1	AT4G33430	68 kDa	22	18	29	23	32	36	35	23	21	20	19	21
BIP	AT5G42020	74 kDa	58	50	51	40	56	68	65	73	66	21	73	74
BSK1	AT4G35230	57 kDa			1					6				
BIR1	AT5G48380	69 kDa					1		1	5				
BIR3	AT3G28450	65 kDa	3	2	3	3	5	1	3	2			2	2
BIR2	AT1G27190	67 kDa	11	8	5	4	17	5	14	16	2	3	10	6
Protein of unknown function	AT2G32240	153kDa					1	7				2	1	3
LRR-RK	AT2G04300 or At2g28960	95 kDa	1	1		1		1		2				
LRR-RK	AT3G14840	112 kDa			1					2				
LRR-RK	AT4G08850	115 kDa			3	1				2				
LRR-RLP	AT1G33600	52 kDa							1	4				
LRR-RLP	AT1G33590	52 kDa			3	3	7		12	15	1		5	

(b)

Annotated as	Accession number	Size	Total coverage	BAK1	BAK1 + spore extract	BAK1-5 -	BAK1-5 + spore extract
BAK1	AT4G33430	68 kDa	> 57%	75	74	83	67
BIP	AT5G42020	74 kDa	> 80 %	180	139	189	187
BSK1	AT4G35230	57 kDa	> 17%	0	0	1	6
BIR1	AT5G48380	69 kDa	> 17%	1	0	1	5
BIR3	AT3G28450	65 kDa	>34 %	8	3	8	7
BIR2	AT1G27190	67 kDa	> 12 %	30	16	29	26
Protein of unknown function	AT2G32240	153kDa	>15%	1	9	1	3
LRR-RK	AT2G04300 or AT2G28960	95 kDa	2 %	1	2	0	3
LRR-RK	AT3G14840	112 kDa	6 %	0	0	1	2
LRR-RK	AT4G08850	115 kDa	4 %	0	0	3	3
LRR-RLP	AT1G33600	52 kDa	13 %	0	0	1	4
LRR-RLP	AT1G33590	52 kDa	> 50%	8	0	20	18

[2] **(a)** List represents results from three independent experiments. **(b)** Peptides identified for the respective protein in the individual samples were pooled from the three individual experiments.

Throughout all of the experiments, the number of AtBAK1 peptides identified was comparable in the water and SE treated samples (Table 4.2). Despite low abundance of proteins on the SDS-PAGE gels, isolation of AtBAK1-YFP and AtBAK1-5-YFP lead to the co-purification of several proteins. Known interactors of AtBAK1 are listed in Table 4.2. Additionally, possible *Pst* receptor candidates and one protein with unknown function (AT2G32240), which showed abundant presence in the SE-treated samples, are listed and specified in bold. Notably, no transmembrane receptors that possess an ectodomain other than an LRR domain were identified. The protein identified with the highest peptide coverage is a binding immunoglobulin protein (BIP), which belongs to the 70 kiloDalton heat shock protein (Hsp70) family.

I identified peptides corresponding to the known BAK1-interacting proteins BIR1, BIR2 and BIR3, as well as from BR-SIGNALING KINASE1 (BSK1) (Tang *et al.*, 2008; Gao *et al.*, 2009; Shi *et al.*, 2013; Halter *et al.*, 2014). I detected a lower number of AtBIR2 corresponding peptides after SE treatment of AtBAK1 IP samples (30 BIR2 peptides for sterile water treated samples, 16 peptides for SE-treated samples). This release was less distinct for AtBAK1-5 IP samples (29 BIR2 peptides for sterile water treated samples, 26 peptides for SE-treated samples). Similar observations have been made previously using flg22 (Halter *et al.*, 2014). Several proteins were represented by a higher number of unique peptides in samples treated with extracts relative to the water control. For a protein with unknown function (AT2G32240), 12 peptides were identified in samples treated with spore extract, whereas only two peptides were found in water treated samples. Another protein, for which a higher number of peptides was found in SE-treated samples (five peptides versus one peptide in samples treated with sterile water), is a LRR-RLK (corresponds to either AT2G04300 or AT2G28960), albeit with sequence coverage of only 2%. All other LRR receptors (AT3G14840, AT4G08850, AT1G33600 and

AT1G33590), were only identified in AtBAK1-5 samples. AtBAK1-5 interacts constitutively with AtFLS2 (Schwessinger *et al.*, 2011) and NbBAK1-5 also binds NbCSPR in the absence of its ligand csp22 (Chapter 3). Thus, the co-isolation of LRR-RLKs by AtBAK1-5 IP does not indicate a SE-specific interaction. As such, the LRR-RLK encoded either by At2g04300 or At2g28960 is the best receptor candidate for components of *Pst* SE. Importantly, according to gene expression data on The Arabidopsis Information Resource (TAIR), AT2G04300 is expressed in the plant sperm cells and AT2G28960 in hypocotyl, pedicel, plant embryo, root, sepal and the stem tissues. As such, neither is likely to act as a fungal PRR. Because a clear PAMP-perceiving PRR candidate for SE could not be identified, the attempt to do so was halted. Further steps to identify such an important receptor and potential improvements in the experimental set-up are discussed below.

4.3. Discussion.

Here, I described the recognition of spores from the wheat stripe rust pathogen *Pst* by the non-host species *A. thaliana* (*Brassicaceae*) and *N. benthamiana* (*Solanaceae*). Although belonging to different families, both plants showed strong similarities in their response to untreated extracts from *Pst* urediniospores as shown by the ROS production profile. The ROS burst assay has been successfully used as a robust, rapid, and highly sensitive method for the detection of PAMP perception by plant cells (Keppler *et al.*, 1989). Additionally, I observed inhibition of seedling growth when *A. thaliana* seedlings were grown in media supplemented with SE, and *N. benthamiana* plants responded to SE with a weak cell death.

Whereas both species react to bacterial extracts or pure PAMPs within seconds to minutes (Felix *et al.*, 1999; Zipfel *et al.*, 2006; Heese *et al.*, 2007; Petutschnig *et al.*, 2010), ROS production after SE treatment started about two hours after extract application and consistently lasted for several hours, with the highest measurable production of ROS at about four to six hours. Thus, the ROS production triggered by *Pst* SE varies in kinetics from responses observed from most known PAMPs. However, the purified elicitor INF1 from the oomycete *Phytophthora infestans* induces a similarly late ROS burst in *N. benthamiana* (Chaparro-Garcia et al., 2011). Plant enzymes potentially process or modify SE derived molecules in the apoplast, which cause the host recognition of those SE components. Such an example has however not been described previously. It is also possible that eliciting host components (DAMPs) are produced in response to SE. *In vivo*, immune responses initiated by DAMPs are a secondary event to microbial detection, and may consequently elicit a delayed defence response (Denoux *et al.*, 2008; Galletti *et al.*, 2008). The production of host DAMPs, as a cause of the delayed ROS burst is thus possible. Notably, initiation of SE induced defence signalling directly after treatment of the plant with SE may not involve the production of ROS. Monitoring additional SE-induced host defence responses such as activation of Mitogen-activated protein kinases (MAPKs) and up-regulation of pathogen-induced genes (PIGs) over time, may clarify this question.

Here, heat treatment of the *Pst* SE caused a robust increase of ROS production in both *A. thaliana* and *N. benthamiana*. When the proteinacous bacterial PAMPs flagellin, cold-shock-protein and elongation factor TU were identified, their ability to elicit extracellular alkalization of plant suspension cultures was also highly enhanced when bacterial cells were heat-treated (Felix *et al.*, 1999; Felix & Boller, 2003; Kunze *et al.*, 2004; Zipfel *et al.*, 2004; Gimenez-Ibanez *et al.*, 2009b). These observations may be due

to a release of the respective PAMPs from the bacterial cells or *Pst* spores or from tertiary protein structures during heat-treatment. Heat-treatment however abolished the cell death response on *N. benthamiana,* suggesting that the cell death is triggered by one or more heat-labile PAMPs. Those PAMP(s) may thus require secondary structures, disrupted by heat-treatment. Whether these components are Proteinase K-resistant remains unknown and a statement about its nature as a protein cannot be made at this stage. In *A. thaliana,* the ROS burst induced by SE originates partly from the recognition of proteinacous components, as treatment of the spore extract with Proteinase K reduced but did not abolish the elicitor activity of the extract. Notably, under the conditions used, PK can inactivate the elicitor activity of 10 µM flg22 (data not shown), and treatment with higher concentrations of PK did not abolish the SE-dependent ROS burst completely (data not shown). Therefore, the incomplete loss of elicitor activity after PK treatment is probably not a result of insufficient PK treatment, and suggests the presence of at least one non-proteinaceous (or PK-resistant) PAMP in the extract. Additional evidence for the presence of more than one PAMP in SE comes from the observation, that the SE-mediated ROS burst is only party dependent on *bak1* and/or *bkk1* in *A. thaliana*. In a complementary approach, the ability of SE to inhibit seedling growth in *A. thaliana* was also partly dependent on the co-receptor BAK1. This result was only observed in two out of four independent experiments. This ambiguity may result from the observation that *Pst* SE is a complex mixture and likely contains more than one PAMP. Consequently, although a mutation in the receptor gene could cause a lower sensitivity to SE, this effect might be masked by the perception of other PAMPs. As such, this approach is not ideal. Nevertheless, I used an *A. thaliana* library, consisting of insertional mutants in genes coding for RLPs and RLKs, to screen for lines impaired in responses to SE. Importantly, some of the T-DNA insertion lines used here

are heterozygous, which again can lead to non-detectable changes if the gene is dominant. Consequently, a receptor candidate for PAMPs present in the SE could not be identified by screening the T-DNA insertion library for non-responsiveness to SE.

The AtBAK1-dependency of at least one putative SE receptor should allow its identification using BAK1 as molecular bait. This method has been described in Chapter 3 using *N. benthamiana* expressing the genes encoding *NbBAK1-GFP* and *NbBAK1-5-GFP*. Here, *A. thaliana* seedlings were used, that express genes for either AtBAK1 or AtBAK1-5 as YFP fusion proteins. As seedlings responded in a partial *bak1 and/or bkk1*-dependent manner to the SE, at least one AtBAK1-dependent receptor is likely expressed at this growth stage. The kinetics of the ROS production in response to SE made it difficult to decide at what time point the interaction of BAK1 with the putative SE receptor occurs. Because the ROS burst peaked four to six hours after treatment, tissue for subsequent protein isolation, coIP and mass-spectrometry (MS) analysis was harvested four hours after treatment. The quality of the samples for MS analysis was questionable as protein concentration was low when resolved on a one-dimensional SDS-PAGE gel (Figure 4.12). Nevertheless, the LC-MS analysis revealed that AtBAK1-YFP and AtBAK1-5-YFP were purified during the experiment. Interestingly, receptor proteins with extracellular domains other than LRR domains were not identified, suggesting that BAK1 specifically regulates LRR-RLPs and LRR-RKs.

A large number of peptides corresponding to the chaperone BIP were found in sterile water and SE-treated samples throughout all three individual experiments (

Figure **4.12**). The key role of BIP is to promote protein folding to prevent accumulation of unfolded proteins under stress conditions (Wang *et al.*, 2004; Eichmann & Schafer, 2012). This in turn reinforces the hypothesis that the *A. thaliana* seedlings

were highly stressed during the extensive incubation time, and that this stress response in turn might be the reason for low abundance of AtBAK1 and AtBAK1-5 in the IP samples (Figure 4.12). Interestingly BIP and other chaperones are required for the RLPs Ve1 and Cf-4, both of which resistance to fungal pathogens (Liebrand *et al.*, 2012; Liebrand *et al.*, 2014). The specificity of such chaperones is unknown, and they are likely required to assist the folding of a multitude of proteins, which are not all involved in plant immunity. In fact, an *A. thaliana* triple mutant of all three HRP70/BIP genes is lethal (Nekrasov *et al.*, 2009).

Despite the low abundance of AtBAK1-YFP and AtBAK1-5-YFP after IP (as determined gel electrophoresis), known BAK1 interactors were identified in these experiments. BR-SIGNALING KINASE1 (BSK1) was isolated by precipitating AtBAK1-5 but not AtBAK1. BSK1 is a positive regulator of several different responses associated with brassinosteroid (BR) signalling and PTI (Tang *et al.*, 2008; Shi *et al.*, 2013). Notably, BSK1 also interacts with FLS2 (Shi *et al.*, 2013) and hence, possibly other PRRs. The data presented here suggests that BSK1 can directly or indirectly interact with AtBAK1-5-YFP. Unlike BAK1, BAK1-5 interacts with FLS2 (Schwessinger *et al.*, 2011) and CSPR (Chapter 3) in the absence of their respective ligands. Hence, other unknown PRRs may bind BAK1-5, which may explain the co-isolation of BSK1 by AtBAK1-5 but not AtBAK1.

The BAK1-INTERACTING RECEPTOR-LIKE KINASES BIR1, BIR2 and BIR3 previously reported to interact with AtBAK1 were also isolated here (Gao *et al.*, 2009; Halter *et al.*, 2014). For BIR1, I found a higher number of corresponding peptides in SE-treated AtBAK1-5-YFP but not AtBAK1-YFP IPs. BIR1 constitutively interacts with BAK1 but its exact role in PTI is currently unknown. The biological function of BIR3 also remains unknown, but BIR2 negatively regulates BAK1 signalling by physical interaction prior to

PAMP perception (Halter *et al.*, 2014). Consistent with these results (at least for BIR2), the number of unique peptides corresponding to BIR2 and BIR3 was reduced in SE-treated samples. BIR2 was also co-precipitated when isolating NbBAK1-GFP in *N. benthamiana*, but a lower number of BIR2 peptides in csp22-treated samples was not detected (Chapter 3). Differences may be due to the different host systems or the expression of *NbBAK1-GFP* from the strong 35S promoter in Chapter 3; here I used seedlings of *A. thaliana* that express AtBAK1-YFP and AtBAK1-5-YFP from the native AtBAK1 promoter (pAtBAK1).

A large number of peptides were identified in SE-treated samples for a protein with unknown function (encoded by At2g32240). The sequence coverage for this large 153 kDa protein was over 15%, but this protein was also identified in IPs of *A. thaliana* proteins where plants have been treated with different PAMPs (PAMP treated and PAMP untreated, Dr Yasuhiro Kadota, personal communication). The protein seems to bind several different proteins without apparent specificity, and is thus not likely to perceive SE components as part of the defence machinery. I also detected more peptides corresponding to the receptors encoded by At1g33600, At1g33590, At3g14840 and At4g08850 in SE treated samples. According to TAIR, all of those receptors are expressed in leaf tissue and predicted to locate to the plasma membrane. Peptides corresponding to proteins encoded by those genes were isolated only by AtBAK1-5, but not AtBAK1 IPs. This is important as BAK1-5 interacts with FLS2 (Schwessinger *et al.*, 2011) and CSPR (Chapter 3) in the absence of their respective ligand. Hence, the receptors encoded by At1g33600, At1g33590, At3g14840 and At4g08850 are likely partners for BAK1, but not necessarily SE receptors. Screening the cognate knockout lines for impaired responses to bacterial and fungal PAMPs or intact pathogens may reveal PTI phenotypes. Another protein, for which peptides were abundant in SE-treated

samples, is an LRR-RK (encoded by At2g04300 or At2g28960) protein. The peptides identified do not distinguish between the proteins encoded by those genes. According to TAIR, At2g04300 and At2g28960 are not expressed in mesophyll cells, where fungal spores would most likely be able to enter the plant leaf through stomata after germination. Identification of these proteins here is likely due to vacuum infiltration of the SE into *A. thaliana* seedlings for subsequent coIP and LC-MS analysis. Nevertheless, an expression analysis may be performed to exclude the expression of either gene in leaves before completely disregarding their potential of acting as receptors in PTI. Alternatively, the genes for each receptor candidate (At2g04300 and At2g28960) could be cloned expressed transiently in *N. benthamiana*, and the interaction of their respective proteins with BAK1 tested after MOCK or SE treatment. Whereas the MS results for the identification of the csp22 receptor were high quality and lead to two clear candidates, the experimental outcomes here were difficult to interpret because of the number and diversity of candidates, and the difficulty of ranking these in importance. The low quality LC-MS data are likely due to the abundance of BIP and lower concentration of isolated AtBAK1-YFP and AtBAK1-5-YFP proteins (as determined by SDS-PAGE) in all samples. This was not observed when isolating NbBAK1, to identify the receptor for csp22, and as such is likely due to the extensive treatment (4 h) of *A. thaliana* seedlings after vacuum infiltration with SE and sterile water. This is further supported by experiments performed by Dr Yasuhiro Kadota using an unrelated PAMP. After treatment of the same *A. thaliana* lines with this pure PAMP for 15 minutes, IP of AtBAK1-YFP and AtBAK1-5-YFP resulted in a clear band corresponding to AtBAK1-YFP and AtBAK1-5-YFP after gel-separation. Peptides corresponding to BIP were not identified by subsequent LC-MS analysis (Dr Yasuhiro Kadota, personal communication).

In conclusion, two different non-host plant families respond to a PAMP preparation from an obligate biotrophic wheat pathogen. Here, I mainly focused on the recognition of *Pst* component by *A. thaliana*. *Pst* SE components are recognised by AtBAK1 and/or AtBKK1-dependent and AtBAK1/AtBKK1-independent receptors. At least one PAMP is heat stable, while another is heat-labile. Proteinase K treatment reduced SE-induced PTI responses suggesting a proteinaceous nature of one or more *Pst* PAMP(s). I was unable to identify a clear *Pst* SE receptor candidate, likely due to the complex nature and mixture of several PAMPs within the SE. The ability to use a pure PAMP as a starting point for purifying novel PRRs would be a distinct advantage in identifying important non-host disease resistance genes. Fractionating the different PAMPs within SE by size and their chemical properties would likely give insight into the number and properties of the different PAMPs present in the SE and may result in fractions with only one PAMP.

5. The structure of the Pto/Prf protein complex.

5.1. Introduction.

Understanding the structures of R proteins and R protein complexes, and mapping the proximal steps in signal transduction leading to resistance, is critical for manipulating these receptor proteins to engineer durable resistance in crop plants. *Pto* was the first *R* gene to be isolated and genetically confers resistance to *Pseudomonas syringae* pathovar *tomato* (*Psto*) in tomato, although resistance is completely dependent on the multi-domain protein Prf. Prf is a nucleotide-binding- leucine-rich-repeats (NB-LRR) protein but contains a large N-terminal extension that doubles the length of the protein to almost 2,000 amino acids (Martin *et al.*, 1993; Salmeron *et al.*, 1996; Oldroyd & Staskawicz, 1998; Mucyn *et al.*, 2006). A predicted Coiled-Coil (CC) domain, followed by a *Solanaceous* domain (SD) and unique N-terminal domain without any sequence similarity to other R proteins, are encoded N-terminal of the NB site. The unique N-terminal domain (N) of Prf is both the interaction site for the effector binding determinant Pto (Mucyn *et al.*, 2006), and a contact surface for Prf oligomerisation. Additionally, N mediates intramolecular interactions with the other moiety of Prf, the SCNL domain (for SD-CC-NB-LRR), through a yet unspecified interaction surface within the SCNL domain (Gutierrez *et al.*, 2010; Ntoukakis *et al.*, 2013).

The interaction sites for both AvrPto and AvrPtoB on Pto have been mapped carefully, and overlay conserved aspects of the kinase domain (Wu *et al.*, 2004; Xing *et al.*, 2007; Dong *et al.*, 2009). In the last few years, advances have been made in understanding the importance of the Pto-Prf interaction surfaces, oligomerisation of the

complex and the role of Pto phosphorylation (Ntoukakis *et al.*, 2014). However, the conformational changes that are thought to activate the R protein complex are still poorly elucidated. Here I investigate the structure of the Prf complex, especially the Prf N dimer, the Pto-Prf interaction surfaces, the ability of N to bind SCNL, and potential changes to these interactions during complex activation.

5.2. Results.

5.2.1. Heterologous expression of Prf N (experiments carried out by Dayna Scott, ANU Summer Scholar under my supervision).

Despite an optimised nucleic acid sequence for expression in *E. coli*, previous attempts to express Prf N in the *E. coli* BL21 strain have been unsuccessful. Here, the novel *E. coli* Shuffle strains B and K12 (New England Biolabs) were tested for their ability to express the Prf N domain. *E. coli* Shuffle B is derived from *E. coli* BL21 and most efficient for expression of proteins from lac promoters, whereas *E. coli* Shuffle K12 is more efficient for expression of proteins from T7 promoters. *E. coli* Shuffle K12 was also able to express proteins toxic to other *E. coli* strains (Lobstein *et al.*, 2012). We tested the expression of N in both strains. It was indeed possible to express the Prf N domain in the *E. coli* Shuffle strains B and K12, but these proteins were not soluble (Fig 1). None of the tested growth conditions and extraction protocols led to expression of N in the soluble fraction (Figure 5.1). This included expression at 16°C, 20°C, or 30°C with induction using different concentrations of Isopropyl β-D-1-thiogalactopyranoside (IPTG) ranging from 0.1 mM to 1 mM. Additionally, expression using auto-induction medium was tested without success. Auto-induction medium induces production of target proteins automatically, usually near saturation at high cell density, which may

help protein folding (Studier, 2005). Conventional protein extraction buffers were used including buffers that have been successfully used to extract the TIR domains of the R proteins RRS1, RPS4 and L6 (Bernoux *et al.*, 2011; Williams *et al.*, 2014); those attempts also remained unsuccessful. Further, co-expression of Pto within the same strain did not affect the solubility of Prf N. Although previous attempts of heterologous expression of Prf N have failed, here N could be expressed successfully, but its absence from the soluble fraction did not allow for purification of a functional protein. This demanded an alternative approach to determine the structure of the Prf complex and activation-dependent changes: I generated deletion fragments of the *Prf* gene and expressed them transiently in *Nicotiana benthamiana* for subsequent co-Immunoprecipitation (coIP) analysis to understand which regions of N are required for intra- and inter-molecular interactions, and potential transducing structures between Pto and Prf.

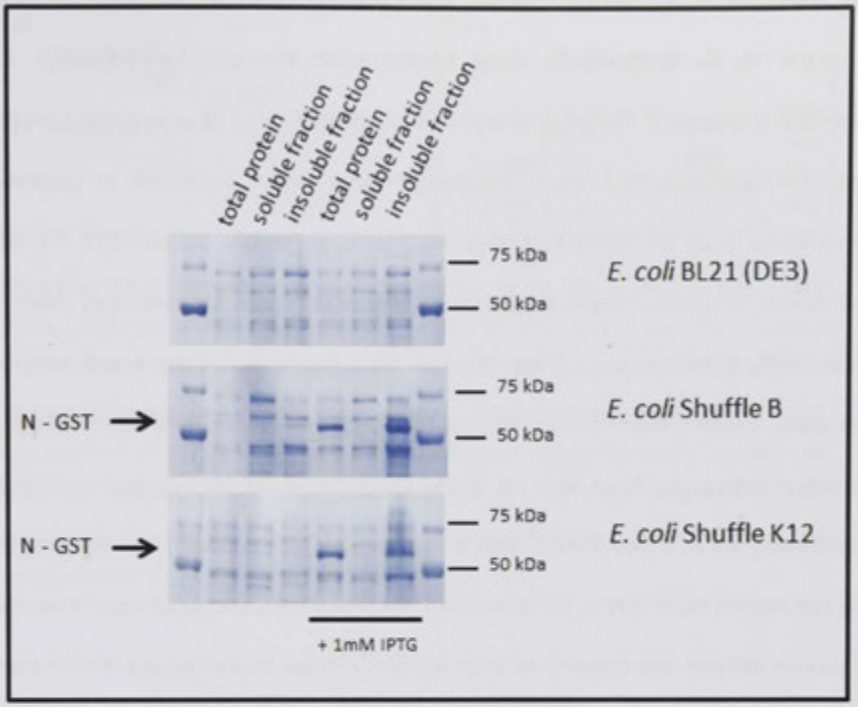

Figure 5.1: Heterologous expression of the Prf N-terminal domain (N) in-frame with a GST tag in *E. coli*. Top panel: Expression of GST-N in *E. coli* strain BL 21. Middle panel: Expression of GST-N in *E. coli* strain ShuffleB. Bottom panel: Expression of GST-N in *E. coli* strain Shuffle K12. In this example, protein was expressed at 20°C for 16 h, under the control of the *lac* promoter after induction of protein expression with 1 mM IPTG. Proteins were extracted as described in Chapter 2 and soluble and insoluble fractions separated on a one dimensional SDS-PAGE gel. Proteins were visualised using Coomassie Brilliant Blue R-250.

5.2.2. Generating deletion fragments of Prf N (N deletants).

The results above precluded an approach to Prf structure using recombinant proteins *in vitro*. As an alternative strategy, I generated successive genetic deletions from the N- and C-termini of N to test for protein interactions by coIP experiments. An overview of the constructs and corresponding areas of each N-terminal domain region can be found in Figure 5.2. Unless otherwise indicated all constructs were cloned into binary vectors

and expressed as 3xHA-FLAG or 5xMyc fusion proteins under the control of the 35S promoter in N. benthamiana using Agrobacterium-transient transformation as described in Chapter 2. The smallest terminal fragments N1 and C4 accumulated poorly and were excluded from most subsequent experiments, or tested in separate experiments when absolutely necessary. All C-terminal deletion proteins (N2, N3 and N4) showed N-terminal fragmentation of about 10 kDa as detected previously (Mucyn et al., 2006; Gutierrez et al., 2010). Whether N1 is N-terminally fragmented remains unknown, as such a fragment is too small to be detected on conventional SDS-PAGE gels. The use of detergent (1% NP-40 or 1% IGEPAL, SIGMA) inhibited this fragmentation (data not shown), but as it may disrupt weak protein:protein interactions it was not used in any subsequent experiments. For all western blot procedures, loading of equal amounts of protein extracts was determined after western analysis by staining the membranes using Coomassie brilliant blue (CBB, data not shown). Molecular weights (MWs) of all proteins were determined on every gel individually but are not indicated in the Figures. The MWs of individual proteins used here are listed in Figure 5.2 and Table 5.1. Exact sizes after electrophoretic separation of proteins on a gel varied depending on the respective epitope tag. All coIPs here were performed at least twice with representative results shown.

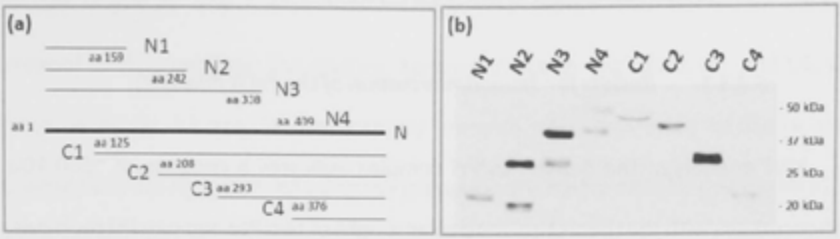

Figure 5.2: The Prf N-terminal deletion constructs. (a) N1, N2, N3, and N4 carry the N-terminus of N with N1 being the shortest fragment. C1, C2, C3 and C4 carry the C-terminus of the N domain with C4 being the shortest fragment. The amino acid (aa) length of each fragment is indicated as a number at the terminus of each fragment. **(b):** N fragments were expressed as 3xHAF fusions in *N. benthamiana* and leaf tissue was harvested two days post infiltration. Proteins were extracted and separated on a SDS-PAGE gel before immune-blotting and immune-detection using Anti-HA. N-terminal fragmentation of ~ 10kDa can be detected for N2, N3, and N4. MW: Molecular weight.

Table 5.1: Molecular weight of proteins used for coIP analysis

Protein	Theoretical molecular weight [kDa]
Prf NmL (N middle long)	32 (aa 125 - 409)
Prf NmS (N middle short)	21 (aa 208 - 409)
Pto	36 (full length)
Fen	35 (full length)
Prf SCNL	146 (aa 530 - 1825)
Prf CNL (SCNL lacking SD)	105 (aa 940 - 1825)
Prf SD	41 (aa 530 - 970)
Prf CC-NBS	59 (aa 940 – 1460)
Prf LRR	46 (aa 1429 – 1825)

5.2.3. Homodimerisation of the Prf N domain.

5.2.3.1. Results for 'homodimerisation of the Prf N domain'.

MW analysis of the native Pto/Prf complex indicates a complex of ~500 kDa, which correlates with the theoretical molecular weight of two Pto and two Prf molecules within the complex (Gutierrez *et al.*, 2010). Prf N mediates auch a homotypic interaction (this site dimerises with the same site of another N molecule) of Prf (Gutierrez *et al.*, 2010). In order to gain insight into this important interaction, the N deletion regions were used for different combinational coIP experiments. Firstly, the N deletion proteins were checked for the ability to homodimerise with the full length N molecule. Only those fragments that carried the C-terminus of N (C1, C2, C3) were able to co-precipitate full length N in the absence of Pto, suggesting that the C-terminus contains an important Prf homodimerisation site (Figure 5.3). Although N2, N3, and N4 did not interact with full-length N in these tests, it is important to consider that N-N homotypic interactions are competitive in such experiments. Indeed, I found that longer exposure times of the western blots revealed interactions between N2, N3 and N4 with N suggesting the presence of a homodimerisation surface at the N-terminus. This is supported by the fact that in a reverse coIP approach, the full length N-terminal domain was able to co-precipitate all three tested regions (N2, N3, N4) (Figure 5.3).

To further investigate N homodimerisation, the longest non-overlapping fragments N2 and C3 were co-expressed and their abilities to self-associate or heterodimerise tested. N2 and C3 were each able to self-associate, supporting the results above that showed each terminus in homodimeric associations. Additionally, N2 co-immunoprecipitated C3, and in the opposite pulldown, C3 co-immunoprecipitated N2 (Figure 5.3 a). Interaction between N2 and C3 demonstrates that non-homologous

surfaces in the N- and C-subdomains interact. To narrow this interaction surface, potential binding between the shortest terminal deletion fragments, N1 and C4, was tested. Although N1 and C4 are normally unstable when expressed in planta, their accumulation can be enhanced using the proteasome inhibitor MG132 (Ntoukakis *et al.*, 2009). N1 interacted with C4 in both forward and reverse pulldowns (Figure 5.3b), suggesting a heterotypic interaction (this site dimerises with a different site of another N molecule) between the N- and C-termini within the Prf N domain, which may explain at least part of the N2-C3 interaction. On the other hand, and in contrast to N2, the N1 fragment consisting of the 159 N-terminal amino acids of N was unable to homodimerise. This defines a further homotypic interaction surface between aa 160-242, in addition to the C4 self-association motif between aa 376-546. The presence of Pto did not affect those interactions (data not shown).

To determine if either the N-termini or C-termini of N are mandatory for Prf dimerisation, I generated two constructs wich lack either end of N and named them NmiddleLong (NmL) and NmiddleShort (NmS). The sequence encoding NmL was amplified from the N template plasmid using N4 forward and C1 reverse primers, thus encoding aa 125-409. NmS was amplified using the N4 forward and C2 reverse primers, thus encoding aa 242-409. In co-immunoprecipitation tests, both NmL and NmS were able to co-isolate the full length N protein, as well as each other and themselves (Figure 5.4), suggesting that at least one N homotypic interaction site is encoded by aa 242-409 (NmS) or that additional homo-interaction sites are contained within Prf residues 242-409.

Taken together, N likely contains multiple dimerisation sites. N1 interacted with C4 in both forward and reverse pulldowns, suggesting a heterotypic interaction between

the N- and C-termini within the Prf N domain, which may explain at least part of the N2-C3 interaction. On the other hand, and in contrast to N2, the N1 fragment consisting of the 159 N-terminal amino acids of N was unable to homodimerise. This defines a further homotypic interaction surface between aa 160-242, in addition to the C4 self-association motif between aa 376-546. The Prf N-terminal domain thus forms a parallel or anti-paralell homodimer that apparently folds over crosswise to provide an interaction surface between either ends of the molecule (Figure 5.5 a and b). At this stage, neither conformation can be ruled out; both are as likely.

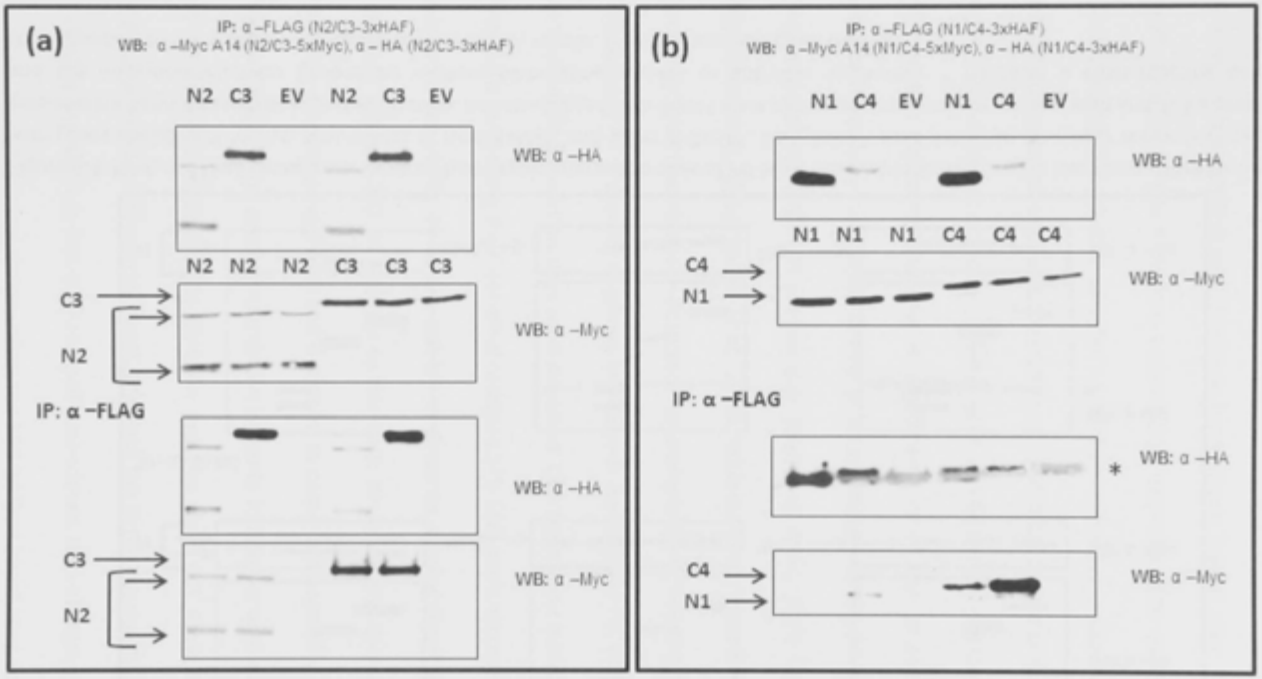

Figure 5.3: The first 259 aa and last 175 aa of N encode a N dimerization site. (a) Interactions between N2 and C3. *N. benthamiana* plants were co-transformed with genes encoding N2-5xMyc or C3-5xMyc, and either N2-3xHAF, C3-3xHAF, or an empty vector (EV). **(b) Interactions between N1 and C4.** *N. benthamiana* plants were transformed with genes encoding N1-5xMyc or C4-5xMyc, and either N1-3xHAF, C4-3xHAF, or EV. Leaf tissues were harvested two days post infiltration. N deletion proteins fused to 3xHAF were recovered from leaf extracts with anti-FLAG beads, and the immunoprecipitates probed by western blots using anti-HA or anti-Myc antibodies. * indicates a cross-reacting band corresponding to the antibody released from the affinity matrix. IP: Immunoprecipitated fraction.

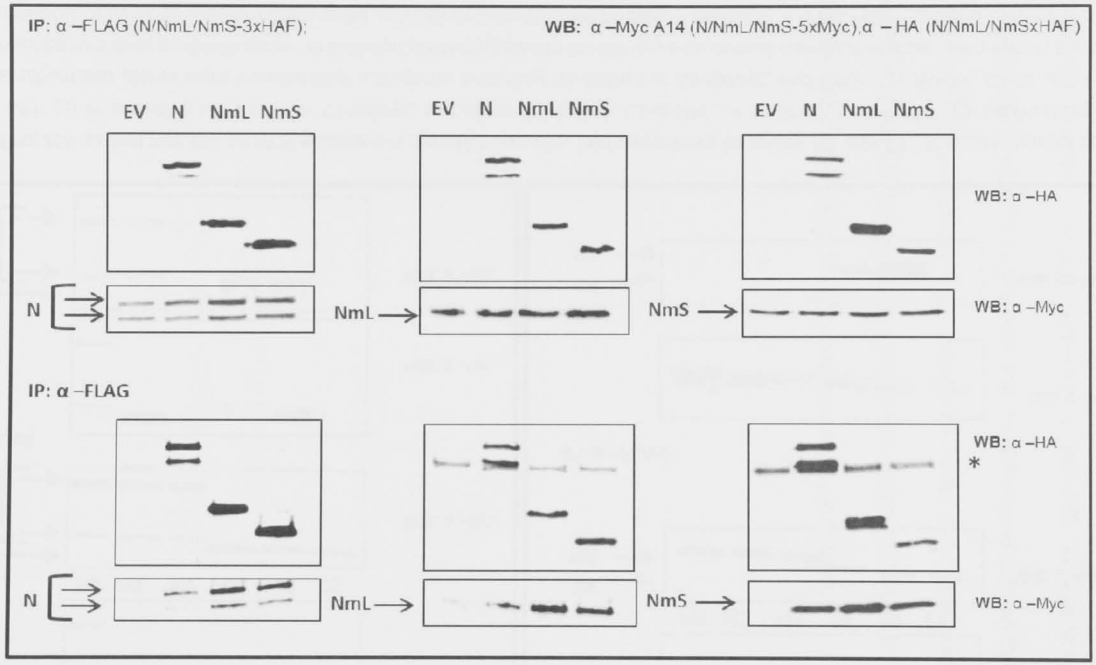

Figure 5.4: NmL and NmS contain one or more homotypic interaction sites of Prf N. *N. benthamiana* plants were transiently transformed with genes encoding N-5xMyc, NmL-5xMyc or NmS-5xMyc, and either N-3xHAF, NmL-3xHAF, NmS-3xHAF or an empty vector (EV). Leaf tissues were harvested two days post infiltration. Proteins tagged with 3xHAF were recovered from protein extracts with anti-FLAG beads, and the immunoprecipitates probed by western blots using anti-HA or anti-Myc antibodies. * indicates a cross-reacting band corresponding to the antibody released from the affinity matrix. IP: Immunoprecipitated fraction.

5.2.3.2. Discussion for 'homodimerisation of the Prf N domain'.

Self-association of NB-LRR proteins is a common occurrence. Crystallographic studies of their N-terminal domains have given insight into the structural basis underlying these interactions in a number of examples. This includes the CC-domain containing protein MLA10, and the TIR-domain containing proteins tobacco N, flax L6, and the heterologous pairs RGA4/RGA5 and RPS4/RRS1 (Bernoux *et al.*, 2011; Maekawa *et al.*, 2011; Cesari *et al.*, 2014; Williams *et al.*, 2014). Neither the structural basis for NB-LRR protein multimerisation nor its significance in ETI can be generalised, as homo-oligomerisation can be found before or after effector recognition depending on the respective effector/NB-LRR protein pair (Gutierrez *et al.*, 2010; Bernoux *et al.*, 2011; Ntoukakis *et al.*, 2013; Cesari *et al.*, 2014; Williams *et al.*, 2014). For some R proteins multimerisation has not been detected, for example the CC-NB-LRR Rx (Hao *et al.*, 2013). The unique Prf N domain mediates homomeric assembly of Prf. In this thesis a number of homotypic interaction sites were detected. One homotypic interface is within the C4 fragment comprising the C-terminal residues 376-546, and a second region by inference based on the ability of N2 but not N1 to dimerise, placing the interaction site within residues 160 and 242. In addition to this basic structure, the domain must fold across the long axis, allowing the N- and C-termini to come into proximity, which is supported by the ability of the smallest terminal fragments to interact with each other. Mapping of the interaction sites using deletion proteins does not allow to narrow them to individual residues. The N deletants, that lack the N-terminus and C-terminus, NmL (aa 125-409) and NmS (aa 242-409) also self-assosciated. NmL at least party contains the N-terminal homotypic interaction suface (aa 160-242) and both NmL and NmS contain part of the C-terminal interaction surface contained by C4 (aa 376-546). I can therefore not

exclude, additional N self-association sites within the residues 243 and 375. A deletion of N lacking the two dimerisation interfaces identified here (encoding aa 243 – 375) would give insight into this but may fail to accumulate, because of its low theoretical molecular weight (~ 13 kDa). Fusion of this protein (and also N1 or C4) with GFP might potentiate higher accumulation of such short deletion proteins. However, the possibility that GFP might interfere with their function would have to be excluded. Ultimately, heterologous expression and subsequent crystallographic analysis of homodimerisation interfaces may reveal the exact residues that underlie these interactions.

Taken together, results here suggest that the unique Prf N-terminal domain exists as a parallel or anti-parallel homodimer (Figure 5.5). In the parallel conformation the N-terminal and C-terminal regions within the same N molecule would interact (Figure 5.5 a), and the homodimerisation would be mediated only by interactions between the N-terminal and C-terminal regions of either N in the dimer (Figure 5.5 a). In an antiparallel conformation, the N-terminal region of one molecule would interact with the C-terminal region of the other molecule (Figure 5.5 b) in the dimer providing additional interactions between two individual N molecules in the N dimer. N homodimerisation would also be mediated by interactions between the N-termini and C-termini of either N in the dimer (Figure 5.5 b). At this stage, I do not have evidence pointing towards one or the other conformation. In (Saur *et al.*, 2015) we show the Prf dimer in a parallel conformation. I will show the Prf dimer from here on in its possible anti-parallel conformation. The likely outcome of Pto-Prf oligomerisation is to bring two kinase molecules into proximity in an inhibited state, ready for effector perception and trans-phosphorylation (Ntoukakis *et al.*, 2013). Whether dimerization changes during effector dependent activation remains to be determined.

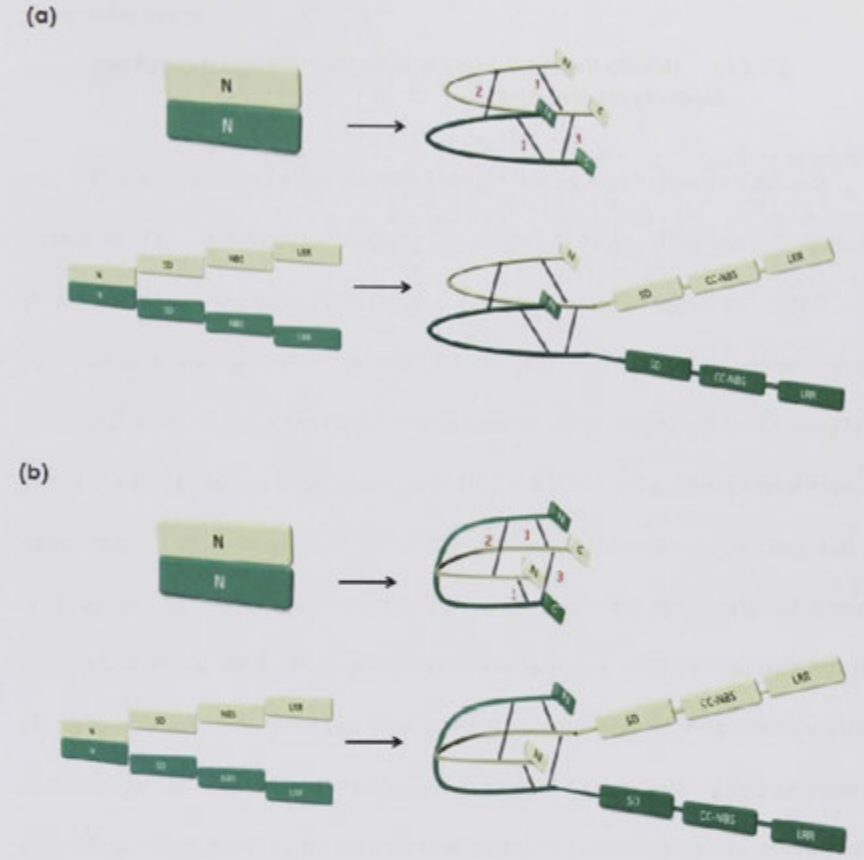

Figure 5.5: A schematic representation of the anti-parallel (a) or parallel (b) Prf N dimer based on results shown in Figure 5.3 and Figure 5.4. (a) Prf N shown as a parallel homodimer, which folds over crosswise. Four interactions sites have been identified within the N dimer. The C-terminal region of one N protein interacts with the C-terminal region of the same N protein (indicated with a red 1). The N-terminal regions (indicated with a red 2) and C-terminal regions (indicated with a red 3) of both N proteins interact. The interaction of two Prf molecules is mediated by the anti-parallel N-terminal dimer of either Prf molecule. **(b)** Prf N shown as an anti-parallel homodimer, which folds over crosswise. Four interactions sites have been identified within the N dimer. The C-terminal regions of one N protein interacts with the N-terminal regions of a second N protein, those interactions are indicated with a red 1. The N-terminal region (indicated with a red 2) and C-terminal regions (indicated with a red 3) of both N proteins interact. The interaction of two Prf molecules is mediated by the anti-parallel N-terminal dimer of either Prf molecule. The two Prf/N molecules can be distinguished from each other by their bright and dark green colors.

5.2.4. Prf N interacts with the Pto kinase through two separate binding sites.

5.2.4.1. Results for 'Prf N interacts with the Pto kinas through two separate binding sites'.

N is the interaction surface for Prf/Pto heterocomplex formation. Thus, Prf acts as a bridge to bring two or more Pto molecules together (Mucyn *et al.*, 2006; Ntoukakis *et al.*, 2013). To further characterise this important association, I assessed the N deletants for the ability to interact with Pto. All tested N deletions were able to co-purify Pto (Figure 5.6). I also stabilised the protein accumulation of C4 and N1 by infiltration of the proteasome inhibitor MG132. C4 and N1 were able to bind Pto, yet, Pto did not alter the ability of C4 to dimerise (data not shown) or the inability of N1 to homodimerise (Figure 5.7). I also tested the regions of N, that lack the N- and C-termini, NmL (aa 125-409) and NmS (aa 242-409), for the ability to interact with Pto. Both proteins interacted weakly with Pto after immune-precipitation of NmL and NmS, and detection of Pto in the immune-precipitates. Using a reverse coIP approach (precipitation of Pto, detection of NmL or NmS co-precipitation) only NmS was co-isolated by Pto, suggesting that this interaction might be slightly more stable (Figure 5.8). However this observation is unexpected because NmL (aa 125-409) actually contains the NmS (aa 242-409) region. The interaction between NmS and Pto in the reverse coIP may be an artefact as in the forward coIP, neither the NmS nor the NmL protein showed a strong interaction with Pto.

Taken together, the ability of internal N fragments NmL and NmS to bind Pto is weak. I conclude that the N-terminus (encoded by N1, aa 1-159) and C-terminus (C4, aa 376-546) of N must encode the major Pto interaction sites, suggesting the presence of at least two interfaces mediating the interaction of Pto and Prf. NmL and NmS may partly

encode those interaction sites. From now on, I will refer to the N-terminal Pto binding site of N (encoded by N1, aa 1-159) to 'Pto/N site 1' and the C-terminal Pto binding site (encoded by C4, aa 376-546) to 'Pto/N site 2'.

In a forward coIP approach, N2, N3 and N4 did not co-precipitate full length N, whereas C1, C2, and C3 were able to bind N. Co-expression of Pto however complemented N2, N3 and N4 to co-precipitate full length N in forward coIP experiments (Figure 5.9). All three were able to bind full length N to similar extent as C1, C2 and C3, when Pto was co-expressed. All N deletants were also able to co-precipitate Pto as shown previously (Figure 5.6). These results suggest that a) Pto brings N2, N3 and N4 into a conformation, which supports homodimerisation with full length N, and/or b) that Pto forms a bridge between N2, N3 and N4 with the full length N-term. Neither of those possibilities can be excluded at this stage (Figure 5.10).

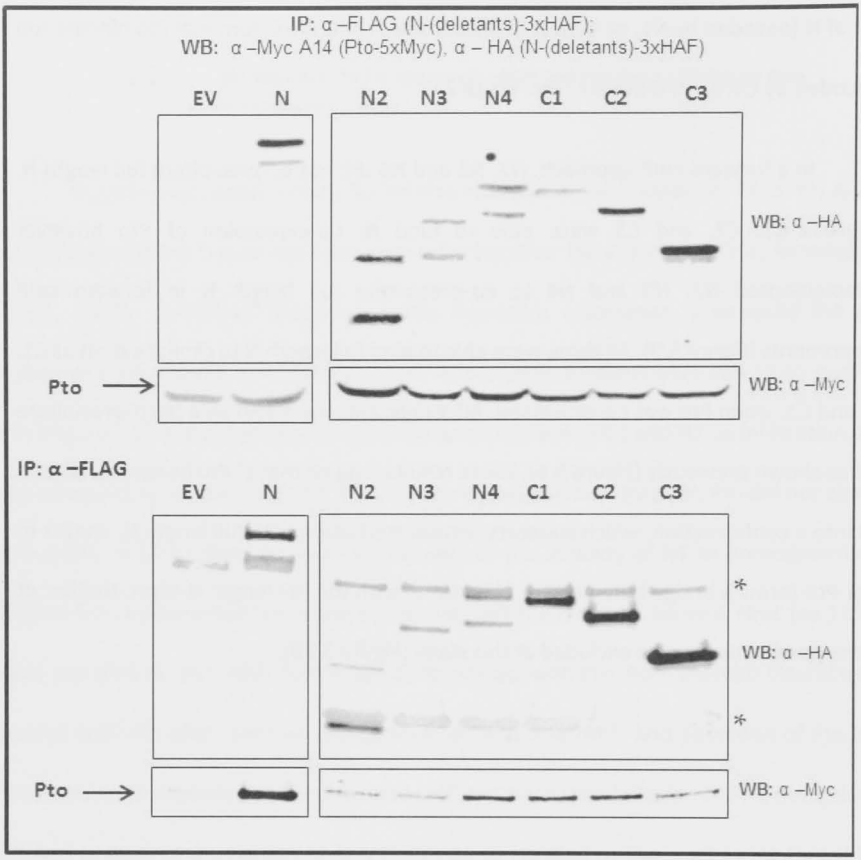

Figure 5.6: All N deletants are able to bind Pto. *N. benthamiana* leaves were co-transformed transiently with genes encoding Pto-5xMyc and one of the C-terminal deletants fused to a 3xHAF tag, or empty vector (EV).Leaf tissues were harvested two days post infiltration. N and its deletants were recovered from protein extracts with anti-FLAG beads, and the immunoprecipitates probed by western blots using anti-HA or anti-Myc antibodies. * indicates a cross-reacting band corresponding to the antibody released from the affinity matrix. IP: Immunoprecipitated fraction.

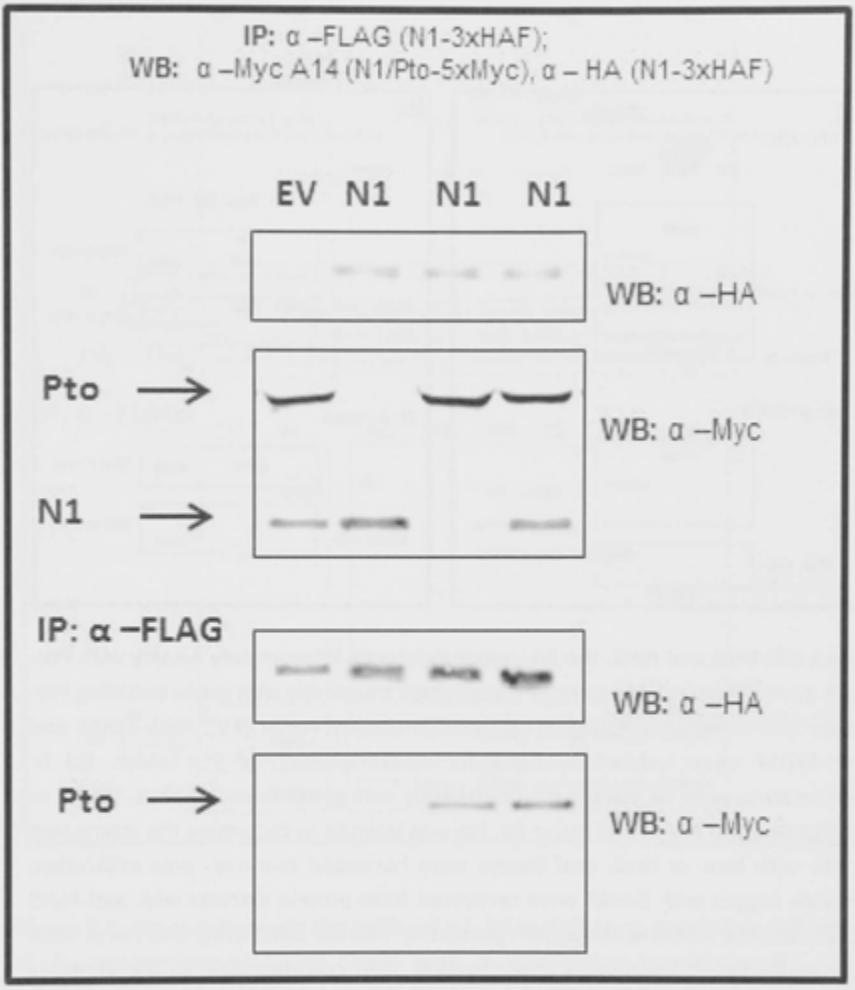

Figure 5.7: Pto binds N1 but does not affect its inability to homodimerise. (a) *N. benthamiana* plants were co-transformed transiently with genes encoding N1-3xHAF, and Pto-5xMyc and/or N1-5xMyc, or empty vector (EV) Leaf tissues were harvested two days post infiltration. N1 was recovered from protein extracts with anti-FLAG beads, and the immunoprecipitates probed by western blots using anti-HA or anti-Myc antibodies. * indicates a cross-reacting band corresponding to the antibody released from the affinity matrix. IP: Immunoprecipitated fraction.

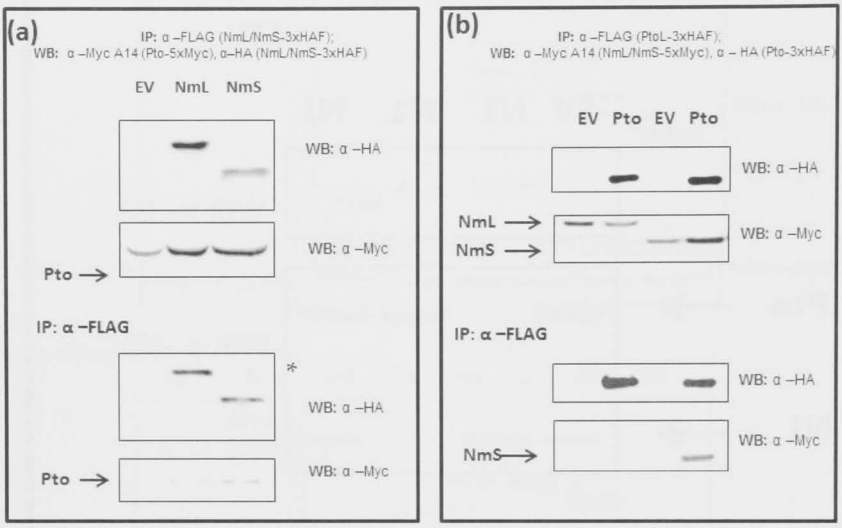

Figure 5.8: NmL and NmS, the internal N deletants, interact only weakly with Pto. **(a)** *N. benthamiana* plants were co-transformed transiently with genes encoding Pto-5xMyc and either NmL-3xHAF, NmS-3xHAF or empty vector (EV). NmL-3xHAF and NmS-3xHAF were isolated to check for co-precipitation of Pto-5xMyc. **(b)** *N. benthamiana* were co-transformed transiently with genes encoding NmL-5xMyc or NmS5xMyc, and Pto-3xHAF tag or EV. Pto was isolated to determine the interaction of Pto with NmL or NmS. Leaf tissues were harvested two days post infiltration. Proteins tagged with 3xHAF were recovered from protein extracts with anti-FLAG beads, and the immunoprecipitates probed by western blots using anti-HA or anti-Myc antibodies. * indicates a cross-reacting band corresponding to the antibody released from the affinity matrix. IP: Immunoprecipitated fraction.

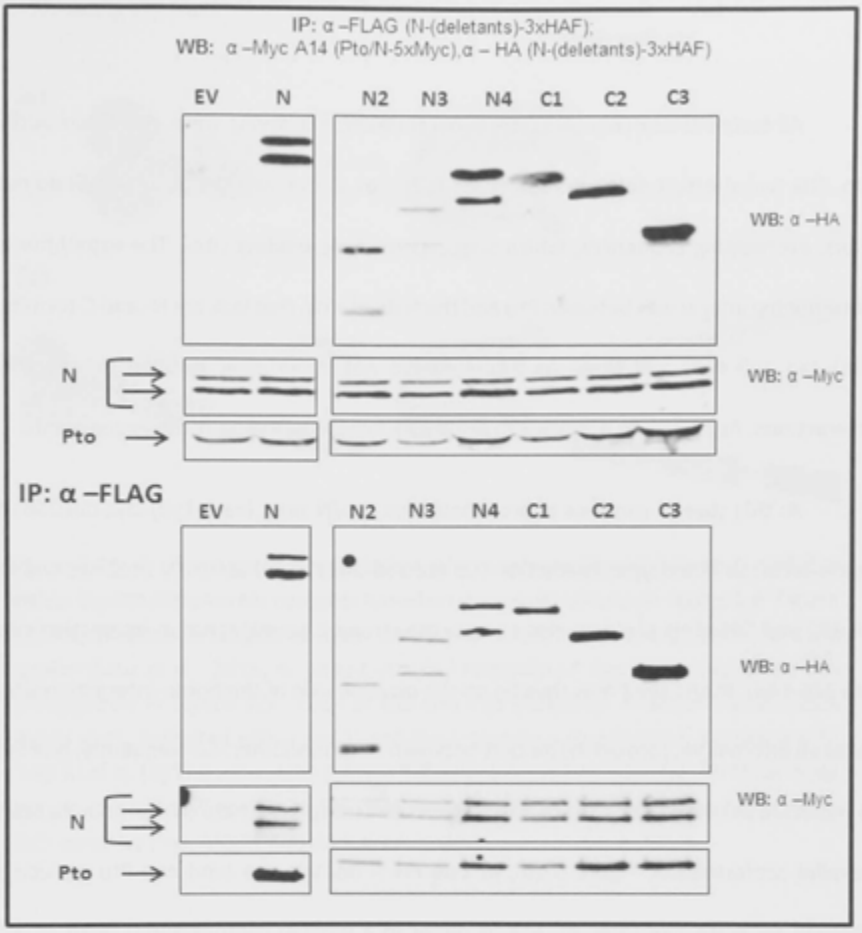

Figure 5.9: Pto complements the ability of N2, N3 and N4 to co-precipitate full length N. *N. benthamiana* wild type plants were co-transformed transiently with genes encoding Pto-5xMyc, N-5xMyc, and N-3xHAF tag or EV. Leaf tissues were harvested two days post infiltration. N and its deletions were recovered from protein extracts with anti-FLAG beads to check for interaction with N-5xMyc and Pto-5xMyc. The immunoprecipitates were probed by western blots using anti-HA or anti-Myc antibodies. IP: Immunoprecipitated fraction.

5.2.4.2. Discussion for 'Prf N interacts with Pto through two separate binding sites'.

All tested N-terminal and C-terminal N deletion proteins were able to co-purify Pto. The two shortest deletants tested here, N1 (aa 1-159) and C4 (aa 376-546) do not share overlapping sequences, which suggests multiple binding sites. The experiments determining interaction between Pto and the N deletants, that lack the N- and C-termini, NmL (aa 125-409) and NmS (aa 242-409) did not show clear positive or negative interactions. As such, I do not want to draw conclusions based on those experiments.

At this stage, I can thus approximate that Pto/N site1 (aa 1-159) lays outside of the N-terminal homotypic interaction site (aa 160-242) and that Pto/N site2 lies within aa 376 and 546. This site may also contain the strong C-terminal homo-interaction site (aa 376-546). Pto/N site2 may thus be on the obverse side of the homo-interaction site, or as an alternative, formed in the cleft between each monomer. Consequently, one Prf N molecule may bind two different Pto molecule as displayed here (N dimer in an anti-parallel conformation, Figure 5.10), or one Prf N domain can bind one Pto molecule through separate interfaces on Pto (N dimer in a parallel conformation) (Saur *et al.*, 2015).

Pto promoted the interaction of fragments lacking the C-terminal homodimerisation site with full length N (Figure 5.9). Pto may place those regions into the right conformation, or act as a bridge between two individual molecules. The latter would promote the idea of N as an anti-parallel homodimer (Pto binds two N molecules). As both hypotheses are possible, it remains unknown if N occurs as a parallel or an anti-parallel homodimer.

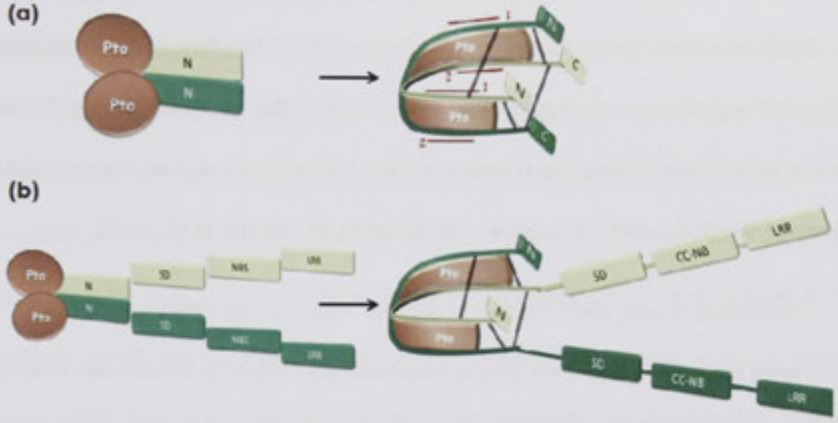

Figure 5.10: A schematic representation of the interactions between N and Pto within the Pto/Prf protein complex based on the results shown in Figure 5.6- Figure 5.9. The N dimer is displayed in an anti-parallel conformation. (a) Prf N forms a parallel (Saur *et al.*, 2015) or an anti-parallel homodimer that folds over crosswise as suggested in Figure 5.5. Each of the two Pto molecules binds the N-terminus (Pto/N site1, indicated with a red 1) and the C-terminus (Pto/N site2, indicated with a red 2) of N. **(b)** The interaction of two Prf molecules is mediated by the N-terminal domain of either Prf molecule. The two Prf/N molecules can be distinguished from each other by their bright and dark green color.

5.2.5. Results 'A P+1 loop mutation in Pto abrogates interaction with the Pto/N site1'.

5.2.5.1. Results for 'A P+1 loop mutation in Pto abrogates interaction with the Pto/N site1'.

Activation of the Prf/Pto resistance protein complex is dependent on two key Pto-mediated events during effector mediated activation: First, on the disruption of the Pto P+1 loop (Pto activation segment) by effector binding, and secondly Pto trans-phosphorylation, which in turn requires a functional NB site within Prf (Wu *et al.*, 2004; Balmuth & Rathjen, 2007; Ntoukakis *et al.*, 2013). Pto is phosphorylated on residues

Serine 198 and Threonine 199, and phosphorylation can be mimicked by the ptoS198D/T199D double mutant. Disruption of the activation segment is mimicked by the L205D mutation, which causes a constitutive gain-of-function (CGF) phenotype when such mutants are expressed in *N. benthamiana* (Wu *et al.*, 2004). The L205D mutants lacks kinase activity, but is phosphorylated *in trans* by the *N. benthamiana* Pto homolog 1 (NbPth1), which is necessary for signalling (Ntoukakis et al., 2013).

Previously it was speculated that the Pto negative-regulatory patch (NRP) in cooperating the P+1 loop is mirrored by a complementary region in an unknown binding protein to inhibit Pto (Wu *et al.*, 2004). As Prf is a constitutive partner of Pto, this sequence likely resides within Prf N. To locate this hypothetical region, genes encoding the N deletion proteins were co-expressed with ptoL205D and tested for interaction. Interestingly, the characteristic N-terminal processing of the N deletants by ~10 kDa was largely absent when *ptoL205D* was co-expressed (Figure 5.11), implying that the cleavage site is no longer accessible perhaps due to a change in N conformation. The fragments N1, N2, N3, and N4, which all lack the C-terminal residues 410-546 but contain the amino acids 1-159 (Pto/N site1), were unable to interact with ptoL205D (Figure 5.11). This suggests that the P+1 loop mutation affects the interaction with Prf residues 1-159, which may interact directly with the Pto catalytic cleft to repress signalling (Wu *et al.*, 2004). Importantly, all of C1, C2, and C3 and even the unstable C4 protein (all containing Pto/N site2) were able to bind both Pto and ptoL205D (Figure 5.11) meaning that this interaction is not affected by the Pto P+1 loop mutation. Considering the lack of N4 (aa 1-409)/ ptoL205D interaction, it narrows the Pto/N site2 to residues 410-546.

To further investigate those interactions, I rationalised that overexpressing the N domain should outcompete NbPrf for Pto binding, causing accumulation of a non-

functional Pto/N complex. This was confirmed by overexpressing tomato *N* or the homologous region from *N. benthamiana Prf* homolog that I termed *NbN* (Attachment 7 and 8). Both N and NbN compromised the cell death induced by the most active form of Pto, ptoS198D/T199D/L205D, after weak expression of this mutant from the native *Pto* promoter (*gPto:ptoS198D/T199D/L205D*). Consistent with their inability to bind to ptoL205D, co-expression of N1, N2, N3 or N4 did not inhibit the ptoS198D/T199D/L205D mediated HR (Figure 5.12). In contrast, the N-terminal deletions C2 and C3 completely inhibited the HR, and C1 partly inhibited the HR (Figure 5.12). C4 was unable to inhibit the ptoL205D CGF phenotype, possibly due to its generally low accumulation (Figure 5.2). These results are thus consistent with the identification of Pto/N site 2 within residues 410-546. The additional Pto/N site1 in turn is disrupted by the activation state of Pto and cannot inhibit Pto molecules containing the L205D mutation.

To extend these observations, I tested the interaction of N4 and C3 with key Pto mutants mimicking the different states of activation. For this, phospho-mimic (S198D/T199D) and phospho-null (S198A/T199A) Pto mutations were combined with or without the kinase inactivation mutation D164N, or the CGF mutant L205D (Wu *et al.*, 2004), and the ability of the composite mutants to bind N4 (containing Pto/N site1) and C3 (containing the Pto/N site2) were tested. Whereas all mutants bound to the full length N domain and the N-terminal deletion C3 (containing Pto/N site2), no mutant containing the L205D mutation (ptoL205D, ptoS198A/T199A/L205D, or ptoS198D/T199D/L205D) was able to co-precipitate N4 (Figure 5.13). Again, N-terminal processing of the 10 kDa fragment was not detected when Pto molecules containing the L205D mutation were paired with Prf N fragments. Interestingly, the phospho-mimic mutant ptoS198D/T198D showed an impaired interaction with N4, but this was not seen

with the triple mutant containing the D164N kinase knock-out mutation, or with the phospho-dead mutant ptoS198A/T198A (Figure 5.13). This implies that the kinase activity of ptoS198D/T198D contributes to the diminished interaction with N4 and thus Pto/N site1.

Overall, the data are suggestive of an interaction between the Pto catalytic cleft mediated particularly by Pto Leu-205, and the first 159 amino acid residues of Prf (Pto/N site 1) as schematically explained in Figure 5.14.

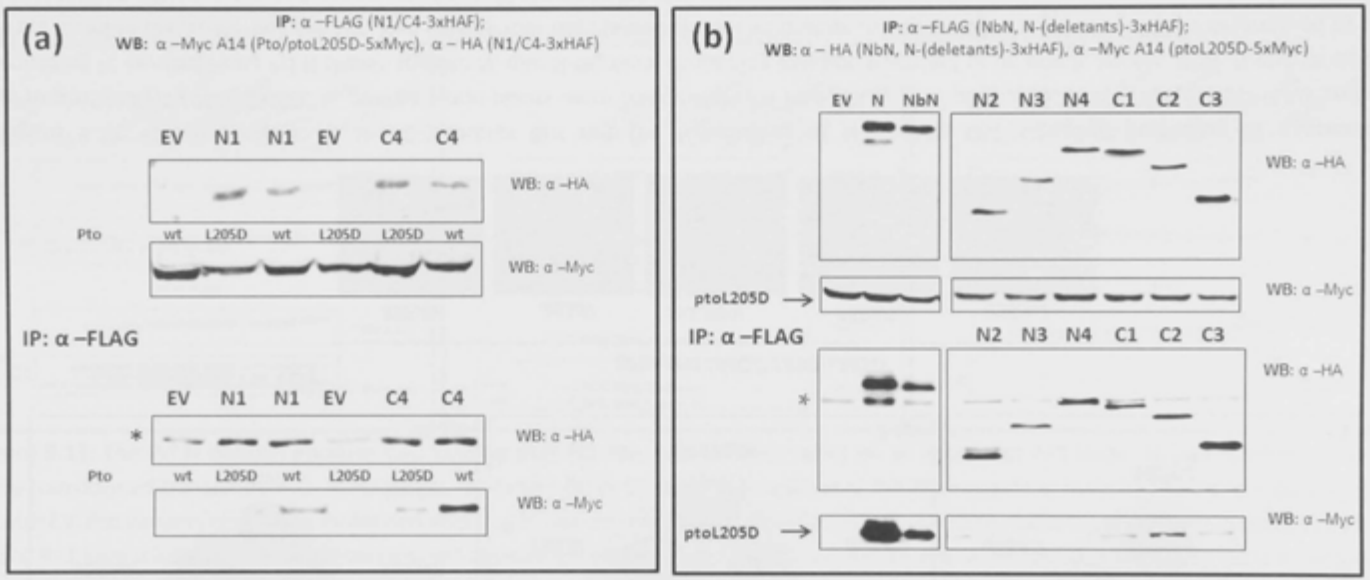

Figure 5.11: N- deletants that lack the C-terminus do not bind ptoL205D. *N. benthamiana* plants were co-transformed transiently with genes encoding Pto-5xMyc **(a)** and /or ptoL205D-5xMyc and NbN, N or one of the N- deletants fused to a 3xHAF tag, or EV. Leaf tissues were harvested two days post infiltration. N and its deletions were recovered from protein extracts with anti-FLAG beads, and the immunoprecipitates probed by western blots using anti-HA or anti-Myc antibodies. * indicates a cross-reacting band corresponding to the antibody released from the affinity matrix. IP: Immunoprecipitated fraction. wt: wild type.

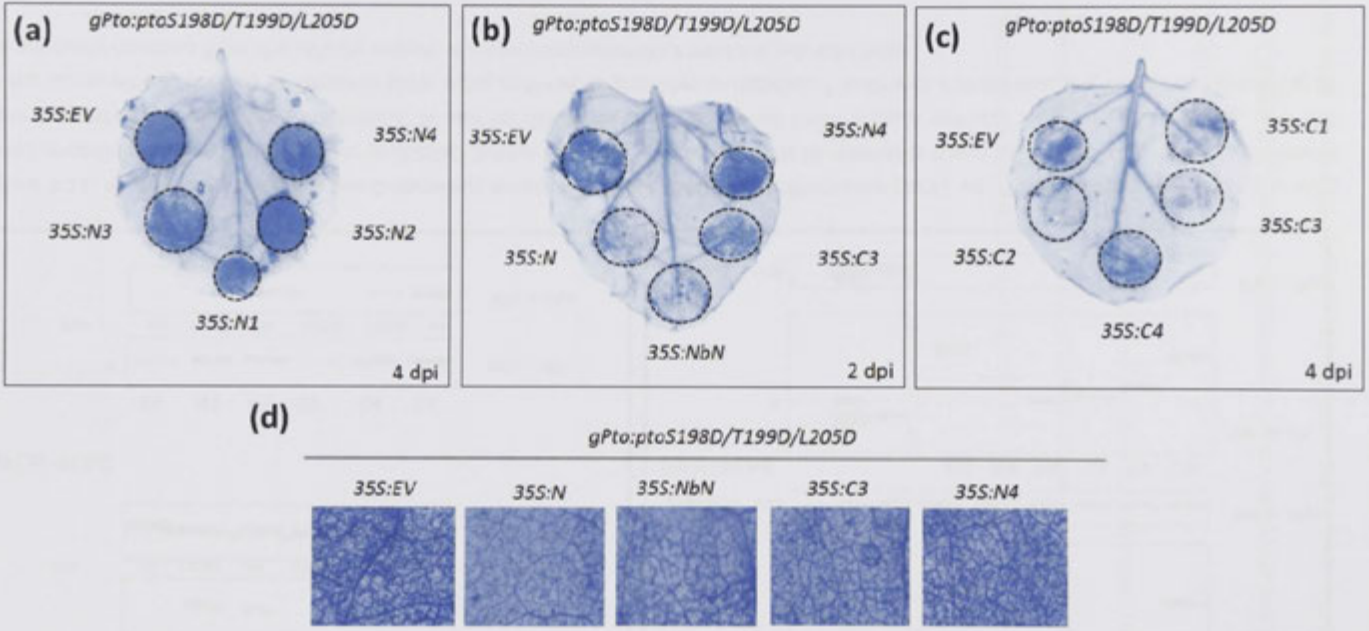

Figure 5.12: Overexpression of the C-terminus but not the N-terminus of N inhibits CGF signaling mediated by expression of *gPto:ptoS198D/T199D/L205D*. *N. benthamiana* plants were co-transformed transiently with *gPto:ptoS198D/T199D/L205D*-FLAG and genes encoding *N. benthamiana* Prf N (NbN), tomato N, one N-terminal containing deletion fragment or an empty vector. NbN, N and its deletants were fused to the 3xHAF epitope tag. Two **(b)** and four days **(a and c)** after infiltration, hypersensitive response (HR)was determined by trypan blue staining. **(d)** microscopic assessment of the HR shown in **(b)**. dpi: days post infiltration.

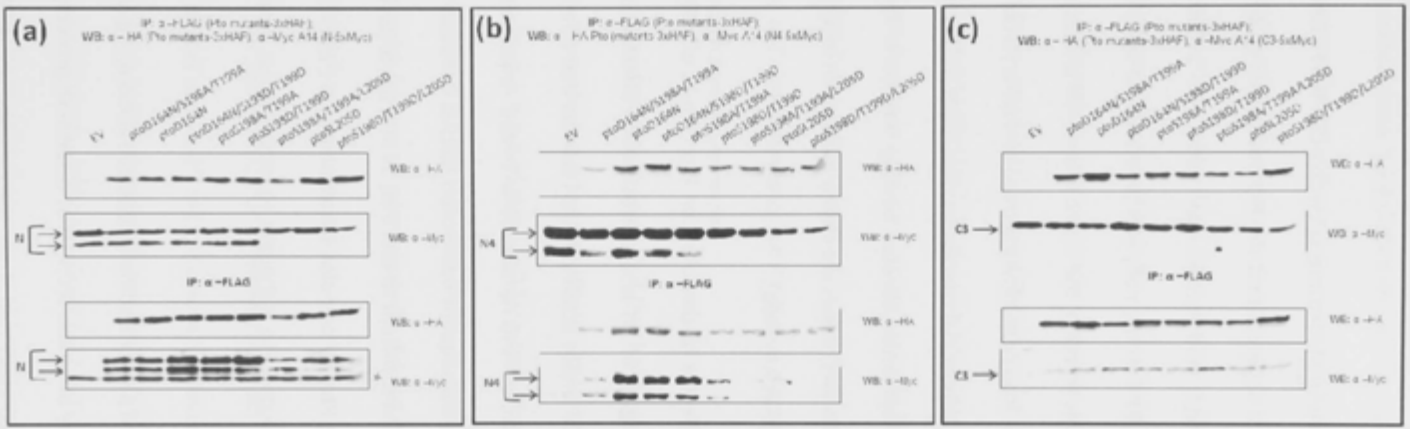

Figure 5.13: The Prf N domain encodes two binding sites for Pto, one of which relies on an intact Pto P+1 loop. *N. benthamiana* plants were transformed transiently with *N-5xMyc* **(a)**, *N4-5xMyc* **(b)** or *C3-5xMyc* **(c)** and one of the *Pto* mutants as indicated fused to a 3xHAF tag, or with EV. Pto variants containing mutations affecting kinase activity (D164N, L205D), phosphorylation status (S198A/T199A, S198D/T199D), or the P+1 loop (L205D). Note the absence of the cleaved form of N **(a)** and N4 **(b)** in the presence of ptoL205D. Leaf tissues were harvested two days post infiltration. Pto and its variants were recovered from protein extracts with anti-FLAG beads, and the immunoprecipitates probed by western blots using anti-HA or anti-Myc antibodies. IP: Immunoprecipitated fraction. * indicates a cross-reacting band corresponding to the antibody released from the affinity matrix.

5.2.5.2. Discussion for 'A P+1 loop mutation in Pto abrogates interaction with the Pto/N site1'.

N fragments lacking Pto/N site 2 were unable to interact with a CGF Pto P+1 loop. This is an intriguing observation because it suggests that the N-terminal region of Prf interacts directly with the Pto P+1 loop, and hence may carry the proposed complementary surface patch to the Pto NRP that normally acts to repress Prf signalling (Wu *et al.*, 2004; Mucyn *et al.*, 2006). In this scenario, the stable C-terminal interaction surface of Prf N (Pto/N site 2) would allow close proximity and trans-phosphorylation of Pto molecules even after disruption of the N-terminal interaction (Pto/N site1). This may explain why loss of the Pto-Prf interaction after effector binding has never been observed, despite the fact that conformational changes are clearly involved in receptor complex activation (Wu *et al.*, 2004; Mucyn *et al.*, 2006).

As the NRP region overlaps the effector binding sites on Pto (Wu *et al.*, 2004; Dong *et al.*, 2009), it is likely that this region of Prf also contacts each effector, and indeed may also play a role in inhibition of kinase activity. It thus follows that effector binding releases the Pto/N site1 interaction, but this remains to be tested. Importantly, co-expression of AvrPtoB and AvrPto and subsequent interaction studies between N4 (containing Pto/N site1) and Pto may not be sufficient to test this, as they are expected to only bind one Pto molecule within the Pto/Prf complex (Ntoukakis *et al.*, 2013). As such, the Pto/N site1 interaction of the second Pto is thought to remain intact despite the presence of either effector.

Unlike Pto/N site2, Pto/N site1 is not part of a homo-interaction surface, implying that it is more mobile. This is supported by the observation that N-terminal proteolysis of N is largely absent when ptoL205D is co-expressed. Thus, the cleavage site is likely

surface exposed before P+1 loop disruption, perhaps by distortion of the respective polypeptide chain. Further evidence that Pto binding at the N-terminal site (Pto/N site1) induces a conformational shift is provided by the observation that Pto complemented the ability of deletion mutants lacking the C-terminus to interact with full length N. The phospho-mimic ptoS198D/T199D mutant retained some ability to maintain the Pto/N site1 interaction, supporting a previous conclusion that Pto trans-phosphorylation alone is not sufficient for activation of the protein complex and requires P+1 loop disruption (Ntoukakis *et al.*, 2014). Despite this, when compared to the kinase inactive form ptoD164N/S198D/T199D or the phospho-null form ptoS198A/T199A, ptoS198D/T199D repeatedly showed reduced interaction with the N-terminal binding site. This suggests that Pto kinase activity plays a further role beyond the known trans-phosphorylation sites, and phosphorylation of Prf is also a possibility. It will be intriguing to test these ideas in future experiments.

Previous result suggested that both full length N and the C3 subdomain lacking the N-terminal interaction site (Pto/N site1) can suppress the autoactivity of ptoL205D. This is likely a result of ptoL205D forming an inactive complex with N and C3, and hence is unavailable to interact with NbPrf. In contrast, the N1, N2, N3 and N4 molecules lacking the C-terminal interaction site did not inhibit ptoL205D because they are unable to bind to it.

In conclusion, the N-terminal domain of Prf binds Pto through two surfaces: Pto/N site1 and Pto/N site2. Because N1 binds Pto but not ptoL205D, Pto/N site1 may be at least partly encoded in the first 159 aa of Prf. The second Pto binding site is contained by C4 (aa 376-546). As N4 (aa 1-409) does not bind the ptoL205D mutant, this binding site must lie C-terminal of N4 and thus within residues 410 – 546.

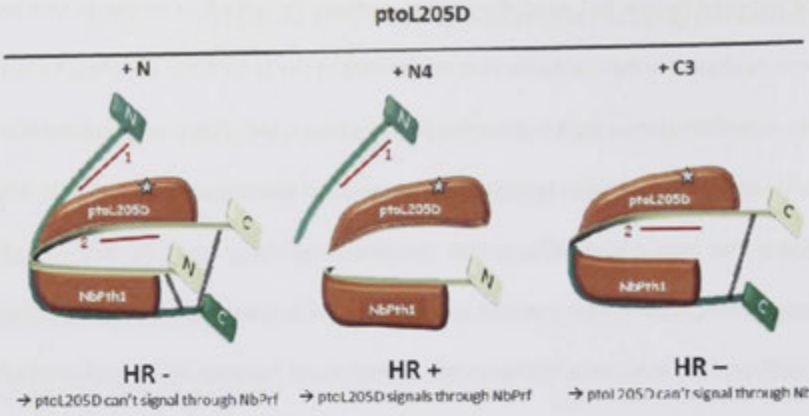

Figure 5.14: A proposed schematic representation of the conformation between the Prf N domain and the P+1 loop mutant ptoL205D based on results shown in Figure 5.11 -Figure 5.13. Pto/N site1 (Prf aa 1-159, red 1) is disrupted by the Pto L205D mutation. Pto/N site1 is encoded by N4 (Prf aa 1-409). Pto/N site2 (Prf aa 410-546, red 2) is not affected by the Pto L205D mutation. Pto/N site2 is encoded by C3 (Prf aa 293-546). The two N (deletion) molecules can be distinguished from each other by their bright and dark green color.

5.2.6. The Fen kinase is regulated by tomato Prf N but not its homolog from *Nicotiana benthamiana* NbN.

5.2.6.1. Results for 'The Fen kinase is regulated by tomato Prf N but not its homolog from Nicotiana benthamiana NbN'.

When expressed transiently in *N. benthamiana* leaves, the Fen kinase causes CGF signalling in the absence of its activating ligand fenthion (Mucyn *et al.*, 2009). Like Pto mutants containing the L205D mutation, it requires *NbPrf*. Fen may however not require trans-phosphorylation by NbPth1 as Fen possesses kinase activity itself, in the absence of the ligand fenthion. Importantly, its kinase activity is required for the CGF HR in *N. benthamiana,* as the kinase dead mutant fenD164N does not cause CGF (Wu *et al.*, 2004; Mucyn *et al.*, 2009; Ntoukakis *et al.*, 2013). Constitutive signalling by Fen is compromised by co-expression of *35S:Prf* suggesting that tomato Prf can regulate Fen appropriately,

whereas NbPrf is unable to do so. Thus, Fen and NbPrf form a mis-regulated complex that signals constitutively. Expression of *N* but not *NbN* inhibited the Fen-induced HR (Figure 5.15), and co-expression of the tomato Prf SCNL domain did not affect this (data not shown), suggesting that the inhibitory effect is encoded by N rather than the SCNL domain. These results suggest that sequence variation between N and NbN affects negative regulation of Fen in *N. benthamiana*.

The Fen-mediated HR was not affected by co-expression of C3, but was supressed by N4, and partly supressed when N1 or C1 were co-expressed (Figure 5.15). In agreement with these data, interaction tests showed that Fen was able to bind NbN, N, and N4, which suppressed the HR, but not C3, which did not (Figure 5.16). Again, the characteristic N-terminal processing of N4 by ~10 kDa was largely absent when *Fen* was co-expressed (Figure 5.16). The inability of C3 to inhibit the Fen-mediated HR can thus be explained by a lack of interaction between C3 and Fen. In contrast to Pto, Fen seems to interact with only the N-terminal interaction site of N (Pto/N site1). In contrast, the Fen HR was not inhibited by co-expression of NbN, despite the physical interaction between Fen and NbN. Thus, in contrast to the non-functional ptoL205D/N, ptoL205D/NbN (Figure 5.14) and Fen/N complexes, the Fen/NbN complex is able to elicit a hypersensitive response. This might suggest that Fen does not require the SCNL domain for signalling, or alternatively, that the Fen/NbN complex can act *in trans* to NbPrf.

To exclude an involvement of NbPrf, virus-induced-gene-silencing (VIGS) of *NbPrf* or the chaperon *NbSGT1,* required for Prf accumulation (Kud *et al.*, 2013), was performed using the tobacco rattle virus (TRV) (Peart *et al.*, 2002). As expected, when the *NbPrf* or *NbSGT1* transcripts are silenced, Fen did not cause CGF cell death (Figure

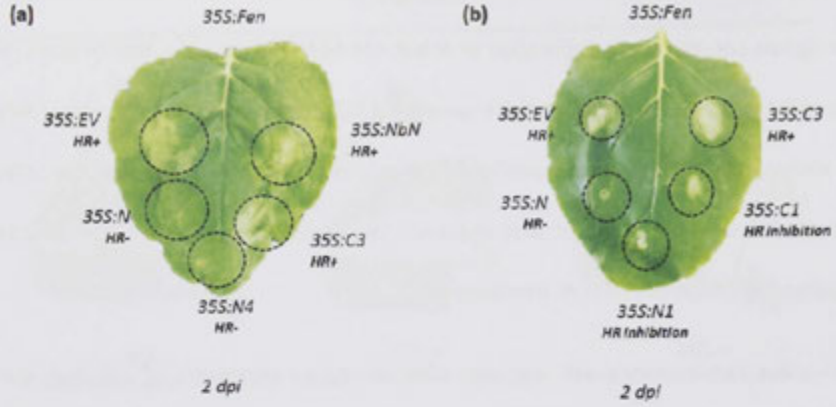

Figure 5.15: Inhibition of the Fen-mediated HR. *N. benthamiana* plants were co-transformed transiently with *35S:Fen*-5xMyc and genes encoding NbN, N, or deletion derivatives of N fused to a 3xHAF tag or EV. **(a)** Expression of *35S:Fen*-3xHA with NbN and full length N and constructs encoding the N-terminal (N4, Prf aa 1-409, Pto/N site1) and C-terminal (C3, Prf aa 293-546, Pto/N site2) Pto binding sites of N. **(b)** Expression of *35S:Fen*-3xHA with full length N as well as constructs encoding the N-terminal (N1, Prf aa 1-159, Pto/N site1) and C-terminal (C1, Prf aa 125-546; C3, Prf aa 293-546, Pto/N site2) Pto binding sites of N. The Fen-mediated hypersensitive response (HR) was detected 2 days post infiltration (dpi) and evaluated by full HR (HR+), inhibition of HR (HR inhibition) and no HR (HR-). Expression levels of the same plants can be observed in the coIP result shown below (Figure 5.16)

5.18). Importantly, co-expression of *NbN* or *C3* did not restore the Fen CGF signalling observed in the *TRV:GFP* silencing control (Figure 5.18). Notably, Fen protein accumulation was reduced in *TRV:NbPrf* and *TRV:NbSGT1* plants and most importantly, no NbN protein can be detected in *TRV:NbPrf* leaves likely due to posttranslational silencing from the *TRV:NbPrf* silencing construct. Neither the tomato Prf deletions, nor NbN accumulated in *TRV:NbSGT1* plants (Figure 5.18). To exclude an involvement of NbPrf in the HR mediated by transient expression of *Fen* and *NbN*, a synthetic sequence of *NbN* needs to be expressed together with *Fen* in *TRV:NbPrf* leaves.

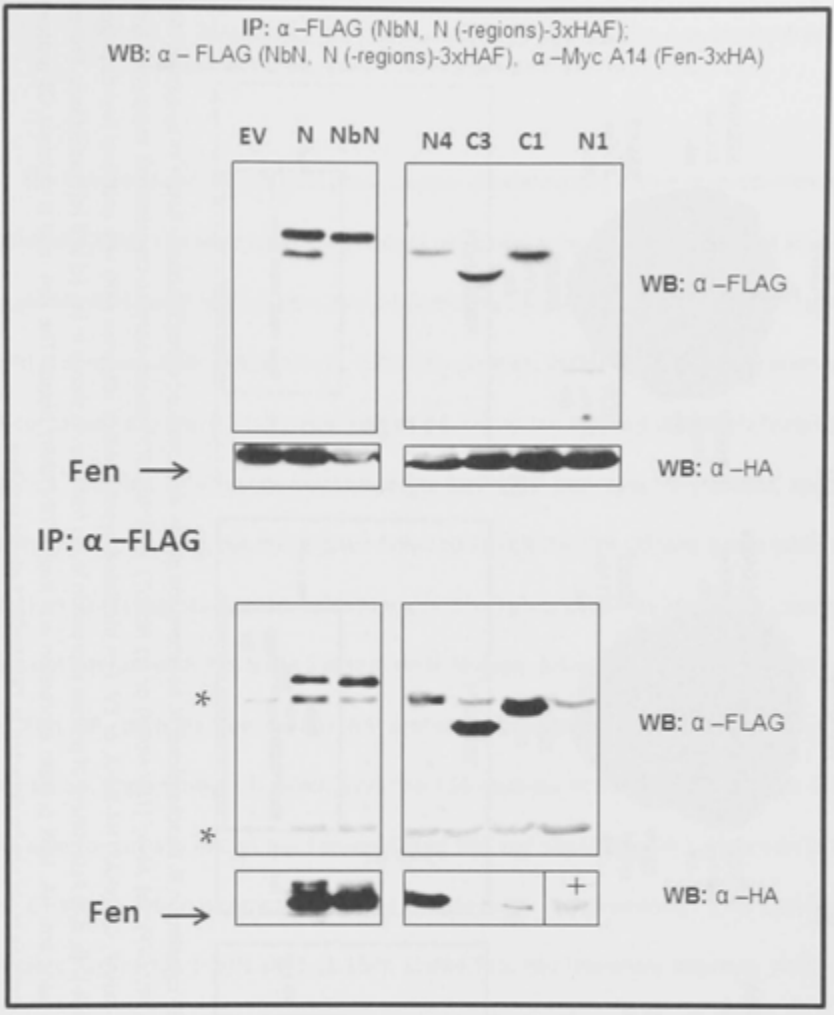

Figure 5.16: N deletants that lack the C-terminus do not bind Fen. *N. benthamiana* plants were co-transformed transiently with *Fen-3*xHA and genes encoding NbN, N, or the N deletants N1, N4, C1, C3 or EV. Leaf tissue was harvested two days post infiltration. NbN, N and its derivatives were recovered from protein extracts with anti-FLAG beads, and the immunoprecipitates probed by western blots using anti-HA or anti-Myc antibodies * indicates a cross-reacting band corresponding to the antibody heavy or light chain released form the affinity matrix. IP: Immunoprecipitated fraction. + indicated longer exposure times for the respective fraction (no band detection of EV control under longer exposure).

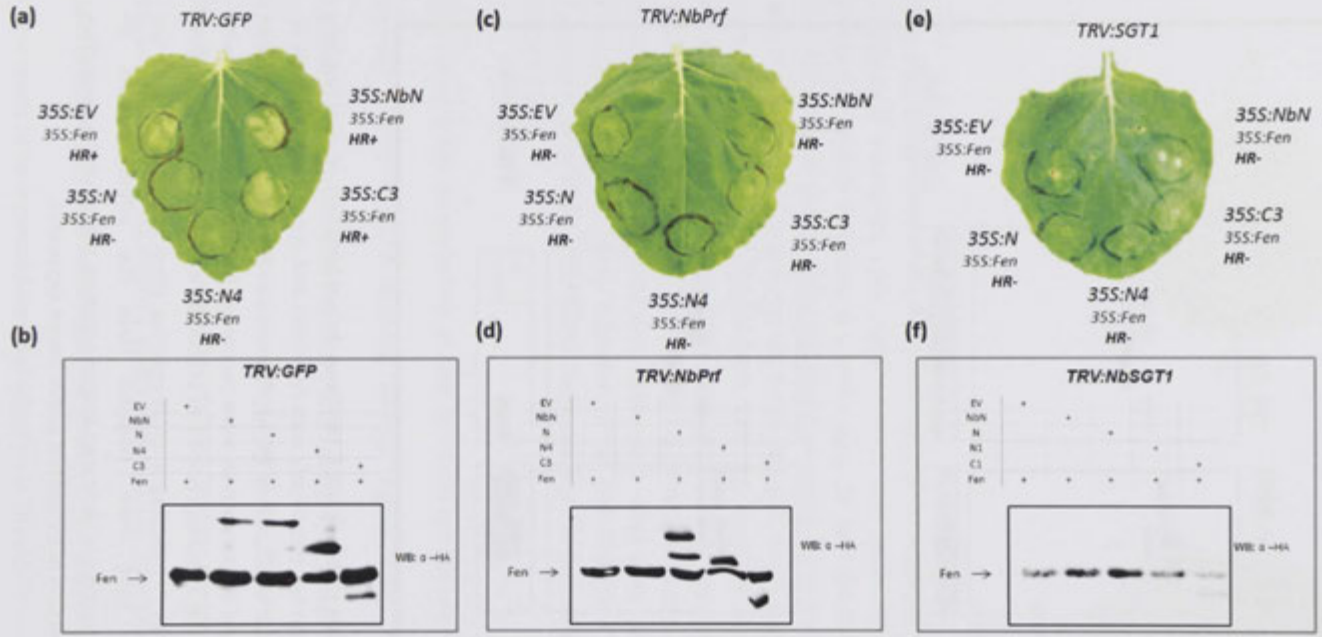

Figure 5.17: *NbPrf* is required for Fen-mediated CGF signaling in *N. benthamiana*. *N. benthamiana* plants were silenced though Tobacco-Rattle Virus-based (TRV) Virus Induced Gene Silencing (VIGS). **(a)** control (*TRV:GFP*), **(b)** *NbPrf* (*TRV:NbPrf*) or **(c)** *NbSGT1* (*TRV:NbSGT1*) plants were co-transformed transiently with *35S:Fen-3xHA* and genes encoding NbN-3xHAF, N-3xHAF, C3-3xHAF, N4-3xHA, or EV. Fen mediated hypersensitive response (HR) was assessed two days post inoculation and evaluated by HR (HR+) and no HR (HR-). **(b, d, f)** Assessment of protein expression levels from leaves shown in (a), (c) and (e) respectively. Protein expression was analysed by immunoblot analysis using anti-HA. NbN protein expression was low in *TRV:NbPrf plants*. The Fen and N deletant C3 proteins accumulated to a low level and NbN, N, N4 and C3 proteins could not be detected in *TRV:NbSGT1* plants was low.

5.2.6.2. Discussion for 'The Fen kinase is regulated by tomato Prf N but not its homolog from N. benthamiana NbN'.

The Fen kinase, similar to ptoL205D, causes HR when expressed in *N. benthamiana*. Unlike ptoL205D, this HR is kinase dependent and compromised by expression of *35S:Prf* suggesting functional and possibly structural differences between the tomato Prf N and NbPrf N domains (NbN) (Mucyn *et al.*, 2006; Mucyn *et al.*, 2009). Similarly, the N deletant N4 containing the Pto/N site1 inhibited Fen HR. N4 bound Fen and thus likely forms an inactive complex with Fen by outcompeting NbPrf for signalling. In contrast, the N deletant C3 containing the Pto/N site2 failed to inhibit the Fen HR and was unable to bind Fen. This suggests that this inhibitory effect is likely encoded by Pto/N site1, as Fen does not interact with Pto/N site 2 of tomato N. Notably, N1 was not able to fully supress the Fen HR, perhaps due to low N1 protein accumulation and thus low N1-Fen interaction. Importantly, C1, which lacks the 124 residues at the N-terminus of N, was also able to partially inhibit the Fen-mediated HR, and showed weak interaction with Fen. C1 accumulation is comparable to N4 protein levels. In agreement, C1 (aa 125-546) contains part of the Pto/N site1 (1-159). Unlike Pto, Fen therefore interacts with Prf through only one interface possibly analogous to the Pto/N site 1 N (Figure 5.18). For Pto, disruption of this site by the L205D mutation and possibly effector binding, leads to complex activation and such distruption may thus be important for Fen signalling. In this case, Prf would completely lose its ability to interact with Fen, unless this also mediates interaction of Fen with Pto/N site 2. It will be intriguing to test this in the future.

Because the Pto/N site2 does not bind Fen, site-directed mutagenesis in-cooperating Fen residues to Pto may lead to the identification of the Pto/N site2. For example, the AvrPto binding site on Pto requires the residues H49 and V51, and

mutation of these to the respective Fen residues (ptoH49E/V51G) conferred CGF to the mutant protein (Wu *et al.*, 2004; Xing *et al.*, 2007). Similar to Fen, ptoH49E/V51G is kinase active. Whether the ptoH49E/V51G CGF phenotype is kinase dependent is however unknown. Similarly, it could be informative to see if the ptoH49E/V51G CGF phenotype was inhibited by co-expression of NbN, N or its deletions N4 and C3. Notably, attempts to clone this construct were unsuccessful as additional mutations were introduced after cloning of the ptoH49E/V51G into plant expression vectors (performed by Madeleine Parker (summer scholar) under my supervision). Similar problems regarding this mutant have been reported previously (Xing *et al.*, 2007). On the other hand, it would be interesting to determine Fen CGF activity when in-cooperating Pto/N site 2 to Fen. A surprising and potentially important result is that the interaction of the isolated NbN domain with Fen does not compromise CGF signalling by Fen in *N. benthamiana*. First of all, this provides an additional opportunity to define important contact sites. Generating NbN deletants corresponding to N4 and C3, domain swaps between NbN and N and comparing polymorphic residues through site-directed mutagenesis, with subsequent functional analysis in signalling with, and binding to Fen and Pto, may reveal the regions responsible for the functional differences between tomato N and NbN. Especially those residues that have apparently co-evolved between *Pto* and *N* as determined by computational analysis (Grzeskowiak *et al.*, 2014) may reveal functionally important residues and should be targets for mutational analysis. Notably, Grzeskowaik *et. al.* 2014 propose co-adaption of Pto P+1 loop residues with C-terminal amino acids of N. Biochemical studies here imply that the N-terminus of Prf binds to the Pto P+1 loop in the resting state complex (Pto/N site1), but an impact of the C-terminal amino acids (Pto/N site2) cannot be excluded, especially because the C3 deletion fragment containing Pto/N site2 was unable to bind Fen.

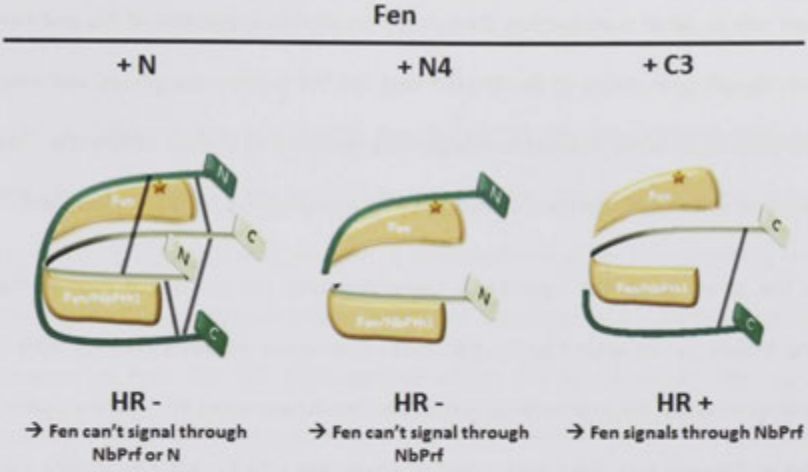

Figure 5.18: A proposed schematic representation of Fen regulation by N and its deletion regions N4 and C3 based on results in Figure 5.15-Figure 5.17. N and N4 but not C3 repress Fen signalling. N therefore only contains one binding site for interaction with Fen. Unlike Pto, the Fen molecule does not require P+1 loop disruption for signalling in *N. benthamiana*, but is kinase-dependent. The two N (deletion) molecules can be distinguished from each other by their bright and dark green colour.

One interpretation of the result that NbN does not inhibit Fen CGF is that Fen, provides the function necessary for downstream signalling. In this scenario, SCNL would act only as a regulatory unit to activate the kinase activity of the associated kinase subunit(s). In this scenario, the N domain is required for close proximity between two Fen (or Pto) molecules and (upon ligand binding to the first kinase, activation of the NB domain of Prf and de-repression of the second kinase) or may be phosphorylated directly by either kinase to cause downstream signalling. Mis-regulation of Fen by NbN may thus overcome the requirement for the NbPrf SCNL domain in activating the second Fen kinase. This is supported by the observation that CGF signalling of the kinase dead phospho-mimic ptoS198D/T199D/L205D is compromised by co-expression of N (Figure

5.12). Importantly, NbN was also able to suppress the HR induced by ptoS198D/T199D/L205D, but not by Fen, enforcing the idea that kinase activity plays an important role in signal transduction. Overall the results are suggestive of Pto and Fen being the signalling moieties of the Pto/Prf and Fen/Prf protein complexes and may phosphorylate N or other downstream-signalling partners to induce resistance. This would explain why so far, a protein transducing Prf signalling has not been identified.

On the other hand, the hypothesis suggesting that Fen (or active Pto) is the signalling moiety, is challenged by the fact that extreme overexpression of Prf from a dexamethasone-inducible promoter causes an NbPth1-independent HR. In this scenario, signalling by Prf seemed to be independent of any kinase activity, but importantly, the HR is repressed when the kinase inactive *ptoD164N* was co-expressed. It is therefore possible that another *N. benthamiana* protein kinase acted together with Prf in this experiment, or that NbPth1 was silenced insufficiently (Mucyn *et al.*, 2006).

Alternatively, Fen and NbN may also act in *trans* with NbPrf. To test this possibility, I silenced *NbPrf* and co-expressed *NbN* and *Fen*. Post-translational silencing however caused strongly reduced NbN protein expression (Figure 5.18). In an alternative approach, I silenced the gene encoding the chaperon NbSGT1, required for accumulation of NB-LRR proteins (Kud *et al.*, 2013). However, NbSGT1 also stabilises NbN and N, as *SGT1* silencing caused abrogated protein levels of NbN, N and the N deletants. To therefore assess Fen/NbN CGF in the absence of NbPrf, *NbPrf* needs to be silenced and a synthetic *NbN* construct co-expressed with *Fen*

5.2.7. The N domain of Prf interacts with SCNL via the LRR domain.

5.2.7.1. Results for 'The N domain of Prf interacts with SCNL via the LRR domain'.

Prf requires both N and SCNL for its function. The interaction between these domains restores the functional Prf molecule when the gene encoding Pto is co-expressed, as transient co-expression of both moieties under the control of the 35S promoter leads to a weak but reliable hypersensitive response in *N. benthamiana* (in the presence of Pto). This HR is thought to reflect the ligand-independent signalling phenotype found when Prf is overexpressed in the presence of Pto but in the absence of the effectors AvrPto or AvrPtoB. The separated molecules interact with each other after transient co-expression to reconstitute Prf (Mucyn *et al.*, 2006). Although no other characterised NB-LRR protein contains a domain homologous to N, reconstitution of function by co-expression of separated domain has been demonstrated extensively for the potato NB-LRR protein Rx (Moffett *et al.*, 2002).

I tested the ability of the N deletions to interact with SCNL and confer CGF when their genes were overexpressed together with *Pto* in the absence (effector independent HR) and presence of the effector AvrPtoB (effector dependent HR). Co-expression of either of the genes encoding the N deletants together with *SCNL* and *Pto* did not lead to HR signalling (Figure 5.19). Co-expression of the *35S:AvrPtoB* construct caused a slight HR, independently of N or its deletants (Figure 5.19). Only when full length *N* was co-expressed together with *Pto, SCNL* and *AvrPtoB* from the strong 35S promoter, a strong HR was detected (Figure 5.19). I conclude that neither N deletion is capable of causing an effector-dependent or effector-independent HR, suggesting that both termini of Prf N are required to reconstitute a functional Prf molecule after co-expression with *SCNL*.

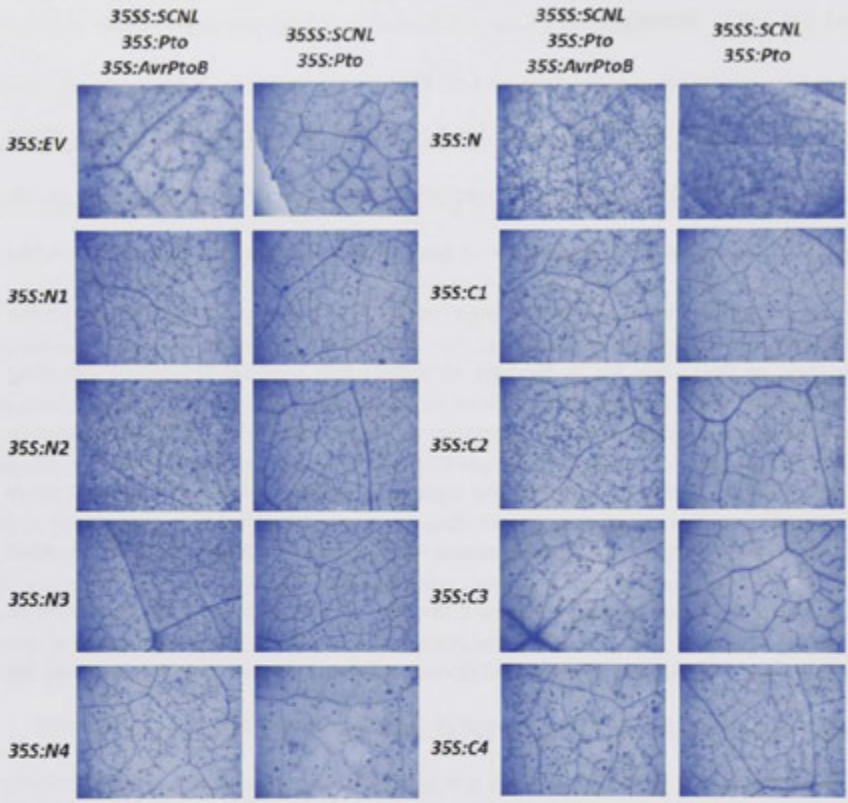

Figure 5.19: None of the N deletants induce effector-independent or effector-dependent signalling in the presence of Pto and SCNL. *N. benthamiana* leaves were transformed as indicated and harvested for trypan blue staining five days after transformation with genes encoding N, SCNL, and Pto. The intensity of the HR was determined by microscopic analysis after trypan blue staining. Overexpression of *N, Pto* and *SCNL* leads to a hypersensitive response (HR, dark blue spots) in *N. benthamiana*. Expression of *AvrPtoB* one day after initial transformation causes a weak HR in the absence of N or its deletants. A stronger HR can be detected when *N* was expressed with *Pto, SCNL* and *AvrPtoB*, but not when *N* was substituted for any of its deletants.

All of the N deletions bound to Pto (Figure 5.6). I thus investigated that a lack of HR after co-expression of the *N* deletants with *Pto* and *SCNL* is caused by a lack of interaction between the N deletants and SCNL. To test this, I isolated the N deletion proteins and checked for co-precipitation of SCNL in the presence of Pto (Figure 5.20). All N deletions interacted with SCNL. C2 and C3 interacted consistently but only weakly with SCNL as longer exposure times were required to detect the interaction (EV still negative after longer exposure) (Figure 5.20). Notably, the presence of SCNL did not alter the ability of any N deletion to bind Pto (Figure 5.20). In a reverse coIP, pull down of SCNL co-isolated N and all N deletants (data not shown). The N deletion proteins N2 and C3 do not overlap, suggesting either two individual interaction sufaces for SCNL within N or one large interaction surface spanning from the N- to the C-terminus. The N middle fragments NmS and NmL co-precipitated SCNL, but SCNL did not co-precipitate NmS or NmL in the corresponing reverse coIP. I therfore conclude that NmL and NmS bind SCNL weakly or not at all (Figure 5.8, Figure 5.21).

Mucyn *et. al.* found that the assembly of Prf from separate N and SCNL components is dependent on Pto (Mucyn *et al.*, 2006). I found that N and its deletion proteins co-isolated SCNL when Pto was absent, but their protein accumulation enhanced by infiltration of the proteasome inhibitor MG132 (Figure 5.22). This implies that the role of Pto in Prf reconstitution is likely related to increasing the accumulation of either interation partner. I also tested the requirement of the Prf SD domain in mediating this interaction. For this, I generated the *CNL* construct (SCNL domain lacking the SD domain) and tested its ability to interact with N and its deletion proteins. Similarly to SCNL, CNL was co-precipitated by N and all of its deletants in the presence or absence of Pto (Figure 5.23, Figure 5.24, Figure 5.27). In contrast, the HR phenotype observed

when N, SCNL and Pto were overexpressed was absent in leaves co-expressing CNL, Pto and N (Figure 5.23) or any of the N deletants (data not shown), suggesting that the SD domain plays an imporant role in reassembling the a functional Prf molecule, but is not required for the physical interaction between N and SCNL. To determine which part of the SCNL physically assembles with N, I generated the Prf domains SD, CC-NB, and LRR. Co-expression of either of those constructs with *N* revealed that reconstitution of Prf by N and SCNL is likely mediated by the Prf LRR domain. The LRR domain, but not SD or CC-NB, bound to N in forward and reverse coIP analyses (Figure 5.25). Again, all N deletants were also able to co-precipitate the LRR domain (Figure 5.26, Figure 5.27).

To test if the Pto P+1 loop mutation L205D affects the interaction underlying the N-SCNL assembly, ptoL205D was co-expressed with N or and SCNL. N bound to SCNL when Pto or ptoL205D were co-expressed (data not shown). Because all N deletants interacted with SCNL, N may contain two interaction sites for SCNL, one on the N- and one on the C-terminus of N. I thus tested if either of those predicted SCNL-N interactions are affected by the co-expression of ptoL205D. N4 and C3 interacted with SCNL in the presence of ptoL205D (Figure 5.28). Notably, N4 did not interact with ptoL205D and thus an effect on N4-SCNL interaction was not expected.

The Prf mutation D1416V causes CGF signalling, which is dependent on *NbPth1* (Ntoukakis *et al.*, 2013). The D1416V mutation lays within the conserved MHD motive in the NB site. The SCNL domain corresponding to the CGF mutant prfD1416V (scnlD888V) does not confer CGF signalling (data not shown). SCNL lacks the Pto bnding mioety N, it can thus not bind NbPth1. I tested if scnlD888V showed differences in the interaction with N and its deltants N4 or C3 in the presence of Pto or its CGF mutant ptoL205D. Full

length N (data not shown), N4 and C3 interacted with scnlD888V in the presence of wild-type Pto and ptoL205D (Figure 5.28).

I thus conclude that Prf is assembled by N and SCNL through an interaction of N with the SCNL LRR domain. The SD domain is not required for this interaction, but for the microscopic HR mediated by co-expression of *Pto, N* and *SCNL*. The L205D mutation of *Pto* and D888V mutation of *scnl* do not change the interaction between full length N or its deletants N4 or C3 with SCNL. N4 does not bind ptoL205D and as such an effect of N4/SCNL interaction or N4/scnlD888V interaction by the P+1 loop mutation L205D is also not expected. Because of this experimental limitation, I cannot make a statement about possible changes in the N/LRR interaction when the Pto/N site1 is distrupted by the Pto L205D mutation.

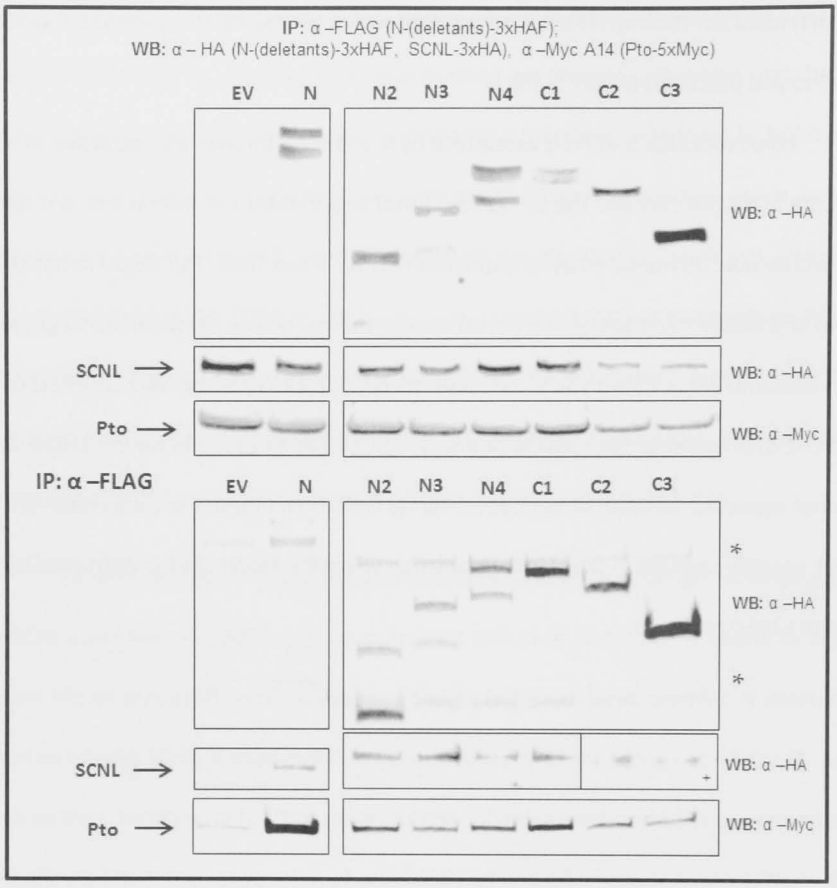

Figure 5.20: N and its deletions co-precipitate SCNL. *N. benthamiana* plants were co-transformed with genes encoding SCNL-5xHA, Pto-5xMyc and N, each of the N deletants fused to a 3xHAF tag, or EV. Only a weak interaction of C2 and C3 with SCNL was detected. Leaf tissues were harvested two days post infiltration. N and its deletants were recovered from protein extracts with anti-FLAG beads, and the immunoprecipitates probed by western blots using anti-HA or anti-Myc antibodies. * indicates a cross-reacting band corresponding to the antibody heavy or light chain released form the affinity matrix. + indicates longer exposure times. IP: Immunoprecipitated fraction.

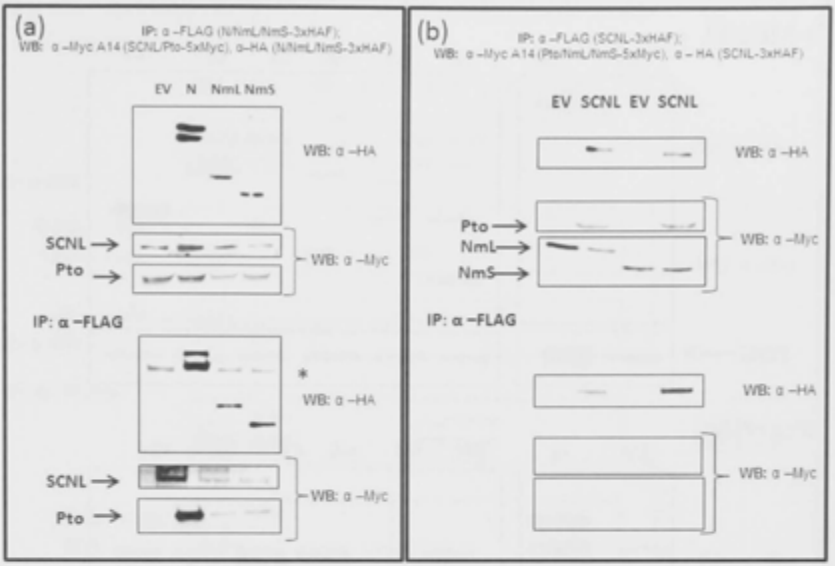

Figure 5.21: Negligible binding of the N middle fragments NmL and NmS with SCNL. (a) *N. benthamiana* plants were co-transformed transiently with genes encoding Pto and SCNL fused to a 5xMyc tag and N, NmL or NmS fused to a 3xHAF tag or EV. **(b)** *N. benthamiana* plants were co-transformed transiently with genes encoding SCNL-3xHAF or EV, and NmL-5xMyc or NmS-5xMyc. All samples with SCNL-3xHAF also contained Pto-5xMyc. Leaf tissues were harvested two days post infiltration. Proteins tagged with 3xHAF were recovered from protein extracts with anti-FLAG beads, and the immunoprecipitates probed by western blots using anti-HA or anti-Myc antibodies. * indicates a cross-reacting band corresponding to the antibody heavy chain released form the affinity matrix. IP: Immunoprecipitated fraction.

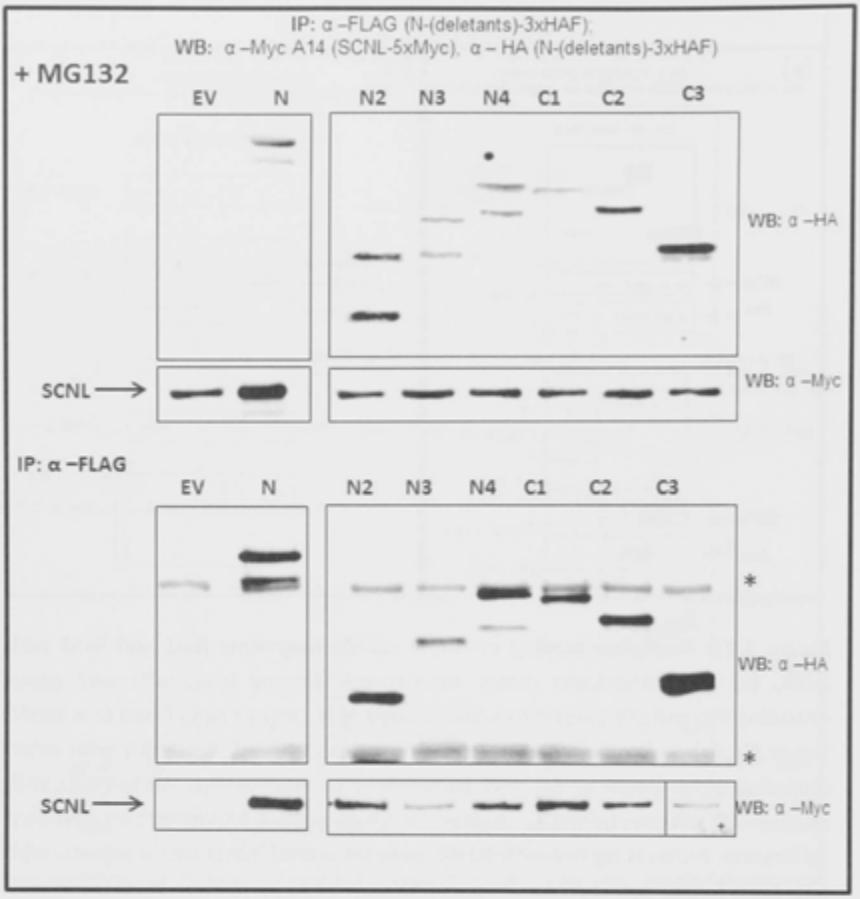

Figure 5.22: The interactions of N and its deletants with SCNL is not dependent on Pto but the accumulation of SCNL. *N. benthamiana* plants were co-transformed transiently with genes encoding SCNL-5xMyc and either N, its deletants fused to a 3xHAF tag, or EV. Leave tissues were harvested two days post infiltration. N and its deletions were recovered from protein extracts with anti-FLAG beads, and the immunoprecipitates probed by western blots using anti-HA or anti-Myc antibodies. * indicates a cross-reacting band corresponding to the antibody released form the affinity matrix. + indicates longer exposure times for the respective reaction when compared to the section next to it. IP: Immunoprecipitated fraction.

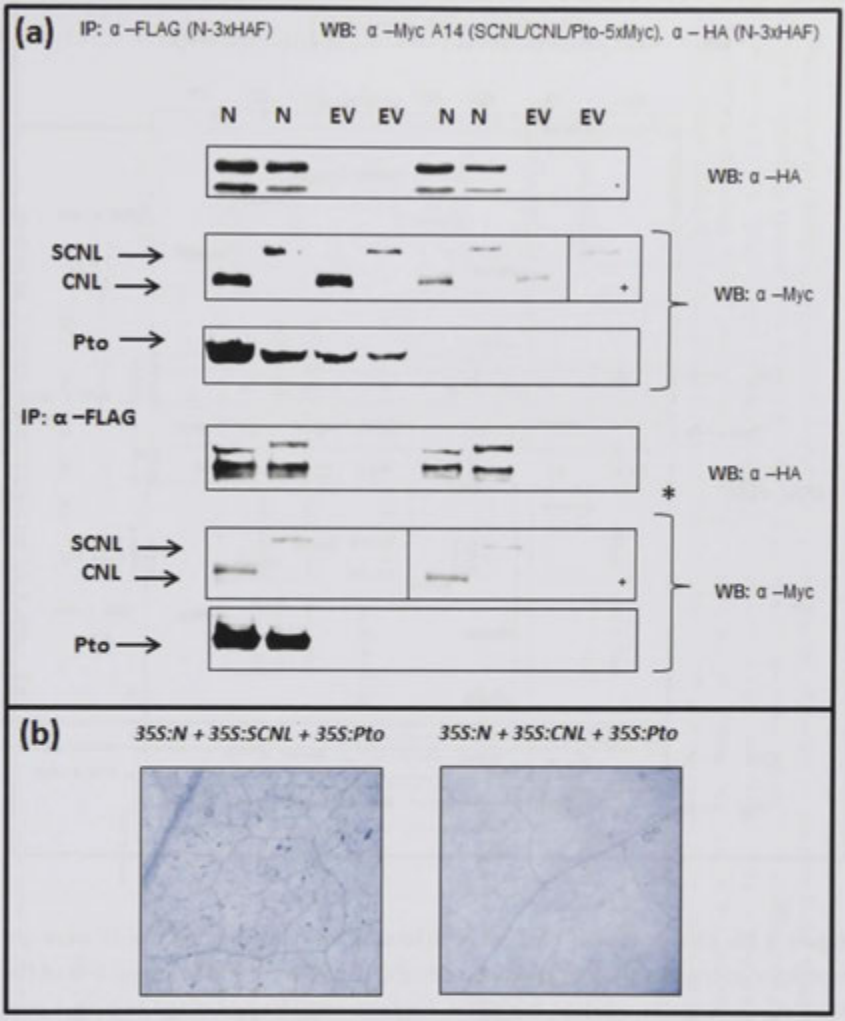

Figure 5.23: N binds the Prf SCNL and CNL domains in the absence and presence of Pto. (a) *N. benthamiana* plants were co-transformed transiently with genes encoding N-5xMyc or EV, and either SCNL-5xMyc or CNL-5xMyc, in the presence or absence of Pto-5xMyc. Leaf tissues were harvested two days post infiltration. N was recovered from protein extracts with anti-FLAG beads, and the immunoprecipitates probed by western blots using anti-HA or anti-Myc antibodies. + indicates longer exposure times. IP: Immunoprecipitated fraction. **(b)** Overexpression of genes encoding N, Pto and SCNL leads to a HR. The HR is absent when genes encoding N and Pto were co-expressed with CNL. For trypan blue staining, whole leaves are harvested and stained 5 days post infiltration.

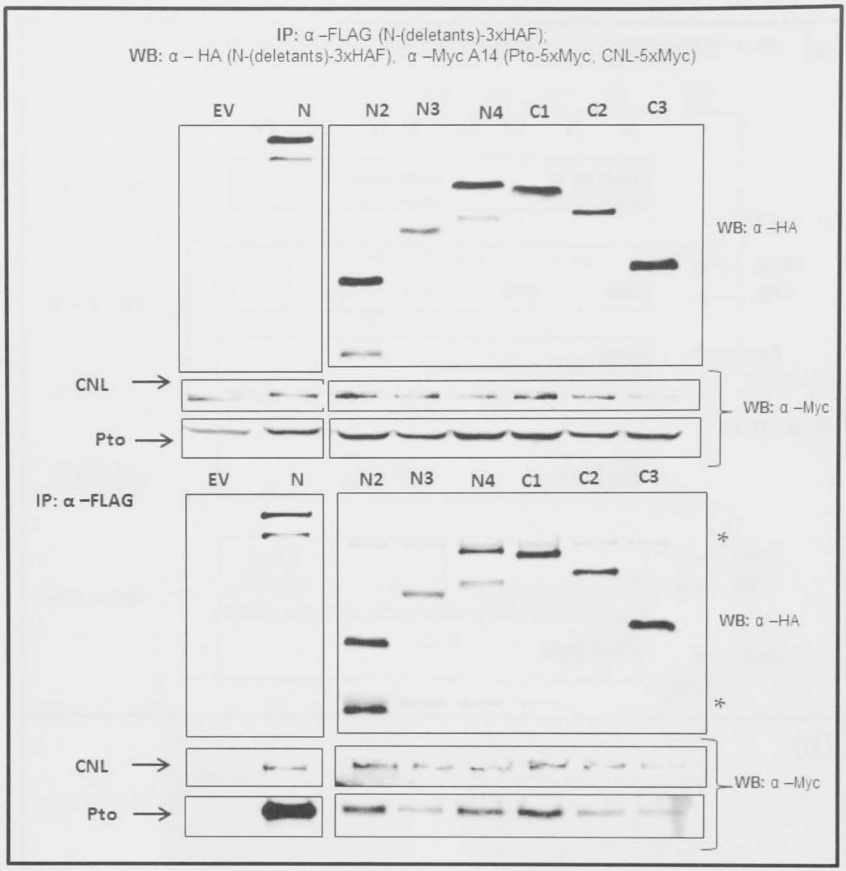

Figure 5.24: CNL is able to bind all N deletants. *N. benthamiana* plants were co-transformed transiently with genes encoding CNL-5xMyc, Pto-5xMyc, and one of the N deletants fused to a 3xHAF tag or EV. Leaf tissues were harvested two days post infiltration. N and its deletants were recovered from protein extracts with anti-FLAG beads, and the immunoprecipitates probed by western blots using anti-HA or anti-Myc antibodies. * indicates a cross-reacting band corresponding to the antibody released form the affinity matrix. IP: Immunoprecipitated fraction.

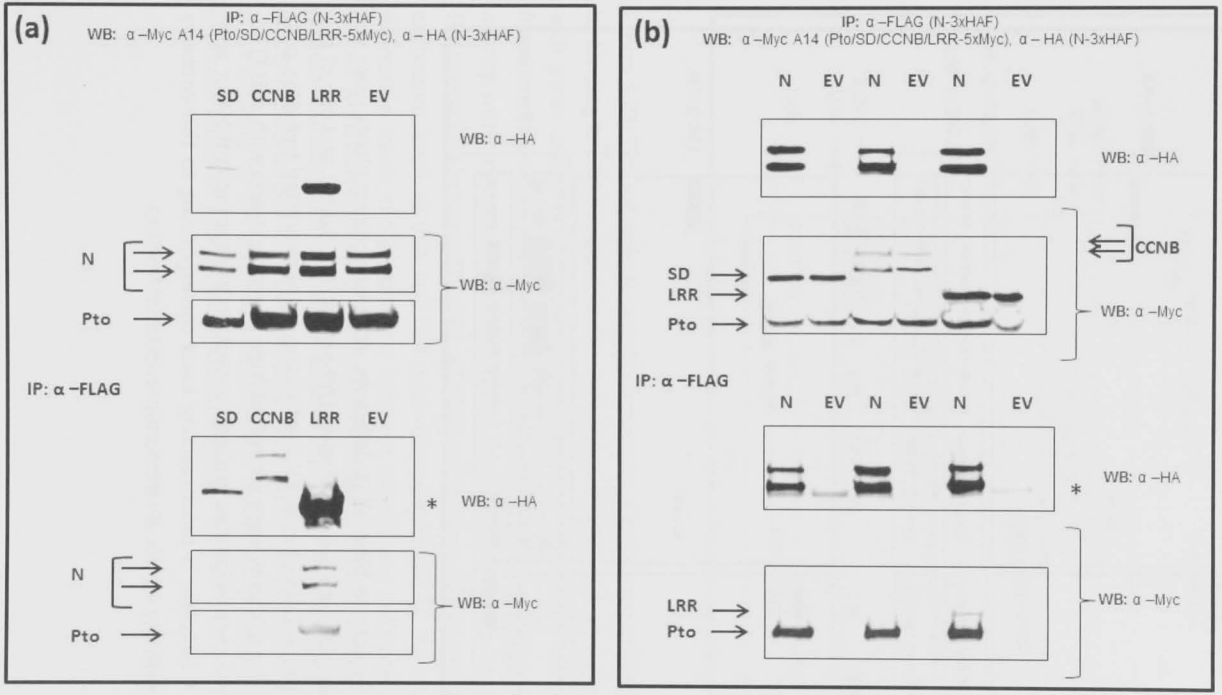

Figure 5.25: Prf N interacts with the LRR domain. (A) *N. benthamiana* plants were co-transformed transiently with genes encoding the SD, CC-NB or LRR domains fused to a 3xHAF tag or EV, Pto-5xMyc and N-5xMyc. (B) *N. benthamiana* plants were co-transformed transiently with genes encoding N-3xHAF or EV, Pto-5xMyc, and either SD-5xMyc, CC-NB-5xMyc or LRR-5xMyc. Leaf tissues were harvested two days post infiltration. Proteins tagged with 3xHAF were recovered from protein extracts with anti-FLAG beads, and the immunoprecipitates probed by western blots using anti-HA or anti-Myc antibodies. * indicates a cross-reacting band corresponding to the antibody heavy chain released from the affinity matrix. IP: Immunoprecipitated fraction.

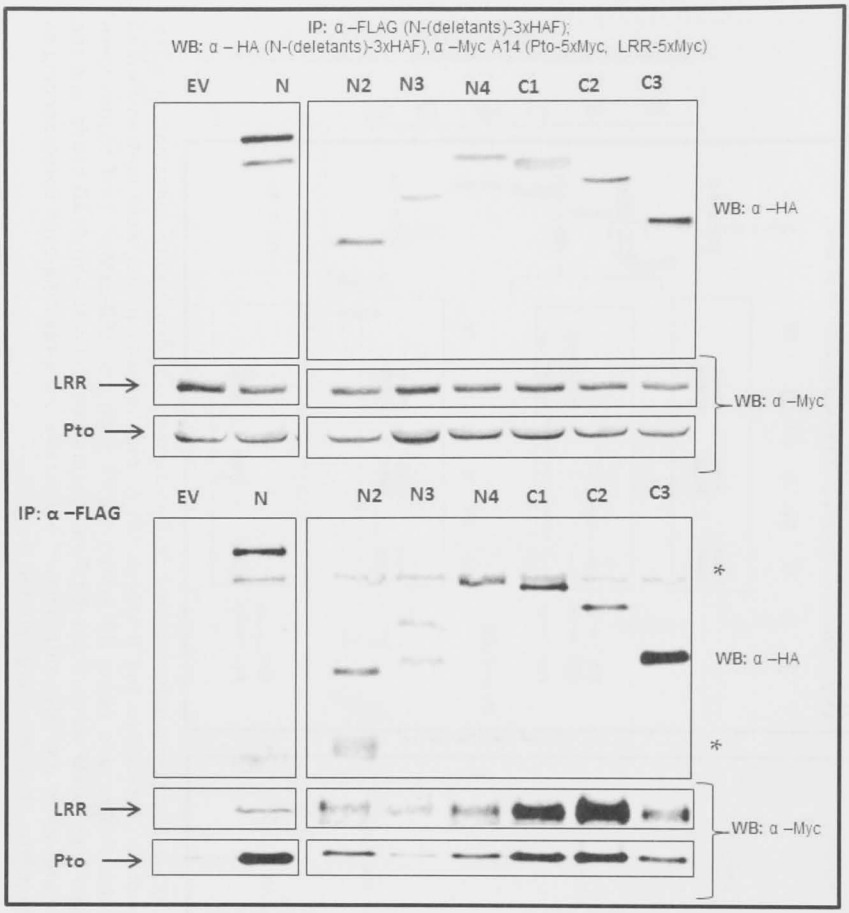

Figure 5.26: LRR is able to bind all N deletants. *N. benthamiana* plants were co-transformed transiently with genes encoding LRR-5xMyc, Pto-5xMyc, and one of the N deletants fused to a 3xHAF tag or EV. Leaf tissues were harvested two days post infiltration. N and its deletants were recovered from protein extracts with anti-FLAG beads, and the immunoprecipitates probed by western blots using anti-HA or anti-Myc antibodies. * indicates a cross-reacting band corresponding to the antibody released form the affinity matrix. IP: Immunoprecipitated fraction.

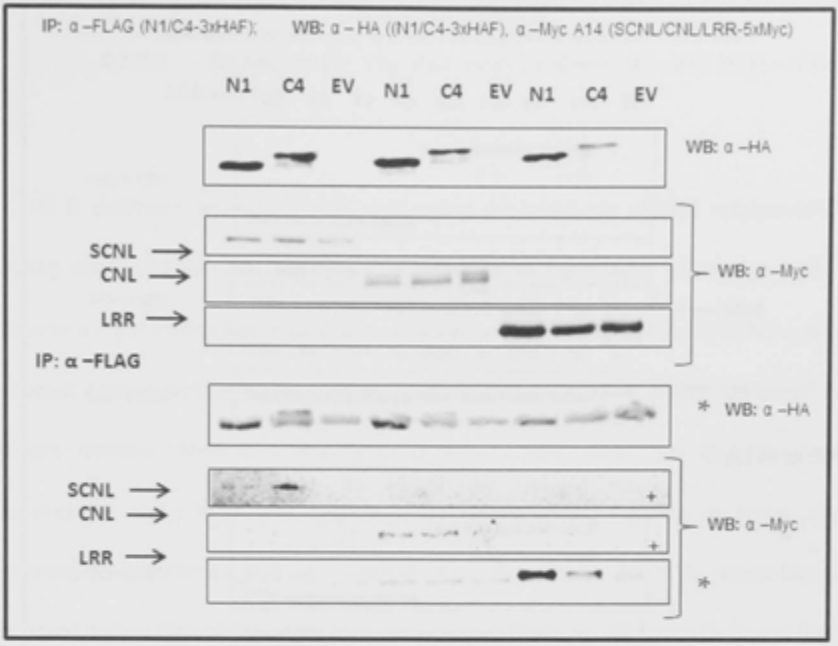

Figure 5.27: The extreme N- and C-termini of Prf N interact with the SCNL domain by binding its LRR structure. *N. benthamiana* plants were co-transformed transiently with genes encoding SCNL-5xMyc, CNL-5xMyc or LRR-5xMyc, and either N1 or C4 fused to a 3xHAF tag, or EV. Although hard to detect due to low expression levels and overlap with cross-reacting bands, N1 and C4 were both able to co-precipitate SCNL. The interaction between N1 or C4 with CNL or LRR were clearer possibly due to higher expression levels of CNL and LRR when compared to SCNL. To ensure detectable expression levels, the proteasome inhibitor MG132 was infiltrated after 24h. Leaf tissues were harvested two days post infiltration. N1 and C4 were recovered from protein extracts with anti-FLAG beads, and the immunoprecipitates probed by western blots using anti-HA or anti-Myc antibodies. * indicates a cross-reacting band corresponding to the antibody released form the affinity matrix. + indicates longer exposure times. IP: Immunoprecipitated fraction.

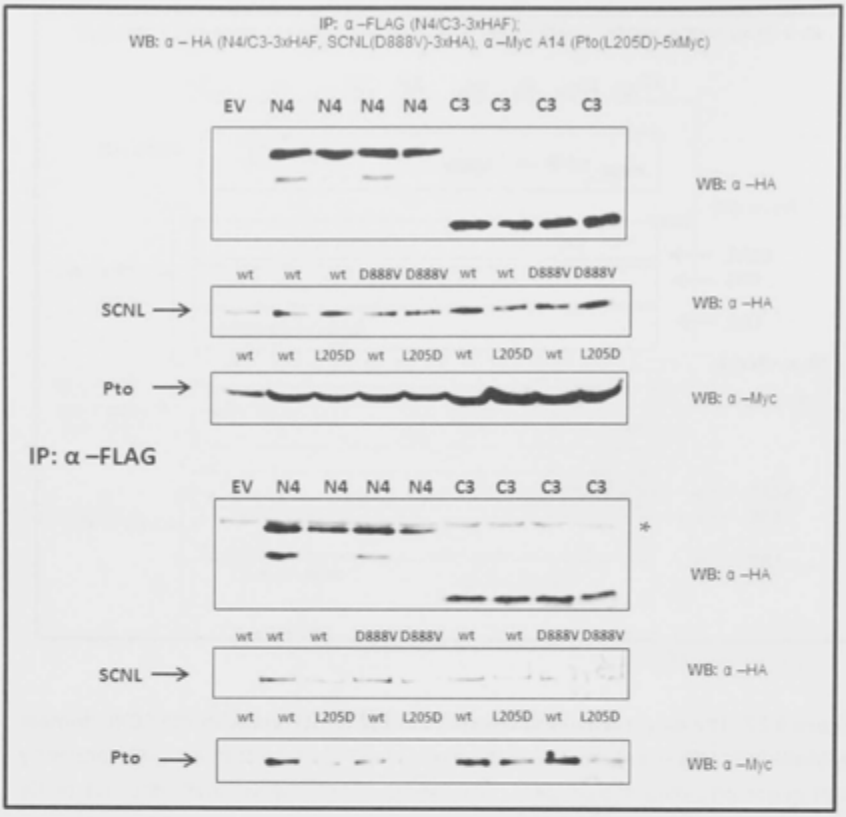

Figure 5.28: The Pto L205D mutation and the SCNL D888V mutation do not change the reconstituted Prf complex. *N. benthamiana* plants were co-transformed transiently with *N4* or *C3* fused to a 3xHAF tag or EV *together* with either *SCNL-3xHA* or *scnlD888V-3xHA* and *Pto-5xMyc* or *ptoL205D-5xMyc*. Leaf tissues were harvested two days post infiltration. N4 and C3 proteins were recovered from extracts with anti-FLAG beads, and the immunoprecipitates probed by western blots using anti-HA or anti-Myc antibodies. * indicates a cross-reacting band corresponding to the antibody released from the affinity matrix. IP: Immunoprecipitated fraction.

5.2.7.2. Discussion for 'The N domain of Prf interacts with SCNL via the LRR domain'.

All N deletants bound to SCNL suggesting the presence of two independent N binding sites for SCNL. Alternatively, N may contain a large SCNL interaction surface. Because a clear interaction of the N middle regions NmL and NmS with SCNL was not detected, I conclude that such a large interaction surface for SCNL on the full length N is unlikely. Notably, the N-terminal deletion protein C3 only bound to SCNL weakly in the presence or absence of Pto (Figure 5.20, Figure 5.22). I repeated those exact experiments four times and can conclude that this weaker C3/SCNL assembly was observed only in 50% of the performed experiments (Figure 5.20, Figure 5.22 and Figure 5.28). It therefore remains questionable, if this weaker interaction is of biological significance.

A lack of co-precipitation of the SCNL domain by Prf (Mucyn *et al.*, 2006) may be explained by the strong N-domain homodimerisation of the intact Prf proteins. In this case, N would not be available to interact with SCNL *in trans*. Additionally, assembly of the Prf holomolecule from N and SCNL components required co-expression of Pto in previous coIP analysis, whereas here it was shown that this is likely due to enhanced protein and complex stability rather than Pto functionally mediating this interaction.

The interaction between the Prf LRR and N domains is likely the interface for functional restoration of the Prf molecule after co-expression of the isolated N and SCNL domains (Figure 5.29). In agreement, N was able to interact with both CNL and the LRR domain, but not the SD or CC-NB domains, and these interactions did not require Pto. Whether the N-LRR interaction occurs in *cis* or *trans* within the dimeric full length Prf

complex remains undetermined. Correspondingly, all N deletants interacted with CNL and LRR. Notably, the interaction between C3 with CNL and LRR was not weaker than the interaction of all other N deletants with CNL and LRR. This is in contrast with the C3/SCNL interaction, which was weaker than the interaction of the other N deletants in 50% of the cases.

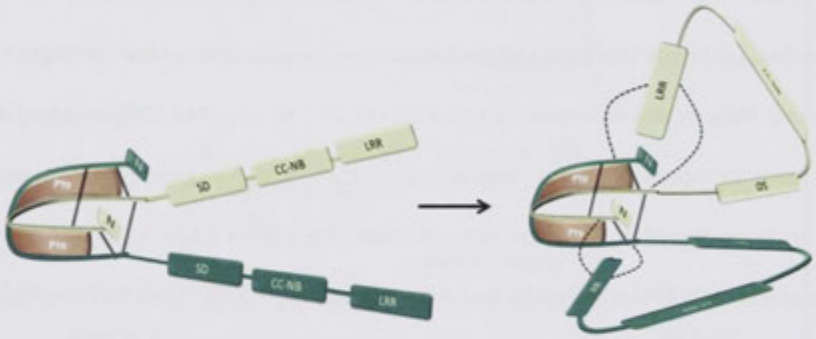

Figure 5.29: A schematic representation of the Pto/Prf complex with the N dimer in an anti-parallel conformation and the LRR domain binding N *in cis*. N forms a parallel (Saur *et. al.*, 2015) or an anti-parallel homodimer that folds over crosswise. Each of the two Pto molecules binds both the N- and C-termini of N. The LRR domain of SCNL binds to the N domain through two binding sites, bringing the N- and C-termini of the intact Prf molecule into close proximity. Note that whether the LRR of one Prf molecule binds the Pto/N site1 *in cis* or *in trans* remains undetermined.

The interactions between N or its deletants and SCNL were not affected by CGF mutations in Pto (L205D) and/or Prf (D1416V). The D1416V mutation lays within the Prf NB site in the MHD motif; D888V is the corresponding mutation within the SCNL moiety of Prf. The MHD motive is highly conserved in plant NB-LRR proteins and mutations within this motif cause CGF of several NB-LRR proteins (DeYoung & Innes, 2006). The D888V mutation did not change the interaction between SCNL and N. Further, the C3 (containing Pto/N site2) protein bound both SCNL and scnlD888V, in the presence of

either Pto or ptoL205D. The same results were found for the C-terminal deletion construct N4. Notably, N4 (containing Pto/N site1) was unable to bind to ptoL205D, which removes its ability to translate the P+1 loop disruption to the SCNL domain. Because of the N-LRR interface must be located so closely to the Pto-N complex, it is possible that this interaction is changed during effector binding or subsequent activation of Pto kinase activity, causing molecular activation of the NB site. Such a change could involve a change of conformation rather than abrogation of the interaction per se. In this case, the Prf LRR domain mediates certain intra-/inter-molecular interactions to regulate the NB domain molecular switch (potentially exchange of ADP to ATP) (Kim, HE *et al.*, 2005; Riedl *et al.*, 2005; Takken *et al.*, 2006). Such a hypothesis may be supported by the inhibitory effect of the Prf lack-of-function mutant prfK1128A (Prf NB P-loop mutation) on the gain-of-function mutants ptoL205D and prfD1416V (Ntoukakis et al., 2013), and inhibition of the prfD1416V by overexpression of the Prf LRR domain (Du et al., 2012). As such, the presence of one non-functional Prf molecule (prfK1128A) or a regulatory unit (LRR) in the Pto/Prf dimeric complex may abrogate signal transduction induced by effector binding to Pto (or its L205D mutation).

I conclude that the use of deletion proteins is insufficient to detect hypothetical conformational changes of the intra-/inter-molecular interaction between Pto/N site1 and LRR. However, if the regulatory residues within the Pto/N site1 (affected by the Pto L205D mutation and likely effector binding) can be identified, mutations within this region in the full length N molecule may allow detecting changes within this interface.

5.3. Conclusion.

The N domain of Prf forms a parallel or anti-parallel homodimer that folds crosswise (5.2.3). The N dimer has two binding sites for one Pto molecule, one on the N-terminus

of Prf N (Pto/N site1) and one on the C-terminus of N (Pto/N site 2) (5.2.4). The Pto L205D mutation, mimicking effector binding, causes loss of the Pto/N site1 interaction surface (residues 1-159). Pto/N site 2 (residues 409-546) remains unaffected by the Pto L205D mutation (5.2.5). Positioning the LRR domain close to the Pto-N regulatory hub (5.2.7) could provide a mechanistic link between effector recognition and regulating the NB switch, which is required for Pto trans-phosphorylation and full complex activation. Two potential signalling pathways through the Pto/Prf complex (with N as an anti-parallel homodimer) by effector-mediated activation are possible: The disruption of the Pto/N site1 (by effector binding or the L205D mutation) translates to Prf through 1. a disruption of the Pto/N site1 interface with LRR (*in trans*, Figure 5.30 a, b1, c) or 2. signalling through the N domain (Figure 5.30 a, b2, c). Subsequent changes in conformation within the SCNL domain may cause activation of one or the other Prf NB domains by exchange of ADP to ATP. The activation of the Prf NB domain activates the second Pto molecule for Pto trans-phosphorylation. In this scenario, a Pto/N site1 interaction with LRR is possible *in cis* and *in trans*. If N however, forms a parallel homodimer (Figure 5.31), the LRR domain likely binds the N domain *in trans* (N of one Prf binds the LRR domain of the second Prf). This is based on the observation that an *in cis* interaction (Figure 5.31, N of one Prf binds LRR of the same Prf) would not allow signal transduction from one Pto molecule (effector binding determinant) to the second Pto molecule (trans-phosphorylation determinant). Both conformations remain same likely at this stage. HR and resistance may be mediated by trans-phosphorylation of the first Pto molecule itself. Alternatively, the activation of the second Pto kinase may induce phosphorylation of N, LRR or downstream signalling components, leading to HR and resistance. Overall, results are suggestive of the idea that the Pto/N complex is the moiety of the Pto/Prf complex that initiates downstream signalling.

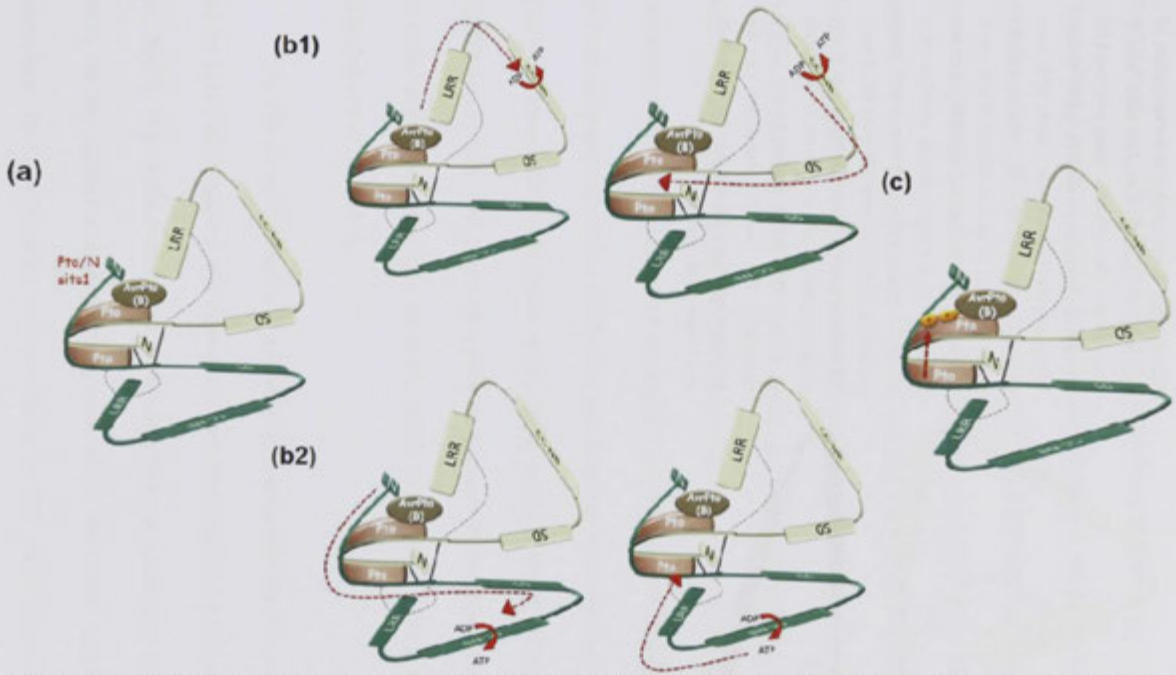

Figure 5.30: A schematic representation of the Pto/Prf protein complex with the N dimer in antiparallel conformation, and the LRR domain binding N in *trans with the Pto/N site1.* **(a)** Prf N may form an anti-parallel homodimer, which folds over crosswise. Formation of the N dimer in parallel is not excluded by this study. Each of the two Pto molecules binds both the N- and C-termini of N. The LRR domain of Prf binds to the N domain, bringing the N- and C-termini of the intact Prf molecule into close proximity. Note that whether the LRR of each Prf molecule binds the Pto/N site1 *in cis or in trans* remains undetermined. Pto/N site 1 (red) is disrupted by effector binding (or the L205D mutation). **(b)** The disruption of the Pto/N site1 (by effector binding or the L205D mutation) translates to one or the other Prf molecule, likely through the N/LRR interaction. Subsequent changes in conformation within the SCNL domain may cause activation of one or the other Prf NB domains by exchange of ADP to ATP. **(c)** The activation of the Prf NB domain activates the second Pto molecule for Pto trans-phosphorylation. The two Prf molecules can be distinguished from each other by their dark and bright green colours.

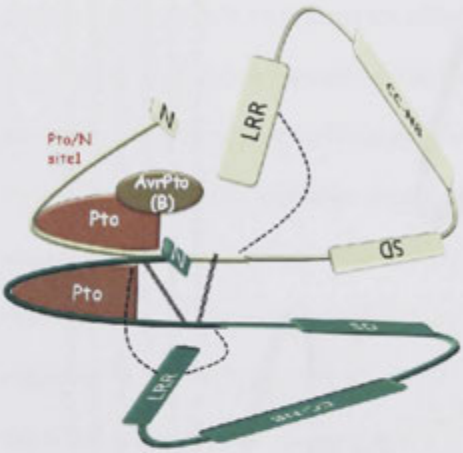

Figure 5.31: A schematic representation of the Pto/Prf protein complex with the N dimer in parallel conformation, and the LRR domain binding N *in cis* with N. (a) Prf N may form a parallel homodimer, which folds over crosswise. Each of the two Pto molecules binds both the N- and C-termini of the same N domain. The LRR domain of Prf binds to the N domain *in cis*, bringing the N- and C-termini of the intact Prf molecule into close proximity. Note that whether the LRR of each Prf molecule binds N *in cis* or *in trans* remains undetermined. Pto/N site 1 (red) is disrupted by effector binding (mimicked by the L205D mutation). The two Prf molecules can be distinguished from each other by their dark and bright green colours.

6. General Conclusions and Discussion.

The work presented here is separated into three independent projects. A central theme in all projects is host receptors recognising the presence of microbes. Pattern-recognition receptors (PRRs) usually belong to the receptor-like protein (RLP) or receptor kinase (RK) class of proteins, and recognise pathogen-associated molecular patterns (PAMPs) leading to PAMP-triggered immunity (PTI). Pathogenic microbes inhibit PTI via their effector molecules, causing host disease susceptibility. Resistant hosts are usually able to detect effectors via resistance (R) proteins leading to effector-triggered immunity (ETI). ETI often relies on dramatic immune responses, such as localised cell death. Whereas effectors are highly diverse, PAMPs are mostly common components for whole classes of microbes. Their recognition by PRRs limits the growth of host-pathogens as well as conferring resistance to non-host pathogens (Reviewed in (Dangl & Jones, 2001; Chisholm *et al.*, 2006; Jones & Dangl, 2006; Dodds & Rathjen, 2010)) and as such, PRR genes may provide a source of durable resistance after transfer to other plant species (Lacombe *et al.*, 2010; Fradin *et al.*, 2011; Holton *et al.*, 2015; Schoonbeek *et al.*, 2015).

As described in Chapter 3, a novel method for PRR identification was developed, which takes advantage of the ligand-induced interaction of BAK1 with PRRs (Heese *et al.*, 2007). The method described here using BAK1 as molecular bait to identify novel PRRs can be applied widely, perhaps even when the active PAMP has not yet been identified. The functionality and specificity of this novel biochemical strategy was demonstrated by the identification of the novel receptor for the cytoplasmic bacterial PAMP cold shock protein (CSP) or its peptide derivative csp22. The receptor was

successfully identified from *Nicotiana benthamiana*, its requirement for CSP perception confirmed and therefore it was named COLD SHOCK PROTEIN RECEPTOR (NbCSPR).

NbCSPR plays a role in restricting growth of host and non-host pathogens. Additionally, the work presented here suggests the possibility of sequential perception of PAMPs during plant innate immunity, as perception of flg22, the peptide derivative of the extracellular PAMP flagellin, potentiates csp22-mediated defence responses. That individual elicitor perception events might influence each other, has been proposed previously (Ma *et al.*, 2012; Hou *et al.*, 2014). Here I propose that different PAMPs are perceived differentially on a temporal basis. In mammalian cells, an efficient immune response often requires such sequential detection events. For example, host-induced bacterial lysis is required for the release of prokaryotic DNA, recognised by cytoplasmic PRRs (Broz & Monack, 2013). A hallmark of PTI is resistance to whole classes of microbes. Frequently, PTI induces moderate defence responses when compared to the cell death often observed during ETI, although these categories are not exclusive. Such moderate defences allow restriction of microbial growth while limiting the possible impact on host fitness. Actively facilitating microbial death by a single dramatic response may affect the host metabolism itself. The sequential recognition of microbial patterns may thus facilitate a sequence of weak responses to gradually inhibit microbial growth without significant impact on host viability. This strategy is used in bacterial disease treatment, where antimicrobial compounds, such as antibiotics, are applied in weak doses, but over a longer period of time (Craig, 1995). As such, the treatment inhibits bacterial growth (bacteriostatic), rather than directly killing bacteria (bactericidal) to avoid host cellular damage. Further research on independent PAMP/PRR pairs may explain exact sequences of recognition events to provide a test of this hypothesis.

My work also revealed an age-dependent perception mechanism for csp22 by NbCSPR. Age-related resistance is a well described phenomenon but the molecular basis is unclear. Age-related innate immunity exists in humans (Kollmann *et al.*, 2012; Shaw *et al.*, 2013) and is an important source of disease resistance in cereal crops. Adult plant resistance to rusts is controlled by single resistance genes expressed in adult plants (Ramburan *et al.*, 2004; Coram *et al.*, 2008; Periyannan *et al.*, 2013; Haruta *et al.*, 2014). In *Arabidopsis thaliana*, mostly the salicylic acid pathway has been implicated in age-related resistance to *Pseudomonas* (Hall *et al.*, 2009). With the exception of the rice immune receptor Xa21 (Century *et al.*, 1999), PRRs have so far not been implicated in age-related resistance. The developmental control of Xa21-mediated immunity may or may not be explained by the expression levels of Xa21 (Century *et al.*, 1999; Park *et al.*, 2010). Importantly, the model plant species *A. thaliana* and *N. benthamiana*, which have been widely used to understand the molecular mechanisms of plant immunity, are commonly studied at specific developmental stages. Usually both plants are four to five weeks of age when used for assaying immune responses. This may explain why such an important aspect has previously not been described in detail. Moving towards other growth stages may lead to the discovery of more receptors involved in age-related resistance. The identification of the specific pathogen elicitor-host receptor pair CSP/NbCSPR in the widely used and easily transformable model species *N. benthamiana* may allow the specific study of this relatively novel mechanism of resistance. In addition to developmental host stages, environmental conditions may influence plant immunity. A number of diseases develop more vigorously at lower temperatures and higher humidity than are usually used for plant growth in a controlled environment. Signalling molecules and perception systems might therefore differ depending on the developmental stage of the plant, the pathogen and environmental factors. This could

potentially also explain discrepancies in experimental outcomes of different research facilities.

NbSOBIR1 interacted with NbCSPR after co-expression in *N. benthamiana*, as shown for other RLPs (Liebrand *et al.*, 2013). I showed that SOBIR1 is however not required for NbCSPR protein accumulation or csp22-mediated immune responses in *N. benthamiana* and *A. thaliana*. NbCSPR may therefore rely only on BAK1 as a signal transducer for csp22-mediated immunity.

Because NbCSPR plays an important role in restricting bacterial growth of host and non-host bacterial pathogens, it is likely a target of bacterial effectors. Possible inhibition of csp22-dependent PTI responses by bacterial effectors, especially by the *Pseudomonas* effector AvrPto, will be interesting to study in the future. The kinase inhibitor AvrPto constrains flg22 initiated immune responses. So far, it is unclear whether AvrPto targets the kinase domain of the flagellin receptor FLS2 and/or the co-receptor BAK1 (Murray *et al.*, 2004; Shan *et al.*, 2008; Xiang *et al.*, 2008). The effect of AvrPto on NbCSPR/NbBAK1 mediated immunity may give insight into this question, as NbCSPR does not carry an intracellular kinase domain.

The possibility that *Pseudomonas* effectors target NbCSPR, may explain why the *35:NbCSPR-5xMyc-5* transgenic *A. thaliana* line is only slightly more resistant to the host pathogen *Pseudomonas syringae* pv. *tomato* DC3000 when compared to the *35:EV-5xMyc-1* line. Mutants deficient in effector delivery of non-adapted bacterial pathogens such as *Pseudomonas syringae* pv. *syringae* (E3 ligase deficient AvrPtoB (Chien *et al.*, 2013)) may be tested for bacterial growth on both lines to clarify this possibility. Alternatively, NbCSPR may recognise *A. thaliana* host proteins with cold shock domains (CSDs), which are highly similar to the CSD of bacterial CSPs. This may be related to the

difficulty in recovering *35S:NbCSPR A. thaliana* transgenics. I could however not detect clear differences between CSD-containing proteins from *N. benthamiana* (responsive to csp22) and the ones from *A. thaliana* (not responsive to csp22). I therefore speculate, that developmental and flagellin-dependent control of CSP perception in *N. benthamiana* avoids autoimmunity by perception of host proteins with CDSs, similar to bacterial CSPs.

Perception of *Agrobacterium* CSP by NbCSPR likely facilitates complex formation of NbBAK1 and NbCSPR and activation of at least some NbBAK1 molecules. This potential activation of BAK1 post transient expression through *Agrobacterium*-mediated transformation, should be kept in mind when studying the role of BAK1 in *N. benthamiana*. Importantly, the perception of *Agrobacterium* CSP by NbCSPR is at least partly responsible for restricted *Agrobacterium*-mediated transformation of flowering *N. benthamiana* plants. Transient transformation is used widely for studies of protein functionality, protein regulation, protein-protein interactions or protein expression (Goodin *et al.*, 2008). Knock out of *NbCSPR* in *N. benthamiana* will allow more efficient and reliable transient protein expression in this species. By analogy, knock out of functional homologs in tomato and potato may allow more efficient transformation of these important agricultural species, which usually show very low transformation rates (Chinchilla *et al.*, 2007b; Bhaskar *et al.*, 2009). The results presented here might therefore not only impact aspects in plant-microbe interactions *per se*, but research on *Nicotiana*, tomato, potato and other *Solanaceae* in general.

An alternative strategy to the identification of PRRs from host plants is the identification of PRRs from non-host plants. The mechanisms underlying non-host resistance (NHR) are hard to break down, and may involve not only active immunity mechanisms but also physiological incompatibilities. Generally, it is believed that

detection of non-host pathogens relies on PRR and NB-LRR receptors (Ron & Avni, 2004; Lacombe *et al.*, 2010; Fradin *et al.*, 2011; Wulff *et al.*, 2011; Dangl *et al.*, 2013). The resistance is thought to be more durable because it is polygenic, and because the pathogen's effectors are not evolved to combat them. Identification of NHR PRRs could thus be a valuable source of resistance genes for cropping species.

Fungal rust pathogens of the genus *Puccinia* cause some of the most devastating diseases on the economically important crop wheat. Here, molecular recognition of elicitors from the wheat stripe rust fungus (*Puccinia striiformis f. sp. tritici*) in the non-hosts species *N. benthamiana* and *A. thaliana* was demonstrated in Chapter 4, suggesting the existence of functional PRRs in species completely unrelated to the wheat host. Both species recognised elicitors present in spore extracts (SE) from stripe rust, and activated typical PAMP-induced responses. Measuring the production of reactive oxygen species (ROS) demonstrated a late immune response when compared to bacterial PAMPs or fungal chitin. Importantly, the pure elicitor INF1 from *Phytophthora infestans* induces a similarly late ROS burst on *N. benthamiana* (Chaparro-Garcia *et al.*, 2011). The biological relevance of this remains unknown, but one possibility is that it may be a feature for elicitors from some eukaryotic pathogens. For example, an elicitor-containing fraction from the necrotrophic fungal pathogen *Sclerotinia sclerotiorum* elicits a slightly delayed ROS burst when compared to the flg22 profile in *A. thaliana* (Zhang et al., 2013). Testing extracts from both biotrophic and necrotrophic fungal pathogens for delayed production of ROS on *A. thaliana* and *N. benthamiana* may provide insight into the conservation of such non-host recognition events, and into the possible biological role(s) of delayed immune responses. Additional PTI assays such as the activation of mitogen-activated protein kinases and up-regulation of pathogen-

induced defence genes may reveal additional information about specificity and kinetics of stripe rust elicitor-induced defences.

The detection of SE in *A. thaliana* and *N. benthamiana* is an important achievement as this is the first demonstration that this obligate biotrophic pathogen is recognized on non-host species. The ultimate goal of this project was the identification of at least one PRR that is capable of recognising a rust elicitor. Because the identity of the respective PAMP(s) is unknown, and the spore extract likely contains more than one PAMP, a screen of RLP and RK mutant lines impaired in responses to SE was unsuccessful. However, host defences activated by at least one of the SE components required the co-receptor BAK1. This provided the opportunity to identify the respective receptor using the novel method of BAK1-dependent PRR identification. Receptor candidates were identified here but their participation in SE recognition remains to be tested. Additionally, potential improvements for this method were discussed, which may facilitate a greater potential for identifying receptors for elicitors that are not yet purified. Overall, this work suggests the existence of PRRs, that recognise a range of non-adapted pathogens, and provides a baseline for the discovery of eliciting components and their respective PRRs. This strategy also allows the relatively easy discovery of such PRRs, because of the genetic amenability of *A. thaliana* and *N. benthamiana,* and thus a more rapid and targeted discovery of genetic material to eventually provide resistance in crops.

All pathogenic microbes are thought to have evolved numbers of effectors to inhibit PTI. This imposes severe selection on the hosts; it promotes pathogenicity of the microbe and leads to disease development on susceptible plants. The recognition of a single effector by intracellular NB-LRR R proteins can initiate ETI, usually associated with the hypersensitive response (HR), a cellular suicide. In contrast to PRRs, NB-LRR protein

complexes only recognise pathogens containing a specific form of a particular effector, which however mediates strong resistance. Because of the dramatic outcome of ETI, NB-LRR proteins have to be tightly regulated and due to the diversity of effectors, their recognition mechanisms are also diverse. Transfer of NB-LRR genes and NB-LRR gene pyramiding as strategy to engineer durable resistance thus requires a more detailed understanding of R protein regulation. This was underlined most recently by research demonstrating the incompatibility of *A. thaliana* NB-LRR proteins (Alcazar *et al.*, 2014). In most described cases, NB-LRRs indirectly recognise effectors through specific accessory proteins (Van der Biezen & Jones, 1998; van der Hoorn & Kamoun, 2008; Collier & Moffett, 2009). Pto acts as an accessory for the NB-LRR protein Prf, which it binds directly to confer recognition of the *Pseudomonas* effectors AvrPto and AvrPtoB (Ntoukakis *et al.*, 2014). The exact mechanism of how effector perception translates into resistance is still unknown, but compared to many other examples, this R protein complex is well understood and described in detail in Chapter 1. Briefly, the unique Prf N-terminal domain (N) is both the interaction site for Pto, and a contact surface for Prf dimerisation (Mucyn *et al.*, 2006; Gutierrez *et al.*, 2010). The R protein complex therefore consists of at least two Pto and two Prf molecules. Pto and Prf can regulate each other, likely through the N domain of Prf, which is the interaction surface for Pto. The same residues in the Pto activation segment which bind the effector molecules, are also required to maintain Prf in the inactive configuration prior to effector perception (Mucyn *et al.*, 2006) and are consequently also called the negative regulatory patch (NRP) (Wu *et al.*, 2004). This idea is in contrast with the fact that the N domain of Prf does not lose its ability to bind Pto after effector perception. The enduring interaction is however extremely important, as the sensor Pto moiety (the molecule that binds the effector) requires a helper Pto kinase for trans-phosphorylation and full complex

activation, leading to cell death and resistance (Ntoukakis *et al.*, 2013). Consequently, a loss of N-Pto interaction by effector binding would abolish these trans-phosphorylation events. The schematic structure of the Pto/Prf complex presented in Chapter 5, has helped to clarify this discrepancy. Co-immunoprecipitation (coIP) based interaction studies of the N-dimer revealed that the N domain forms either a parallel or an antiparallel homo-dimer. Such a structural arrangement allows binding of at least two Pto molecules. Using the same deletion molecule for interaction studies of Pto and important Pto mutants, which mimic effector binding and trans-phosphorylation, I demonstrated the existence of two independent Pto binding sites on each N molecule (Pto/N site1, encoded by Prf aa 1-159; and Pto/N site2, encoded by Prf aa 410-546). Pto/N site1 most likely encodes the surface complementary to the Pto NRP as the N deletants containing this site cannot bind a Pto mutant with a disrupted NRP (L205D mutation). The second interaction site is not disrupted by P+1 loop mutation and may thus continue to facilitate close proximity of the helper Pto kinase for trans-phosphorylation. Notably, disruption of the Pto P+1 loop (mimicked by the L205D mutation) is facilitated by the effectors AvrPto or AvrPtoB. It would therefore be interesting to determine the interaction sites between N and Pto in the presence of either effector. Importantly, the effectors only target one of the two Pto molecules present within the Pto/Prf dimer (Ntoukakis *et al.*, 2013) and thus, effector mediated disruption of the Pto/N site1 may not be detected.

Importantly, an intact Prf NB site is required for Pto trans-phosphorylation events (Ntoukakis *et al.*, 2013). This implies that the effector binding signal (to the detector Pto kinase) has to transduce to the Prf NB site, and from there to the helper Pto kinase. The likely region for translating the disruption of Pto P+1 loop is the Pto/N site1, as it likely identifies recognition of either effector by Pto, through loss of

interaction with Pto NRP. Pto/N site2 may then facilitate the translation of NB-LRR changes to the helper Pto kinase for trans-phosphorylation. Evidence for the latter hypothesis is so far lacking. Importantly, the schematic model developed here shows an interaction of N with the LRR domain of Prf, suggesting that this interaction may be used to regulate the Prf NB domain. A precedent for this type of interaction is given by the NB domain of Rx, which can physically interact with CC and LRR domains. These interactions reconstitute the Rx protein, but were disrupted in the presence of the effector protein (Rairdan & Moffett, 2006). Similarly, the RPS5 NB domain also associates with both its CC and LRR domains (Ade *et al.*, 2007; Qi *et al.*, 2012). The linkage of N and the remaining moieties of Prf through the LRR domain also functionally reconstructs Prf, but this is not affected by Pto CGF mutations, which are thought to mimic effector binding. Because of the dimeric occurrence of the complex, effector binding might rather mediate conformational changes within the protein complex, than loss of N/LRR interaction.

So far it is unknown whether Pto or Prf encodes the function for downstream signalling. I propose here that the last step in activation of the complex is the trans-phosphorylation of Pto. Studies on the Fen kinase in this work gave insight into this important question. Fen is activated by the insecticide fenthion in tomato but is mis-regulated when overexpressed in *N. benthamiana,* which results in a constitutive-gain of function (CGF) HR (Mucyn *et al.*, 2009). The reason for this mis-regulation is unclear but results presented here indicate that this is due to differences between N from tomato Prf and N from *N. benthamiana* Prf (NbN). Co-expression of genes encoding N but not NbN with Fen inhibited the HR. Constructs of tomato N containing Pto/N site1 bound and inhibited Fen CGF, but this was not the case for the N deletants lacking Pto/N site1. NbN may lack the important control residues of the Pto/N site1 although it

strongly bound Fen in coIP analysis after transient expression. Further comparative studies of N and NbN may identify the exact residues required for regulation of Pto and Fen.

In the Fen/N and Fen/NbN complexes, the NB of Prf is absent, yet the Fen/NbN complex caused signalling leading to the HR, but this was not the case for the Fen/N complex. At this stage, it is important to note that although the NbN/Fen interaction seems to be as stable as the N/Fen interaction, a role for NbPrf in the Fen/NbN mediated HR cannot be excluded. For this, a re-synthesised *NbN* nucleotide sequence has to be expressed together with Fen in plants silenced for native *NbPrf*. The kinase-inactive, phospho-mimic CGF Pto mutant ptoS198D/T199D/L205D formed inactive complexes with both N and NbN. Pto CGF signalling is usually associated with a disrupted activation segment and therefore lack of kinase activity. Kinase-active Fen however caused the CGF phenotype, and kinase activity is mandatory for Fen CGF activity (Mucyn *et al.*, 2009). Kinase activity may thus overcome the requirement for intact Prf NB in complex activation, and may be required for signalling beyond Pto trans-phosphorylation. That is to say, the final stage of Pto (or Fen) activation is an active kinase poised for substrate phosphorylation. On the other hand, only a single Pto CGF molecule mutated within the NRP (ptoI214D) remained kinase active (Wu *et al.*, 2004). It will be extremely interesting to test the ptoI214D CGF activity in the presence of NbN. At this point however, results indicate that Fen and by analogy Pto are responsible for signalling downstream, and for this may phosphorylate a downstream target or even Prf itself. Due to its close proximity, Prf N would be the most likely target for such Pto phosphorylation. Similarly, the TIR homo-dimers of L6 TIR, CC homo-dimer of MLA10 CC and TIR hetero-dimer of the RRS1/RPS4 proteins provide structures that are capable of inducing HR when expressed in *N. benthamiana* and/or *N. tabacum* (Bernoux *et al.*, 2011; Maekawa *et al.*,

2011; Williams *et al.*, 2014). Although N does not show similarity, either to TIR or CC domains, it might act similarly in the sense that it is the point of downstream signalling controlled by the NB-LRR domain of Prf, as well as by Pto.

The schematic structure of Pto/Prf developed here provides a basis to compare functional and structural differences between Pto and Fen as well as tomato N and NbN. Altogether, those studies have the potential to discover the component(s) required for downstream signalling. This may give insight into NB-LRR protein downstream signalling components, a mechanism that remains elusive not only for Pto/Prf but also other NB-LRR resistance protein complexes.

Literature

Aarts N, Metz M, Holub E, Staskawicz BJ, Daniels MJ, Parker JE. 1998. Different requirements for EDS1 and NDR1 by disease resistance genes define at least two R gene-mediated signaling pathways in Arabidopsis. *Proceedings of the National Academy of Sciences of the United States of America* **95**(17): 10306-10311.

Ade J, DeYoung BJ, Golstein C, Innes RW. 2007. Indirect activation of a plant nucleotide binding site-leucine-rich repeat protein by a bacterial protease. *Proceedings of the National Academy of Sciences of the United States of America* **104**(7): 2531-2536.

Albrecht C, Boutrot F, Segonzac C, Schwessinger B, Gimenez-Ibanez S, Chinchilla D, Rathjen JP, de Vries SC, Zipfel C. 2012. Brassinosteroids inhibit pathogen-associated molecular pattern-triggered immune signaling independent of the receptor kinase BAK1. *Proceedings of the National Academy of Sciences of the United States of America* **109**(1): 303-308.

Albrecht C, Russinova E, Kemmerling B, Kwaaitaal M, de Vries SC. 2008. Arabidopsis SOMATIC EMBRYOGENESIS RECEPTOR KINASE proteins serve brassinosteroid-dependent and -independent signaling pathways. *Plant Physiology* **148**(1): 611-619.

Albrecht M, Takken FL. 2006. Update on the domain architectures of NLRs and R proteins. *Biochemical and Biophysical Research Communications* **339**(2): 459-462.

Alcazar R, von Reth M, Bautor J, Chae E, Weigel D, Koornneef M, Parker JE. 2014. Analysis of a plant complex resistance gene locus underlying immune-related hybrid incompatibility and its occurrence in nature. *Public Library of Science genetics* **10**(12): e1004848.

Andreasson E, Jenkins T, Brodersen P, Thorgrimsen S, Petersen NH, Zhu S, Qiu JL, Micheelsen P, Rocher A, Petersen M, Newman MA, Bjorn Nielsen H, Hirt H, Somssich I, Mattsson O, Mundy J. 2005. The MAP kinase substrate MKS1 is a regulator of plant defense responses. *The EUROPEAN MOLECULAR BIOLOGY ORGANIZATION Journal* **24**(14): 2579-2589.

Andriotis VM, Rathjen JP. 2006. The Pto kinase of tomato, which regulates plant immunity, is repressed by its myristoylated N terminus. *The Journal of Biological Chemistry* **281**(36): 26578-26586.

Anikster Y, Eilam T, Manisterski J, Leonard KJ. 2003. Self-fertility and other distinguishing characteristics of a new morphotype of Puccinia coronata pathogenic on smooth brome grass. *Mycologia* **95**(1): 87-97.

Arnold DL, Lovell HC, Jackson RW, Mansfield JW. 2011. Pseudomonas syringae pv. phaseolicola: from 'has bean' to supermodel. *Molecular Plant Pathology* **12**(7): 617-627.

Asai S, Ohta K, Yoshioka H. 2008. MAPK signaling regulates nitric oxide and NADPH oxidase-dependent oxidative bursts in Nicotiana benthamiana. *The Plant Cell* **20**(5): 1390-1406.

Asai T, Tena G, Plotnikova J, Willmann MR, Chiu WL, Gomez-Gomez L, Boller T, Ausubel FM, Sheen J. 2002. MAP kinase signalling cascade in *Arabidopsis* innate immunity. *Nature* **415**(6875): 977-983.

Atkinson MM, Keppler LD, Orlandi EW, Baker CJ, Mischke CF. 1990. Involvement of plasma membrane calcium influx in bacterial induction of the k/h and hypersensitive responses in tobacco. *Plant Physiology* **92**(1): 215-221.

Axtell MJ, Staskawicz BJ. 2003. Initiation of RPS2-specified disease resistance in *Arabidopsis* is coupled to the AvrRpt2-directed elimination of RIN4. *Cell* **112**(3): 369-377.

Azevedo C, Sadanandom A, Kitagawa K, Freialdenhoven A, Shirasu K, Schulze-Lefert P. 2002. The RAR1 interactor SGT1, an essential component of R gene-triggered disease resistance. *Science* **295**(5562): 2073-2076.

Bailey-Serres J, Mittler R. 2006. The roles of reactive oxygen species in plant cells. *Plant Physiology* **141**(2): 311.

Bailey BA, Dean JF, Anderson JD. 1990. An Ethylene Biosynthesis-Inducing Endoxylanase Elicits Electrolyte Leakage and Necrosis in Nicotiana tabacum cv Xanthi Leaves. *Plant Physiology* **94**(4): 1849-1854.

Bailey BA, Korcak RF, Anderson JD. 1993. Sensitivity to an Ethylene Biosynthesis-Inducing Endoxylanase in Nicotiana tabacum L. cv Xanthi Is Controlled by a Single Dominant Gene. *Plant Physiology* **101**(3): 1081-1088.

Balmuth A, Rathjen JP. 2007. Genetic and molecular requirements for function of the Pto/Prf effector recognition complex in tomato and Nicotiana benthamiana. *The Plant Journal : for cell and molecular biology* **51**(6): 978-990.

Banerjee D, Zhang X, Bent AF. 2001. The leucine-rich repeat domain can determine effective interaction between RPS2 and other host factors in *Arabidopsis* RPS2-mediated disease resistance. *Genetics* **158**(1): 439-450.

Bar M, Sharfman M, Ron M, Avni A. 2010. BAK1 is required for the attenuation of ethylene-inducing xylanase (Eix)-induced defense responses by the decoy receptor LeEix1. *The Plant Journal : for cell and molecular biology* **63**(5): 791-800.

Bargmann BO, Laxalt AM, Riet BT, Schouten E, van Leeuwen W, Dekker HL, de Koster CG, Haring MA, Munnik T. 2006. LePLDbeta1 activation and relocalization in suspension-cultured tomato cells treated with xylanase. *The Plant Journal : for cell and molecular biology* **45**(3): 358-368.

Bauer Z, Gomez-Gomez L, Boller T, Felix G. 2001. Sensitivity of different ecotypes and mutants of Arabidopsis thaliana toward the bacterial elicitor flagellin correlates with the presence of receptor-binding sites. *The Journal of Biological Chemistry* **276**(49): 45669-45676.

Belkhadir Y, Jaillais Y, Epple P, Balsemao-Pires E, Dangl JL, Chory J. 2012. Brassinosteroids modulate the efficiency of plant immune responses to microbe-associated molecular patterns. *Proceedings of the National Academy of Sciences of the United States of America* **109**(1): 297-302.

Belkhadir Y, Subramaniam R, Dangl JL. 2004. Plant disease resistance protein signaling: NBS-LRR proteins and their partners. *Current Opinion in Plant Biology* **7**(4): 391-399.

Bella J, Hindle KL, McEwan PA, Lovell SC. 2008. The leucine-rich repeat structure. *Cellular and Molecular Life Sciences* **65**(15): 2307-2333.

Bendahmane A, Farnham G, Moffett P, Baulcombe DC. 2002. Constitutive gain-of-function mutants in a nucleotide binding site-leucine rich repeat protein encoded at the Rx locus of potato. *The Plant Journal* **32**(2): 195-204.

Bender CL, Cooksey DA. 1987. Molecular cloning of copper resistance genes from *Pseudomonas syringae* pv. *tomato*. *Journal of Bacteriology* **169**(2): 470-474.

Bent AF, Mackey D. 2007. Elicitors, effectors, and R genes: The new paradigm and a lifetime supply of questions. *Annual Review of Phytopathology* **45**: 399-436.

Bernoux M, Ve T, Williams S, Warren C, Hatters D, Valkov E, Zhang X, Ellis JG, Kobe B, Dodds PN. 2011. Structural and Functional Analysis of a Plant Resistance Protein TIR Domain Reveals Interfaces for Self-Association, Signaling, and Autoregulation. *Cell Host & Microbe* **9**(3): 200-211.

Bestwick CS, Brown IR, Bennett MHR, Mansfield JW. 1997. Localization of hydrogen peroxide accumulation during the hypersensitive reaction of lettuce cells to Pseudomonas syringae pv phaseolicola. *The Plant Cell* **9**(2): 209-221.

Bhaskar PB, Venkateshwaran M, Wu L, Ane JM, Jiang J. 2009. Agrobacterium-mediated transient gene expression and silencing: a rapid tool for functional gene assay in potato. *Public Library of Science One* **4**(6): e5812.

Bhattacharjee S, Halane MK, Kim SH, Gassmann W. 2011. Pathogen effectors target Arabidopsis EDS1 and alter its interactions with immune regulators. *Science* **334**(6061): 1405-1408.

Bieri S, Mauch S, Shen QH, Peart J, Devoto A, Casais C, Ceron F, Schulze S, Steinbiss HH, Shirasu K, Schulze-Lefert P. 2004. RAR1 positively controls steady state levels of barley MLA resistance proteins and enables sufficient MLA6 accumulation for effective resistance. *The Plant Cell* **16**(12): 3480-3495.

Birker D, Heidrich K, Takahara H, Narusaka M, Deslandes L, Narusaka Y, Reymond M, Parker JE, O'Connell R. 2009. A locus conferring resistance to Colletotrichum higginsianum is shared by four geographically distinct Arabidopsis accessions. *Plant Journal* **60**(4): 602-613.

Bittel P, Robatzek S. 2007. Microbe-associated molecular patterns (MAMPs) probe plant immunity. *Current Opinion in Plant Biology* **10**(4): 335-341.

Boller T, Felix G. 2009. A renaissance of elicitors: perception of microbe-associated molecular patterns and danger signals by pattern-recognition receptors. *Annual Review Plant Biology* **60**: 379-406.

Botella MA, Parker JE, Frost LN, Bittner-Eddy PD, Beynon JL, Daniels MJ, Holub EB, Jones JD. 1998. Three genes of the *Arabidopsis* RPP1 complex resistance locus recognize distinct *Peronospora parasitica* avirulence determinants. *The Plant Cell* **10**(11): 1847-1860.

Boter M, Amigues B, Peart J, Breuer C, Kadota Y, Casais C, Moore G, Kleanthous C, Ochsenbein F, Shirasu K, Guerois R. 2007. Structural and functional analysis of SGT1 reveals that its interaction with HSP90 is required for the accumulation of Rx, an R protein involved in plant immunity. *The Plant Cell* **19**(11): 3791-3804.

Boudsocq M, Willmann MR, McCormack M, Lee H, Shan L, He P, Bush J, Cheng SH, Sheen J. 2010. Differential innate immune signalling via Ca(2+) sensor protein kinases. *Nature* **464**(7287): 418-422.

Broz P, Monack DM. 2013. Newly described pattern recognition receptors team up against intracellular pathogens. *Nature Review Immunoloy* **13**(8): 551-565.

Brutus A, Sicilia F, Macone A, Cervone F, De Lorenzo G. 2010. A domain swap approach reveals a role of the plant wall-associated kinase 1 (WAK1) as a receptor of oligogalacturonides. *Proceedings of the National Academy of Sciences of the United States of America* **107**(20): 9452-9457.

Buttner D, Bonas U. 2002. Getting across--bacterial type III effector proteins on their way to the plant cell. *The EUROPEAN MOLECULAR BIOLOGY ORGANIZATION Journal* **21**(20): 5313-5322.

Cao Y, Liang Y, Tanaka K, Nguyen CT, Jedrzejczak RP, Joachimiak A, Stacey G. 2014. The kinase LYK5 is a major chitin receptor in Arabidopsis and forms a chitin-induced complex with related kinase CERK1. *Elife* **3**.

Cao Z, Henzel WJ, Gao X. 1996. IRAK: a kinase associated with the interleukin-1 receptor. *Science* **271**(5252): 1128-1131.

Caplan JL, Mamillapalli P, Burch-Smith TM, Czymmek K, Dinesh-Kumar SP. 2008. Chloroplastic protein NRIP1 mediates innate immune receptor recognition of a viral effector. *Cell* **132**(3): 449-462.

Caplan JL, Zhu X, Mamillapalli P, Marathe R, Anandalakshmi R, Dinesh-Kumar SP. 2009. Induced ER chaperones regulate a receptor-like kinase to mediate antiviral innate immune response in plants. *Cell Host & Microbe* **6**(5): 457-469.

Carland FM, Staskawicz BJ. 1993. Genetic characterization of the Pto locus of tomato: semi-dominance and cosegregation of resistance to Pseudomonas syringae pathovar tomato and sensitivity to the insecticide Fenthion. *Molecular Genetics and Genomics* **239**(1-2): 17-27.

Catanzariti AM, Dodds PN, Ve T, Kobe B, Ellis JG, Staskawicz BJ. 2010. The AvrM Effector from Flax Rust Has a Structured C-Terminal Domain and Interacts Directly with the M Resistance Protein. *Molecular Plant-Microbe Interactions* **23**(1): 49-57.

Century KS, Lagman RA, Adkisson M, Morlan J, Tobias R, Schwartz K, Smith A, Love J, Ronald PC, Whalen MC. 1999. Short communication: developmental control of Xa21-mediated disease resistance in rice. *The Plant Journal : for cell and molecular biology* **20**(2): 231-236.

Cesari S, Kanzaki H, Fujiwara T, Bernoux M, Chalvon V, Kawano Y, Shimamoto K, Dodds P, Terauchi R, Kroj T. 2014. The NB-LRR proteins RGA4 and RGA5 interact functionally and physically to confer disease resistance. *The EUROPEAN MOLECULAR BIOLOGY ORGANIZATION Journal* **33**(17): 1941-1959.

Cesari S, Thilliez G, Ribot C, Chalvon V, Michel C, Jauneau A, Rivas S, Alaux L, Kanzaki H, Okuyama Y, Morel JB, Fournier E, Tharreau D, Terauchi R, Kroj T. 2013. The rice resistance protein pair RGA4/RGA5 recognizes the Magnaporthe oryzae effectors AVR-Pia and AVR1-CO39 by direct binding. *The Plant Cell* **25**(4): 1463-1481.

Chang C, Yu D, Jiao J, Jing S, Schulze-Lefert P, Shen QH. 2013. Barley MLA immune receptors directly interfere with antagonistically acting transcription factors to initiate disease resistance signaling. *The Plant Cell* **25**(3): 1158-1173.

Chang JH, Tai YS, Bernal AJ, Lavelle DT, Staskawicz BJ, Michelmore RW. 2002. Functional analyses of the Pto resistance gene family in tomato and the identification of a minor resistance determinant in a susceptible haplotype. *Molecular Plant-Microbe interactions* **15**(3): 281-291.

Chaparro-Garcia A, Wilkinson RC, Gimenez-Ibanez S, Findlay K, Coffey MD, Zipfel C, Rathjen JP, Kamoun S, Schornack S. 2011. The receptor-like kinase SERK3/BAK1 is required for basal resistance against the late blight pathogen phytophthora infestans in Nicotiana benthamiana. *Public Library of Science ONE* **6**(1): e16608.

Cheng W, Munkvold KR, Gao H, Mathieu J, Schwizer S, Wang S, Yan YB, Wang J, Martin GB, Chai J. 2011. Structural analysis of Pseudomonas syringae AvrPtoB bound to host BAK1 reveals two similar kinase-interacting domains in a type III Effector. *Cell Host & Microbe* **10**(6): 616-626.

Chien CF, Mathieu J, Hsu CH, Boyle P, Martin GB, Lin NC. 2013. Nonhost resistance of tomato to the bean pathogen Pseudomonas syringae pv. syringae B728a is due to a defective E3 ubiquitin ligase domain in avrptobb728a. *Molecular Plant-Microbe Interactions* **26**(4): 387-397.

Chinchilla D, Bauer Z, Regenass M, Boller T, Felix G. 2006. The *Arabidopsis* receptor kinase FLS2 binds flg22 and determines the specificity of flagellin perception. *The Plant Cell* **18**(2): 465-476.

Chinchilla D, Boller T, Robatzek S. 2007a. Flagellin signalling in plant immunity. *Advances in Experimental Medicine and Biology* **598**: 358-371.

Chinchilla D, Zipfel C, Robatzek S, Kemmerling B, Nurnberger T, Jones JD, Felix G, Boller T. 2007b. A flagellin-induced complex of the receptor FLS2 and BAK1 initiates plant defence. *Nature* **448**(7152): 497-500.

Chisholm ST, Coaker G, Day B, Staskawicz BJ. 2006. Host-microbe interactions: shaping the evolution of the plant immune response. *Cell* **124**(4): 803-814.

Clarke CR, Chinchilla D, Hind SR, Taguchi F, Miki R, Ichinose Y, Martin GB, Leman S, Felix G, Vinatzer BA. 2013. Allelic variation in two distinct Pseudomonas syringae flagellin epitopes modulates the strength of plant immune responses but not bacterial motility. *New Phytologist* **200**(3): 847-860.

Clough SJ, Bent AF. 1998. Floral dip: a simplified method for Agrobacterium-mediated transformation of Arabidopsis thaliana. *The Plant Journal* **16**(6): 735-743.

Cohn J, Sessa G, Martin GB. 2001. Innate immunity in plants. *Current Opinion in Immunology* **13**(1): 55-62.

Colcombet J, Boisson-Dernier A, Ros-Palau R, Vera CE, Schroeder JI. 2005. Arabidopsis SOMATIC EMBRYOGENESIS RECEPTOR KINASES1 and 2 are essential for tapetum development and microspore maturation. *The Plant Cell* **17**(12): 3350-3361.

Collier SM, Moffett P. 2009. NB-LRRs work a "bait and switch" on pathogens. *Trends in Plant Science* **14**(10): 521-529.

Coram TE, Settles ML, Chen X. 2008. Transcriptome analysis of high-temperature adult-plant resistance conditioned by Yr39 during the wheat-*Puccinia striiformis f. sp. tritici* interaction. *Molecular Plant Pathology* **9**(4): 479-493.

Correia JD, Miranda Y, Leonard N, Ulevitch R. 2007. SGT1 is essential for Nod1 activation. *Proceedings of the National Academy of Sciences of the United States of America* **104**(16): 6764-6769.

Craig WA. 1995. Kinetics of antibiotics in relation to effective and convenient outpatient parenteral therapy. *International journal of antimicrobial agents* **5**(1): 19-22.

D'Haeze W, De Rycke R, Mathis R, Goormachtig S, Pagnotta S, Verplancke C, Capoen W, Holsters M. 2003. Reactive oxygen species and ethylene play a positive role in lateral root base nodulation of a semiaquatic legume. *Proceedings of the National Academy of Sciences of the United States of America* **100**(20): 11789-11794.

da Cunha L, Sreerekha MV, Mackey D. 2007. Defense suppression by virulence effectors of bacterial phytopathogens. *Current Opinion in Plant Biology* **10**(4): 349-357.

Daegelen P, Studier FW, Lenski RE, Cure S, Kim JF. 2009. Tracing ancestors and relatives of Escherichia coli B, and the derivation of B strains REL606 and BL21(DE3). *Journal of Molecular Biology* **394**(4): 634-643.

Dagenais M, Dupaul-Chicoine J, Saleh M. 2010. Function of NOD-like receptors in immunity and disease. *Current Opinion in Investigating Drugs* **11**(11): 1246-1255.

Dangl JL, Horvath DM, Staskawicz BJ. 2013. Pivoting the plant immune system from dissection to deployment. *Science* **341**(6147): 746-751.

Dangl JL, Jones JD. 2001. Plant pathogens and integrated defence responses to infection. *Nature* **411**(6839): 826-833.

Danna CH, Millet YA, Koller T, Han SW, Bent AF, Ronald PC, Ausubel FM. 2011. The Arabidopsis flagellin receptor FLS2 mediates the perception of Xanthomonas Ax21 secreted peptides. *Proceedings of the National Academy of Sciences of the United States of America* **108**(22): 9286-9291.

Day B, Dahlbeck D, Huang J, Chisholm ST, Li D, Staskawicz BJ. 2005. Molecular basis for the RIN4 negative regulation of RPS2 disease resistance. *The Plant Cell* **17**(4): 1292-1305.

de Jonge R, van Esse HP, Kombrink A, Shinya T, Desaki Y, Bours R, van der Krol S, Shibuya N, Joosten MH, Thomma BP. 2010. Conserved fungal LysM effector Ecp6 prevents chitin-triggered immunity in plants. *Science* **329**(5994): 953-955.

de Vries JS, Andriotis VM, Wu AJ, Rathjen JP. 2006. Tomato Pto encodes a functional N-myristoylation motif that is required for signal transduction in Nicotiana benthamiana. *The Plant Journal : for cell and molecular biology* **45**(1): 31-45.

DebRoy S, Thilmony R, Kwack YB, Nomura K, He SY. 2004. A family of conserved bacterial effectors inhibits salicylic acid-mediated basal immunity and promotes disease necrosis in plants. *Proceedings of the National Academy of Sciences of the United States of America* **101**(26): 9927-9932.

del Pozo O, Pedley KF, Martin GB. 2004. MAPKKKalpha is a positive regulator of cell death associated with both plant immunity and disease. *The EUROPEAN MOLECULAR BIOLOGY ORGANIZATION Journal* **23**(15): 3072-3082.

Denoux C, Galletti R, Mammarella N, Gopalan S, Werck D, De Lorenzo G, Ferrari S, Ausubel FM, Dewdney J. 2008. Activation of defense response pathways by OGs and Flg22 elicitors in Arabidopsis seedlings. *Molecular Plant* **1**(3): 423-445.

Deslandes L, Olivier J, Peeters N, Feng DX, Khounlotham M, Boucher C, Somssich I, Genin S, Marco Y. 2003. Physical interaction between RRS1-R, a protein conferring resistance to bacterial wilt, and PopP2, a type III effector targeted to the plant nucleus. *Proceedings of the National Academy of Sciences of the United States of America* **100**(13): 8024-8029.

Deslandes L, Olivier J, Theulieres F, Hirsch J, Feng DX, Bittner-Eddy P, Beynon J, Marco Y. 2002. Resistance to Ralstonia solanacearum in Arabidopsis thaliana is conferred by the recessive RRS1-R gene, a member of a novel family of resistance genes. *Proceedings of the National Academy of Sciences of the United States of America* **99**(4): 2404-2409.

Deslandes L, Rivas S. 2012. Catch me if you can: bacterial effectors and plant targets. *Trends in Plant Science* **17**(11): 644-655.

Devallavieillepope C, Huber L, Leconte M, Goyeau H. 1995. Comparative Effects of Temperature and Interrupted Wet Periods on Germination, Penetration, and Infection of Puccinia-Recondita F Sp Tritici and P-Striiformis on Wheat Seedlings. *Phytopathology* **85**(4): 409-415.

Devarenne TP, Ekengren SK, Pedley KF, Martin GB. 2006. Adi3 is a Pdk1-interacting AGC kinase that negatively regulates plant cell death. *The EUROPEAN MOLECULAR BIOLOGY ORGANIZATION Journal* **25**(1): 255-265.

DeYoung BJ, Innes RW. 2006. Plant NBS-LRR proteins in pathogen sensing and host defense. *Nature Immunology* **7**(12): 1243-1249.

Dodd AN, Kudla J, Sanders D. 2010. The language of calcium signaling. *Annual Review of Plant Biology* **61**: 593-620.

Dodds PN, Lawrence GJ, Catanzariti AM, Teh T, Wang CI, Ayliffe MA, Kobe B, Ellis JG. 2006. Direct protein interaction underlies gene-for-gene specificity and coevolution of the flax resistance genes and flax rust avirulence genes. *Proceedings of the National Academy of Sciences of the United States of America* **103**(23): 8888-8893.

Dodds PN, Rathjen JP. 2010. Plant immunity: towards an integrated view of plant-pathogen interactions. *Nature Reviews Genetics* **11**(8): 539-548.

Dong J, Xiao F, Fan F, Gu L, Cang H, Martin GB, Chai J. 2009. Crystal structure of the complex between Pseudomonas effector AvrPtoB and the tomato Pto kinase reveals both a shared and a unique interface compared with AvrPto-Pto. *The Plant Cell* **21**(6): 1846-1859.

Dong Y, Burch-Smith TM, Liu Y, Mamillapalli P, Dinesh-Kumar SP. 2007. A ligation-independent cloning tobacco rattle virus vector for high-throughput virus-induced gene silencing identifies roles for NbMADS4-1 and -2 in floral development. *Plant Physiology* **145**(4): 1161-1170.

Dow M, Newman MA, von Roepenack E. 2000. The Induction and Modulation of Plant Defense Responses by Bacterial Lipopolysaccharides. *Annual Review Phytopathology* **38**: 241-261.

Du X, Miao M, Ma X, Liu Y, Kuhl JC, Martin GB, Xiao F. 2012. Plant programmed cell death caused by an autoactive form of Prf is suppressed by co-expression of the Prf LRR domain. *Molecular Plant* **5**(5): 1058-1067.

Durrant WE, Dong X. 2004. Systemic acquired resistance. *Annual Review Phytopathology* **42**: 185-209.

Eichmann R, Schafer P. 2012. The endoplasmic reticulum in plant immunity and cell death. *Frontiers in Plant Science* **3**: 200.

Eitas TK, Dangl JL. 2010. NB-LRR proteins: pairs, pieces, perception, partners, and pathways. *Current Opinion in Plant Biology* **13**(4): 472-477.

Ekengren SK, Liu Y, Schiff M, Dinesh-Kumar SP, Martin GB. 2003. Two MAPK cascades, NPR1, and TGA transcription factors play a role in Pto-mediated disease resistance in tomato. *The Plant Journal : for cell and molecular biology* **36**(6): 905-917.

Enkerli J, Felix G, Boller T. 1999. The enzymatic activity of fungal xylanase is not necessary for its elicitor activity. *Plant Physiology* **121**(2): 391-397.

Erbs G, Newman MA. 2003. The role of lipopolysaccharides in induction of plant defence responses. *Molecular Plant Pathology* **4**(5): 421-425.

Eulgem T, Somssich IE. 2007. Networks of WRKY transcription factors in defense signaling. *Current Opinion in Plant Biology* **10**(4): 366-371.

Falk A, Feys BJ, Frost LN, Jones JD, Daniels MJ, Parker JE. 1999. EDS1, an essential component of R gene-mediated disease resistance in Arabidopsis has homology to eukaryotic lipases. *Proceedings of the National Academy of Sciences of the United States of America* **96**(6): 3292-3297.

Fan M, Bai MY, Kim JG, Wang T, Oh E, Chen L, Park CH, Son SH, Kim SK, Mudgett MB, Wang ZY. 2014. The bHLH transcription factor HBI1 mediates the trade-off between growth and pathogen-associated molecular pattern-triggered immunity in Arabidopsis. *The Plant Cell* **26**(2): 828-841.

Felix G, Boller T. 2003. Molecular sensing of bacteria in plants. The highly conserved RNA-binding motif *RNP-1* of bacterial cold shock proteins is recognized as an elicitor signal in tobacco. *The Journal of Biological Chemistry* **278**(8): 6201-6208.

Felix G, Duran JD, Volko S, Boller T. 1999. Plants have a sensitive perception system for the most conserved domain of bacterial flagellin. *The Plant Journal* **18**(3): 265-276.

Felix G, Grosskopf DG, Regenass M, Basse CW, Boller T. 1991. Elicitor-induced ethylene biosynthesis in tomato cells: characterization and use as a bioassay for elicitor action. *Plant Physiology* **97**(1): 19-25.

Ferrari S, Galletti R, Pontiggia D, Manfredini C, Lionetti V, Bellincampi D, Cervone F, De Lorenzo G. 2008. Transgenic expression of a fungal endo-polygalacturonase increases plant resistance to pathogens and reduces auxin sensitivity. *Plant Physiology* **146**(2): 669-681.

Feys BJ, Moisan LJ, Newman MA, Parker JE. 2001. Direct interaction between the Arabidopsis disease resistance signaling proteins, EDS1 and PAD4. *The EUROPEAN MOLECULAR BIOLOGY ORGANIZATION Journal* **20**(19): 5400-5411.

Feys BJ, Wiermer M, Bhat RA, Moisan LJ, Medina-Escobar N, Neu C, Cabral A, Parker JE. 2005. Arabidopsis SENESCENCE-ASSOCIATED GENE101 stabilizes and signals within an ENHANCED DISEASE SUSCEPTIBILITY1 complex in plant innate immunity. *The Plant Cell* **17**(9): 2601-2613.

Flor HH. 1956. Mutations in Flax Rust Induced by Ultraviolet Radiation. *Science* **124**(3227): 888-889.

Fradin EF, Abd-El-Haliem A, Masini L, van den Berg GC, Joosten MH, Thomma BP. 2011. Interfamily transfer of tomato Ve1 mediates Verticillium resistance in *Arabidopsis*. *Plant Physiology* **156**(4): 2255-2265.

Fradin EF, Zhang Z, Juarez Ayala JC, Castroverde CD, Nazar RN, Robb J, Liu CM, Thomma BP. 2009. Genetic dissection of Verticillium wilt resistance mediated by tomato Ve1. *Plant Physiology* **150**(1): 320-332.

Franchi L, Warner N, Viani K, Nunez G. 2009. Function of Nod-like receptors in microbial recognition and host defense. *Immunology Reviews* **227**(1): 106-128.

Frederick RD, Thilmony RL, Sessa G, Martin GB. 1998. Recognition specificity for the bacterial avirulence protein AvrPto is determined by Thr-204 in the activation loop of the tomato Pto kinase. *Molecular Cell* **2**(2): 241-245.

Freialdenhoven A, Scherag B, Hollricher K, Collinge DB, Thordal-Christensen H, Schulze-Lefert P. 1994. Nar-1 and Nar-2, Two Loci Required for Mla12-Specified Race-Specific Resistance to Powdery Mildew in Barley. *The Plant Cell* **6**(7): 983-994.

Fritz-Laylin LK, Krishnamurthy N, Tor M, Sjolander KV, Jones JD. 2005. Phylogenomic analysis of the receptor-like proteins of rice and Arabidopsis. *Plant Physiology* **138**(2): 611-623.

Frost D, Way H, Howles P, Luck J, Manners J, Hardham A, Finnegan J, Ellis J. 2004. Tobacco transgenic for the flax rust resistance gene *L* expresses allele-specific activation of defense responses. *Molecular Plant-Microbe Interactions* **17**(2): 224-232.

Fuchs Y, Saxena A, Gamble HR, Anderson JD. 1989. Ethylene biosynthesis-inducing protein from cellulysin is an endoxylanase. *Plant Physiology* **89**(1): 138-143.

Furman-Matarasso N, Cohen E, Du Q, Chejanovsky N, Hanania U, Avni A. 1999. A point mutation in the ethylene-inducing xylanase elicitor inhibits the beta-1-4-endoxylanase activity but not the elicitation activity. *Plant Physiology* **121**(2): 345-351.

Gabriels SHEJ, Vossen JH, Ekengren SK, van Ooijen G, Abd-El-Haliem AM, van den Berg GCM, Rainey DY, Martin GB, Takken FLW, de Wit PJGM, Joosten MHAJ. 2007. An NB-LRR protein required for HR signalling mediated by both extra- and intracellular resistance proteins. *The Plant Journal* **50**(1): 14-28.

Galletti R, Denoux C, Gambetta S, Dewdney J, Ausubel FM, De Lorenzo G, Ferrari S. 2008. The AtrbohD-mediated oxidative burst elicited by oligogalacturonides in Arabidopsis is dispensable for the activation of defense responses effective against Botrytis cinerea. *Plant Physiology* **148**(3): 1695-1706.

Gao M, Wang X, Wang D, Xu F, Ding X, Zhang Z, Bi D, Cheng YT, Chen S, Li X, Zhang Y. 2009. Regulation of cell death and innate immunity by two receptor-like kinases in Arabidopsis. *Cell Host & Microbe* **6**(1): 34-44.

Garnica DP, Upadhyaya NM, Dodds PN, Rathjen JP. 2013. Strategies for Wheat Stripe Rust Pathogenicity Identified by Transcriptome Sequencing. *Public Library of Science One* **8**(6): e67150.

Gimenez-Ibanez S, Boter M, Fernandez-Barbero G, Chini A, Rathjen JP, Solano R. 2014. The bacterial effector HopX1 targets JAZ transcriptional repressors to activate jasmonate signaling and promote infection in Arabidopsis. *Public Library of Science Biology* **12**(2): e1001792.

Gimenez-Ibanez S, Hann DR, Ntoukakis V, Petutschnig E, Lipka V, Rathjen JP. 2009a. AvrPtoB targets the LysM receptor kinase CERK1 to promote bacterial virulence on plants. *Current Biology* **19**(5): 423-429.

Gimenez-Ibanez S, Ntoukakis V, Rathjen JP. 2009b. The LysM receptor kinase CERK1 mediates bacterial perception in Arabidopsis. *Plant Signaling & Behavior* **4**(6): 539-541.

Glazebrook J. 2005. Contrasting mechanisms of defense against biotrophic and necrotrophic pathogens. *Annual Review Phytopathology* **43**: 205-227.

Gohre V, Spallek T, Haweker H, Mersmann S, Mentzel T, Boller T, de Torres M, Mansfield JW, Robatzek S. 2008. Plant pattern-recognition receptor FLS2 is directed for degradation by the bacterial ubiquitin ligase AvrPtoB. *Current Biology* **18**(23): 1824-1832.

Gomez-Gomez L, Boller T. 2000. FLS2: an LRR receptor-like kinase involved in the perception of the bacterial elicitor flagellin in *Arabidopsis*. *Molecular Cell* **5**(6): 1003-1011.

Gomez-Gomez L, Felix G, Boller T. 1999. A single locus determines sensitivity to bacterial flagellin in *Arabidopsis thaliana*. *The Plant Journal : for cell and molecular biology* **18**(3): 277-284.

Goodin MM, Zaitlin D, Naidu RA, Lommel SA. 2008. Nicotiana benthamiana: Its history and future as a model for plant-pathogen interactions. *Molecular Plant-Microbe Interactions* **21**(8): 1015-1026.

Grant M, Lamb C. 2006. Systemic immunity. *Current Opinion in Plant Biology* **9**(4): 414-420.

Grant MR, Godiard L, Straube E, Ashfield T, Lewald J, Sattler A, Innes RW, Dangl JL. 1995. Structure of the *Arabidopsis RPM1* gene enabling dual specificity disease resistance. *Science* **269**(5225): 843-846.

Grant SR, Fisher EJ, Chang JH, Mole BM, Dangl JL. 2006. Subterfuge and manipulation: type III effector proteins of phytopathogenic bacteria. *Annual Review of Microbiology* **60**: 425-449.

Greenberg JT, Yao N. 2004. The role and regulation of programmed cell death in plant-pathogen interactions. *Cellular Microbiology* **6**(3): 201-211.

Grzeskowiak L, Stephan W, Rose LE. 2014. Epistatic selection and coadaptation in the Prf resistance complex of wild tomato. *Infection, Genetics and Evolution*.

Gust AA, Biswas R, Lenz HD, Rauhut T, Ranf S, Kemmerling B, Gotz F, Glawischnig E, Lee J, Felix G, Nurnberger T. 2007. Bacteria-derived peptidoglycans constitute pathogen-associated molecular patterns triggering innate immunity in Arabidopsis. *The Journal of Biological Chemistry* **282**(44): 32338-32348.

Gust AA, Felix G. 2014. Receptor like proteins associate with SOBIR1-type of adaptors to form bimolecular receptor kinases. *Current Opinion in Plant Biology* **21C**: 104-111.

Gutierrez JR, Balmuth AL, Ntoukakis V, Mucyn TS, Gimenez-Ibanez S, Jones AM, Rathjen JP. 2010. Prf immune complexes of tomato are oligomeric and contain multiple Pto-like kinases that diversify effector recognition. *The Plant Journal : for cell and molecular biology* **61**(3): 507-518.

Hall SA, Allen RL, Baumber RE, Baxter LA, Fisher K, Bittner-Eddy PD, Rose LE, Holub EB, Beynon JL. 2009. Maintenance of genetic variation in plants and pathogens involves complex networks of gene-for-gene interactions. *Molecular Plant Pathology* **10**(4): 449-457.

Halter T, Imkampe J, Mazzotta S, Wierzba M, Postel S, Bucherl C, Kiefer C, Stahl M, Chinchilla D, Wang X, Nurnberger T, Zipfel C, Clouse S, Borst JW, Boeren S, de Vries SC, Tax F, Kemmerling B. 2014. The Leucine-Rich Repeat Receptor Kinase BIR2 Is a Negative Regulator of BAK1 in Plant Immunity. *Current biology : CB* **24**(2): 134-143.

Hanahan D. 1983. Studies on transformation of *Escherichia coli* with plasmids. *The Journal of Molecular Biology* **166**(4): 557-580.

Hann DR, Gimenez-Ibanez S, Rathjen JP. 2010. Bacterial virulence effectors and their activities. *Current Opinion in Plant Biology* **13**(4): 388-393.

Hao W, Collier SM, Moffett P, Chai J. 2013. Structural Basis for the Interaction between the Potato Virus X Resistance Protein (Rx) and its Co-factor Ran GTPase-Activating Protein 2 (RanGAP2). *The Journal of Biological Chemistry*.

Haruta M, Sabat G, Stecker K, Minkoff BB, Sussman MR. 2014. A peptide hormone and its receptor protein kinase regulate plant cell expansion. *Science* **343**(6169): 408-411.

Hauck P, Thilmony R, He SY. 2003. A *Pseudomonas syringae* type III effector suppresses cell wall-based extracellular defense in susceptible *Arabidopsis* plants. *Proceedings of the National Academy of Sciences of the United States of America* **100**(14): 8577-8582.

He K, Gou X, Yuan T, Lin H, Asami T, Yoshida S, Russell SD, Li J. 2007. BAK1 and BKK1 regulate brassinosteroid-dependent growth and brassinosteroid-independent cell-death pathways. *Current Biology* **17**(13): 1109-1115.

He P, Shan L, Lin NC, Martin GB, Kemmerling B, Nurnberger T, Sheen J. 2006. Specific bacterial suppressors of MAMP signaling upstream of MAPKKK in *Arabidopsis* innate immunity. *Cell* **125**(3): 563-575.

Hecht V, Vielle-Calzada JP, Hartog MV, Schmidt ED, Boutilier K, Grossniklaus U, de Vries SC. 2001. The Arabidopsis SOMATIC EMBRYOGENESIS RECEPTOR KINASE 1 gene is expressed in developing ovules and embryos and enhances embryogenic competence in culture. *Plant Physiology* **127**(3): 803-816.

Heese A, Hann DR, Gimenez-Ibanez S, Jones AM, He K, Li J, Schroeder JI, Peck SC, Rathjen JP. 2007. The receptor-like kinase SERK3/BAK1 is a central regulator of innate immunity in plants. *Proceedings of the National Academy of Sciences of the United States of America* **104**(29): 12217-12222.

Heidrich K, Wirthmueller L, Tasset C, Pouzet C, Deslandes L, Parker JE. 2011. Arabidopsis EDS1 connects pathogen effector recognition to cell compartment-specific immune responses. *Science* **334**(6061): 1401-1404.

Hinsch M, Staskawicz B. 1996. Identification of a new Arabidopsis disease resistance locus, RPs4, and cloning of the corresponding avirulence gene, avrRps4, from Pseudomonas syringae pv. pisi. *Molecular Plant-Microbe Interactions* **9**(1): 55-61.

Holton N, Nekrasov V, Ronald PC, Zipfel C. 2015. The phylogenetically-related pattern recognition receptors EFR and XA21 recruit similar immune signaling components in monocots and dicots. *Public Library of Science Pathogens* **11**(1): e1004602.

Hou SG, Wang X, Chen DH, Yang X, Wang M, Turra D, Di Pietro A, Zhang W. 2014. The Secreted Peptide PIP1 Amplifies Immunity through Receptor-Like Kinase 7. *Public Library of Science Pathogens* **10**(9).

Houterman PM, Ma L, van Ooijen G, de Vroomen MJ, Cornelissen BJC, Takken FLW, Rep M. 2009. The effector protein Avr2 of the xylem-colonizing fungus Fusarium oxysporum activates the tomato resistance protein I-2 intracellularly. *The Plant Journal : for cell and molecular biology* **58**(6): 970-978.

Hu G, deHart AK, Li Y, Ustach C, Handley V, Navarre R, Hwang CF, Aegerter BJ, Williamson VM, Baker B. 2005. EDS1 in tomato is required for resistance mediated by TIR-class R genes and the receptor-like R gene Ve. *The Plant Journal : for cell and molecular biology* **42**(3): 376-391.

Hueck CJ. 1998. Type III protein secretion systems in bacterial pathogens of animals and plants. *Microbiology and Molecular Biology Reviews* **62**(2): 379-433.

Huffaker A, Pearce G, Ryan CA. 2006. An endogenous peptide signal in Arabidopsis activates components of the innate immune response. *Proceedings of the National Academy of Sciences of the United States of America* **103**(26): 10098-10103.

Iizasa E, Mitsutomi M, Nagano Y. 2010. Direct binding of a plant LysM receptor-like kinase, LysM RLK1/CERK1, to chitin in vitro. *The Journal of Biological Chemistry* **285**(5): 2996-3004.

Imlay JA. 2003. Pathways of oxidative damage. *Annual Review of Microbiology* **57**: 395-418.

Jacobs AK, Lipka V, Burton RA, Panstruga R, Strizhov N, Schulze-Lefert P, Fincher GB. 2003. An Arabidopsis Callose Synthase, GSL5, Is Required for Wound and Papillary Callose Formation. *The Plant Cell* **15**(11): 2503-2513.

Jalali BL, Bhargava S, Kamble A. 2006. Signal transduction and transcriptional regulation of plant defence responses. *Journal of Phytopathology* **154**(2): 65-74.

Janjusevic R, Abramovitch RB, Martin GB, Stebbins CE. 2006. A bacterial inhibitor of host programmed cell death defenses is an E3 ubiquitin ligase. *Science* **311**(5758): 222-226.

Jebanathirajah JA, Peri S, Pandey A. 2002. Toll and interleukin-1 receptor (TIR) domain-containing proteins in plants: a genomic perspective. *Trends in Plant Science* **7**(9): 388-391.

Jehle AK, Furst U, Lipschis M, Albert M, Felix G. 2013a. Perception of the novel MAMP eMax from different Xanthomonas species requires the Arabidopsis receptor-like protein ReMAX and the receptor kinase SOBIR. *Plant Signaling & Behavior* **8**(12).

Jehle AK, Lipschis M, Albert M, Fallahzadeh-Mamaghani V, Furst U, Mueller K, Felix G. 2013b. The receptor-like protein ReMAX of Arabidopsis detects the microbe-associated molecular pattern eMax from Xanthomonas. *The Plant Cell* **25**(6): 2330-2340.

Jeong YJ, Shang Y, Kim BH, Kim SY, Song JH, Lee JS, Lee MM, Li J, Nam KH. 2010. BAK7 displays unequal genetic redundancy with BAK1 in brassinosteroid signaling and early senescence in Arabidopsis. *Molecular Cells* **29**(3): 259-266.

Jeworutzki E, Roelfsema MR, Anschutz U, Krol E, Elzenga JT, Felix G, Boller T, Hedrich R, Becker D. 2010. Early signaling through the Arabidopsis pattern recognition receptors FLS2 and EFR involves Ca-associated opening of plasma membrane anion channels. *The Plant Journal : for cell and molecular biology* **62**(3): 367-378.

Jia Y, McAdams SA, Bryan GT, Hershey HP, Valent B. 2000. Direct interaction of resistance gene and avirulence gene products confers rice blast resistance. *The EUROPEAN MOLECULAR BIOLOGY ORGANIZATION Journal* **19**(15): 4004-4014.

Jo KR, Kim CJ, Kim SJ, Kim TY, Bergervoet M, Jongsma MA, Visser RG, Jacobsen E, Vossen JH. 2014. Development of late blight resistant potatoes by cisgene stacking. *BMC Biotechnology* **14**: 50.

Johnson LN, Noble ME, Owen DJ. 1996. Active and inactive protein kinases: structural basis for regulation. *Cell* **85**(2): 149-158.

Jones JD, Dangl JL. 2006. The plant immune system. *Nature* **444**(7117): 323-329.

Jones JD, Shlumukov L, Carland F, English J, Scofield SR, Bishop GJ, Harrison K. 1992. Effective vectors for transformation, expression of heterologous genes, and assaying transposon excision in transgenic plants. *Transgenic Research* **1**(6): 285-297.

Jones JD, Witek K, Verweij W, Jupe F, Cooke D, Dorling S, Tomlinson L, Smoker M, Perkins S, Foster S. 2014. Elevating crop disease resistance with cloned genes. *Philosophical transactions of the Royal Society* **369**(1639): 20130087.

Joosten MH, Vogelsang R, Cozijnsen TJ, Verberne MC, De Wit PJ. 1997. The biotrophic fungus Cladosporium fulvum circumvents Cf-4-mediated resistance by producing unstable AVR4 elicitors. *The Plant Cell* **9**(3): 367-379.

Kadota Y, Sklenar J, Derbyshire P, Stransfeld L, Asai S, Ntoukakis V, Jones JD, Shirasu K, Menke F, Jones A, Zipfel C. 2014. Direct Regulation of the NADPH Oxidase RBOHD by the PRR-Associated Kinase BIK1 during Plant Immunity. *Molecular Cell* **54**(1): 43-55.

Kaelin WG, Jr., Krek W, Sellers WR, DeCaprio JA, Ajchenbaum F, Fuchs CS, Chittenden T, Li Y, Farnham PJ, Blanar MA, et al. 1992. Expression cloning of a cDNA encoding a retinoblastoma-binding protein with E2F-like properties. *Cell* **70**(2): 351-364.

Kaku H, Nishizawa Y, Ishii-Minami N, Akimoto-Tomiyama C, Dohmae N, Takio K, Minami E, Shibuya N. 2006. Plant cells recognize chitin fragments for defense signaling through a plasma membrane receptor. *Proceedings of the National Academy of Sciences of the United States of America* **103**(29): 11086-11091.

Kamoun S. 2006. A catalogue of the effector secretome of plant pathogenic oomycetes. *Annual Review of Phytopathology* **44**: 41-60.

Kang HG, Kuhl JC, Kachroo P, Klessig DF. 2008. CRT1, an Arabidopsis ATPase that interacts with diverse resistance proteins and modulates disease resistance to turnip crinkle virus. *Cell Host & Microbe* **3**(1): 48-57.

Kang HG, Oh CS, Sato M, Katagiri F, Glazebrook J, Takahashi H, Kachroo P, Martin GB, Klessig DF. 2010. Endosome-associated CRT1 functions early in resistance gene-mediated defense signaling in Arabidopsis and tobacco. *The Plant Cell* **22**(3): 918-936.

Karlova R, Boeren S, Russinova E, Aker J, Vervoort J, de Vries S. 2006. The Arabidopsis SOMATIC EMBRYOGENESIS RECEPTOR-LIKE KINASE1 protein complex includes BRASSINOSTEROID-INSENSITIVE1. *The Plant Cell* **18**(3): 626-638.

Karlova R, de Vries SC. 2006. Advances in understanding brassinosteroid signaling. *Science's Signal Transduction Knowledge Environment* **2006**(354): pe36.

Kavanagh T, Goulden M, Santa Cruz S, Chapman S, Barker I, Baulcombe D. 1992. Molecular analysis of a resistance-breaking strain of potato virus X. *Virology* **189**(2): 609-617.

Keller T, Damude HG, Werner D, Doerner P, Dixon RA, Lamb C. 1998. A plant homolog of the neutrophil NADPH oxidase gp91phox subunit gene encodes a plasma membrane protein with Ca2+ binding motifs. *The Plant Cell* **10**(2): 255-266.

Kemen E, Kemen AC, Rafiqi M, Hempel U, Mendgen K, Hahn M, Voegele RT. 2005. Identification of a protein from rust fungi transferred from haustoria into infected plant cells. *Molecular Plant-Microbe Interactions* **18**(11): 1130-1139.

Kemmerling B, Schwedt A, Rodriguez P, Mazzotta S, Frank M, Qamar SA, Mengiste T, Betsuyaku S, Parker JE, Mussig C, Thomma BP, Albrecht C, de Vries SC, Hirt H, Nurnberger T. 2007. The BRI1-associated kinase 1, BAK1, has a brassinolide-independent role in plant cell-death control. *Current Biology : CB* **17**(13): 1116-1122.

Keppler LD, Baker CJ, Atkinson MM. 1989. Active Oxygen Production during a Bacteria-Induced Hypersensitive Reaction in Tobacco Suspension Cells. *Phytopathology* **79**(9): 974-978.

Keshavarzi M, Soylu S, Brown I, Bonas U, Nicole M, Rossiter J, Mansfield J. 2004. Basal defenses induced in pepper by lipopolysaccharides are suppressed by *Xanthomonas campestris* pv. *vesicatoria*. *Molecular Plant-Microbe Interactions* **17**(7): 805-815.

Kim HE, Du F, Fang M, Wang X. 2005. Formation of apoptosome is initiated by cytochrome c-induced dATP hydrolysis and subsequent nucleotide exchange on Apaf-1. *Proceedings of the National Academy of Sciences of the United States of America* **102**(49): 17545-17550.

Kim HS, Desveaux D, Singer AU, Patel P, Sondek J, Dangl JL. 2005. The *Pseudomonas syringae* effector AvrRpt2 cleaves its C-terminally acylated target, RIN4, from *Arabidopsis* membranes to block RPM1 activation. *Proceedings of the National Academy of Sciences of the United States of America* **102**(18): 6496-6501.

Kim YJ, Lin NC, Martin GB. 2002. Two distinct *Pseudomonas* effector proteins interact with the Pto kinase and activate plant immunity. *Cell* **109**(5): 589-598.

Knight MR, Campbell AK, Smith SM, Trewavas AJ. 1991. Transgenic plant aequorin reports the effects of touch and cold-shock and elicitors on cytoplasmic calcium. *Nature* **352**(6335): 524-526.

Kobe B, Deisenhofer J. 1994. The leucine-rich repeat: a versatile binding motif. *Trends Biochemical Science* **19**(10): 415-421.

Kobe B, Kajava AV. 2001. The leucine-rich repeat as a protein recognition motif. *Current Opinion Structural Biology* **11**(6): 725-732.

Koller T, Bent AF. 2014. FLS2-BAK1 extracellular domain interaction sites required for defense signaling activation. *Public Library of Science One* **9**(10): e111185.

Kollmann TR, Levy O, Montgomery RR, Goriely S. 2012. Innate immune function by Toll-like receptors: distinct responses in newborns and the elderly. *Immunity* **37**(5): 771-783.

Kolmer J OM, Groth J 2009. The Rust Fungi. *Encyclopedia of Life Sciences*

Koncz C, Schell J. 1986. The Promoter of TI-DNA Gene 5 Controls the Tissue-Specific Expression of Chimeric Genes Carried by a Novel Type of Agrobacterium Binary Vector. *Molecular & General Genetics* **204**(3): 383-396.

Krasileva KV, Dahlbeck D, Staskawicz BJ. 2010. Activation of an *Arabidopsis* resistance protein is specified by the in planta association of its leucine-rich repeat domain with the cognate oomycete effector. *The Plant Cell* **22**(7): 2444-2458.

Krol E, Mentzel T, Chinchilla D, Boller T, Felix G, Kemmerling B, Postel S, Arents M, Jeworutzki E, Al-Rasheid KA, Becker D, Hedrich R. 2010. Perception of the Arabidopsis danger signal peptide 1 involves the pattern recognition receptor AtPEPR1 and its close homologue AtPEPR2. *The Journal of Biological Chemistry* **285**(18): 13471-13479.

Kud J, Zhao Z, Du X, Liu Y, Zhao Y, Xiao F. 2013. SGT1 interacts with the Prf resistance protein and is required for Prf accumulation and Prf-mediated defense signaling. *Biochemical and Biophysical Research Communications* **431**(3): 501-505.

Kudla J, Batistic O, Hashimoto K. 2010. Calcium signals: the lead currency of plant information processing. *The Plant Cell* **22**(3): 541-563.

Kunkel BN, Bent AF, Dahlbeck D, Innes RW, Staskawicz BJ. 1993. RPS2, an *Arabidopsis* disease resistance locus specifying recognition of *Pseudomonas syringae* strains expressing the avirulence gene *avrRpt2*. *The Plant Cell* **5**(8): 865-875.

Kunze G, Zipfel C, Robatzek S, Niehaus K, Boller T, Felix G. 2004. The N terminus of bacterial elongation factor Tu elicits innate immunity in Arabidopsis plants. *The Plant Cell* **16**(12): 3496-3507.

Lacombe S, Rougon-Cardoso A, Sherwood E, Peeters N, Dahlbeck D, van Esse HP, Smoker M, Rallapalli G, Thomma BP, Staskawicz B, Jones JD, Zipfel C. 2010. Interfamily transfer of a plant pattern-recognition receptor confers broad-spectrum bacterial resistance. *Nature Biotechnology* **28**(4): 365-369.

Laluk K, Luo H, Chai M, Dhawan R, Lai Z, Mengiste T. 2011. Biochemical and genetic requirements for function of the immune response regulator BOTRYTIS-INDUCED KINASE1 in plant growth, ethylene signaling, and PAMP-triggered immunity in Arabidopsis. *The Plant Cell* **23**(8): 2831-2849.

Le Roux C, Huet G, Jauneau A, Camborde L, Tremousaygue D, Kraut A, Zhou B, Levaillant M, Adachi H, Yoshioka H, Raffaele S, Berthome R, Coute Y, Parker JE, Deslandes L. 2015. A receptor pair with an integrated decoy converts pathogen disabling of transcription factors to immunity. *Cell* **161**(5): 1074-1088.

Lehti-Shiu MD, Zou C, Hanada K, Shiu SH. 2009. Evolutionary History and Stress Regulation of Plant Receptor-Like Kinase/Pelle Genes. *Plant Physiology* **150**(1): 12-26.

Leipe DD, Koonin EV, Aravind L. 2004. STAND, a class of P-loop NTPases including animal and plant regulators of programmed cell death: multiple, complex domain architectures, unusual phyletic patterns, and evolution by horizontal gene transfer. *Journal of Molecular Biology* **343**(1): 1-28.

Leister RT, Dahlbeck D, Day B, Li Y, Chesnokova O, Staskawicz BJ. 2005. Molecular genetic evidence for the role of SGT1 in the intramolecular complementation of Bs2 protein activity in *Nicotiana benthamiana*. *The Plant Cell* **17**(4): 1268-1278.

Li J, Nam KH. 2002. Regulation of brassinosteroid signaling by a GSK3/SHAGGY-like kinase. *Science* **295**(5558): 1299-1301.

Li J, Zhao-Hui C, Batoux M, Nekrasov V, Roux M, Chinchilla D, Zipfel C, Jones JD. 2009. Specific ER quality control components required for biogenesis of the plant innate immune receptor EFR. *Proceedings of the National Academy of Sciences of the United States of America* **106**(37): 15973-15978.

Liebrand TW, Kombrink A, Zhang Z, Sklenar J, Jones AM, Robatzek S, Thomma BP, Joosten MH. 2014. Chaperones of the endoplasmic reticulum are required for Ve1-mediated resistance to Verticillium. *Molecular Plant Pathology* **15**(1): 109-117.

Liebrand TW, Smit P, Abd-El-Haliem A, de Jonge R, Cordewener JH, America AH, Sklenar J, Jones AM, Robatzek S, Thomma BP, Tameling WI, Joosten MH. 2012. Endoplasmic reticulum-quality control chaperones facilitate the biogenesis of Cf receptor-like proteins involved in pathogen resistance of tomato. *Plant Physiology* **159**(4): 1819-1833.

Liebrand TW, van den Berg GC, Zhang Z, Smit P, Cordewener JH, America AH, Sklenar J, Jones AM, Tameling WI, Robatzek S, Thomma BP, Joosten MH. 2013. Receptor-like kinase SOBIR1/EVR interacts with receptor-like proteins in plant immunity against fungal infection. *Proceedings of the National Academy of Sciences of the United States of America* **110**(24): 10010-10015.

Lipka V, Dittgen J, Bednarek P, Bhat R, Wiermer M, Stein M, Landtag J, Brandt W, Rosahl S, Scheel D, Llorente F, Molina A, Parker J, Somerville S, Schulze-Lefert P. 2005. Pre- and postinvasion defenses both contribute to nonhost resistance in Arabidopsis. *Science* **310**(5751): 1180-1183.

Liu T, Liu Z, Song C, Hu Y, Han Z, She J, Fan F, Wang J, Jin C, Chang J, Zhou JM, Chai J. 2012. Chitin-induced dimerization activates a plant immune receptor. *Science* **336**(6085): 1160-1164.

Liu X, Grabherr HM, Willmann R, Kolb D, Brunner F, Bertsche U, Kuhner D, Franz-Wachtel M, Amin B, Felix G, Ongena M, Nurnberger T, Gust AA. 2014. Host-induced bacterial cell wall decomposition mediates pattern-triggered immunity in Arabidopsis. *Elife* **3**.

Lobstein J, Emrich CA, Jeans C, Faulkner M, Riggs P, Berkmen M. 2012. SHuffle, a novel Escherichia coli protein expression strain capable of correctly folding disulfide bonded proteins in its cytoplasm. *Microbial Cell Factories* **11**: 56.

Lozano-Duran R, Macho AP, Boutrot F, Segonzac C, Somssich IE, Zipfel C. 2013. The transcriptional regulator BZR1 mediates trade-off between plant innate immunity and growth. *Elife* **2**.

Lu D, Lin W, Gao X, Wu S, Cheng C, Avila J, Heese A, Devarenne TP, He P, Shan L. 2011. Direct ubiquitination of pattern recognition receptor FLS2 attenuates plant innate immunity. *Science* **332**(6036): 1439-1442.

Lu D, Wu S, Gao X, Zhang Y, Shan L, He P. 2010. A receptor-like cytoplasmic kinase, BIK1, associates with a flagellin receptor complex to initiate plant innate immunity. *Proceedings of the National Academy of Sciences of the United States of America* **107**(1): 496-501.

Ma Y, Walker RK, Zhao Y, Berkowitz GA. 2012. Linking ligand perception by PEPR pattern recognition receptors to cytosolic Ca2+ elevation and downstream immune signaling in plants. *Proceedings of the National Academy of Sciences of the United States of America* **109**(48): 19852-19857.

Macho AP, Zipfel C. 2014. Plant PRRs and the activation of innate immune signaling. *Molecular Cell* **54**(2): 263-272.

Mackey D, Holt BF, 3rd, Wiig A, Dangl JL. 2002. RIN4 interacts with *Pseudomonas syringae* type III effector molecules and is required for RPM1-mediated resistance in *Arabidopsis*. *Cell* **108**(6): 743-754.

Maekawa T, Cheng W, Spiridon LN, Toller A, Lukasik E, Saijo Y, Liu P, Shen QH, Micluta MA, Somssich IE, Takken FL, Petrescu AJ, Chai J, Schulze-Lefert P. 2011. Coiled-Coil Domain-Dependent Homodimerization of Intracellular Barley Immune Receptors Defines a Minimal Functional Module for Triggering Cell Death. *Cell Host & Microbe* **9**(3): 187-199.

Martin GB, Bogdanove AJ, Sessa G. 2003. Understanding the functions of plant disease resistance proteins. *Annual Reviev Plant Biology* **54**: 23-61.

Martin GB, Brommonschenkel SH, Chunwongse J, Frary A, Ganal MW, Spivey R, Wu T, Earle ED, Tanksley SD. 1993. Map-based cloning of a protein kinase gene conferring disease resistance in tomato. *Science* **262**(5138): 1432-1436.

Mathieu J, Schwizer S, Martin GB. 2014. Pto kinase binds two domains of AvrPtoB and its proximity to the effector E3 ligase determines if it evades degradation and activates plant immunity. *Public Library of Science Pathogens* **10**(7): e1004227.

Matzinger P. 2002. The danger model: a renewed sense of self. *Science* **296**(5566): 301-305.

McCann HC, Guttman DS. 2008. Evolution of the type III secretion system and its effectors in plant-microbe interactions. *New Phytologist* **177**(1): 33-47.

Medzhitov R, Janeway CA, Jr. 1997. Innate immunity: the virtues of a nonclonal system of recognition. *Cell* **91**(3): 295-298.

Melotto M, Underwood W, Koczan J, Nomura K, He SY. 2006. Plant stomata function in innate immunity against bacterial invasion. *Cell* **126**(5): 969-980.

Mestre P, Baulcombe DC. 2006. Elicitor-mediated oligomerization of the tobacco N disease resistance protein. *The Plant Cell* **18**(2): 491-501.

Meszaros T, Helfer A, Hatzimasoura E, Magyar Z, Serazetdinova L, Rios G, Bardoczy V, Teige M, Koncz C, Peck S, Bogre L. 2006. The Arabidopsis MAP kinase kinase MKK1 participates in defence responses to the bacterial elicitor flagellin. *The Plant Journal : for cell and molecular biology* **48**(4): 485-498.

Meyers BC, Dickerman AW, Michelmore RW, Sivaramakrishnan S, Sobral BW, Young ND. 1999. Plant disease resistance genes encode members of an ancient and diverse protein family within the nucleotide-binding superfamily. *The Plant Journal : for cell and molecular biology* **20**(3): 317-332.

Mishina TE, Zeier J. 2007. Pathogen-associated molecular pattern recognition rather than development of tissue necrosis contributes to bacterial induction of systemic acquired resistance in Arabidopsis. *The Plant Journal* **50**(3): 500-513.

Miya A, Albert P, Shinya T, Desaki Y, Ichimura K, Shirasu K, Narusaka Y, Kawakami N, Kaku H, Shibuya N. 2007. CERK1, a LysM receptor kinase, is essential for chitin elicitor signaling in *Arabidopsis*. *Proceedings of the National Academy of Sciences of the United States of America* **104**(49): 19613-19618.

Moffett P, Farnham G, Peart J, Baulcombe DC. 2002. Interaction between domains of a plant NBS-LRR protein in disease resistance-related cell death. *The EUROPEAN MOLECULAR BIOLOGY ORGANIZATION Journal* **21**(17): 4511-4519.

Monaghan J, Matschi S, Shorinola O, Rovenich H, Matei A, Segonzac C, Malinovsky FG, Rathjen JP, MacLean D, Romeis T, Zipfel C. 2014. The calcium-dependent protein kinase CPK28 buffers plant immunity and regulates BIK1 turnover. *Cell Host & Microbe* **16**(5): 605-615.

Monaghan J, Zipfel C. 2012. Plant pattern recognition receptor complexes at the plasma membrane. *Current Opinion in Plant Biology* **15**(4): 349-357.

Morel JB, Dangl JL. 1997. The hypersensitive response and the induction of cell death in plants. *Cell Death and Differentiation* **4**(8): 671-683.

Mucyn TS, Clemente A, Andriotis VM, Balmuth AL, Oldroyd GE, Staskawicz BJ, Rathjen JP. 2006. The tomato NBARC-LRR protein Prf interacts with Pto kinase in vivo to regulate specific plant immunity. *The Plant Cell* **18**(10): 2792-2806.

Mucyn TS, Wu AJ, Balmuth AL, Arasteh JM, Rathjen JP. 2009. Regulation of tomato Prf by Pto-like protein kinases. *Molecular Plant-Microbe Interactions* **22**(4): 391-401.

Mudgett MB. 2005. New insights to the function of phytopathogenic bacterial type III effectors in plants. *Annual Review of Plant Biology* **56**: 509-531.

Mukherjee M, Larrimore KE, Ahmed NJ, Bedick TS, Barghouthi NT, Traw MB, Barth C. 2010. Ascorbic acid deficiency in arabidopsis induces constitutive priming that is dependent on hydrogen peroxide, salicylic acid, and the NPR1 gene. *Molecular Plant-Microbe Interactions* **23**(3): 340-351.

Murashige T, Skoog F. 1962. A Revised Medium for Rapid Growth and Bio Assays with Tobacco Tissue Cultures. *Physiologia Plantarum* **15**(3): 473-497.

Murray F, Brettell R, Matthews P, Bishop D, Jacobsen J. 2004. Comparison of Agrobacterium-mediated transformation of four barley cultivars using the GFP and GUS reporter genes. *Plant Cell Reports* **22**(6): 397-402.

Muskett PR, Kahn K, Austin MJ, Moisan LJ, Sadanandom A, Shirasu K, Jones JD, Parker JE. 2002. Arabidopsis RAR1 exerts rate-limiting control of R gene-mediated defenses against multiple pathogens. *The Plant Cell* **14**(5): 979-992.

Nagarajan S, Singh DV. 1990. Long-distance dispersion of rust pathogens. *Annual Review of Phytopathology* **28**: 139-153.

Nakagawa T, Nakamura S, Tanaka K, Kawamukai M, Suzuki T, Nakamura K, Kimura T, Ishiguro S. 2008. Development of R4 gateway binary vectors (R4pGWB) enabling high-throughput promoter swapping for plant research. *Bioscience Biotechnology Biochemistry* **72**(2): 624-629.

Nam KH, Li J. 2002. BRI1/BAK1, a receptor kinase pair mediating brassinosteroid signaling. *Cell* **110**(2): 203-212.

Naqvi S, Farre G, Sanahuja G, Capell T, Zhu C, Christou P. 2010. When more is better: multigene engineering in plants. *Trends in Plant Science* **15**(1): 48-56.

Narusaka M, Shirasu K, Noutoshi Y, Kubo Y, Shiraishi T, Iwabuchi M, Narusaka Y. 2009. RRS1 and RPS4 provide a dual Resistance-gene system against fungal and bacterial pathogens. *Plant Journal* **60**(2): 218-226.

Navarro L, Dunoyer P, Jay F, Arnold B, Dharmasiri N, Estelle M, Voinnet O, Jones JD. 2006. A plant miRNA contributes to antibacterial resistance by repressing auxin signaling. *Science* **312**(5772): 436-439.

Navarro L, Zipfel C, Rowland O, Keller I, Robatzek S, Boller T, Jones JD. 2004. The transcriptional innate immune response to flg22. Interplay and overlap with Avr gene-dependent defense responses and bacterial pathogenesis. *Plant Physiology* **135**(2): 1113-1128.

Nekrasov V, Li J, Batoux M, Roux M, Chu ZH, Lacombe S, Rougon A, Bittel P, Kiss-Papp M, Chinchilla D, van Esse HP, Jorda L, Schwessinger B, Nicaise V, Thomma BP, Molina A, Jones JD, Zipfel C. 2009. Control of the pattern-recognition receptor EFR by an ER protein complex in plant immunity. *The EUROPEAN MOLECULAR BIOLOGY ORGANIZATION Journal* **28**(21): 3428-3438.

Nimchuk Z, Eulgem T, Holt BF, 3rd, Dangl JL. 2003. Recognition and response in the plant immune system. *Annual Review Genetics* **37**: 579-609.

Nothnagel EA, McNeil M, Albersheim P, Dell A. 1983. Host-Pathogen Interactions : XXII. A Galacturonic Acid Oligosaccharide from Plant Cell Walls Elicits Phytoalexins. *Plant Physiology* **71**(4): 916-926.

Ntoukakis V, Balmuth AL, Mucyn TS, Gutierrez JR, Jones AM, Rathjen JP. 2013. The tomato Prf complex is a molecular trap for bacterial effectors based on Pto transphosphorylation. *Public Library of Science Pathogens* **9**(1): e1003123.

Ntoukakis V, Mucyn TS, Gimenez-Ibanez S, Chapman HC, Gutierrez JR, Balmuth AL, Jones AM, Rathjen JP. 2009. Host inhibition of a bacterial virulence effector triggers immunity to infection. *Science* **324**(5928): 784-787.

Ntoukakis V, Saur IM, Conlan B, Rathjen JP. 2014. The changing of the guard: the Pto/Prf receptor complex of tomato and pathogen recognition. *Current Opinion in Plant Biology* **20C**: 69-74.

Nurnberger T, Kemmerling B. 2006. Receptor protein kinases--pattern recognition receptors in plant immunity. *Trends in Plant Science* **11**(11): 519-522.

Nurnberger T, Lipka V. 2005. Non-host resistance in plants: new insights into an old phenomenon. *Molecular Plant Pathology* **6**(3): 335-345.

Oh CS, Pedley KF, Martin GB. 2010. Tomato 14-3-3 protein 7 positively regulates immunity-associated programmed cell death by enhancing protein abundance and signaling ability of MAPKKK {alpha}. *The Plant Cell* **22**(1): 260-272.

Oldroyd GE, Staskawicz BJ. 1998. Genetically engineered broad-spectrum disease resistance in tomato. *Proceedings of the National Academy of Sciences of the United States of America* **95**(17): 10300-10305.

Olson EL, Rouse MN, Pumphrey MO, Bowden RL, Gill BS, Poland JA. 2013. Simultaneous transfer, introgression, and genomic localization of genes for resistance to stem rust

race TTKSK (Ug99) from Aegilops tauschii to wheat. *Theoretic and Applied Genetics* **126**(5): 1179-1188.

Ostergaard L, Petersen M, Mattsson O, Mundy J. 2002. An Arabidopsis callose synthase. *Plant Molecular Biology* **49**(6): 559-566.

Padmanabhan M, Cournoyer P, Dinesh-Kumar SP. 2009. The leucine-rich repeat domain in plant innate immunity: a wealth of possibilities. *Cellular Microbiology* **11**(2): 191-198.

Pandey SP, Somssich IE. 2009. The role of WRKY transcription factors in plant immunity. *Plant Physiology* **150**(4): 1648-1655.

Panstruga R, Dodds PN. 2009. Terrific protein traffic: the mystery of effector protein delivery by filamentous plant pathogens. *Science* **324**(5928): 748-750.

Park CJ, Lee SW, Chern M, Sharma R, Canlas PE, Song MY, Jeon JS, Ronald PC. 2010. Ectopic expression of rice Xa21 overcomes developmentally controlled resistance to Xanthomonas oryzae pv. oryzae. *Plant Science* **179**(5): 466-471.

Peart JR, Cook G, Feys BJ, Parker JE, Baulcombe DC. 2002. An EDS1 orthologue is required for N-mediated resistance against tobacco mosaic virus. *Plant Journal* **29**(5): 569-579.

Pedley KF, Martin GB. 2005. Role of mitogen-activated protein kinases in plant immunity. *Current Opinion in Plant Biology* **8**(5): 541-547.

Periyannan S, Moore J, Ayliffe M, Bansal U, Wang X, Huang L, Deal K, Luo M, Kong X, Bariana H, Mago R, McIntosh R, Dodds P, Dvorak J, Lagudah E. 2013. The gene Sr33, an ortholog of barley Mla genes, encodes resistance to wheat stem rust race Ug99. *Science* **341**(6147): 786-788.

Petersen M, Brodersen P, Naested H, Andreasson E, Lindhart U, Johansen B, Nielsen HB, Lacy M, Austin MJ, Parker JE, Sharma SB, Klessig DF, Martienssen R, Mattsson O, Jensen AB, Mundy J. 2000. Arabidopsis map kinase 4 negatively regulates systemic acquired resistance. *Cell* **103**(7): 1111-1120.

Petutschnig EK, Jones AM, Serazetdinova L, Lipka U, Lipka V. 2010. The lysin motif receptor-like kinase (LysM-RLK) CERK1 is a major chitin-binding protein in Arabidopsis thaliana and subject to chitin-induced phosphorylation. *The Journal of Biological Chemistry* **285**(37): 28902-28911.

Postel S, Kemmerling B. 2009. Plant systems for recognition of pathogen-associated molecular patterns. *Seminars in Cell & Developmental Biology* **20**(9): 1025-1031.

Postel S, Kufner I, Beuter C, Mazzotta S, Schwedt A, Borlotti A, Halter T, Kemmerling B, Nurnberger T. 2010. The multifunctional leucine-rich repeat receptor kinase BAK1 is implicated in Arabidopsis development and immunity. *European Journal of Cell Biology* **89**(2-3): 169-174.

Preston GM. 2000. *Pseudomonas syringae* pv. *tomato*: the right pathogen, of the right plant, at the right time. *Molecular Plant Pathology* **1**(5): 263-275.

Qi D, DeYoung BJ, Innes RW. 2012. Structure-function analysis of the coiled-coil and leucine-rich repeat domains of the RPS5 disease resistance protein. *Plant Physiology* **158**(4): 1819-1832.

Qiu JL, Zhou L, Yun BW, Nielsen HB, Fiil BK, Petersen K, Mackinlay J, Loake GJ, Mundy J, Morris PC. 2008. Arabidopsis mitogen-activated protein kinase kinases MKK1 and MKK2 have overlapping functions in defense signaling mediated by MEKK1, MPK4, and MKS1. *Plant Physiology* **148**(1): 212-222.

Rafiqi M, Gan PHP, Ravensdale M, Lawrence GJ, Ellis JG, Jones DA, Hardham AR, Dodds PN. 2010. Internalization of Flax Rust Avirulence Proteins into Flax and Tobacco Cells Can Occur in the Absence of the Pathogen. *The Plant Cell* **22**(6): 2017-2032.

Rairdan GJ, Moffett P. 2006. Distinct domains in the ARC region of the potato resistance protein Rx mediate LRR binding and inhibition of activation. *The Plant Cell* **18**(8): 2082-2093.

Ramburan VP, Pretorius ZA, Louw JH, Boyd LA, Smith PH, Boshoff WH, Prins R. 2004. A genetic analysis of adult plant resistance to stripe rust in the wheat cultivar Kariega. *TAG. Theoretical and Applied Genetics* **108**(7): 1426-1433.

Ranf S, Gisch N, Schaffer M, Illig T, Westphal L, Knirel YA, Sanchez-Carballo PM, Zahringer U, Huckelhoven R, Lee J, Scheel D. 2015. A lectin S-domain receptor kinase mediates lipopolysaccharide sensing in Arabidopsis thaliana. *Nature Immunology*.

Rapilly F. 1979. Yellow Rust Epidemiology. *Annual Review of Phytopathology* **17**: 59-73.

Rathjen JP, Chang JH, Staskawicz BJ, Michelmore RW. 1999. Constitutively active Pto induces a Prf-dependent hypersensitive response in the absence of avrPto. *The EUROPEAN MOLECULAR BIOLOGY ORGANIZATION Journal* **18**(12): 3232-3240.

Riedl SJ, Li W, Chao Y, Schwarzenbacher R, Shi Y. 2005. Structure of the apoptotic protease-activating factor 1 bound to ADP. *Nature* **434**(7035): 926-933.

Roelfs AP, Huertaespino J, Marshall D. 1992. Barley Stripe Rust in Texas. *Plant Disease* **76**(5): 538-538.

Rommens CM, Salmeron JM, Oldroyd GE, Staskawicz BJ. 1995. Intergeneric transfer and functional expression of the tomato disease resistance gene Pto. *Plant Cell* **7**(10): 1537-1544.

Ron M, Avni A. 2004. The receptor for the fungal elicitor ethylene-inducing xylanase is a member of a resistance-like gene family in tomato. *The Plant Cell* **16**(6): 1604-1615.

Rosebrock TR, Zeng L, Brady JJ, Abramovitch RB, Xiao F, Martin GB. 2007. A bacterial E3 ubiquitin ligase targets a host protein kinase to disrupt plant immunity. *Nature* **448**(7151): 370-374.

Roux M, Schwessinger B, Albrecht C, Chinchilla D, Jones A, Holton N, Malinovsky FG, Tor M, de Vries S, Zipfel C. 2011. The Arabidopsis leucine-rich repeat receptor-like kinases BAK1/SERK3 and BKK1/SERK4 are required for innate immunity to hemibiotrophic and biotrophic pathogens. *The Plant Cell* **23**(6): 2440-2455.

Russinova E, Borst JW, Kwaaitaal M, Cano-Delgado A, Yin Y, Chory J, de Vries SC. 2004. Heterodimerization and endocytosis of Arabidopsis brassinosteroid receptors BRI1 and AtSERK3 (BAK1). *The Plant Cell* **16**(12): 3216-3229.

Saari EE, and Prescott, J. M. 1985. World distribution in relation to economic losses. *The Cereal Rusts* **II**: 259-298

Sagi M, Fluhr R. 2001. Superoxide production by plant homologues of the gp91(phox) NADPH oxidase. Modulation of activity by calcium and by tobacco mosaic virus infection. *Plant Physiology* **126**(3): 1281-1290.

Salmeron JM, Oldroyd GE, Rommens CM, Scofield SR, Kim HS, Lavelle DT, Dahlbeck D, Staskawicz BJ. 1996. Tomato Prf is a member of the leucine-rich repeat class of plant disease resistance genes and lies embedded within the *Pto* kinase gene cluster. *Cell* **86**(1): 123-133.

Salmeron JM, Staskawicz BJ. 1993. Molecular characterization and hrp dependence of the avirulence gene avrPto from *Pseudomonas syringae* pv. *tomato*. *Molecular and General Genetics* **239**(1-2): 6-16.

Saur IM, Conlan BF, Rathjen JP. 2015. The N-Terminal Domain of the Tomato Immune Protein Prf Contains Multiple Homotypic and Pto Kinase Interaction Sites. *The Journal of Biological Chemistry* **290**(18): 11258-11267.

Schoonbeek HJ, Wang HH, Stefanato FL, Craze M, Bowden S, Wallington E, Zipfel C, Ridout CJ. 2015. Arabidopsis EF-Tu receptor enhances bacterial disease resistance in transgenic wheat. *New Phytologist*.

Schulze B, Mentzel T, Jehle AK, Mueller K, Beeler S, Boller T, Felix G, Chinchilla D. 2010. Rapid heteromerization and phosphorylation of ligand-activated plant transmembrane receptors and their associated kinase BAK1. *The Journal of Biological Chemistry* **285**(13): 9444-9451.

Schwessinger B, Roux M, Kadota Y, Ntoukakis V, Sklenar J, Jones A, Zipfel C. 2011. Phosphorylation-dependent differential regulation of plant growth, cell death, and innate immunity by the regulatory receptor-like kinase BAK1. *Public Library of Science Genetics* **7**(4): e1002046.

Scofield SR, Tobias CM, Rathjen JP, Chang JH, Lavelle DT, Michelmore RW, Staskawicz BJ. 1996. Molecular Basis of Gene-for-Gene Specificity in Bacterial Speck Disease of Tomato. *Science* **274**(5295): 2063-2065.

Searle BC. 2010. Scaffold: a bioinformatic tool for validating MS/MS-based proteomic studies. *Proteomics* **10**(6): 1265-1269.

Seeholzer S, Tsuchimatsu T, Jordan T, Bieri S, Pajonk S, Yang WX, Jahoor A, Shimizu KK, Keller B, Schulze-Lefert P. 2010. Diversity at the Mla Powdery Mildew Resistance Locus from Cultivated Barley Reveals Sites of Positive Selection. *Molecular Plant-Microbe Interactions* **23**(4): 497-509.

Segonzac C, Feike D, Gimenez-Ibanez S, Hann DR, Zipfel C, Rathjen JP. 2011. Hierarchy and roles of pathogen-associated molecular pattern-induced responses in Nicotiana benthamiana. *Plant Physiology* **156**(2): 687-699.

Segonzac C, Macho AP, Sanmartin M, Ntoukakis V, Sanchez-Serrano JJ, Zipfel C. 2014. Negative control of BAK1 by protein phosphatase 2A during plant innate immunity. *The EUROPEAN MOLECULAR BIOLOGY ORGANIZATION Journal* **33**(18): 2069-2079.

Segonzac C, Zipfel C. 2011. Activation of plant pattern-recognition receptors by bacteria. *Current Opinion in Microbiology* **14**(1): 54-61.

Sessa G, D'Ascenzo M, Martin GB. 2000a. The major site of the pti1 kinase phosphorylated by the pto kinase is located in the activation domain and is required for pto-pti1 physical interaction. *European Journal of Biochemistry* **267**(1): 171-178.

Sessa G, D'Ascenzo M, Martin GB. 2000b. Thr38 and Ser198 are Pto autophosphorylation sites required for the AvrPto-Pto-mediated hypersensitive response. *The EUROPEAN MOLECULAR BIOLOGY ORGANIZATION Journal* **19**(10): 2257-2269.

Shamloul M, Trusa J, Mett V, Yusibov V. 2014. Optimization and utilization of Agrobacterium-mediated transient protein production in Nicotiana. *Journal of Visualized Experiments* (86).

Shan L, He P, Li J, Heese A, Peck SC, Nurnberger T, Martin GB, Sheen J. 2008. Bacterial effectors target the common signaling partner BAK1 to disrupt multiple MAMP receptor-signaling complexes and impede plant immunity. *Cell Host & Microbe* **4**(1): 17-27.

Shan L, Thara VK, Martin GB, Zhou JM, Tang X. 2000. The *Pseudomonas* AvrPto protein is differentially recognized by tomato and tobacco and is localized to the plant plasma membrane. *The Plant Cell* **12**(12): 2323-2338.

Shao F, Golstein C, Ade J, Stoutemyer M, Dixon JE, Innes RW. 2003. Cleavage of Arabidopsis PBS1 by a bacterial type III effector. *Science* **301**(5637): 1230-1233.

Shaw AC, Goldstein DR, Montgomery RR. 2013. Age-dependent dysregulation of innate immunity. *Nature reviews Immunology* **13**(12): 875-887.

Shelton CA, Wasserman SA. 1993. pelle encodes a protein kinase required to establish dorsoventral polarity in the *Drosophila* embryo. *Cell* **72**(4): 515-525.

Shen QH, Saijo Y, Mauch S, Biskup C, Bieri S, Keller B, Seki H, Ulker B, Somssich IE, Schulze-Lefert P. 2007. Nuclear activity of MLA immune receptors links isolate-specific and basal disease-resistance responses. *Science* **315**(5815): 1098-1103.

Shen QH, Schulze-Lefert P. 2007. Rumble in the nuclear jungle: compartmentalization, trafficking, and nuclear action of plant immune receptors. *The EUROPEAN MOLECULAR BIOLOGY ORGANIZATION Journal* **26**(20): 4293-4301.

Shi H, Shen Q, Qi Y, Yan H, Nie H, Chen Y, Zhao T, Katagiri F, Tang D. 2013. BR-SIGNALING KINASE1 physically associates with FLAGELLIN SENSING2 and regulates plant innate immunity in Arabidopsis. *The Plant Cell* **25**(3): 1143-1157.

Shimizu R, Taguchi F, Marutani M, Mukaihara T, Inagaki Y, Toyoda K, Shiraishi T, Ichinose Y. 2003. The DeltafliD mutant of Pseudomonas syringae pv. tabaci, which secretes flagellin monomers, induces a strong hypersensitive reaction (HR) in non-host tomato cells. *Molecular Genetics & Genomics* **269**(1): 21-30.

Shimizu T, Nakano T, Takamizawa D, Desaki Y, Ishii-Minami N, Nishizawa Y, Minami E, Okada K, Yamane H, Kaku H, Shibuya N. 2010. Two LysM receptor molecules, CEBiP and

OsCERK1, cooperatively regulate chitin elicitor signaling in rice. *The Plant Journal* **64**(2): 204-214.

Shirasu K, Schulze-Lefert P. 2003. Complex formation, promiscuity and multi-functionality: protein interactions in disease-resistance pathways. *Trends in Plant Science* **8**(6): 252-258.

Shiu SH, Bleecker AB. 2001. Receptor-like kinases from Arabidopsis form a monophyletic gene family related to animal receptor kinases. *Proceedings of the National Academy of Sciences of the United States of America* **98**(19): 10763-10768.

Smith JM, Salamango DJ, Leslie ME, Collins CA, Heese A. 2014. Sensitivity to Flg22 Is Modulated by Ligand-Induced Degradation and de Novo Synthesis of the Endogenous Flagellin-Receptor FLAGELLIN-SENSING2. *Plant Physiology* **164**(1): 440-454.

Stam R, Mantelin S, McLellan H, Thilliez G. 2014. The role of effectors in nonhost resistance to filamentous plant pathogens. *Frontiers Plant Science* **5**: 582.

Staskawicz BJ. 2001. Genetics of plant-pathogen interactions specifying plant disease resistance. *Plant Physiology* **125**(1): 73-76.

Storozhenko S, Belles-Boix E, Babiychuk E, Herouart D, Davey MW, Slooten L, Van Montagu M, Inze D, Kushnir S. 2002. Gamma-glutamyl transpeptidase in transgenic tobacco plants. Cellular localization, processing, and biochemical properties. *Plant Physiology* **128**(3): 1109-1119.

Stubbs RW. 1985. Stripe rust. *The Cereal Rusts* **II**: 61-101.

Studier FW. 2005. Protein production by auto-induction in high-density shaking cultures. *Protein Expression and Purification* **41**(1): 207-234.

Su SH, Suarez-Rodriguez MC, Krysan P. 2007. Genetic interaction and phenotypic analysis of the Arabidopsis MAP kinase pathway mutations mekk1 and mpk4 suggests signaling pathway complexity. *Federation of European Biochemical Societies letters* **581**(17): 3171-3177.

Suarez-Rodriguez MC, Adams-Phillips L, Liu Y, Wang H, Su SH, Jester PJ, Zhang S, Bent AF, Krysan PJ. 2007. MEKK1 is required for flg22-induced MPK4 activation in Arabidopsis plants. *Plant Physiology* **143**(2): 661-669.

Sun F, Zhang P, Guo M, Yu W, Chen K. 2013. Burdock fructooligosaccharide induces fungal resistance in postharvest Kyoho grapes by activating the salicylic acid-dependent pathway and inhibiting browning. *Food Chemistry* **138**(1): 539-546.

Sun Y, Li L, Macho AP, Han Z, Hu Z, Zipfel C, Zhou JM, Chai J. 2013. Structural basis for flg22-induced activation of the Arabidopsis FLS2-BAK1 immune complex. *Science* **342**(6158): 624-628.

Swiderski MR, Birker D, Jones JD. 2009. The TIR domain of TIR-NB-LRR resistance proteins is a signaling domain involved in cell death induction. *Molecular Plant-Microbe Interactions* **22**(2): 157-165.

Swiderski MR, Innes RW. 2001. The *Arabidopsis PBS1* resistance gene encodes a member of a novel protein kinase subfamily. *The Plant Journal : for cell and molecular biology* **26**(1): 101-112.

Tai TH, Dahlbeck D, Clark ET, Gajiwala P, Pasion R, Whalen MC, Stall RE, Staskawicz BJ. 1999. Expression of the Bs2 pepper gene confers resistance to bacterial spot disease in tomato. *Proceedings of the National Academy of Sciences of the United States of America* **96**(24): 14153-14158.

Takahashi A, Casais C, Ichimura K, Shirasu K. 2003. HSP90 interacts with RAR1 and SGT1 and is essential for RPS2-mediated disease resistance in Arabidopsis. *Proceedings of the National Academy of Sciences of the United States of America* **100**(20): 11777-11782.

Takken FL, Albrecht M, Tameling WI. 2006. Resistance proteins: molecular switches of plant defence. *Current Opinion in Plant Biology* **9**(4): 383-390.

Tameling WI, Elzinga SD, Darmin PS, Vossen JH, Takken FL, Haring MA, Cornelissen BJ. 2002. The tomato *R* gene products I-2 and MI-1 are functional ATP binding proteins with ATPase activity. *The Plant Cell* **14**(11): 2929-2939.

Tameling WI, Nooijen C, Ludwig N, Boter M, Slootweg E, Goverse A, Shirasu K, Joosten MH. 2010. RanGAP2 mediates nucleocytoplasmic partitioning of the NB-LRR immune receptor Rx in the Solanaceae, thereby dictating Rx function. *The Plant Cell* **22**(12): 4176-4194.

Tameling WI, Vossen JH, Albrecht M, Lengauer T, Berden JA, Haring MA, Cornelissen BJ, Takken FL. 2006. Mutations in the NB-ARC domain of I-2 that impair ATP hydrolysis cause autoactivation. *Plant Physiology* **140**(4): 1233-1245.

Tanabe T, Chamaillard M, Ogura Y, Zhu L, Qiu S, Masumoto J, Ghosh P, Moran A, Predergast MM, Tromp G, Williams CJ, Inohara N, Nunez G. 2004. Regulatory regions and critical residues of NOD2 involved in muramyl dipeptide recognition. *The EUROPEAN MOLECULAR BIOLOGY ORGANIZATION Journal* **23**(7): 1587-1597.

Tang W, Kim TW, Oses-Prieto JA, Sun Y, Deng Z, Zhu S, Wang R, Burlingame AL, Wang ZY. 2008. BSKs mediate signal transduction from the receptor kinase BRI1 in Arabidopsis. *Science* **321**(5888): 557-560.

Tang X, Frederick RD, Zhou J, Halterman DA, Jia Y, Martin GB. 1996. Initiation of Plant Disease Resistance by Physical Interaction of AvrPto and Pto Kinase. *Science* **274**(5295): 2060-2063.

Tang X, Xie M, Kim YJ, Zhou J, Klessig DF, Martin GB. 1999. Overexpression of *Pto* activates defense responses and confers broad resistance. *The Plant Cell* **11**(1): 15-29.

Tao Y, Yuan F, Leister RT, Ausubel FM, Katagiri F. 2000. Mutational analysis of the Arabidopsis nucleotide binding site-leucine-rich repeat resistance gene RPS2. *Plant Cell* **12**(12): 2541-2554.

Taylor SS, Knighton DR, Zheng J, Sowadski JM, Gibbs CS, Zoller MJ. 1993. A template for the protein kinase family. *Trends Biochemical Science* **18**(3): 84-89.

Tobias CM, Oldroyd GE, Chang JH, Staskawicz BJ. 1999. Plants expressing the Pto disease resistance gene confer resistance to recombinant PVX containing the avirulence gene AvrPto. *The Plant Journal : for cell and molecular biology* **17**(1): 41-50.

Tor M, Gordon P, Cuzick A, Eulgem T, Sinapidou E, Mert-Turk F, Can C, Dangl JL, Holub EB. 2002. Arabidopsis SGT1b is required for defense signaling conferred by several downy mildew resistance genes. *Plant Cell* **14**(5): 993-1003.

Tornero P, Merritt P, Sadanandom A, Shirasu K, Innes RW, Dangl JL. 2002. RAR1 and NDR1 contribute quantitatively to disease resistance in Arabidopsis, and their relative contributions are dependent on the R gene assayed. *Plant Cell* **14**(5): 1005-1015.

Torres MA, Dangl JL. 2005. Functions of the respiratory burst oxidase in biotic interactions, abiotic stress and development. *Current Opinion in Plant Biology* **8**(4): 397-403.

Torres MA, Dangl JL, Jones JD. 2002. Arabidopsis gp91phox homologues AtrbohD and AtrbohF are required for accumulation of reactive oxygen intermediates in the plant defense response. *Proceedings of the National Academy of Sciences of the United States of America* **99**(1): 517-522.

Tsuda K, Sato M, Glazebrook J, Cohen JD, Katagiri F. 2008. Interplay between MAMP-triggered and SA-mediated defense responses. *The Plant Journal : for cell and molecular biology* **53**(5): 763-775.

Underhill DM, Ozinsky A. 2002. Toll-like receptors: key mediators of microbe detection. *Current Opinion Immunology* **14**(1): 103-110.

Van der Biezen EA, Jones JD. 1998. Plant disease-resistance proteins and the gene-for-gene concept. *Trends Biochemical Science* **23**(12): 454-456.

van der Hoorn RA, Kamoun S. 2008. From Guard to Decoy: a new model for perception of plant pathogen effectors. *The Plant Cell* **20**(8): 2009-2017.

van Doorn WG, Woltering EJ. 2005. Many ways to exit? Cell death categories in plants. *Trends in Plant Science* **10**(3): 117-122.

Veronese P, Nakagami H, Bluhm B, Abuqamar S, Chen X, Salmeron J, Dietrich RA, Hirt H, Mengiste T. 2006. The membrane-anchored BOTRYTIS-INDUCED KINASE1 plays distinct roles in Arabidopsis resistance to necrotrophic and biotrophic pathogens. *The Plant Cell* **18**(1): 257-273.

Wan J, Zhang XC, Neece D, Ramonell KM, Clough S, Kim SY, Stacey MG, Stacey G. 2008a. A LysM receptor-like kinase plays a critical role in chitin signaling and fungal resistance in Arabidopsis. *The Plant Cell* **20**(2): 471-481.

Wan J, Zhang XC, Stacey G. 2008b. Chitin signaling and plant disease resistance. *Plant Signaling & Behavior* **3**(10): 831-833.

Wan JR, Tanaka K, Zhang XC, Son GH, Brechenmacher L, Tran HNN, Stacey G. 2012. LYK4, a Lysin Motif Receptor-Like Kinase, Is Important for Chitin Signaling and Plant Innate Immunity in Arabidopsis. *Plant Physiology* **160**(1): 396-406.

Wang D, Pajerowska-Mukhtar K, Culler AH, Dong X. 2007. Salicylic acid inhibits pathogen growth in plants through repression of the auxin signaling pathway. *Current Biology* **17**(20): 1784-1790.

Wang G, Ellendorff U, Kemp B, Mansfield JW, Forsyth A, Mitchell K, Bastas K, Liu CM, Woods-Tor A, Zipfel C, de Wit PJ, Jones JD, Tor M, Thomma BP. 2008. A genome-wide functional investigation into the roles of receptor-like proteins in *Arabidopsis*. *Plant Physiology* **147**(2): 503-517.

Wang W, Vinocur B, Shoseyov O, Altman A. 2004. Role of plant heat-shock proteins and molecular chaperones in the abiotic stress response. *Trends Plant Sci* **9**(5): 244-252.

Warren RF, Henk A, Mowery P, Holub E, Innes RW. 1998. A mutation within the leucine-rich repeat domain of the *Arabidopsis* disease resistance gene *RPS5* partially suppresses multiple bacterial and downy mildew resistance genes. *The Plant Cell* **10**(9): 1439-1452.

Weaver ML, Swiderski MR, Li Y, Jones JD. 2006. The *Arabidopsis thaliana* TIR-NB-LRR R-protein, RPP1A; protein localization and constitutive activation of defence by truncated alleles in tobacco and *Arabidopsis*. *The Plant Journal : for cell and molecular biology* **47**(6): 829-840.

Wellings CR, Mcintosh RA. 1990. Puccinia-Striiformis F Sp Tritici in Australasia - Pathogenic Changes during the 1st 10 Years. *Plant Pathology* **39**(2): 316-325.

Williams SJ, Sohn KH, Wan L, Bernoux M, Sarris PF, Segonzac C, Ve T, Ma Y, Saucet SB, Ericsson DJ, Casey LW, Lonhienne T, Winzor DJ, Zhang X, Coerdt A, Parker JE, Dodds PN, Kobe B, Jones JD. 2014. Structural basis for assembly and function of a heterodimeric plant immune receptor. *Science* **344**(6181): 299-303.

Willmann R, Lajunen HM, Erbs G, Newman MA, Kolb D, Tsuda K, Katagiri F, Fliegmann J, Bono JJ, Cullimore JV, Jehle AK, Gotz F, Kulik A, Molinaro A, Lipka V, Gust AA, Nurnberger T. 2011. Arabidopsis lysin-motif proteins LYM1 LYM3 CERK1 mediate bacterial peptidoglycan sensing and immunity to bacterial infection. *Proceedings of the National Academy of Sciences of the United States of America* **108**(49): 19824-19829.

Wirthmueller L, Maqbool A, Banfield MJ. 2013. On the front line: structural insights into plant-pathogen interactions. *Nature Reviews Microbiology* **11**(11): 761-776.

Wu AJ, Andriotis VM, Durrant MC, Rathjen JP. 2004. A patch of surface-exposed residues mediates negative regulation of immune signaling by tomato Pto kinase. *The Plant Cell* **16**(10): 2809-2821.

Wulf J, Pascuzzi PE, Fahmy A, Martin GB, Nicholson LK. 2004. The solution structure of type III effector protein AvrPto reveals conformational and dynamic features important for plant pathogenesis. *Structure* **12**(7): 1257-1268.

Wulff BBH, Horvath DM, Ward ER. 2011. Improving immunity in crops: new tactics in an old game. *Current Opinion in Plant Biology* **14**(4): 468-476.

Xiang T, Zong N, Zou Y, Wu Y, Zhang J, Xing W, Li Y, Tang X, Zhu L, Chai J, Zhou JM. 2008. *Pseudomonas syringae* effector AvrPto blocks innate immunity by targeting receptor kinases. *Current Biology* **18**(1): 74-80.

Xiao F, Lu M, Li J, Zhao T, Yi SY, Thara VK, Tang X, Zhou JM. 2003. *Pto* mutants differentially activate Prf-dependent, avrPto-independent resistance and gene-for-gene resistance. *Plant Physiology* **131**(3): 1239-1249.

Xing W, Zou Y, Liu Q, Liu J, Luo X, Huang Q, Chen S, Zhu L, Bi R, Hao Q, Wu JW, Zhou JM, Chai J. 2007. The structural basis for activation of plant immunity by bacterial effector protein AvrPto. *Nature* **449**(7159): 243-247.

Yamaguchi Y, Pearce G, Ryan CA. 2006. The cell surface leucine-rich repeat receptor for AtPep1, an endogenous peptide elicitor in Arabidopsis, is functional in transgenic tobacco cells. *Proceedings of the National Academy of Sciences of the United States of America* **103**(26): 10104-10109.

Yasuda M, Ishikawa A, Jikumaru Y, Seki M, Umezawa T, Asami T, Maruyama-Nakashita A, Kudo T, Shinozaki K, Yoshida S, Nakashita H. 2008. Antagonistic interaction between systemic acquired resistance and the abscisic acid-mediated abiotic stress response in Arabidopsis. *The Plant Cell* **20**(6): 1678-1692.

Zeng L, Velasquez AC, Munkvold KR, Zhang J, Martin GB. 2012. A tomato LysM receptor-like kinase promotes immunity and its kinase activity is inhibited by AvrPtoB. *The Plant Journal : for cell and molecular biology* **69**(1): 92-103.

Zeng W, He SY. 2010. A prominent role of the flagellin receptor FLAGELLIN-SENSING2 in mediating stomatal response to Pseudomonas syringae pv tomato DC3000 in Arabidopsis. *Plant Physiology* **153**(3): 1188-1198.

Zeng W, Melotto M, He SY. 2010. Plant stomata: a checkpoint of host immunity and pathogen virulence. *Current Opinion in Biotechnology* **21**(5): 599-603.

Zhang J, Li W, Xiang T, Liu Z, Laluk K, Ding X, Zou Y, Gao M, Zhang X, Chen S, Mengiste T, Zhang Y, Zhou JM. 2010. Receptor-like cytoplasmic kinases integrate signaling from multiple plant immune receptors and are targeted by a Pseudomonas syringae effector. *Cell Host & Microbe* **7**(4): 290-301.

Zhang L, Kars I, Essenstam B, Liebrand TW, Wagemakers L, Elberse J, Tagkalaki P, Tjoitang D, van den Ackerveken G, van Kan JA. 2014. Fungal endopolygalacturonases are recognized as microbe-associated molecular patterns by the arabidopsis receptor-like protein RESPONSIVENESS TO BOTRYTIS POLYGALACTURONASES1. *Plant Physiology* **164**(1): 352-364.

Zhang LS, Kars I, Essenstam B, Liebrand TWH, Wagemakers L, Elberse J, Tagkalaki P, Tjoitang D, van den Ackerveken G, van Kan JAL. 2014. Fungal Endopolygalacturonases Are Recognized as Microbe-Associated Molecular Patterns by the Arabidopsis Receptor-Like Protein RESPONSIVENESS TO BOTRYTIS POLYGALACTURONASES1. *Plant Physiology* **164**(1): 352-364.

Zhang M, Kadota Y, Prodromou C, Shirasu K, Pearl LH. 2010. Structural basis for assembly of Hsp90-Sgt1-CHORD protein complexes: implications for chaperoning of NLR innate immunity receptors. *Molecular Cell* **39**(2): 269-281.

Zhang W, Fraiture M, Kolb D, Loffelhardt B, Desaki Y, Boutrot FF, Tor M, Zipfel C, Gust AA, Brunner F. 2013. Arabidopsis receptor-like protein30 and receptor-like kinase suppressor of BIR1-1/EVERSHED mediate innate immunity to necrotrophic fungi. *The Plant Cell* **25**(10): 4227-4241.

Zhang X, Dai Y, Xiong Y, DeFraia C, Li J, Dong X, Mou Z. 2007. Overexpression of Arabidopsis MAP kinase kinase 7 leads to activation of plant basal and systemic acquired resistance. *The Plant Journal : for cell and molecular biology* **52**(6): 1066-1079.

Zheng Z, Qamar SA, Chen Z, Mengiste T. 2006. Arabidopsis WRKY33 transcription factor is required for resistance to necrotrophic fungal pathogens. *The Plant Journal : for cell and molecular biology* **48**(4): 592-605.

Zhou J, Loh YT, Bressan RA, Martin GB. 1995. The tomato gene *Pti1* encodes a serine/threonine kinase that is phosphorylated by Pto and is involved in the hypersensitive response. *Cell* **83**(6): 925-935.

Zhu Z, Xu F, Zhang Y, Cheng YT, Wiermer M, Li X. 2010. Arabidopsis resistance protein SNC1 activates immune responses through association with a transcriptional corepressor. *Proceedings of the National Academy of Sciences of the United States of America* **107**(31): 13960-13965.

Zipfel C. 2009. Early molecular events in PAMP-triggered immunity. *Current Opinion in Immunology* **12**(4): 414-420.

Zipfel C. 2014. Plant pattern-recognition receptors. *Trends in Immunology* **35**(7): 345-351.

Zipfel C, Kunze G, Chinchilla D, Caniard A, Jones JD, Boller T, Felix G. 2006. Perception of the bacterial PAMP EF-Tu by the receptor EFR restricts Agrobacterium-mediated transformation. *Cell* **125**(4): 749-760.

Zipfel C, Robatzek S, Navarro L, Oakeley EJ, Jones JD, Felix G, Boller T. 2004. Bacterial disease resistance in *Arabidopsis* through flagellin perception. *Nature* **428**(6984): 764-767.

Attachments

Attachment 1

Table containing all proteins with their corresponding unique peptides identified by LC-MS of proteins isolated from *Nicotiana benthamiana* that transiently expressed either NbBAK1-FLAG (control -), NbBAK1-GFP (BAK1) or NbBAK1-5-GFP (BAK1-GFP) treated for ten minutes with sterile MQ-water or 100 nM csp22 peptide by vacuum infiltration.[3]

annotated as	Accession Number	Unique peptides				
		control	BAK1	BAK1 + csp22	BAK1-5	BAK1-5 + csp22
NbBAK1	NICBE_048965.1_TGAC (+1)	30	163	163	152	163
NbBIR2b	NICBE_138628.1_TGAC	5	122	123	36	60
NbSERK1	NICBE_063035.1_TGAC (+4)	2	8	9	7	9
NbBIR1	NbS00052609g0002.1_SGN	0	44	56	41	56
NbBIR2a	NICBE_309719.1_TGAC	0	26	28	6	11
NbCSPRC2	**NICBE_271375.1_TGAC (+1)**	**0**	**2**	**6**	**1**	**4**
NbCSPRC1	**NbS00035240g0005.1_SGN**	**0**	**1**	**6**	**1**	**4**
GFP_TAG enhanced green fluorescent protein, Gateway binary vector pK7WGF2	Vector_pK7WGF2	6	76	78	72	89
sp_Q8GHE2_Q8GHE2_AZOVI_Green_fluorescence_protein.	cont186	0	9	9	6	10
Tubulin alpha chain len=507 E=0.0 (blastp), pfam_domain=Tubulin Tubulin/FtsZ family, GTPase domain E=6.8e-70 score=235.1	NICBE_021799.1_TGAC (+1)	8	33	30	27	28
Calcium binding protein Calnexin	NbS00004679g0009.1_SGN	0	41	38	21	38

Luminal-binding protein 5 len=727 E=0.0 (blastp), pfam_domain=HSP70 Hsp70 protein E=3.7e-267 score=887.0	NICBE_009952.1_TGAC	0	13	12	11	12
Subtilisin protease (The same sequence as NICBE_198665.1 in TGAC db)	NbS00016367g0001.1_SGN	15	13	6	16	18
ADP,ATP carrier protein, mitochondrial len=483 E=0.0 (blastp), pfam_domain=Mito_carr Mitochondrial carrier protein E=1.1e-71 score=236.4	NICBE_374223.1_TGAC (+3)	0	13	12	11	18
78 kDa glucose-regulated protein len=629 E=0.0 (blastp), pfam_domain=HSP70 Hsp70 protein E=1.9e-281 score=934.2	NICBE_307468.2_TGAC (+2)	0	14	23	12	25
Luminal-binding protein 4 len=666 E=0.0 (blastp), pfam_domain=HSP70 Hsp70 protein E=1.1e-269 score=895.3	NICBE_362411.1_TGAC	0	10	11	11	16
5 epi aristolochene synthase 2	NbS00055581g0001.1_SGN	0	25	23	8	18
Cell division protein FtsZ homolog 2-2, chloroplastic len=468 E=0.0 (blastp), pfam_domain=Tubulin Tubulin/FtsZ family, GTPase domain E=3.7e-35 score=121.6	NICBE_231362.1_TGAC (+1)	2	20	22	12	12
UDP-glucose:glycoprotein glucosyltransferase len=1644 E=0.0 (blastp),	NICBE_234796.1_TGAC	0	20	22	6	5
Histone deacetylase 14 len=466 E=1e-164 (blastp), pfam_domain=Hist_deacetyl Histone deacetylase domain E=6.5e-85 score=285.0	NICBE_096164.1_TGAC	9	15	11	12	7
Receptor kinase RLK	NbS00021170g0013.1_SGN	0	10	11	4	2
Cysteine desulfurase 1, mitochondrial len=409 E=0.0 (blastp), pfam_domain=Aminotran_5 Aminotransferase class-V E=7.6e-89 score=297.9	NICBE_002939.1_TGAC (+1)	2	12	14	11	11
Heat shock cognate 70 kDa protein 2 len=417 E=0.0 (blastp), pfam_domain=HSP70 Hsp70 protein E=8.9e-202 score=671.0	NICBE_129182.1_TGAC	0	7	9	14	10
Tubulin beta 1 chain	NbS00056603g0002.1_SGN	2	9	7	7	8
Subtilisin protease (The same sequence as NICBE_126600.1 in TGAC db)	NbS00009728g0003.1_SGN	6	7	2	7	9
Calnexin homolog 1 len=492 E=0.0 (blastp), pfam_domain=Calreticulin Calreticulin family E=4.7e-116 score=387.3	NICBE_276058.1_TGAC	0	11	8	9	10
CASB_BOVIN_BETA_CASEIN_PRECURSOR_-_BOS_TAURUS_(BOVINE).	cont21	3	10	0	3	2
DnaJ protein homolog len=420 E=0.0 (blastp), pfam_domain=DnaJ DnaJ domain E=3.2e-25 score=87.5	NICBE_201478.1_TGAC	0	5	9	6	7
Premnaspirodiene oxygenase len=472 E=8e-177 (blastp), pfam_domain=p450 Cytochrome P450 E=2.8e-96 score=322.7	NICBE_256456.1_TGAC (+1)	0	11	13	0	2
Tubulin beta-1 chain len=447 E=0.0 (blastp), pfam_domain=Tubulin Tubulin/FtsZ family, GTPase domain E=9.8e-72 score=241.1	NICBE_319602.1_TGAC	1	6	7	3	7
Puromycin-sensitive aminopeptidase len=876 E=0.0 (blastp), pfam_domain=Peptidase_M1 Peptidase family M1 E=8.2e-136 score=453.0	NICBE_198526.1_TGAC	0	7	5	8	6
cytochrome P450	NbS00006716g0007.1_SGN	0	10	12	8	8
Glucose-1-phosphate adenylyltransferase large subunit 3, chloroplastic/amyloplastic len=520 E=0.0 (blastp),	NICBE_399345.1_TGAC	3	8	7	5	5
Proline-rich receptor-like protein kinase PERK10 len=634 E=8e-49 (blastp), pfam_domain=Pkinase Protein kinase domain E=1.8e-43 score=148.5	NICBE_162664.1_TGAC	0	9	7	7	4
Calcium binding protein Calnexin	NbS00025205g0024.1_SGN	0	10	7	5	6

Isoflavone 2'-hydroxylase len=511 E=5e-131 (blastp), pfam_domain=p450 Cytochrome P450 E=3.5e-94 score=315.8	NICBE_376221.1_TGAC (+1)	0	7	7	7	7
Cathepsin B cysteine proteinase 5	NbS00025385g0005.1_SGN	0	11	9	2	6
gi_229552_prf__754920A_albumin_[Bos_primigenius_taurus]	cont15	4	1	2	3	4
26S protease regulatory subunit 7 homolog A len=482 E=0.0 (blastp),	NICBE_287309.1_TGAC	0	10	9	5	6
F box protein PP2 B1	NbS00010457g0003.1_SGN	0	13	11	2	3
(The same sequence as NICBE_062837.1 in TGAC db)	NbS00004447g0101.1_SGN	0	6	9	1	5
Tubulin beta-5 chain len=438 E=0.0 (blastp), pfam_domain=Tubulin Tubulin/FtsZ family, GTPase domain E=7.3e-72 score=241.5	NICBE_087279.1_TGAC (+1)	1	4	5	4	6
Sieve element occluding protein 3 (The same sequence as NICBE_075244.1 in TGAC db)	NbS00005491g0018.1_SGN	5	0	1	7	4
CAS2_BOVIN_ALPHA-S2_CASEIN_PRECURSOR_-_BOS_TAURUS_(BOVINE).	cont20	2	11	0	1	0
PTI1-like tyrosine-protein kinase 3 len=584 E=8e-177 (blastp), pfam_domain=Pkinase_Tyr Protein tyrosine kinase E=4.4e-46 score=156.9	NICBE_253622.1_TGAC (+1)	0	8	4	5	6
Diacylglycerol kinase 7 (The same sequence as NICBE_115113.1 in TGAC db)	NbS00008692g0009.1_SGN	0	7	6	5	10
Ribulose bisphosphate carboxylase large chain	NbS00034416g0005.1_SGN	2	6	6	4	5
Glutamyl-tRNA(Gln) amidotransferase subunit A, chloroplastic/mitochondrial len=534 E=0.0 (blastp), pfam_domain=Amidase Amidase E=1.3e-140 score=468.9	NICBE_169742.1_TGAC (+1)	0	8	5	7	6
Subtilisin protease (The same sequence as NICBE_198666.1 in TGAC db)	NbS00016367g0002.1_SGN	2	5	2	4	6
S adenosyl L methionine dependent methyltransferases (The same sequence as NICBE_040365.1 in TGAC db)	NbS00002899g0003.1_SGN	0	4	2	9	8
No hits found in SwissProt (blastp), pfam_domain=DUF642 Protein of unknown function, DUF642 E=2.4e-162 score=538.9	NICBE_120003.1_TGAC	1	4	6	4	4
Cytochrome P450	NbC25673618g0001.1_SGN	0	7	9	1	1
Aspartic proteinase nepenthesin-2 len=457 E=7e-37 (blastp), pfam_domain=Asp Eukaryotic aspartyl protease E=2.4e-22 score=79.5	NICBE_147615.1_TGAC	0	6	3	4	9
Calreticulin-3 len=423 E=1e-179 (blastp), pfam_domain=Calreticulin Calreticulin family E=1.2e-107 score=359.6	NICBE_002915.1_TGAC	0	6	2	10	4
ABC transporter B family member 11 len=1352 E=0.0 (blastp), pfam_domain=ABC_membrane ABC transporter transmembrane region E=4.2e-107 score=357.5	NICBE_232772.1_TGAC	0	8	3	2	3
CASK_BOVIN_KAPPA_CASEIN_PRECURSOR_-_BOS_TAURUS_(BOVINE).	cont22	3	6	1	5	1
Hydroxycinnamoyl-Coenzyme A shikimate/quinate hydroxycinnamoyltransferase len=488 E=7e-13 (blastp),	NICBE_186668.1_TGAC (+1)	0	2	3	1	4
Auxin transport protein BIG	NbS00009154g0017.1_SGN	0	6	3	1	0

CBL-interacting serine/threonine-protein kinase 23 len=454 E=0.0 (blastp), pfam_domain=Pkinase Protein kinase domain E=2.4e-76 score=256.2	NICBE_153230.1_TGAC (+2)	0	5	5	2	1
ABC transporter C family member 2 len=1797 E=0.0 (blastp), pfam_domain=ABC_membrane ABC transporter transmembrane region E=5.9e-70 score=235.6	NICBE_342595.1_TGAC (+1)	0	4	8	0	4
ABC transporter C family member 14 len=1504 E=0.0 (blastp), pfam_domain=ABC_membrane ABC transporter transmembrane region E=6.5e-55 score=186.3	NICBE_284760.1_TGAC (+2)	0	3	5	1	5
Glucose-1-phosphate adenylyltransferase small subunit, chloroplastic/amyloplastic len=520 E=0.0 (blastp),	NICBE_062133.1_TGAC (+2)	1	2	2	3	5
Histone deacetylase 5 len=1154 E=0.0 (blastp), pfam_domain=Hist_deacetyl Histone deacetylase domain E=1.1e-95 score=320.4	NICBE_186109.1_TGAC (+1)	2	1	2	5	5
3-isopropylmalate dehydrogenase 2, chloroplastic len=405 E=0.0 (blastp),	NICBE_281987.1_TGAC (+1)	0	3	4	2	1
Calnexin homolog 1 len=539 E=0.0 (blastp), pfam_domain=Calreticulin Calreticulin family E=8.1e-140 score=465.5	NICBE_004710.1_TGAC (+1)	0	4	2	3	2
Proteasome activator subunit 4	NbS00037122g0006.1_SGN	0	6	7	0	0
Malate dehydrogenase [NADP], chloroplastic len=440 E=0.0 (blastp),	NICBE_251983.1_TGAC (+3)	2	3	2	4	4
Chaperone protein DnaJ len=491 E=7e-109 (blastp), pfam_domain=DnaJ_C DnaJ C terminal domain E=7.2e-28 score=96.2	NICBE_265694.1_TGAC (+1)	0	3	4	4	6
Dolichyl-diphosphooligosaccharide--protein glycosyltransferase 48 kDa subunit len=663 E=8e-106 (blastp),	NICBE_284653.1_TGAC (+1)	0	7	3	1	3
Methionine S-methyltransferase len=353 E=2e-103 (blastp), pfam_domain=Aminotran_1_2 Aminotransferase class I and II E=3e-11 score=42.7	NICBE_365772.1_TGAC	0	1	1	6	2
Probable rhamnose biosynthetic enzyme 1 len=674 E=0.0 (blastp),	NICBE_334461.1_TGAC (+1)	0	1	2	1	4
Dihydrolipoyllysine-residue acetyltransferase component of pyruvate dehydrogenase complex len=499 E=2e-51 (blastp),	NICBE_285076.1_TGAC (+1)	4	3	2	3	2
Cell division protein FtsZ homolog 2-1, chloroplastic len=478 E=0.0 (blastp), pfam_domain=Tubulin Tubulin/FtsZ family, GTPase domain E=3e-34 score=118.6	NICBE_170179.1_TGAC	0	6	5	0	2
Chaperone protein DnaJ len=525 E=1e-106 (blastp), pfam_domain=DnaJ_C DnaJ C terminal domain E=9.3e-29 score=99.0	NICBE_159486.1_TGAC	0	2	4	4	1
Protein TOC75-3, chloroplastic len=810 E=0.0 (blastp), pfam_domain=Bac_surface_Ag Surface antigen E=6.7e-30 score=104.5	NICBE_392596.1_TGAC (+2)	0	1	2	2	6
Subtilisin protease	NbS00019460g0003.1_SGN	2	1	0	3	4
Phytosulfokine receptor 1 len=1017 E=0.0 (blastp), pfam_domain=Pkinase Protein kinase domain E=3.8e-46 score=157.2	NICBE_247532.1_TGAC (+1)	0	3	3	2	3
Receptor protein kinase (The same sequence as NICBE_103863.1 in TGAC db)	NbS00007578g0028.1_SGN (+1)	0	1	1	3	2
26S protease regulatory subunit 8 homolog A len=417 E=0.0 (blastp),	NICBE_417606.1_TGAC	0	4	3	1	0
Uncharacterized aarF domain containing protein kinase chloroplastic (The same sequence as NICBE_235177.1 in TGAC db)	NbS00020204g0014.1_SGN	0	3	3	1	2
C2 domain containing protein	NbS00047459g0007.1_SGN	0	3	3	0	1

Mitochondrial carnitine/acylcarnitine carrier-like protein len=335 E=4e-119 (blastp),	NICBE_365272.1_TGAC (+1)	0	2	1	1	4
Phospholipase D alpha 1 len=832 E=0.0 (blastp), pfam_domain=PLD_C Phospholipase D C terminal E=4.9e-32 score=109.1	NICBE_192899.1_TGAC (+1)	0	2	2	3	0
Actin	NbS00041237g0007.1_SGN	0	1	1	1	4
Phospholipase D beta 1 len=835 E=0.0 (blastp), pfam_domain=PLD_C Phospholipase D C terminal E=3.9e-31 score=106.2	NICBE_065700.1_TGAC (+3)	0	3	3	1	1
Presequence protease 1, chloroplastic/mitochondrial len=1072 E=0.0 (blastp), pfam_domain=M16C_assoc Peptidase M16C associated E=2e-67 score=226.5	NICBE_142969.1_TGAC (+1)	0	6	1	0	2
O methyltransferase (The same sequence as NICBE_049372.1 in TGAC db)	NbS00003479g0020.1_SGN	0	4	3	0	2
Serine/threonine-protein kinase PBS1 len=411 E=4e-141 (blastp), pfam_domain=Pkinase Protein kinase domain E=3.9e-54 score=183.4	NICBE_424866.1_TGAC (+1)	0	1	2	2	0
Tubulin beta 1 chain	NbS00019798g0005.1_SGN	0	4	3	0	0
Dihydrolipoyllysine-residue succinyltransferase component of 2-oxoglutarate dehydrogenase complex 1, mitochondrial len=471 E=0.0 (blastp),	NICBE_156418.1_TGAC (+1)	2	1	0	0	0
Translational activator gcn1	NbS00008510g0009.1_SGN	0	4	1	0	1
Sister chromatid cohesion protein PDS5 B B	NbS00015555g0001.1_SGN	0	5	0	2	0
Coatomer subunit beta-1 len=563 E=0.0 (blastp), pfam_domain=Coatamer_beta_C Coatamer beta C-terminal region E=2.1e-90 score=302.2	NICBE_298878.1_TGAC (+1)	0	2	3	0	1
Probable protein disulfide-isomerase A6 len=359 E=1e-160 (blastp), pfam_domain=Thioredoxin Thioredoxin E=2.3e-71 score=235.9	NICBE_207600.1_TGAC	0	4	3	0	0
Photosystem II CP47 chlorophyll apoprotein	NbS00021832g0023.1_SGN	0	2	3	0	2
Proline rich receptor protein kinase PERK1 (The same sequence as NICBE_213949.1 in TGAC db)	NbS00017789g0029.1_SGN	0	4	2	0	1
Probable 26S proteasome non-ATPase regulatory subunit 3 len=488 E=0.0 (blastp),	NICBE_198688.1_TGAC (+1)	0	1	3	0	1
Cytochrome P450	NbC24805505g0002.1_SGN	0	3	4	0	0
Uncharacterized oxidoreductase ygbJ len=1382 E=3e-53 (blastp), pfam_domain=F_bP_aldolase Fructose-bisphosphate aldolase class-II E=1.2e-87 score=293.5	NICBE_367990.1_TGAC (+1)	0	1	2	0	3
Aldehyde dehydrogenase expressed (The same sequence as NICBE_389073.1 in TGAC db)	NbS00047628g0009.1_SGN	0	0	1	3	2
NADP-dependent glyceraldehyde-3-phosphate dehydrogenase len=496 E=0.0 (blastp),	NICBE_047708.1_TGAC (+1)	0	0	5	0	1
BURP domain-containing protein 3 len=434 E=1e-51 (blastp), pfam_domain=BURP BURP domain E=7.7e-74 score=247.3	NICBE_011791.1_TGAC (+1)	1	1	3	1	1
3-ketoacyl-CoA thiolase 2, peroxisomal len=528 E=0.0 (blastp), pfam_domain=Thiolase_N Thiolase, N-terminal domain E=3.1e-79 score=265.5	NICBE_083849.1_TGAC (+1)	0	4	1	1	1
Stomatin-like protein 2 len=421 E=5e-90 (blastp), pfam_domain=Band_7 SPFH domain / Band 7 family E=6.3e-30 score=104.2	NICBE_303626.1_TGAC	0	0	0	3	1

Pyruvate kinase, cytosolic isozyme len=528 E=0.0 (blastp), pfam_domain=PK Pyruvate kinase, barrel domain E=9.8e-157 score=520.8	NICBE_002849.1_TGAC (+1)	0	2	3	0	0
Premnaspirodiene oxygenase len=364 E=3e-131 (blastp), pfam_domain=p450 Cytochrome P450 E=1.2e-79 score=267.9	NICBE_007240.1_TGAC (+1)	0	1	0	0	4
NADP-dependent malic enzyme len=636 E=0.0 (blastp), pfam_domain=Malic_M Malic enzyme, NAD binding domain E=3.4e-90 score=301.9	NICBE_297967.1_TGAC (+1)	0	0	3	0	2
Glyceraldehyde-3-phosphate dehydrogenase, cytosolic len=337 E=0.0 (blastp),	NICBE_167948.1_TGAC	0	1	2	3	0
Villin-2 len=950 E=0.0 (blastp), pfam_domain=Gelsolin Gelsolin repeat E=1.7e-78 score=258.1	NICBE_314436.1_TGAC	0	3	1	0	2
Heat shock 70 kDa protein 15 len=836 E=0.0 (blastp), pfam_domain=HSP70 Hsp70 protein E=5.1e-148 score=493.5	NICBE_282017.1_TGAC	0	1	0	1	3
Cullin-1 len=699 E=0.0 (blastp), pfam_domain=Cullin Cullin family E=4e-182 score=606.7	NICBE_368924.1_TGAC (+1)	0	1	4	0	0
Serine/threonine-protein kinase PBS1 len=403 E=3e-135 (blastp), pfam_domain=Pkinase Protein kinase domain E=6.2e-49 score=166.3	NICBE_345253.1_TGAC (+2)	0	2	0	5	0
E3 ubiquitin protein ligase KEG	NbS00023657g0017.1_SGN	0	1	2	0	0
mRNA turnover protein 4	NbC25881068g0003.1_SGN	0	0	0	4	1
14-3-3-like protein 16R len=316 E=1e-143 (blastp), pfam_domain=14-3-3 14-3-3 protein E=1.7e-115 score=383.9	NICBE_092857.1_TGAC (+8)	0	1	1	0	3
Phototropin-2 len=962 E=0.0 (blastp), pfam_domain=Pkinase Protein kinase domain E=5e-61 score=206.0	NICBE_349345.1_TGAC (+3)	0	1	3	1	0
50S ribosomal protein L19 1 chloroplastic (The same sequence as NICBE_325423.1 in TGAC db)	NbS00032684g0004.1_SGN	0	0	0	3	1
50S ribosomal protein L15 (The same sequence as NICBE_240170.1 in TGAC db)	NbS00020743g0011.1_SGN	0	0	0	2	1
Chaperone protein dnaJ (The same sequence as NICBE_091486.1 in TGAC db)	NbS00006769g0021.1_SGN	0	0	0	3	0
Subtilisin protease	NbS00054116g0012.1_SGN	3	0	0	0	0
Cell division protein FtsZ homolog 1, chloroplastic len=414 E=7e-157 (blastp), pfam_domain=Tubulin Tubulin/FtsZ family, GTPase domain E=1.9e-39 score=135.6	NICBE_295989.1_TGAC	0	3	0	0	0
Phosphate carrier protein, mitochondrial len=343 E=5e-49 (blastp), pfam_domain=Mito_carr Mitochondrial carrier protein E=1.8e-17 score=62.6	NICBE_139054.1_TGAC (+1)	0	1	0	0	2
Sec7 guanine nucleotide exchange factor	NbS00049277g0005.1_SGN	0	2	0	0	0
Glucan endo-1,3-beta-glucosidase, basic vacuolar isoform GLB len=540 E=0.0 (blastp),	NICBE_051963.1_TGAC (+1)	0	0	0	0	3
Glutamate decarboxylase len=495 E=0.0 (blastp), pfam_domain=Pyridoxal_deC Pyridoxal-dependent decarboxylase conserved domain E=9.5e-109 score=363.1	NICBE_266679.1_TGAC	0	0	0	0	3
DNA-directed RNA polymerase subunit beta len=214 E=9e-46 (blastp), pfam_domain=RNA_pol_Rpb2_6 RNA polymerase Rpb2, domain 6 E=8.9e-13 score=47.6	NICBE_265089.1_TGAC	0	2	0	1	0
Serine hydroxymethyltransferase 1 len=471 E=2e-173 (blastp), pfam_domain=SHMT Serine hydroxymethyltransferase E=3.9e-187 score=621.4	NICBE_152763.1_TGAC (+1)	0	2	1	2	2

Methionine s methyltransferase	NbS00040816g0010.1_SGN	4	10	6	15	14
DEAD-box ATP-dependent RNA helicase 42 len=1142 E=0.0 (blastp), pfam_domain=DEAD DEAD/DEAH box helicase E=1.2e-46 score=158.1	NICBE_121384.1_TGAC (+1)	0	0	0	3	7
Polyubiquitin (Fragment) len=305 E=1e-171 (blastp), pfam_domain=ubiquitin Ubiquitin family E=6.3e-136 score=441.7	NICBE_329062.1_TGAC	0	26	27	22	34
1 aminocyclopropane 1 carboxylate oxidase (The same sequence as NICBE_280936.1 in TGAC db)	NbS00025918g0006.1_SGN	0	4	3	1	0
Pleiotropic drug resistance protein 1	NbS00038421g0004.1_SGN (+1)	0	26	17	9	13
Proliferation-associated protein 2G4 len=379 E=2e-92 (blastp), pfam_domain=Peptidase_M24 Metallopeptidase family M24 E=2.6e-31 score=108.7	NICBE_416164.1_TGAC (+1)	0	3	1	0	0
60S ribosomal protein L26-1 len=146 E=4e-70 (blastp), pfam_domain=KOW KOW motif E=1.6e-10 score=39.9	NICBE_022973.1_TGAC (+1)	0	0	2	1	1
Aspartic proteinase nepenthesin-1 len=536 E=2e-43 (blastp), pfam_domain=Asp Eukaryotic aspartyl protease E=2e-15 score=56.7	NICBE_349639.1_TGAC (+1)	3	4	3	6	6
Glyoxysomal fatty acid beta oxidation multifunctional protein MFP a	NbS00017976g0006.1_SGN	0	0	0	0	3
Cell division protease ftsH 3	NbS00033465g0001.1_SGN	0	8	7	3	4
Auxin-binding protein ABP19a len=242 E=6e-76 (blastp), pfam_domain=Cupin_1 Cupin E=1.2e-22 score=79.7	NICBE_136581.1_TGAC (+1)	0	5	1	2	2
Nucleolin 2 len=686 E=2e-67 (blastp), pfam_domain=RRM_1 RNA recognition motif. (a.k.a. RRM, RBD, or RNP domain) E=3.7e-29 score=100.0	NICBE_168419.1_TGAC	0	2	3	0	0
Eukaryotic translation initiation factor 3 subunit B len=717 E=0.0 (blastp), pfam_domain=eIF2A Eukaryotic translation initiation factor eIF2A E=2.2e-76 score=255.8	NICBE_266107.1_TGAC (+3)	0	1	2	2	0
Alanine--tRNA ligase len=1041 E=0.0 (blastp), pfam_domain=tRNA-synt_2c tRNA synthetases class II (A) E=1.4e-222 score=739.7	NICBE_289218.1_TGAC	1	2	4	1	1
No hits found in SwissProt (blastp), pfam_domain=SR-25 Nuclear RNA-splicing-associated protein E=0.013 score=14.8	NICBE_413146.1_TGAC	1	2	0	0	0
Heat shock cognate 70 kDa protein 2 len=648 E=0.0 (blastp), pfam_domain=HSP70 Hsp70 protein E=7.7e-271 score=899.1	NICBE_361081.1_TGAC	1	12	11	12	19
ATP dependent Zn protease cell division protein FtsH	NbC25032573g0001.1_SGN	1	5	0	1	1
Protein CHUP1 chloroplastic (The same sequence as NICBE_304626.1 in TGAC db)	NbS00029380g0012.1_SGN	1	0	3	1	1
DEAD-box ATP-dependent RNA helicase 40 len=1315 E=0.0 (blastp), pfam_domain=DEAD DEAD/DEAH box helicase E=4.6e-49 score=166.0	NICBE_303585.1_TGAC (+1)	1	2	1	0	0
30S ribosomal protein S1, chloroplastic len=500 E=0.0 (blastp), pfam_domain=S1 S1 RNA binding domain E=1.3e-48 score=162.8	NICBE_341475.1_TGAC	2	3	3	4	7
Staphylococcal nuclease domain-containing protein 1 len=1020 E=7e-140 (blastp),	NICBE_059654.1_TGAC	1	15	7	3	5
26S proteasome non-ATPase regulatory subunit 2 1A len=900 E=0.0 (blastp), pfam_domain=PC_rep Proteasome/cyclosome repeat E=5.6e-25 score=86.0	NICBE_172900.1_TGAC	1	16	11	8	11
Delta-1-pyrroline-5-carboxylate synthase len=717 E=0.0 (blastp), pfam_domain=AA_kinase Amino acid kinase family E=5.5e-35 score=120.9	NICBE_256585.1_TGAC	1	5	14	8	4

Cell division cycle protein 48 homolog len=805 E=0.0 (blastp),	NICBE_349021.1_TGAC (+2)	1	6	11	3	8
Pleiotropic drug resistance protein 1 len=1413 E=0.0 (blastp), pfam_domain=ABC2_membrane ABC-2 type transporter E=2.2e-83 score=278.3	NICBE_136035.1_TGAC	2	4	6	4	5
Endoplasmin homolog len=812 E=3e-169 (blastp), pfam_domain=HSP90 Hsp90 protein E=8.7e-177 score=588.6	NICBE_008861.1_TGAC	2	5	7	4	3
Signal recognition particle protein SRP72	NbS00014259g0005.1_SGN	1	1	1	2	3
Biotin carboxylase 1, chloroplastic len=802 E=0.0 (blastp),	NICBE_147919.1_TGAC (+1)	2	7	11	8	11
L-ascorbate oxidase homolog len=704 E=3e-162 (blastp), pfam_domain=Cu-oxidase Multicopper oxidase E=3.2e-40 score=137.5	NICBE_327572.1_TGAC	4	0	2	6	5
RuBisCO large subunit-binding protein subunit beta, chloroplastic len=760 E=0.0 (blastp),	NICBE_002070.1_TGAC (+3)	1	1	2	0	3
D-3-phosphoglycerate dehydrogenase, chloroplastic len=599 E=0.0 (blastp),	NICBE_255774.1_TGAC (+3)	1	0	3	0	1
Tubulin beta-1 chain len=447 E=0.0 (blastp), pfam_domain=Tubulin Tubulin/FtsZ family, GTPase domain E=1.8e-71 score=240.3	NICBE_313142.1_TGAC	7	51	47	35	41
CAS1_BOVIN_ALPHA-S1_CASEIN_PRECURSOR_-_BOS_TAURUS_(BOVINE).	cont19	6	17	9	11	11
Glyceraldehyde 3 phosphate dehydrogenase B	NbS00029815g0004.1_SGN	4	20	20	14	16
26S protease regulatory subunit 6B homolog len=563 E=0.0 (blastp),	NICBE_268659.1_TGAC (+2)	1	11	12	14	10
Ribulose 1 5 bisphosphate carboxylase/oxygenase activase 1	NbS00009714g0011.1_SGN	1	11	11	12	11
DNA-damage-repair/toleration protein DRT100 len=365 E=2e-113 (blastp), pfam_domain=LRR_1 Leucine Rich Repeat E=7e-21 score=70.9	NICBE_399931.1_TGAC	3	8	7	15	11
Mannose-1-phosphate guanylyltransferase 1 len=361 E=0.0 (blastp),	NICBE_362172.1_TGAC	2	8	9	7	3
26S protease regulatory subunit S10B homolog B len=390 E=0.0 (blastp),	NICBE_351398.1_TGAC (+2)	1	6	8	3	6
Actin len=365 E=0.0 (blastp), pfam_domain=Actin Actin E=4e-150 score=499.5	NICBE_053462.1_TGAC (+1)	2	3	5	7	6
Rhodanese related sulfurtransferase (The same sequence as NICBE_299086.1 in TGAC db)	NbS00028552g0005.1_SGN	1	9	6	3	6
Isocitrate dehydrogenase [NADP] len=415 E=0.0 (blastp), pfam_domain=Iso_dh Isocitrate/isopropylmalate dehydrogenase E=4.1e-90 score=302.1	NICBE_042890.1_TGAC	1	6	8	2	4
26S proteasome non ATPase regulatory subunit 11	NbS00016436g0001.1_SGN (+1)	1	5	3	4	5
Serine--glyoxylate aminotransferase len=432 E=0.0 (blastp), pfam_domain=Aminotran_5 Aminotransferase class-V E=3.1e-32 score=111.6	NICBE_230315.2_TGAC (+2)	2	5	1	2	4
Fructose bisphosphate aldolase (The same sequence as NICBE_113095.1 in TGAC db)	NbS00008558g0004.1_SGN	2	3	2	4	5
UDP-glucose 6-dehydrogenase len=464 E=0.0 (blastp),	NICBE_010507.1_TGAC (+4)	1	3	5	0	1
Phosphoglycerate kinase, chloroplastic len=486 E=0.0 (blastp), pfam_domain=PGK Phosphoglycerate kinase E=1.8e-160 score=533.6	NICBE_091738.1_TGAC	1	2	1	0	3

Early fruit mRNA (The same sequence as NICBE_256285.1 in TGAC db)	NbS00022676g0014.1_SGN	1	2	1	0	1
Uncharacterized RNA pseudouridine synthase aq_1464 len=415 E=1e-33 (blastp),	NICBE_281882.1_TGAC	1	2	1	0	0
(The same sequence as NICBE_060391.1 in TGAC db)	NbS00004321g0109.1_SGN (+1)	1	6	3	4	5
Putative mitochondrial 2-oxoglutarate/malate carrier protein len=273 E=6e-58 (blastp),	NICBE_412941.1_TGAC (+1)	1	4	8	2	8
Serine/arginine-rich splicing factor RSZ22 len=285 E=2e-51 (blastp),	NICBE_143524.1_TGAC (+2)	1	2	1	2	3
Disease resistance response (The same sequence as NICBE_382720.1 in TGAC db)	NbS00045727g0001.1_SGN	1	2	2	4	2
Small heat shock protein C2 len=247 E=6e-10 (blastp), pfam_domain=HSP20 Hsp20/alpha crystallin family E=2.7e-13 score=49.5	NICBE_104588.1_TGAC	1	2	1	1	0
29 kDa ribonucleoprotein A, chloroplastic len=304 E=8e-121 (blastp),	NICBE_134078.1_TGAC (+2)	1	1	0	3	3
ATP-dependent Clp protease proteolytic subunit-related protein 3, chloroplastic len=418 E=3e-141 (blastp),	NICBE_184152.1_TGAC (+3)	1	3	1	1	2
60S ribosomal protein L21 protein	NbS00056343g0003.1_SGN	1	0	1	2	2
No hits found in SwissProt (blastp), pfam_domain=Rieske_2 Rieske-like [2Fe-2S] domain E=1.1e-20 score=73.1	NICBE_080531.1_TGAC (+1)	1	3	1	1	1
Oxygen-evolving enhancer protein 2-2, chloroplastic len=265 E=1e-153 (blastp),	NICBE_035651.1_TGAC (+3)	1	3	1	1	1
Transmembrane emp24 domain-containing protein A len=218 E=1e-21 (blastp),	NICBE_138070.1_TGAC (+1)	1	1	0	1	3
Glycine rich protein 2 (The same sequence as NICBE_258347.1 in TGAC db)	NbS00023063g0001.1_SGN	1	3	1	0	0
Ribulose bisphosphate carboxylase small chain 8B, chloroplastic len=159 E=7e-91 (blastp),	NICBE_352940.1_TGAC (+3)	2	3	4	2	2
rRNA biogenesis protein rrp5 len=1855 E=4e-112 (blastp), pfam_domain=S1 S1 RNA binding domain E=5.8e-72 score=237.6	NICBE_351986.1_TGAC (+1)	1	2	0	0	0
Glutamine synthetase, chloroplastic len=404 E=0.0 (blastp), pfam_domain=Gln-synt_C Glutamine synthetase, catalytic domain E=9.9e-62 score=208.2	NICBE_060321.1_TGAC (+3)	2	5	2	0	2
Photosystem II CP43 chlorophyll apoprotein len=158 E=1e-66 (blastp), pfam_domain=PSII Photosystem II protein E=1.9e-52 score=178.2	NICBE_123771.1_TGAC	1	0	2	0	2
Fructose 1 6 bisphosphatase class 1 (The same sequence as NICBE_081880.1 in TGAC db)	NbS00005953g0021.1_SGN	2	1	1	2	3
Uncharacterized protein ycf39 len=449 E=2e-93 (blastp), pfam_domain=NmrA NmrA-like family E=2e-24 score=86.0	NICBE_119443.1_TGAC (+1)	1	8	3	2	4
Alpha-glucan phosphorylase, H isozyme len=842 E=0.0 (blastp), pfam_domain=Phosphorylase Carbohydrate phosphorylase E=0 score=1132.5	NICBE_252898.1_TGAC (+1)	1	0	4	0	1
Histidine--tRNA ligase len=857 E=0.0 (blastp), pfam_domain=tRNA-synt_His Histidyl-tRNA synthetase E=1.6e-48 score=165.2	NICBE_397186.1_TGAC (+2)	1	1	4	0	1
Eukaryotic initiation factor 4A-15 len=458 E=0.0 (blastp), pfam_domain=DEAD DEAD/DEAH box helicase E=1.5e-40 score=138.3	NICBE_012093.1_TGAC	2	6	9	7	7
Translational activator gcn1	NbS00008510g0008.1_SGN	1	14	13	4	4

50S ribosomal protein L4, chloroplastic len=296 E=4e-153 (blastp), pfam_domain=Ribosomal_L4 Ribosomal protein L4/L1 family E=5.5e-54 score=182.3	NICBE_226009.1_TGAC	1	3	4	7	4
Histone deacetylase HDT1 len=301 E=1e-29 (blastp), pfam_domain=Daxx Daxx Family E=0.029 score=12.7	NICBE_141903.1_TGAC	1	2	1	0	3
No hits found in SwissProt (blastp), pfam_domain=DUF642 Protein of unknown function, DUF642 E=2.3e-145 score=483.1	NICBE_283707.1_TGAC (+3)	5	2	1	5	2
40S ribosomal protein S15 (The same sequence as NICBE_200898.1 in TGAC db)	NbS00046450g0014.1_SGN	1	0	1	4	3
H/ACA ribonucleoprotein complex subunit 1 protein 1	NbS00002940g0010.1_SGN (+3)	1	0	0	3	3
unknown protein	NbS00017375g0002.1_SGN	1	2	1	1	2
Chloroplast stem-loop binding protein of 41 kDa a, chloroplastic len=402 E=3e-171 (blastp),	NICBE_268212.1_TGAC (+1)	1	2	1	0	2
Subtilisin protease (The same sequence as NICBE_385290.1 in TGAC db)	NbS00046532g0005.1_SGN	1	3	1	6	2
Protein TIC 62, chloroplastic len=509 E=4e-12 (blastp), pfam_domain=NAD_binding_10 NADH(P)-binding E=2.9e-09 score=37.0	NICBE_373424.1_TGAC	1	2	3	3	0
Transketolase 1	NbS00008412g0009.1_SGN	1	3	2	0	4
Triosephosphate isomerase cytosolic (The same sequence as NICBE_141621.1 in TGAC db)	NbS00011031g0007.1_SGN	1	0	0	0	3
Elongation factor 1-beta 1 len=285 E=7e-80 (blastp), pfam_domain=EF1_GNE EF-1 guanine nucleotide exchange domain E=2.3e-31 score=107.2	NICBE_112194.1_TGAC (+1)	1	3	0	0	1
60S ribosomal protein L6	NbS00031098g0006.1_SGN	1	0	2	0	2
Coatomer alpha subunit protein	NbS00031319g0001.1_SGN	1	16	16	8	13
Monodehydroascorbate reductase NADH protein	NbS00032372g0009.1_SGN	1	2	2	0	2
Histone-lysine N-methyltransferase, H3 lysine-9 specific SUVH1 len=710 E=0.0 (blastp), pfam_domain=YDG_SRA YDG/SRA domain E=9.5e-57 score=190.5	NICBE_236417.1_TGAC (+1)	1	3	0	0	1
H/ACA ribonucleoprotein complex subunit 2-like protein len=175 E=2e-59 (blastp),	NICBE_312609.1_TGAC (+1)	1	0	1	3	3
Uncharacterized protein C16C10.8 len=312 E=4e-10 (blastp), pfam_domain=zf-LYAR LYAR-type C2HC zinc finger E=9.4e-14 score=50.7	NICBE_139823.1_TGAC (+1)	1	2	0	1	1
Ribosomal RNA large subunit methyltransferase J (The same sequence as NICBE_169513.1 in TGAC db)	NbS00013355g0004.1_SGN	1	0	0	0	2
ATP synthase subunit alpha, chloroplastic len=286 E=2e-74 (blastp),	NICBE_177665.1_TGAC (+1)	4	6	5	4	7
V-type proton ATPase subunit B 2 len=479 E=0.0 (blastp),	NICBE_088201.1_TGAC (+1)	3	7	8	6	8
Aquaporin 1 (The same sequence as NICBE_408907.1 in TGAC db)	NbS00054890g0003.1_SGN	2	2	2	3	4
Replication factor C subunit 3 len=409 E=2e-105 (blastp), pfam_domain=Rep_fac_C Replication factor C C-terminal domain E=1.1e-14 score=54.0	NICBE_128371.1_TGAC	2	1	2	2	3

Actin-7 len=641 E=0.0 (blastp), pfam_domain=Actin Actin E=4.9e-159 score=528.8	NICBE_128693.1_TGAC (+3)	2	6	8	7	9
Clathrin heavy chain 1 len=1749 E=0.0 (blastp), pfam_domain=Clathrin Region in Clathrin and VPS E=4.3e-191 score=626.0	NICBE_383105.1_TGAC (+1)	8	14	30	16	22
Glyceraldehyde-3-phosphate dehydrogenase, cytosolic len=337 E=0.0 (blastp),	NICBE_182820.1_TGAC	4	27	14	23	12
ATP synthase subunit beta, chloroplastic len=185 E=7e-81 (blastp),	NICBE_187671.1_TGAC (+1)	4	8	8	7	9
Heat shock 70 kDa protein 15 len=867 E=0.0 (blastp), pfam_domain=HSP70 Hsp70 protein E=1.1e-154 score=515.5	NICBE_391986.1_TGAC	2	9	6	11	14
Nbs00006907g0117.1_SGN	Nbs00006907g0117.1_SGN	2	11	16	13	14
S-adenosylmethionine synthase 2 len=460 E=0.0 (blastp),	NICBE_172027.1_TGAC (+3)	4	4	4	7	7
26S proteasome non-ATPase regulatory subunit 2 1A len=898 E=0.0 (blastp), pfam_domain=PC_rep Proteasome/cyclosome repeat E=2.3e-26 score=90.4	NICBE_166405.1_TGAC	2	8	8	3	4
Aminomethyltransferase, mitochondrial len=422 E=0.0 (blastp), pfam_domain=GCV_T Aminomethyltransferase folate-binding domain E=1.4e-66 score=223.7	NICBE_358374.1_TGAC (+2)	3	5	4	3	10
No hits found in SwissProt (blastp), pfam_domain=Thioredoxin_8 Thioredoxin-like E=0.0082 score=16.1	NICBE_356266.1_TGAC	3	4	4	1	2
COBW domain-containing protein 2 len=451 E=2e-61 (blastp), pfam_domain=cobW CobW/HypB/UreG, nucleotide-binding domain E=2.5e-54 score=183.2	NICBE_126990.1_TGAC	2	3	2	8	3
Signal peptide peptidase SppA type (The same sequence as NICBE_029938.1 in TGAC db)	Nbs00002109g0019.1_SGN	2	4	2	2	6
Eukaryotic translation initiation factor 3 subunit A len=958 E=0.0 (blastp), pfam_domain=PCI PCI domain E=2.7e-19 score=69.2	NICBE_387795.1_TGAC (+1)	2	5	3	2	3
ATP-citrate synthase beta chain protein 1 len=583 E=0.0 (blastp), pfam_domain=Citrate_synt Citrate synthase E=5.1e-20 score=71.4	NICBE_252166.1_TGAC (+2)	2	6	4	1	1
Malate dehydrogenase 2, mitochondrial len=395 E=2e-167 (blastp),	NICBE_023572.1_TGAC (+3)	2	4	2	0	6
Aquaporin PIP2-1 len=283 E=1e-133 (blastp), pfam_domain=MIP Major intrinsic protein E=2.5e-87 score=291.9	NICBE_207950.1_TGAC (+2)	2	2	1	3	3
Ribosomal L9 protein (The same sequence as NICBE_070385.1 in TGAC db)	Nbs00005152g0006.1_SGN	2	0	2	4	1
Eukaryotic translation initiation factor 6-2 len=245 E=1e-131 (blastp), pfam_domain=eIF-6 eIF-6 family E=5.8e-85 score=283.2	NICBE_406359.1_TGAC (+1)	2	1	2	2	2
2-Cys peroxiredoxin BAS1-like, chloroplastic len=298 E=1e-109 (blastp), pfam_domain=AhpC-TSA AhpC/TSA family E=4.1e-42 score=142.6	NICBE_256348.1_TGAC (+3)	2	4	2	0	3
Polyadenylate-binding protein 2 len=667 E=0.0 (blastp), pfam_domain=RRM_1 RNA recognition motif. (a.k.a. RRM, RBD, or RNP domain) E=3.3e-89 score=292.4	NICBE_065459.1_TGAC (+1)	2	0	2	3	2
Chlorophyll a-b binding protein 36, chloroplastic len=265 E=9e-152 (blastp), pfam_domain=Chloroa_b-bind Chlorophyll A-B binding protein E=7.9e-51 score=172.2	NICBE_005654.1_TGAC (+5)	2	3	1	1	1
50S ribosomal protein L9, chloroplastic len=194 E=2e-68 (blastp), pfam_domain=Ribosomal_L9_C Ribosomal protein L9, C-terminal domain E=1.3e-20 score=73.1	NICBE_117476.1_TGAC (+1)	2	0	0	4	1

H/ACA ribonucleoprotein complex subunit 2-like protein len=214 E=1e-60 (blastp),	NICBE_343209.1_TGAC (+1)	2	1	0	3	3
Malate dehydrogenase, glyoxysomal len=391 E=2e-179 (blastp),	NICBE_324750.1_TGAC (+2)	2	3	1	0	2
60S ribosomal protein L5 1	NbS00010892g0008.1_SGN	2	0	3	0	2
C-terminal binding protein AN len=632 E=0.0 (blastp),	NICBE_326115.1_TGAC (+1)	2	0	0	2	0
Delta-aminolevulinic acid dehydratase, chloroplastic len=367 E=0.0 (blastp),	NICBE_204651.1_TGAC (+1)	2	4	0	0	0
High mobility group B protein 1 (The same sequence as NICBE_291299.1 in TGAC db)	NbS00027305g0007.1_SGN	2	6	3	3	3
Genomic DNA chromosome 3 TAC clone K15M2 (The same sequence as NICBE_384309.1 in TGAC db)	NbS00046219g0002.1_SGN	2	0	0	1	0
Histone-lysine N-methyltransferase, H3 lysine-9 specific SUVH1 len=756 E=0.0 (blastp), pfam_domain=YDG_SRA YDG/SRA domain E=2.5e-70 score=234.6	NICBE_066109.1_TGAC (+1)	2	0	2	6	3
Pinin len=424 E=1e-07 (blastp), pfam_domain=Pinin_SDK_memA pinin/SDK/memA/ protein conserved region E=1.7e-23 score=82.5	NICBE_098178.1_TGAC (+1)	2	0	1	1	3
40S ribosomal protein S10	NbS00033943g0010.1_SGN (+6)	2	1	1	3	2
DNA gyrase subunit A, chloroplastic/mitochondrial len=949 E=0.0 (blastp),	NICBE_010625.1_TGAC (+1)	3	2	3	5	1
Uncharacterized protein At3g06530 len=1939 E=0.0 (blastp), pfam_domain=BP28CT BP28CT (NUC211) domain E=9.5e-42 score=142.1	NICBE_102434.1_TGAC	2	0	1	0	3
Nucleolar protein 5 (The same sequence as NICBE_404600.1 in TGAC db)	NbS00053191g0001.1_SGN	2	1	1	4	5
AT3G05680 protein Fragment	NbS00017403g0022.1_SGN	2	0	0	0	3
Remorin 2 (The same sequence as NICBE_013071.1 in TGAC db)	NbS00000986g0012.1_SGN (+1)	2	1	1	0	1
Nucleolar and coiled body phosphoprotein 1 (The same sequence as NICBE_412554.1 in TGAC db)	NbS00056367g0006.1_SGN	2	2	2	0	0
ATP dependent zinc metalloprotease FtsH 3	NbS00021959g0006.1_SGN	2	2	1	0	0
40S ribosomal protein S2-2 len=280 E=1e-117 (blastp), pfam_domain=Ribosomal_S5 Ribosomal protein S5, N-terminal domain E=1.1e-29 score=101.8	NICBE_203773.1_TGAC (+3)	2	4	7	7	8
60S ribosomal protein L11 len=316 E=2e-98 (blastp), pfam_domain=Ribosomal_L5_C ribosomal L5P family C-terminus E=5.4e-22 score=77.2	NICBE_087570.1_TGAC (+10)	2	1	2	2	2
sensitive to freezing 6	NbS00009035g0012.1_SGN	2	0	0	2	0
S adenosyl L methionine dependent methyltransferases (The same sequence as NICBE_382672.1 in TGAC db)	NbS00045721g0004.1_SGN	2	2	0	0	0
DNA polymerase V	NbS00012580g0015.1_SGN	2	1	2	0	0
BAG family molecular chaperone regulator 7 len=406 E=2e-84 (blastp), pfam_domain=BAG BAG domain E=0.001 score=19.0	NICBE_351556.1_TGAC	4	2	1	3	3

Pleiotropic drug resistance protein 1 len=1436 E=0.0 (blastp), pfam_domain=ABC2_membrane ABC-2 type transporter E=1.9e-98 score=327.6	NICBE_357824.1_TGAC (+2)	2	72	64	40	62
Fructokinase-2 len=691 E=2e-41 (blastp), pfam_domain=PfkB pfkB family carbohydrate kinase E=6e-28 score=97.7	NICBE_417695.1_TGAC (+1)	2	0	1	0	0
Charged multivesicular body protein 1 len=203 E=8e-50 (blastp), pfam_domain=Snf7 Snf7 E=8.9e-19 score=67.3	NICBE_204427.1_TGAC (+2)	2	4	1	0	0
(The same sequence as NICBE_048582.1 in TGAC db)	NbS00003380g0113.1_SGN	2	0	1	1	1
Nucleolar protein 14 len=933 E=3e-81 (blastp), pfam_domain=Nop14 Nop14-like family E=1.5e-207 score=691.2	NICBE_195703.1_TGAC (+1)	2	3	0	1	0
Cell division cycle and apoptosis regulator protein 1	NbS00014940g0015.1_SGN	3	2	1	2	2
Nuclear export mediator factor Nemf (The same sequence as NICBE_028753.1 in TGAC db)	NbS00002000g0019.1_SGN	2	0	2	1	0
NbS00005026g0127.1_SGN	NbS00005026g0127.1_SGN (+1)	2	1	1	1	1
WD-40 repeat-containing protein MSI4 len=492 E=0.0 (blastp), pfam_domain=WD40 WD domain, G-beta repeat E=2.1e-26 score=90.6	NICBE_250325.1_TGAC (+1)	2	1	2	0	0
5 methyltetrahydropteroyltriglutamate homocysteine methyltransferase	NbS00022063g0009.1_SGN	2	3	5	3	4
chaperonin	NbS00019145g0009.1_SGN	2	6	8	6	7
Chlorophyll a b binding protein 8 chloroplastic (The same sequence as NICBE_092693.1 in TGAC db)	NbS00006820g0015.1_SGN (+1)	2	6	5	2	4
Sedoheptulose-1,7-bisphosphatase, chloroplastic len=393 E=0.0 (blastp), pfam_domain=FBPase Fructose-1-6-bisphosphatase E=9.2e-105 score=349.9	NICBE_289927.1_TGAC	2	0	0	2	4
Chlorophyll a/b binding protein	NbS00014580g0002.1_SGN	2	9	3	6	2
Protein LTV1 (The same sequence as NICBE_152379.1 in TGAC db)	NbS00011921g0001.1_SGN	2	0	0	0	0
ATP synthase subunit gamma mitochondrial (The same sequence as NICBE_088581.1 in TGAC db)	NbS00006501g0003.1_SGN	2	0	2	1	3
RNA-binding protein 25 len=1082 E=5e-24 (blastp), pfam_domain=PWI PWI domain E=5.1e-17 score=61.6	NICBE_371593.1_TGAC (+1)	2	2	2	2	0
60S ribosomal protein L8 len=339 E=8e-149 (blastp), pfam_domain=Ribosomal_L2_C Ribosomal Proteins L2, C-terminal domain E=6e-41 score=139.1	NICBE_003339.1_TGAC (+3)	2	4	8	1	4
Catalase isozyme 1 (Fragment) len=502 E=0.0 (blastp), pfam_domain=Catalase Catalase E=9.8e-181 score=600.4	NICBE_161360.1_TGAC	4	1	2	1	3
Protein DEK len=569 E=2e-06 (blastp), pfam_domain=DEK_C DEK C terminal domain E=2.3e-11 score=43.1	NICBE_067933.1_TGAC (+1)	2	2	0	0	0
Ribulose bisphosphate carboxylase large chain	NbS00004956g0015.1_SGN	6	17	18	13	11
ATP synthase subunit alpha	NbS00036430g0009.1_SGN	2	11	12	4	8
Ferredoxin-dependent glutamate synthase, chloroplastic len=503 E=0.0 (blastp), pfam_domain=GXGXG GXGXG motif E=4.2e-65 score=218.4	NICBE_017437.1_TGAC	2	7	8	6	8

116 kDa U5 small nuclear ribonucleoprotein component len=925 E=0.0 (blastp),	NICBE_377725.1_TGAC	2	2	3	1	1
RNA and export factor-binding protein 2 len=249 E=2e-30 (blastp),	NICBE_276569.1_TGAC	2	1	2	0	0
tRNA pseudouridine synthase B len=682 E=2e-39 (blastp), pfam_domain=TruB_N TruB family pseudouridylate synthase (N terminal domain) E=4.2e-50 score=169.6	NICBE_397176.1_TGAC (+2)	2	0	2	1	1
Pentatricopeptide repeat-containing protein At1g74850, chloroplastic len=641 E=0.0 (blastp), pfam_domain=PPR_2 PPR repeat family E=1.5e-94 score=309.7	NICBE_194681.1_TGAC (+1)	2	1	1	1	0
Probable cation-transporting ATPase len=1043 E=0.0 (blastp), pfam_domain=Hydrolase haloacid dehalogenase-like hydrolase E=2.7e-17 score=63.8	NICBE_034499.1_TGAC (+1)	2	0	2	0	0
WD repeat-containing protein 75 len=790 E=7e-48 (blastp), pfam_domain=WD40 WD domain, G-beta repeat E=7.2e-15 score=54.1	NICBE_031349.1_TGAC	2	0	0	0	0
60S ribosomal protein L10a-1 len=267 E=7e-101 (blastp), pfam_domain=Ribosomal_L1 Ribosomal protein L1p/L10e family E=1.3e-49 score=168.4	NICBE_115071.1_TGAC (+3)	2	0	1	2	1
U3 small nucleolar RNA interacting protein 2 (The same sequence as NICBE_009839.1 in TGAC db)	NbS00000729g0012.1_SGN	2	0	1	0	2
Phosphate carrier protein, mitochondrial len=550 E=2e-99 (blastp), pfam_domain=Mito_carr Mitochondrial carrier protein E=6.5e-43 score=144.2	NICBE_219137.1_TGAC (+1)	2	3	6	3	9
V-type proton ATPase catalytic subunit A len=623 E=0.0 (blastp),	NICBE_332932.1_TGAC	5	10	13	9	14
DEAD-box ATP-dependent RNA helicase 28 len=744 E=0.0 (blastp), pfam_domain=DEAD DEAD/DEAH box helicase E=2.7e-47 score=160.3	NICBE_046448.1_TGAC (+2)	2	0	1	1	0
Nucleolar GTP-binding protein 2 len=505 E=5e-146 (blastp), pfam_domain=NGP1NT NGP1NT (NUC091) domain E=1e-44 score=151.5	NICBE_143481.1_TGAC (+2)	2	0	1	1	1
Aconitate hydratase, cytoplasmic len=998 E=0.0 (blastp), pfam_domain=Aconitase Aconitase family (aconitate hydratase) E=7.9e-149 score=495.9	NICBE_106906.1_TGAC (+1)	2	1	9	0	2
Ribosomal protein L15	NbS00049696g0008.1_SGN	2	0	1	1	2
Glycine-rich RNA-binding protein 7 len=204 E=6e-24 (blastp), pfam_domain=RRM_1 RNA recognition motif. (a.k.a. RRM, RBD, or RNP domain) E=9.3e-23 score=79.5	NICBE_142135.1_TGAC	2	0	0	0	0
UDP N acetylmuramoyl L alanyl D glutamate 2 6 diaminopimelate ligase	NbS00003467g0022.1_SGN	2	1	0	2	1
Protein MAK16 homolog B len=305 E=9e-61 (blastp), pfam_domain=Ribosomal_L28e Ribosomal L28e protein family E=1.7e-32 score=112.1	NICBE_113791.1_TGAC (+3)	2	0	0	1	1
50S ribosomal protein L3, chloroplastic (Fragment) len=213 E=3e-119 (blastp), pfam_domain=Ribosomal_L3 Ribosomal protein L3 E=4.2e-43 score=147.5	NICBE_269820.1_TGAC (+2)	2	1	1	1	0
50S ribosomal protein L5, chloroplastic len=301 E=7e-104 (blastp), pfam_domain=Ribosomal_L5_C ribosomal L5P family C-terminus E=1.4e-33 score=114.3	NICBE_117685.1_TGAC (+3)	2	2	1	4	4
Plasma membrane ATPase 4 len=952 E=0.0 (blastp), pfam_domain=E1-E2_ATPase E1-E2 ATPase E=2.1e-58 score=196.9	NICBE_026307.1_TGAC	3	37	32	22	26
26S proteasome regulatory subunit 4 homolog A len=446 E=0.0 (blastp),	NICBE_024250.1_TGAC (+1)	3	20	9	3	15
Geranylgeranyl diphosphate reductase chloroplastic	NbS00008675g0003.1_SGN (+1)	4	21	12	13	16

Long chain acyl-CoA synthetase 9, chloroplastic len=668 E=0.0 (blastp), pfam_domain=AMP-binding AMP-binding enzyme E=2.5e-88 score=296.1	NICBE_289931.1_TGAC (+1)	5	4	7	17	12
Glutamate-1-semialdehyde 2,1-aminomutase, chloroplastic len=477 E=0.0 (blastp), pfam_domain=Aminotran_3 Aminotransferase class-III E=5.4e-65 score=219.3	NICBE_415385.1_TGAC	5	11	4	5	7
Elongation factor 1 alpha	NbS00037026g0004.1_SGN (+1)	5	5	5	6	7
50S ribosomal protein L19 1 chloroplastic (The same sequence as NICBE_080995.1 in TGAC db)	NbS00006002g0007.1_SGN	3	1	3	7	6
Dolichyl-diphosphooligosaccharide--protein glycosyltransferase subunit STT3 len=772 E=0.0 (blastp),	NICBE_386230.1_TGAC (+1)	3	0	4	2	3
Adenosylhomocysteinase len=485 E=0.0 (blastp), pfam_domain=AdoHcyase S-adenosyl-L-homocysteine hydrolase E=1.1e-144 score=480.2	NICBE_406153.1_TGAC (+2)	3	2	7	1	2
No hits found in SwissProt (blastp), pfam_domain=Tom37_C Tom37 C-terminal domain E=0.015 score=15.0	NICBE_317247.1_TGAC (+1)	3	3	2	3	4
H/ACA ribonucleoprotein complex subunit 4 len=604 E=0.0 (blastp), pfam_domain=DKCLD DKCLD (NUC011) domain E=1.5e-29 score=101.6	NICBE_162868.1_TGAC (+1)	3	0	2	1	3
Eukaryotic translation initiation factor 2 subunit alpha len=490 E=1e-40 (blastp),	NICBE_097140.1_TGAC (+1)	3	2	1	2	3
Myosin protein	NbS00008970g0007.1_SGN	3	2	3	2	2
Dihydrolipoyl dehydrogenase 1 mitochondrial (The same sequence as NICBE_125227.1 in TGAC db)	NbS00009495g0011.1_SGN	3	2	4	0	2
Replication factor C subunit 2 len=332 E=4e-133 (blastp), pfam_domain=Rep_fac_C Replication factor C C-terminal domain E=8.1e-22 score=76.9	NICBE_270465.1_TGAC (+1)	3	4	2	0	1
Protein argonaute 1A len=992 E=0.0 (blastp), pfam_domain=Piwi Piwi domain E=7.9e-113 score=376.2	NICBE_130339.1_TGAC (+3)	3	1	0	4	1
Splicing factor 3B subunit 3 len=1211 E=0.0 (blastp), pfam_domain=CPSF_A CPSF A subunit region E=1.4e-100 score=336.4	NICBE_269313.1_TGAC	3	2	2	2	0
ATP dependent RNA helicase	NbS00027294g0010.1_SGN	3	0	2	1	0
ATP-dependent zinc metalloprotease FtsH len=1087 E=3e-39 (blastp),	NICBE_005818.1_TGAC (+1)	3	1	1	1	0
ATP-dependent zinc metalloprotease FtsH len=1289 E=9e-88 (blastp),	NICBE_141731.1_TGAC (+1)	3	1	1	1	0
U5 small nuclear ribonucleoprotein 200 kDa helicase len=1777 E=0.0 (blastp), pfam_domain=Sec63 Sec63 Brl domain E=3.6e-110 score=367.9	NICBE_347175.1_TGAC (+1)	3	3	0	1	1
DEAD-box ATP-dependent RNA helicase 3, chloroplastic len=853 E=0.0 (blastp), pfam_domain=DEAD DEAD/DEAH box helicase E=4.9e-47 score=159.4	NICBE_245177.1_TGAC (+1)	3	3	0	1	1
Delta24 sterol reductase (The same sequence as NICBE_370630.1 in TGAC db)	NbS00042036g0008.1_SGN	3	0	1	0	1
Cysteine-rich repeat secretory protein 55 len=262 E=1e-65 (blastp), pfam_domain=Stress-antifung Salt stress response/antifungal E=2.5e-44 score=149.8	NICBE_331337.1_TGAC (+1)	3	2	0	2	0
60S ribosomal protein L5 len=391 E=8e-144 (blastp), pfam_domain=Ribosomal_L18p Ribosomal L18p/L5e family E=5.9e-45 score=152.2	NICBE_211126.1_TGAC	3	0	3	0	0
Pentatricopeptide repeat containing protein	NbS00033609g0005.1_SGN	3	1	1	0	0

Replication factor C subunit 5 len=360 E=1e-110 (blastp), pfam_domain=Rep_fac_C Replication factor C C-terminal domain E=1.7e-16 score=59.8	NICBE_156927.1_TGAC (+1)	3	1	1	0	0
DEAD-box ATP-dependent RNA helicase 10 len=432 E=1e-162 (blastp), pfam_domain=DEAD DEAD/DEAH box helicase E=2.5e-36 score=124.6	NICBE_105739.1_TGAC (+1)	3	1	0	0	1
60S ribosomal protein L5 len=346 E=2e-139 (blastp), pfam_domain=Ribosomal_L18p Ribosomal L18p/L5e family E=2e-44 score=150.5	NICBE_250495.1_TGAC (+1)	3	0	2	0	0
Splicing factor U2af large subunit A (The same sequence as NICBE_326312.1 in TGAC db)	NbS00032866g0003.1_SGN (+1)	3	0	1	0	1
WD40 repeat-containing protein SMU1 len=514 E=0.0 (blastp), pfam_domain=WD40 WD domain, G-beta repeat E=6.8e-42 score=139.7	NICBE_017933.1_TGAC (+2)	3	0	1	0	0
Acetyl-coenzyme A carboxylase carboxyl transferase subunit alpha, chloroplastic len=621 E=0.0 (blastp),	NICBE_407139.1_TGAC (+1)	3	0	1	0	0
Root phototropism protein 3 len=630 E=0.0 (blastp), pfam_domain=NPH3 NPH3 family E=1.4e-104 score=348.9	NICBE_132316.1_TGAC (+2)	3	0	0	0	0
Ribosome production factor 1 len=353 E=2e-76 (blastp), pfam_domain=Brix Brix domain E=5.8e-47 score=159.7	NICBE_268853.1_TGAC	3	0	0	0	0
No hits found in SwissProt (blastp), pfam_domain=PORR Plant organelle RNA recognition domain E=4.7e-116 score=387.1	NICBE_282735.1_TGAC (+1)	3	0	0	0	0
Transcription elongation factor spt5	NbS00003996g0016.1_SGN	3	0	0	0	0
Phosphoribulokinase, chloroplastic len=407 E=0.0 (blastp), pfam_domain=PRK Phosphoribulokinase / Uridine kinase family E=7.2e-81 score=270.2	NICBE_317910.1_TGAC (+2)	4	4	3	1	2
Uncharacterized protein At2g40430 len=358 E=1e-60 (blastp), pfam_domain=Nop53 Nop53 (60S ribosomal biogenesis) E=9.8e-48 score=162.9	NICBE_198190.1_TGAC (+1)	3	1	1	0	1
No hits found in SwissProt (blastp), pfam_domain=Rubredoxin Rubredoxin E=0.00021 score=20.9	NICBE_086447.1_TGAC	3	3	4	6	3
Protease Do 9	NbS00027506g0012.1_SGN	3	0	0	0	0
Catalase isozyme 1 len=534 E=0.0 (blastp), pfam_domain=Catalase Catalase E=6.6e-174 score=577.9	NICBE_172990.1_TGAC	7	8	12	3	13
ATP-dependent Clp protease proteolytic subunit-related protein 1, chloroplastic len=385 E=8e-151 (blastp),	NICBE_014546.1_TGAC	3	3	2	4	3
U3 small nucleolar RNA-associated protein 6 homolog len=700 E=4e-40 (blastp),	NICBE_175812.1_TGAC (+1)	3	1	0	0	0
SDA1 (The same sequence as NICBE_045705.1 in TGAC db)	NbS00003297g0005.1_SGN	3	1	0	0	0
Apoptosis inhibitor 5	NbS00008232g0008.1_SGN	3	0	1	0	1
ATPase family AAA domain-containing protein 3-A len=681 E=2e-99 (blastp),	NICBE_106346.1_TGAC (+2)	3	2	6	3	6
H2B histone fold protein Fragment	NbS00020531g0029.1_SGN	3	1	0	1	0
Phototropic responsive NPH3 (The same sequence as NICBE_123251.1 in TGAC db)	NbS00009404g0009.1_SGN	3	0	0	1	1
Ribosomal RNA processing protein 36 homolog len=232 E=8e-29 (blastp), pfam_domain=DUF947 Domain of unknown function (DUF947) E=6.6e-42 score=143.0	NICBE_142976.1_TGAC	3	0	0	0	2

Chromodomain-helicase-DNA-binding protein 3 len=1598 E=5e-11 (blastp), pfam_domain=PHD PHD-finger E=1.3e-10 score=40.7	NICBE_286607.1_TGAC (+1)	3	5	1	2	2
60S ribosomal protein L4/L1	Nbs00039797g0003.1_SGN	3	0	0	0	2
No hits found in SwissProt (blastp), pfam_domain=FliD_C Flagellar hook-associated protein 2 C-terminus E=0.16 score=11.1	NICBE_006483.1_TGAC	4	0	2	3	0
Protein DEK len=548 E=5e-12 (blastp), pfam_domain=DEK_C DEK C terminal domain E=3.4e-13 score=49.0	NICBE_322028.1_TGAC	3	1	3	0	1
Dynamin related protein 1E	Nbs00056353g0008.1_SGN	3	2	2	3	5
P loop containing nucleoside triphosphate hydrolases (The same sequence as NICBE_163642.1 in TGAC db)	Nbs00013004g0003.1_SGN	3	0	2	0	1
Kelch domain containing protein 4 (The same sequence as NICBE_146663.1 in TGAC db)	Nbs00011309g0028.1_SGN	3	3	3	3	1
No hits found in SwissProt (blastp), pfam_domain=TPX2 Targeting protein for Xklp2 (TPX2) E=1.5e-21 score=76.0	NICBE_238670.1_TGAC	3	0	0	0	0
Replication factor C subunit 1 len=1064 E=8e-111 (blastp), pfam_domain=RFC1 Replication factor RFC1 C terminal domain E=7.6e-46 score=155.5	NICBE_157453.1_TGAC (+1)	3	3	1	1	2
(The same sequence as NICBE_109097.1 in TGAC db)	Nbs00007993g0305.1_SGN	3	2	1	9	6
40S ribosomal protein S3 3 (The same sequence as NICBE_006406.1 in TGAC db)	Nbs00000485g0008.1_SGN (+1)	3	1	4	5	4
Eukaryotic translation initiation factor 2 subunit beta len=309 E=1e-111 (blastp), pfam_domain=eIF-5_eIF-2B Domain found in IF2B/IF5 E=1e-47 score=160.7	NICBE_297688.1_TGAC (+5)	3	0	0	0	0
60S ribosomal protein L19-2 len=259 E=9e-91 (blastp), pfam_domain=Ribosomal_L19e Ribosomal protein L19e E=5.7e-67 score=223.9	NICBE_266755.1_TGAC (+1)	3	0	3	0	0
ATP-dependent zinc metalloprotease FTSH, chloroplastic len=754 E=0.0 (blastp), pfam_domain=Peptidase_M41 Peptidase family M41 E=2.6e-82 score=275.3	NICBE_282794.1_TGAC	3	17	14	13	16
Ribosomal L1 domain containing protein 1	Nbs00000440g0015.1_SGN	3	0	5	1	2
Importin alpha 1b subunit (The same sequence as NICBE_088005.1 in TGAC db)	Nbs00006541g0003.1_SGN	3	1	0	1	1
Pumilio domain containing protein KIAA0020	Nbs00023485g0006.1_SGN	3	0	0	0	0
SWI4 1 Peter Pan protein suppressor	Nbs00047940g0012.1_SGN (+1)	3	1	1	0	0
Protein IWS1 homolog len=516 E=9e-33 (blastp), pfam_domain=Med26 TFIIS helical bundle-like domain E=6.6e-18 score=63.8	NICBE_003736.1_TGAC (+1)	4	1	2	2	2
Uncharacterized protein C57A7.06 len=967 E=3e-29 (blastp), pfam_domain=Utp14 Utp14 protein E=1.8e-172 score=575.1	NICBE_271454.1_TGAC (+1)	4	2	2	2	4
pectin methylesterase 3	Nbs00011496g0007.1_SGN	4	2	1	0	3
Luminal-binding protein 4 len=753 E=0.0 (blastp), pfam_domain=HSP70 Hsp70 protein E=1e-268 score=892.1	NICBE_321257.1_TGAC (+1)	9	86	92	77	89
Ferredoxin dependent glutamate synthase 1 chloroplastic (The same sequence as NICBE_234363.1 in TGAC db)	Nbs00020069g0017.1_SGN	6	15	14	10	15

ATP synthase gamma chain, chloroplastic len=377 E=0.0 (blastp), pfam_domain=ATP-synt ATP synthase E=8.3e-98 score=327.1	NICBE_159540.1_TGAC (+1)	4	10	5	7	6
DNA directed RNA polymerase	NbS00004369g0012.1_SGN	4	9	5	3	3
50S ribosomal protein L6, chloroplastic len=243 E=2e-98 (blastp), pfam_domain=Ribosomal_L6 Ribosomal protein L6 E=2.7e-39 score=133.4	NICBE_404581.1_TGAC (+1)	4	1	1	5	4
Ribosomal protein L12 (The same sequence as NICBE_209894.1 in TGAC db)	NbS00017357g0001.1_SGN (+5)	4	2	2	4	2
No hits found in SwissProt (blastp), pfam_domain=NusG Transcription termination factor nusG E=4.9e-10 score=39.3	NICBE_094835.1_TGAC (+1)	4	5	4	3	2
ABC transporter F family member 1 len=624 E=0.0 (blastp), pfam_domain=ABC_tran ABC transporter E=8e-32 score=109.9	NICBE_291529.1_TGAC	4	2	2	4	0
high mobility group A (The same sequence as NICBE_232060.1 in TGAC db)	NbS00019948g0003.1_SGN	4	3	1	2	2
60S ribosomal protein L18-2 len=227 E=1e-87 (blastp), pfam_domain=Ribosomal_L18e Ribosomal protein L18e/L15 E=4.7e-25 score=88.3	NICBE_242674.1_TGAC (+1)	4	0	2	0	2
Replication factor C subunit 2 (The same sequence as NICBE_384152.1 in TGAC db)	NbS00045861g0008.1_SGN	4	3	2	1	2
No hits found in SwissProt (blastp), pfam_domain=DUF1311 Protein of unknown function (DUF1311) E=0.57 score=10.2	NICBE_161767.1_TGAC (+1)	4	0	1	1	0
RRP15 protein (The same sequence as NICBE_088756.1 in TGAC db)	NbS00006493g0017.1_SGN	4	1	0	0	1
RNA and export factor-binding protein 2 len=549 E=6e-27 (blastp),	NICBE_103488.1_TGAC (+1)	4	1	1	0	0
DNA topoisomerase	NbS00050706g0009.1_SGN	4	0	0	2	0
Peptidyl-prolyl cis-trans isomerase FKBP53 len=644 E=5e-94 (blastp), pfam_domain=FKBP_C FKBP-type peptidyl-prolyl cis-trans isomerase E=5.9e-29 score=99.8	NICBE_337606.1_TGAC	4	0	0	0	0
gi_136429_sp_P00761_TRYP_PIG_TRYPSIN_PRECURSOR.	cont10	12	19	17	18	17
Red (The same sequence as NICBE_418698.1 in TGAC db)	NbS00058940g0004.1_SGN	4	0	0	0	1
DNA directed RNA polymerase I subunit rpa1	NbS00011273g0004.1_SGN	4	6	2	1	5
Heterogeneous nuclear ribonucleoprotein Q len=797 E=4e-33 (blastp),	NICBE_107290.1_TGAC	4	1	1	3	0
Importin subunit alpha-1 len=528 E=0.0 (blastp), pfam_domain=Arm Armadillo/beta-catenin-like repeat E=3.8e-88 score=286.5	NICBE_295401.1_TGAC (+2)	4	0	4	1	5
Uncharacterized protein At5g49945 len=511 E=8e-160 (blastp), pfam_domain=DUF1682 Protein of unknown function (DUF1682) E=3.1e-87 score=292.2	NICBE_119228.1_TGAC (+3)	4	1	1	0	1
Pumilio homolog 23 len=324 E=5e-79 (blastp), pfam_domain=PUF Pumilio-family RNA binding repeat E=4.2e-07 score=28.9	NICBE_363680.1_TGAC (+1)	4	0	0	0	0
60S ribosomal protein L24 (The same sequence as NICBE_093608.1 in TGAC db)	NbS00006878g0022.1_SGN	4	2	0	0	0
Ribosomal RNA-processing protein 7 homolog A len=323 E=1e-10 (blastp), pfam_domain=RRP7 Ribosomal RNA-processing protein 7 (RRP7) E=1.4e-35 score=122.0	NICBE_417997.1_TGAC	4	0	0	0	1

Histone H1 len=516 E=2e-12 (blastp), pfam_domain=Linker_histone linker histone H1 and H5 family E=4.7e-19 score=68.1 U4/U6 small nuclear ribonucleoprotein Prp3 len=888 E=4e-69 (blastp), pfam_domain=PRP3 pre-mRNA processing factor 3 (PRP3) E=2.6e-67 score=226.3	NICBE_295653.1_TGAC (+1)	4	0	1	1	0
Dynamin 2B (The same sequence as NICBE_320416.1 in TGAC db)	NICBE_141826.1_TGAC (+1)	4	0	1	0	1
60S ribosomal protein L4/L1	NbS00031648g0011.1_SGN	4	2	3	4	3
Myosin-J heavy chain len=1529 E=0.0 (blastp), pfam_domain=Myosin_head Myosin head (motor domain) E=4.3e-241 score=801.6	NbS00002612g0002.1_SGN	4	0	2	1	3
Elongation factor EF 2	NICBE_063800.1_TGAC (+1)	4	18	14	27	20
NAD dependent epimerase/dehydratase (The same sequence as NICBE_146150.1 in TGAC db) Pentatricopeptide repeat-containing protein At5g50280, chloroplastic len=709 E=0.0 (blastp), pfam_domain=PPR_2 PPR repeat family E=6.8e-80 score=262.7	NbS00016832g0010.1_SGN (+1)	4	10	13	7	11
60S ribosomal protein L13a protein (The same sequence as NICBE_204521.1 in TGAC db)	NbS00011313g0004.1_SGN (+1)	4	0	0	1	0
Serine/threonine protein kinase RIO1 (The same sequence as NICBE_050649.1 in TGAC db) 60S ribosomal protein L18a len=178 E=5e-94 (blastp), pfam_domain=Ribosomal_L18ae Ribosomal L18ae/LX protein domain E=2.9e-58 score=195.0	NICBE_173836.1_TGAC (+1)	4	0	1	2	2
Retrovirus-related Pol polyprotein from transposon TNT 1-94 len=846 E=9e-43 (blastp), 50S ribosomal protein L1, chloroplastic len=340 E=5e-129 (blastp), pfam_domain=Ribosomal_L1 Ribosomal protein L1p/L10e family E=1.8e-46 score=158.1	NbS00016948g0018.1_SGN (+1)	4	2	4	4	2
Nucleolar complex protein 3 homolog len=877 E=7e-70 (blastp), pfam_domain=CBF CBF/Mak21 family E=2.6e-29 score=101.6	NbS00003704g0004.1_SGN	4	0	1	0	0
60S ribosomal protein L7-1 len=243 E=1e-64 (blastp), pfam_domain=Ribosomal_L30_N Ribosomal L30 N-terminal domain E=3.7e-12 score=45.9	NICBE_117769.1_TGAC (+3)	4	1	3	3	2
FAD dependent oxidoreductase	NICBE_210744.1_TGAC (+1)	4	0	1	3	0
DEAD-box ATP-dependent RNA helicase 7 len=690 E=0.0 (blastp), pfam_domain=DEAD DEAD/DEAH box helicase E=8.8e-45 score=152.1	NICBE_080914.1_TGAC (+3)	4	1	3	1	2
Heat shock 70 kDa protein mitochondrial	NICBE_339139.1_TGAC	4	1	0	0	2
DBIRD complex subunit KIAA1967 homolog len=1499 E=3e-09 (blastp), pfam_domain=DBC1 DBC1 E=2.6e-33 score=114.1	NICBE_336006.1_TGAC (+1)	4	1	2	1	1
DNA topoisomerase 1 len=1172 E=0.0 (blastp), pfam_domain=Topoisom_bac DNA topoisomerase E=2.2e-115 score=385.5	NbS00001587g0027.1_SGN	4	0	1	1	1
Tetratricopeptide repeat TPR (The same sequence as NICBE_012154.1 in TGAC db)	NICBE_138855.1_TGAC (+1)	4	0	0	0	2
RRP12-like protein len=1299 E=3e-95 (blastp), pfam_domain=NUC173 NUC173 domain E=6.5e-59 score=198.5 U4/U6 small nuclear ribonucleoprotein PRP4-like protein len=649 E=0.0 (blastp), pfam_domain=WD40 WD domain, G-beta repeat E=3.5e-69 score=226.3	NbS00012368g0006.1_SGN	7	13	14	10	9
	NICBE_184038.1_TGAC	7	6	5	4	3
	NICBE_179178.1_TGAC (+1)	4	4	1	3	4
	NbS00000891g0006.1_SGN	4	1	2	1	1
	NICBE_025729.1_TGAC	4	2	2	1	1
	NICBE_341899.1_TGAC (+3)	4	0	2	1	3

B2 protein len=732 E=9e-12 (blastp), pfam_domain=Dev_Cell_Death Development and cell death domain E=1e-42 score=144.6	NICBE_071823.1_TGAC (+1)	5	2	2	0	0
40S ribosomal protein S6	NbS00005003g0014.1_SGN	5	0	7	3	6
30S ribosomal protein S5, chloroplastic len=327 E=5e-112 (blastp), pfam_domain=Ribosomal_S5_C Ribosomal protein S5, C-terminal domain E=1.6e-26 score=91.2	NICBE_028588.1_TGAC (+3)	7	6	4	9	7
Protein IQ-DOMAIN 31 len=563 E=5e-74 (blastp), pfam_domain=DUF4005 Protein of unknown function (DUF4005) E=7.3e-11 score=42.0	NICBE_109894.1_TGAC	5	0	0	0	0
DEAD-box ATP-dependent RNA helicase 31 len=867 E=0.0 (blastp), pfam_domain=DEAD DEAD/DEAH box helicase E=1.2e-44 score=151.6	NICBE_399551.1_TGAC (+1)	5	4	4	5	3
Developmentally-regulated GTP-binding protein 1 len=368 E=3e-156 (blastp), pfam_domain=TGS TGS domain E=4.4e-25 score=87.1	NICBE_382396.1_TGAC	5	4	6	6	6
Alpha-1,4 glucan phosphorylase L-2 isozyme, chloroplastic/amyloplastic len=967 E=0.0 (blastp),	NICBE_232534.1_TGAC (+1)	5	6	5	3	6
DEAD-box ATP-dependent RNA helicase 51 len=540 E=0.0 (blastp), pfam_domain=DEAD DEAD/DEAH box helicase E=7e-45 score=152.4	NICBE_107491.1_TGAC	5	0	4	1	9
Heterogeneous nuclear ribonucleoprotein 27C len=346 E=9e-39 (blastp),	NICBE_159125.1_TGAC	5	5	1	5	3
60S acidic ribosomal protein P0 len=321 E=6e-147 (blastp), pfam_domain=Ribosomal_60s 60s Acidic ribosomal protein E=1.6e-22 score=79.5	NICBE_417286.1_TGAC	5	4	3	3	3
60S ribosomal protein L7	NbS00039066g0008.1_SGN (+1)	5	2	3	2	0
Transmembrane protein 214-A len=586 E=7e-11 (blastp), pfam_domain=DUF2359 Uncharacterised conserved protein (DUF2359) E=1.2e-15 score=56.8	NICBE_213163.1_TGAC	5	0	2	0	5
Ribosomal L9 protein (The same sequence as NICBE_069621.1 in TGAC db)	NbS00005119g0003.1_SGN	5	0	2	3	1
WD repeat-containing protein 3 len=950 E=0.0 (blastp), pfam_domain=WD40 WD domain, G-beta repeat E=2.4e-76 score=248.9	NICBE_002958.1_TGAC (+1)	5	2	1	2	0
Ribonuclease P protein subunit p25	NbS00001259g0009.1_SGN	5	3	2	1	1
RNA binding KH domain containing protein (The same sequence as NICBE_314670.1 in TGAC db)	NbS00030879g0008.1_SGN	5	1	1	1	1
No hits found in SwissProt (blastp), pfam_domain=HABP4_PAI-RBP1 Hyaluronan / mRNA binding family E=9.6e-28 score=96.6	NICBE_023495.1_TGAC	5	0	0	0	1
ATP dependent RNA helicase	NbS00003134g0011.1_SGN	5	0	0	0	1
Beta D glucosidase (The same sequence as NICBE_143374.1 in TGAC db)	NbS00011140g0006.1_SGN	6	5	2	5	2
Chaperone protein ClpD, chloroplastic len=967 E=0.0 (blastp), pfam_domain=AAA_2 AAA domain (Cdc48 subfamily) E=1.2e-53 score=181.4	NICBE_346879.1_TGAC (+2)	5	0	2	2	2
Dynamin related protein 1E (The same sequence as NICBE_331790.1 in TGAC db)	NbS00033686g0006.1_SGN	5	0	1	3	1
Ribosome production factor 2 (The same sequence as NICBE_146953.1 in TGAC db)	NbS00011371g0021.1_SGN (+1)	5	1	0	0	1
gi_113574_sp_P02769_ALBU_BOVIN_SERUM_ALBUMIN_PRECURSOR.	cont16	40	33	36	45	51

26S protease regulatory subunit 6A homolog len=423 E=0.0 (blastp),	NICBE_021292.1_TGAC	5	24	24	16	20
Glyceraldehyde-3-phosphate dehydrogenase B, chloroplastic len=465 E=0.0 (blastp),	NICBE_329039.1_TGAC (+1)	12	28	17	21	16
Chloroplast stem-loop binding protein of 41 kDa b, chloroplastic len=374 E=0.0 (blastp),	NICBE_347493.1_TGAC	5	10	5	2	2
Chlorophyll a-b binding protein CP26, chloroplastic len=274 E=9e-120 (blastp),	NICBE_056958.1_TGAC (+1)	5	6	2	5	4
Ferredoxin--NADP reductase, leaf-type isozyme, chloroplastic len=362 E=0.0 (blastp),	NICBE_003502.1_TGAC (+2)	5	1	3	3	4
Nuclear RNA binding protein Fragment	NbS00030061g0007.1_SGN	5	4	2	0	0
Pre-mRNA-processing protein 40A len=1175 E=0.0 (blastp), pfam_domain=FF FF domain E=5.4e-45 score=151.0	NICBE_177227.1_TGAC	5	2	1	3	2
ATP dependent RNA helicase (The same sequence as NICBE_394444.1 in TGAC db)	NbS00049120g0015.1_SGN	5	0	0	0	3
Elongation factor Tu chloroplastic	NbS00027807g0002.1_SGN	8	30	23	29	23
Carbonic anhydrase, chloroplastic len=321 E=6e-180 (blastp), pfam_domain=Pro_CA Carbonic anhydrase E=8.2e-42 score=142.5	NICBE_048578.1_TGAC	5	11	4	6	13
Phosphoenolpyruvate carboxylase, housekeeping isozyme len=987 E=0.0 (blastp),	NICBE_222157.1_TGAC (+1)	5	5	6	3	5
60S ribosomal protein L17-1 len=175 E=2e-85 (blastp), pfam_domain=Ribosomal_L22 Ribosomal protein L22p/L17e E=1.6e-34 score=117.8	NICBE_346362.1_TGAC	5	3	5	8	6
Translation initiation factor IF 2 (The same sequence as NICBE_311728.1 in TGAC db)	NbS00030345g0007.1_SGN	5	1	2	1	1
chloroplast photosystem II 22 kDa component (The same sequence as NICBE_342246.1 in TGAC db)	NbS00035687g0007.1_SGN	5	6	2	4	2
No hits found in SwissProt (blastp), pfam_domain=MORN MORN repeat E=7.1e-09 score=34.7	NICBE_379768.1_TGAC (+1)	5	1	0	4	3
40S ribosomal protein S4 len=542 E=7e-151 (blastp), pfam_domain=Ribosomal_S4e Ribosomal family S4e E=2.2e-30 score=104.0	NICBE_160362.1_TGAC (+1)	5	1	4	1	5
Proton pump interactor 1	NbS00002945g0006.1_SGN	5	1	4	2	0
Ribonuclease P protein subunit p25	NbS00030156g0009.1_SGN	5	2	2	2	3
Microfibrillar associated protein 1 (The same sequence as NICBE_138983.1 in TGAC db)	NbS00010569g0009.1_SGN (+1)	5	0	3	1	1
Importin subunit alpha len=532 E=0.0 (blastp), pfam_domain=Arm Armadillo/beta-catenin-like repeat E=5.4e-91 score=295.5	NICBE_177267.1_TGAC (+1)	5	0	0	0	4
Pre-mRNA-processing factor 19 homolog 1 len=578 E=0.0 (blastp), pfam_domain=WD40 WD domain, G-beta repeat E=2.7e-39 score=131.5	NICBE_187838.1_TGAC (+2)	5	0	2	0	1
Chloroplastic group IIA intron splicing facilitator CRS1, chloroplastic len=833 E=4e-121 (blastp),	NICBE_211802.1_TGAC (+3)	5	0	0	1	0
Heat shock cognate 70 kDa protein 2 len=626 E=0.0 (blastp), pfam_domain=HSP70 Hsp70 protein E=4.4e-252 score=837.2	NICBE_276570.1_TGAC	10	42	42	55	49
Protein ASPARTIC PROTEASE IN GUARD CELL 2 len=451 E=2e-47 (blastp), pfam_domain=Asp Eukaryotic aspartyl protease E=4.9e-19 score=68.6	NICBE_289334.1_TGAC (+1)	6	3	1	3	4

Glyceraldehyde-3-phosphate dehydrogenase, cytosolic (Fragment) len=340 E=0.0 (blastp),	NICBE_080780.1_TGAC	14	56	58	67	48
Plasma membrane ATPase 1 len=956 E=0.0 (blastp), pfam_domain=E1-E2_ATPase E1-E2 ATPase E=2.8e-59 score=199.8	NICBE_251440.1_TGAC	9	48	46	34	45
Peroxisomal S 2 hydroxy acid oxidase	NbS00025736g0004.1_SGN	15	15	14	20	16
ATP synthase subunit beta mitochondrial (The same sequence as NICBE_226947.1 in TGAC db)	NbS00019305g0027.1_SGN	6	15	20	11	29
Flotillin-like protein 1 len=479 E=0.0 (blastp), pfam_domain=Band_7 SPFH domain / Band 7 family E=2.9e-14 score=53.2	NICBE_035591.1_TGAC	6	11	12	4	15
Serine hydroxymethyltransferase	NbS00027670g0006.1_SGN	6	8	7	3	11
Respiratory burst oxidase homolog protein C len=938 E=0.0 (blastp), pfam_domain=NAD_binding_6 Ferric reductase NAD binding domain E=1.6e-49 score=167.4	NICBE_086010.1_TGAC	6	6	10	6	6
Sister chromatid cohesion protein PDS5 B	NbS00024877g0006.1_SGN	6	8	5	6	7
Putative chromatin-remodeling complex ATPase chain len=1075 E=0.0 (blastp), pfam_domain=SNF2_N SNF2 family N-terminal domain E=5.7e-93 score=310.9	NICBE_260676.1_TGAC	6	7	6	4	5
60S ribosomal protein L21 protein	NbS00024029g0004.1_SGN	6	3	8	6	6
Probable histone H2B.1 len=203 E=3e-68 (blastp), pfam_domain=Histone Core histone H2A/H2B/H3/H4 E=2e-23 score=82.1	NICBE_351965.1_TGAC (+1)	6	2	1	11	5
Extracellular calcium sensing receptor (The same sequence as NICBE_281604.1 in TGAC db)	NbS00026008g0003.1_SGN	6	6	3	5	9
NbS00016243g0202.1_SGN	NbS00016243g0202.1_SGN	6	3	5	3	4
Nucleolar protein (The same sequence as NICBE_265210.1 in TGAC db)	NbS00023900g0001.1_SGN	6	1	3	2	8
Pentatricopeptide repeat-containing protein At2g17140 len=810 E=2e-11 (blastp), pfam_domain=PPR_3 Pentatricopeptide repeat domain E=1.8e-16 score=58.8	NICBE_005272.1_TGAC (+1)	6	5	4	5	1
RNA binding RNA binding	NbS00006878g0032.1_SGN	6	5	2	1	3
Single stranded DNA binding protein (The same sequence as NICBE_193207.1 in TGAC db)	NbS00015816g0008.1_SGN	6	4	1	3	3
DEAD box ATP dependent RNA helicase 21	NbS00027428g0011.1_SGN (+1)	6	1	4	6	3
Pre rRNA processing protein TSR1 (The same sequence as NICBE_309764.1 in TGAC db)	NbS00030132g0010.1_SGN	6	2	2	2	1
MKI67 FHA domain-interacting nucleolar phosphoprotein-like len=257 E=6e-33 (blastp),	NICBE_404304.1_TGAC (+1)	6	1	1	2	3
Protein unc-45 homolog B len=800 E=2e-11 (blastp), pfam_domain=TPR_11 TPR repeat E=7.4e-21 score=73.4	NICBE_148117.1_TGAC	6	2	1	2	0
Uncharacterized protein C19orf29 len=722 E=1e-105 (blastp), pfam_domain=CactinC_cactus Cactus-binding C-terminus of cactin protein E=6.9e-76 score=251.7	NICBE_210415.1_TGAC (+1)	6	0	2	2	2
40S ribosomal protein S3a (The same sequence as NICBE_002254.1 in TGAC db)	NbS00000177g0011.1_SGN	7	4	4	18	6

ATP-dependent Clp protease ATP-binding subunit clpA homolog CD4B, chloroplastic len=1046 E=0.0 (blastp),	NICBE_271692.1_TGAC	9	43	50	28	24
Ribulose bisphosphate carboxylase/oxygenase activase 1, chloroplastic len=442 E=0.0 (blastp),	NICBE_380342.1_TGAC	9	23	21	22	16
Signal recognition particle 72 kDa protein len=777 E=1e-81 (blastp), pfam_domain=SRP72 SRP72 RNA-binding domain E=1.6e-16 score=60.3	NICBE_351226.1_TGAC (+1)	7	2	8	7	12
Endoplasmin homolog len=811 E=0.0 (blastp), pfam_domain=HSP90 Hsp90 protein E=1.6e-244 score=812.1	NICBE_174581.1_TGAC (+1)	7	13	12	7	6
40S ribosomal protein S9-2 len=197 E=3e-97 (blastp), pfam_domain=Ribosomal_S4 Ribosomal protein S4/S9 N-terminal domain E=2e-27 score=95.2	NICBE_254538.1_TGAC (+1)	7	2	9	7	7
40S ribosomal protein S7 len=226 E=8e-91 (blastp), pfam_domain=Ribosomal_S7e Ribosomal protein S7e E=3.9e-84 score=280.7	NICBE_390275.1_TGAC	7	2	3	7	10
60S ribosomal protein L24 len=164 E=4e-68 (blastp), pfam_domain=Ribosomal_L24e Ribosomal protein L24e E=1.5e-36 score=123.9	NICBE_165355.1_TGAC (+3)	7	4	5	3	4
CCAAT/enhancer binding protein zeta (The same sequence as NICBE_296600.1 in TGAC db)	NbS00028065g0009.1_SGN	7	6	3	3	7
Magnesium chelatase subunit chlD chloroplastic	NbS00040120g0009.1_SGN	7	2	4	5	0
60S ribosomal protein L5 len=455 E=6e-144 (blastp), pfam_domain=Ribosomal_L18p Ribosomal L18p/L5e family E=1.8e-44 score=150.6	NICBE_122339.1_TGAC	7	1	4	1	2
Translation initiation factor IF-3 len=294 E=1e-32 (blastp), pfam_domain=IF3_N Translation initiation factor IF-3, N-terminal domain E=8.3e-27 score=92.8	NICBE_175630.1_TGAC (+1)	7	1	1	3	1
Uncharacterized protein C9orf114 len=448 E=7e-75 (blastp), pfam_domain=Methyltrn_RNA_3 Putative RNA methyltransferase E=7.6e-93 score=310.9	NICBE_355725.1_TGAC (+1)	7	7	1	0	1
60S ribosomal protein L28	NbS00005975g0012.1_SGN (+1)	7	0	2	1	0
Protein LTV1 homolog len=509 E=4e-15 (blastp), pfam_domain=DUF1399 Protein of unknown function (DUF1399) E=0.057 score=13.5	NICBE_353788.1_TGAC	7	1	1	1	3
No hits found in SwissProt (blastp), pfam_domain=HATPase_c_2 Histidine kinase-like ATPase domain E=0.26 score=10.9	NICBE_168331.1_TGAC (+1)	7	0	2	1	1
Actin-97 len=360 E=0.0 (blastp), pfam_domain=Actin Actin E=9.2e-152 score=504.8	NICBE_141623.1_TGAC (+1)	23	63	69	77	66
Chaperonin 60 subunit beta 2 chloroplastic	NbS00034791g0001.1_SGN	11	12	20	5	30
RuBisCO large subunit-binding protein subunit alpha, chloroplastic len=657 E=0.0 (blastp),	NICBE_329880.1_TGAC	8	17	13	3	20
Chlorophyll a b binding protein 6A chloroplastic (The same sequence as NICBE_291298.1 in TGAC db)	NbS00027305g0008.1_SGN	8	7	6	15	11
Nucleolin 2 len=657 E=4e-70 (blastp), pfam_domain=RRM_1 RNA recognition motif. (a.k.a. RRM, RBD, or RNP domain) E=2.7e-27 score=94.0	NICBE_382164.1_TGAC	8	9	15	6	2
ATP dependent transporter	NbS00001134g0008.1_SGN	8	7	7	8	6
DEAD-box ATP-dependent RNA helicase 53 len=660 E=8e-177 (blastp), pfam_domain=DEAD DEAD/DEAH box helicase E=4.8e-43 score=146.4	NICBE_235039.1_TGAC (+1)	8	8	8	2	8
UPF0202 protein At1g10490 len=1030 E=0.0 (blastp), pfam_domain=GNAT_acetyltr_2 GNAT acetyltransferase 2 E=6.9e-75 score=250.5	NICBE_125808.1_TGAC	8	8	8	4	6

Metalloendopeptidase family saccharolysin %26amp thimet oligopeptidase ISS (The same sequence as NICBE_071405.1 in TGAC db)	NbS00005259g0004.1_SGN	8	4	1	5	4
No hits found in SwissProt (blastp), pfam_domain=HABP4_PAI-RBP1 Hyaluronan / mRNA binding family E=1.2e-27 score=96.3	NICBE_286507.1_TGAC	8	6	8	4	1
B2 protein len=862 E=2e-13 (blastp), pfam_domain=Dev_Cell_Death Development and cell death domain E=1.1e-40 score=138.0	NICBE_397973.1_TGAC (+1)	8	3	5	4	2
RNA splicing factor (The same sequence as NICBE_311022.1 in TGAC db)	NbS00030134g0011.1_SGN	8	2	0	4	5
60S ribosomal protein L23a (The same sequence as NICBE_211196.1 in TGAC db)	NbS00017699g0003.1_SGN (+1)	8	2	3	3	3
Serrate RNA effector molecule len=780 E=0.0 (blastp), pfam_domain=DUF3546 Domain of unknown function (DUF3546) E=7e-27 score=93.5	NICBE_151251.1_TGAC (+1)	8	2	2	5	2
DEAD-box ATP-dependent RNA helicase 30 len=701 E=0.0 (blastp), pfam_domain=DEAD DEAD/DEAH box helicase E=3.9e-46 score=156.5	NICBE_021652.1_TGAC (+1)	8	1	2	3	1
Transketolase, chloroplastic len=741 E=0.0 (blastp),	NICBE_378457.1_TGAC (+1)	13	11	14	14	20
5 methyltetrahydropteroyltriglutamate homocysteine methyltransferase	NbS00012577g0009.1_SGN	9	14	18	13	22
Glycine dehydrogenase (The same sequence as NICBE_256942.1 in TGAC db)	NbS00022684g0008.1_SGN	13	13	10	12	22
Probable fructose-bisphosphate aldolase 2, chloroplastic len=396 E=0.0 (blastp),	NICBE_095186.1_TGAC (+1)	10	18	12	13	12
Importin alpha 1b subunit	NbS00022414g0008.1_SGN (+1)	9	8	10	4	13
(The same sequence as NICBE_089742.1 in TGAC db)	NbS00006338g0323.1_SGN (+2)	9	8	9	4	8
Nucleolar protein 8 len=792 E=8e-09 (blastp), pfam_domain=RRM_6 RNA recognition motif (a.k.a. RRM, RBD, or RNP domain) E=1.3e-07 score=31.3	NICBE_251121.1_TGAC (+1)	9	4	4	4	4
Dek protein	NbS00041042g0010.1_SGN	9	9	0	3	1
60S ribosomal protein L13	NbS00026051g0013.1_SGN	9	1	4	4	2
Pescadillo homolog len=599 E=2e-135 (blastp), pfam_domain=Pescadillo_N Pescadillo N-terminus E=2.3e-111 score=371.4	NICBE_421321.1_TGAC	9	1	2	4	4
Ribosome biogenesis regulatory protein homolog len=331 E=3e-116 (blastp),	NICBE_146357.1_TGAC (+1)	9	1	2	1	2
Ribulose bisphosphate carboxylase/oxygenase activase 2, chloroplastic len=439 E=0.0 (blastp),	NICBE_389439.1_TGAC	31	105	85	93	80
Heat shock cognate protein 80 len=772 E=0.0 (blastp), pfam_domain=HSP90 Hsp90 protein E=1.2e-263 score=875.2	NICBE_184285.1_TGAC (+1)	11	30	30	10	17
RNA-binding protein 25 len=932 E=3e-24 (blastp), pfam_domain=PWI PWI domain E=3.7e-17 score=62.0	NICBE_368002.1_TGAC (+1)	10	9	4	8	9
Transmembrane protein 214-A len=585 E=2e-11 (blastp), pfam_domain=DUF2359 Uncharacterised conserved protein (DUF2359) E=1.1e-16 score=60.3	NICBE_014082.1_TGAC	10	9	13	1	13
60S ribosomal protein L10 len=317 E=4e-123 (blastp), pfam_domain=Ribosomal_L16 Ribosomal protein L16p/L10e E=1.5e-32 score=112.0	NICBE_341346.1_TGAC (+2)	11	2	7	6	5

Nucleolar GTP binding protein	NbS00005100g0009.1_SGN	10	5	8	4	5
ATP dependent zinc metalloprotease FTSH 12 chloroplastic	NbS00029765g0015.1_SGN	10	3	3	6	1
DEAD box ATP dependent RNA helicase 16 (The same sequence as NICBE_115085.1 in TGAC db)	NbS00008609g0018.1_SGN	10	1	2	2	4
NbS00004583g0120.1_SGN	NbS00004583g0120.1_SGN	10	1	1	0	1
Elongation factor 1 alpha	NbS00019623g0001.1_SGN (+1)	19	27	23	21	23
Catalase isozyme 1 (Fragment) len=553 E=0.0 (blastp), pfam_domain=Catalase Catalase E=8.5e-181 score=600.6	NICBE_083774.1_TGAC	16	18	14	10	18
60S ribosomal protein L7 50S ribosomal protein L15, chloroplastic (Fragment) len=228 E=2e-86 (blastp), pfam_domain=Ribosomal_L18e Ribosomal protein L18e/L15 E=1.2e-24 score=87.0	NbS00024868g0008.1_SGN	11	3	9	15	10
Signal recognition particle 68 kDa protein len=640 E=1e-72 (blastp), pfam_domain=Med7 MED7 protein E=0.12 score=11.9 Ribosome biogenesis protein BOP1 homolog len=759 E=1e-177 (blastp), pfam_domain=BOP1NT BOP1NT (NUC169) domain E=9.7e-104 score=346.5	NICBE_179113.1_TGAC (+1)	11	3	11	9	6
Protein TIC 62, chloroplastic len=509 E=2e-12 (blastp), pfam_domain=NAD_binding_10 NADH(P)-binding E=8.9e-09 score=35.4	NICBE_318398.1_TGAC	11	1	1	6	6
Stromal 70 kDa heat shock-related protein, chloroplastic len=707 E=0.0 (blastp), pfam_domain=HSP70 Hsp70 protein E=3.1e-264 score=877.3 Peptidyl-prolyl cis-trans isomerase FKBP53 len=563 E=3e-90 (blastp), pfam_domain=FKBP_C FKBP-type peptidyl-prolyl cis-trans isomerase E=1.7e-29 score=101.5	NICBE_347263.1_TGAC	11	3	4	6	7
Glyceraldehyde-3-phosphate dehydrogenase A, chloroplastic (Fragment) len=1143 E=0.0 (blastp),	NICBE_372855.1_TGAC	12	27	35	19	27
Phosphoglycerate kinase, chloroplastic len=407 E=0.0 (blastp), pfam_domain=PGK Phosphoglycerate kinase E=2.7e-160 score=532.9	NICBE_403996.1_TGAC (+1)	21	19	26	24	34
DNA REPLICATION FACTOR C SUBUNIT DEAD-box ATP-dependent RNA helicase 3, chloroplastic len=740 E=0.0 (blastp), pfam_domain=DEAD DEAD/DEAH box helicase E=2.4e-46 score=157.2	NICBE_110782.1_TGAC (+1)	12	1	2	4	6
NbS00002134g0112.1_SGN Protein KIAA0664 homolog len=1854 E=3e-58 (blastp), pfam_domain=eIF3_p135 Translation initiation factor eIF3 subunit 135 E=7e-37 score=126.7	NICBE_228497.1_TGAC	21	56	37	51	45
(The same sequence as NICBE_323200.1 in TGAC db)	NICBE_025234.1_TGAC	14	29	16	11	14
DNA helicase	NbS00001587g0026.1_SGN	13	15	8	9	13
Large subunit GTPase 1 homolog len=588 E=1e-92 (blastp), pfam_domain=MMR_HSR1 50S ribosome-binding GTPase E=6.9e-19 score=67.8	NICBE_417924.1_TGAC	14	9	7	10	8
Dynamin-related protein 1E len=579 E=0.0 (blastp), pfam_domain=Dynamin_M Dynamin central region E=1.1e-70 score=237.7	NbS00002134g0112.1_SGN	14	4	9	17	13
	NICBE_186375.1_TGAC	14	6	7	7	4
	NbS00032025g0111.1_SGN	14	6	9	6	5
	NbS00016240g0009.1_SGN	14	2	2	4	0
	NICBE_019427.1_TGAC	14	1	4	1	5
	NICBE_407487.1_TGAC	22	8	11	15	26

50S ribosomal protein L6 (The same sequence as NICBE_016472.1 in TGAC db)	NbS00001075g0014.1_SGN	15	5	14	16	13
Nucleolar GTP binding protein 2 (The same sequence as NICBE_361271.1 in TGAC db)	NbS00039776g0013.1_SGN	15	1	14	4	8
Dynamin-related protein 5A len=609 E=0.0 (blastp), pfam_domain=Dynamin_M Dynamin central region E=8.2e-72 score=241.3	NICBE_191552.1_TGAC (+1)	19	11	16	15	28
DEAD box ATP dependent RNA helicase 37 (The same sequence as NICBE_028095.1 in TGAC db)	NbS00001988g0005.1_SGN	20	10	11	18	14
Polyadenylate binding protein	NbS00001538g0002.1_SGN	16	9	8	6	8
Luminal-binding protein 5 len=717 E=0.0 (blastp), pfam_domain=HSP70 Hsp70 protein E=9.8e-270 score=895.5	NICBE_365796.1_TGAC	44	236	239	233	246
U4/U6.U5 tri-snRNP-associated protein 1 len=910 E=2e-24 (blastp), pfam_domain=SART-1 SART-1 family E=4.7e-87 score=292.6	NICBE_095692.1_TGAC	17	15	12	15	12
Nucleolar and coiled body phosphoprotein 1 (The same sequence as NICBE_412031.1 in TGAC db)	NbS00056206g0005.1_SGN	17	10	7	6	4
Mediator of RNA polymerase II transcription subunit 36a len=314 E=3e-132 (blastp), pfam_domain=Fibrillarin Fibrillarin E=6.6e-114 score=378.4	NICBE_038627.1_TGAC	18	12	13	15	15
60S ribosomal protein L4/L1 (The same sequence as NICBE_387030.1 in TGAC db)	NbS00047015g0005.1_SGN	18	12	16	8	19
Heat shock cognate 70 kDa protein 2 len=658 E=0.0 (blastp), pfam_domain=HSP70 Hsp70 protein E=2.7e-270 score=897.3	NICBE_217133.1_TGAC	29	115	134	151	156
Nucleolar protein 56 len=572 E=5e-149 (blastp), pfam_domain=Nop Putative snoRNA binding domain E=5.2e-60 score=200.9	NICBE_082659.1_TGAC	21	5	11	7	30
DEAD-box ATP-dependent RNA helicase 31 len=896 E=0.0 (blastp), pfam_domain=DEAD DEAD/DEAH box helicase E=1.2e-44 score=151.7	NICBE_292858.1_TGAC	22	14	20	16	4
Nucleolar protein 6	NbS00048975g0006.1_SGN	31	40	27	27	35
Dynamin-2B len=916 E=0.0 (blastp), pfam_domain=Dynamin_N Dynamin family E=2.9e-28 score=98.6	NICBE_074039.1_TGAC	36	40	39	41	53

[3] List represents results from four independent experiments. Peptides identified for the respective protein in the individual samples were summed up from the four individual experiments. Protein identifications were accepted if they could be established at greater than 95.0% probability and contained at least 2 identified peptides.

Attachment 2.

Identity between protein sequences of BAK1-interacting receptors (BIR) from *Arabidopsis thaliana* and BAK1-interacting receptors identified here in *Nicotiana benthamiana*. Protein sequences were aligned pairwise using NCBI blastp (http://blast.ncbi.nlm.nih.gov/blast/Blast.cgi?PROGRAM=blastp&PAGE_TYPE=BlastSearch&LINK_LOC=blasthome).

Protein	AtBIR1	AtBIR2	AtBIR3	NbBIR1	NbBIR2a	NbBIR2b
AtBIR1	100%	43%	44%	60%	45%	45%
AtBIR2	43%	100%	57%	46%	63%	63%
AtBIR3	44%	57%	100%	45%	61%	60%
NbBIR1	60%	46%	45%	100%	46%	46%
NbBIR2a	45%	63%	61%	46%	100%	98%
NbBIR2b	45%	63%	60%	46%	98%	100%

Attachment 3.

Predicted cDNA sequence of the NbCSPR candidate 1. NbCSPRC1 was identified by LC-MS of proteins isolated from *Nicotiana benthamiana* that transiently expressed either NbBAK1-FLAG (control -), NbBAK1-GFP or NbBAK1-5-GFP treated for ten minutes with sterile MQ-water or 100 nM csp22 peptide by vacuum infiltration.

> NbCSPRC1 (NbS00035240g0005.1 Niben044Scf00035240:1443..3354 disease resistance/LRR [*Arabidopsis thaliana*])

ATGAGAGGGCCATTACCAGATTTAGCATTGTTTCCATCATTGAGAGAGTTGCATCTTGGATTTC
AATGGAGGATACCACAAGAATTTTGGGTCTCGTCCAATAGACTGGAAGGATTACCAAAAAGT
ATGGGACAACTATCAAACTTGGAAAGTATTGATGCCTCTTACAATGTCCTGAAGGGTATAATC
ATTGAGTCCCACCTTTCAAACCTCTCTAGTTTAGTAGATTTGGACTTATCGTTCAACTCGTTGGC
TTTGAAGACAAGCTTCGATTGGCTTCCTCCTTTTCAGCTTCAATTTATAAACCTTCCATCTTGCA
ATTTGGGACCTTCTTTCCCCAAGTGGCTTCACAGTCAAAACAACTGTACTGTTCTTGAAATCTCT
CTTGCAAATCTATCAGATGCGTTACCAAGTTGGTTCTCTGATCTTCCTCTCAATTTAAAGATTCT
GACTCTCTCTAACAACCATATCAGTGGAAGAGTTTCTGAGTTGATAGTGAATAAACAAGACTA
CATGGTTATAGATTTAAGTTCTAACAACTTTTCAGGACCTTTGCCACAAGTTCCTACCAATGTG
CGAATATTTTACCTACATAAAAATAAGTTTTCCGGATCCACTTCTTCCATTTGTAAAAGTACAAC
AGGAGCGGCCACTTCCCTTGACTTGTCACACAACCTATTTTCAGGAGAACTTCCTGATTGTTGG
ATGAATATGAGTAATCTAGTTGTTCTTAATCTAGCCTTTAACAATTTCTCTGGAAAACTTCCACA
CGGGATTTTGCCTTCTTTCTCACAATGTCAATTATTGCAAATCTTGGACCTTGGAGGGAATAAG
TTGACAGGAAGAATCCCAGCATGGATAGGTACTGATCTACTCAACTTGCGTATTCTAAGCCTA
CGGTTCAACAAATTCTATGGCAGCATTCTATTTATCATTTGTCAGCTTCAATTTCTTCAGATACT
GGACCTTTCAGCAAATGGATTATCTGAACAATGCTTTAACAATTTTACTTTATTGCATCAAGAA
AATGGTTCTGGTGAGTCAATGAATTTTTCAGTCCAATATGACTATATGCCTCGATCATACTTGT
ACATAGGCAATTTATTGGTTCAATGGAAAAACCAGGAGGCTGAGTACAAGAATCCTTTATTAT
ATCTGAAGGCTATTGATCTTTCAAGTAATAAATTGGTTGGAGGTATTCCTAAAGAGATAGCTG
AAATGAGAGGATTGAAATCTTTGAACCTTTCAAGAAATGATCTGAATGGAAGTATCATTGAAG
GAATAGGTCAAATGAAGATGTTGGAGTCACTTGACCTGTCAAGAAACCAGCTTTCTGGTATGA
TTCCTAAAGACCTTGCTAACTTGACTTTTATTGGTGTGTTGGACTTGTCAAACAACCACTTATCA
GGGAGAATTCCATCAAGCACTCAACTCCAAACTTTTGAGAGATCATCCTACAGTGGTAACGCT
AAACTCTGCGGTCCTCCTCTTCAAGAATGTCCCGGATATGCTCCCCCTAGCCCATGTATCGATC
ATAACAGCAACATGAATCCTCAAGAACTTGACGATGATGATGATTTTCCATCTCTATGTCCCGG
ATATGCTCCCCCTAGCCCACGTATCGATCATAACAGCAACATGAATCCTCAAGAACTTGACGTT
GATGATGATTTTCCATCTCTAGAGTTTTATATATCGATGGTGCTAGGTTTCTTTGTTGCATTCTG
GGGAATCTTGGGCTCTTTAATTGTCAATCATTCTTGGAGGAATGCCTACTTCATATTCTTAATG
GACGTGAAGAATTGGCTCGCTATGATATCAAGAGTCTGA

Attachment 4.

cDNA sequence of the NbCSPR (NbCSPR candidate 2). NbCSPR was identified by LC-MS of proteins isolated from *Nicotiana benthamiana* that transiently expressed either NbBAK1-FLAG (control -), NbBAK1-GFP or NbBAK1-5-GFP treated for ten minutes with sterile MQ-water or 100 nM csp22 peptide by vacuum infiltration. Nucleotide sequences used for the TRV-based VIGS constructs are indicated in blue for *TRV1:NbCSPR* and red for *TRV2:NbCSPR*.

>*NbCSPR (NbCSPRC2* NbS00024693g0004.1 Niben044Scf00024693:42211..45051 LRR receptor serine/threonine protein kinase RLP [*Solanum lycopersicum*])

ATGAAAAGTGAGAGATTTTTATTTCTCAATATTGCATTTTCAGCGTTCATCG
GACTTGTTATTGGAACAAGTTCAGGAGGGGATGGTCGAACTACTTTGTGCAT
TGAGAGGGAGAGGGAAGCTCTTCTCAAGTTCAAGCAAGGTCTGATAGATAA
CTACGGTATCCTCTCGTCATGGGGGAGAGAAGAAGAGAAAGAAGAATGCTG
TGGTTGGAAAGGTGTGCAGTGTAGCAATAGAACAGGTCATGTTGTGGTTCTT
GATATTCATGCTCCGTCCTATAGTCAACATTTGAGAGGTAACATTACTCCTT
CATTGCTTGAATTGCAACATCTGAAGCACCTAGACCTTAGTTACAATGATTT
TGGTACAAGTCGAATACCAAATTTCATTGGTTCTTTTCCAAGACTGGAATAT
CTTTTTCTTGAGGATGCTAGCTTGTCAGGGGAAATTCCTCACGCTCTTGGGA
ACCTTACCCATTTGCAGATTCTTGACCTTAGCCTGAACTCCCGTCTAGTAGT
GAAGAACCTTGAGTGGCTTCCTCGTCTTGCTTTTTTACGCGACCTTGGCCTCT
CTTTGGTTCATATTGAAACAGTCAATTGGTTACAACAAATAATTAAGTCCCC
TTCTTTAGAACAATTGGATTTGAAACATTGCAACGTCCCCGAGCCAATCATA
TCAATATCTCATCTCTCATCCAATGTCTCTTCCCGTTTGCTTTCCAGCCTCAA
CCTTGCTGACACTGGGCTTTCCTCTTCTGCATTTCGGTGGTTGTTCAACTTGA
GTACGAGATTTACTTCCATAGATCTCTCTTCTAACAATTTAGCAGGTTGCAT
CCCTGAAGCCTTTGGGTATATGCAACATCTTGAGTTCATTGACCTTAATACA
AATATTCTAGAAGGTGGATTGCCCAAATCTTTTGGCAACTTGAGCCACTTAA
GAGCCCTTGATTTATCAACTAATAACTTGAACCAACCACTTCCTGAATTGTT
TCTGAGCTTATCTGATAAAGCAGAAAAATCACTTGAAGAATTGCATTTATCT
AACAATCATCTTAGTGGTTCATTGCCTGACATCACCAGATTTTCATCTTTGA
AAAGTTTGTACCTGCAAGAGAATCAACTGAATGGATCTTTCTTTGAAAGCTA
CGGGCAGATTTCCAAGATCGAATTCCTCGATTTATCTTTGAATCAGTTAACA
GGACCTTTGCCAAACTTAACAGCATTTTCAGCATTAAGAGAGTTGCATTTGA
ACAATAACCAATTCAAAGGGAGGTTACCCCAAAGTATAGGACGACTTTCAA
AGCTTGAGATGTTGAGGGTCGAATCAAATTTCATGGAAGGTCCAATCACAG
AGTCACATCTTTCAAACCTTTCCAGCTTAAGAGTGTTGGACTTGTCATATAA
CTCCTTCTCTTTTCAGTTGGGACTTAATTGGCTTCCTCCTTTTGAATTAGATG
TTATAAGTCTCTCCCATTGTAAAATGGGGCCTCATTTCCCACAGTGGCTACG
AACTCAGAAGAATTACTCACATCTTGATATCTCTTTTGCTGGTATATCAGGC
GTTGCACCTAACTGGTTTTGGGATCTTTCTCCTGAAATGATGCACTTTAGTAT
TTCCAATAACCAAATAAGTGGAGAGGTCCCTGATTTATCTTCCAAGTTTGTA

AAGGAAACTAATTATCCGACAATGGATTTTAGTTCGAATAATTTCTCAGGTT
TAGTGCCATCATTCTCATCCAACTTGGAATCATTGAACCTTTCCAAAAACAA
GTTTGTTGGATCAATTTCTTTCCTGTGCAAAATAGCCAACGCGTTGTTCCGC
ACCATTGACCTCTCAAATAACCTACTTTCAGGAGAACTTCACAATTGTTTGA
TGGGATTTGAAGAACTAGCCATTCTTAATTTAGCTAACAACAATCTATATGG
TAAAATTCCCAGTTCCATTGGTTCTTTGTGGGATATCCAATCTCTACAGTTGC
GGAACAACAATTTTACTGGTGATCTGCCTACCTCTTTGAAAAACTGCGGAAT
ATTGCAAATCTTGGATGTAGGAGGAAATAAGCTAAGTGGAGAAATACCATT
ATGGATTGGCTCACACTTAACATTCTTGGTTGTCTTAAGTTTGAGACTCAAC
AAGTTCAATGGAAGCATACCTCAAAATTTCTGTCATCTGAATAAAATCCATA
TTTTGGATCTTTCTCAGAACAGCTTATCAGGAGAAATCCCCCGATGTCTCAA
CAATATCACATCTTTGCTTCAGAATAATAATAGTTCAGACCCAAGCATCCTT
TTTGCATTAGGTGGAGACAGTCACAATGGCTATTCTTATTATGAAGAATACT
TGGGGGATGCATTAGTTCAATGGAAAAGCAGTGAGTCTGTGTACAATAAGA
CACTCGGGTTGTTGAAGATCATCGATTTTTCAAATAATGAGTTATCTGGAAA
TGTTCCTGAAGAAATCGCGCAACTGAATGGAGTGCTTTCACTAAACCTCTCG
AGAAATAATTTAACAGGAAATGTAATACAAGGAATTGGGAAGATGGAAAA
GTTAGAGTCCCTTGATTTGTCCGGAAATCGGCTCACTGGTCGAATTCCCACA
AGTCTTGCTCAACTACATTTCCTAAGTGTCTTAGACTTGTCGAGTAACAACT
TATCGGGGAAAATTCCTTCAAGCACACAATTGCAGAGTTTTGATCCTTCATC
ATATGAAGGAAACAATGAACTTTGTGGCCCACCACTTGCAGAATGTCCCGA
AGATAGAAATACTCAAAGCCCTTCTGCTGATCATAGCAAAATCAACAATCT
TGATGAAGATGACAAGATTCTGTCGTTTGAGTTTTA

Attachment 5

NbCSPR and *NtCSPR* nucleotide sequence alignment. The *NbCSPR* nucleotide sequence was obtained by the Sol Genomics Network genome and predicted cDNA database v0.4.4 tblastn using the protein sequence (http://solgenomics.net/tools/blast/). The *NtCSPR* nucleotide sequence was obtained by alignment of the *NbCSPR* nucleotide sequence against the *Nicotiana tabacum* whole-genome shotgun sequence database (http://blast.ncbi.nlm.nih.gov/Blast.cgi).

```
NtCSPR          ATGAAAAGTGAGATATTTTTATTTCTCAATATTGCATTTTCAGTGTTCATAGGACTTGTT 60
NbCSPR          ATGAAAAGTGAGAGATTTTTATTTCTCAATATTGCATTTTCAGCGTTCATCGGACTTGTT 60
                ************ ***************************** ****** *********

NtCSPR          ATTGGAACAAGTTCAGGAGGGGATGGTCGTACTACTTTGTGCATTGAGAGGGAGAGGGAA 120
NbCSPR          ATTGGAACAAGTTCAGGAGGGGATGGTCGAACTACTTTGTGCATTGAGAGGGAGAGGGAA 120
                ***************************** *****************************

NtCSPR          GCTCTTCTCAAGTTCAAGCAAGGTCTGATAGATAACTACGGTATCCTCTCGTCATGGGGG 180
NbCSPR          GCTCTTCTCAAGTTCAAGCAAGGTCTGATAGATAACTACGGTATCCTCTCGTCATGGGGG 180
                ************************************************************

NtCSPR          AGAGAAGAAGAGAAAGAAGAATGCTGTGGTTGGAAAGGTGTGCAGTGTAGCAATATAACA 240
NbCSPR          AGAGAAGAAGAGAAAGAAGAATGCTGTGGTTGGAAAGGTGTGCAGTGTAGCAATAGAACA 240
                ************************************************** ****

NtCSPR          GGTCATGTTGTGGTTCTTGATATTCATGCTCCGTCCTATAGTCAACATTTGAGAGGTAAC 300
NbCSPR          GGTCATGTTGTGGTTCTTGATATTCATGCTCCGTCCTATAGTCAACATTTGAGAGGTAAC 300
                ************************************************************

NtCSPR          ATTACTCCTTCATTGCTTGAATTGCAACATCTGAAGCACCTAGACCTTAGTTACAATAAT 360
NbCSPR          ATTACTCCTTCATTGCTTGAATTGCAACATCTGAAGCACCTAGACCTTAGTTACAATGAT 360
                ************************************************************ **

NtCSPR          TTTGGTACAAGTCGAATACCGAATTTCATTGGTTCTTTTCCAAGACTGGAATATCTTTTT 420
NbCSPR          TTTGGTACAAGTCGAATACCAAATTTCATTGGTTCTTTTCCAAGACTGGAATATCTTTTT 420
                ******************* ************************************

NtCSPR          CTTGAGTATGCTAACTTGTCAGGTGAAATTCCTCACGCTCTTGGGAAACTTACCCATTTG 480
NbCSPR          CTTGAGGATGCTAGCTTGTCAGGGGAAATTCCTCACGCTCTTGGGAACCTTACCCATTTG 480
                ****** ****** ********* ********************** ************

NtCSPR          CAGATTCTTGACCTTAGCCTGAACTCCCGTCTAGTAGTGAAGAACCTTGAGTGGCTTCCT 540
NbCSPR          CAGATTCTTGACCTTAGCCTGAACTCCCGTCTAGTAGTGAAGAACCTTGAGTGGCTTCCT 540
                ************************************************************

NtCSPR          CGTCTTGTTTTTTTACTTGACCTTGACCTTTCTGGGGTTCATATTGAAACAGTCAATTGG 600
NbCSPR          CGTCTTGCTTTTTTACGCGACCTTGGCCTCTCTTTGGTTCATATTGAAACAGTCAATTGG 600
                ******* ********  ******* *** ***  ************************

NtCSPR          TTGCAACAAATAATTAAGTCCCCTTCTTTAGAACAATTGAATTTGGAACATTGCAACGTC 660
NbCSPR          TTACAACAAATAATTAAGTCCCCTTCTTTAGAACAATTGGATTTGAAACATTGCAACGTC 660
                ** ************************************ ***** *************


NtCSPR          CCCGAGCCAATCATATCAATATCTCATCTCTCATCCAATGTCTCTTCCCGTTTGCTTTCC 720
```

```
NbCSPR          CCCGAGCCAATCATATCAATATCTCATCTCTCATCCAATGTCTCTTCCCGTTTGCTTTCC 720
                ************************************************************

NtCSPR          AGCCTCAACCTTGCTGATACTGGGCTTTCCTCTTCTGCATTTCGGTGGTTGTTCAACTTG 780
NbCSPR          AGCCTCAACCTTGCTGACACTGGGCTTTCCTCTTCTGCATTTCGGTGGTTGTTCAACTTG 780
                ********** ************************************************

NtCSPR          AGTACGAGATTTACTTCCATAGATCTCTCTTCTAACCATTTAGCAGGCCGCATCCCTGAA 840
NbCSPR          AGTACGAGATTTACTTCCATAGATCTCTCTTCTAACAATTTAGCAGGTTGCATCCCTGAA 840
                ************************************ ********** ***********

NtCSPR          GCCTTTGGGTATATGCAACATCTTGAGTTCATTGACCTTGCTACAAATATTCTAGAAGGT 900
NbCSPR          GCCTTTGGGTATATGCAACATCTTGAGTTCATTGACCTTAATACAAATATTCTAGAAGGT 900
                ************************************ ********** ***********

NtCSPR          GGATTGCCCAAATCTTTTGGCAACTTGAGTCACTTAAGAGCCCTTGATTTATCAACTAAT 960
NbCSPR          GGATTGCCCAAATCTTTTGGCAACTTGAGCCACTTAAGAGCCCTTGATTTATCAACTAAT 960
                ************************** **************************** ***

NtCSPR          AACTTGAACCAACCACTTCCTGAATTATTTCTGAGCTTATCTGGTAAAGCAGAAAAATCA 1020
NbCSPR          AACTTGAACCAACCACTTCCTGAATTGTTTCTGAGCTTATCTGATAAAGCAGAAAAATCA 1020
                ************************ *************** ***************

NtCSPR          CTTGAAGAATTGCATTTATCTAACAATCATTTTAGTGGTTCATTGCCTGACATCACCAGA 1080
NbCSPR          CTTGAAGAATTGCATTTATCTAACAATCATCTTAGTGGTTCATTGCCTGACATCACCAGA 1080
                ***************************** ***************************** ***

NtCSPR          TTTTCATCCTTAAAAAGTTTGTACCTGCAAGAGAATCAACTGAATGGATCTTTCTTAGAA 1140
NbCSPR          TTTTCATCTTTGAAAAGTTTGTACCTGCAAGAGAATCAACTGAATGGATCTTTCTTTGAA 1140
                ******** ** ********************************************* ***

NtCSPR          AGCTATGGGCAGACTTCCAAGATCGAATTCCTCGATTTATCTTTGAATCAAATAACAGGA 1200
NbCSPR          AGCTACGGGCAGATTTCCAAGATCGAATTCCTCGATTTATCTTTGAATCAGTTAACAGGA 1200
                ***** ******* ************************************ ********

NtCSPR          CCTTTGCCAAACTTAACAGCATTTTCAGCATTAAGAGAGTTGCATTTGAACAATAACCAA 1260
NbCSPR          CCTTTGCCAAACTTAACAGCATTTTCAGCATTAAGAGAGTTGCATTTGAACAATAACCAA 1260
                ************************************************************

NtCSPR          TTCAAAGGGAGGTTACCCCAAAGTATAGGACGACTTTCAAAGCTTGAGATGTTGAGGGTC 1320
NbCSPR          TTCAAAGGGAGGTTACCCCAAAGTATAGGACGACTTTCAAAGCTTGAGATGTTGAGGGTC 1320
                ************************************************************

NtCSPR          GAATCAAATTTCATGGAAGGTCCAATCACAGAGTCACATCTTTCTAACCTTTCCAGCTTA 1380
NbCSPR          GAATCAAATTTCATGGAAGGTCCAATCACAGAGTCACATCTTTCAAACCTTTCCAGCTTA 1380
                ******************************************* **************

NtCSPR          AGAGTGTTGGACTTGTCATATAACTCCTTCTCTTTTCAGTTGGGACTTAATTGGCTTCCT 1440
NbCSPR          AGAGTGTTGGACTTGTCATATAACTCCTTCTCTTTTCAGTTGGGACTTAATTGGCTTCCT 1440
                ************************************************************


NtCSPR          CCTTTTGAATTAGATGTTATAGGTCTCTCCCATTGTAAAATGGGGCCTCATTTCCCACAG 1500
NbCSPR          CCTTTTGAATTAGATGTTATAAGTCTCTCCCATTGTAAAATGGGGCCTCATTTCCCACAG 1500
                ******************** ***************************************
```

```
NtCSPR          TGGCTACGAACTCAGAAGAGTTACTCACATCTTGATATCTCTTTCGCTGGTATATCAGGC 1560
NbCSPR          TGGCTACGAACTCAGAAGAATTACTCACATCTTGATATCTCTTTTGCTGGTATATCAGGC 1560
                ******************* ********************** ***************

NtCSPR          GTAGCACCTAACTGGTTTTGGGATCTTTCTCCTGAAATGATGCACTTTAGTATTTCCAAT 1620
NbCSPR          GTTGCACCTAACTGGTTTTGGGATCTTTCTCCTGAAATGATGCACTTTAGTATTTCCAAT 1620
                ** ************************************************************

NtCSPR          AACCAAATAAGTGGAGAGGTCCCTGATTTGTCTTCCAAGTTTGTAAAGGAAACTAATTAC 1680
NbCSPR          AACCAAATAAGTGGAGAGGTCCCTGATTTATCTTCCAAGTTTGTAAAGGAAACTAATTAT 1680
                ***************************** ****************************

NtCSPR          CCGACAATGGATTTTAGTTCGAATAATTTCTCGGGTTTAGTGCCATCATTCTCATCCAAC 1740
NbCSPR          CCGACAATGGATTTTAGTTCGAATAATTTCTCAGGTTTAGTGCCATCATTCTCATCCAAC 1740
                ******************************** ****************************

NtCSPR          TTGGAATCATTGAACCTTTCCAAAAACAAGTTTGTTGGATCAATTTCTTTCCTGTGCAAA 1800
NbCSPR          TTGGAATCATTGAACCTTTCCAAAAACAAGTTTGTTGGATCAATTTCTTTCCTGTGCAAA 1800
                ************************************************************

NtCSPR          ATAGCCAACGCTTTGTTCCGCACCATTGACCTCTCAAATAACCTACTTTCAGGAGAACTT 1860
NbCSPR          ATAGCCAACGCGTTGTTCCGCACCATTGACCTCTCAAATAACCTACTTTCAGGAGAACTT 1860
                ********** ************************************************

NtCSPR          CACAATTGTTTGATGGGATTTGAAGAACTAGCCATTCTTAATTTAGCTAACAACAATCTA 1920
NbCSPR          CACAATTGTTTGATGGGATTTGAAGAACTAGCCATTCTTAATTTAGCTAACAACAATCTA 1920
                ************************************************************

NtCSPR          TATGGTAAAATTCCCAGTTCCATTGGTTCTTTGTCGGATATCCAATCTCTACAGTTGCGG 1980
NbCSPR          TATGGTAAAATTCCCAGTTCCATTGGTTCTTTGTGGGATATCCAATCTCTACAGTTGCGG 1980
                ******************************** ************************

NtCSPR          AACAACAATTTTACTGGTGATCTGCCTACCTCTTTGAAAAACTGCGGAATATTGCAAATC 2040
NbCSPR          AACAACAATTTTACTGGTGATCTGCCTACCTCTTTGAAAAACTGCGGAATATTGCAAATC 2040
                ************************************************************

NtCSPR          TTGGACGTAGGAGGAAATAAGCTAAGTGGAGAAATACCATTATGGATTGGCTCACACTTA 2100
NbCSPR          TTGGATGTAGGAGGAAATAAGCTAAGTGGAGAAATACCATTATGGATTGGCTCACACTTA 2100
                ***** ******************************************************

NtCSPR          ACATTCTTGGTTGTCTTAAGTTTGAGACTCAACAAGTTCAATGGAAGCATACCTCAAAAT 2160
NbCSPR          ACATTCTTGGTTGTCTTAAGTTTGAGACTCAACAAGTTCAATGGAAGCATACCTCAAAAT 2160
                ************************************************************

NtCSPR          TTGTGTCATCTGAATAAAATCCATATTTTGGATCTTTCTCAGAACAGCTTATCTGGAGAA 2220
NbCSPR          TTCTGTCATCTGAATAAAATCCATATTTTGGATCTTTCTCAGAACAGCTTATCAGGAGAA 2220
                ** ********************************************** ******

NtCSPR          ATCCCCCGATGTCTCAACAATATCACATCTTTGCTTCAGAATAATAATAGTTCAACCCCA 2280
NbCSPR          ATCCCCCGATGTCTCAACAATATCACATCTTTGCTTCAGAATAATAATAGTTCAGACCCA 2280
                ************************************************  ****

NtCSPR          AGCATCCTTTTTGAATTAGGTGGAGACAGTCACAATGGCTATTCTTATTTTGAAGAATAC 2340
NbCSPR          AGCATCCTTTTTGCATTAGGTGGAGACAGTCACAATGGCTATTCTTATTATGAAGAATAC 2340
                ************ ********************************** **********
```

```
NtCSPR          TTGGGGGATGCATTAGTTCAATGGAAAAGCAGTGAATCTGTGTACAATAAGACACTCGGG 2400
NbCSPR          TTGGGGGATGCATTAGTTCAATGGAAAAGCAGTGAGTCTGTGTACAATAAGACACTCGGG 2400
                ********************************** ************************

NtCSPR          TTGTTGAAGATCATCGATTTTTCTAATAACGAGTTAGCTGGAAATGTTCCTGAAGAAATC 2460
NbCSPR          TTGTTGAAGATCATCGATTTTTCAAATAATGAGTTATCTGGAAATGTTCCTGAAGAAATC 2460
                ************************ ***** ****** ************************

NtCSPR          GCGCAACTGGATGGAGTGCTTTCACTAAACCTCTCGAGAAATAATTTAACAGGAAATGTA 2520
NbCSPR          GCGCAACTGAATGGAGTGCTTTCACTAAACCTCTCGAGAAATAATTTAACAGGAAATGTA 2520
                ********* ************************************************

NtCSPR          ATACAAGGAATTGGGAAGATGGAAAAGTTAGAGTCCCTTGATTTGTCTGGAAATCAGTTC 2580
NbCSPR          ATACAAGGAATTGGGAAGATGGAAAAGTTAGAGTCCCTTGATTTGTCCGGAAATCGGCTC 2580
                ************************************************ ******* * **

NtCSPR          ACTGGTCGAATTCCCACAAGTCTTGCTCAACTACATTTCCTAAGTGTCTTAGACTTGTCG 2640
NbCSPR          ACTGGTCGAATTCCCACAAGTCTTGCTCAACTACATTTCCTAAGTGTCTTAGACTTGTCG 2640
                ************************************************************

NtCSPR          AGTAACAACTTATCGGGGAAAATTCCTTCAAGCACTCAATTGCAGAGTTTTGATCCTTCA 2700
NbCSPR          AGTAACAACTTATCGGGGAAAATTCCTTCAAGCACACAATTGCAGAGTTTTGATCCTTCA 2700
                ********************************** ************************

NtCSPR          TCATATGAAGGAAACAATGAACTTTGTGGCCCACCACTTGCAGAATGTCCTGAAGATAGA 2760
NbCSPR          TCATATGAAGGAAACAATGAACTTTGTGGCCCACCACTTGCAGAATGTCCCGAAGATAGA 2760
                ************************************************ *********

NtCSPR          AATACTCAAAGCCTTTCTGCTGATCATAGCAAAATCAACAATCTTGATGAAGATGACAAG 2820
NbCSPR          AATACTCAAAGCCCTTCTGCTGATCATAGCAAAATCAACAATCTTGATGAAGATGACAAG 2820
                ************ ************************************************

NtCSPR          ATTCTGTCGTTTGGGTTTTATGTATGTGTGGCAAGTGGCTTCATTCTTGGATTTTGGGGA 2880
NbCSPR          ATTCTGTCGTTTGAGTTTTATGTATGTGTGGAAAGTGGCTTCATTCTTGGATTTTGGGGA 2880
                ************ ***************** ****************************

NtCSPR          GTAATATTTACTTTAGCCCTCAAGCAATCATTTAGAGATGCTTACTTTCAGAAGTTGACC 2940
NbCSPR          GTAGTATTCTCTTTAGTCCTCAACCAATCATTTAGAGATGCTTACTTTCAGAAGTTGACC 2940
                *** ****  ****** ****** ************************************

NtCSPR          AATTTCGCAAACTGGATCTTTGTGACAATAATAATGTCTCTACACAGATTGAAGATGATG 3000
NbCSPR          AATTTTGCAATTTGGATCTCTGCAACAATAGTAATGTTTCTTCACAGATTGAAGGTGCTC 3000
                ***** ****  ******* **  ****** ****** *** ************ ** *

NtCSPR          TGGAGCTAG 3009
NbCSPR          TGGAGTTAG 3009
                ***** ***
```

Attachment 6.

Table containing all proteins with their corresponding unique peptides identified by LC-MS/MS of proteins isolated from *Arabidopsis thaliana bak1-4*/35S::AtBAK1-YFP (BAK1) or *bak1-4*/35S::AtBAK1-5-YFP (BAK1-5) treated with sterile MQ-water or extract from *Puccinia striiformis* f. sp. *tritici* (spore extract). [4]

annotated as	Accession Number/ annotation	Molecular Weight	Unique Peptides			
			BAK1	BAK1 + spore extract	BAK1-5	BAK1-5 + spore extract
BAK1	AT4G33430	68 kDa	75	74	83	67
BIP	AT5G42020	74 kDa	180	139	189	187
BSK1	AT4G35230	57 kDa	0	0	1	6
BIR1	AT5G48380	69 kDa	1	0	1	5
BIR2	AT3G28450	65 kDa	8	3	8	7
BIR3	AT1G27190	67 kDa	30	16	29	26
LRR-RLK	AT2G04300	95 kDa	1	2	0	3
Protein of unknown function	AT2G32240	153kDa	1	9	1	3
LRR-RLK	AT3G14840	112 kDa	0	0	1	2
LRR-RLK	AT4G08850	115 kDa	0	0	3	3
LRR-RLP	AT1G33600	52 kDa	0	0	1	4
LRR-RLP	AT1G33590	52 kDa	8	0	20	18

LRR-RLP	AT5G23400	64 kDa	1	0	3	2
LRR-RLP	AT3G20820	40 kDa	12	10	8	11
Calnexin	AT5G61790	60 kDa	0	0	1	17
PEPR1	AT1G73080	123 kDa	1	3	4	1
Protein of unknown function	AT1G70770	67 kDa	0	0	4	8
__Symbols:_AAC1___ADP/ATP_carrier_1___chr3:2605706-2607030_REVERSE_LENGTH=381	AT3G08580.1 (+1)	41 kDa	15	25	2	1
__Symbols:_ACCD___acetyl-CoA_carboxylase_carboxyl_transferase_subunit_beta___chrC:57075-58541_FORWARD_LENGTH=488	ATCG00500.1	56 kDa	1	0	5	1
__Symbols:_ACLA-3___ATP-citrate_lyase_A-3___chr1:3042135-3044978_FORWARD_LENGTH=424	AT1G09430.1	47 kDa	0	0	0	2
__Symbols:_ACLB-2___ATP_citrate_lyase_subunit_B_2___chr5:20055048-20058195_FORWARD_LENGTH=608	AT5G49460.1	66 kDa	1	1	1	8
__Symbols:_ACT1,_AAc1___actin_1___chr2:15779761-15781241_FORWARD_LENGTH=377	AT2G37620.1 (+2)	42 kDa	1	2	0	1
__Symbols:_ACT7___actin_7___chr5:3052809-3054220_FORWARD_LENGTH=377	AT5G09810.1	42 kDa	37	26	23	35
__Symbols:_ACT8___actin_8___chr1:18216539-18217947_FORWARD_LENGTH=377	AT1G49240.1 (+1)	42 kDa	18	11	12	16
__Symbols:_ACX1,_ATACX1___acyl-CoA_oxidase_1___chr4:9424930-9428689_REVERSE_LENGTH=664	AT4G16760.1	74 kDa	0	0	2	2
__Symbols:_ADG1,_APS1___ADP_glucose_pyrophosphorylase__1___chr5:19570326-19572557_FORWARD_LENGTH=520	AT5G48300.1	57 kDa	4	1	5	1
__Symbols:_ADG2,_APL1___ADP_glucose_pyrophosphorylase_large_subunit_1___chr5:6463931-6466775_REVERSE_LENGTH=522	AT5G19220.1	58 kDa	2	0	5	1
__Symbols:_ADH1,_ADH,_ATADH,_ATADH1___alcohol_dehydrogenase_1___chr1:28975509-28977216_FORWARD_LENGTH=379	AT1G77120.1	41 kDa	0	0	2	2
__Symbols:_ADL1,_ADL1A,_AG68,_DRP1A,_RSW9,_DL1___dynamin-like_protein___chr5:16820661-16824536_REVERSE_LENGTH=610	AT5G42080.1 (+1)	68 kDa	0	0	3	3
__Symbols:_ADL3,_CF1,_DRP2B,_DL3___dynamin-like_3___chr1:21893413-21900780_FORWARD_LENGTH=920	AT1G59610.1	100 kDa	0	0	2	1
__Symbols:_AGT,_AGT1,_SGAT___alanine:glyoxylate_aminotransferase___chr2:5539417-5540902_REVERSE_LENGTH=401	AT2G13360.1 (+1)	44 kDa	2	1	4	3
__Symbols:_AHA1,_PMA,_OST2,_HA1___H(+)-ATPase_1___chr2:8221858-8227268_FORWARD_LENGTH=949	AT2G18960.1	104 kDa	3	4	9	3
__Symbols:_AIM1___Enoyl-CoA_hydratase/isomerase_family___chr4:14297312-14302016_REVERSE_LENGTH=721	AT4G29010.1	78 kDa	7	7	10	7
__Symbols:_AIR3___Subtilisin-like_serine_endopeptidase_family_protein___chr2:1401450-1407694_REVERSE_LENGTH=772	AT2G04160.1	83 kDa	0	1	1	3
__Symbols:_ALB1,_ALB-1V,_V157,_PDE166,_CHLD___ALBINA_1___chr1:2696538-2700819_FORWARD_LENGTH=760	AT1G08520.1	83 kDa	0	0	8	0
__Symbols:_ALDH2C4,_ALDH1A,_REF1___aldehyde_dehydrogenase_2C4___chr3:8919732-8923029_REVERSE_LENGTH=501	AT3G24503.1	54 kDa	4	0	4	8
__Symbols:_ANNAT4___annexin_4___chr2:16196582-16198431_REVERSE_LENGTH=319	AT2G38750.1	36 kDa	2	2	0	0

__Symbols:_AOS,_CYP74A,_DDE2___allene_oxide_synthase___chr5:17097803-17099359_REVERSE_LENGTH=518	AT5G42650.1	58 kDa	1	1	4	3
__Symbols:_APM1,_ATAPM1___aminopeptidase_M1___chr4:15965915-15970418_REVERSE_LENGTH=879	AT4G33090.1	98 kDa	0	0	3	2
__Symbols:_ARA12___Subtilase_family_protein___chr5:26872192-26874465_REVERSE_LENGTH=757	AT5G67360.1	79 kDa	31	30	30	29
__Symbols:_ARP1,_emb2207,_RPL3A,_RP1___ribosomal_protein_1___chr1:16266992-16268631_FORWARD_LENGTH=389	AT1G43170.1 (+7)	45 kDa	4	3	4	4
__Symbols:_ASN2___asparagine_synthetase_2___chr5:25969224-25972278_FORWARD_LENGTH=578	AT5G65010.1 (+1)	65 kDa	8	2	4	12
__Symbols:_ASP2,_AAT2___aspartate_aminotransferase_2___chr5:6598201-6601597_FORWARD_LENGTH=405	AT5G19550.1	44 kDa	1	1	2	3
__Symbols:_ATAMY3,_AMY3___alpha-amylase-like_3___chr1:26288518-26293003_REVERSE_LENGTH=887	AT1G69830.1	100 kDa	3	0	0	0
__Symbols:_ATBBC1,_BBC1,_RSU2___breast_basic_conserved_1___chr3:18166971-18168047_REVERSE_LENGTH=206	AT3G49010.1 (+3)	24 kDa	3	4	2	4
__Symbols:_ATBETA-AMY,_AT-BETA-AMY,_RAM1,_BMY1,_BAM5___beta-amylase_5___chr4:8666734-8669357_REVERSE_LENGTH=498	AT4G15210.1 (+1)	56 kDa	0	0	2	0
__Symbols:_ATCIMS,_ATMETS,_ATMS1___Cobalamin-independent_synthase_family_protein___chr5:5935771-5939195_FORWARD_LENGTH=765	AT5G17920.1 (+1)	84 kDa	8	12	29	35
__Symbols:_ATCWINV1,_ATBFRUCT1___Glycosyl_hydrolases_family_32_protein___chr3:4533084-4535831_REVERSE_LENGTH=584	AT3G13790.1 (+1)	66 kDa	3	4	8	2
__Symbols:_ATG2,_EBP1,_ATEBP1___metallopeptidase_M24_family_protein___chr3:19211261-19213568_REVERSE_LENGTH=392	AT3G51800.1 (+2)	43 kDa	1	0	1	6
__Symbols:_ATGCN1,_GCN1___ABC_transporter_family_protein___chr5:24453760-24455767_REVERSE_LENGTH=595	AT5G60790.1	67 kDa	0	0	6	2
__Symbols:_ATGCN4,_GCN4___general_control_non-repressible_4___chr3:20190393-20192564_FORWARD_LENGTH=723	AT3G54540.1	80 kDa	0	3	17	8
__Symbols:_ATHXK1,_GIN2,_HXK1___hexokinase_1___chr4:14352338-14354865_REVERSE_LENGTH=496	AT4G29130.1	54 kDa	1	0	4	2
__Symbols:_ATIMD1,_IMD1___isopropylmalate_dehydrogenase_1___chr5:4576220-4578111_FORWARD_LENGTH=409	AT5G14200.1 (+2)	44 kDa	0	0	0	2
__Symbols:_ATJ2,_J2___DNAJ_homologue_2___chr5:7303798-7305668_REVERSE_LENGTH=419	AT5G22060.1	46 kDa	0	0	2	1
__Symbols:_ATJ3,_ATJ___DNAJ_homologue_3___chr3:15869115-15871059_REVERSE_LENGTH=420	AT3G44110.1	46 kDa	4	0	6	4
__Symbols:_ATKRS-1___lysyl-tRNA_synthetase_1___chr3:3702359-3705613_REVERSE_LENGTH=626	AT3G11710.1	71 kDa	1	0	6	9
__Symbols:_ATL5,_PGY3,_OLI5,_RPL5A___ribosomal_protein_L5___chr3:9269573-9271327_REVERSE_LENGTH=301	AT3G25520.1	34 kDa	4	4	2	2
__Symbols:_ATMDAR1,_MDAR1___monodehydroascorbate_reductase_1___chr3:19601477-19604366_REVERSE_LENGTH=434	AT3G52880.1 (+1)	46 kDa	0	0	1	2
__Symbols:_ATMES14,_MES14___methyl_esterase_14___chr1:12355909-12357894_FORWARD_LENGTH=348	AT1G33990.1	39 kDa	2	0	0	0
__Symbols:_ATMLP-470,_NSP1,_ATNSP1___nitrile_specifier_protein_1___chr3:5566516-5568330_FORWARD_LENGTH=470	AT3G16400.1 (+2)	52 kDa	4	3	3	6
__Symbols:_ATNADP-ME2,_NADP-ME2___NADP-malic_enzyme_2___chr5:3754456-3758040_FORWARD_LENGTH=588	AT5G11670.1	64 kDa	0	0	3	6

__Symbols:_ATNIFS1,_NIFS1,_NFS1,_ATNFS1___nitrogen_fixation_S_(NIFS)-like_1___chr5:26296349-26297710_FORWARD_LENGTH=453	AT5G65720.1	50 kDa	0	0	2	2
__Symbols:_ATPS8IPK,_PS8IPK___homolog_of_mamallian_PS8IPK___chr5:750286-752671_FORWARD_LENGTH=482	AT5G03160.1	54 kDa	0	0	0	2
__Symbols:_ATPA___ATP_synthase_subunit_alpha___chrC:9938-11461_REVERSE_LENGTH=507	ATCG00120.1	55 kDa	47	31	40	46
__Symbols:_ATPB,_PB___ATP_synthase_subunit_beta___chrC:52660-54156_REVERSE_LENGTH=498	ATCG00480.1	54 kDa	40	36	60	56
__Symbols:_ATPC1___ATPase,_F1_complex,_gamma_subunit_protein___chr4:2350761-2351882_REVERSE_LENGTH=373	AT4G04640.1	41 kDa	3	2	0	1
__Symbols:_ATPDIL1-1,_ATPDI5,_PDI5,_PDIL1-1___PDI-like_1-1___chr1:7645767-7648514_FORWARD_LENGTH=501	AT1G21750.1	56 kDa	0	0	0	10
__Symbols:_ATPDIL1-2,_PDI6,_ATPDI6,_PDIL1-2___PDI-like_1-2___chr1:29126742-29129433_FORWARD_LENGTH=508	AT1G77510.1	56 kDa	0	0	0	8
__Symbols:_ATPDIL2-1,_UNE5,_MEE30,_PDI11,_ATPDI11___thioredoxin_family_protein___chr2:19481503-19483683_FORWARD_LENGTH=361	AT2G47470.1 (+1)	39 kDa	8	4	4	10
__Symbols:_ATPDIL2-3,_PDI9,_ATPDI9,_PDIL2-3___PDI-like_2-3___chr2:13962502-13965406_REVERSE_LENGTH=440	AT2G32920.1	48 kDa	2	0	3	9
__Symbols:_ATPME3,_PME3___pectin_methylesterase_3___chr3:4772214-4775095_REVERSE_LENGTH=592	AT3G14310.1	64 kDa	2	1	0	0
__Symbols:_ATPPC1,_PEPC1,_ATPEPC1,_PPC1___phosphoenolpyruvate_carboxylase_1___chr1:19884261-19888070_REVERSE_LENGTH=967	AT1G53310.1 (+2)	110 kDa	1	3	6	6
__Symbols:_ATRAB8D,_ATRABE1B,_RABE1b___RAB_GTPase_homolog_E1B___chr4:10990036-10991466_FORWARD_LENGTH=476	AT4G20360.1	52 kDa	36	35	25	30
__Symbols:_ATSPS1F,_SPS1F___sucrose_phosphate_synthase_1F___chr5:6844994-6849997_REVERSE_LENGTH=1043	AT5G20280.1	117 kDa	0	0	2	0
__Symbols:_ATTIC110,_TIC110___translocon_at_the_inner_envelope_membrane_of_chloroplasts_110___chr1:2130303-2135563_REVERSE_LENGTH=1016	AT1G06950.1	112 kDa	2	1	5	7
__Symbols:_ATTLL1,_TLL1___triacylglycerol_lipase-like_1___chr1:17123889-17128462_FORWARD_LENGTH=479	AT1G45201.1 (+1)	55 kDa	2	2	1	2
__Symbols:_ATXYL1,_XYL1,_TRG1___alpha-xylosidase_1___chr1:25734435-25737897_REVERSE_LENGTH=915	AT1G68560.1	102 kDa	0	4	4	3
__Symbols:_AXR4,_RGR,_RGR1___alpha/beta-Hydrolases_superfamily_protein___chr1:20511565-20513489_FORWARD_LENGTH=473	AT1G54990.1	52 kDa	0	0	0	2
__Symbols:_AtGLDP1,_GLDP1___glycine_decarboxylase_P-protein_1___chr4:15926852-15931150_REVERSE_LENGTH=1037	AT4G33010.1	113 kDa	2	7	9	1
__Symbols:_AtGUS2,_GUS2___glucuronidase_2___chr5:2504168-2506567_FORWARD_LENGTH=543	AT5G07830.1	60 kDa	4	0	2	2
__Symbols:_B73,_SIR4,_CNX,_CHL6,_CNX1___molybdopterin_biosynthesis_CNX1_protein_/_molybdenum_cofactor_biosynthesis_enzyme_CNX1_(CNX1)___chr5:7128737-7133397_REVERSE_LENGTH=670	AT5G20990.1	71 kDa	0	0	2	4
__Symbols:_BGAL1___beta_galactosidase_1___chr3:4511192-4515756_FORWARD_LENGTH=847	AT3G13750.1	94 kDa	12	13	17	15
__Symbols:_BGL1,_BGLU18,_ATBG1___beta_glucosidase_18___chr1:19515250-19517930_FORWARD_LENGTH=528	AT1G52400.1 (+1)	60 kDa	1	0	4	8
__Symbols:_BGLU21___Glycosyl_hydrolase_superfamily_protein___chr1:24700110-24702995_REVERSE_LENGTH=524	AT1G66270.1 (+1)	60 kDa	0	0	7	12

__Symbols:_BGLU22___Glycosyl_hydrolase_superfamily_protein___chr1:24706759-24709737_REVERSE_LENGTH=524	AT1G66280.1	60 kDa	0	1	4	6
__Symbols:_BGLU34,_TGG4___beta_glucosidase_34___chr1:17491771-17494589_FORWARD_LENGTH=511	AT1G47600.1 (+1)	58 kDa	0	0	1	2
__Symbols:_BGLU35,_TGG5___beta_glucosidase_35___chr1:19087424-19090248_FORWARD_LENGTH=511	AT1G51470.1	57 kDa	1	0	2	2
__Symbols:_BGLU44___B-S_glucosidase_44___chr3:6191586-6194124_FORWARD_LENGTH=512	AT3G18080.1	59 kDa	9	10	21	24
__Symbols:_BIP1___heat_shock_protein_70_(Hsp_70)_family_protein___chr5:10540665-10543274_REVERSE_LENGTH=669	AT5G28540.1	74 kDa	14	13	13	10
__Symbols:_BXL1,_ATBXL1___beta-xylosidase_1___chr5:20012179-20016659_REVERSE_LENGTH=774	AT5G49360.1	84 kDa	13	9	18	20
__Symbols:_CAB3,_AB180,_LHCB1.2___chlorophyll_A/B_binding_protein_3___chr1:10472443-10473246_REVERSE_LENGTH=267	AT1G29910.1 (+3)	28 kDa	2	3	3	0
__Symbols:_CAC2___acetyl_Co-enzyme_a_carboxylase_biotin_carboxylase_subunit___chr5:13584300-13588268_FORWARD_LENGTH=537	AT5G35360.1 (+1)	58 kDa	7	1	9	5
__Symbols:_CAC3___acetyl_Co-enzyme_a_carboxylase_carboxyltransferase_alpha_subunit___chr2:15917612-15920749_FORWARD_LENGTH=769	AT2G38040.1 (+1)	85 kDa	2	1	6	4
__Symbols:_CAT2___catalase_2___chr4:16700937-16703215_REVERSE_LENGTH=492	AT4G35090.1	57 kDa	18	4	19	16
__Symbols:_CAT3,_SEN2,_ATCAT3___catalase_3___chr1:7143142-7146193_FORWARD_LENGTH=492	AT1G20620.1	57 kDa	44	30	62	52
__Symbols:_CDC48,_ATCDC48,_CDC48A___cell_division_cycle_48___chr3:3019494-3022832_FORWARD_LENGTH=809	AT3G09840.1	89 kDa	0	0	2	4
__Symbols:_CDPK6,_CPK3___calcium-dependent_protein_kinase_6___chr4:12324967-12327415_REVERSE_LENGTH=529	AT4G23650.1	59 kDa	1	1	3	2
__Symbols:_CLPC,_ATHSP93-V,_HSP93-V,_DCA1,_CLPC1___CLPC_homologue_1___chr5:20715710-20719800_REVERSE_LENGTH=929	AT5G50920.1	?	16	19	34	24
__Symbols:_CNX1,_ATCNX1___calnexin_1___chr5:24827394-24829642_REVERSE_LENGTH=530	AT5G61790.1	60 kDa	0	0	1	17
__Symbols:_CORI3,_JR2___Tyrosine_transaminase_family_protein___chr4:12310657-12312885_FORWARD_LENGTH=422	AT4G23600.1	47 kDa	10	1	2	9
__Symbols:_CPHSC70-2EAT_SHOCK_PROTEIN_70-2,_HSC70-7,_cpHsc70-2___chloroplast_heat_shock_protein_70-2___chr5:20303470-20306295_FORWARD_LENGTH=718	AT5G49910.1	77 kDa	2	4	4	3
__Symbols:_CPN60A,_CH-CPN60A,_SLP___chaperonin-60alpha___chr2:11926603-11929184_FORWARD_LENGTH=586	AT2G28000.1	62 kDa	13	11	13	24
__Symbols:_CPN60B,_LEN1___chaperonin_60_beta___chr1:20715717-20718673_REVERSE_LENGTH=600	AT1G55490.1 (+1)	64 kDa	16	7	17	24
__Symbols:_CR88,_EMB1956,_HSP90.5,_Hsp88.1,_AtHsp90.5___Chaperone_protein_htpG_family_protein___chr2:1281983-1285909_FORWARD_LENGTH=780	AT2G04030.1 (+1)	89 kDa	6	6	9	9
__Symbols:_CRB,_CSP41B,_HIP1.3___chloroplast_RNA_binding___chr1:3015473-3018035_FORWARD_LENGTH=378	AT1G09340.1	43 kDa	6	0	3	1
__Symbols:_CRT1,_CRT1a,_AtCRT1a___calreticulin_1a___chr1:21090022-21092630_REVERSE_LENGTH=424	AT1G56340.2	49 kDa	2	1	1	12
__Symbols:_CRT1b,_AtCRT1b___calreticulin_1b___chr1:2973217-2976655_REVERSE_LENGTH=424	AT1G09210.1	48 kDa	0	0	1	13

__Symbols:_CRT3,_PSL1,_EBS2,_AtCRT3___calreticulin_3___chr1:2668008-2671800_REVERSE_LENGTH=424	AT1G08450.1	50 kDa	0	0	3	9
__Symbols:_CRU3,_CRC___cruciferin_3___chr4:14087596-14089617_FORWARD_LENGTH=524	AT4G28520.1 (+3)	58 kDa	0	2	0	0
__Symbols:_CSI1___binding___chr2:9406793-9414223_FORWARD_LENGTH=2150	AT2G22125.1	231 kDa	0	1	0	2
__Symbols:_CYP706A1___cytochrome_P450,_family_706,_subfamily_A,_polypeptide_1___chr4:11929847-11931520_FORWARD_LENGTH=557	AT4G22690.1 (+1)	63 kDa	0	0	2	0
__Symbols:_CaS___calcium_sensing_receptor___chr5:7736760-7738412_REVERSE_LENGTH=387	AT5G23060.1	41 kDa	6	6	1	1
__Symbols:_DGL1___dolichyl-diphosphooligosaccharide-protein_glycosyltransferase_48kDa_subunit_family_protein___chr5:26617840-26620581_REVERSE_LENGTH=437	AT5G66680.1	49 kDa	0	0	0	5
__Symbols:_DHS1___3-deoxy-D-arabino-heptulosonate_7-phosphate_synthase_1___chr4:18539654-18541832_FORWARD_LENGTH=525	AT4G39980.1	58 kDa	9	3	7	7
__Symbols:_DIN10___Raffinose_synthase_family_protein___chr5:6834207-6836635_FORWARD_LENGTH=749	AT5G20250.1 (+3)	83 kDa	0	0	2	0
__Symbols:_DPE2___disproportionating_enzyme_2___chr2:17045368-17050779_FORWARD_LENGTH=955	AT2G40840.1	110 kDa	0	2	4	0
__Symbols:_DRH1,_ATDRH1___DEAD_box_RNA_helicase_1___chr3:213077-216142_REVERSE_LENGTH=618	AT3G01540.1 (+3)	68 kDa	0	0	0	2
__Symbols:_DWF1,_DIM,_EVE1,_DIM1,_CBB1___cell_elongation_protein_/_DWARF1_/_DIMINUTO_(DIM)___chr3:6879835-6881616_REVERSE_LENGTH=561	AT3G19820.1 (+2)	65 kDa	3	4	10	10
__Symbols:_ECT2___evolutionarily_conserved_C-terminal_region_2___chr3:4385274-4388220_REVERSE_LENGTH=667	AT3G13460.1 (+2)	72 kDa	2	0	0	4
__Symbols:_EDA38,_SBP2___selenium-binding_protein_2___chr4:8100691-8102828_REVERSE_LENGTH=487	AT4G14040.1	54 kDa	4	0	4	6
__Symbols:_EDA9___D-3-phosphoglycerate_dehydrogenase___chr4:16374041-16376561_REVERSE_LENGTH=603	AT4G34200.1	63 kDa	1	0	4	6
__Symbols:_EIF2_GAMMA___eukaryotic_translation_initiation_factor_2_gamma_subunit___chr1:1097423-1099702_FORWARD_LENGTH=465	AT1G04170.1	51 kDa	7	2	15	5
__Symbols:_EIF3A,_ATEIF3A-1,_EIF3A-1,_ATTIF3A1,_TIF3A1___eukaryotic_translation_initiation_factor_3A___chr4:6947834-6952053_REVERSE_LENGTH=987	AT4G11420.1	?	0	1	9	10
__Symbols:_EIF3C,_ATEIF3C-1,_EIF3C-1,_ATTIF3C1,_TIF3C1___eukaryotic_translation_initiation_factor_3C___chr3:20833790-20836820_REVERSE_LENGTH=900	AT3G56150.1 (+1)	103 kDa	2	4	6	4
__Symbols:_EIF3E,_TIF3E1,_ATEIF3E-1,_INT-6,_ATINT6,_INT6___eukaryotic_translation_initiation_factor_3E___chr3:21196786-21199073_REVERSE_LENGTH=441	AT3G57290.1	52 kDa	0	0	4	0
__Symbols:_EIF4A1,_RH4,_TIF4A1___eukaryotic_translation_initiation_factor_4A1___chr3:4592635-4594128_REVERSE_LENGTH=412	AT3G13920.1 (+1)	47 kDa	15	6	8	16
__Symbols:_EIF4B2___eukaryotic_initiation_factor_4B2___chr1:4440927-4443520_REVERSE_LENGTH=549	AT1G13020.1	59 kDa	0	4	0	3
__Symbols:_EMB1290,_DUF26-21,_RKC1,_CRK17___kinases;protein_kinases___chr4:12162004-12167026_REVERSE_LENGTH=1035	AT4G23250.1	116 kDa	0	0	0	3
__Symbols:_EMB1467,_CI76___NADH-ubiquinone_dehydrogenase,_mitochondrial,_putative___chr5:14897490-14900352_FORWARD_LENGTH=745	AT5G37510.1 (+1)	81 kDa	0	1	4	5

__Symbols:_EMB2296___Ribosomal_protein_L2_family___chr2:7837151-7838160_FORWARD_LENGTH=258	AT2G18020.1	28 kDa	6	2	4	4
__Symbols:_EMB2719,_HAP15___PAM_domain_(PCI/PINT_associated_module)_protein___chr1:7001409-7004154_REVERSE_LENGTH=488	AT1G20200.1	56 kDa	1	0	2	2
__Symbols:_EMB2753___tetratricopeptide_repeat_(TPR)-containing_protein___chr1:30227963-30234832_REVERSE_LENGTH=897	AT1G80410.1 (+1)	102 kDa	6	9	19	6
__Symbols:_EMB3003___2-oxoacid_dehydrogenases_acyltransferase_family_protein___chr1:12588027-12590084_REVERSE_LENGTH=465	AT1G34430.1	48 kDa	10	3	9	8
__Symbols:_ESM1___epithiospecifier_modifier_1___chr3:4729886-4731562_FORWARD_LENGTH=392	AT3G14210.1	44 kDa	11	4	10	12
__Symbols:_FBA1___fructose-bisphosphate_aldolase_1___chr2:9128416-9130152_REVERSE_LENGTH=399	AT2G21330.1 (+1)	43 kDa	2	2	1	2
__Symbols:_FBA2___fructose-bisphosphate_aldolase_2___chr4:18163714-18165659_REVERSE_LENGTH=398	AT4G38970.1 (+1)	43 kDa	8	6	3	4
__Symbols:_FDH___formate_dehydrogenase___chr5:4777043-4779190_FORWARD_LENGTH=384	AT5G14780.1	42 kDa	1	0	4	2
__Symbols:_FUM1___fumarase_1___chr2:19498614-19502020_FORWARD_LENGTH=492	AT2G47510.1 (+1)	53 kDa	1	0	7	5
__Symbols:_FVE,_ACG1,_MSI4,_NFC4,_NFC04,_ATMSI4___Transducin_family_protein_/_WD-40_repeat_family_protein___chr2:8456006-8459235_FORWARD_LENGTH=507	AT2G19520.1	56 kDa	0	1	2	2
__Symbols:_GAD2___glutamate_decarboxylase_2___chr1:24552094-24557253_FORWARD_LENGTH=494	AT1G65960.2	56 kDa	0	0	2	2
__Symbols:_GAPA,_GAPA-1___glyceraldehyde_3-phosphate_dehydrogenase_A_subunit___chr3:9795226-9796848_FORWARD_LENGTH=396	AT3G26650.1	42 kDa	11	3	2	2
__Symbols:_GAPA-2___glyceraldehyde_3-phosphate_dehydrogenase_A_subunit_2___chr1:4392634-4394283_REVERSE_LENGTH=399	AT1G12900.1	43 kDa	2	0	0	0
__Symbols:_GAPB___glyceraldehyde-3-phosphate_dehydrogenase_B_subunit___chr1:16127552-16129584_FORWARD_LENGTH=447	AT1G42970.1	48 kDa	42	27	26	34
__Symbols:_GAPC-2,_GAPC2___glyceraldehyde-3-phosphate_dehydrogenase_C2___chr1:4608465-4610494_REVERSE_LENGTH=338	AT1G13440.1	37 kDa	14	10	8	16
__Symbols:_GDH2___glutamate_dehydrogenase_2___chr5:2356153-2358012_FORWARD_LENGTH=411	AT5G07440.1 (+1)	45 kDa	9	3	7	9
__Symbols:_GGT1,_AOAT1,_GGAT1___glutamate:glyoxylate_aminotransferase___chr1:8268720-8271329_REVERSE_LENGTH=481	AT1G23310.1	53 kDa	1	0	3	1
__Symbols:_GLU1,_GLS1,_GLUS,_FD-GOGAT___glutamate_synthase_1___chr5:1130031-1138186_FORWARD_LENGTH=1622	AT5G04140.1 (+1)	177 kDa	0	15	6	5
__Symbols:_GME___GDP-D-mannose_3',5'-epimerase___chr5:10862472-10864024_REVERSE_LENGTH=377	AT5G28840.1 (+1)	43 kDa	1	0	1	2
__Symbols:_GS2,_GLN2,_ATGSL1___glutamine_synthetase_2___chr5:13831220-13833239_FORWARD_LENGTH=430	AT5G35630.1 (+2)	47 kDa	7	3	6	9
__Symbols:_HAP6___ribophorin_II_(RPN2)_family_protein___chr4:11278646-11283599_FORWARD_LENGTH=691	AT4G21150.1 (+2)	75 kDa	1	1	1	4
__Symbols:_HCEF1___high_cyclic_electron_flow_1___chr3:20016951-20018527_FORWARD_LENGTH=417	AT3G54050.1 (+1)	45 kDa	14	1	4	8
__Symbols:_HDA05,_HDA5,_ATHDA5___histone_deacetylase_5___chr5:24567137-24570917_REVERSE_LENGTH=660	AT5G61060.1 (+1)	73 kDa	7	12	11	4

__Symbols:_HEMB1___Aldolase_superfamily_protein___chr1:26232197-26234713_FORWARD_LENGTH=430	AT1G69740.1 (+1)	47 kDa	0	0	0	2
__Symbols:_HOG1,_EMB1395,_SAHH1,_MEE58,_ATSAHH1___S-adenosyl-L-homocysteine_hydrolase___chr4:8054931-8056676_FORWARD_LENGTH=485	AT4G13940.1	53 kDa	6	2	9	11
__Symbols:_HPR,_ATHPR1___hydroxypyruvate_reductase___chr1:25493418-25495720_FORWARD_LENGTH=386	AT1G68010.1 (+1)	42 kDa	3	1	5	4
__Symbols:_HSC70-1,_HSP70-1,_AT-HSC70-1,_HSC70___heat_shock_cognate_protein_70-1___chr5:554055-556334_REVERSE_LENGTH=651	AT5G02500.1	71 kDa	52	53	55	49
__Symbols:_HSP60,_HSP60-3B___heat_shock_protein_60___chr3:8669013-8672278_FORWARD_LENGTH=577	AT3G23990.1	61 kDa	5	3	2	19
__Symbols:_HSP60-2___heat_shock_protein_60-2___chr2:14075093-14078568_REVERSE_LENGTH=585	AT2G33210.1 (+1)	62 kDa	1	0	0	3
__Symbols:_HSP60-3A___heat_shock_protein_60-3A___chr3:4561704-4565133_REVERSE_LENGTH=572	AT3G13860.1	60 kDa	0	0	0	2
__Symbols:_HSP70,_ATHSP70___heat_shock_protein_70___chr3:3991487-3993689_REVERSE_LENGTH=650	AT3G12580.1	71 kDa	0	1	1	10
__Symbols:_HSP81-1,_ATHS83,_HSP81.1,_HSP83,_ATHSP90.1,_AtHsp90-1,_HSP90.1___heat_shock_protein_90.1___chr5:21352542-21355147_FORWARD_LENGTH=705	AT5G52640.1	81 kDa	0	1	3	9
__Symbols:_HSP81-2,_ERD8,_HSP90.2,_AtHsp90.2___heat_shock_protein_81-2___chr5:22686923-22689433_FORWARD_LENGTH=699	AT5G56030.1	80 kDa	13	10	24	50
__Symbols:_HSP81-3,_Hsp81.3,_AtHsp90-3,_AtHsp90.3___heat_shock_protein_81-3___chr5:22681410-22683911_FORWARD_LENGTH=699	AT5G56010.1	80 kDa	1	0	1	5
__Symbols:_Hsp70b___heat_shock_protein_70B___chr1:5502386-5504326_REVERSE_LENGTH=646	AT1G16030.1	71 kDa	0	2	1	1
__Symbols:_IBR3___acyl-CoA_dehydrogenase-related___chr3:2146534-2150654_FORWARD_LENGTH=824	AT3G06810.1	92 kDa	0	10	6	1
__Symbols:_IMPA-2___importin_alpha_isoform_2___chr4:9134450-9137134_REVERSE_LENGTH=535	AT4G16143.1 (+1)	59 kDa	1	1	0	2
__Symbols:_JAL22___jacalin-related_lectin_22___chr2:16414262-16416323_REVERSE_LENGTH=458	AT2G39310.1 (+1)	50 kDa	0	0	4	5
__Symbols:_JAL23___jacalin-related_lectin_23___chr2:16419787-16421573_REVERSE_LENGTH=459	AT2G39330.1	50 kDa	0	0	2	0
__Symbols:_JR1___Mannose-binding_lectin_superfamily_protein___chr3:5596096-5597709_REVERSE_LENGTH=451	AT3G16470.1 (+1)	48 kDa	5	0	10	8
__Symbols:_KASI,_KAS1___3-ketoacyl-acyl_carrier_protein_synthase_I___chr5:18774439-18776629_REVERSE_LENGTH=473	AT5G46290.1 (+2)	50 kDa	0	0	0	2
__Symbols:_KAS_III___3-ketoacyl-acyl_carrier_protein_synthase_III___chr1:23192502-23194737_FORWARD_LENGTH=404	AT1G62640.1 (+1)	43 kDa	2	0	0	0
__Symbols:_LACS4___AMP-dependent_synthetase_and_ligase_family_protein___chr4:12403720-12408263_REVERSE_LENGTH=666	AT4G23850.1	75 kDa	0	0	3	3
__Symbols:_LACS6,_ATLACS6___long-chain_acyl-CoA_synthetase_6___chr3:1786510-1791746_REVERSE_LENGTH=701	AT3G05970.1	77 kDa	0	1	0	3
__Symbols:_LOS1___Ribosomal_protein_S5/Elongation_factor_G/III/V_family_protein___chr1:20968245-20971077_REVERSE_LENGTH=843	AT1G56070.1	94 kDa	10	12	33	40
__Symbols:_LOS2,_ENO2___Enolase___chr2:15321081-15323786_REVERSE_LENGTH=444	AT2G36530.1	48 kDa	7	0	14	11

__Symbols:_LOX2,_ATLOX2___lipoxygenase_2___chr3:16525437-16529233_FORWARD_LENGTH=896	AT3G45140.1	102 kDa	25	41	51	26
__Symbols:_LPD1,_ptlpd1___lipoamide_dehydrogenase_1___chr3:5786761-5790383_REVERSE_LENGTH=570	AT3G16950.1	61 kDa	2	0	2	3
__Symbols:_LTA2,_PLE2___2-oxoacid_dehydrogenases_acyltransferase_family_protein___chr3:9460632-9462585_FORWARD_LENGTH=480	AT3G25860.1	50 kDa	23	11	23	17
__Symbols:_LTA3___Dihydrolipoamide_acetyltransferase,_long_form_protein___chr3:19360317-19366091_FORWARD_LENGTH=637	AT3G52200.1 (+1)	69 kDa	2	2	1	2
__Symbols:_LTI29,_LTI45,_ERD10___Dehydrin_family_protein___chr1:7088235-7089107_REVERSE_LENGTH=260	AT1G20450.1 (+1)	30 kDa	2	0	0	1
__Symbols:_MAB1___Transketolase_family_protein___chr5:20689671-20692976_FORWARD_LENGTH=363	AT5G50850.1	39 kDa	2	0	1	0
__Symbols:_MAML-4,_IPMS1___methylthioalkylmalate_synthase-like_4___chr1:6369347-6372861_FORWARD_LENGTH=631	AT1G18500.1	69 kDa	4	0	0	3
__Symbols:_MAT3___methionine_adenosyltransferase_3___chr2:15479721-15480893_REVERSE_LENGTH=390	AT2G36880.1 (+1)	42 kDa	1	0	0	2
__Symbols:_MEE5,_CLO,_GFA1___Ribosomal_protein_S5/Elongation_factor_G/III/V_family_protein___chr1:1900524-1904583_FORWARD_LENGTH=987	AT1G06220.1 (+1)	110 kDa	0	0	2	2
__Symbols:_MFP2,_ATMFP2___multifunctional_protein_2___chr3:2161926-2166009_FORWARD_LENGTH=725	AT3G06860.1	79 kDa	0	0	5	1
__Symbols:_MPPBETA___Insulinase_(Peptidase_family_M16)_protein___chr3:365624-368526_FORWARD_LENGTH=531	AT3G02090.1	59 kDa	8	12	9	13
__Symbols:_MTHFR1___methylenetetrahydrofolate_reductase_1___chr3:22151303-22154323_FORWARD_LENGTH=592	AT3G59970.3	66 kDa	0	0	0	4
__Symbols:_MTHSC70-2,_HSC70-5___mitochondrial_HSO70_2___chr5:2975721-2978508_FORWARD_LENGTH=682	AT5G09590.1	73 kDa	3	5	6	11
__Symbols:_MTO3,_SAMS3,_MAT4___S-adenosylmethionine_synthetase_family_protein___chr3:5952484-5953665_REVERSE_LENGTH=393	AT3G17390.1	43 kDa	10	7	8	17
__Symbols:_NAI2___DNA_topoisomerase-related___chr3:5397783-5402610_REVERSE_LENGTH=772	AT3G15950.1	85 kDa	2	8	10	13
__Symbols:_NAP1;1,_ATNAP1;1___nucleosome_assembly_protein1;1___chr4:13232712-13235502_FORWARD_LENGTH=372	AT4G26110.1 (+1)	43 kDa	2	0	4	5
__Symbols:_NFA02,_NFA2,_NAP1;2___nucleosome_assembly_protein_1;2___chr2:8438601-8441040_FORWARD_LENGTH=379	AT2G19480.1 (+2)	44 kDa	3	1	7	5
__Symbols:_NHL3___NDR1/HIN1-like_3___chr5:1931016-1931711_REVERSE_LENGTH=231	AT5G06320.1	26 kDa	1	2	0	0
__Symbols:_NIT1,_ATNIT1,_NIT1___nitrilase_1___chr3:15986901-15988841_FORWARD_LENGTH=346	AT3G44310.1 (+1)	38 kDa	8	1	1	1
__Symbols:_NOP56___homolog_of_nucleolar_protein_NOP56___chr1:20984544-20986893_REVERSE_LENGTH=522	AT1G56110.1	59 kDa	0	0	0	2
__Symbols:_NQR___ARP_protein_(REF)___chr1:18381591-18386021_REVERSE_LENGTH=629	AT1G49670.1 (+1)	68 kDa	0	0	2	0
__Symbols:_NTRC___NADPH-dependent_thioredoxin_reductase_C___chr2:17376349-17379028_REVERSE_LENGTH=529	AT2G41680.1	58 kDa	2	0	1	3
__Symbols:_OPR1,_ATOPR1___12-oxophytodienoate_reductase_1___chr1:28776982-28778271_FORWARD_LENGTH=372	AT1G76680.1 (+1)	41 kDa	3	2	0	4
__Symbols:_P40,_AP40,_RP40,_RPSAA___40s_ribosomal_protein_SA___chr1:27243148-27244842_REVERSE_LENGTH=298	AT1G72370.1 (+1)	32 kDa	2	0	1	0

__Symbols:_P5CS1,_ATP5CS___delta1-pyrroline-5-carboxylate_synthase_1___chr2:16598516-16602939_REVERSE_LENGTH=717	AT2G39800.1 (+3)	78 kDa	0	0	2	4
__Symbols:_PAB2,_PABP2,_ATPAB2___poly(A)_binding_protein_2___chr4:16336732-16339892_FORWARD_LENGTH=629	AT4G34110.1	69 kDa	0	0	0	2
__Symbols:_PAB8,_PABP8___poly(A)_binding_protein_8___chr1:18416740-18419753_FORWARD_LENGTH=671	AT1G49760.1 (+1)	73 kDa	4	2	1	10
__Symbols:_PATL1___PATELLIN_1___chr1:27148558-27150652_FORWARD_LENGTH=573	AT1G72150.1	64 kDa	0	2	3	16
__Symbols:_PATL2___PATELLIN_2___chr1:7955773-7958326_REVERSE_LENGTH=683	AT1G22530.1	76 kDa	0	0	0	3
__Symbols:_PBP1,_JAL30___PYK10-binding_protein_1___chr3:5579560-5580674_FORWARD_LENGTH=298	AT3G16420.1 (+2)	32 kDa	3	0	0	0
__Symbols:_PCK1,_PEPCK___phosphoenolpyruvate_carboxykinase_1___chr4:17802974-17806332_REVERSE_LENGTH=671	AT4G37870.1	73 kDa	2	2	1	4
__Symbols:_PDC2___pyruvate_decarboxylase-2___chr5:22310858-22312681_REVERSE_LENGTH=607	AT5G54960.1	66 kDa	3	2	1	4
__Symbols:_PDH-E1_ALPHA___pyruvate_dehydrogenase_E1_alpha___chr1:47705-49166_REVERSE_LENGTH=428	AT1G01090.1	47 kDa	4	2	3	7
__Symbols:_PDH-E1_BETA___pyruvate_dehydrogenase_E1_beta___chr1:10584350-10586477_REVERSE_LENGTH=406	AT1G30120.1	44 kDa	2	0	0	0
__Symbols:_PEN3,_PDR8,_ATPDR8,_ABCG36,_ATABCG36___ABC-2_and_Plant_PDR_ABC-type_transporter_family_protein___chr1:22034661-22039844_FORWARD_LENGTH=1469	AT1G59870.1	165 kDa	0	0	3	3
__Symbols:_PGIP1,_ATPGIP1___polygalacturonase_inhibiting_protein_1___chr5:2132373-2133434_FORWARD_LENGTH=330	AT5G06860.1	37 kDa	1	0	0	4
__Symbols:_PGIP2,_ATPGIP2___polygalacturonase_inhibiting_protein_2___chr5:2133941-2135016_FORWARD_LENGTH=330	AT5G06870.1	37 kDa	3	1	2	1
__Symbols:_PGK1___phosphoglycerate_kinase_1___chr3:4061127-4063140_REVERSE_LENGTH=481	AT3G12780.1	50 kDa	7	4	14	12
__Symbols:_PGK___phosphoglycerate_kinase___chr1:29924347-29926295_REVERSE_LENGTH=401	AT1G79550.1 (+1)	42 kDa	0	0	2	1
__Symbols:_PGM3___Phosphoglucomutase/phosphomannomutase_family_protein___chr1:8219946-8224186_FORWARD_LENGTH=583	AT1G23190.1	63 kDa	0	0	0	4
__Symbols:_PHT3;1___phosphate_transporter_3;1___chr5:4531059-4532965_REVERSE_LENGTH=375	AT5G14040.1	40 kDa	2	0	0	0
__Symbols:_PKT3,_PED1,_KAT2___peroxisomal_3-ketoacyl-CoA_thiolase_3___chr2:14047814-14050983_REVERSE_LENGTH=462	AT2G33150.1	49 kDa	4	1	7	4
__Symbols:_PLDALPHA1,_PLD___phospholipase_D_alpha_1___chr3:5330835-5333474_FORWARD_LENGTH=810	AT3G15730.1	92 kDa	18	18	34	37
__Symbols:_PLDGAMMA1,_MEE54___phospholipase_D_gamma_1___chr4:7129352-7132937_REVERSE_LENGTH=858	AT4G11850.1	96 kDa	0	1	3	3
__Symbols:_PMH1,_ATRH9___putative_mitochondrial_RNA_helicase_1___chr3:7887382-7889806_FORWARD_LENGTH=610	AT3G22310.1	64 kDa	0	0	0	2
__Symbols:_PMH2,_ATRH53___putative_mitochondrial_RNA_helicase_2___chr3:7892641-7895145_FORWARD_LENGTH=616	AT3G22330.1	65 kDa	0	3	0	6
__Symbols:_POP2,_GABA-T,_HER1___Pyridoxal_phosphate_(PLP)-dependent_transferases_superfamily_protein___chr3:7835286-7838863_FORWARD_LENGTH=504	AT3G22200.1 (+1)	55 kDa	0	1	2	0
__Symbols:_PPI1___proton_pump_interactor_1___chr4:13743614-13745900_FORWARD_LENGTH=612	AT4G27500.1	?	1	7	15	15

__Symbols:_PRK___phosphoribulokinase___chr1:11532668-11534406_FORWARD_LENGTH=395	AT1G32060.1	44 kDa	2	0	1	4
__Symbols:_PSAF___photosystem_I_subunit_F___chr1:11215011-11215939_REVERSE_LENGTH=221	AT1G31330.1	24 kDa	2	3	0	0
__Symbols:_PSAT___phosphoserine_aminotransferase___chr4:16904205-16905497_FORWARD_LENGTH=430	AT4G35630.1	47 kDa	0	0	1	2
__Symbols:_PSBB___photosystem_II_reaction_center_protein_B___chrC:72371-73897_FORWARD_LENGTH=508	ATCG00680.1	56 kDa	8	5	2	3
__Symbols:_PSBC___photosystem_II_reaction_center_protein_C___chrC:33720-35141_FORWARD_LENGTH=473	ATCG00280.1	52 kDa	6	4	4	4
__Symbols:_PSBD___photosystem_II_reaction_center_protein_D___chrC:32711-33772_FORWARD_LENGTH=353	ATCG00270.1	40 kDa	0	4	1	0
__Symbols:_PTAC16___plastid_transcriptionally_active_16___chr3:17228766-17231021_FORWARD_LENGTH=510	AT3G46780.1	54 kDa	13	10	17	8
__Symbols:_PYD2___pyrimidine_2___chr5:3941700-3944727_REVERSE_LENGTH=531	AT5G12200.1	58 kDa	0	0	2	0
__Symbols:_PYK10,_PSR3.1,_BGLU23,_LEB___Glycosyl_hydrolase_superfamily_protein___chr3:2840657-2843730_REVERSE_LENGTH=524	AT3G09260.1	?	18	8	19	23
__Symbols:_Phox2___Octicosapeptide/Phox/Bem1p_(PB1)_domain-containing_protein_/_tetratricopeptide_repeat_(TPR)-containing_protein___chr1:23084632-23086887_REVERSE_LENGTH=751	AT1G62390.1	83 kDa	0	0	2	0
__Symbols:_Prx37___Peroxidase_superfamily_protein___chr4:5598259-5600262_REVERSE_LENGTH=346	AT4G08770.1	38 kDa	0	0	0	2
__Symbols:_RBCL___ribulose-bisphosphate_carboxylases___chrC:54958-56397_FORWARD_LENGTH=479	ATCG00490.1	53 kDa	56	36	63	59
__Symbols:_RCA___rubisco_activase___chr2:16571046-16573345_REVERSE_LENGTH=446	AT2G39730.2	49 kDa	56	41	44	65
__Symbols:_RD21,_RD21A___Granulin_repeat_cysteine_protease_family_protein___chr1:17283139-17285609_REVERSE_LENGTH=462	AT1G47128.1	51 kDa	2	3	0	0
__Symbols:_RHM1,_ROL1,_ATRHM1___rhamnose_biosynthesis_1___chr1:29550110-29552207_FORWARD_LENGTH=669	AT1G78570.1	75 kDa	3	1	3	10
__Symbols:_RLM3___disease_resistance_protein_(TIR-NBS_class),_putative___chr4:9560155-9565225_FORWARD_LENGTH=796	AT4G16990.2	91 kDa	0	0	2	0
__Symbols:_RML1,_PAD2,_GSH1,_CAD2,_ATECS1,_GSHA___glutamate-cysteine_ligase___chr4:12103458-12106751_REVERSE_LENGTH=522	AT4G23100.1 (+1)	59 kDa	5	1	5	4
__Symbols:_RPN1A,_ATRPN1A___26S_proteasome_regulatory_subunit_S2_1A___chr2:8859211-8864699_FORWARD_LENGTH=891	AT2G20580.1	?	2	8	5	5
__Symbols:_RPS11___ribosomal_protein_S11___chrC:78960-79376_REVERSE_LENGTH=138	ATCG00750.1	15 kDa	1	3	1	0
__Symbols:_RPS6,_RPS6A___ribosomal_protein_S6___chr4:15346306-15347714_REVERSE_LENGTH=250	AT4G31700.1 (+1)	28 kDa	2	2	1	2
__Symbols:_RPT1A___regulatory_particle_triple-A_1A___chr1:20065921-20068324_REVERSE_LENGTH=426	AT1G53750.1	48 kDa	0	1	1	4
__Symbols:_RPT3___regulatory_particle_triple-A_ATPase_3___chr5:23569155-23571116_FORWARD_LENGTH=408	AT5G58290.1	46 kDa	0	0	0	2
__Symbols:_RPT5A,_ATS6A.2___regulatory_particle_triple-A_ATPase_5A___chr3:1603540-1605993_FORWARD_LENGTH=424	AT3G05530.1	47 kDa	1	1	4	6

__Symbols:_SAM1,_SAM-1,_MAT1,_AtSAM1___S-adenosylmethionine_synthetase_1___chr1:519037-520218_FORWARD_LENGTH=393	AT1G02500.1 (+1)	43 kDa	3	1	0	4
__Symbols:_SBE2.2___starch_branching_enzyme_2.2___chr5:931924-937470_FORWARD_LENGTH=805	AT5G03650.1	93 kDa	4	2	7	3
__Symbols:_SBP1___selenium-binding_protein_1___chr4:8098121-8100165_REVERSE_LENGTH=490	AT4G14030.1 (+1)	54 kDa	8	1	9	10
__Symbols:_SDH1-1___succinate_dehydrogenase_1-1___chr5:26653776-26657224_FORWARD_LENGTH=634	AT5G66760.1	70 kDa	16	7	7	12
__Symbols:_SEC6___SEC6___chr1:27010022-27016745_FORWARD_LENGTH=752	AT1G71820.1	86 kDa	0	0	2	0
__Symbols:_SE___C2H2_zinc-finger_protein_SERRATE_(SE)___chr2:11572587-11576357_FORWARD_LENGTH=720	AT2G27100.1	81 kDa	0	1	3	1
__Symbols:_SFR2,_ATSFR2___Glycosyl_hydrolase_superfamily_protein___chr3:2016450-2019533_FORWARD_LENGTH=622	AT3G06510.1 (+1)	71 kDa	2	4	3	5
__Symbols:_SHD,_HSP90.7,_AtHsp90.7,_AtHsp90-7___Chaperone_protein_htpG_family_protein___chr4:12551902-12555851_REVERSE_LENGTH=823	AT4G24190.1 (+1)	94 kDa	4	5	20	31
__Symbols:_SHM1,_STM,_SHMT1___serine_transhydroxymethyltransferase_1___chr4:17831891-17834742_REVERSE_LENGTH=517	AT4G37930.1	57 kDa	5	1	19	15
__Symbols:_SHM4___serine_hydroxymethyltransferase_4___chr4:8048013-8050021_REVERSE_LENGTH=471	AT4G13930.1	52 kDa	3	1	3	3
__Symbols:_SLP2___subtilisin-like_serine_protease_2___chr4:16656929-16659223_REVERSE_LENGTH=764	AT4G34980.1	81 kDa	27	38	30	32
__Symbols:_SNG1,_SCPL8___sinapoylglucose_1___chr2:9786393-9789925_FORWARD_LENGTH=433	AT2G22990.1 (+4)	49 kDa	0	0	1	3
__Symbols:_ST1,_ATMST1,_MST1,_ATRDH1,_STR1___mercaptopyruvate_sulfurtransferase_1___chr1:29800824-29803679_FORWARD_LENGTH=379	AT1G79230.1 (+1)	42 kDa	2	0	0	0
__Symbols:_STT3A___staurosporin_and_temperature_sensitive_3-like_A___chr5:6652649-6658214_FORWARD_LENGTH=779	AT5G19690.1	86 kDa	2	1	1	3
__Symbols:_SUS1,_ASUS1,_atsus1___sucrose_synthase_1___chr5:7050599-7054032_REVERSE_LENGTH=808	AT5G20830.1 (+1)	93 kDa	0	0	5	1
__Symbols:_SYNC1,_EMB2755,_SYNC1_ARATH___Class_II_aminoacyl-tRNA_and_biotin_synthetases_superfamily_protein___chr5:22936645-22938841_FORWARD_LENGTH=572	AT5G56680.1	64 kDa	0	0	0	2
__Symbols:_TGG1,_BGLU38___thioglucoside_glucohydrolase_1___chr5:9079678-9082347_REVERSE_LENGTH=541	AT5G26000.1	61 kDa	5	15	12	9
__Symbols:_TGG2,_BGLU37___glucoside_glucohydrolase_2___chr5:9072730-9075477_FORWARD_LENGTH=547	AT5G25980.2	63 kDa	2	2	5	5
__Symbols:_TIF3B1,_EIF3B,_ATEIF3B-1,_EIF3B-1,_ATTIF3B1___translation_initiation_factor_3B1___chr5:9781207-9784759_REVERSE_LENGTH=712	AT5G27640.1 (+1)	82 kDa	3	2	5	8
__Symbols:_TOC75-III,_MAR1___translocon_at_the_outer_envelope_membrane_of_chloroplasts_75-III___chr3:17216104-17219296_REVERSE_LENGTH=818	AT3G46740.1	89 kDa	4	6	3	4
__Symbols:_TPP2___tripeptidyl_peptidase_ii___chr4:11160935-11169889_REVERSE_LENGTH=1380	AT4G20850.1	152 kDa	12	22	9	15
__Symbols:_TRIP-1,_TIF3I1___TGF-beta_receptor_interacting_protein_1___chr2:19003656-19005393_REVERSE_LENGTH=328	AT2G46280.1 (+2)	36 kDa	2	0	0	0
__Symbols:_TROL___thylakoid_rhodanese-like___chr4:455874-458175_FORWARD_LENGTH=466	AT4G01050.1	49 kDa	2	0	0	0

__Symbols:_TUA3___tubulin_alpha-3___chr5:6682761-6684474_REVERSE_LENGTH=450	AT5G19770.1 (+1)	50 kDa	5	0	5	6
__Symbols:_TUA4,_TOR2___tubulin_alpha-4_chain___chr1:1356421-1358266_REVERSE_LENGTH=450	AT1G04820.1 (+1)	50 kDa	15	9	23	18
__Symbols:_TUB2___tubulin_beta_chain_2___chr5:25181560-25183501_FORWARD_LENGTH=450	AT5G62690.1 (+1)	51 kDa	27	13	33	24
__Symbols:_TUB4___tubulin_beta_chain_4___chr5:17859442-17860994_REVERSE_LENGTH=444	AT5G44340.1	50 kDa	3	1	7	3
__Symbols:_TUB5___tubulin_beta-5_chain___chr1:6938033-6940481_REVERSE_LENGTH=449	AT1G20010.1	50 kDa	6	4	7	5
__Symbols:_TUB6___beta-6_tubulin___chr5:3961317-3962971_REVERSE_LENGTH=449	AT5G12250.1	51 kDa	2	1	3	2
__Symbols:_TUB7___tubulin_beta-7_chain___chr2:12644258-12645932_REVERSE_LENGTH=449	AT2G29550.1	51 kDa	2	0	4	2
__Symbols:_TWN2,_VALRS___valyl-tRNA_synthetase_/_valine--tRNA_ligase_(VALRS)___chr1:5008502-5014486_REVERSE_LENGTH=1108	AT1G14610.1	126 kDa	0	0	2	5
__Symbols:_Tudor1,_AtTudor1,_TSN1___TUDOR-SN_protein_1___chr5:2320344-2324892_REVERSE_LENGTH=991	AT5G07350.1 (+1)	108 kDa	3	1	7	17
__Symbols:_Tudor2,_AtTudor2,_TSN2___TUDOR-SN_protein_2___chr5:24822012-24826641_FORWARD_LENGTH=985	AT5G61780.1	108 kDa	0	0	2	3
__Symbols:_UGP,_UGP1,_AtUGP1___UDP-GLUCOSE_PYROPHOSPHORYLASE_1___chr3:749761-754014_REVERSE_LENGTH=469	AT3G03250.1	52 kDa	0	0	0	2
__Symbols:_VAR1,_FTSH5___FtsH_extracellular_protease_family___chr5:16902659-16905102_FORWARD_LENGTH=704	AT5G42270.1	75 kDa	1	4	3	4
__Symbols:_VAR2,_FTSH2___FtsH_extracellular_protease_family___chr2:13174692-13177064_FORWARD_LENGTH=695	AT2G30950.1	74 kDa	0	2	6	7
__Symbols:_VHA-A3___vacuolar_proton_ATPase_A3___chr4:18209513-18214752_FORWARD_LENGTH=821	AT4G39080.1	93 kDa	2	2	4	4
__Symbols:_VHA-A___vacuolar_ATP_synthase_subunit_A___chr1:29660463-29664575_FORWARD_LENGTH=623	AT1G78900.1 (+1)	69 kDa	12	10	11	27
__Symbols:_YAO___Transducin/WD40_repeat-like_superfamily_protein___chr4:2743229-2745521_REVERSE_LENGTH=504	AT4G05410.1	57 kDa	0	0	0	2
__Symbols:_ZW9___TRAF-like_family_protein___chr1:21612394-21614089_REVERSE_LENGTH=396	AT1G58270.1	45 kDa	3	1	1	7
__Symbols:____2-oxoglutarate_(2OG)_and_Fe(II)-dependent_oxygenase_superfamily_protein___chr2:16012723-16014666_REVERSE_LENGTH=353	AT2G38240.1	40 kDa	6	2	1	0
__Symbols:____2-oxoglutarate_dehydrogenase,_E1_component___chr3:20541897-20545728_FORWARD_LENGTH=1017	AT3G55410.1	115 kDa	7	5	17	4
__Symbols:____6-phosphogluconate_dehydrogenase_family_protein___chr3:482498-483958_FORWARD_LENGTH=486	AT3G02360.1 (+1)	54 kDa	1	0	1	2
__Symbols:____AAA-type_ATPase_family_protein___chr2:8692736-8694837_FORWARD_LENGTH=443	AT2G20140.1	49 kDa	2	0	3	5
__Symbols:____AAA-type_ATPase_family_protein___chr5:5568578-5571565_FORWARD_LENGTH=644	AT5G16930.1	71 kDa	0	1	1	2
__Symbols:____AMP-dependent_synthetase_and_ligase_family_protein___chr3:18159031-18161294_REVERSE_LENGTH=514	AT3G48990.1	56 kDa	1	0	1	10
__Symbols:____ARM_repeat_superfamily_protein___chr5:21714016-21716709_FORWARD_LENGTH=870	AT5G53480.1	96 kDa	0	0	1	3

__Symbols:____ATP_binding;leucine-tRNA_ligases;aminoacyl-tRNA_ligases;nucleotide_binding;ATP_binding;aminoacyl-tRNA_ligases___chr1:3113077-3116455_REVERSE_LENGTH=1091	AT1G09620.1	123 kDa	0	0	3	6
__Symbols:____ATP_synthase_alpha/beta_family_protein___chr5:2818395-2821149_REVERSE_LENGTH=556	AT5G08670.1 (+2)	60 kDa	20	13	22	31
__Symbols:____ATPase,_F1_complex,_alpha_subunit_protein___chr2:3361474-3364028_FORWARD_LENGTH=777	AT2G07698.1	86 kDa	14	14	16	25
__Symbols:____ATPase,_V1_complex,_subunit_B_protein___chr1:7016971-7020290_FORWARD_LENGTH=487	AT1G20260.1 (+1)	54 kDa	8	0	7	15
__Symbols:____ATPase,_V1_complex,_subunit_B_protein___chr4:18011155-18014789_REVERSE_LENGTH=487	AT4G38510.1 (+4)	54 kDa	0	0	2	3
__Symbols:____Aldolase-type_TIM_barrel_family_protein___chr3:4821804-4823899_FORWARD_LENGTH=367	AT3G14420.1 (+2)	40 kDa	16	11	18	15
__Symbols:____Aldolase-type_TIM_barrel_family_protein___chr5:4302080-4304212_REVERSE_LENGTH=438	AT5G13420.1	48 kDa	0	0	1	2
__Symbols:____Aldolase_superfamily_protein___chr2:15296929-15298387_REVERSE_LENGTH=358	AT2G36460.1	38 kDa	0	1	0	2
__Symbols:____Aldolase_superfamily_protein___chr3:19627383-19628874_REVERSE_LENGTH=358	AT3G52930.1	39 kDa	9	2	13	18
__Symbols:____Calreticulin_family_protein___chr5:2317300-2319458_FORWARD_LENGTH=532	AT5G07340.1 (+1)	60 kDa	0	0	0	5
__Symbols:____Carbohydrate-binding-like_fold___chr3:23073020-23080455_REVERSE_LENGTH=1227	AT3G62360.1	133 kDa	0	0	0	2
__Symbols:____Chitinase_family_protein___chr2:18088058-18089184_REVERSE_LENGTH=281	AT2G43610.1	30 kDa	2	3	0	0
__Symbols:____Class-II_DAHP_synthetase_family_protein___chr1:7912120-7914742_FORWARD_LENGTH=527	AT1G22410.1	58 kDa	12	3	13	6
__Symbols:____Class_II_aaRS_and_biotin_synthetases_superfamily_protein___chr3:23001227-23003849_REVERSE_LENGTH=530	AT3G62120.1 (+1)	61 kDa	8	4	7	8
__Symbols:____Class_II_aminoacyl-tRNA_and_biotin_synthetases_superfamily_protein___chr4:13505381-13507619_FORWARD_LENGTH=532	AT4G26870.1	60 kDa	2	1	3	4
__Symbols:____Class_II_aminoacyl-tRNA_and_biotin_synthetases_superfamily_protein___chr4:15156696-15159362_FORWARD_LENGTH=558	AT4G31180.1 (+1)	63 kDa	0	0	0	3
__Symbols:____Class_I_glutamine_amidotransferase-like_superfamily_protein___chr3:5047510-5049621_FORWARD_LENGTH=392	AT3G14990.1	42 kDa	14	10	3	18
__Symbols:____Clathrin,_heavy_chain___chr3:3482575-3491667_REVERSE_LENGTH=1705	AT3G11130.1	193 kDa	48	51	47	38
__Symbols:____Clathrin_light_chain_protein___chr2:8943279-8945108_REVERSE_LENGTH=338	AT2G20760.1	37 kDa	1	1	3	1
__Symbols:____Coatomer,_alpha_subunit___chr2:9152428-9156577_FORWARD_LENGTH=1218	AT2G21390.1	136 kDa	4	2	8	9
__Symbols:____Coatomer,_beta_subunit___chr4:15264145-15267384_FORWARD_LENGTH=948	AT4G31480.1 (+2)	106 kDa	0	0	2	4
__Symbols:____Copper_amine_oxidase_family_protein___chr2:17691600-17695526_REVERSE_LENGTH=776	AT2G42490.1	87 kDa	0	1	6	0
__Symbols:____Curculin-like_(mannose-binding)_lectin_family_protein___chr1:29637141-29638508_REVERSE_LENGTH=455	AT1G78830.1	50 kDa	5	4	1	3
__Symbols:____Cytosol_aminopeptidase_family_protein___chr2:10287017-10289450_REVERSE_LENGTH=520	AT2G24200.1 (+1)	55 kDa	0	0	0	4

__Symbols:____D-mannose_binding_lectin_protein_with_Apple-like_carbohydrate-binding_domain___chr1:29642072-29643397_REVERSE_LENGTH=441	AT1G78850.1	49 kDa	20	11	24	25
__Symbols:____DEA(D/H)-box_RNA_helicase_family_protein___chr3:21640608-21643464_FORWARD_LENGTH=612	AT3G58510.1 (+2)	66 kDa	0	1	7	6
__Symbols:____Dihydrolipoamide_acetyltransferase,_long_form_protein___chr1:20246460-20250208_REVERSE_LENGTH=539	AT1G54220.1 (+1)	58 kDa	2	1	4	3
__Symbols:____Dihydrolipoamide_acetyltransferase,_long_form_protein___chr3:4596240-4600143_FORWARD_LENGTH=539	AT3G13930.1	58 kDa	13	1	11	17
__Symbols:____Dihydrolipoamide_succinyltransferase___chr4:13520127-13522889_REVERSE_LENGTH=464	AT4G26910.1 (+2)	50 kDa	1	0	1	3
__Symbols:____Dihydrolipoamide_succinyltransferase___chr5:22347637-22350409_FORWARD_LENGTH=464	AT5G55070.1	50 kDa	4	1	1	6
__Symbols:____Eukaryotic_aspartyl_protease_family_protein___chr1:3157541-3158960_FORWARD_LENGTH=449	AT1G09750.1	48 kDa	3	4	3	4
__Symbols:____Eukaryotic_aspartyl_protease_family_protein___chr1:787143-788444_FORWARD_LENGTH=433	AT1G03220.1	46 kDa	11	5	12	14
__Symbols:____Eukaryotic_aspartyl_protease_family_protein___chr1:790110-791414_FORWARD_LENGTH=434	AT1G03230.1	46 kDa	3	1	3	4
__Symbols:____Eukaryotic_aspartyl_protease_family_protein___chr3:20140291-20142599_REVERSE_LENGTH=425	AT3G54400.1	45 kDa	14	9	8	20
__Symbols:____Eukaryotic_aspartyl_protease_family_protein___chr5:2183600-2185717_REVERSE_LENGTH=455	AT5G07030.1	49 kDa	0	0	0	4
__Symbols:____Eukaryotic_aspartyl_protease_family_protein___chr5:6411720-6413170_REVERSE_LENGTH=405	AT5G19110.1	43 kDa	5	1	3	10
__Symbols:____Eukaryotic_translation_initiation_factor_2_subunit_1___chr2:16829030-16830889_REVERSE_LENGTH=344	AT2G40290.1	39 kDa	4	1	2	6
__Symbols:____FAD-binding_Berberine_family_protein___chr4:11155486-11157577_FORWARD_LENGTH=570	AT4G20830.1 (+1)	64 kDa	0	0	3	1
__Symbols:____FAD-linked_oxidases_family_protein___chr4:17197265-17200472_FORWARD_LENGTH=559	AT4G36400.1 (+1)	61 kDa	32	14	47	34
__Symbols:____FG-GAP_repeat-containing_protein___chr3:18954023-18957698_FORWARD_LENGTH=698	AT3G51050.1	78 kDa	0	1	2	2
__Symbols:____GDSL-like_Lipase/Acylhydrolase_superfamily_protein___chr1:10375843-10377717_FORWARD_LENGTH=363	AT1G29670.1	40 kDa	9	6	0	0
__Symbols:____GDSL-like_Lipase/Acylhydrolase_superfamily_protein___chr1:12267918-12269690_FORWARD_LENGTH=370	AT1G33811.1	42 kDa	8	8	6	10
__Symbols:____GDSL-like_Lipase/Acylhydrolase_superfamily_protein___chr1:20154548-20156365_REVERSE_LENGTH=391	AT1G54000.1	43 kDa	2	0	8	7
__Symbols:____GDSL-like_Lipase/Acylhydrolase_superfamily_protein___chr1:20158854-20160747_REVERSE_LENGTH=386	AT1G54010.1	43 kDa	4	1	8	11
__Symbols:____GTP-binding_protein-related___chr4:18371329-18374000_REVERSE_LENGTH=369	AT4G39520.1	41 kDa	3	1	3	6
__Symbols:____GTP_binding_Elongation_factor_Tu_family_protein___chr1:2455559-2457001_FORWARD_LENGTH=449	AT1G07920.1 (+5)	50 kDa	44	28	46	40
__Symbols:____GTP_binding_Elongation_factor_Tu_family_protein___chr4:1295751-1298354_REVERSE_LENGTH=454	AT4G02930.1	49 kDa	4	1	2	4
__Symbols:____GTP_binding___chr1:10831953-10835454_REVERSE_LENGTH=394	AT1G30580.1	44 kDa	0	0	0	3

__Symbols:____Galactose_mutarotase-like_superfamily_protein___chr3:17634971-17636998_FORWARD_LENGTH=358	AT3G47800.1	40 kDa	1	1	2	6
__Symbols:____Glycine_cleavage_T-protein_family___chr1:4001801-4003245_FORWARD_LENGTH=408	AT1G11860.1 (+2)	44 kDa	7	5	4	8
__Symbols:____Glycosyl_hydrolase_family_protein___chr5:7107609-7110775_REVERSE_LENGTH=624	AT5G20950.1 (+1)	68 kDa	4	4	6	7
__Symbols:____Glycosyl_hydrolase_superfamily_protein___chr4:9200180-9201441_REVERSE_LENGTH=344	AT4G16260.1	38 kDa	2	0	0	0
__Symbols:____Glycosyl_hydrolases_family_31__protein___chr5:3776840-3780025_FORWARD_LENGTH=902	AT5G11720.1	101 kDa	16	15	19	19
__Symbols:____Glycosyl_hydrolases_family_32_protein___chr1:23199949-23203515_FORWARD_LENGTH=648	AT1G62660.1	72 kDa	5	1	5	5
__Symbols:____HXXXD-type_acyl-transferase_family_protein___chr5:84554-85981_FORWARD_LENGTH=475	AT5G01210.1	52 kDa	1	0	3	0
__Symbols:____Heat_shock_protein_70_(Hsp_70)_family_protein___chr1:30058935-30062224_REVERSE_LENGTH=831	AT1G79920.1 (+3)	92 kDa	0	3	3	2
__Symbols:____Heat_shock_protein_70_(Hsp_70)_family_protein___chr3:2903434-2905632_REVERSE_LENGTH=649	AT3G09440.1 (+1)	71 kDa	2	6	9	14
__Symbols:____Histone_superfamily_protein___chr1:2369212-2369523_FORWARD_LENGTH=103	AT1G07660.1 (+8)	11 kDa	0	7	2	0
__Symbols:____Histone_superfamily_protein___chr3:2914890-2915270_REVERSE_LENGTH=126	AT3G09480.1	14 kDa	2	4	1	2
__Symbols:____Histone_superfamily_protein___chr4:18555840-18556827_REVERSE_LENGTH=164	AT4G40030.2	19 kDa	0	2	2	0
__Symbols:____Hyaluronan_/_mRNA_binding_family___chr4:9771496-9773313_FORWARD_LENGTH=360	AT4G17520.1	39 kDa	0	2	0	2
__Symbols:____Hyaluronan_/_mRNA_binding_family___chr5:19169222-19171012_REVERSE_LENGTH=357	AT5G47210.1	38 kDa	3	7	3	7
__Symbols:____INVOLVED_IN:_protein_processing;_LOCATED_IN:_mitochondrion,_endoplasmic_reticulum,_plasma_membrane,	AT3G44330.1	62 kDa	0	0	0	3
__Symbols:____Insulinase_(Peptidase_family_M16)_family_protein___chr1:2115155-2120635_REVERSE_LENGTH=1024	AT1G06900.1	?	0	0	2	0
__Symbols:____Insulinase_(Peptidase_family_M16)_protein___chr1:19323692-19326771_REVERSE_LENGTH=503	AT1G51980.1	54 kDa	3	3	5	3
__Symbols:____Lactate/malate_dehydrogenase_family_protein___chr1:1189418-1191267_REVERSE_LENGTH=332	AT1G04410.1	36 kDa	5	0	0	1
__Symbols:____Leucine-rich_repeat_(LRR)_family_protein___chr3:7280930-7282027_FORWARD_LENGTH=365	AT3G20820.1	40 kDa	14	12	7	9
__Symbols:____Mannose-binding_lectin_superfamily_protein___chr3:5593029-5595522_FORWARD_LENGTH=705	AT3G16460.1 (+1)	72 kDa	14	3	33	29
__Symbols:____NAD(P)-binding_Rossmann-fold_superfamily_protein___chr3:6511169-6514729_FORWARD_LENGTH=641	AT3G18890.1	68 kDa	0	0	0	3
__Symbols:____NAD(P)-binding_Rossmann-fold_superfamily_protein___chr4:16771401-16773269_REVERSE_LENGTH=395	AT4G35250.1	44 kDa	2	0	0	0
__Symbols:____NOP56-like_pre_RNA_processing_ribonucleoprotein___chr3:1413174-1415564_REVERSE_LENGTH=533	AT3G05060.1	59 kDa	0	0	0	2
__Symbols:____O-Glycosyl_hydrolases_family_17_protein___chr3:20549806-20552004_REVERSE_LENGTH=449	AT3G55430.1	48 kDa	4	3	1	3
__Symbols:____O-fucosyltransferase_family_protein___chr1:1388101-1391074_REVERSE_LENGTH=519	AT1G04910.1	59 kDa	0	0	0	2

__Symbols:____P-loop_containing_nucleoside_triphosphate_hydrolases_superfamily_protein___chr2:14265679-14267880_REVERSE_LENGTH=733	AT2G33730.1	85 kDa	0	1	2	2
__Symbols:____P-loop_containing_nucleoside_triphosphate_hydrolases_superfamily_protein___chr2:17705382-17708744_FORWARD_LENGTH=633	AT2G42520.1	68 kDa	3	8	12	10
__Symbols:____Pectin_lyase-like_superfamily_protein___chr4:12397217-12400050_REVERSE_LENGTH=444	AT4G23820.1	49 kDa	6	2	3	4
__Symbols:____Pectin_lyase-like_superfamily_protein___chr4:12770631-12772227_REVERSE_LENGTH=408	AT4G24780.1 (+1)	45 kDa	3	3	1	1
__Symbols:____Pectinacetylesterase_family_protein___chr4:10582188-10584766_REVERSE_LENGTH=391	AT4G19410.1 (+1)	42 kDa	19	19	10	15
__Symbols:____Pectinacetylesterase_family_protein___chr5:18346862-18349488_FORWARD_LENGTH=391	AT5G45280.2	42 kDa	1	1	2	3
__Symbols:____Peroxidase_superfamily_protein___chr1:26964359-26966557_FORWARD_LENGTH=358	AT1G71695.1	40 kDa	0	2	4	1
__Symbols:____Peroxidase_superfamily_protein___chr3:7673345-7674661_FORWARD_LENGTH=329	AT3G21770.1	36 kDa	1	0	0	3
__Symbols:____Peroxidase_superfamily_protein___chr4:13200653-13201688_FORWARD_LENGTH=310	AT4G26010.1	34 kDa	0	2	0	0
__Symbols:____Peroxidase_superfamily_protein___chr5:25650824-25652062_REVERSE_LENGTH=331	AT5G64100.1	36 kDa	2	0	0	0
__Symbols:____Phosphofructokinase_family_protein___chr1:4050159-4053727_REVERSE_LENGTH=566	AT1G12000.1	61 kDa	2	0	2	5
__Symbols:____Phosphoglycerate_mutase,_2,3-bisphosphoglycerate-independent___chr1:3165550-3167812_REVERSE_LENGTH=557	AT1G09780.1	61 kDa	0	0	0	5
__Symbols:____Phosphorylase_superfamily_protein___chr4:12609637-12611328_FORWARD_LENGTH=336	AT4G24350.1 (+1)	37 kDa	4	0	0	2
__Symbols:____Phototropic-responsive_NPH3_family_protein___chr5:26884754-26887083_FORWARD_LENGTH=604	AT5G67385.1	68 kDa	0	0	0	4
__Symbols:____Protein_kinase_protein_with_tetratricopeptide_repeat_domain___chr1:23556015-23558403_FORWARD_LENGTH=487	AT1G63500.1	55 kDa	0	0	0	2
__Symbols:____Protein_of_unknown_function_(DUF1012)___chr5:17569435-17574954_REVERSE_LENGTH=817	AT5G43745.1	92 kDa	11	5	18	7
__Symbols:____Pyridine_nucleotide-disulphide_oxidoreductase_family_protein___chr1:27991248-27992845_FORWARD_LENGTH=467	AT1G74470.1	52 kDa	2	2	2	4
__Symbols:____Pyruvate_kinase_family_protein___chr5:22820254-22822529_REVERSE_LENGTH=498	AT5G56350.1	54 kDa	1	0	3	2
__Symbols:____Pyruvate_kinase_family_protein___chr5:25490507-25492530_FORWARD_LENGTH=510	AT5G63680.1	55 kDa	0	0	1	4
__Symbols:____RNA-binding_(RRM/RBD/RNP_motifs)_family_protein___chr3:5052844-5054058_FORWARD_LENGTH=404	AT3G15010.1 (+1)	42 kDa	3	0	1	0
__Symbols:____RNA_polymerase_I-associated_factor_PAF67___chr5:8953564-8955511_FORWARD_LENGTH=514	AT5G25754.1 (+1)	60 kDa	2	0	1	3
__Symbols:____Ribosomal_protein_L10_family_protein___chr3:2823364-2825020_REVERSE_LENGTH=320	AT3G09200.1 (+1)	34 kDa	3	0	0	1
__Symbols:____Ribosomal_protein_L4/L1_family___chr3:2953813-2955444_FORWARD_LENGTH=406	AT3G09630.1	45 kDa	19	9	16	33

__Symbols:____Ribosomal_protein_L4/L1_family___chr5:657830-659526_FORWARD_LENGTH=407	AT5G02870.1	45 kDa	2	0	3	6
__Symbols:____Ribosomal_protein_L6_family_protein___chr1:27847256-27848680_REVERSE_LENGTH=233	AT1G74050.1	26 kDa	3	3	0	0
__Symbols:____Ribosomal_protein_L7Ae/L30e/S12e/Gadd45_family_protein___chr2:19529854-19531401_FORWARD_LENGTH=257	AT2G47610.1 (+1)	29 kDa	2	0	0	0
__Symbols:____Ribosomal_protein_S3Ae___chr3:1329751-1331418_FORWARD_LENGTH=262	AT3G04840.1	30 kDa	3	3	0	0
__Symbols:____Ribosomal_protein_S4___chr5:4935124-4936334_REVERSE_LENGTH=198	AT5G15200.1 (+1)	23 kDa	2	0	0	1
__Symbols:____Rubisco_methyltransferase_family_protein___chr5:4601139-4603873_FORWARD_LENGTH=514	AT5G14260.1 (+2)	58 kDa	4	0	4	3
__Symbols:____S-adenosyl-L-methionine-dependent_methyltransferases_superfamily_protein___chr3:8333521-8335902_FORWARD_LENGTH=611	AT3G23300.1	69 kDa	5	6	4	1
__Symbols:____SPFH/Band_7/PHB_domain-containing_membrane-associated_protein_family___chr2:1066717-1068934_FORWARD_LENGTH=356	AT2G03510.1	41 kDa	0	0	0	3
__Symbols:____SPFH/Band_7/PHB_domain-containing_membrane-associated_protein_family___chr4:13766984-13769832_REVERSE_LENGTH=411	AT4G27585.1	45 kDa	1	0	1	3
__Symbols:____SPFH/Band_7/PHB_domain-containing_membrane-associated_protein_family___chr5:8749774-8751430_FORWARD_LENGTH=470	AT5G25250.1	52 kDa	0	1	2	4
__Symbols:____SRP72_RNA-binding_domain___chr1:25365962-25368464_REVERSE_LENGTH=664	AT1G67680.1	73 kDa	0	0	0	5
__Symbols:____Subtilase_family_protein___chr2:2269831-2272207_REVERSE_LENGTH=754	AT2G05920.1	80 kDa	14	15	14	20
__Symbols:____Subtilase_family_protein___chr3:4658421-4660754_REVERSE_LENGTH=777	AT3G14067.1	82 kDa	28	13	22	27
__Symbols:____Subtilase_family_protein___chr3:4741637-4743964_REVERSE_LENGTH=775	AT3G14240.1	83 kDa	13	9	18	11
__Symbols:____Sugar_isomerase_(SIS)_family_protein___chr5:17136080-17140622_FORWARD_LENGTH=560	AT5G42740.1	62 kDa	0	0	0	2
__Symbols:____TCP-1/cpn60_chaperonin_family_protein___chr3:1024432-1027604_FORWARD_LENGTH=549	AT3G03960.1	59 kDa	2	1	2	3
__Symbols:____TCP-1/cpn60_chaperonin_family_protein___chr3:3732734-3736156_FORWARD_LENGTH=557	AT3G11830.1	60 kDa	0	0	1	3
__Symbols:____TCP-1/cpn60_chaperonin_family_protein___chr3:4389685-4392624_FORWARD_LENGTH=596	AT3G13470.1	63 kDa	2	0	0	1
__Symbols:____TCP-1/cpn60_chaperonin_family_protein___chr3:528806-532457_REVERSE_LENGTH=535	AT3G02530.1 (+1)	59 kDa	1	0	1	4
__Symbols:____TCP-1/cpn60_chaperonin_family_protein___chr3:6232226-6233836_FORWARD_LENGTH=536	AT3G18190.1	58 kDa	1	0	0	4
__Symbols:____TCP-1/cpn60_chaperonin_family_protein___chr5:7087020-7089906_REVERSE_LENGTH=527	AT5G20890.1	57 kDa	0	0	3	2
__Symbols:____TCP-1/cpn60_chaperonin_family_protein___chr5:9255561-9258891_REVERSE_LENGTH=555	AT5G26360.1	60 kDa	0	0	0	3
__Symbols:____Tetratricopeptide_repeat_(TPR)-like_superfamily_protein___chr1:121582-130099_REVERSE_LENGTH=1797	AT1G01320.1 (+1)	199 kDa	3	6	5	2

__Symbols:____Thiamine_pyrophosphate_dependent_pyruvate_decarboxylase_family_protein___chr5:5724920-5726720_REVERSE_LENGTH=572	AT5G17380.1	61 kDa	1	0	3	5
__Symbols:____Threonyl-tRNA_synthetase___chr5:9437351-9441568_FORWARD_LENGTH=709	AT5G26830.1	81 kDa	0	0	0	4
__Symbols:____Transketolase___chr3:22454004-22456824_FORWARD_LENGTH=741	AT3G60750.1 (+1)	80 kDa	14	13	21	17
__Symbols:____Translation_elongation_factor_EF1B,_gamma_chain___chr1:21377873-21380114_FORWARD_LENGTH=413	AT1G57720.1 (+1)	46 kDa	6	2	5	9
__Symbols:____Translation_elongation_factor_EF1B,_gamma_chain___chr1:3120162-3122152_FORWARD_LENGTH=414	AT1G09640.1	47 kDa	4	2	7	19
__Symbols:____UDP-glucose_6-dehydrogenase_family_protein___chr3:11267375-11268817_REVERSE_LENGTH=480	AT3G29360.1 (+1)	53 kDa	1	0	2	5
__Symbols:____Ubiquitin_supergroup;Ribosomal_protein_L40e___chr2:15172153-15173046_FORWARD_LENGTH=128	AT2G36170.1 (+1)	15 kDa	0	2	2	7
__Symbols:____cellular_apoptosis_susceptibility_protein,_putative_/_importin-alpha_re-exporter,_putative___chr2:19096867-19099785_FORWARD_LENGTH=972	AT2G46520.1	109 kDa	0	2	0	0
__Symbols:____coatomer_gamma-2_subunit,_putative_/_gamma-2_coat_protein,_putative_/_gamma-2_COP,_putative___chr4:16471956-16476795_FORWARD_LENGTH=886	AT4G34450.1	98 kDa	1	1	3	6
__Symbols:____dehydrin_family_protein___chr1:20310305-20310601_REVERSE_LENGTH=98	AT1G54410.1	11 kDa	2	1	0	0
__Symbols:____dihydrolipoyl_dehydrogenases___chr4:9153570-9157322_REVERSE_LENGTH=630	AT4G16155.1	67 kDa	13	4	8	15
__Symbols:____glycine-rich_protein___chr1:9404041-9406098_REVERSE_LENGTH=420	AT1G27090.1	?	0	0	3	3
__Symbols:____glycyl-tRNA_synthetase_/_glycine--tRNA_ligase___chr1:10459662-10462781_REVERSE_LENGTH=729	AT1G29880.1	82 kDa	1	0	6	2
__Symbols:____ketol-acid_reductoisomerase___chr3:21671561-21674639_FORWARD_LENGTH=591	AT3G58610.1 (+2)	64 kDa	0	0	0	2
__Symbols:____lactate/malate_dehydrogenase_family_protein___chr5:23580010-23582287_REVERSE_LENGTH=443	AT5G58330.1 (+1)	48 kDa	7	5	3	7
__Symbols:____myosin_heavy_chain-related___chr4:15205662-15208895_FORWARD_LENGTH=420	AT4G31340.2	?	0	0	0	4
__Symbols:____phosphoribosylaminoimidazole_carboxylase,_putative_/_AIR_carboxylase,_putative___chr2:15806111-15810240_FORWARD_LENGTH=642	AT2G37690.1	70 kDa	0	0	0	2
__Symbols:____protein_serine/threonine_phosphatases;protein_kinases;catalytics;cAMP-dependent_protein_kinase_regulators;ATP_binding;protein_serine/threonine_phosphatases___chr2:8649779-8654193_REVERSE_LENGTH=1094	AT2G20050.1 (+1)	121 kDa	0	0	0	4
__Symbols:____signal_recognition_particle-related_/_SRP-related___chr5:24888920-24893079_FORWARD_LENGTH=605	AT5G61970.1	69 kDa	0	0	0	2
__Symbols:____tRNA_synthetase_beta_subunit_family_protein___chr1:27319947-27323908_REVERSE_LENGTH=598	AT1G72550.1 (+1)	68 kDa	0	0	0	2
__Symbols:____tRNA_synthetase_class_I_(I,_L,_M_and_V)_family_protein___chr4:6397526-6404509_REVERSE_LENGTH=1190	AT4G10320.1	135 kDa	0	0	1	4
__Symbols:____tetratricopeptide_repeat_(TPR)-containing_protein___chr3:19333232-19341295_FORWARD_LENGTH=1403	AT3G52140.1 (+3)	153 kDa	0	1	0	4

__Symbols:____transducin_family_protein_/_WD-40_repeat_family_protein___chr3:23431009-23437241_REVERSE_LENGTH=1104	AT3G63460.1 (+2)	120 kDa	0	0	2	3
__Symbols:____unknown_protein;_CONTAINS_InterPro_DOMAIN/s:_Protein_of_unknown_function_DUF2042_	AT3G46220.1 (+2)	89 kDa	0	0	0	3
__Symbols:____unknown_protein;_FUNCTIONS_IN:_molecular_function_unknown;_INVOLVED_IN:_biological_process_unknown;_LOCATED_IN:_chloroplast;_EXPRESSED_IN:_23_plant_structures;_EXPRESSED_DURING:_13_growth_stages;_CONTAINS_InterPro_DOMAIN/s:_Uncharacterised_protein_family_UPF0061_(InterPro:IPR003846);_Has_5046_Blast_hits_to_4997_proteins_in_1211_species:_Archae_-_8;_Bacteria_-_2327;_Metazoa_-_120;_Fungi_-_134;_Plants_-_48;_Viruses_-_0;_Other_Eukaryotes_-_2409_(source:_NCBI_BLink).___chr5:4133216-4136461_FORWARD_LENGTH=633	AT5G13030.1	71 kDa	1	0	2	6
__Symbols:____xylose_isomerase_family_protein___chr5:23347030-23349805_FORWARD_LENGTH=477	AT5G57655.2	54 kDa	20	4	24	23
__Symbols:____zinc_finger_(C3HC4-type_RING_finger)_family_protein___chr1:6421433-6425565_FORWARD_LENGTH=486	AT1G18660.1 (+3)	55 kDa	1	2	5	2
__Symbols:_cICDH___cytosolic_NADP+-dependent_isocitrate_dehydrogenase___chr1:24539088-24541861_FORWARD_LENGTH=410	AT1G65930.1	46 kDa	1	0	1	6
__Symbols:_cpHsc70-1___chloroplast_heat_shock_protein_70-1___chr4:12590094-12593437_FORWARD_LENGTH=718	AT4G24280.1	77 kDa	23	21	19	21
__Symbols:_emb1138___DEAD_box_RNA_helicase_(RH3)___chr5:9285540-9288871_REVERSE_LENGTH=747	AT5G26742.1 (+1)	81 kDa	1	9	8	10
__Symbols:_emb2734___ARM_repeat_superfamily_protein___chr5:6695731-6701247_REVERSE_LENGTH=1116	AT5G19820.1	124 kDa	1	0	1	9
__Symbols:_hda14,_ATHDA14___histone_deacetylase_14___chr4:16102774-16105439_REVERSE_LENGTH=423	AT4G33470.1	46 kDa	40	37	38	46
__Symbols:_mtHsc70-1___mitochondrial_heat_shock_protein_70-1___chr4:17825368-17828099_REVERSE_LENGTH=682	AT4G37910.1	73 kDa	10	11	8	19
__Symbols:_mtLPD1___mitochondrial_lipoamide_dehydrogenase_1___chr1:17717432-17719141_REVERSE_LENGTH=507	AT1G48030.1 (+1)	54 kDa	1	0	4	6
__Symbols:_sks15___SKU5__similar_15___chr4:17494820-17497124_REVERSE_LENGTH=541	AT4G37160.1	61 kDa	0	0	0	2
__Symbols:_sks16___SKU5__similar_16___chr2:10052581-10055311_REVERSE_LENGTH=541	AT2G23630.1	61 kDa	0	0	2	1
__Symbols:_sks4___SKU5__similar_4___chr4:11663429-11666463_FORWARD_LENGTH=541	AT4G22010.1	60 kDa	3	5	6	4
__Symbols:_sks5___SKU5_similar_5___chr1:28578211-28581020_REVERSE_LENGTH=541	AT1G76160.1	60 kDa	8	7	10	12
added_for_Lennart	AtAPC8-YFP	96 kDa	33	37	41	23
cont68-DECOY	cont68-DECOY	?	4	4	3	4
cont68-DECOY	cont68-DECOY	4	0	0	0	0

[4] List represents results from three independent experiments. Peptides identified for the respective protein in the individual samples were summed up from the four individual experiments. Protein identifications were accepted if they could be established at greater than 95.0% probability and contained at least 2 identified peptides.

Attachment 7.

The *NbPrf* nucleotide sequence was obtained by blasting the tomato Prf sequence against the Sol Genomics Network *Nicotiana benthamiana* genome predicted cDNA v0.4.4 database (http://solgenomics.net/tools/blast/).

>*NbPrf* (NbS00001223g0007.1:1-6000 Niben044Scf00001223:79024..88954 Cc nbs lrr%2C resistance protein with an R1 specific domain [Solanum lycopersicum])

ATGGCCGAGGAGTGTCGCGCTGTGATAGGTGCCATAAACCTTGTGAAGGGCCAGCATTTAGG
TATAACGACCATTAATCAATTGGAGGATGCTACAAAGCACCTAACGCGTGTAGCTGTATTTCTC
ACTAATCTGGAGAAGCGCTACCCTGAGAATGGGATATCTGGACAACTTAGGCCCCTATTTCTA
GAAGCTCATGATGGATTTTCTGAGATATGTTCTCGCTTTCCTCGTTTCAACCTTACCATTAAAAT
GGCTGAGAAATTCAAAGCTTCAAAGGCATCAAAGCTTCAAATGATTTCAGAGGTGCTGAATAT
AATTGAACATGAGAATATTGCTGAGCGAGTCAGAGCTTCAAAGCCATTAAGATCACCTAGTCG
AATCACTATGGAGATGGTGGGGTTTGTTGAATCTTTGCTTGGTTCTGTTCATCGTGCTCTGTTC
TTTATTAGTGTAGGGCCTGCTGCATCTTTGCTTGACAAGAAGCTCCGACATCTACGAGTCTTCT
TCACATTAATTGCAAAGCGGTGCATTGAGCATGAGAGTATGGAGGATCTCTTCACCCATGTTG
AGGATGTAGCTTATACTGCAGCATACCTATGTTTCTTGGGGTCGAACTGGAATATGGATGGCG
AGTTCTCTGAATTGCTGGAAAGGGTAAGTCGTCCCTTTATCCCAGAGTTGAGGCAGATTTATCT
GAGTGCCTTGATAGGGTTAAAGTCATCAACCTCTGAGACTACTACAATATTGAATGCCAAATA
TATGCTGGATTTTGTTAGTGCTCTCCGGGAGGATCTAAGACTTGGATGTGATGATCGAATTAG
GTGGCTCCAAAGAGGACTTTCTTACCTTTCTCGATTTCTCAGGGACATAGAATCTTATCCCCTTC
CACATGAAGAAGTGATTTCTCTTCGATTAAATATGGAAGCTCTGGCCATTGGGGCAGCAAATG
CTATCTACTCCTCGTATGATGAGGAAATGCACAACACTACTGAAACAGACGATGTGCTATTTCA
TTTGCAACTGAAGTTTAATTATGTCAAGGTGGAAGTCGATCTGATTCAGCTACTAACCCGTCAA
GCTGCCATCACAATAGGTCCTATGAAATCTCTGATTGACTATGTTTGGAGGGAGCTGATATTCT
TTAGAAATTATTTCATGGATGCATTAAAGCAGTGTAAAGAGAAGACTAACATAACTGTTATTTT
GACCTCGATTCAATCTGCAATTAGCCAAGCATGGTCAATCTGTGATTCTCTTTGTCATGGCTCG
GAGCAAGAGGACTATTTTTCTGATGATACGGAGCAAGAAGACCCACTGGTCGGGGAAATGAT
TAATTGCTTGCATTTTCAGTTGCTTCTTAAGTTCAAGTTTATTAAGGCAGCAATTAGACAGATG
TATCCCAGCATTTCTGCATCATCAACATTAGACCATCCCACGATAAGTCTGCTGAGCTTTCTTCC
TATGAACTTTGAGGTCATTGATTCCTATTTCAGCATGCTAAAATCCTCCAATACATCATCCTCAC
ACAGGCCCATGATGGATGAGGTTTTGATGGGGTTTCATGAATATATTCTCGAAAATCTGCTAC

TGAAGGATGAAACCAATTTGACGTTTACTATTGCAGATGAGATCAAAAAGTTTTATGGTGGGT
TATTGCTCCTGGTAACATATCATATTGAAACTCTAGTTCCTCACATTGAATGTAGGAAGCAAAA
TAATCTCTCGACGGGATTTGGAACCATCGCAATTGAGGCGCAATCTGCTATGTGTTTATCGTAT
GAGGATTTGATGAATAGCAACAACTGTAGGGAGGCCAATCTTGTTCTTCAATTTTTGACTGTG
GCTTTCTGGCTTATCAAGTCTGAAGGAAGCTTGATGGATATACTAAAGCACAAAGCCACTTTG
GAATATCAAGTTCTGGATCTGATTCAGAGTGCTCGTGAAGAGCTTATTTTCATTAGATCTATCC
TCATGGATCTTGTCAGGCAACACACAGAAGTTAAGAAATTGGATGATATCTTAATGCATGCTG
AAGTGACTGCGAAACGGTTAGCAATACTCAGTGATTCTTGTTATGAAATTTTCAAGGATGGAA
GCAGCACTGACAAAATGAGGCCTTGGTTATCTGATTCTCTACAAGAGATTGAGTCTATCAAGG
TAGAGTTCAGAAAAGTATGCTTTCAAGTTCTGGATGTATCACCTTTAACCATGACAGATGGAG
AAGGCCTTATTAATTTCTTATTAAACCACCAGGACAAGGTGCCGAACGATGAAGCTGTTTCTTT
TAACGGAAGTTTCATGGATGGAAGCAGCAGTGAGAATATGGAACTTTCATCATTTGATTTTCT
AGGGGAGACTCAGTCTGTCAAGGTAGAGGAGGTCAGAAATGCATGCAATCAAGCTGTGGAT
GCATCACCCTATGAGATGCGTAAGACCGATGGAGAAGGCTTTATCAATCTTCTGTTAACCCAA
CAGGACAAGCTGCTGGACTATGATACTGGTTCAATCTCTTTTCTGCATAATCAAATCTCAGCAG
TTAAAGACAAACTATTGGACATGGGATCTTTACTTGTAGATACTGTACAGTACCGCAATATGCA
TCTTGAACTCAAAGATCTTGCTATACGTCTTCAAGATAAAAACTACATTTGTTTCTTTTCCATCA
AGGGGTATATTCCTGCTTGGTATTACACATTATATCTCTCTGATGTCAAGCAGTTGTATAAGTT
TGTTGAGGCAGAGGTAAAGACGATTTGTCTGAAAGTTCCAGATTCTTCAAGTTATAGCTTCCC
CAAGACAAATGGACTAGGATTTCTAAATTGCTTTTTGGGCAAATTGGAGGAGCTTTTATGTTCT
AAGCTTGATTTGGCTGTCGACTTAAATCATCAGATTGGGTCAGTCAAGGAGGGCTTACTGTAT
CTAACATCATTGATTGATTATTTTTCAGAAAACTATGATGAGCATGATGAAGTTTATAGTCTTG
TAACAAGTGTTACTGTAATGGTATACAAGGCCGAGTATGTCATTGACTCGTGCTTGGCCTATTC
TCATCCACTCTGGTACAAAGTTCTTTGGATTTCTGAAGTTGTTGAGAATATTAAGATTGTAAAT
AAAGTTGTTAGGGAGACTTGTGAAAAAAAGAAGATTGAAGTGACAGTGCATGATGTTGCAAA
GACCTCCACTAATCTTGCACCATCGTTTTCAGATAATACTCAAAGAACAGACGAAGAAATGGA
GGGTTTCCAGGATACAATGGACGAATTAAAGGAGCAGCTACTTGGAGGATCGCCTCAACTTG
ATGTCATCTCAATCGTTGGCATGCCAGGATTGGGCAAGACTACACTAGCAAAGAAGATTTACA
ATGATCCAACAGTCACCTCTCACTTTGATGTCCATGCTCAATGTCTTGTGACTCAAATATATTCA
TGGAGGGAGTTGTTGCTGACCATCTTGAACGATGTTCTTGAGCCTGCTGATCGCAATGAAAAA
GAAGATAGTGAATTAGCTGATGAGCTACGTCGATTTTTGTTGACGAAGAGATTCTTGATTCTC
ATTGATGATGTGTGGGACAACAAAGTGTGGGACAATTTACATATGTGCATCAGAGATGTTCG
GAATGGGAGTAGAATTATTCTAACAACCCGGCTGAGTGACATTGCCAATTATGTTAAATGTGA
AAGTGCTCCCCATCATCTTCGTTTATTCAGAGATGATGAGAGTTGGGCATTGTTACAGAAAGA
GGTATTTCAAGGGGAGACCTGTCCACCTGAACTTGCAGATGTGGGATCTCGGATAGCGAGGC
GTTGTAGAGGGTTGCCTCTCTCAGTGGTGTTAGTAGCTGGTGTTCTGAAACAGAAAAAGAAG
AAACTAGATTCATGGAAAGTAGTAGAAGAAGGTCTAGGTTCCCAGAGCATAGGCAGCTTAGA
AGAGAGCATGTCTATAATTGGATTCAGTTACAAGAATTTACCTCACTATCTTAAGCCTTGTTTTC
TCTATTTTGGAGGTTTTTTGCAGGGAAAGGATATTCATGTCTCAAAATTGACTCGGTTGTGGG
AAGCCGAAGGGTTTGTACAAGCAAACAAGGAAAAAGGACAGCAAGATGCCGCACAAGGTTT
CTTGGAAGATCTTATTCGTAGAAATCTAGTAATGGGCATGGAGAAGAGACCCAATGCCAAGG
TGAAAACGTGCCGCATTCATGATTTGTTGCATAAATTCTGCATGGAAAAGGCCAAACAAGAGA

ATTTCCTTCTCCAGATCAATAGTGGAGAGGATGTGTTCCCTGAACAGCTGGAGGAATACCGAT
TGTTCGTTCACTCTTACCAAGATGAAATTGATTTGTGGCGGCCATCTCGCTCAAATATCCGCTC
TTTACTATTCAATGCAATTGACCTGGATAACTTGTTATGGCCGCGCGATATCTCCTTCATCTTTG
ACAGTTTCAAACTTGTTAAAGTGTTGGATTTAGAGTCTTTCAACATTGGTGGCACGTTTCCCAG
TGAAATACAATATCTAATTCAGATGAGGTACTTCGCTGCTCAAACTGATGCAAATTCAATTCCT
TCATGTATAGCTAAGCTTGGGAATCTTGAGACTTTTGTGGTTAGAGGATTGGGAGGCGAGAT
GATTTTACCTTGTTCATTTCTGAAGATGGTGAAATTGAGGCATATACATGTAAACCATCGGGTT
TCATTTGGTTTGCATGAGAACATGGATGAATCCCTTTCTCACTCTCAATTAGCTAATTTGGAAA
CCTTTTCTACTCCACGTCTCTCTTATGGTGGAGACGCGGAGAAGATTTTGAGGAAGATGCCAA
AACTGAGAAAGTTGAGTTGCATATTTTCAGGGACATTTGGTTATTCAAGGAAAGTGATGGGTA
GGTGCGTTCGTTTTCCCAGATTAGAGTTTCTAAGCCACCTTGAGTCCCTCAAGCTGGTTTCCAA
CAGCTATCCAGCTAAACTTCCTCACAAGTTCAATTTCCCCTCGCAACTAAGGGAATTGACTATG
TCCAAGTTTCGTTTACCTTGGACCCAAATTTCGACCATTGCAGAACTGCCCAACTTGGTGATTC
TTAAGTTATGTCTCAGAGCCTTTGAAGGGGATCACTGGGAAGTGAAAGATTCAGATTTCCCTG
AACTCAAATACTTAAAACTGGATAACCTCAAAATTGCACAATGGTCTGTCTCTTGTGATGCTTT
TCCTAAGCTTGAACATTTGGTTTTAACGAAATGTAAGCATCTTGGGAAAATCCCTTCTCATTTC
GATGATGCTGTATCTCTGAAAAGAATTGAGGTAAACTGGTGCAACTGGTGTGTTGCCAATTCA
GCCCAAGAAATTCAAACAACACAACGTGAAGATATGGCAAATGATTCATTCACAGTTACCATA
CAGCCTCCAGATTGGGCTAAAAGATCATCTCCTTGACTCATATCTGTAACAGCAACCAAAGCA
AAAGATTCTACTTCAGCAAGAGGCGTTCTGTCTATTTCTAGAACAAGTGAAGTTATTATGTTGA
ATTTTTGCAAAGAAGAAGAATCAGGACAGGGATGCCAGCATTTTCAACATGGGAGAGTAGAG
GAATTGTTTGATCCAAATCTTATGTTGTACAACTACAACACTATCAATGTAAAAAAATGAGATT
CTACGAGTGGTACATGTCAGACTTCTGTGCACACAAGAGGTTCTGGGATTAAGACCATCCATG
TCTTAAGGCATGAGGCATTGCAGATGCGAGTAAAGAAAGAAGTGTTTCCTTCACCAACTAATC
CTCCCTTTATAGATGAGAAAACGATGGAGAAGGTGATTCAGCTTCAATTTGCCAGGATTTCTC
ATAGTTCTTTCTAGATGATGCTTCAGTGGCCTCAAACTGAGAAATAACATAAATCTGTGATAGA
GTGAATTTTGCATTTCAAGTATCTTCTTGCCTCTTGTTCCTCTTTTGCACACTCTGGAAGCAGAT
GTTTCGTTTGCAACAAGTTGCTTTTATCATTGTAATAGTTA

Attachment 8.

Tomato Prf N-terminal domain (LePrfN) and *Nicotiana benthamiana* Prf N-terminal domain (NbPrfN) protein sequence alignment (ClustalW, http://www.ebi.ac.uk/Tools/msa/clustalw2/).

```
LePrfN          MAKECRDAIGTINLVKGQHLDRRTTNQLEDAIKHLTHVAVFLTNLEKRHPANGISVHLRP 60
NbPrfN          MAEECRAVIGAINLVKGQHLGITTINQLEDATKHLTRVAVFLTNLEKRYPENGISGQLRP 60
                **:*** .**:*********.  * ****** ****:***********:* **** :***

LePrfN          LFLEAHDGFSLMCSHPPRSQFTVKLDNIAEKFKSAKASRSTRQVIPELLQIIEPENIAKR 120
NbPrfN          LFLEAHDGFSEICSRFPRFNLTIK---MAEKFKASKASK--LQMISEVLNIIEHENIAER 115
                ********** :**: ** ::*:*   :*****::***:   *:*.*:*:*** ****:*

LePrfN          IKASKPSRSSSPITVDMVGFIESLLGSVHRALFFISAGPPVSMLDKKLRHLQVFFRLISK 180
NbPrfN          VRASKPLRSPSRITMEMVGFVESLLGSVHRALFFISVGPAASLLDKKLRHLRVFFTLIAK 175
                ::**** **.* **::****:***************.**..*:********:*** **:*

LePrfN          RGIEHESMKDLFYHVEDVAYTAAQLCVLGSSCHMDNEFSKLLERISRPFSPGLRLVYLNA 240
NbPrfN          RCIEHESMEDLFTHVEDVAYTAAYLCFLGSNWNMDGEFSELLERVSRPFIPELRQIYLSA 235
                * ******:*** ********** **.***. :**.***:****:**** * ** :**.*

LePrfN          LIGLNSSRSKTT--MNAKYMLDFVSALQDDLRLRCDNRIRWLQRGLSYLCRFLRDIESYP 298
NbPrfN          LIGLKSSTSETTTILNAKYMLDFVSALREDLRLGCDDRIRWLQRGLSYLSRFLRDIESYP 295
                ****:** *:**  :************::**** **:************.**********

LePrfN          VSHRQLISLQLNMEDLAIGSANAIYS-YDEDMDKTSEIDHELFHLQMKFNYVKVEVDLIR 357
NbPrfN          LPHEEVISLRLNMEALAIGAANAIYSSYDEEMHNTTETDDVLFHLQLKFNYVKVEVDLIQ 355
                :.*.::***:**** ****:****** ***:*.:*:* *. *****:***********:

LePrfN          LQNIQGTIIV-PMKDLIDYVWEELMFFRSYFMDAFDQCKEQTRITVILNYIQSAVSQAWS 416
NbPrfN          LLTRQAAITIGPMKSLIDYVWRELIFFRNYFMDALKQCKEKTNITVILTSIQSAISQAWS 415
                * . *.:* : ***.******.**:***.*****:.****:*.*****. ****:*****

LePrfN          VCDSLCHDLNQND------------LAREINCLHFQLLLKFKFIKVAIRQMCPSISASST 464
NbPrfN          ICDSLCHGSEQEDYFSDDTEQEDPLVGEMINCLHFQLLLKFKFIKAAIRQMYPSISASST 475
                :******. :*:*            :.. ****************.***** ********

LePrfN          PDHPMIDLLNFLPMNFEAIDSYSSMLKASFPSSSHRPNKDAESPNTSFLCGPNTDVYSFY 524
NbPrfN          LDHPTISLLSFLPMNFEVIDSYFSMLKSSNTSSSHR---------------------- 511
                 *** *.**.*******.**** ****:* .*****

LePrfN          SSSSRIPKMDEILKRFHEYILVNLL 549
NbPrfN          ------PMMDEVLMGFHEYILENLL 530
                      * ***:*  ****** ***
```